KANSAS GEOLOGICAL SURVEY
OPEN-FILE REPORT 91-44

CHARACTERIZATION AND RESERVOIR PERFORMANCE OF THE LANSING-KANSAS CITY "I" AND "J" ZONES (UPPER PENNSYLVANIAN) IN THE PEN OIL FIELD, GRAHAM COUNTY, KANSAS

by

Rod A. Phares

Kansas Geological Survey
1930 Constant Avenue
University of Kansas
Lawrence, KS 66047-3726

CHARACTERIZATION AND RESERVOIR PERFORMANCE OF THE LANSING-KANSAS CITY "I" AND "J" ZONES (UPPER PENNSYLVANIAN) IN THE PEN OIL FIELD, GRAHAM COUNTY, KANSAS

by

Rod A. Phares

A.B., Harvard University, 1986

Submitted to the Department of Geology and the Faculty of the Graduate School of the University of Kansas in partial fulfillment of the requirements for the degree of Master of Science.

Anthony W. Walton
Professor in Charge

Robert H. Goldstein

Paul Wellstead
Committee Members

Anthony W. Walton
for the Department

ABSTRACT

The Pen Field produces oil from several intervals in the Lansing and Kansas City groups (Upper Pennsylvanian). An extraordinary amount of information is available for this field: numerous cores, modern log suites, drillstem tests, and accurate production records. The lithofacies and paragenetic features in the two main producing zones ("I" and "J") were comprehensively examined using slabbed cores and impregnated and stained thin sections.

The "J" zone contains two carbonates units, both of which formed in a shallow, open marine environment. These carbonate units exhibit a great variety of paragenetic features from several diagenetic environments. Severe alteration of the top of the upper carbonate unit occurred during subaerial exposure. Most of the paragenetic features formed during this exposure event. After burial, subsidence of the depositional basin and an evolving pore water chemistry led to formation of burial cements, as well as replacive mineralization.

The "I" zone exhibits a simpler sequence of depositional units with a single carbonate unit, overlain by a shale unit. This carbonate unit also exhibits a great variety of paragenetic features, and is capped by

a subaerial exposure surface. The shale unit contains a second, unrelated subaerial exposure surface. The paragenetic features in the "I" carbonate unit that post-date burial and compaction closely resemble the analogous features in the "J" carbonates, indicating the two zones were essentially part of the same diagenetic environment after significant burial.

A grainstone interval in the "J" zone, termed the alpha grainstone, is the main producing horizon in the field. A crossplot of reservoir pressure versus cumulative production indicates the alpha grainstone has excellent continuity and communication between producing wells. A crossplot constructed from core measurements reveals a good correlation between porosity and permeability. Water saturation also appears to be a function of porosity.

The nature of the pore network in the alpha grainstone can significantly alter the relationship between porosity and permeability. The grainstone typically exhibits abundant interparticle porosity supplemented by skeletal molds and oomolds. However, some small areas of the grainstone body exhibit abundant molds and significant reduction of the interparticle pores with a marine phreatic cement. The resulting "mold-dominated" pore network exhibits very low

permeability for a given porosity. This type of pore network appears to be volumetrically insignificant in the main body of the alpha grainstone, except for the southwest corner of the field.

The relationship between porosity and permeability in the grainstones of the "I" zone is significantly different than the alpha grainstone relationship, but again shows a high degree of correlation. The "I" zone water saturation correlation also shows a marked difference to the "J" alpha grainstone correlation. Porosity is erratically developed in the "I" zone, and there may be very poor continuity between producing wells.

A three-dimensional simulation grid was constructed for the entire field. Porosity values were assigned to every cell by linear interpolation from the adjacent wells. Permeability and water saturation values were derived from the porosity correlations. Analysis of individual well production suggests the values of porosity, permeability, and water saturation in the inter-well areas are generally very accurate. However, the analysis identifies several wells with drainage anomalies. The anomalies were easily resolved because the nature of the anomaly typically coincided with the reservoir characterization.

Analysis of the production by zone indicates the "J" alpha grainstone contributes by far the most Pen Field production, although the "I" zone makes a significant contribution. Both of these zones are attractive waterflood candidates. The "K" zone contributes some production, but is poorly exploited by the original completions. The "L" zone has good porosity and saturation on the logs and in the available cores. However, this pore network exhibits very poor continuity, so the "L" zone probably does not form a commercial reservoir in the Pen Field.

ACKNOWLEDGEMENTS

I would like to thank PanCanadian Petroleum for access to all records pertaining to the Pen Field, as well as the cores. The availability of these items so soon after the field was discovered is a positive step toward greater cooperation between industry and academia.

My chairman, Dr. Anthony Walton, has been instrumental in this thesis project, and very patient throughout its many permutations. Dr. Robert Goldstein was always available to discuss the endless surprises of carbonate diagenesis. Dr. Paul Wilhite ensured that the union between petroleum geology and petroleum engineering remained smooth despite the differing "ideologies".

I would also like to thank the numerous contributors that were not part of the official committee. Dr. Lynn Watney provided insights to both the sedimentology and diagenesis, and was always eager to discuss any aspect of Kansas cyclothem deposits. Dr. John Doveton aided in the log interpretation, and his colorful language provided a much needed change of pace. Dr. Don Green fielded diverse questions, even when it was less than convenient. Lanny Schoeling was helpful in the drillstem test analysis.

Financial support for the protracted gestation of

this thesis was provided by the Tertiary Oil Recovery Project (T.O.R.P.). Texas Oil and Gas Corporation (TXO) also contributed a much welcomed scholarship. This investigation would not have been possible without this generous support.

"But sleep? On a night like this? What an idea! Just think how many thoughts a blanket smothers while one lies alone in bed, and how many unhappy dreams it keeps warm."

Franz Kafka
Description of a Struggle [1905]

"I have grown to believe a stone is a better pillow than many visions."

Robinson Jeffers
Clouds of Evening [1930]

TABLE OF CONTENTS

LIST OF ILLUSTRATIONS

LIST OF TABLES

INTRODUCTION

PURPOSE OF INVESTIGATION

Accurate reservoir characterization is necessary to maximize oil production. Determining the continuity and heterogeneity of petroleum reservoirs is imperative in optimizing primary recovery from compartmentalized reservoirs and in predicting flow patterns in enhanced oil recovery (EOR) projects.

The Pen Field is ideal for comprehensive reservoir characterization for two reasons. First, extensive research in the region provides a solid background for reservoir studies. Pen Field is part of a well-studied, mature trend of oil fields on the Central Kansas Uplift that produce from the Lansing and Kansas City Groups (Fig. 1). Second, an extraordinary amount of information is available on the Pen Field: accurate production records with monthly barrel tests, cores from the productive interval in eight producing wells and three dry holes, modern log suites designed to evaluate carbonate lithologies, and drillstem tests of the reservoir unit in almost every well.

The objectives of this investigation are:
1. describe and interpret the lithofacies and paragenetic features of the main producing zones; 2. analyze the available reservoir engineering data; 3. combine this

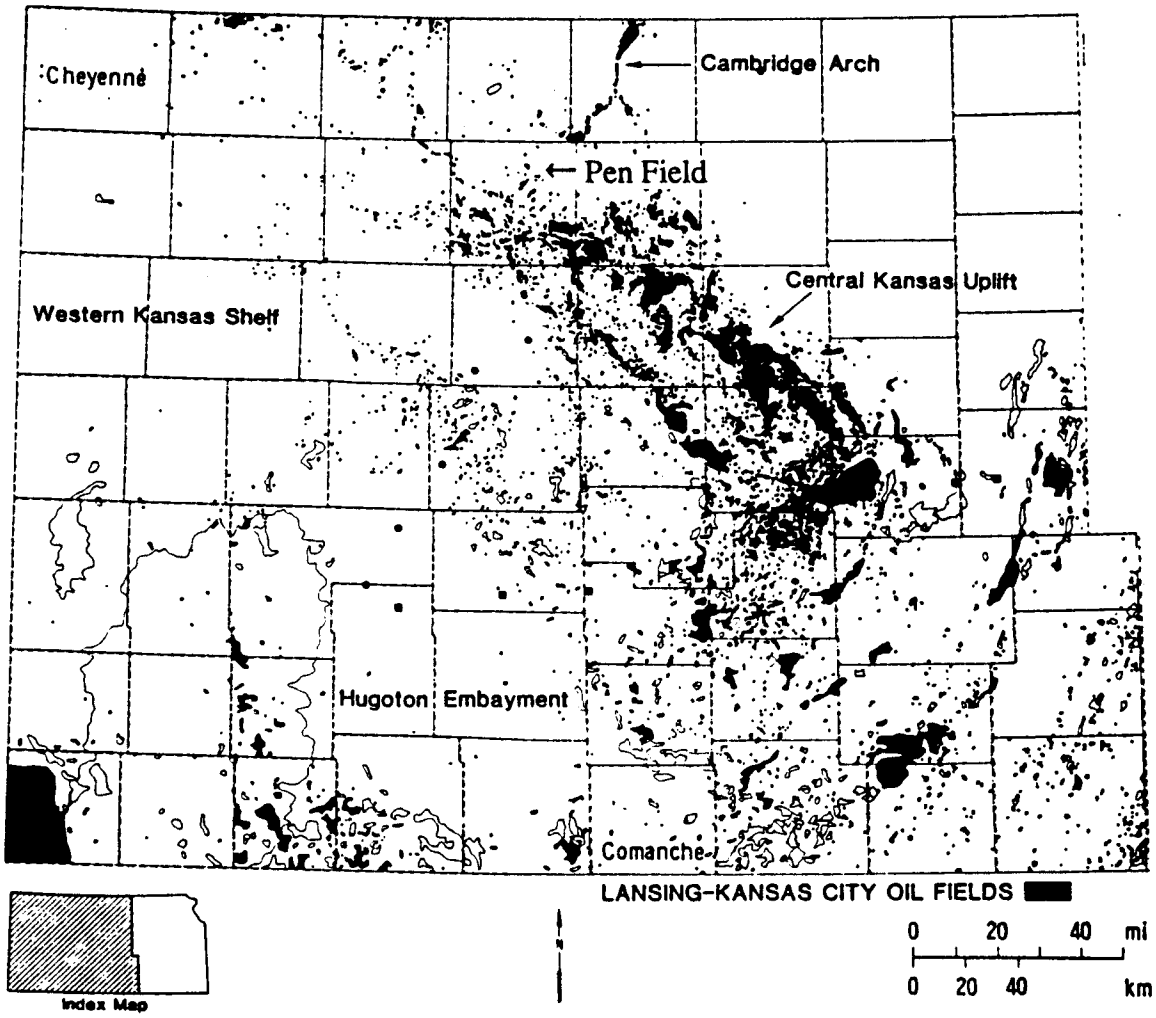

Figure 1. Location map of the Pen Field, with oil and gas fields in central and western Kansas. Fields producing from the Lansing and Kansas City groups are solid black, whereas fields with other pay zones are only outlined. (Adapted from Watney, 1984).

disparate information to determine the continuity and heterogeneity of the reservoir; 4. divide the field into grid blocks and assign values for porosity, permeability, and fluid saturation.

This study is the first part of a multidisciplinary investigation of the Pen Field, conducted under the auspices of the Tertiary Oil Recovery Project (T.O.R.P.). Work is currently underway to simulate the primary production history. The field operator has recently implemented a waterflood project in the "I" and "J" zones. Injection into four converted producing wells began November 25, 1990. This secondary recovery project will provide information for a second reservoir simulation.

GEOLOGIC SETTING AND PREVIOUS INVESTIGATIONS

The Lansing Group and the underlying Kansas City Group are part of the Missourian Stage, Upper Pennsylvanian Series, Pennsylvanian System. Most subsurface workers combine the two groups and refer to them as the Lansing-Kansas City, which is divided into a simple alphabetic series of zones (Fig. 2; Morgan, 1952).

The Lansing-Kansas City strata generally consist of repetitive sequences of interbedded carbonates and shales, which were termed cyclothems by early workers (Moore, 1936; 1949). Most studies attributed the cyclicity to glacio-eustatic changes in sea level

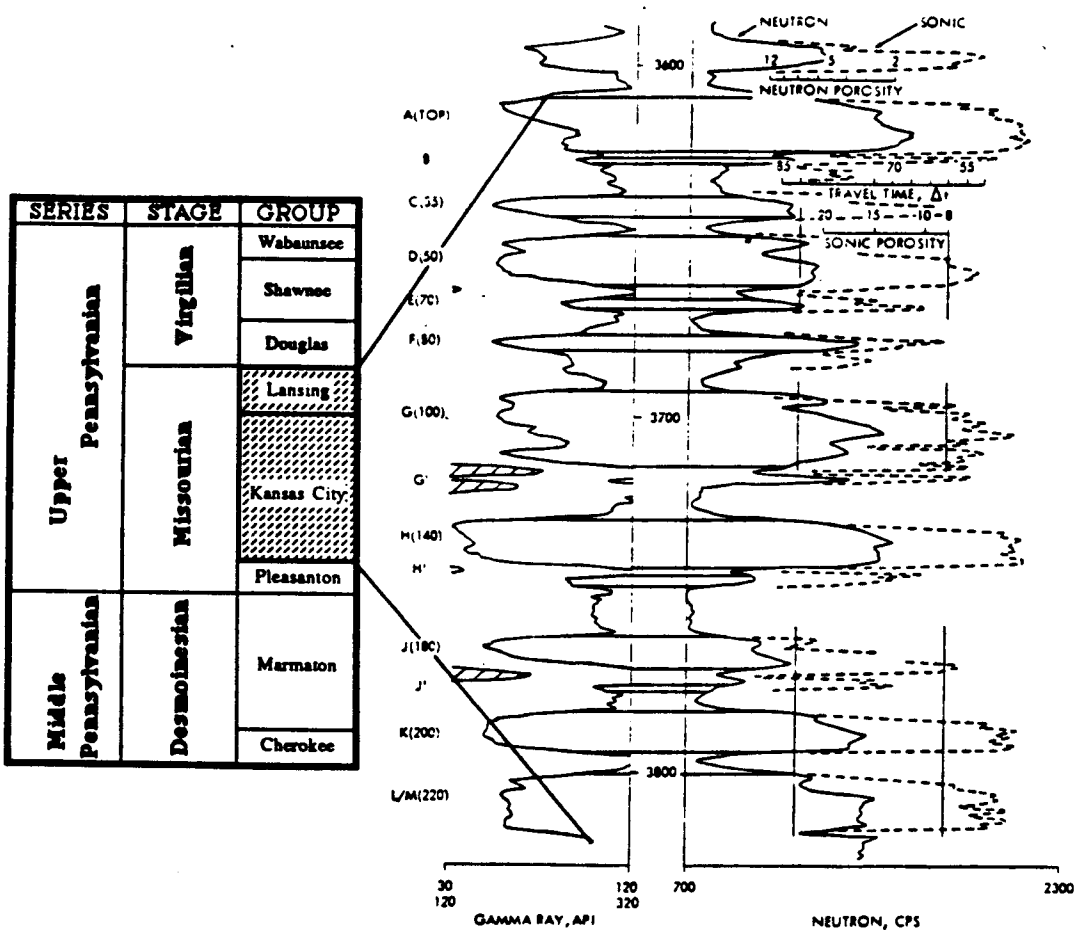

Figure 2. Stratigraphy of the Upper Pennsylvanian Series and well log of the Conoco Adell L-KC Unit 406 from section 2, T6S-R27W. Letter system of correlation of carbonate zones is similar to that of Morgan (1952). Numbers indicate correlation system based on depth (in feet) below the top of the Lansing Group. (Adapted from Watney, 1980).

(Wanless and Shepard, 1936; Heckel, 1977; Watney, 1985).

The ideal cyclothem consists of a lower carbonate, lower shale, upper carbonate, and upper shale (Fig. 3). This ideal four-component cyclothem is interpreted to reflect a general transgression and regression of the sea across a broad shelf; the lower carbonate deposited during the initial transgression, the lower shale deposited at maximum inundation, the upper carbonate deposited during regression, and the upper shale deposited at maximum regression (Fig. 4) (Heckel, 1977; Watney, 1980). Many of the upper carbonates were subjected to subaerial exposure that typically altered the sediments by paleosol development and contact with undersaturated meteoric waters (Dubois, 1979; Heckel, 1983; Prather, 1981; Watney, 1980).

The upper carbonates are the main reservoir units of the Lansing-Kansas City, but confusion sometimes arises because the stratigraphic letter designations are not based on the occurrence of upper carbonates. Rather, each lettered zone marks a carbonate unit that can be correlated over a broad region. According to Watney (1980), the "A", "C", "D", "F", "G", "H", "J", "K", and "M" zones are upper carbonates, whereas the "B", "E", "G'", "H'", and "J'" zones are lower carbonates.

In northwest Kansas, many of the lower carbonate units are thinner than the vertical resolution of the

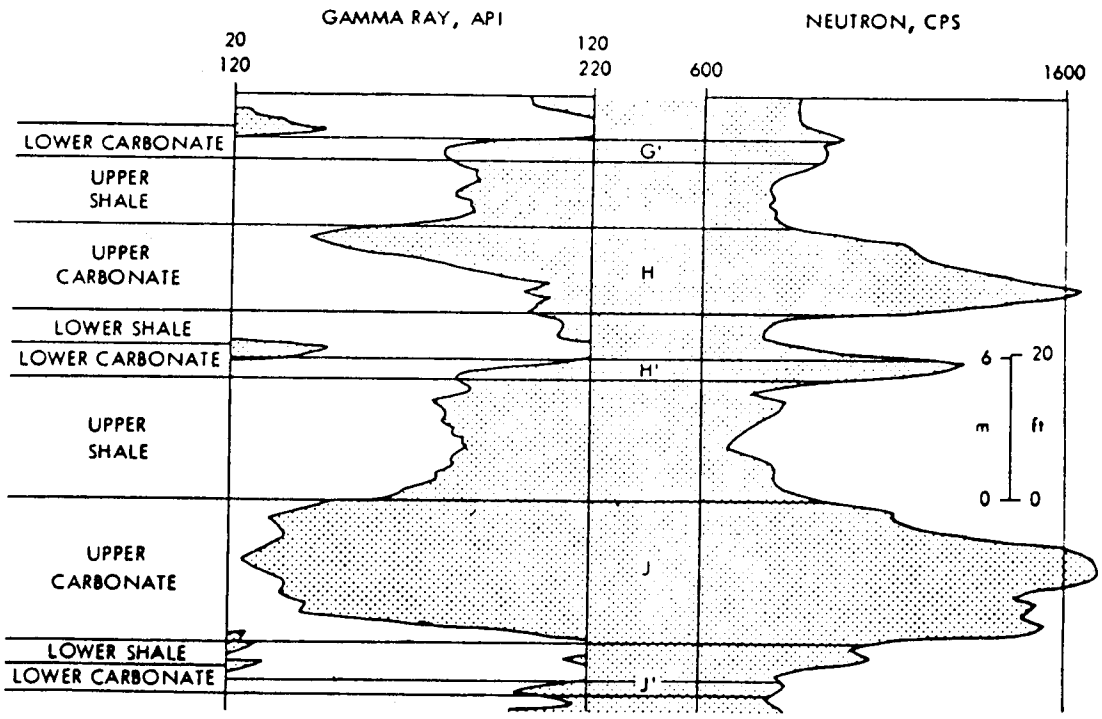

Figure 3. Gamma ray-neutron well log signature of the units in typical four-component cyclothems of the Lansing and Kansas City groups. From bottom to top of a single ideal cycle: lower carbonate - lower shale - upper carbonate - upper shale. Log of the Chief Drlg. Co., VAP A-1, 21-1S-33W (Watney, 1980).

Figure 4. Ideal (basic) four-component cyclothem. Environmental interpretations are based mainly on lithology and gross biotic distribution (Heckel, 1977). [Heckel's terminology for the four components (positional members) differs from the usage adopted for this study. His middle limestone is equivalent to the lower carbonate; the core shale is equivalent to the lower shale; the upper limestone is equivalent to the upper carbonate; the outside shale is equivalent to the upper shale.]

Basic Cyclothem
(simplified megacyclothem)
in Kansas-Iowa outcrop belt
Lithology
Positional Member
Approx. thickness
OUTSIDE SHALE
UPPER LIMESTONE
CORE SHALE
MIDDLE LIMEST.
OUTSIDE SHALE
Gray to green, locally red, Sandy shale w. siltstone sparse fossils
Laminated unfoss. bird's-eye calcilutite to Oolite
loc. cross-bedded Skel. calcarenite w. marine biota
Gray shaly Skel. calcilutite w. abundant marine biota
Gray-brown Shale w. abund. to sparse mar. fauna
Black fissile Shale w. PO_4, pelagic fauna
Dense, dark Skel. calcilutite w. marine biota; loc. Calcarenite at base
Sandy shale w. marine biota
Gray to brown Sandy shale w. loc Coal, Sandstone
5
4
3
2
1
0
m.
Depositional Environment
Nonmarine
Near-shore
Shoreline
Shoal
Shallow w.
Eff. wave base
Intermediate depth
Offshore
Eff. lwr. limit of algal CO_3 production
Deep water
① Detrital influx after carbonate shoal formed
② Detrital influx before shoal conditions reached
Fossil Distribution
Algae (preserved)
Invertebrates
Conodonts
Adetognathus spp.
Ozarkodina minuta
Aethotaxis advena
Idiognathodus spp.
Idioprioniodus lex.
Gondolella spp.
Phase of Deposition
Direction of sea-level change
Dominant processes
Depositional member
Maximum Regression
Regression
Transgression
Maxi-mum
Stillstand
Max. Regr'sn
Stillstd
Sub-sed.
Detrital influx
NEARSHORE SHALE
Stillstand
Subsid.<sedimenth
Detrital influx
NEARSHORE SHALE
Eustatic lowering of sea level
Subsidence probably < sedimentation
CO_3 product'n~"Basin filling"
REGRESSIVE LIMESTONE
Eustatic s.l. rise
Subsid. > sediment'n.
CO_3 prod.
Sed.starv'n
OFFSHORE SHALE
TRANSGR. LIMEST.

logging tools; non-ideal cyclothems, such as the "I" zone strata, also occur in this region. These two factors result in the irregular nomenclature. However, the rare luxury of abundant cores in the Pen Field (Fig. 5) allows each cyclothem to be fully described and compared to the ideal sequence. Therefore, in this study each lettered zone includes all components of the cyclothem, not just the main carbonate unit.

The Lansing-Kansas City strata are important petroleum reservoirs in central and western Kansas and parts of Nebraska, and have stimulated abundant research focusing on the petroleum geology of these sediments: Anderson (1989), Brown (1962; 1963; 1984a; 1984b), Dubois (1979; 1985), Ebanks and Watney (1985), Harbaugh and Davie (1964), Hopkins (1977), Kintner (1984), Prather (1981; 1984; 1985a; 1985b), Rascoe (1962), Rascoe and Adler (1983), and Watney (1980; 1984; 1985; 1986).

Most of these studies covered areas along the Cambridge Arch and the Central Kansas Uplift, both of which are particularly rich in Lansing-Kansas City oil fields. The Pen Field occurs in the saddle between these two positive relief structures (Fig. 6). The major uplift of these structures was post-Mississippian and pre-Middle Pennsylvanian (Merriam, 1963).

Lansing-Kansas City sediments generally thicken toward the shelf margin in southern Kansas (Fig. 6). The

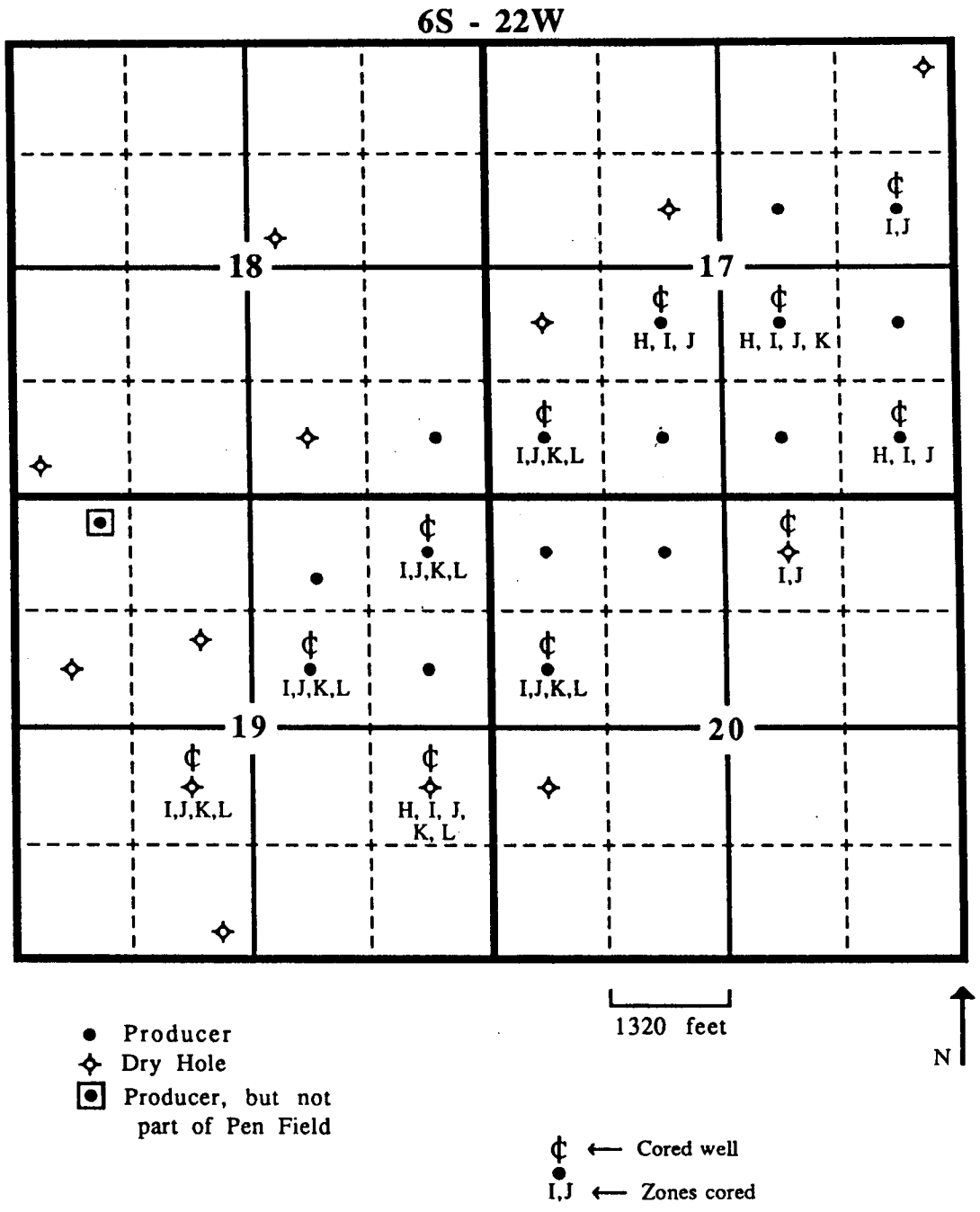

Figure 5. Map of the Pen Field, with cored wells and the Lansing-Kansas City zones covered by these cores.

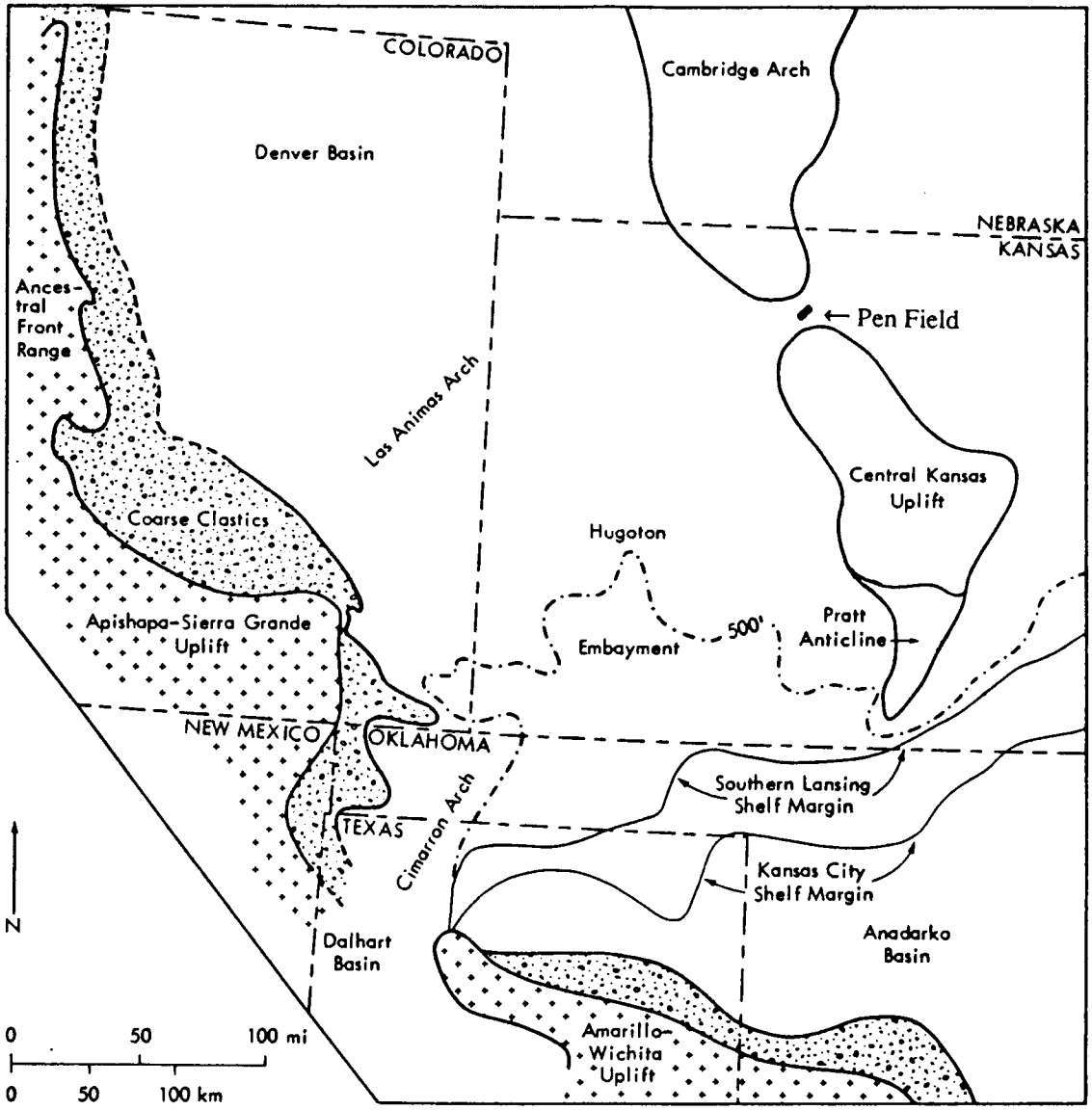

Figure 6. Missourian (Late Pennsylvanian) paleogeographic map of western Kansas and adjacent areas. The Pen Field (not to scale) lies in the saddle between two positive structural elements, the Cambridge Arch and the Central Kansas Uplift. The southern shelf hinge-line, defining the northern limit of the Anadarko Basin, is based on the position of the abrupt decrease in carbonate thickness to the south. Data for the map are from Rascoe (1962), Maher (1953), and Martin (1965). The 500 foot Missourian interval isopach is after Rascoe (1962). (Adapted from Watney, 1980).

Missourian Stage (Lansing, Kansas City, and Pleasanton Groups) is slightly more than 200 feet thick in the Pen Field, but is over 500 feet thick in the Hugoton Embayment (Fig. 7). A paleoenvironment reconstruction shows the extent of the open marine environment that prevailed during the Missourian transgressions (Fig. 7).

FIELD HISTORY

Pen field lies in sections 17, 18, 19, and 20 of township 6S-22W in Graham County, Kansas. The PanCanadian Petroleum Company's Pennington #1 (SW-NE, sec. 17, 6S-22W) was completed in May, 1985 to open the field (Fig. 8). It had an initial potential of 60 barrels of oil per day (BOPD) with no water, from perforations at a depth of 3707 to 3723 feet in the Lansing-Kansas City "I" and "J" zones. Twelve more producing wells were completed over the next year. The field was fully developed on 40 acre spacing by March, 1988 with a total of seventeen producing wells and eight dry holes (Fig. 9). Cumulative production through April, 1990 was 524,000 stock tank barrels of oil. Gravity of the oil sampled during initial production tests varied from 37 to 41 degrees API gravity.

Most of the wells were drilled to the Arbuckle Group, but the only production to date is from the Lansing-Kansas City Groups. The majority of the

Figure 7. Missourian (Late Pennsylvanian) paleoenvironment map of Kansas and adjacent areas, and thickness of Missourian rocks (in feet). This idealized reconstruction shows the vast extent of the open marine environment surrounding the Pen Field (not to scale) that existed during the Missourian transgressions. These marine transgressions inundated the highest areas of the Central Kansas and Nemaha uplifts. The Missourian Stage (Lansing, Kansas City, and Pleasanton Groups) is slightly more than 200 feet thick in the Pen Field, but is over 500 feet thick in the Hugoton Embayment. (Adapted from Rascoe and Adler, 1983).

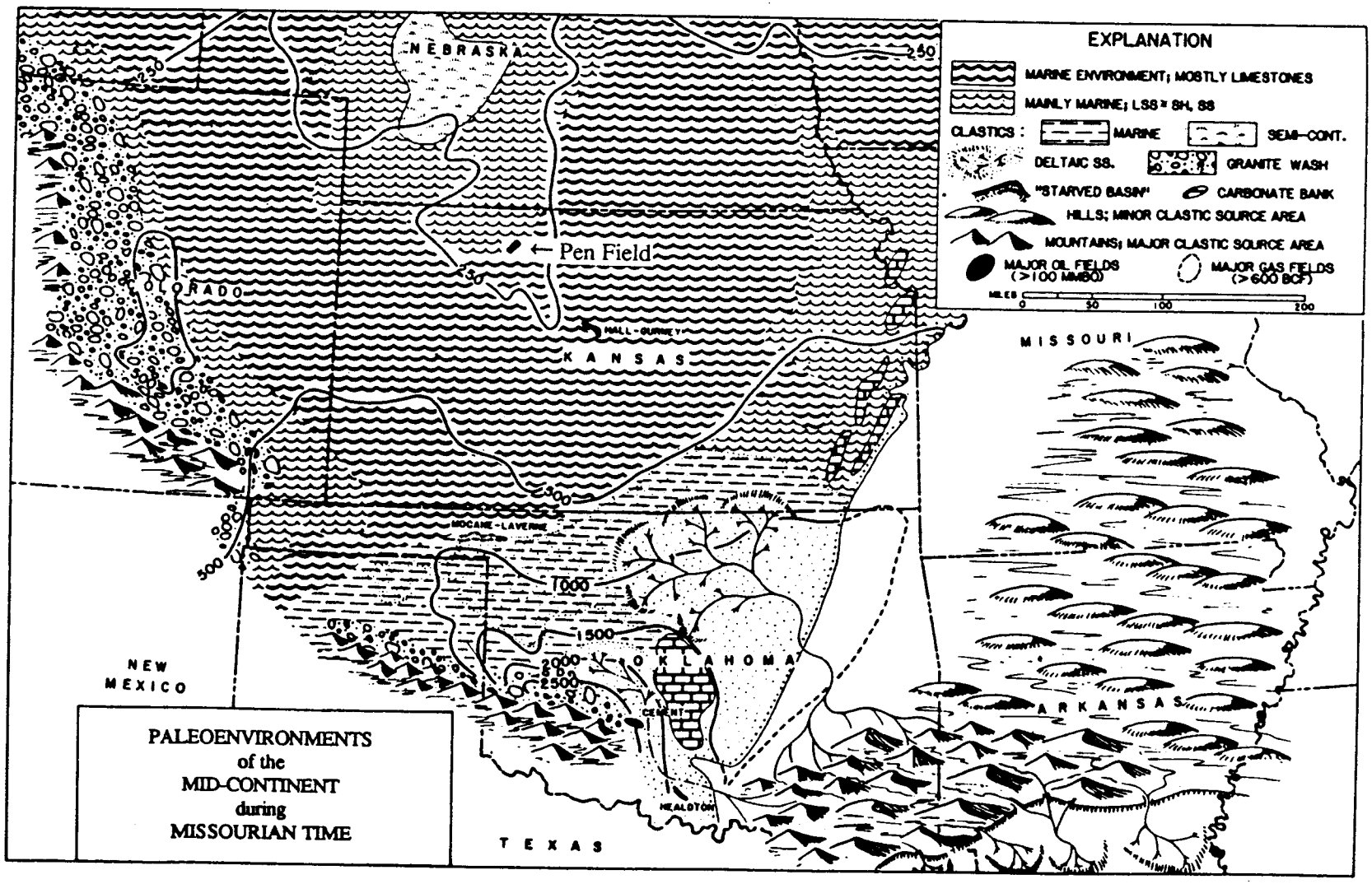
EXPLANATION
MARINE ENVIRONMENT; MOSTLY LIMESTONES
MAINLY MARINE; LSS > SH, SS
CLASTICS :
MARINE
SEMI-CONT.
DELTAIC SS.
GRANITE WASH
"STARVED BASIN"
CARBONATE BANK
HILLS; MINOR CLASTIC SOURCE AREA
MOUNTAINS; MAJOR CLASTIC SOURCE AREA
MAJOR OIL FIELDS (>100 MMBO)
MAJOR GAS FIELDS (>600 BCF)
MILES
0
50
100
200
NEBRASKA
COLORADO
KANSAS
MISSOURI
OKLAHOMA
ARKANSAS
NEW MEXICO
TEXAS
← Pen Field
HALL-GURNEY
MOCANE-LAVERNE
CEMENT
HEALDTON
250
200
300
1000
1500
2000
2500
PALEOENVIRONMENTS
of the
MID-CONTINENT
during
MISSOURIAN TIME

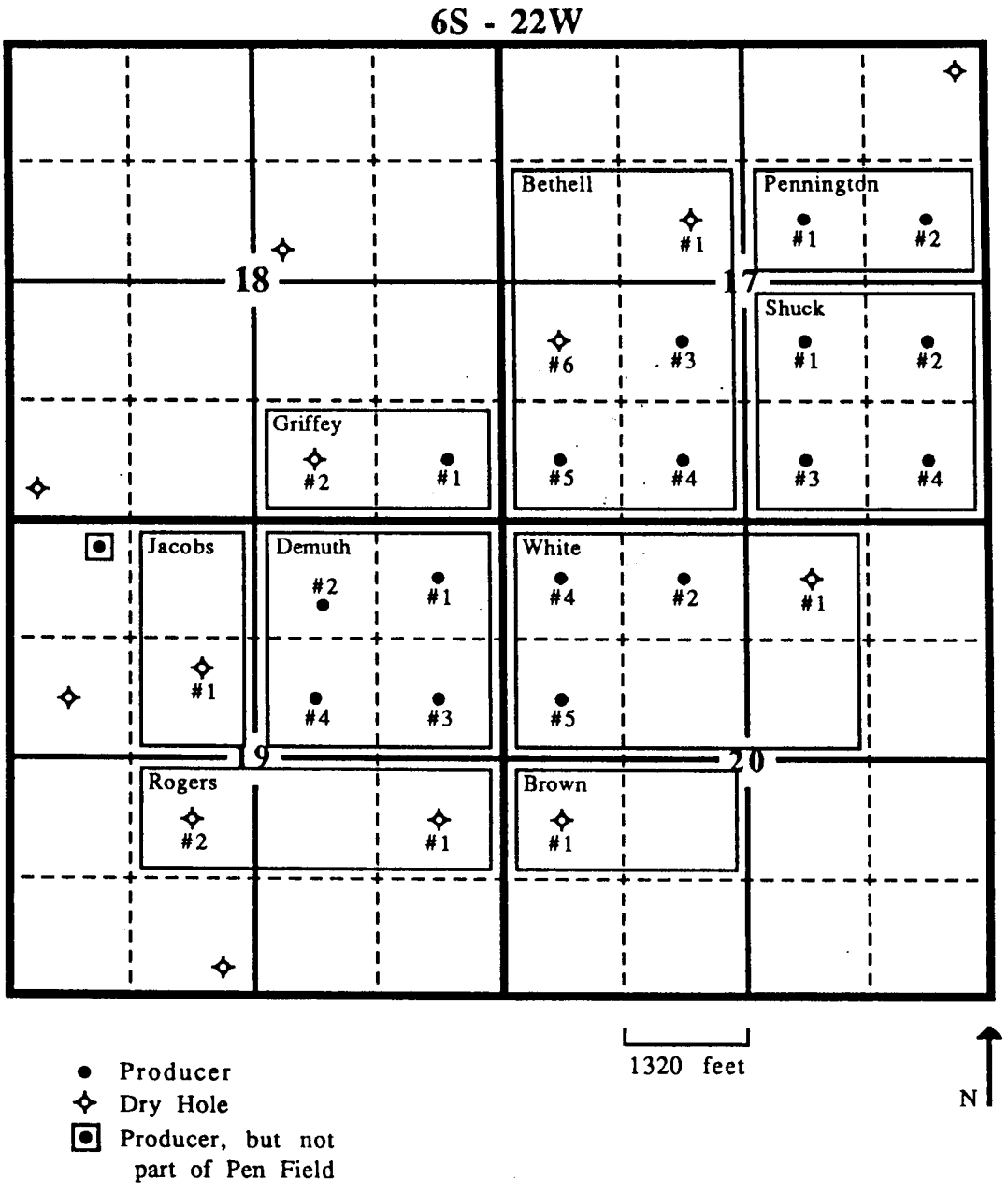

Figure 8. Lease names and well numbers in the Pen Field. All leases, except the Griffey lease, were originally operated by PanCanadian Petroleum Company. The Griffey lease was originally operated by Ritchie Exploration Company.

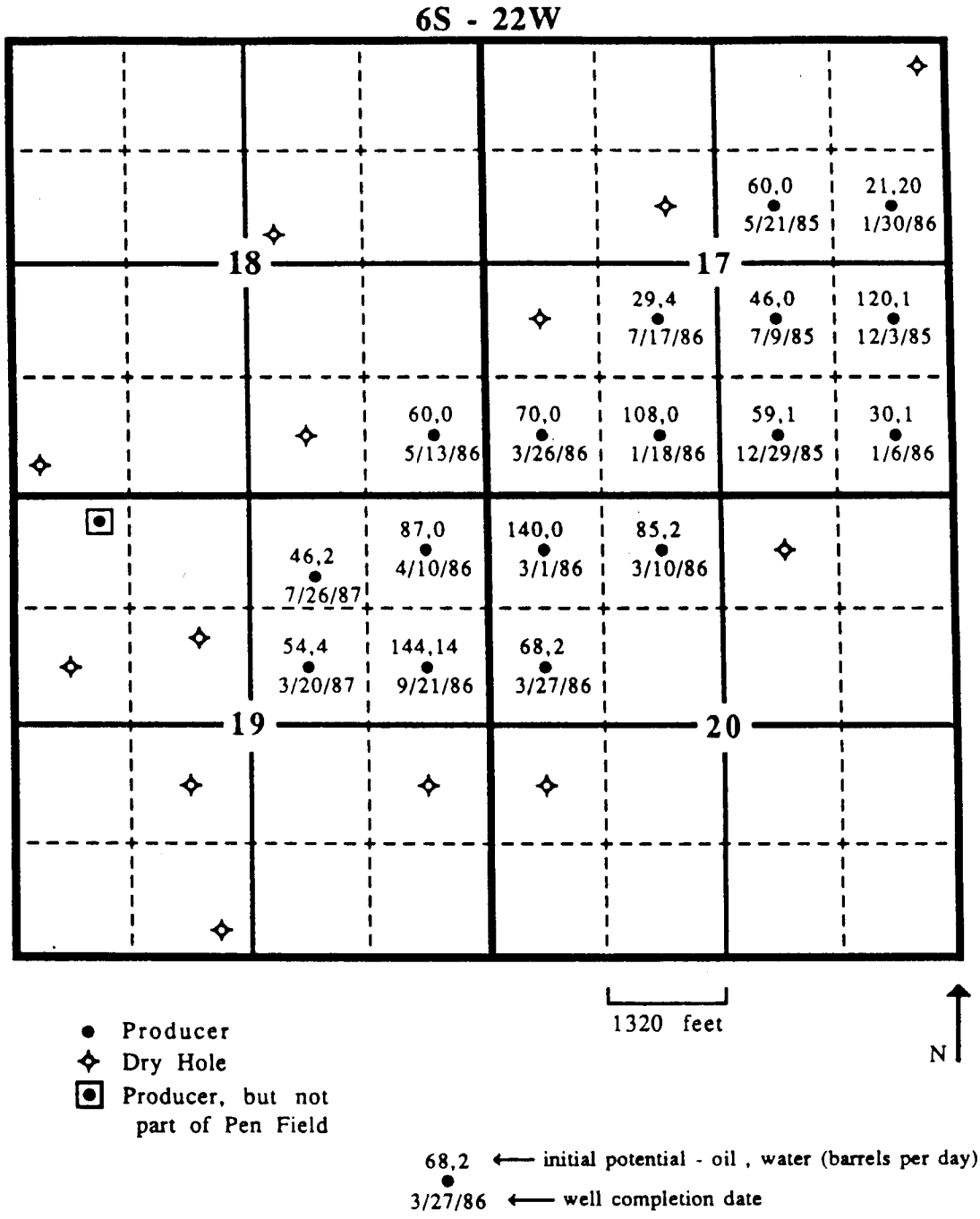

Figure 9. Initial potential and completion date of Pen Field producing wells.

production is from the "J" zone, with a significant contribution from the "I" zone. The "D", "K", and "L" zones are productive in a few wells (Fig. 10). All wells with multiple pay-zones are commingled in the well-bore, making it impossible to assign exact zone production values.

All of the producing wells were completed with a long string of 4 1/2 inch casing run a few feet off the bottom to the surface and either cemented to the surface or set with a two stage cement job. The entire "pay" interval in each productive zone was perforated, usually with two shots per foot.

All wells were stimulated with acid, but the exact treatment procedures were variable. In general, the perforations were treated in 1/2 or 1 foot intervals using a pinpoint injection (PPI) tool. Acid volumes varied from 45 to 250 gallons per foot and usually utilized 15% hydrochloric acid, although other acids were used. Small amounts of de-emulsifier, corrosion inhibitor, clay stabilizer, silt suspender, or KCl water were added to the acid in a few wells. Wells treated with small volumes of acid during the PPI stimulation were given a conventional follow-up acid job of 1,000 to 2,000 gallons. After the acid stimulations, all wells were swabbed back to recover the treatment load. Tubing and rods were run in the hole and then hung on a beam

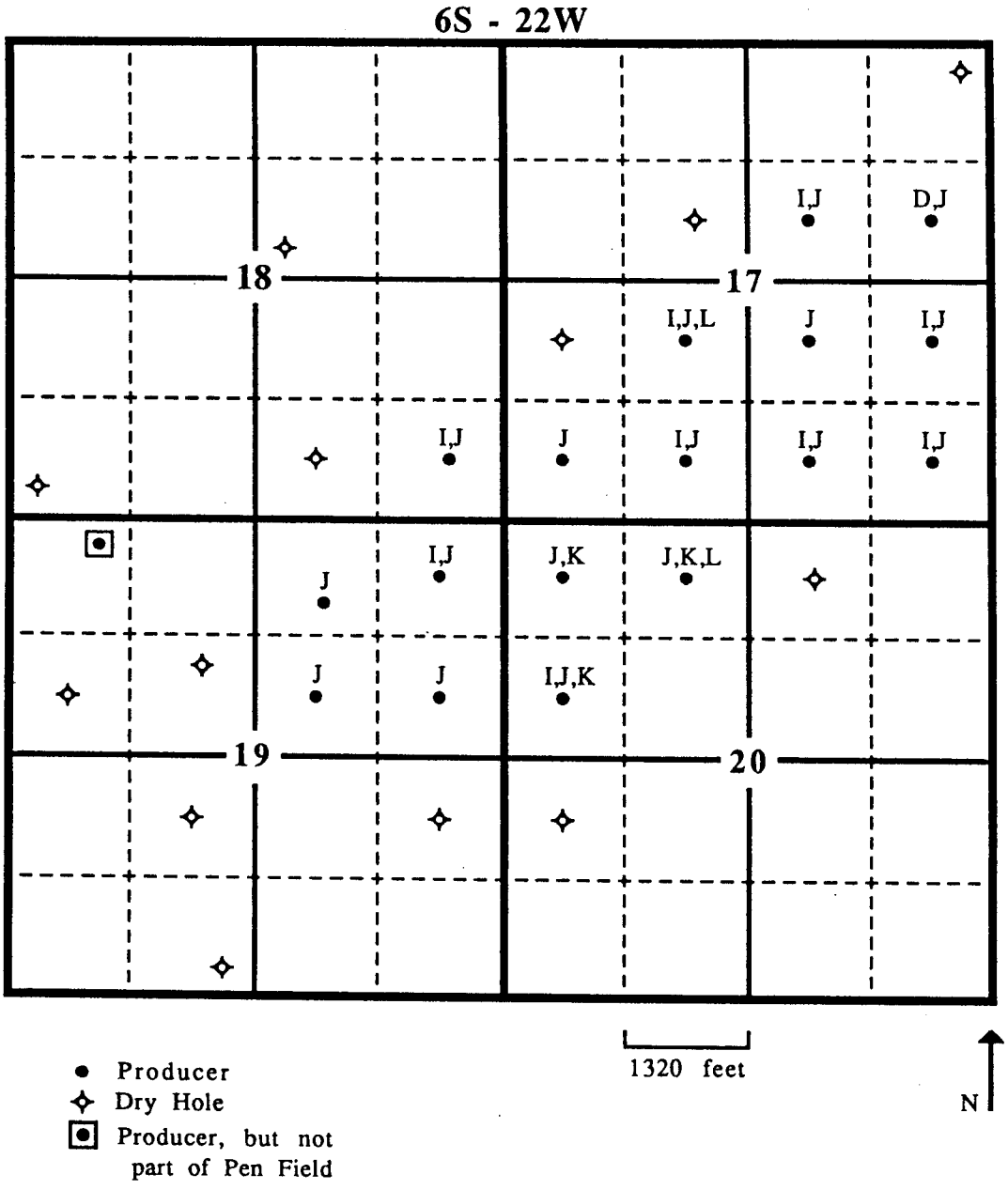

Figure 10. Lansing-Kansas City producing zones of each Pen Field well. The Ritchie Exploration Company, Jacobs #1 in NE-NW-NW of section 19 is a marginal producer from the Lansing-Kansas City "E" zone, and is not part of the Pen Field. This well occurs in the three-well Mt. Vernon North Field, which lies to the west of the mapped area (see Appendix 7).

pumping unit, since all wells required artificial lift.

Pen Field is a stratigraphic trap, with production controlled by the local development and preservation of porous carbonates. The field did not exhibit a gas cap or a water leg. Consequently, production was driven by fluid expansion until the bubble point, and driven by solution gas and fluid expansion after that point. Gas production has been negligible throughout the life of the field.

The drive mechanism in the "D" zone is a minor exception. This zone is only productive in one well, where it is commingled with the "J" zone. This is the only well in the field that has had any significant water production, presumably from the "D" zone. The well initially produced 21 barrels of oil and 20 barrels of water per day, and water production declined to 11 barrels per day by December, 1988. The drive mechanism in the "D" zone is therefore supplemented by a partial water drive, but this drive is necessarily limited because the development of "D" zone porosity surrounding this well forms only a limited reservoir.

STUDY AREA AND METHODS

This investigation was of a very narrow areal scope, including only the productive wells in the Pen Field and the adjacent dry holes. Intensive study of the

depositional and paragenetic features focused on only the "J" and "I" zones because they are the two dominant producing horizons.

The depositional textures, component allochems, sedimentary structures, and facies contacts were described in detail by examination of slabbed cores, supplemented by more than 150 blue epoxy-impregnated and stained thin sections (Dickson, 1965). Petrography of the thin sections was then performed using transmitted and reflected light, blue-light and ultra-violet epifluorescence, cathodoluminescence, and scanning electron microscopy with x-ray energy dispersive analysis (EDS). Reconnaissance microthermometric analysis of fluid inclusions in selected cement samples was also performed to determine the origin of these cements.

Only three cores of the "K" and "L" zones were available for study, although PanCanadian Petroleum did take additional cores of these zones. The three cores were briefly examined and described, but no thin sections were taken.

GEOLOGY OF THE LANSING-KANSAS CITY "J" ZONE IN THE PEN FIELD

LITHOLOGY OF THE "J" ZONE

In the Pen Field, the "J" zone ranges in thickness from 11 to 22 feet (3.4 - 6.7 m) (Fig. 11), and can be subdivided into four apparently conformable but distinct stratigraphic units (Fig. 12; 13). These are in ascending order; the lower carbonate, lower shale, upper carbonate, and upper shale. All four units are present in every cored well that cut through the entire zone. The lower shale unit is thinner than the vertical resolution of wire-line logs, so the upper and lower carbonates can only be distinguished in cores. Appendix 1 contains complete core descriptions.

Lower Carbonate Unit

The lower carbonate unit is uniformly developed, ranging in thickness from 7 to 11 inches (18 - 28 cm). Color ranges from medium brown to medium gray. Most commonly, this unit consists of intermixed packstone and grainstone, although intervals composed entirely of grainstone or packstone do occur (Fig. 14).

The most abundant allochems are Osagia-coated grains and peloids (Fig. 15). Skeletal grains are generally common, and include articulate brachiopods, bivalves, fusilinids, and echinoderm and bryozoan fragments.

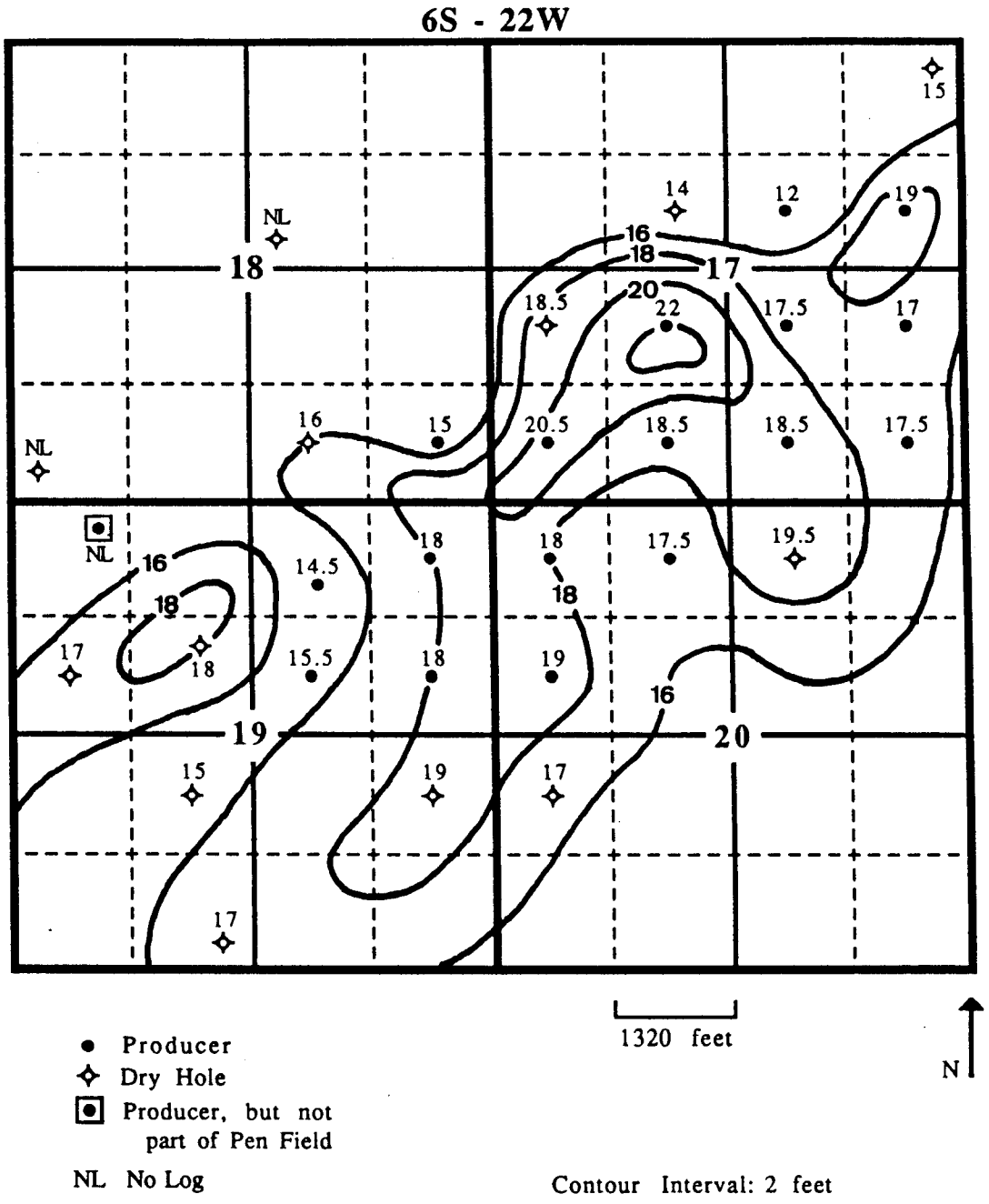

Figure 11. Isopach map of the entire "J" zone interval.

Figure 12. Lithologic subdivisions of the "I", "J", "K", and "L" zones. Numbers in parentheses refer to the thickness ranges of the intervals. These ranges are field wide for the thicker intervals that can be resolved with wire-line logs. The following subdivisions can only be resolved with cores: the subunits within the "J" zone except for the alpha grainstone, the lower shale and lower carbonate units of the "J" zone, the lower shale and lower carbonate units of the "K" zone, and the upper shale, lower shale, and lower carbonate units of the "L" zone. The thickness ranges for these subdivisions may not accurately express the thickness variations in the uncored wells.

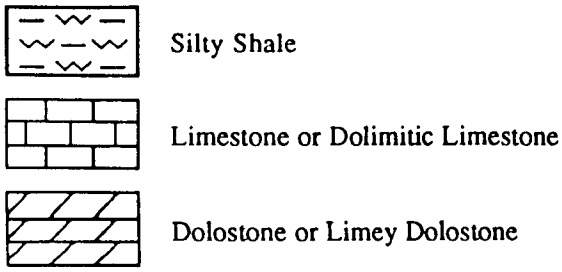

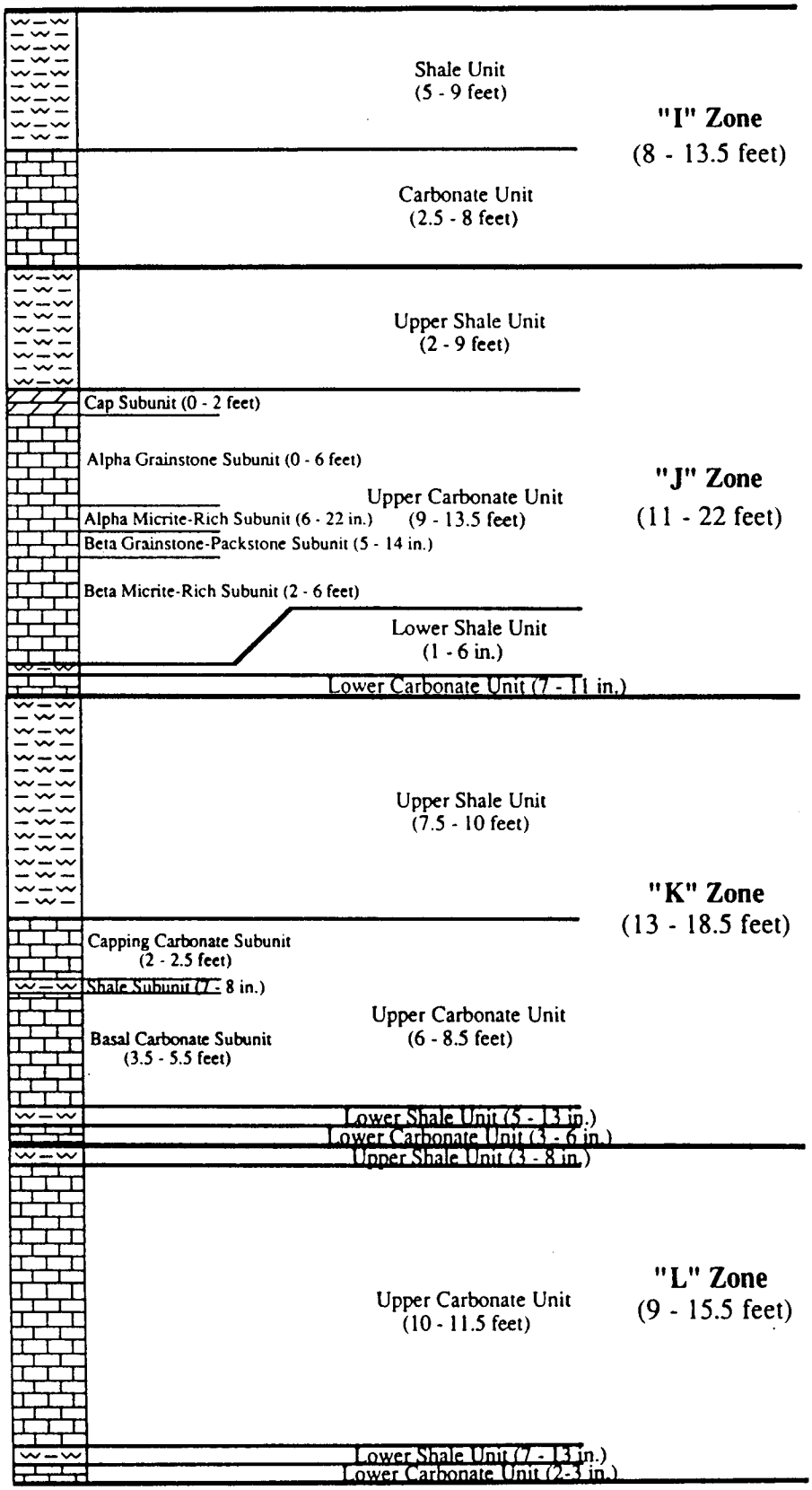
Shale Unit
(5 - 9 feet)
"I" Zone
(8 - 13.5 feet)
Carbonate Unit
(2.5 - 8 feet)
Upper Shale Unit
(2 - 9 feet)
Cap Subunit (0 - 2 feet)
Alpha Grainstone Subunit (0 - 6 feet)
"J" Zone
(11 - 22 feet)
Upper Carbonate Unit
(9 - 13.5 feet)
Alpha Micrite-Rich Subunit (6 - 22 in.)
Beta Grainstone-Packstone Subunit (5 - 14 in.)
Beta Micrite-Rich Subunit (2 - 6 feet)
Lower Shale Unit
(1 - 6 in.)
Lower Carbonate Unit (7 - 11 in.)
Upper Shale Unit
(7.5 - 10 feet)
"K" Zone
(13 - 18.5 feet)
Capping Carbonate Subunit
(2 - 2.5 feet)
Shale Subunit (7 - 8 in.)
Upper Carbonate Unit
(6 - 8.5 feet)
Basal Carbonate Subunit
(3.5 - 5.5 feet)
Lower Shale Unit (5 - 13 in.)
Lower Carbonate Unit (3 - 6 in.)
Upper Shale Unit (3 - 8 in.)
"L" Zone
(9 - 15.5 feet)
Upper Carbonate Unit
(10 - 11.5 feet)
Lower Shale Unit (7 - 13 in.)
Lower Carbonate Unit (2-3 in.)

Figure 13. Type log for the Pen Field. Picks denote the top of the indicated lithologic subdivision, except for the alpha grainstone where the entire subunit is marked. Subdivision abbreviations: I_S - "I" shale unit, I_C - "I" carbonate unit, J_{US} - "J" upper shale unit, J_{UC} - "J" upper carbonate unit, ag - alpha grainstone subunit, K_{US} - "K" upper shale unit, K_{UC-CC} - "K" upper carbonate unit-capping carbonate subunit, K_{UC-S} - "K" upper carbonate unit-shale subunit, K_{UC-BC} - "K" upper carbonate unit-basal carbonate subunit, L_{UC} - "L" upper carbonate unit, PLS - Pleasanton Group. Log abbreviations: GR - gamma ray, NPHI - neutron porosity, DPHI - density porosity.

The pick for the top of the "K" upper shale unit appears to be too low. However, core examination reveals the pick is correct. The lowermost two feet of the "J" zone in the Bethell #5 core exhibits abundant clay, resulting in the "shaley" gamma ray response. The base of the "J" beta micrite-rich subunit, and the "J" lower carbonate unit, both contain abundant clay-filled microstylolite swarms. The high gamma ray response reflects this clay-filling, and the clay within the "J" lower shale unit. The Bethell #3 is the only other cored well that exhibits a similar response. The pick at the base of the "L" zone exhibits a similar response across the field, for analogous reasons. Even with the irregularity at the base of the "J" zone, the Bethell #5 provides the most representative type log from the group of wells with available cores for the "I", "J", "K", and "L" zones. (Bethell #5, SW SW 17-6S-22W.)

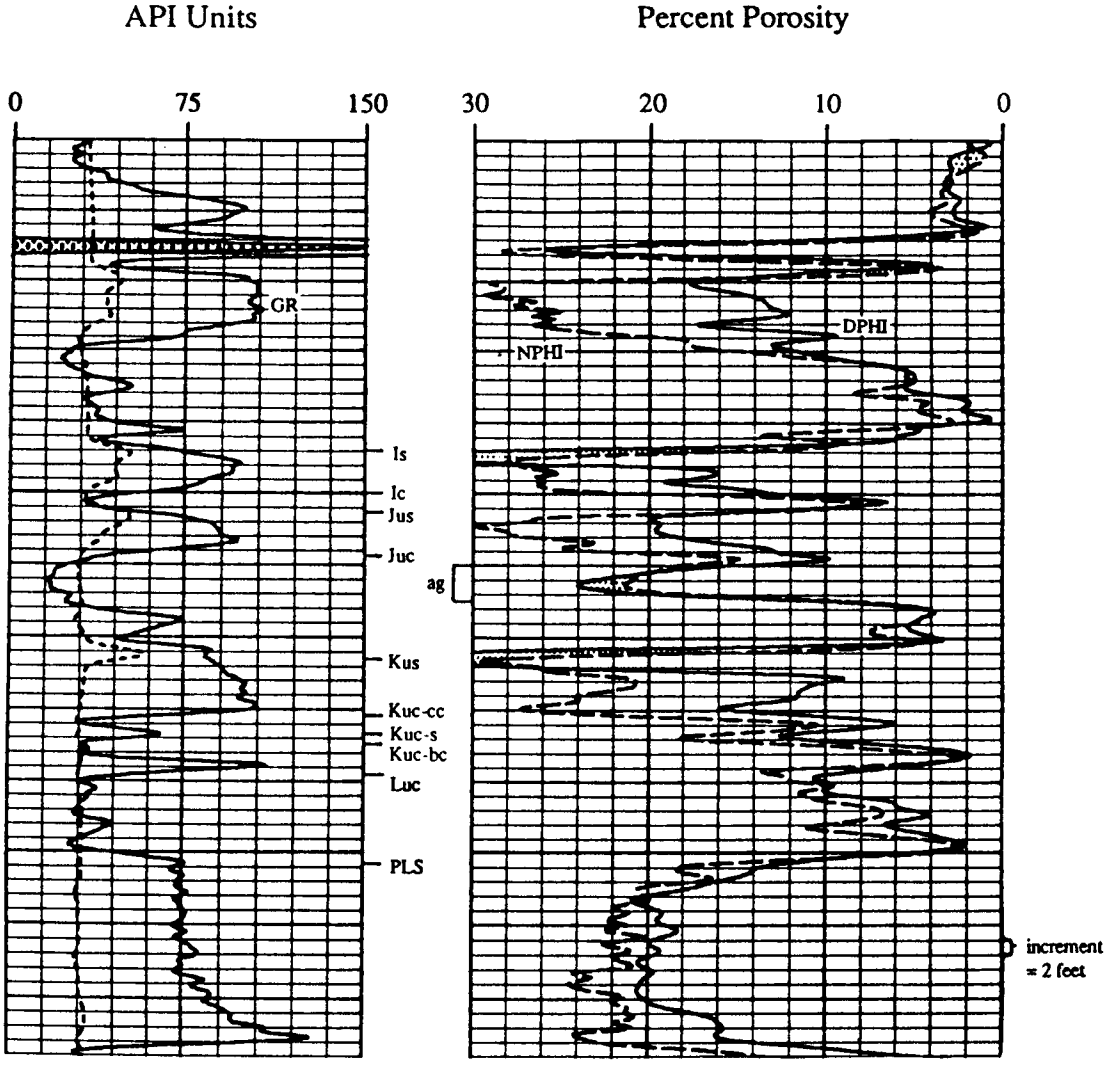
API Units
Percent Porosity
0
75
150
30
20
10
0
GR
NPHI
DPHI
Is
Ic
Jus
Juc
ag
Kus
Kuc-cc
Kuc-s
Kuc-bc
Luc
PLS
increment
= 2 feet

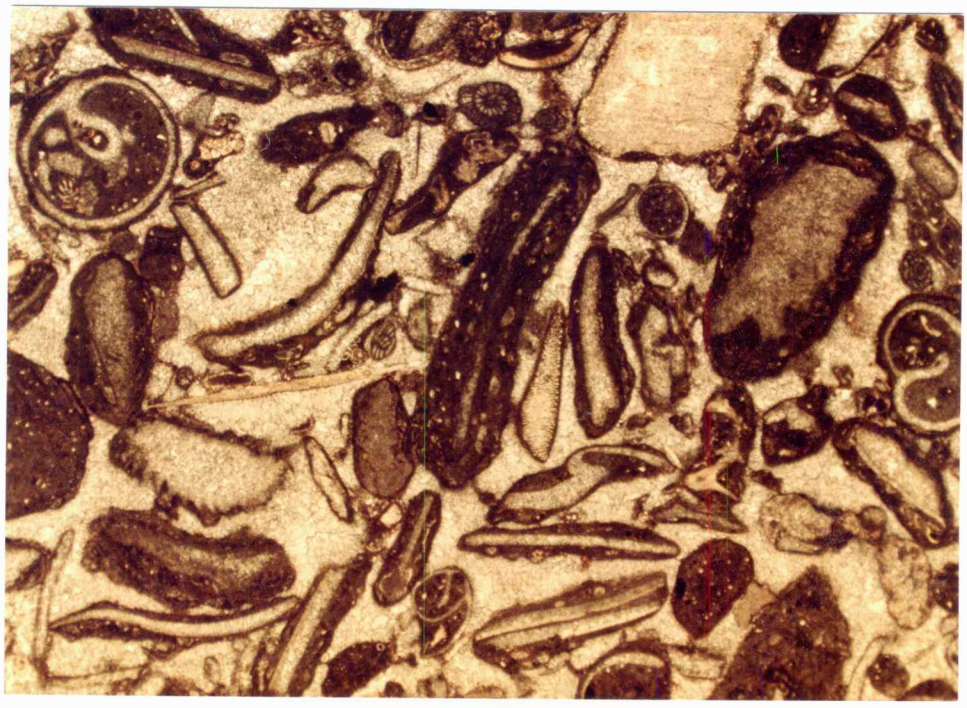

Figure 14. Plane polarized-light photomicrograph of a coarse grainstone lithology in the lower carbonate unit. Osagia-coated grains and peloids are the predominant allochems in the unit, but brachiopods, bivalves, fusilinids, intraclasts, and echinoderm and bryozoan fragments are also present. (Lower carbonate unit, "J" zone; Rogers #1, 3810 feet.)

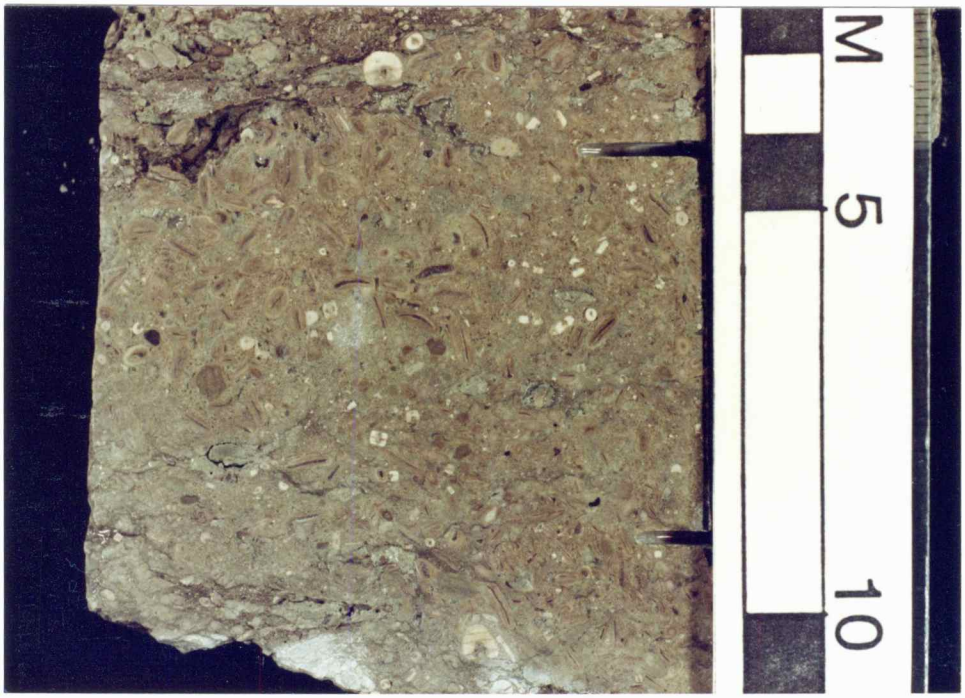

Stratigraphic Up

Blocks on scale equal one centimeter.

Figure 15. Core photo of a packstone lithology in the lower carbonate unit. Skeletal fragments with thick Osagia coatings are the predominant allochem in this sample. (Lower carbonate unit, "J" zone; Rogers #2, 3835 feet.)

Intraclasts are present in a few locations (Fig. 14). The core from the Pennington #2 exhibits a few phosphatized grains.

The matrix in the packstones consists of slightly argillaceous micrite with sub-angular to angular quartz silt and clay mineral laths. The lower carbonate unit commonly exhibits microstylolite swarms and clay seams.

Lower Shale Unit

The lower shale unit is remarkably persistent, it is present in every cored well, yet is only 1 to 2 inches (2.5 - 5.1 cm) thick except in the Rogers #2 where it thickens to 6 inches (15 cm). The contact with the underlying lower carbonate unit is typically very sharp (Fig. 16).

Color of the shale ranges from dark green to dark gray. The unit is composed of silty shale which effervesces mildly in dilute hydrochloric acid. In most wells, the shale exhibits laminations, which range from wavy and discontinuous to uniform and planar, although the shale is not typically fissile. A few large articulate brachiopods are present in many locations.

Upper Carbonate Unit

The upper carbonate unit ranges in thickness from 9 to 13.5 feet (2.7 - 4.1 m) (Fig. 17). This unit exhibits

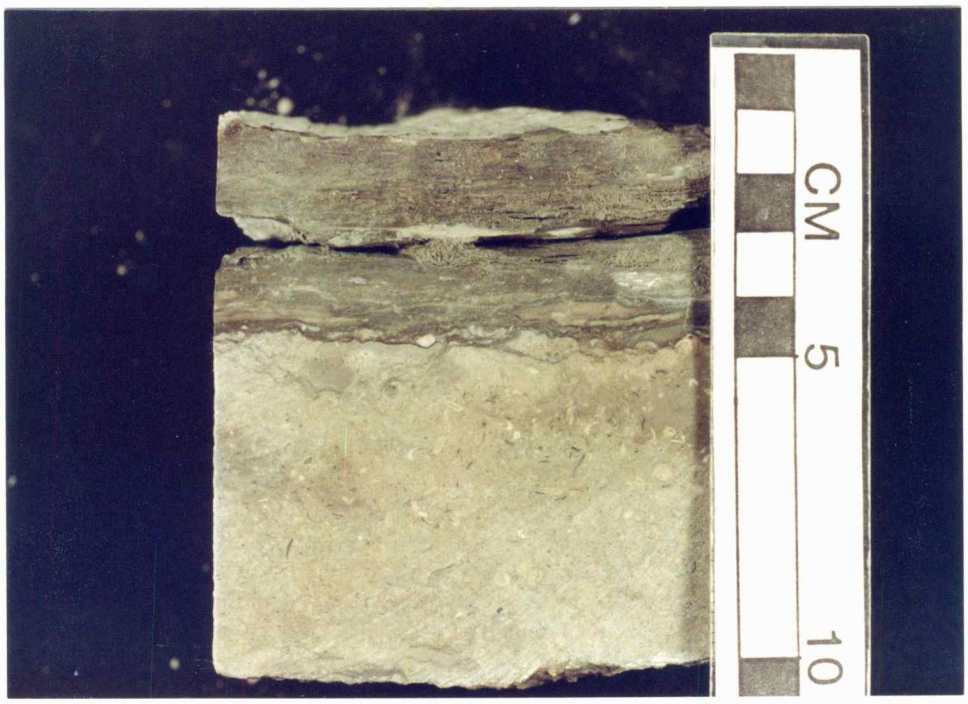

Stratigraphic Up

Blocks on scale equal one centimeter.

Figure 16. Core photo of the lower shale unit. The color of this shale ranges from dark green to dark gray. The contact with the underlying lower carbonate unit is usually very sharp. (Lower carbonate unit - lower shale unit, "J" zone; Bethell #3, 3758 feet.)

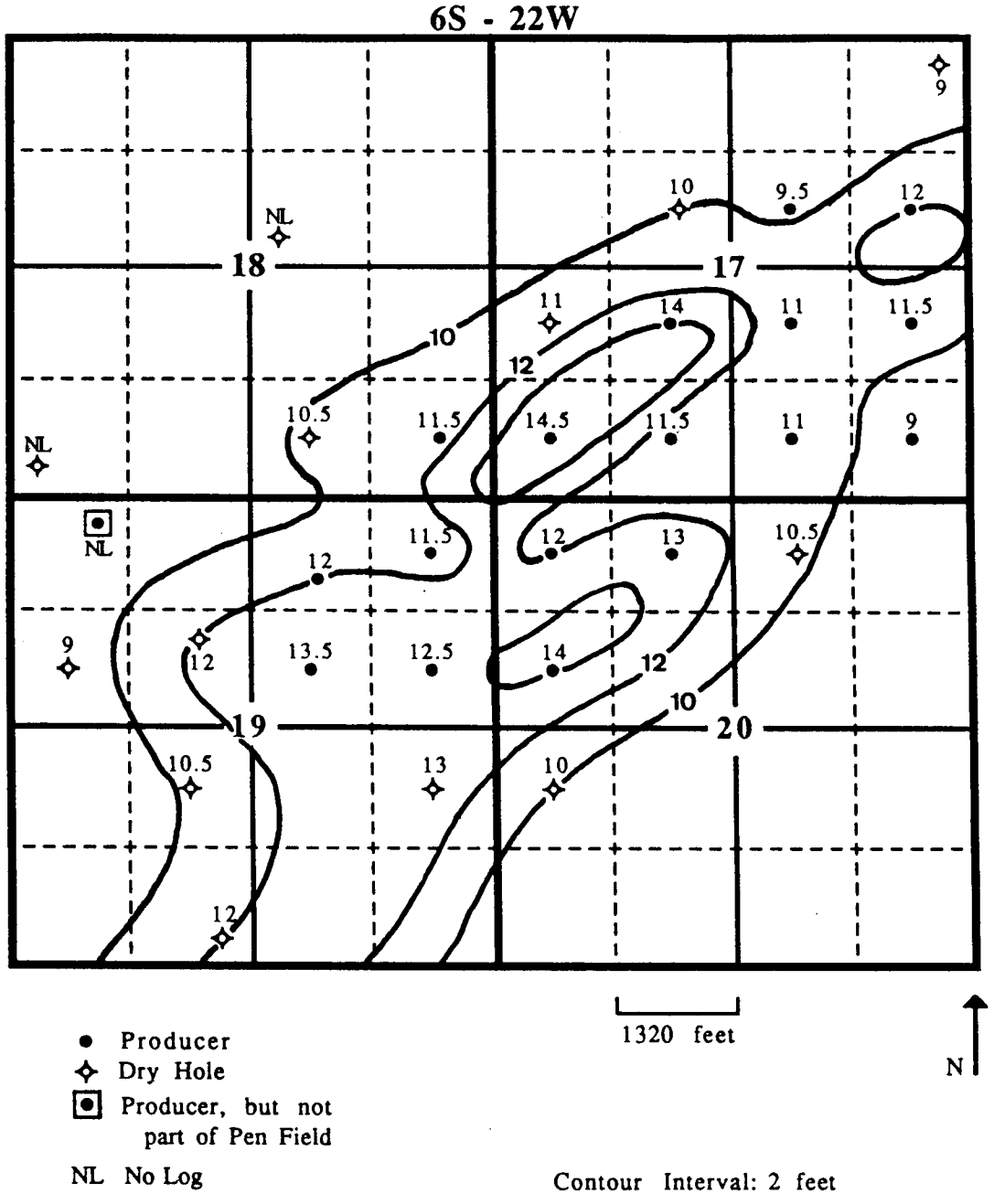

Figure 17. Isopach map of the interval composed of the upper carbonate unit, lower shale unit, and lower carbonate unit of the "J" zone. The observed variation is primarily due to thickness changes in the upper carbonate unit because the lower two units are thin and of relatively uniform thickness. A field wide map of just the upper carbonate unit is not possible because the two lower units cannot be resolved with wire-line logs.

a regular vertical sequence of lithologies, and can be subdivided into five subunits (Fig. 12).

Beta Micrite-Rich Subunit

The lowermost lithologies constitute the beta micrite-rich subunit. This subunit ranges in thickness from 2 to 6 feet (.6 - 1.8 m) and conformably overlies the lower shale unit. Wackestone, packstone, and mottled wackestone-packstone are the dominant lithologies, hence the "micrite-rich" modifier in the subunit name. Many wells show a regular upward gradation from packstone, to a mottled interval, to wackestone. A carbonate mudstone lithology is developed in a few locations. In the Bethell #3, one foot (.3 m) of intermixed packstone and grainstone occurs at the base of the subunit and grades upward into the typical assemblage of muddier lithologies.

The beta micrite-rich subunit is generally light brown or light gray, but a few intervals are cream, light green, or medium to dark brown. This subunit typically exhibits a solution seam every 2 to 4 inches (5.1 - 10.2 cm). Microstylolites and microstylolite swarms predominate, but a few stylolites and clay seams do occur. The allochems in this subunit consist of peloids, fusilinids, articulate brachiopods, bivalves, echinoderm fragments, gastropods, bryozoans, phyloid and

dasycladacean algae, intraclasts, foraminifera-encrusted grains, and ostracodes. A few skeletal particles are composed of (replacement or mold-filling?) phosphatic material whereas others exhibit phosphatic material filling intraparticle pores (Fig. 18).

The beta micrite-rich subunit exhibits an interval with an elevated gamma ray response in most wells in the Pen Field (Fig. 19). This "hot" interval occurs in the stratigraphic position where the radioactive lower shale unit normally occurs in typical Missourian cyclothems (Fig. 3). In the Pen Field, the thin lower shale unit is not apparent on wire-line logs, and the elevated gamma ray response corresponds to an interval of non-shaley carbonate containing phosphatic material. Even though the phosphatic skeletal particles are striking in thin section, they make up less than 1% of the total rock volume. Uranium is commonly a constituent of phosphatic minerals (Blatt, et al., 1980, p. 587), but it is unclear whether the observed phosphate could account for the entire gamma ray response.

Beta Grainstone-Packstone Subunit

The beta grainstone-packstone subunit conformably overlies the beta micrite-rich subunit. The grainstone-packstone interval is only 5 to 14 inches (12.7 - 35.6 cm) thick, but is present in every cored well. This

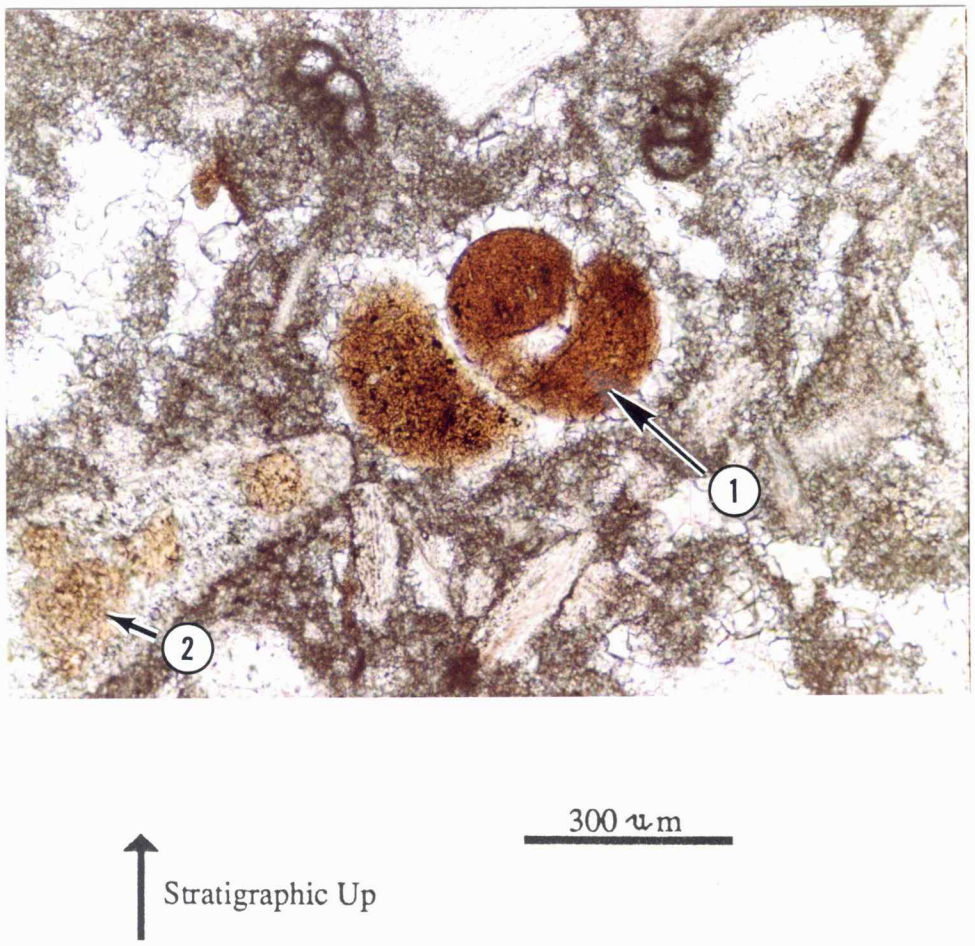

Figure 18. Plane polarized-light photomicrograph of phosphatic material. Arrow 1 points to a gastropod with phosphatic material filling the intraparticle porosity. Arrow 2 points to an irregular bleb of chalcedony replacement. The phosphatic material in the thin sections is striking since it appears virtually isotropic under crossed polars due to the very low order interference (Scholle, 1978). (Beta micrite-rich subunit, upper carbonate unit, "J" zone; Rogers #2, 3833 feet.)

Figure 19. Logs from two wells at opposite ends of the field that exhibit an interval with an elevated gamma ray response in the stratigraphic position where the radioactive lower shale unit normally occurs in typical Missourian cyclothems. Core examination reveals that the two inch thick lower shale unit is not apparent on wire-line logs, and the "hot" interval occurs in relatively "clean" carbonate in the beta micrite-rich subunit. Subdivision abbreviations: J_{US} - "J" upper shale unit, J_{UC} - "J" upper carbonate unit, K_{US} - "K" upper shale unit. Log abbreviations: GR - gamma ray, NPHI - neutron porosity, DPHI - density porosity. (Bethell #5, SW SW 17-6S-22W; Rogers #1, NE SE 19-6S-22W.)

Bethell #5

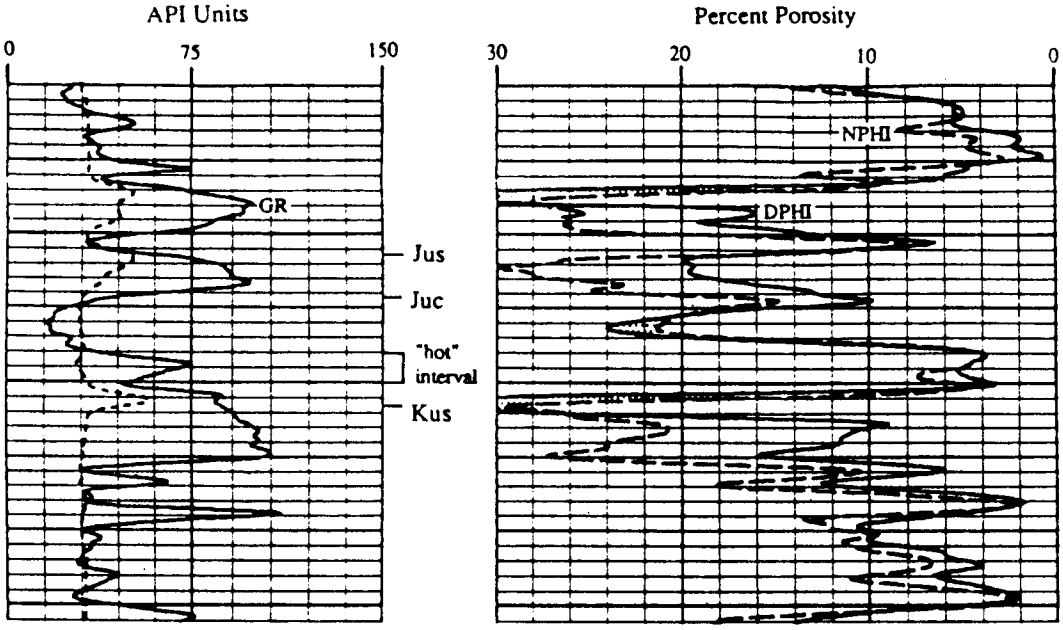

Rogers #1

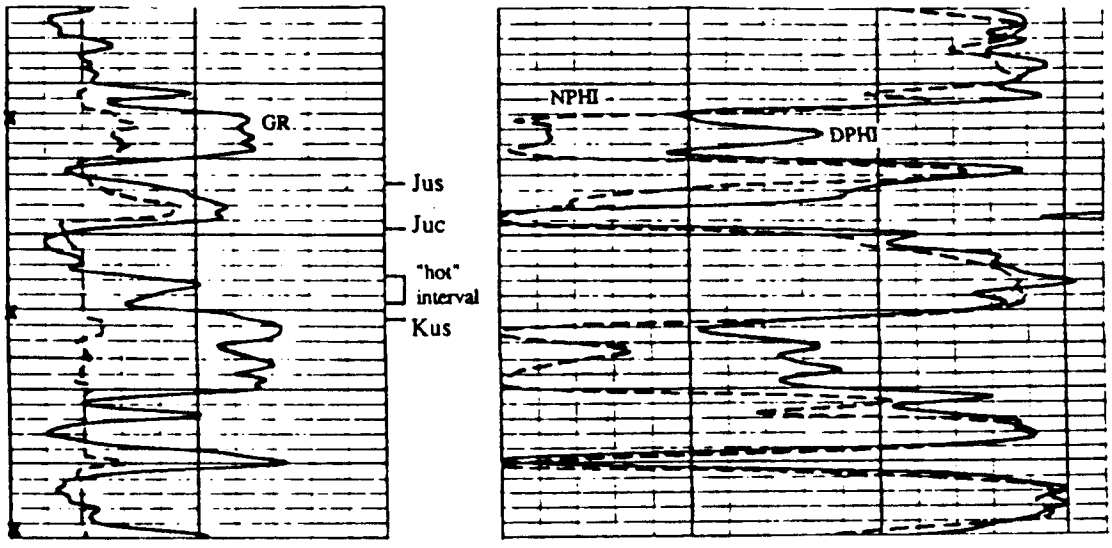

subunit most commonly consists of grainstone, which by definition contains no micrite (Dunham, 1962). However, many wells exhibit micrite in a few of the interparticle pores, which constitutes a packstone lithology. The amount of micrite ranges from a light coating at the bottom of pores to pore filling. The occurrence of micrite is erratic, but typically forms patches of packstone from the scale of thin sections to hand samples. The subunit name is based on these patches of packstone that occur throughout the grainstone in most wells.

The color of this subunit ranges from light to medium brown. Development of solution seams is variable; the subunit lacks seams in some wells, shows only one or two microstylolites in other wells, and exhibits stylolites every 2 - 4 inches (5.1 - 10.2 cm) in a few wells. Peloids, fusilinids, articulate brachiopods, and echinoderm fragments are the dominant allochems, but the subunit also contains bivalves, foraminifera-encrusted grains, phyloid algae, bryozoans, gastropods, and intraclasts.

Alpha Micrite-Rich Subunit

The beta grainstone-packstone subunit is conformably overlain by the alpha micrite-rich subunit. This subunit is 6 to 22 inches (15.2 - 55.9 cm) thick, and ranges in

color from light brown to light gray to cream. It is typically composed of wackestone or intermixed wackestone and mudstone, but an intermixed wackestone and packstone occurs in the Bethell #5.

Solution seams are varied and common; microstylolites, microstylolite swarms, stylolites, and clay seams all occur in this subunit. The alpha micrite-rich subunit contains peloids, bivalves, fusilinids, articulate brachiopods, echinoderm fragments, phyloid algae, ostracodes, bryozoans, and foraminifera-encrusted grains. It also exhibits well-preserved vertical and horizontal burrows.

Alpha Grainstone Subunit

The alpha grainstone subunit conformably overlies the alpha micrite-rich subunit. All underlying subunits are present in every well, but the alpha grainstone subunit is absent in several locations. Thickness ranges from 0 to 6 feet (0 - 1.8 m) (Fig. 20).

In the northeastern portion of the field, the lower third of the subunit typically is composed of skeletal, peloid grainstones whereas the upper two-thirds consists of grainstones containing ooids as one of the principal allochems. Two peripheral wells in the northeast exhibit a relatively thin alpha grainstone subunit that completely lacks ooids and consists of peloids, skeletal

Figure 20. Isopach map of the alpha grainstone subunit of the "J" zone. The interval thickness in uncored wells was determined from wire-line logs. Most of the lithologies in the upper half of the upper carbonate unit are "tight" and exhibit porosities in the 1-3% range. Porosities in the alpha grainstone exceed 5%, except in the White #1. Therefore, any interval with porosity $\geq$ 5% was interpreted as alpha grainstone. However, a few lithologies in the cap subunit exhibit porosity greater than 5%. These porous lithologies are present in only three cored wells, and range from 0.5-1.0 feet in thickness. These porous intervals are excluded from the thickness of the alpha grainstone interval in the cored wells, but a porous interval of this type may be included in the alpha grainstone interval measured from wire-line logs. This circumstance would produce an error of one foot or less, and would result in an overestimation of the thickness of the alpha grainstone.

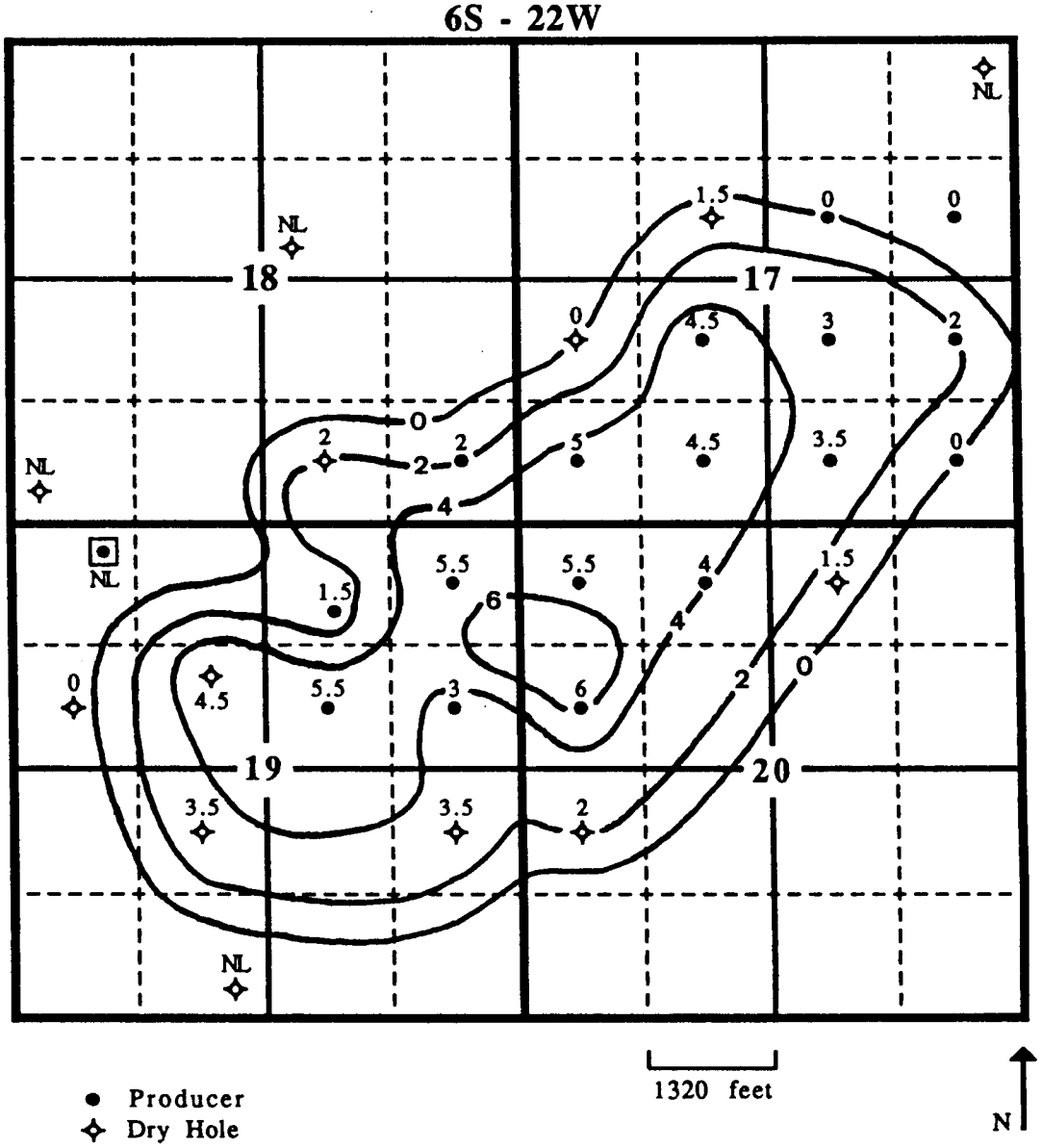
6S - 22W
18
17
19
20
NL
1.5
0
0
4.5
3
2
2
2
5
4.5
3.5
0
4
5.5
5.5
4
1.5
6
1.5
4.5
5.5
3
6
2
0
3.5
3.5
2
1320 feet
N
Producer
Dry Hole
Producer, but not part of Pen Field
NL No Log
Contour Interval: 2 feet

grains, and intraclasts. The thickest grainstones occur in the southwestern portion of the field. These grainstones include ooids throughout the entire interval.

The alpha grainstone subunit does contain packstone and intermixed grainstone and packstone in the Rogers #2. The packstone and grainstone-packstone intervals contain ooids and are overlain by an interval composed entirely of grainstone, so they are included in the alpha grainstone subunit.

The alpha grainstone subunit exhibits cross-bedding at several locations. Stylolites and microstylolites occur every 2 to 4 inches (5.1 - 10.2 cm) in roughly half of the wells, whereas the other wells exhibit intervals of 2 to 3 feet (.6 - .9 m) without any solution seams. A few vertical fractures are present in some of the wells. The fractures range from completely cemented, to open with only minor cement crystals. The alpha grainstone subunit is typically light brown in color. Allochems include ooids, peloids, fusilinids, articulate brachiopods, bivalves, echinoderm fragments, intraclasts, gastropods, and rarely, grapestone.

Cap Subunit

The uppermost subunit shows a great range of lithologies, so instead of being named for the dominant rock type, it is simply called the cap subunit. This

subunit conformably overlies the alpha grainstone subunit where grainstone is present. It is not possible to positively differentiate between the alpha micrite-rich subunit and the cap subunit in the areas lacking grainstone.

The cap subunit ranges in thickness from 0 to 2 feet (0 - .6 m). The most common lithologies are wackestones with a diverse fauna and a few ooids, and carbonate mudstones with very few allochems. However, in a few wells, these muddy intervals contain layers a few centimeters thick consisting of intermixed packstone and grainstone, clean grainstone with ooids and peloids, or laminated crusts. One location exhibits a wackestone containing abundant tubules and spicules. Color of the cap subunit ranges from light to medium brown.

The cap subunit commonly exhibits microstylolites, microstylolite swarms, and clay seams every 2 to 3 inches (5.1 - 7.6 cm). However, most of these solution seams are related to shale-infilling in pores formed during subaerial exposure. The exposure features will be more fully discussed in the paragenesis section.

Upper Shale Unit

The thickness of the upper shale unit ranges from 2 to 9 feet (.6 - 2.7 m) (Fig. 21). This unit consists of red, green, and mottled red-green silty shales which

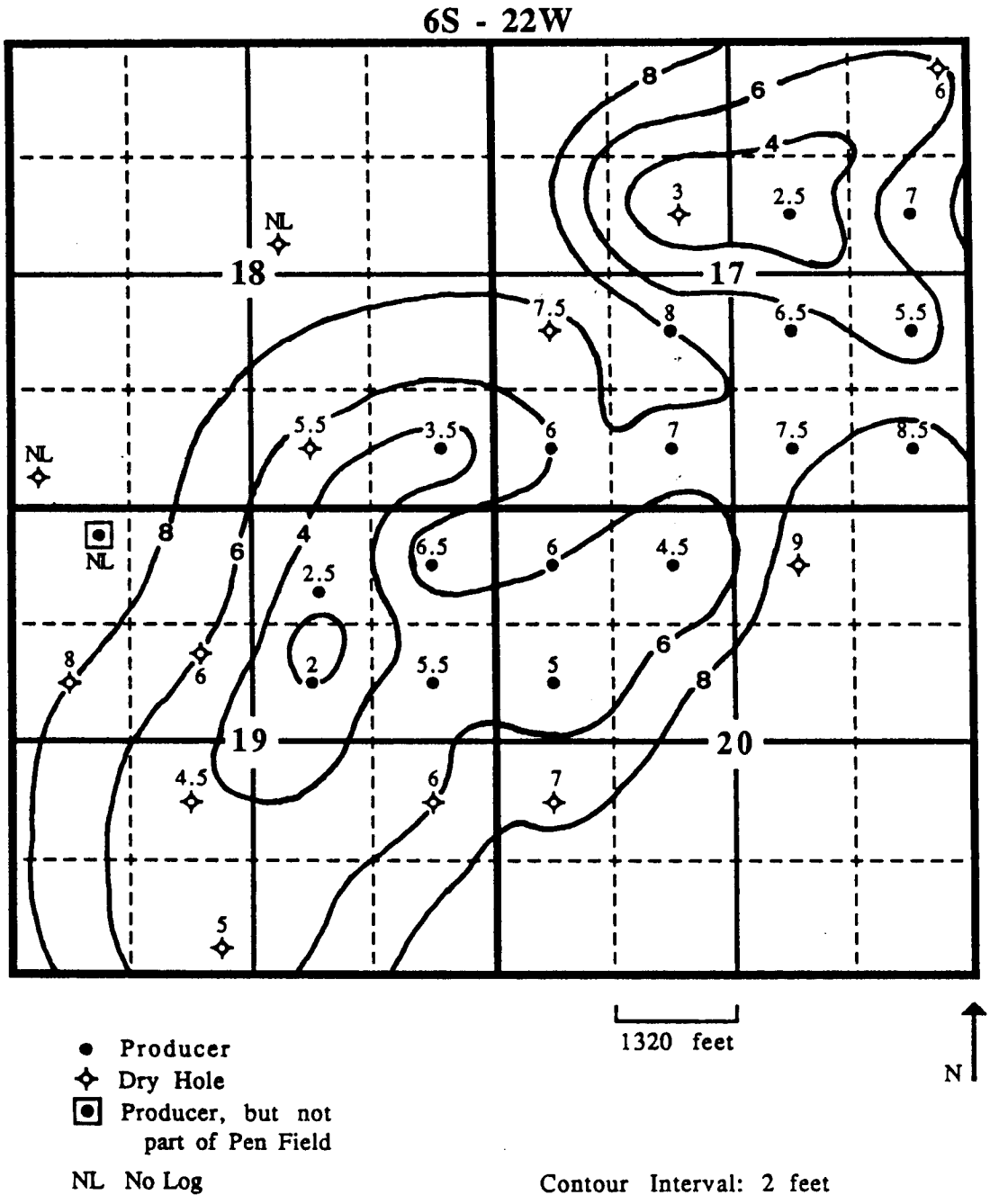

Figure 21. Isopach map of the upper shale unit of the "J" zone.

exhibit mild effervescence in dilute hydrochloric acid. The shales typically contain black carbonate clasts .5 - 2 mm in length that exhibit polished, concave facets. The upper shale unit is devoid of fossils. This unit is commonly blocky, but most wells exhibit intervals with slickensides that penetrate the width of the core.

The basal portion of the unit is typically medium green in color and reaches a maximum thickness of 3 feet (.9 m). This green interval is less than a foot thick in most wells, and is absent in one well, the Pennington #2. The bulk of the upper shale is brick red to maroon in color. The upper foot or less of the upper shale is generally medium green, but this upper green interval is absent from many wells. The contacts at the color changes are mottled in several wells, and color mottles occur in the central portion of either the red or green intervals in a few wells.

INTERPRETATION OF THE DEPOSITIONAL ENVIRONMENTS OF THE "J" ZONE

A broad, low-relief, open marine shelf is the environment of deposition generally ascribed to the carbonates of the Lansing-Kansas City cyclothems of the Midcontinent (Brown, 1984b; Dubois, 1979; Kintner, 1984; Watney, 1980). The local evidence from the Pen Field is consistent with this regional model.

Lower Carbonate Unit

The grainstone and packstone textures indicate the lower carbonate unit of the "J" zone formed in a relatively high energy environment (Fig. 14). Osagia coatings and intraclasts indicate very shallow water (Watney, 1980). The presence of abundant allochems of stenohaline fauna such as articulate brachiopods and crinoids show this environment occurred in an open marine setting (Wilson and Jordan, 1983).

The features and interpretation of this unit are consistent with Watney's (1980) analysis of the bottom portion of the lower carbonate unit. However, in an ideal cyclothem the grainstone and packstone grade upward to wackestone and carbonate mudstone in the top portion of the lower carbonate unit. According to the model for an ideal cyclothem, the top of the lower carbonate unit formed in a low energy, subtidal environment of increasing turbidity eventually resulting in deposition

of the lower shale as relative sea level rose toward the point of maximum transgression (Watney, 1980; Heckel, 1983). This interpretation is based on the occurrence of increasingly muddy carbonate sediments in the lower carbonate unit, and the gradational contact with overlying shale.

These features are absent in the upper portion of the "J" lower carbonate unit of the Pen Field. Abundant Osagia-coated grains exist in the unit up to the shale contact, indicating shallow water conditions persisted at least until deposition of the shale unit. The lower carbonate unit in the Pen Field therefore does not fit the ideal cyclothem model.

Lower Shale Unit

The cyclothem deposits of the Lansing-Kansas City outcrop belt have been intensively studied, and most workers interpret the lower shale units to have formed during maximum transgression (Wanless, 1967; Heckel, 1977; Malinky, 1982). This interpretation is commonly extended to the lower shale units in the subsurface of central and western Kansas. The lower shale units in the outcrop belt are typically nonsandy, and most contain a characteristic phosphatic, black, fissile facies. The "J" lower shale unit in the Pen Field contains abundant quartz silt and lacks a phosphatic, black, fissile

facies, and may therefore be unrelated to the lower shales that typically form during maximum transgression.

The "J" lower shale unit in the Pen Field contains articulate brachiopods which are which are considered to be stenohaline. The brachiopods indicate the shale unit probably formed in a normal marine environment, and may have formed in shallow water, as suggested by the high silt content. More cores in the region would be required to determine the distribution of this shale and its exact origin. If the lower shale unit was deposited in a shallow, open marine environment, it supports the earlier interpretation of divergence from the ideal cyclothem model for the lower portions of the "J" zone in the Pen Field.

Upper Carbonate Unit

The diversity of facies in the "J" upper carbonate unit in the Pen Field appears to be a normal occurrence in accordance with Watney's (1980) regional work. He found that the upper carbonate unit of a typical cyclothem could be divided into a lower and upper interval. The lower interval consisted of lime mudstone and wackestone with a diversity of fossils, including phyloid algae. In places, the lower interval contains thin beds of mixed skeletal grainstone and packstone. The beta micrite-rich, beta grainstone-packstone, and

alpha micrite-rich subunits of the "J" zone would make up the lower interval in Watney's terminology. He interpreted these rocks to have formed in a low energy, subtidal, marine environment. The thin grainstones and packstones formed as the result of occasional strong currents, perhaps caused by storms.

The aforementioned three subunits are continuous across the Pen Field and probably reflect regional depositional patterns. The nature of these subunits in the Pen Field supports Watney's (1980) depositional environment interpretation for the region.

Watney noted that the upper interval of the upper carbonate unit in a typical cyclothem tends to be much more variable than the lower interval, with textures ranging from lime mudstone to grainstone. The locally developed alpha grainstone subunit and the variety of lithologies in the cap subunit show this high degree of variability occurs in the Pen Field. Most authors interpret the upper interval of the upper carbonate unit as a high energy, shallowing-upward, marine deposit (Brown, 1963; Payton, 1966; Mossler, 1973; Watney, 1980). This shallowing-upward sequence is commonly capped by a subaerial exposure surface (Watney and Ebanks, 1978; Watney, 1980). The presence of coarse grainstone containing ooids and abraded skeletal allochems, indicates the Pen Field alpha grainstone subunit formed

in a shallow water, high energy environment. The restricted distribution of the grainstone (Fig. 20) suggests a localized body.

Structure maps were drawn on the top of the Arbuckle Group and a number of shallower horizons to evaluate the paleostructure in the Pen Field area. Isopach maps were drawn on a variety of intervals to evaluate controls on sedimentation during deposition of the lower Lansing-Kansas City zones. These maps failed to reveal any obvious reason for the localized formation of an ooid grainstone deposit in the Pen Field area.

The "J" cap subunit exhibits a variety of lithologies but is predominantly muddy, indicating lower energy conditions. The decrease in energy probably results from some type of restriction that limits wave and tidal action, but the nature of restriction is difficult to determine with the available subsurface data.

A subaerial exposure surface at the top of the upper carbonate unit is indicated by several alteration features. The exposure features will be more fully discussed in the paragenesis section.

Upper Shale Unit

In the Pen Field, the upper shale unit is devoid of fossils and is primarily red in color. Watney (1980)

noted these features as typical of the upper shales in his regional study. He also noted possible paleosol features in these shales and concluded that the evidence of paleosols, combined with the absence of fossils and the oxidized appearance, indicated the upper shales were probably subaerially exposed continental deposits.

In this local study of the Pen Field, no distinctive fossils or sedimentary features were observed in the "J" upper shale, so it is not possible to interpret the specific depositional environment of the upper shale unit. However, there is no evidence to contradict Watney's interpretation.

PARAGENESIS OF THE "J" ZONE

The "J" zone exhibits ten generations of cement, several different types of primary and secondary pores, a variety of replacive minerals, several episodes of sediment infilling, and the development of a range of alteration features (Fig. 22). Cement generations that occur exclusively within the "J" zone are given a J prefix. Cements that are present in multiple Lansing-Kansas City zones are given an M prefix.

Pervasive shale infilling (Fig. 23; 24; 25) provides the best means of determining relative timing of the paragenetic features in the upper carbonate unit. This infilling of clay and silt probably marks the onset of deposition of the upper shale unit, which eventually resulted in burial of the upper carbonate unit. Consequently, this section is subdivided into pre-burial and post-burial features.

Pre-burial Features

These features pre-date deposition of the "J" upper shale unit, and also pre-date compaction. Most features are described individually, but the descriptions are grouped for features that typically form in close association.

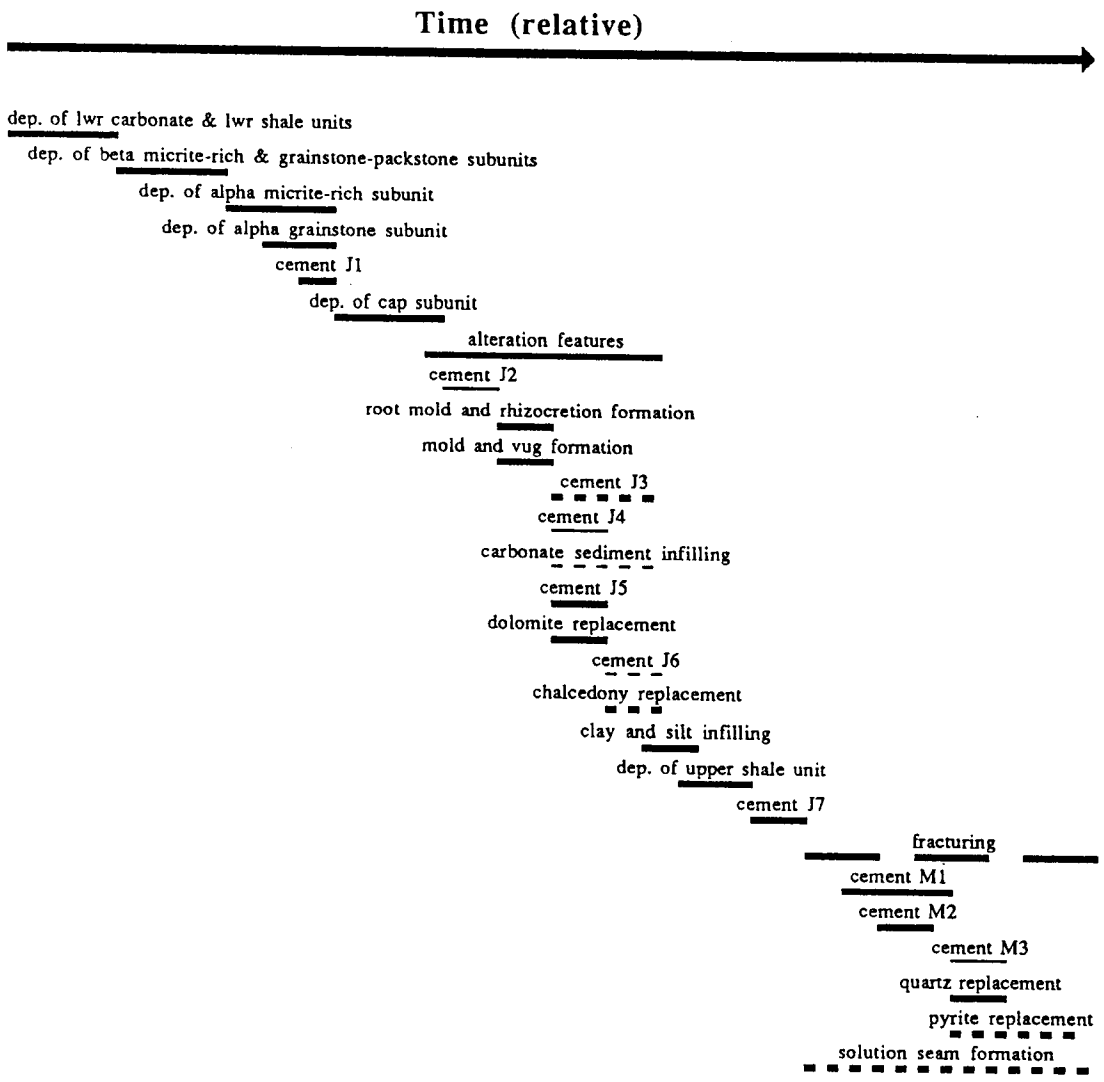

Figure 22. Paragenetic sequence of the "J" zone. The thick lines denote "major" features, that are either pervasive throughout the zone or particularly abundant. The thin lines denote "minor" features.

Cement J1

Cement J1 forms fairly uniform, isopachous rims of finely bladed, nonferroan calcite that commonly exhibit polygonal sutures where rims intersect (Fig. 26). The blades range from 3 to 90 micrometers in length, and 3 to 20 micrometers in width. The cement blades typically exhibit moderately bright luminescence, but in places the rims are speckled with dark areas (Fig. 27).

Cement J1 only occurs in the interparticle porosity of the alpha grainstone subunit, and is commonly absent in the upper 3 to 8 inches (7.6 - 20.3 cm) of the grainstone. Where present, cement abundance ranges from a thin rim only 3 micrometers thick, to completely pore-filling. This cement clearly post-dates compaction because the cement rim may be spalled around the substrate allochem, or fractured where the allochem was leached and the mold crushed (Fig. 28).

Alteration Features

A variety of alteration features are present in the cap subunit throughout the field, and in the alpha grainstone subunit in several wells. These pervasive features are also very useful in establishing the relative timing of paragenetic features in the "J" zone. No occurrence of cement J1 post-dates any of the alteration features.

Figure 23. Core photo of alteration "fissures" and shale infilling. A large vertical fissure runs down the left side of the sample. This fissure was filled with light green, silty shale, but most of this sediment was washed out during slabbing. The vertical fissure intersects a horizontal fissure filled with the same sediment. (Cap subunit, upper carbonate unit, "J" zone; Shuck #1, 3744 feet.)

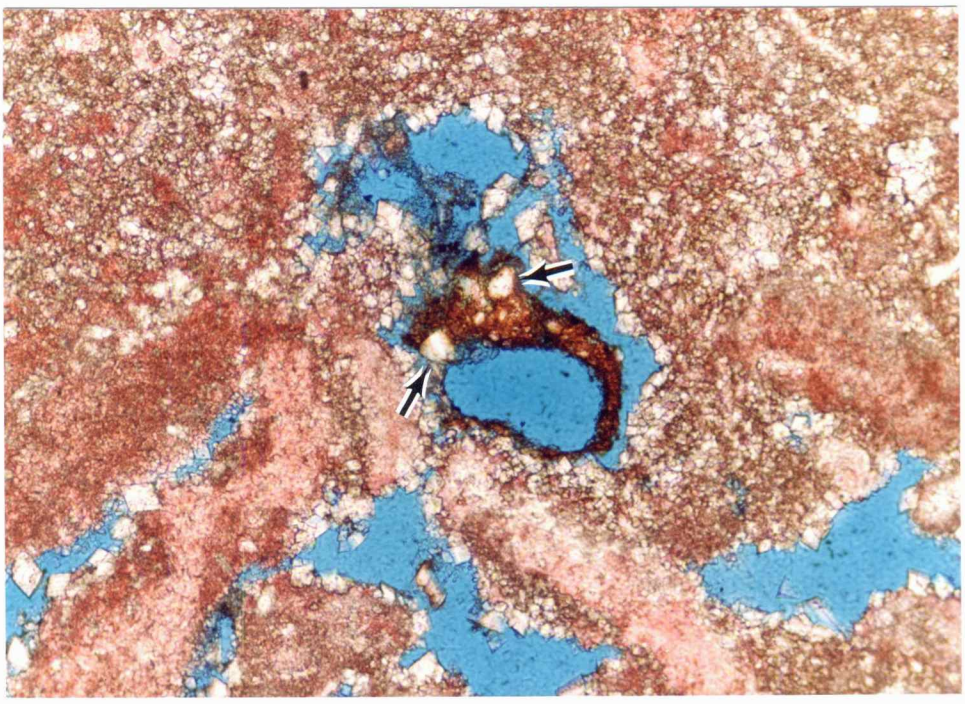

Figure 24. Unpolarized-light photomicrograph of clay and quartz silt coating dolomite cement J5. (Thin section impregnated with blue epoxy and stained with Alizarin Red-S and potassium ferricyanide.) The arrows point to two grains of quartz silt in the infilling sediment. The unusual shape of the sediment infill is probably the result of wash-out that occurred during slabbing of the core and trimming of the billet. (Alpha grainstone subunit, upper carbonate unit, "J" zone; Bethell #5, 3762 feet.)

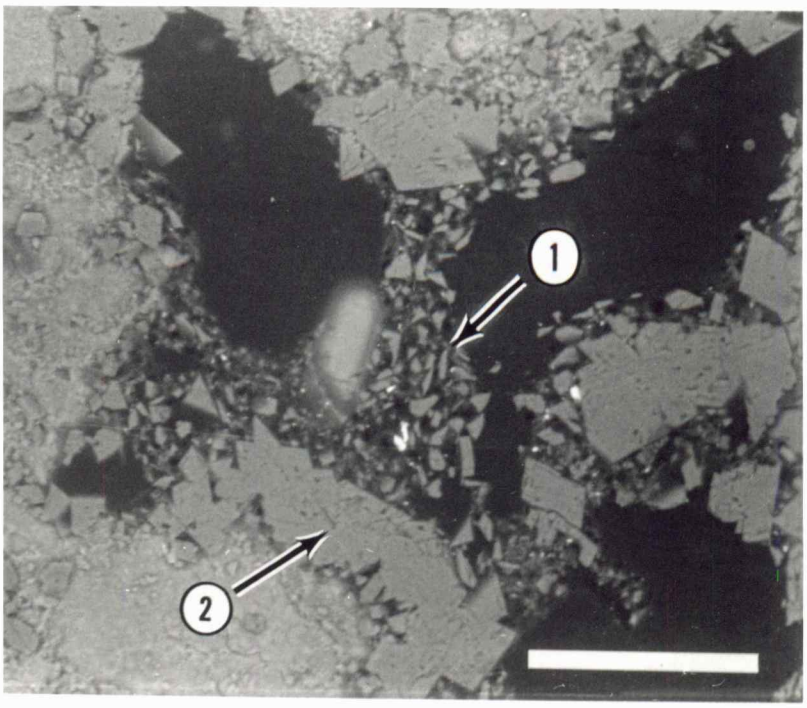

Figure 25. Scanning electron microscope (SEM) photomicrograph (backscattered electron image) of clay and quartz silt (arrow 1) coating dolomite cement J5 (arrow 2). The quartz silt exhibits very sharp, angular outlines. (Scale bar equals 100 micrometers.) (Alpha grainstone subunit, upper carbonate unit, "J" zone; Bethell #5, 3762 feet.)

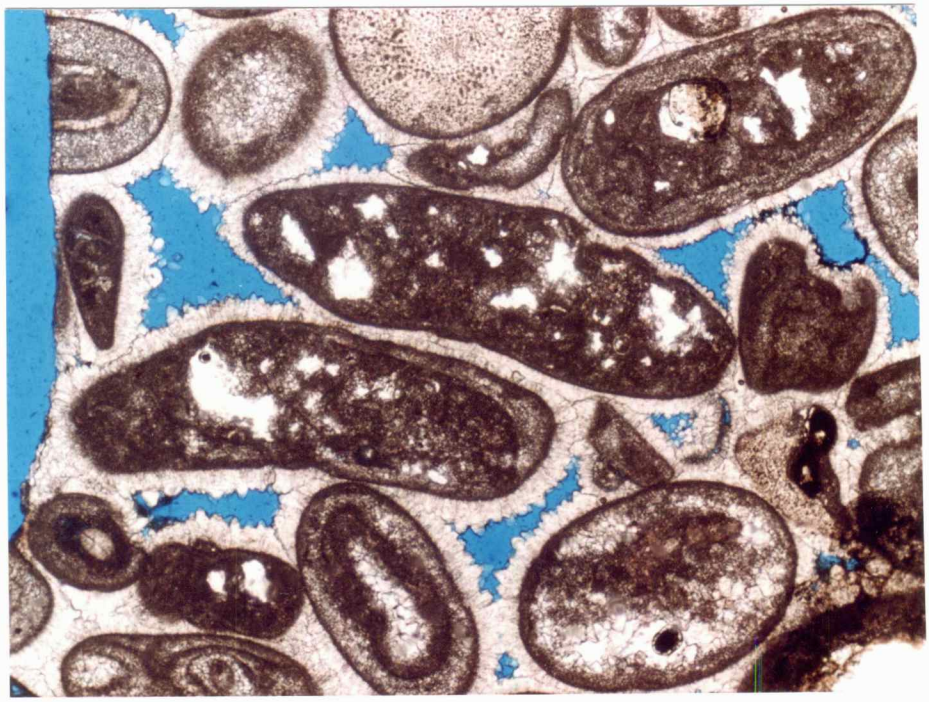

Figure 26. Unpolarized-light photomicrograph of cement J1. (Thin section impregnated with blue epoxy.) The finely bladed cement forms fairly uniform isopachous rims. These rims exhibit polygonal sutures where they intersect. (Alpha grainstone subunit, upper carbonate unit, "J" zone; Demuth #1, 3813 feet.)

Figure 27. Paired plane polarized-light (A) and cathodoluminescent (B) photomicrographs of cement J1. (Thin section impregnated with blue epoxy.) The rims of cement blades (arrows marked 1) typically exhibit moderately bright luminescence, but in places the rims are speckled with patches of dark luminescence (arrows marked 2). (Alpha grainstone subunit, upper carbonate unit, "J" zone; White #5, 3794 feet.)

A

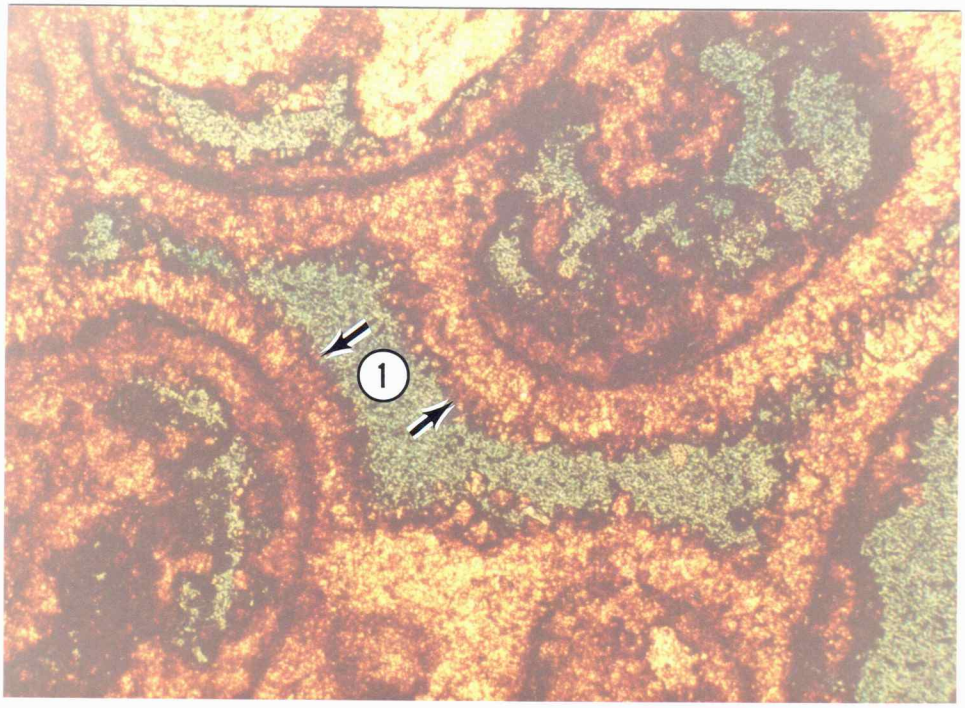

B

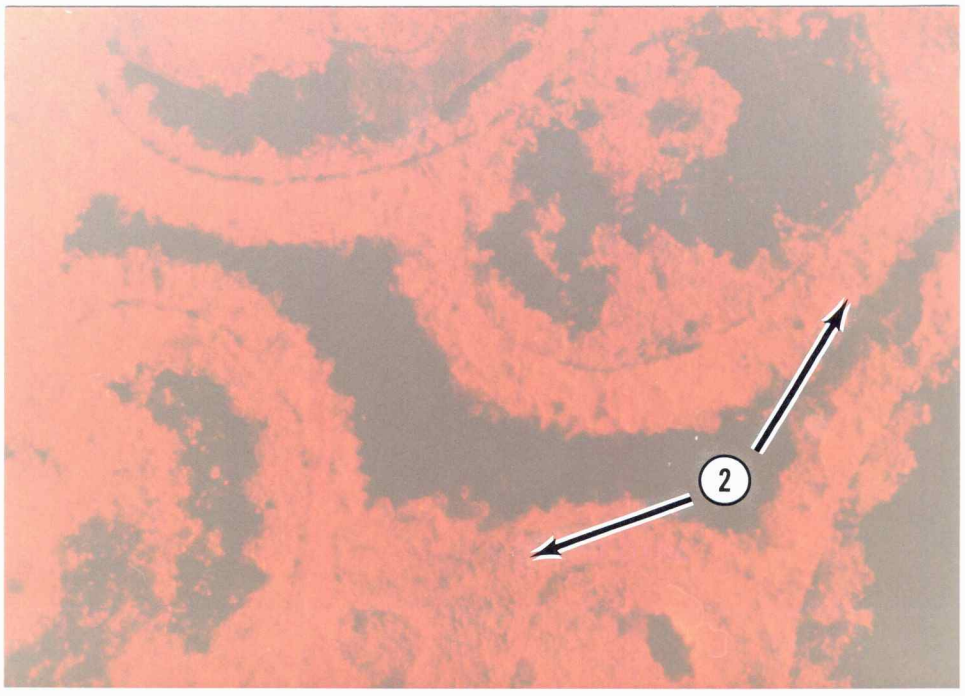

200 μm

Stratigraphic Up

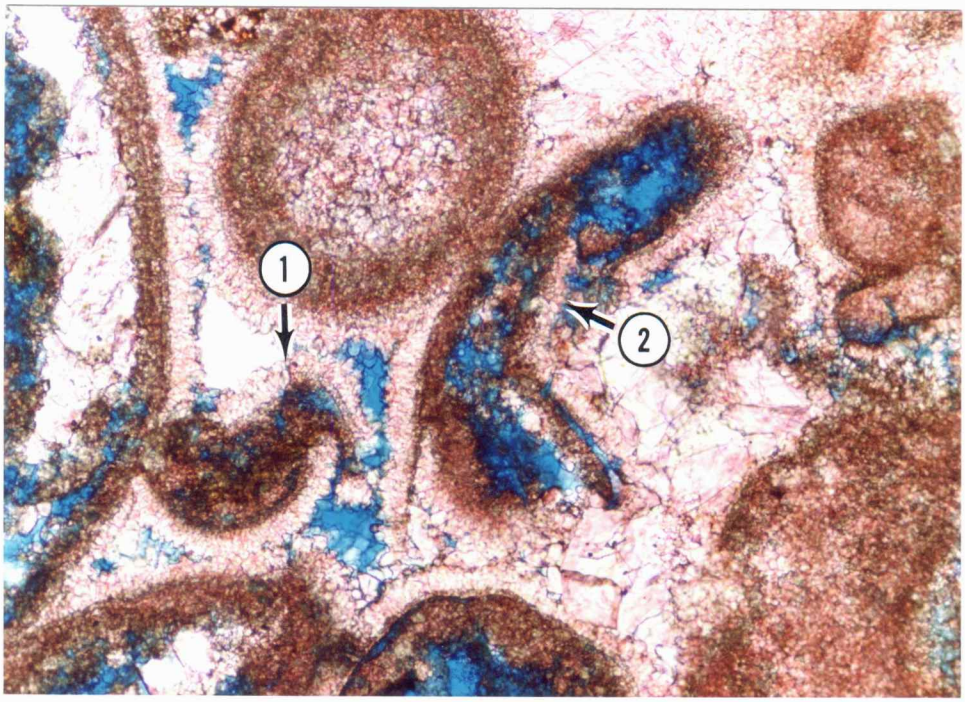

Figure 28. Unpolarized-light photomicrograph showing two crushed molds with fractured and spalled rims of cement J1 (arrows 1 and 2). (Thin section impregnated with blue epoxy and stained with Alizarin Red-S and potassium ferricyanide.) Precipitation of cement J1 obviously predates compaction. Coarse, equant crystals of cement M1 were precipitated after compaction, and reduced much of the remaining pore space in this sample (arrows 3 and 4). (Alpha grainstone subunit, upper carbonate unit, "J" zone; Rogers #1, 3801 feet.)

Autoclastic brecciation is the most pervasive alteration feature, and is observed to some degree in every well with a cap subunit (Fig. 29). Autoclastic brecciation to the extent that the clasts retain a fitted texture with only minor rotation is common, but chaotic, completely unfitted textures with angular to rounded clasts occur in several wells.

Autoclastic brecciation extends below the cap subunit in only two cored wells, the Bethell #3 and the White #1. Circumgranular cracks are present in a few locations, and appear to be intimately associated with the autoclastic brecciation. The factors causing brecciation were apparently recurrent, as evidenced by the cracking and rotation of cements that fill previously formed alteration pores (Fig. 30).

The upper carbonate unit commonly exhibits two other alteration features here termed "fissures" and "pipes". These features extend below the cap subunit in only three wells.

Fissures are generally tabular features from .5 to 4 cm wide, and primarily have a vertical orientation (Fig. 23). Where the fissure edges are irregular, the two adjacent edges typically cannot be re-fitted. The vertical fissures may intersect roughly horizontal fissures of approximately the same dimensions. These horizontal fissures generally continue to the core edges.

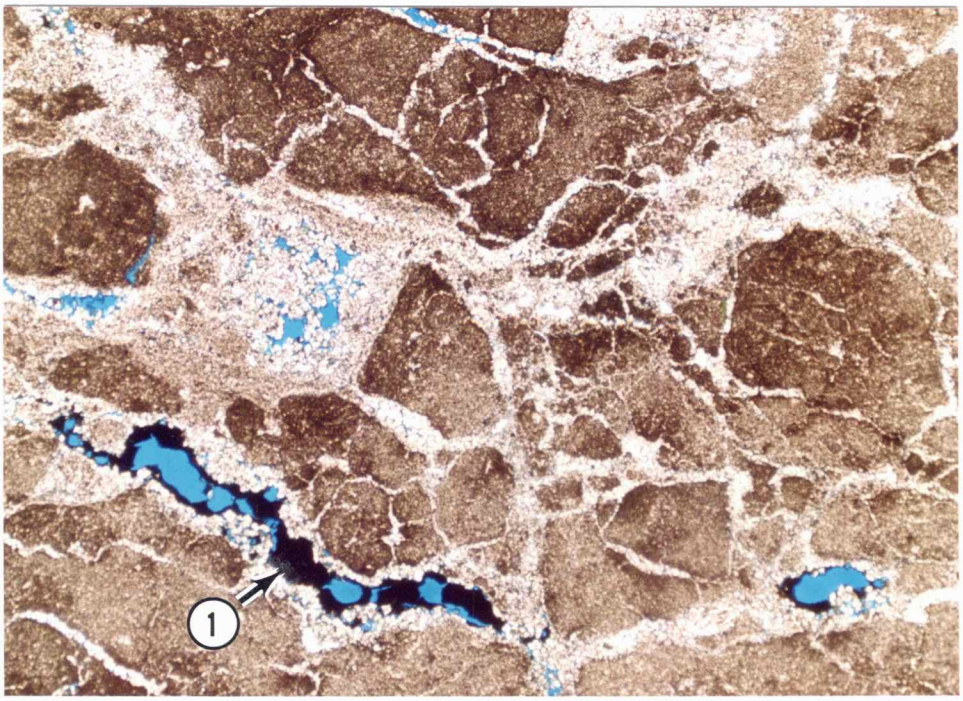

Figure 29. Unpolarized-light photomicrograph showing pervasive autoclastic brecciation. (Thin section impregnated with blue epoxy.) Many of the clasts retain a fitted texture, whereas others are obviously rotated. The clasts consist of completely dolomitized carbonate mudstone. Dolomite rhombohedra of cement J5 reduce or fill the breccia porosity. The black material lining the large pore in the lower left is hydrocarbon residue (arrow 1). (Cap subunit, upper carbonate unit, "J" zone; Shuck #1, 3843 feet.)

Figure 30. Photomicrographs of cracked cement J4 and minor infilling of micritic sediment in an alteration pore; unpolarized-light (A) photomicrograph of a stained section in oil with a cover slip, and paired plane polarized-light (B) and cathodoluminescent (C) photomicrographs. (Thin section impregnated with blue epoxy and stained with Alizarin Red-S. The large white areas in photo A are the result of plucking during thin section preparation.) In these photos, cement J4 reduces a crack formed by autoclastic brecciation. The rim of cement J4 between the arrows marked 1 in photo A does not exhibit euhedral crystal terminations, instead the cement rings the entire pore and exhibits smooth, undulose bands that are also continuous around the pore. Under cathodoluminescence, these undulose bands form alternating moderately bright and dark bands. Arrows 2 and 3 point to bands composed of dolomite cement. Under cathodoluminescence, the thick outer band of dolomite cement exhibits a dark inner band and dully luminescent outer band. Arrow 4 points to an area where the cement layers were cracked during a second episode of autoclastic brecciation. Arrow 5 points to a pore bridge of infilling micritic sediment. The crack and the pore center were subsequently filled with cement J7. (Cap subunit, upper carbonate unit, "J" zone; White #1, 3780 feet.)

A

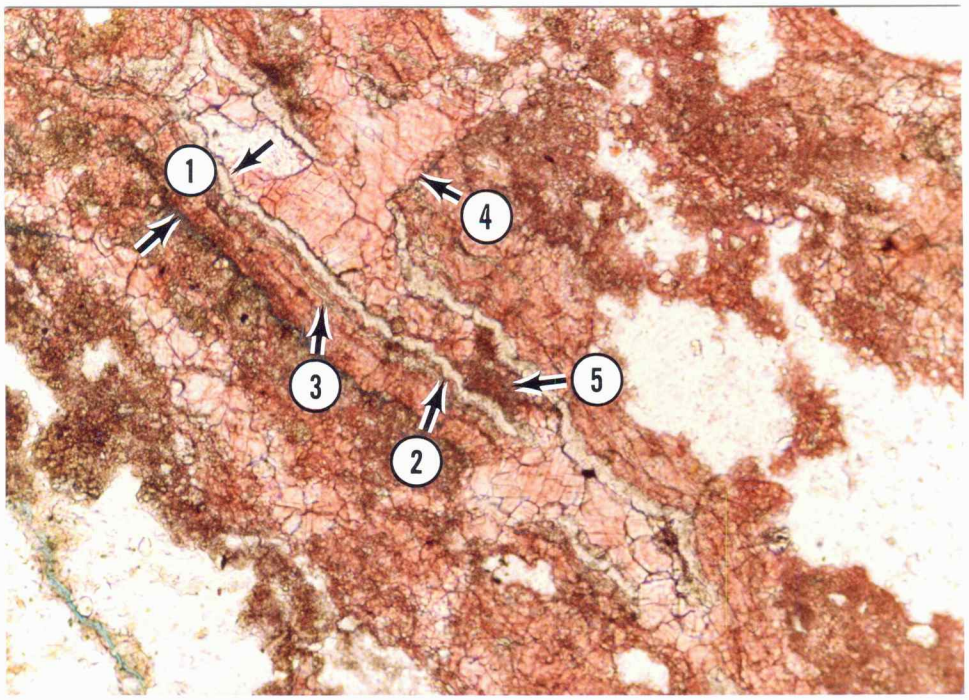

300 μm

Stratigraphic Up

B

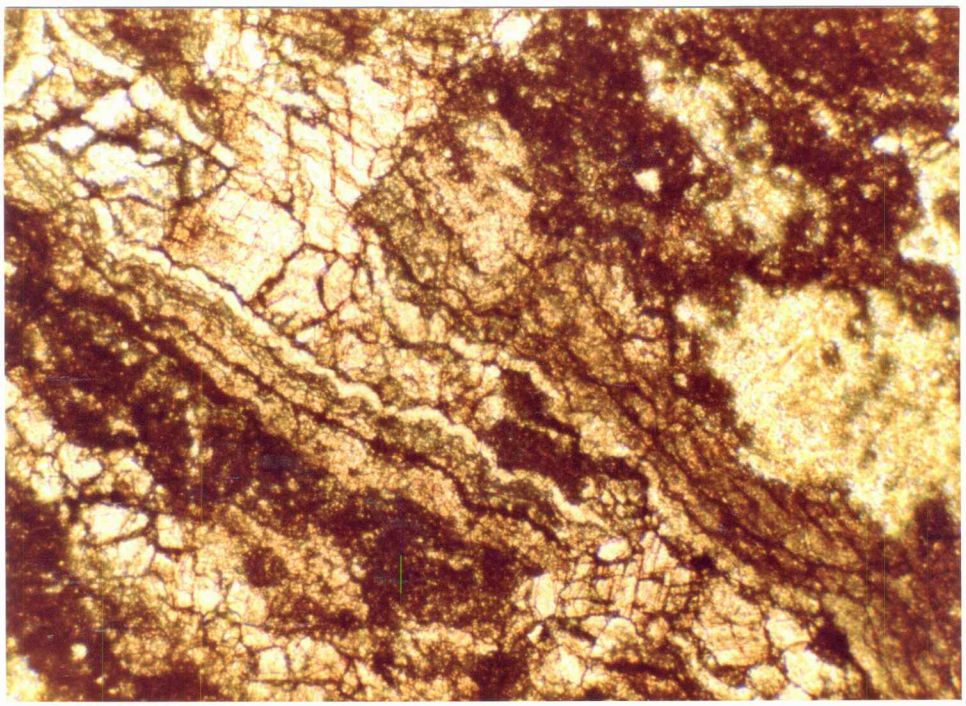

C

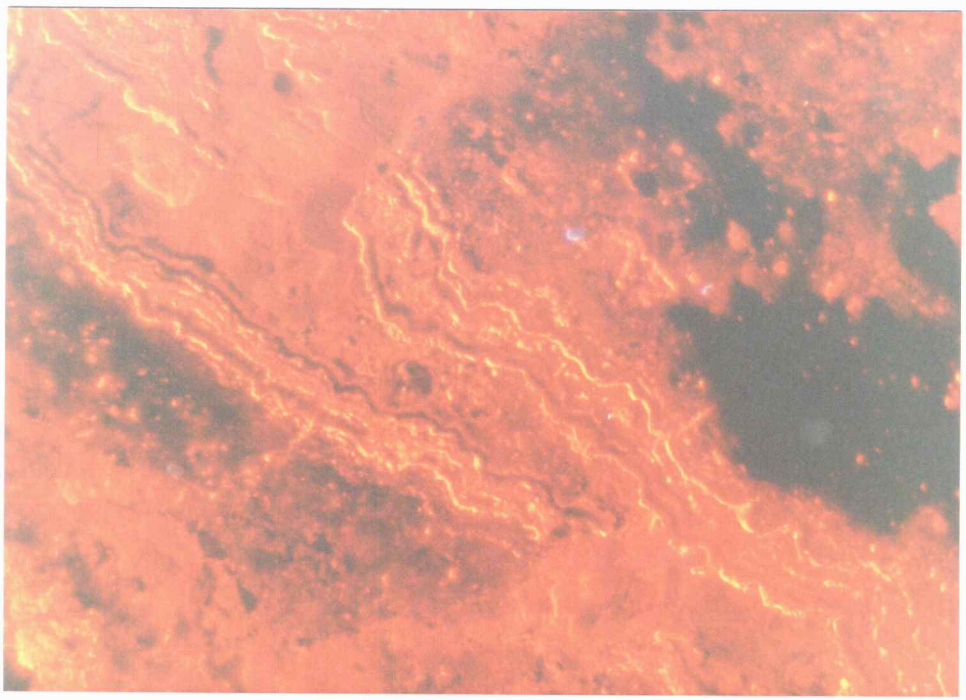

200 μm

Stratigraphic Up

The original nature of the contact between the fissures and the host material cannot be determined because every observed contact now forms a solution seam. Several fissures contain root molds or rhizocretions, others exhibit circumgranular cracking of the infilling sediment.

Pipes are nearly cylindrical vertical features exhibiting diameters of 1 to 3 cm. Pipes are much rarer than fissures. The only pipe cut for a significant length by a core was only partially intersected (Fig. 31), but the horizontal section of this pipe is nearly perfectly circular. This pipe is at least 2.5 feet (.76 m) long.

The autoclastic breccias, circumgranular cracks, fissures, and pipes created significant secondary porosity in the upper carbonate unit. These four pore types are here termed "alteration pores". However, all four types of alteration pores are almost completely occluded throughout the field, and do not make a significant contribution to the extant porosity.

Cement J2

A brown, aphanocrystalline cement (J2) with a point-contact and meniscus distribution occurs in the alteration pores of the cap subunit in several wells, and is rarely present at the top of the alpha grainstone

Stratigraphic Up

Blocks on scale equal one centimeter.

Figure 31. Core photo of an alteration "pipe". The pipe runs down the left side of the sample, and is filled with ooid, peloid, skeletal wackestone. The carbonate mud matrix in the pipe is completely dolomitized. The core intersected 2.5 feet (.76 m) of this pipe, which exhibited a nearly perfectly circular horizontal section prior to slabbing. (Alpha grainstone subunit, upper carbonate unit, "J" zone; Bethell #3, 3747 feet.)

subunit (Fig. 32). This cement is now completely composed of dolomite, with no relict texture. The cement typically exhibits uniform, moderately bright luminescence, but in places exhibits a few dark speckles (Fig. 33).

Root Molds and Rhizocretions

Cylindrical molds and rhizocretions are a common paragenetic feature of the cap subunit, and occur in alteration pores as well as unaltered rock. The molds primarily show a vertical orientation although horizontal orientations are present (Fig. 34). Many molds exhibit a sinuous path through the rock, and may be discordant to the rock fabric, suggesting the molds are post-depositional. The sinuous paths indicate the molds are probably formed by root action. The diameters of the round to elliptical mold sections range from .3 to 3 mm. Bifurcations are only rarely present, but the branches generally show a decrease in diameter. Decreasing bifurcations differentiate root-formed structures from animal burrows (Klappa, 1980), confirming the root mold interpretation. Rhizocretions are relatively rare, and always exhibit the same distinctive pattern of cement accretion (Fig. 35). They do not form in association with the root molds.

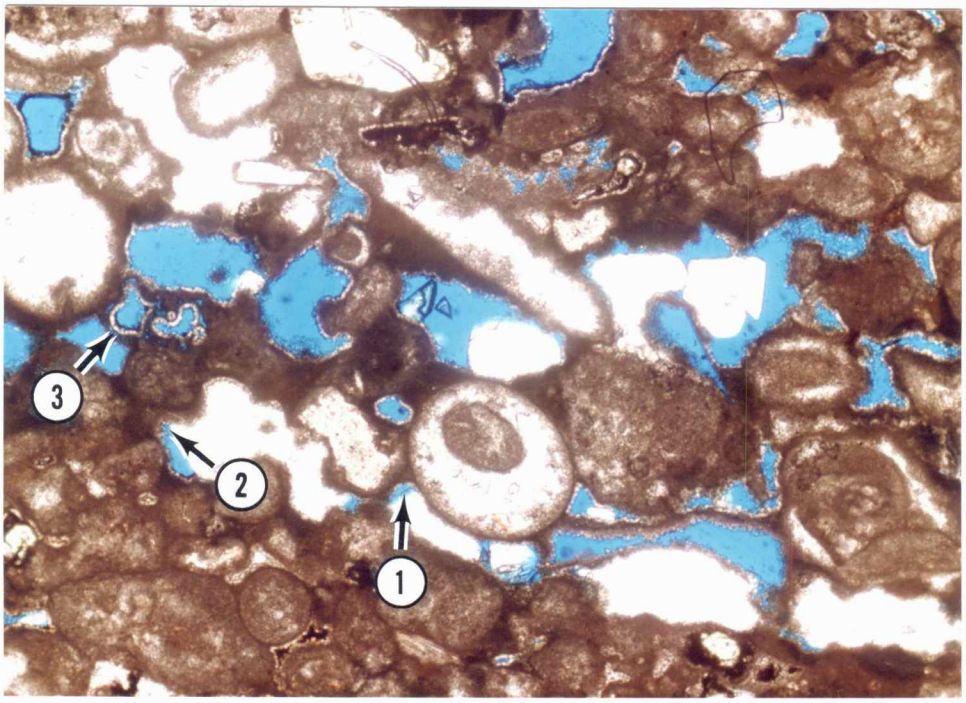

Figure 32. Unpolarized-light photomicrograph of cement J2. (Thin section impregnated with blue epoxy.) The brown, aphanocrystalline cement exhibits an irregular distribution, but is most abundant at the point-contacts between grains. The cement in the point-contacts commonly exhibits a curved meniscus face (arrows 1 and 2). Cement J2 is now completely composed of dolomite. In this sample, dolomite cement J5 forms a thin rim of small crystals coating cement J2 (arrow 3). The coarse, equant spar consists of cements J7 and M1. (Alpha grainstone subunit, upper carbonate unit, "J" zone; Rogers #1, 3799 feet.)

Figure 33. Paired plane polarized-light (A) and cathodoluminescent (B) photomicrographs of cement J2. (Thin section impregnated with blue epoxy.) The cement typically exhibits uniform, moderately bright luminescence (arrow 1), but some areas show dark speckling (arrow 2). In this sample, fine crystals of cement J5 coat cement J2 (arrow 3), and the coarse, equant spar consists of cements J7 and M1. (Alpha grainstone subunit, upper carbonate unit, "J" zone; Rogers #1, 3799 feet.)

A

B

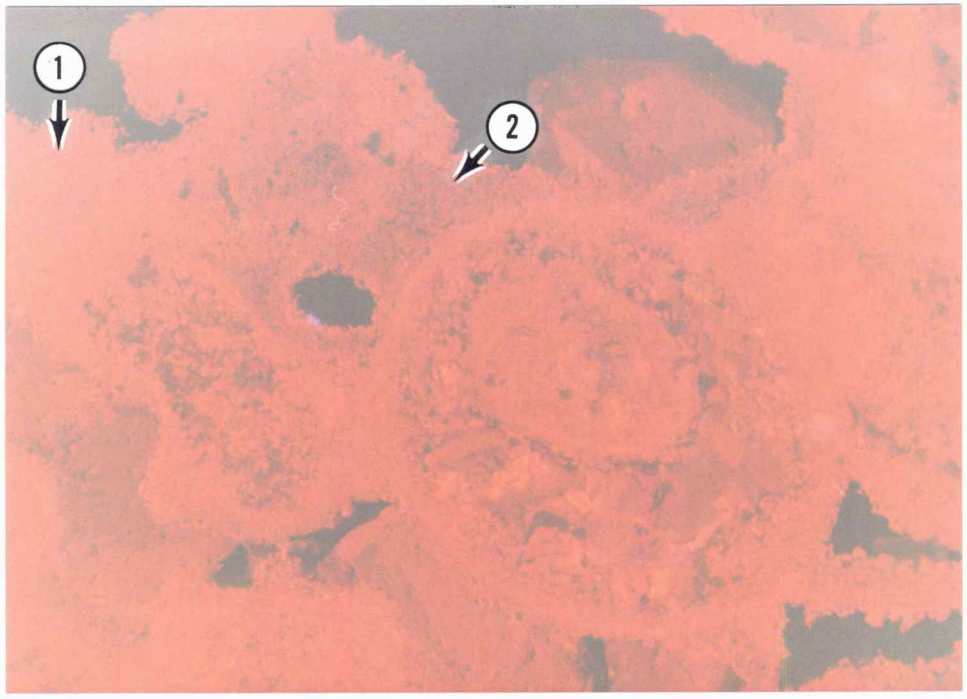

300 μm

Stratigraphic Up

Figure 34. Core photo of abundant root molds in a carbonate mudstone. Several of the root molds in the sample exhibit bifurcations (arrow 1). The molds with circular or elliptical aspects are the result of the slab face intersecting cylindrical root molds formed by horizontal roots, or vertical roots that weave in and out of the plane of the slab. (Cap subunit, upper carbonate unit, "J" zone; Pennington #2, 3773 feet.)

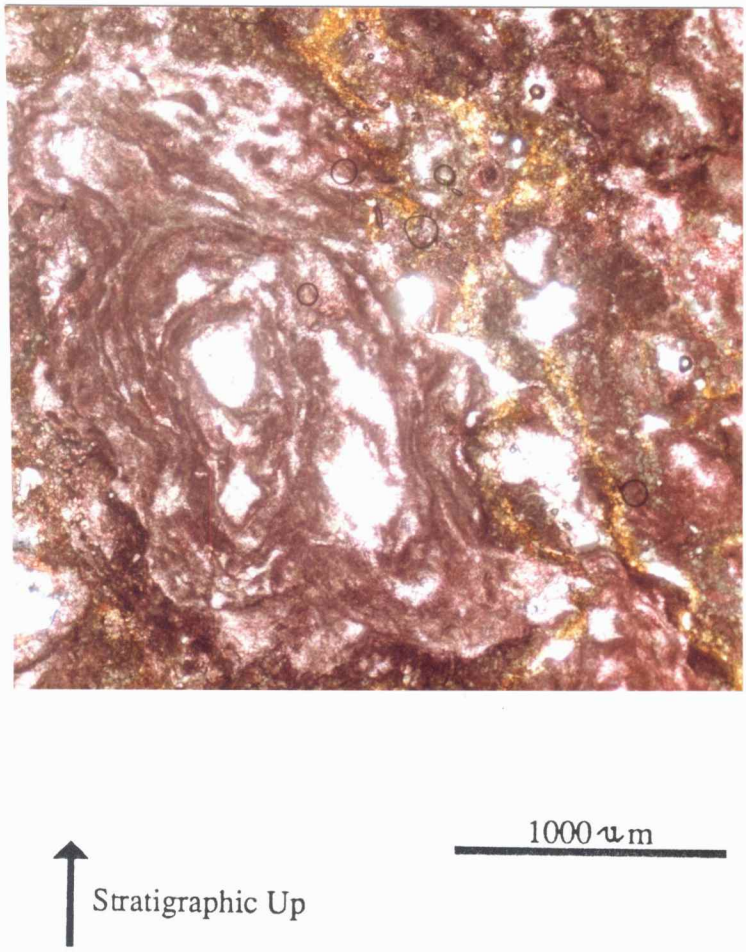

Figure 35. Unpolarized-light photomicrograph of a rhizocretion showing a distinctive pattern of cement accretion (in a heavily altered portion of the alpha grainstone). (Thin section stained with Alizarin Red-S and potassium ferricyanide.) (Alpha grainstone subunit, upper carbonate unit, "J" zone; Bethell #3, 3746 feet.)

Skeletal Molds, Oomolds, and Vugs

Abundant skeletal molds, oomolds, and a few rare vugs all exhibit a sequence of cement infilling that closely resembles that of the root molds. The dissolution event that formed the molds and vugs was widespread both vertically and laterally. Skeletal molds of algal fragments, bivalves, and gastropods, from the cap subunit through the beta micrite-rich subunit, all show the same general sequence of cements across the entire field.

Many oomolds also formed during this dissolution event, but the dissolution was far from uniform. In several wells the vast majority of ooids were leached, whereas in other wells, only a small percentage of ooids were leached. The unleached ooids exhibit a neomorphic texture with the original concentric layers preserved. Oomold formation was not even uniform at the scale of thin sections; oomolds can commonly be observed adjacent to neomorphosed ooids (Fig. 36). The ooids generally exhibit only thin micritized rims, or lack them entirely.

Vugs are relatively rare, but they show the same sequence of cements as the skeletal molds and oomolds. The vugs appear to be of two distinct types. The first type occurs only in the intervals with root molds. These vugs are primarily vertical, and typically show slightly larger dimensions than the root molds. A few of the vugs

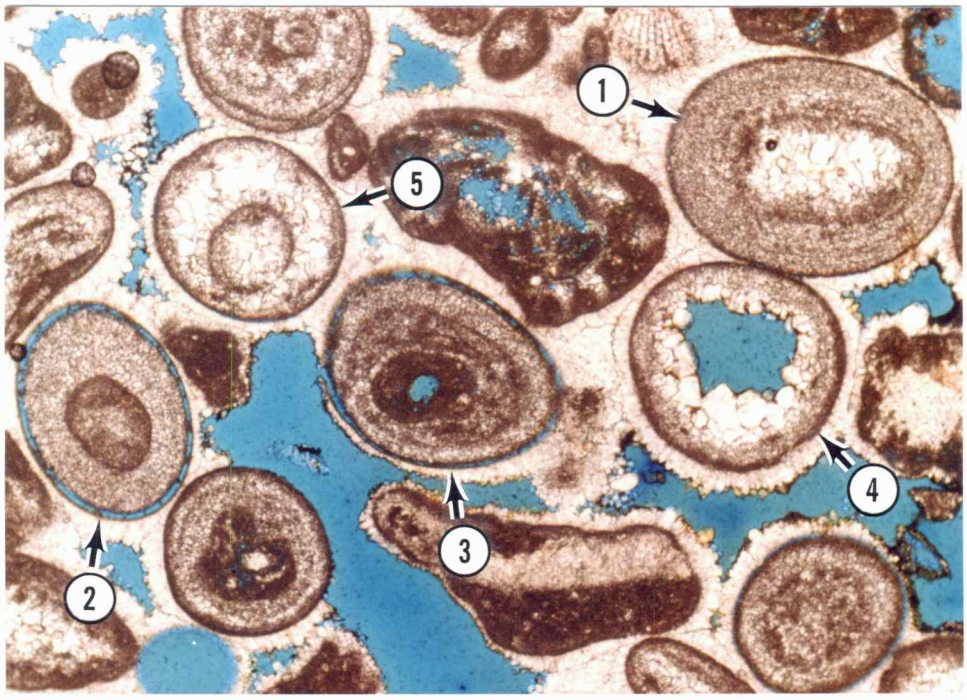

1000 µm

Stratigraphic Up

Figure 36. Unpolarized-light photomicrograph of ooid textures and preservation. (Thin section impregnated with blue epoxy.) Arrow 1 points to an ooid that was completely neomorphosed except for the leached and filled nucleus. Arrows 2 and 3 point to ooids that were completely neomorphosed except for the outermost layer which was leached. Arrow 4 points to an ooid that exhibits neomorphosed outer layers, with leached inner layers and a leached nucleus. The leached portion was later reduced by cement. Arrow 5 points to an ooid that was completely leached except for the micritized rims around the nucleus and the ooid. The nucleus "dropped" before the oomold was filled with cement. The ooids in the alpha grainstone subunit typically exhibit only thin micritized rims, or lack them entirely. (Alpha grainstone subunit, upper carbonate unit, "J" zone; Demuth #1, 3813 feet.)

are more irregular and larger, ranging from 1 to 3 cm in length and .5 to 1 cm in width.

The second type of vug is roughly equant, exhibits an irregular outline, and occurs only in the muddy lithologies. These vugs are generally rare, but they may be locally abundant, giving the rock a "moth-eaten" appearance (Fig. 37). Cement J2 was not observed in the root molds, skeletal molds, oomolds, or vugs and probably pre-dates these dissolution features.

Cement J3

The interparticle pores and skeletal molds of the lower carbonate unit are partially to totally filled with a generation of bladed to equant, nonferroan calcite cement (J3), which occurs only in the lower carbonate unit. This cement is generally clear, but exhibits many bands of solid and fluid inclusions that mimic the shape of the grain boundaries. The long axes of the cement blades range from 15 to 415 micrometers, whereas the short axes range from 10 to 400 micrometers. This cement shows a very distinctive pattern of alternating moderately bright and dark bands under cathodoluminescence (Fig. 38).

None of the alteration features are present in the lower carbonate unit, therefore no direct cross-cutting relationships exist to date cement J3 relative to the

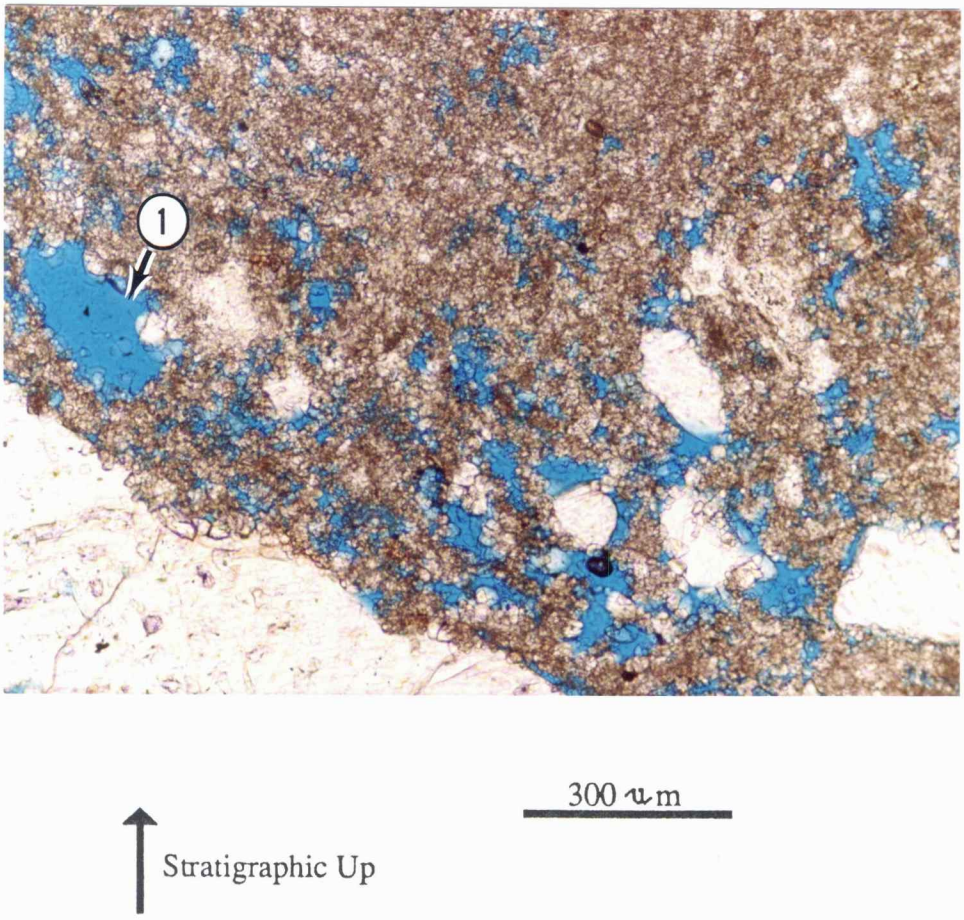

Figure 37. Unpolarized-light photomicrograph of small vugs which give the rock a "moth-eaten" appearance. (Thin section impregnated with blue epoxy.) The pore marked by arrow 1 is probably a skeletal mold, but the rest of the pores exhibit irregular shapes and outlines and are probably vugs. The calcite spar in the southwest corner of the photo is cement M1 filling a large skeletal mold. (Beta micrite-rich subunit, upper carbonate unit, "J" zone; Bethell #5, 3771 feet.)

Figure 38. Paired plane polarized-light (A) and cathodoluminescent (B) photomicrographs of cements J3 and M1. Cement J3 consists of bladed crystals which line the pore walls. These blades exhibit alternating bands of dark and moderately bright luminescence (arrows 1 and 2). A few coarse crystals of cement M1 fill the center of the pore and exhibit moderately bright luminescence (arrow 3). (Lower carbonate unit, "J" zone; Shuck #1, 3756 feet.)

A

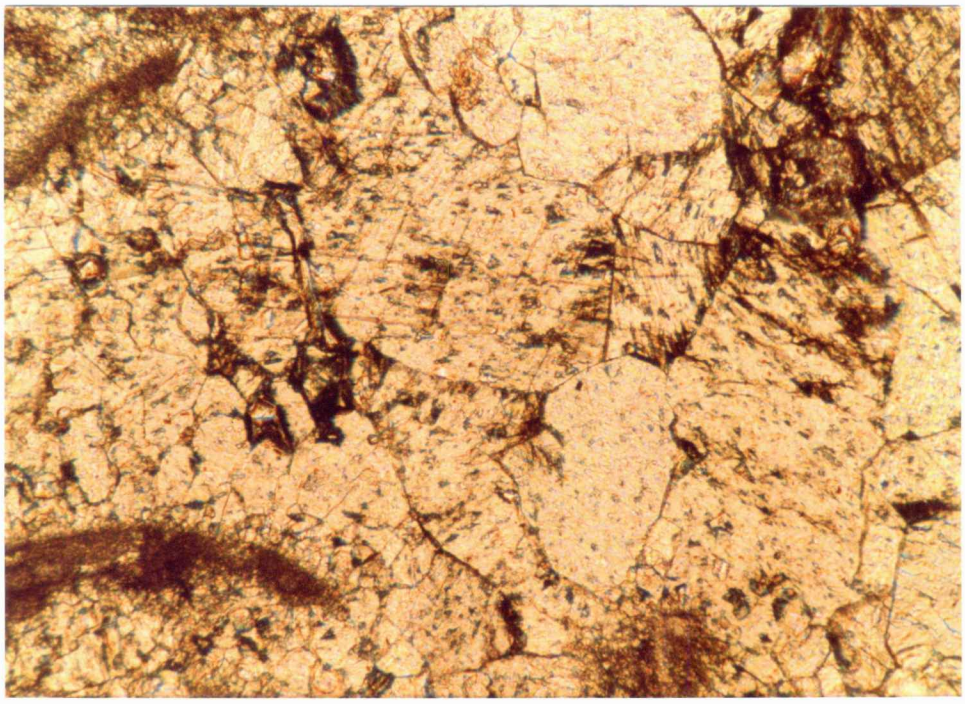

B

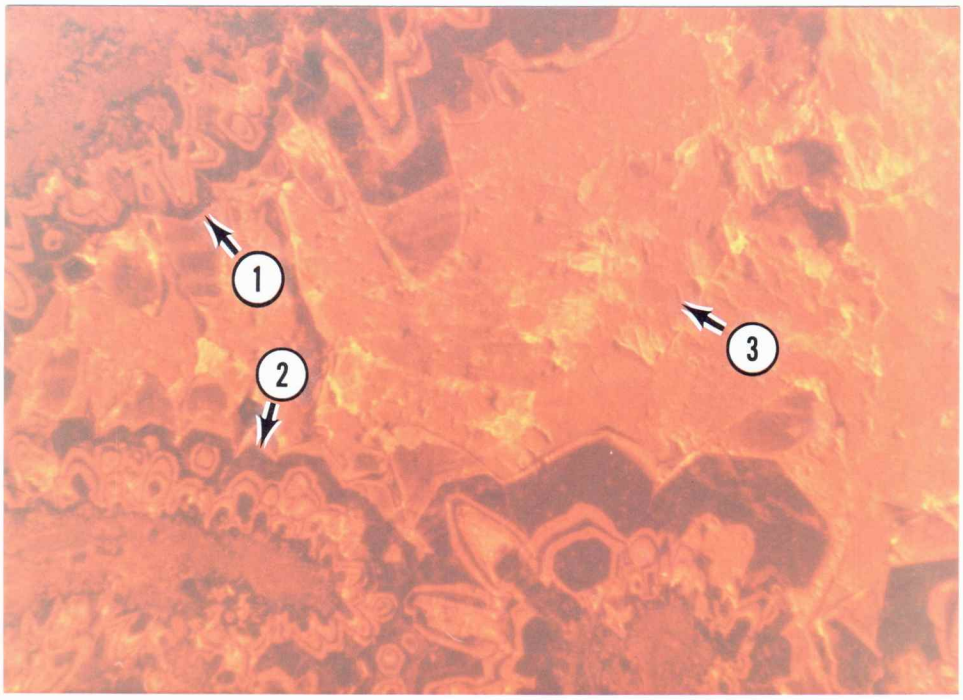

300 μm

Stratigraphic Up

alteration features. Likewise, cement J3 does not occur in the upper carbonate unit and none of the other J-prefix cement generations occur in the lower carbonate unit, so the formation of cement J3 relative to the other J cement generations cannot be determined. However, cement J3 does post-date the dissolution event that formed skeletal molds, and based on fluid inclusion data is interpreted to have formed during the event that caused the alteration features. This interpretation will be clarified in the sections covering the fluid inclusion study and diagenetic environment interpretations.

Cement J4

Continuous, isopachous rims of nonferroan calcite are the first cement (J4) to appear in both the alteration pores and the root molds, skeletal molds, and vugs. The rims exhibit smooth, undulose bands with no evidence of euhedral crystal terminations. A few continuous bands of dolomite occur within cement J4, and exhibit optical continuity with the calcite. Cement J4 exhibits continuous, alternating moderately bright and dark bands under cathodoluminescence (Fig. 30). This rare cement is only present in the cap subunit, and then only in a few wells.

Carbonate Sediment Infilling

Partial to complete infilling of alteration pores with carbonate sediment is a rare occurrence, but carbonate infilling is present throughout the cap subunit. Sparsely fossiliferous micrite is the most common sediment, but some features are filled with skeletal, ooid wackestone, or even intraclast, skeletal, ooid grainstone. The infill sediment occurs as a coating on several generations of J-cements (Fig. 30; 39). However, in other places skeletal molds and oomolds in the infill sediment contain the same generations of cement. The evidence that carbonate sediment infilling may both pre-date and post-date certain cement generations indicates the infilling was episodic, rather than a single discrete event.

Cement J5

Cement J5 is pervasive vertically and is found in every well. This cement typically consists of well-developed rhombohedra of nonferroan dolomite that form a scattered distribution in interparticle pores that lack precursor cements, alteration pores, root molds, skeletal molds, and oomolds. Cement rhombohedra range in size from 10 to 50 micrometers. Luminescence ranges from dark cores with thin moderately bright rims, to alternating moderately bright and dark bands, to rhombohedra

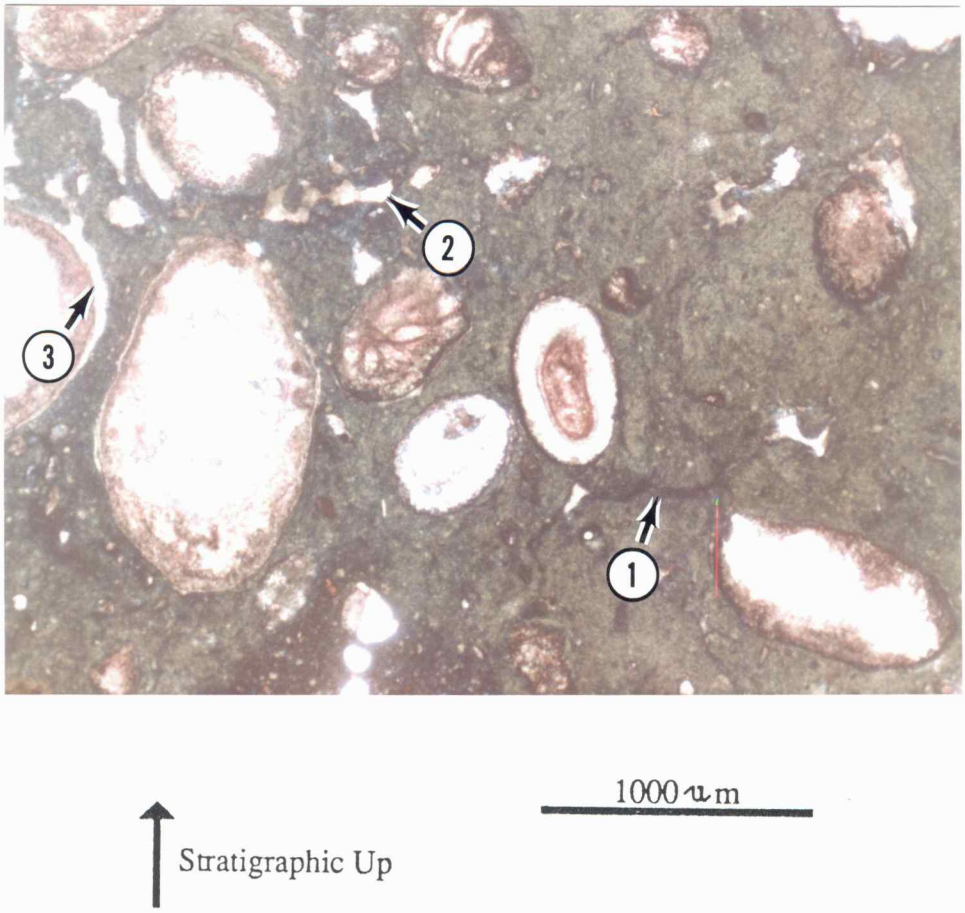

Figure 39. Unpolarized-light photomicrograph of ooid, skeletal wackestone filling an alteration pipe. (Thin section stained with Alizarin Red-S and potassium ferricyanide.) The matrix of the pipe-fill is completely dolomitized and exhibits a vaguely clotted texture (arrow 1), fenestral pores (arrow 2), and circumgranular cracks (arrow 3). The ooids, intraclasts, and rounded fusilinid fragments of the wackestone infilling are all typical allochems of the alpha grainstone. (Alpha grainstone subunit, upper carbonate unit, "J" zone; Bethell #3, 3746 feet.)

exhibiting completely moderately bright luminescence (Fig. 40). The abundance of this cement decreases downwards. It is abundant in the cap subunit, relatively common in the alpha grainstone subunit, and much rarer in the lower subunits of the upper carbonate unit.

Cement J5 is substrate selective to a degree. It is well developed in the molds of the alpha grainstone where a micrite rim forms the substrate, but it does not form on the isopachous rims of cement J1, even where significant interparticle porosity exists beyond the cement rims. The dolomite cement does form roughly isopachous rims in the interparticle pore space of the alpha grainstone where the bladed calcite rims of cement J1 are absent (Fig. 41).

Dolomite Replacement

Dolomite replacement of micrite was also a pervasive event, and also shows a decrease in abundance downwards. The micrite in the muddy lithologies of the cap subunit is completely dolomitized, or almost so, in most of the wells. The mudstone intraclasts and thick micrite envelopes in the alpha grainstone usually show at least partial dolomite replacement. The matrix of the alpha and beta micrite-rich subunits shows varying degrees of dolomite replacement. Dolomite replacement in the micrite-rich subunits does occur in the few wells that

Figure 40. Paired plane polarized-light (A) and cathodoluminescent (B) photomicrographs of dolomite cement (J5) and dolomite replacement showing the variability of luminescence patterns. (Thin section impregnated with blue epoxy.) Many cement rhombohedra exhibit dark cores with thin moderately bright rims (arrows 1 and 2), as do several replacement rhombohedra (arrows 3 and 4). However, some cement rhombohedra exhibit moderately bright cores with alternating dark and moderately bright bands (arrows 5 and 6). Other cement rhombohedra exhibit moderately bright luminescence across the entire crystal (arrows 7 and 8). (Alpha grainstone subunit, upper carbonate unit, "J" zone; Bethell #5, 3762 feet.)

A

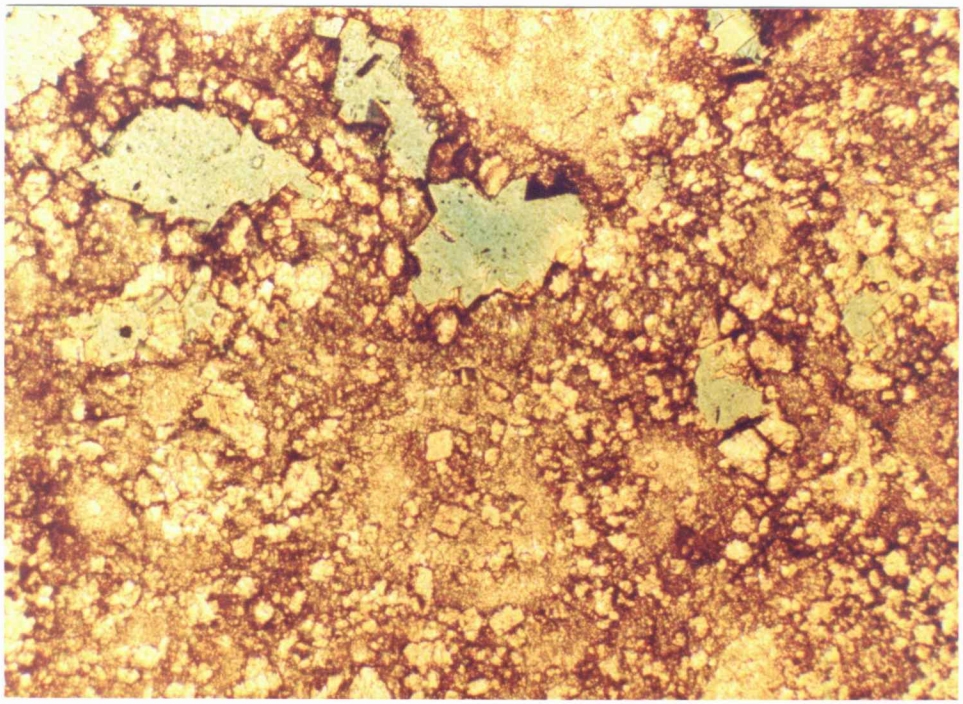

B

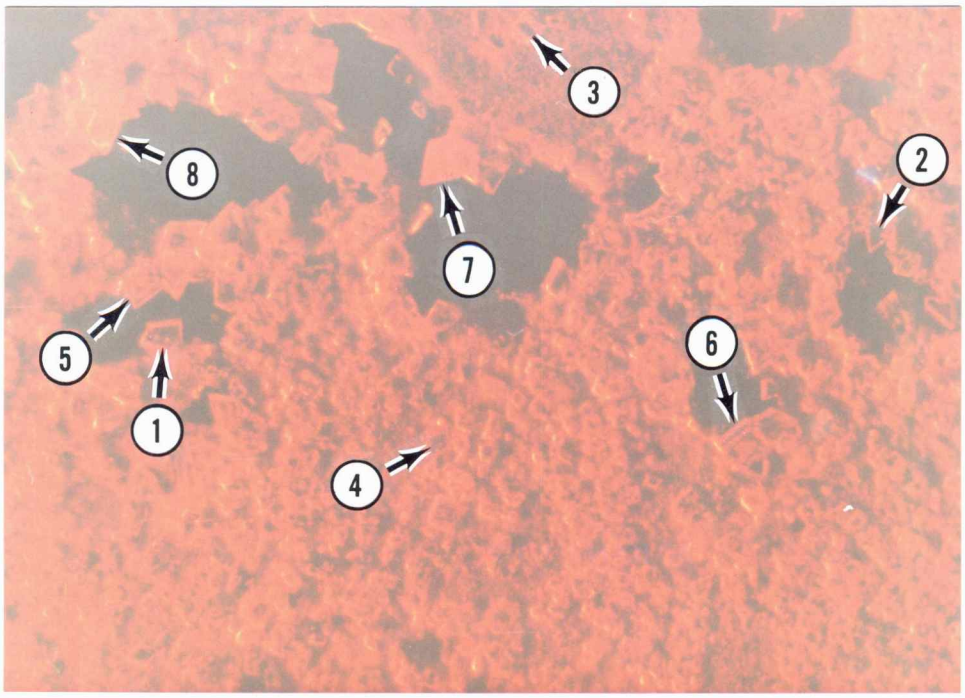

200 μm

Stratigraphic Up

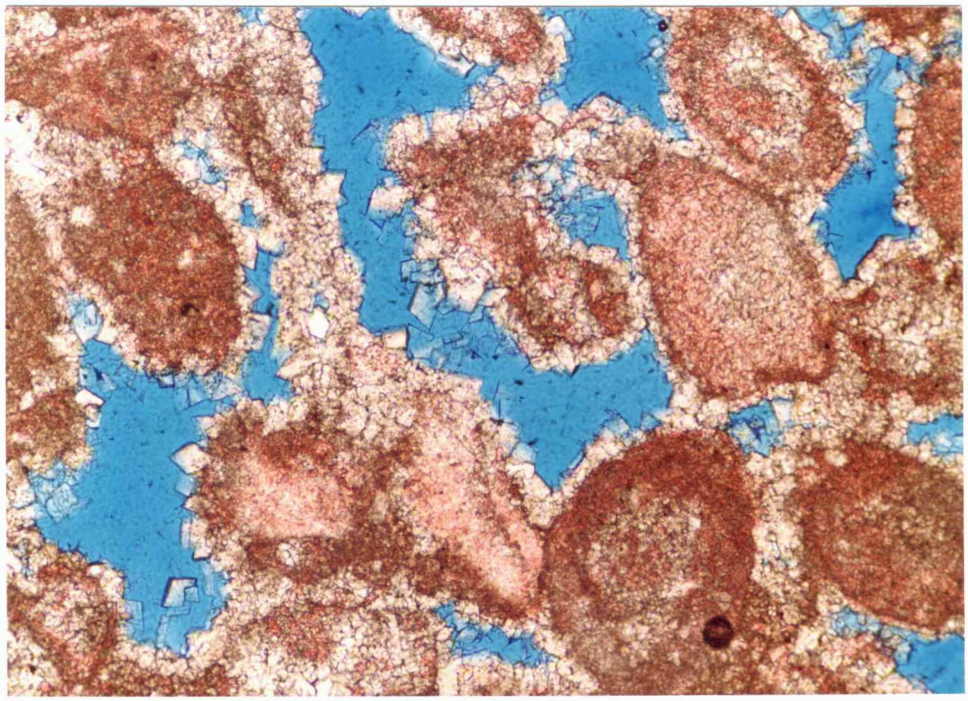

Figure 41. Unpolarized-light photomicrograph of dolomite cement (J5) forming roughly isopachous rims in interparticle porosity. (Thin section impregnated with blue epoxy and stained with Alizarin Red-S.) (Alpha grainstone subunit, upper carbonate unit, "J" zone; Bethell #5, 3762 feet.)

lack dolomite cement in the lowest portions of the alpha grainstone.

The replacement rhombohedra are well developed, and of roughly the same size as the rhombohedra of cement J5 (Fig. 42). Luminescence patterns of the replacement rhombohedra are also similar to those in the cement (Fig. 40).

Cement J6

Chalcedony cement and chalcedony replacement are present in the "J" zone strata. Very minor amounts of aphanocrystalline, chalcedony cement (J6) occur in the cap subunit, typically as the final bit of pore-fill (Fig. 43).

Chalcedony Replacement

Unlike the cement, chalcedony replacement is a common feature, and can be found in almost every well. This replacement was observed in the alpha and beta micrite-rich subunits, the beta grainstone-packstone subunit, and the lower carbonate unit. Replacement is highly selective and occurs only in brachiopod shells, echinoderm fragments, and in cement J3. The skeletal grains typically show roughly circular, irregular blebs of replacement. In many places, the chalcedony blebs contain small spheres of hematite (Fig. 44). The

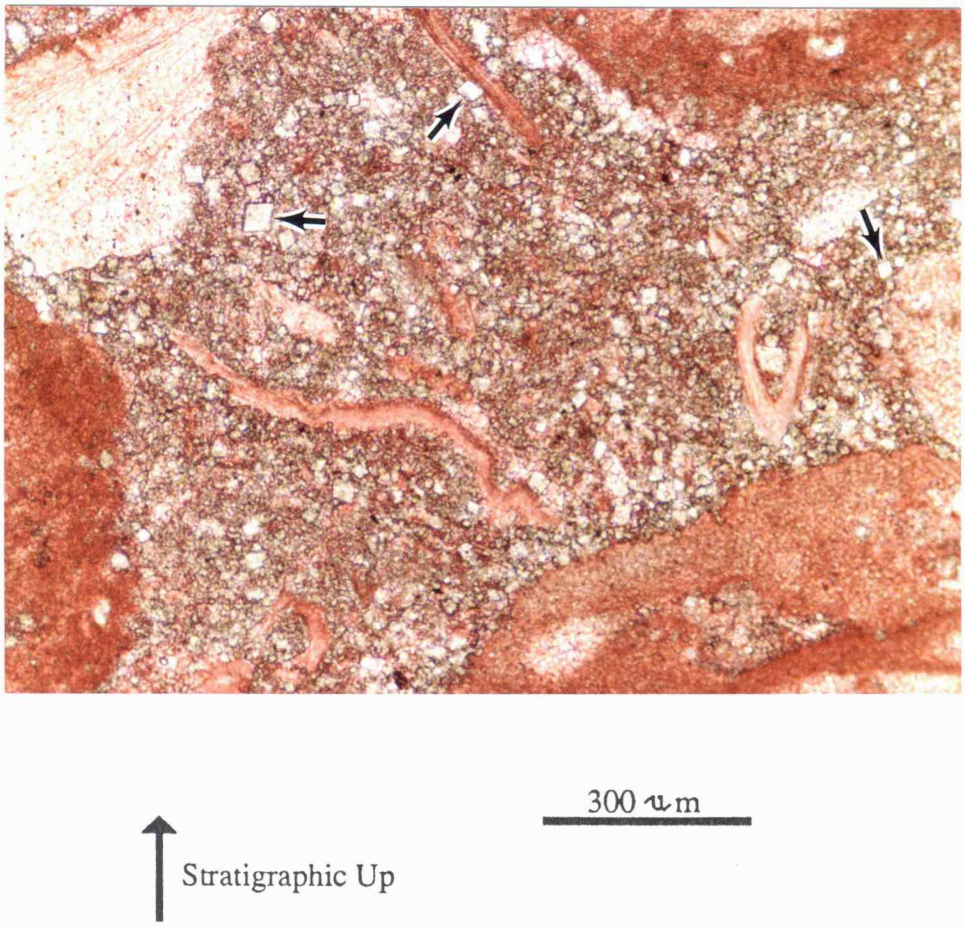

Figure 42. Unpolarized-light photomicrograph of dolomite replacement rhombohedra (arrows) in micrite matrix of a skeletal packstone. (Thin section stained with Alizarin Red-S and potassium ferricyanide.) The rhombohedra are roughly the same size as those of cement J5. The rhombohedra are generally well-formed, with no signs of abrasion, indicating they are replacive rather than part of the depositional matrix. (Beta grainstone-packstone subunit, upper carbonate unit, "J" zone; Pennington #2, 3777 feet.)

Figure 43. Paired plane polarized-light (A) and crosspolarized-light (B) photomicrographs of chalcedony cement J6. (Thin section stained with Alizarin Red-S and potassium ferricyanide.) The arrows point to two pores where the final fill consists of cement J6. Cement J5 forms the isopachous rims that line the pore walls. (Cap subunit, upper carbonate unit, "J" zone; Bethell #3, 3745 feet.)

A

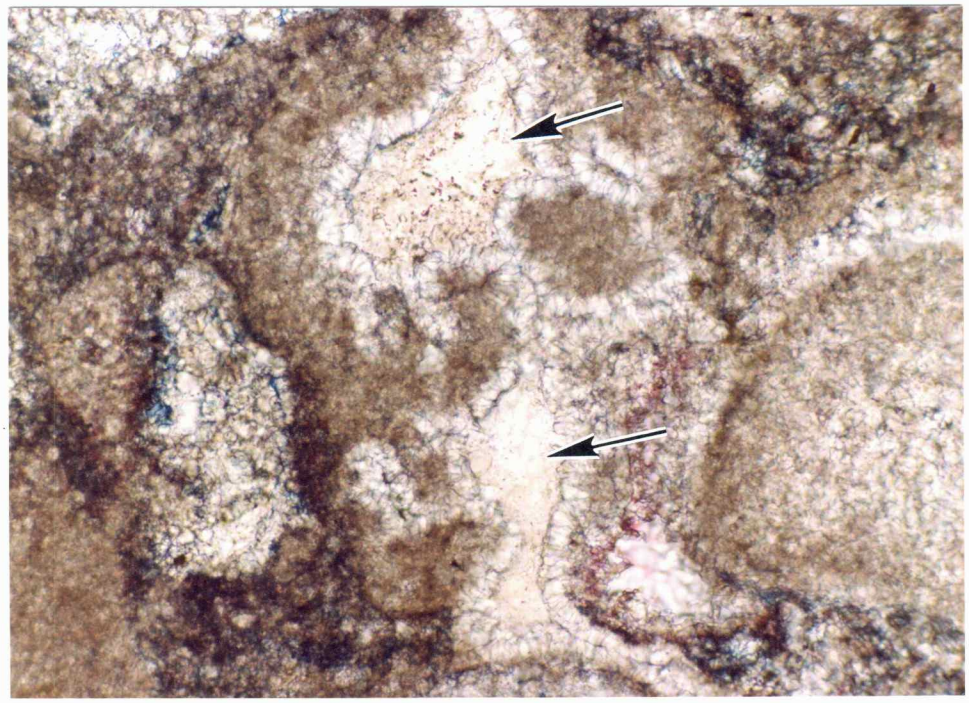

B

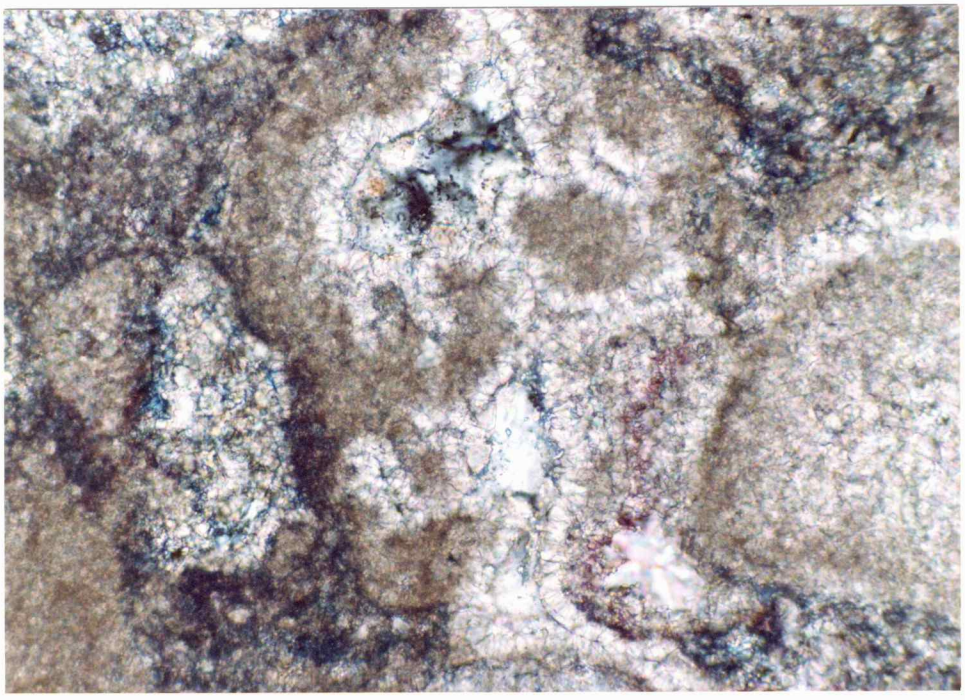

150 μm

Stratigraphic Up

Figure 44. Paired unpolarized-light (A) and crosspolarized-light (B) photomicrographs of chalcedony replacement (arrow 1). (Thin section impregnated with blue epoxy.) The chalcedony shows an irregular replacement front into a brachiopod shell. The chalcedony contains many blood-red to opaque spheres of hematite (arrow 2). (Beta micrite-rich subunit, upper carbonate unit, "J" zone; Bethell #5, 3769 feet.)

A

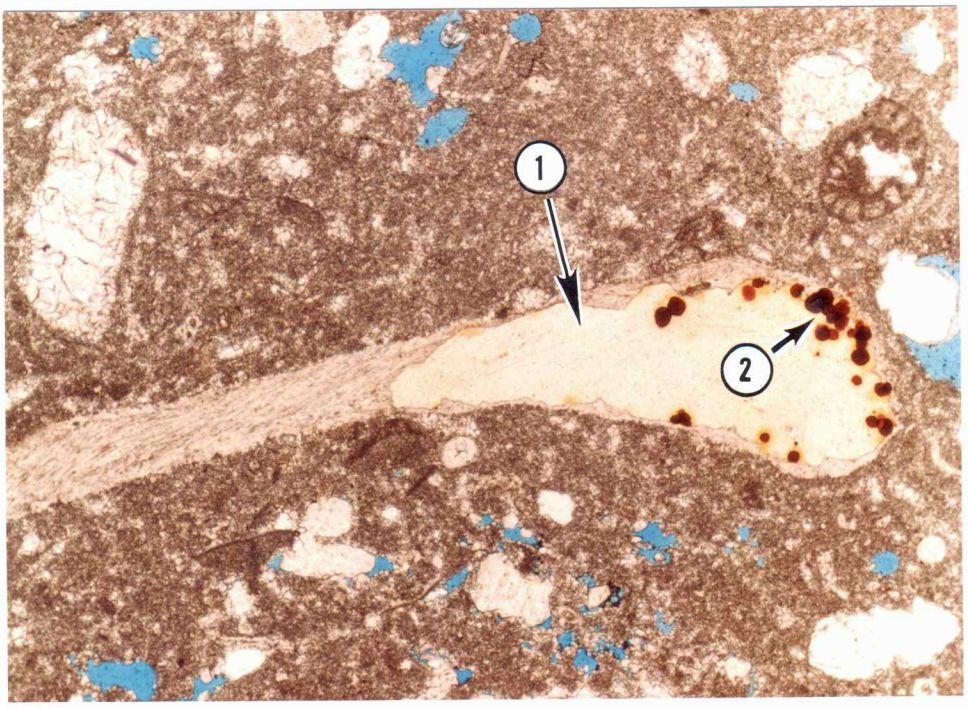

B

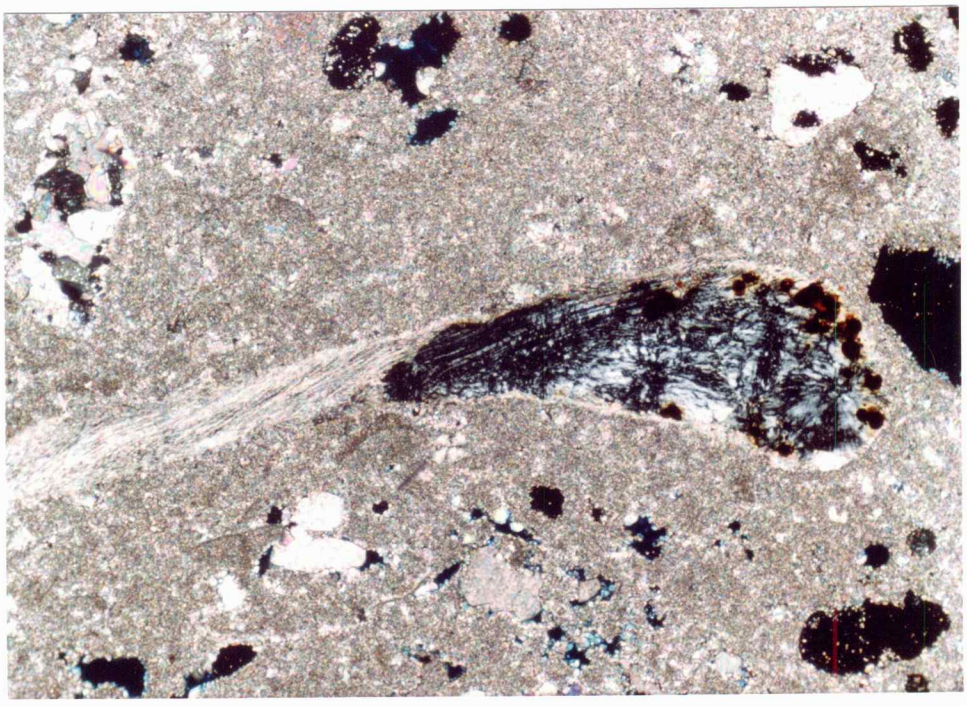

1000 μm

Stratigraphic Up

replacement chalcedony in cement J3 is of roughly the same shape and size as that in the skeletal grains, and clearly truncates luminescence bands in the calcite cement (Fig 45). Chalcedony formation clearly post-dates cements J3 and J5.

Post-burial Features

The upper shale unit is regionally extensive and forms a seal over the "J" zone carbonates, effectively isolating them from near-surface diagenetic environments. Shale infilling marks the onset of burial, but not necessarily the onset of significant compaction.

Shale Infilling

Scattered clay and quartz silt infilling occurs across the entire field. This infill sediment closely resembles the sediment of the upper shale unit (Fig. 23). The majority of the alteration pores that resulted from autoclastic brecciation and fissure formation are filled with light green silty shale. Clay and silt infilling of root molds and vugs in the cap subunit also occurs in several wells. Clay and silt filtered into the alpha grainstone in a few wells, and in places covers dolomite cement J5 (Fig. 24; 25).

Figure 45. Paired plane polarized-light (A) and cathodoluminescent (B) photomicrographs of chalcedony replacement (arrow 1) of cement J3 (arrow 2). The chalcedony bleb is completely dark under cathodoluminescence. The replacement front of the chalcedony clearly truncates luminescence zones in the cement (arrow 3). (Lower carbonate unit, "J" zone; Bethell #5, 3774 feet.)

A

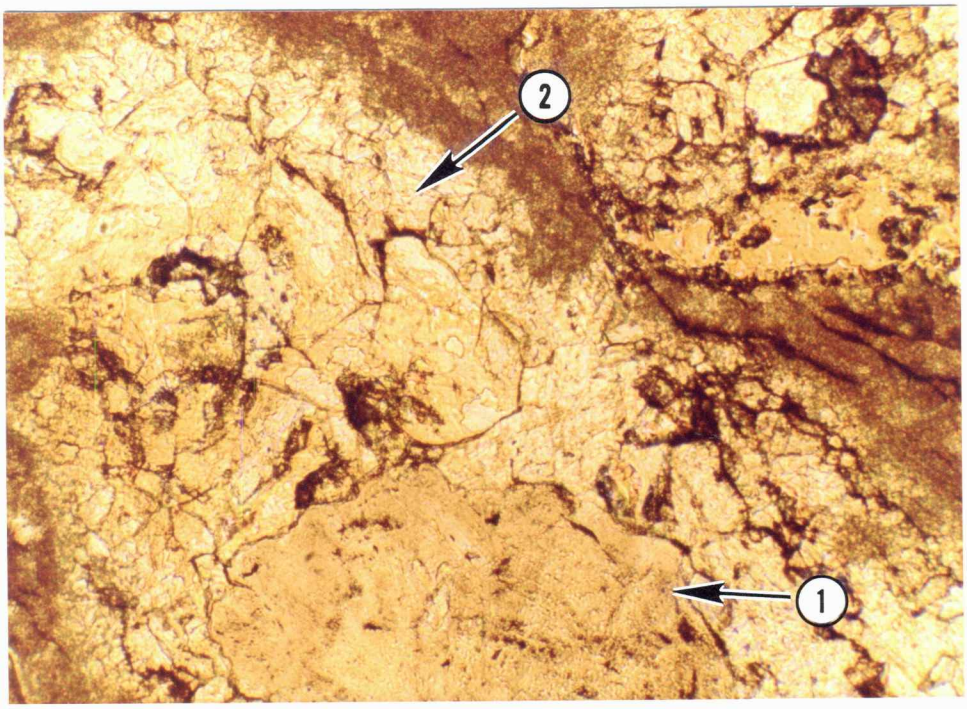

B

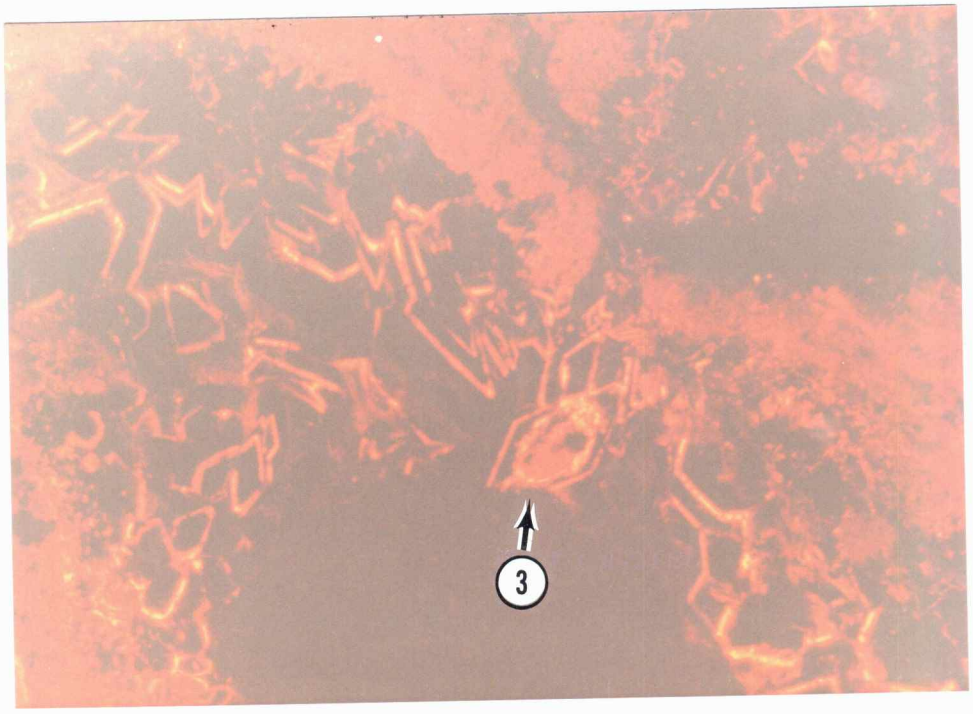

200 μm

Stratigraphic Up

Cement J7

Cement J7 consists of equant to bladed, nonferroan calcite. This cement is pervasive, although generally of only minor abundance. Crystals range in size from 7 to 460 micrometers. Under cathodoluminescence, cement J7 exhibits an initial dark zone, then relatively broad, alternating bands of dull and very dull luminescence (Fig. 46). This cement clearly pre-dates compaction (Fig. 47).

Filled Fractures

A few fractures occur throughout the "J" zone. These fractures are primarily vertical and are typically less than 2 mm wide. They are generally filled with cements M1 and M2.

Cement M1

The formation of equant, moderately to highly ferroan calcite cement (M1) post-dates shale infilling, cement J7, and compaction. Cement M1 is pervasive and is found in moldic and interparticle pores, in fractures, and rarely in alteration pores that were incompletely filled with shale. Occurrences of cement M1 vary from a single crystal, to small groups of crystals that partially occlude or fill large pores. Crystals may be as small as 15 micrometers in the groups, but large,

Figure 46. Paired plane polarized-light (A) and cathodoluminescent (B) photomicrographs of cement J7 filling interparticle pores and a skeletal mold (arrow). (Thin section stained with Alizarin Red-S.) Under cathodoluminescence, the cement exhibits a broad, initial dark zone, then alternating bands of dull and very dull luminescence. (Beta grainstone-packstone subunit, upper carbonate unit, "J" zone; White #1, 3784 feet.)

A

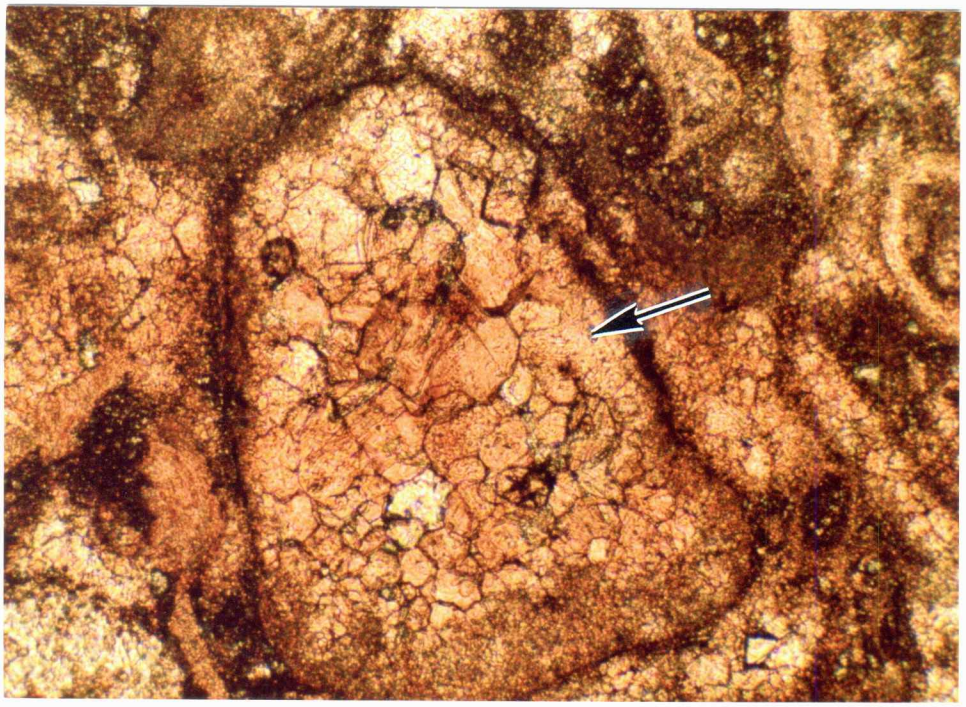

B

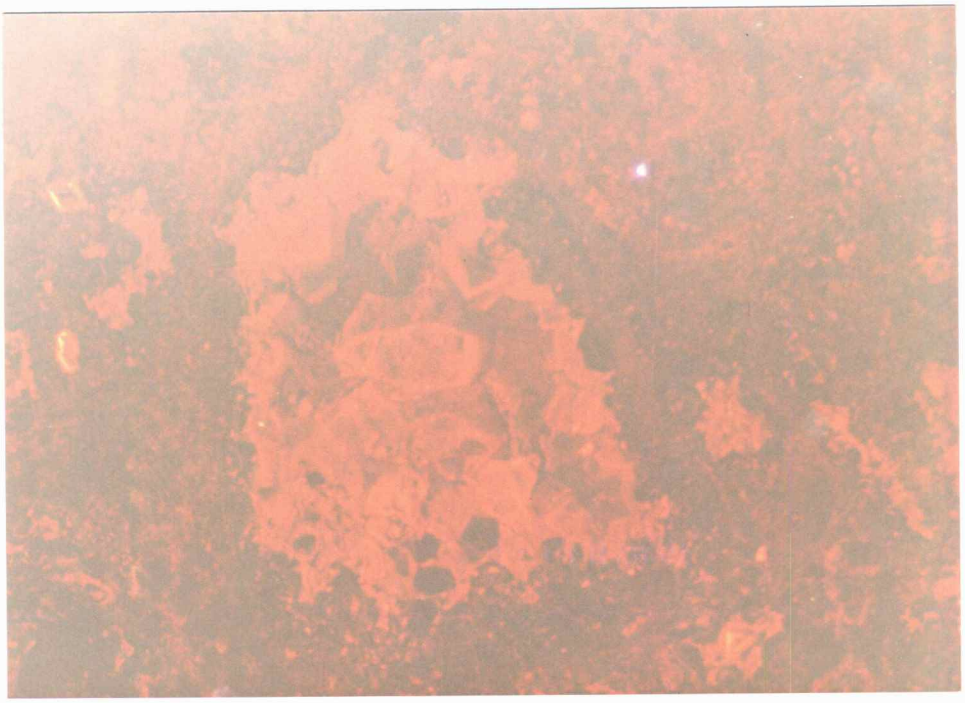

200 μm

Stratigraphic Up

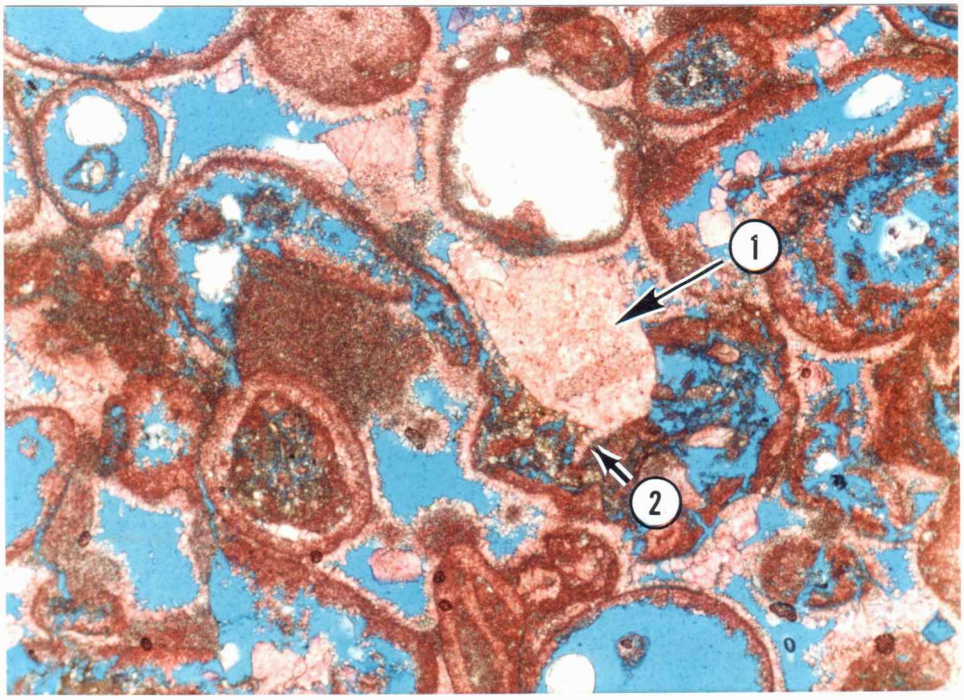

Figure 47. Unpolarized-light photomicrograph of cement J7, showing the cement pre-dates compaction. (Thin section impregnated with blue epoxy and stained with Alizarin Red-S and potassium ferricyanide.) Arrow 1 points to a crystal of cement J7 that was growing in an interparticle pore. During compaction this crystal punctured the adjacent mold, pushing the mold wall and rim of cement J1 (arrow 2) into the center of the mold. (Alpha grainstone subunit, upper carbonate unit, "J" zone; White #5, 3796 feet.)

poikilotopic crystals greater than 4000 micrometers in length do occur (Fig. 48). In thin sections stained with Alizarin Red-S and potassium ferricyanide (Dickson, 1965), cement M1 exhibits colors ranging from reddish-purple to lavender to deep purple to blue, indicating a variable iron content.

Cement M1 also exhibits a wide range of luminescence patterns. Uniform, dull to moderately bright luminescence is the most common pattern (Fig. 38), but areas of cement with very dull luminescence (Fig. 71), completely dark luminescence, or moderately bright luminescence with patches of dull luminescence (Fig. 49) also occur.

Cement M2

Equant, highly ferroan, baroque dolomite cement (M2) occurs in roughly the same pore types as the ferroan calcite cement M1. Cement M2 may occur as single crystals, but typically forms a pore-filling mosaic in molds where a rim of dolomite cement J5 is the only precursor (Fig. 50). The baroque dolomite cement post-dates compaction and typically post-dates the ferroan calcite cement, but it can be shown to clearly pre-date ferroan calcite cement in a few pores. The ambiguous relationship to cement M1 is probably the result of an extended period of formation for cement generation M1.

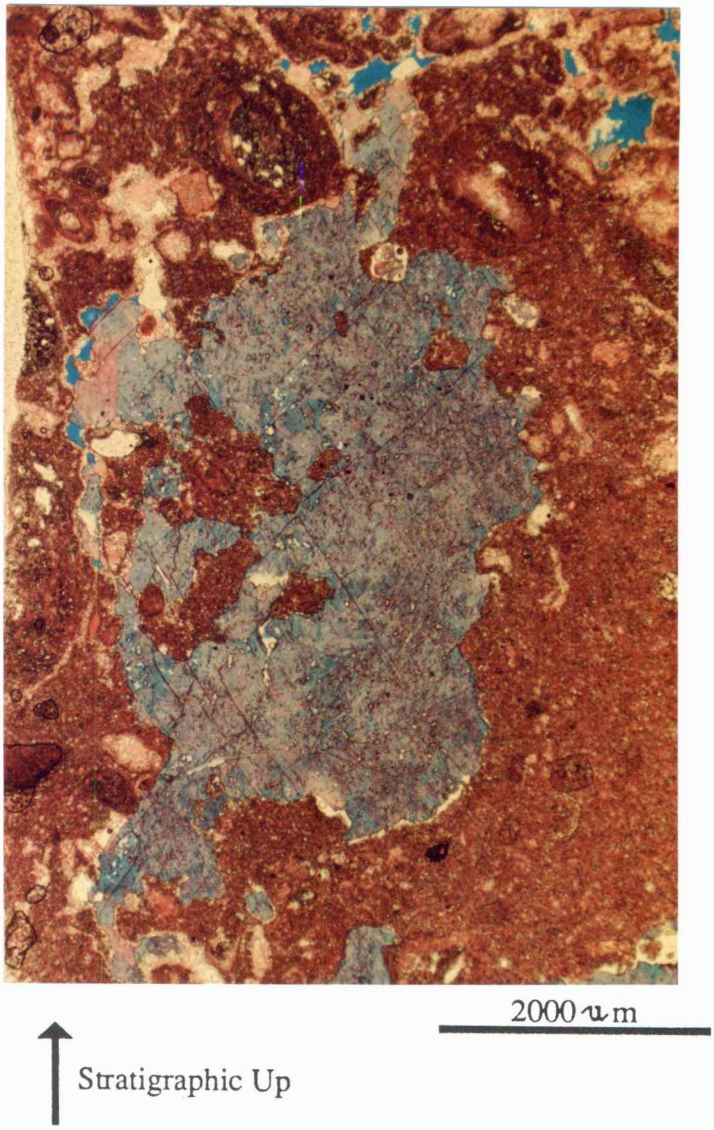

Figure 48. Plane polarized-light photomicrograph of cement M1. (Thin section impregnated with blue epoxy and stained with Alizarin Red-S and potassium ferricyanide.) This large, poikilotopic crystal fills a large vug. The crystal shows mottling of the lavender and blue staining colors. (Carbonate unit, "I" zone; Shuck #4, 3782 feet.)

Figure 49. Paired plane polarized-light (A) and cathodoluminescent (B) photomicrographs of a large crystal of cement M1 (crystal fill entire field of view). Under cathodoluminescence, the cement exhibits irregular patches of dull luminescence in a field of moderately bright luminescence. (Carbonate unit, "I" zone; Demuth #1, 3801 feet.)

A

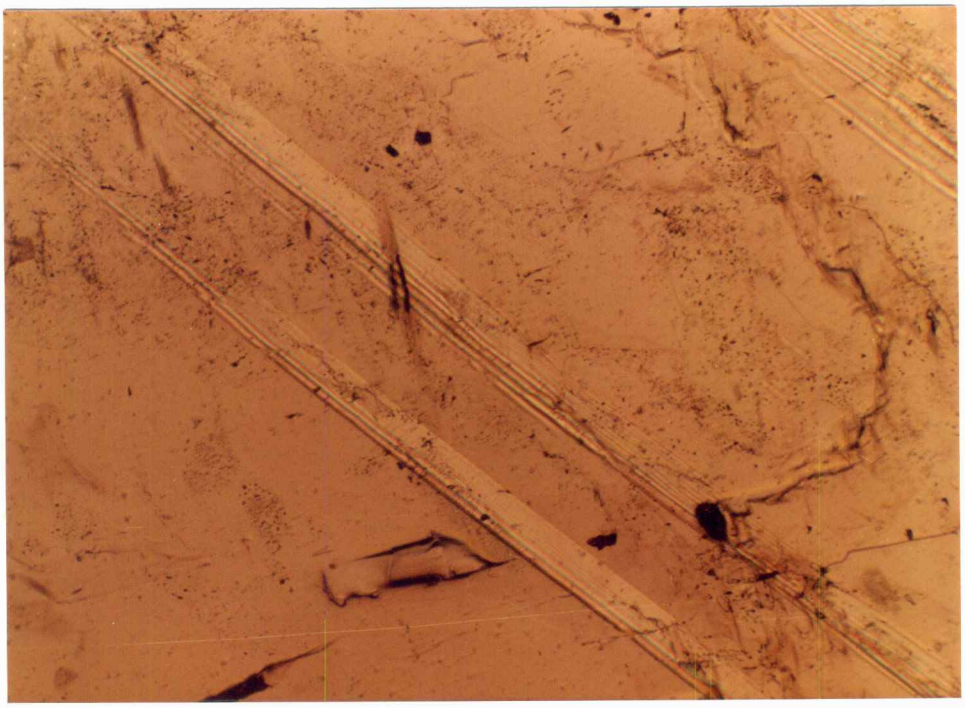

B

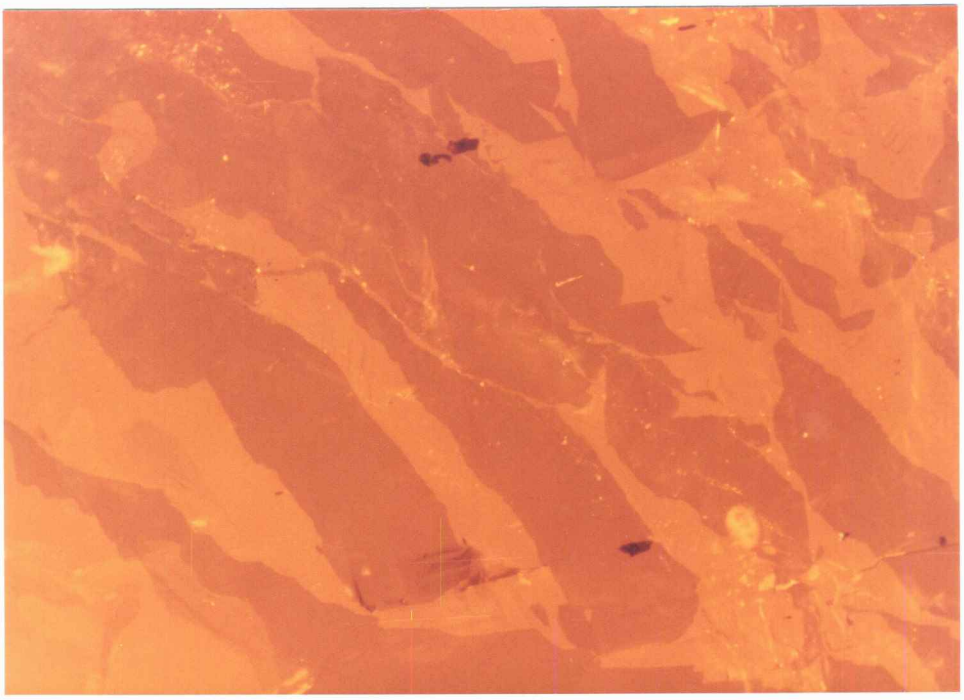

500 μm

Stratigraphic Up

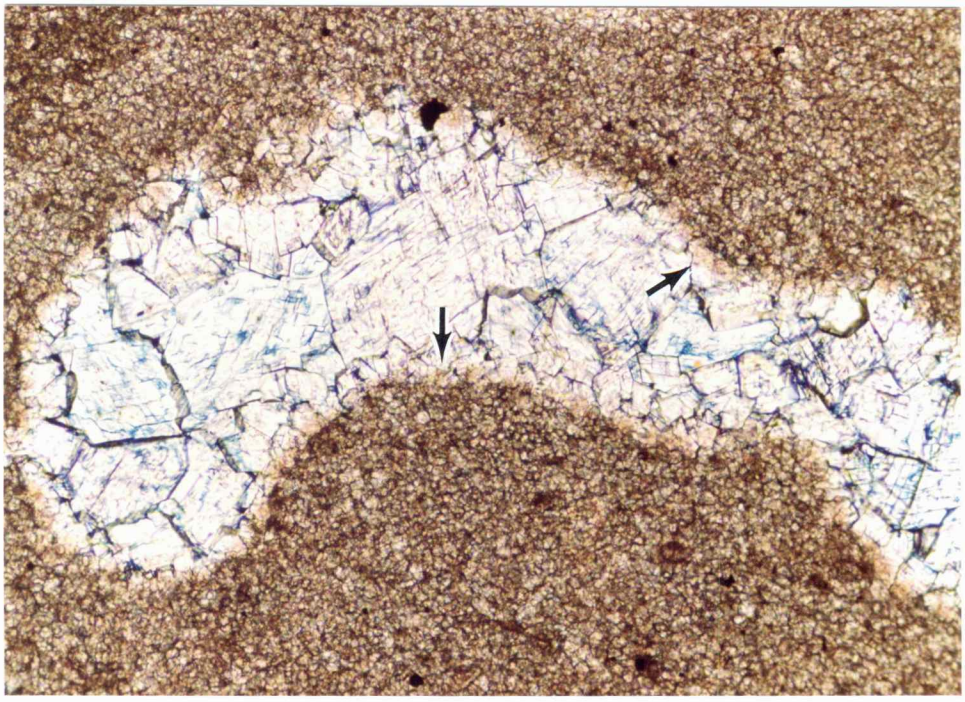

Figure 50. Unpolarized-light photomicrograph of cement M2 filling a root mold. (Thin section stained with Alizarin Red-S and potassium ferricyanide.) The carbonate mudstone matrix is completely dolomitized. A thin, isopachous rim of dolomite cement J5 lines the pore and appears as small, light brown rhombohedra (arrows). Baroque dolomite cement M2 overgrows cement J5 and completely fills the pore. The blue color is due to potassium ferricyanide staining, and indicates that cement M2 is ferroan, whereas the matrix and cement J5 exhibit no stains. (Cap subunit, upper carbonate unit, "J" zone; Shuck #1, 3744 feet.)

Open Fractures

A few fractures post-date cements M1 and M2 (Fig. 51). Like the earlier fractures, these fractures are generally vertical, but fracture widths are only .1 - .3 mm so the fractures can be considered only marginally open.

Cement M3

A generation of equant, quartz cement (M3) forms the final pore fill in a few pores, clearly post-dating the ferroan calcite cement M1 (Fig. 52). Crystals range in size from 20 to 575 micrometers.

Quartz Replacement

Quartz replacement of micrite matrix was observed in every well, although it is volumetrically insignificant. The quartz typically forms highly irregular blebs, but well developed hexagonal and hexagonal dipyramid aspects are present (Fig. 53). The blebs and crystals are generally very small, from 1 to 20 micrometers in size, but range up to 45 micrometers.

Quartz replacement occurs in the cap subunit, in micrite envelopes and intraclasts in the alpha grainstone subunit, and in both the alpha and beta micrite-rich subunits. These quartz blebs generally lack cross-cutting relationships, but they do bridge fractures that

Figure 51. Unpolarized-light photomicrograph of vertical fractures that post-date cement M1. (Thin section impregnated with blue epoxy and stained with Alizarin Red-S and potassium ferricyanide.) (The cement in the fracture exhibited a mauve coloration after staining, but this color has faded due to handling of the thin section.) (Cap subunit, upper carbonate unit, "J" zone; Shuck #1, 3744 feet.)

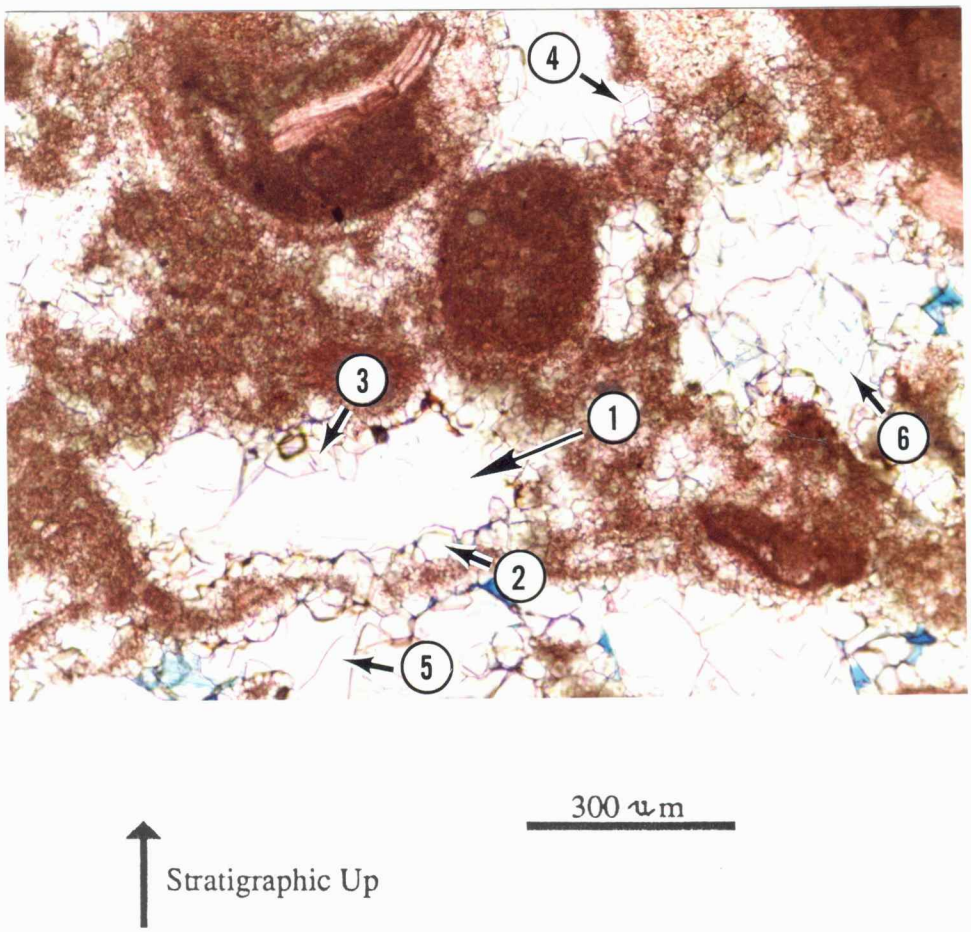

Figure 52. Unpolarized-light photomicrograph of quartz cement M3. (Thin section impregnated with blue epoxy and stained with Alizarin Red-S and potassium ferricyanide.) Arrow 1 points to a large quartz crystal that fills a pore lined with crystals of cement M1 (arrows 2 and 3). This photo shows several of the other cements present in the "J" zone: non-stained rhombohedra of dolomite cement J5 (arrow 4), light purple stained cement M1 (arrow 5), and light blue stained baroque dolomite cement M2 (arrow 6). (Staining colors are faded in this photo due to handling of the thin section.) (Beta grainstone-packstone subunit, upper carbonate unit, "J" zone; Bethell #3, 3752 feet.)

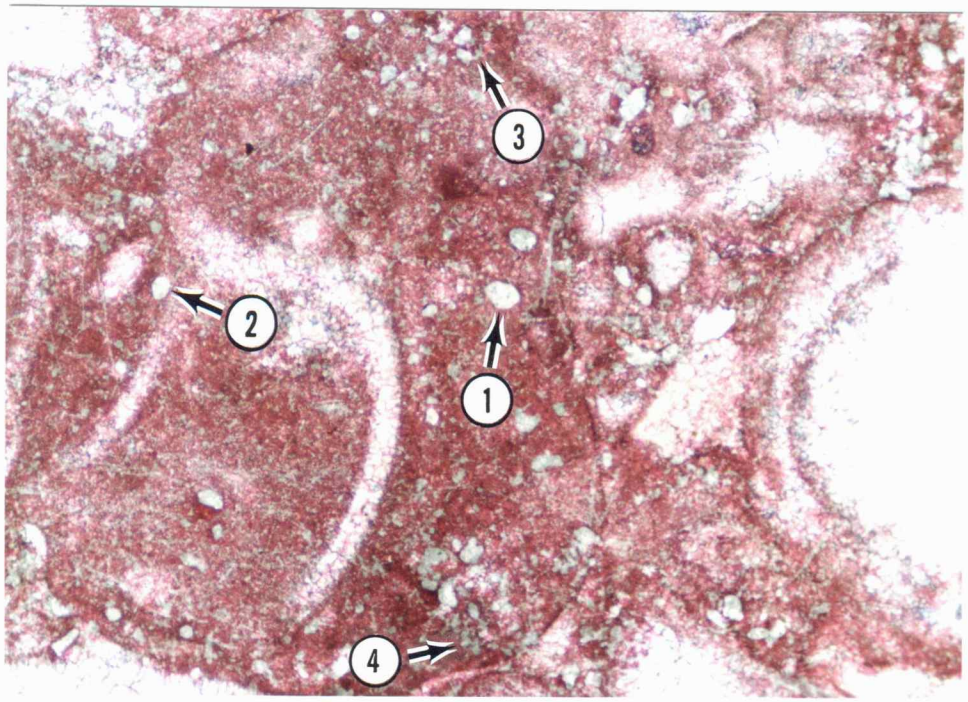

Figure 53. Plane polarized-light photomicrograph of replacement quartz. (Thin section stained with Alizarin Red-S and potassium ferricyanide.) This sample contains quartz with well-developed hexagonal aspects (arrows 1 and 2), as well as irregular bleb shapes (arrows 3 and 4). (Alpha grainstone subunit, upper carbonate unit, "J" zone; Bethell #3, 3746 feet.)

cross-cut cement M1 (Fig. 54).

Pyrite Replacement

Pyrite replacement is pervasive, although generally minor volumetrically. Well defined cubic, hexagonal, or octahedral crystal aspects are most common, and they typically cut across grain and cement boundaries (Fig. 55). The crystals range in size from 20 to 750 micrometers. Well-developed, euhedral pyrite crystals show irregular "tendrils" of replacement along the intercrystalline boundaries of ferroan calcite cement M1, indicating the pyrite replacement post-dates the cement (Fig. 56).

Solution Seams

Solution seams are ubiquitous in the "J" zone. They show a great variety of forms including: stylolites, microstylolites, microstylolite swarms, and clay seams. Grain to grain sutures are also present. The solution seams post-date the ferroan calcite cement M1, as indicated by cross-cutting relationships such as cement within sutures (Fig. 57). However, this indicates only the latest dissolution along the seams. No relationships were observed that indicate the onset of solution seam formation.

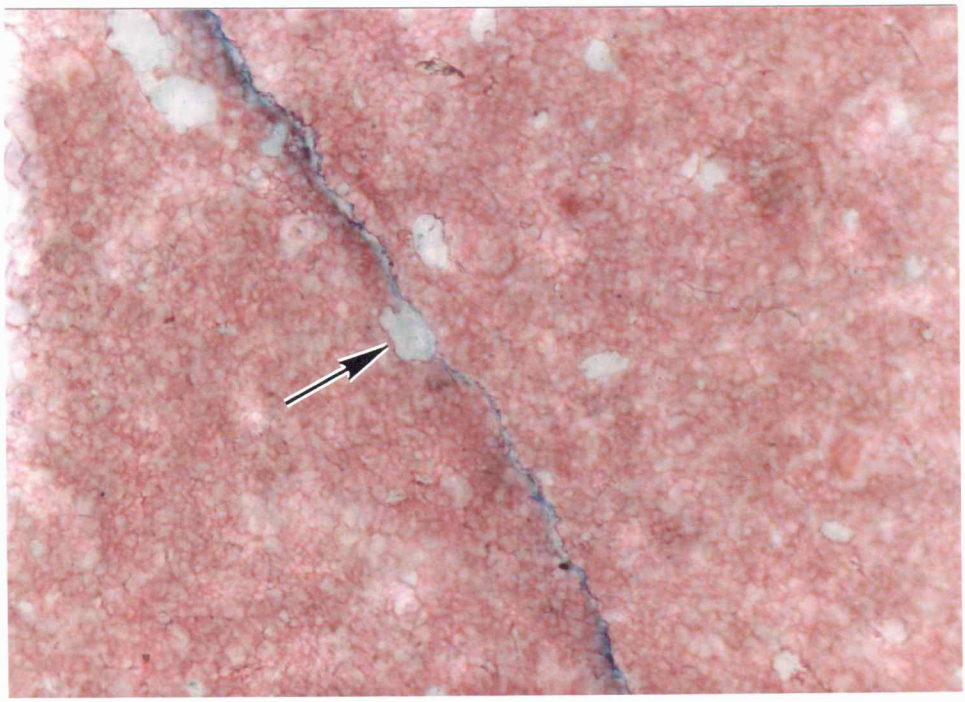

Figure 54. Unpolarized-light photomicrograph of quartz replacement blebs, one of which is bridging a fracture (arrow). (Thin section impregnated with blue epoxy and stained with Alizarin Red-S and potassium ferricyanide.) These fractures cross-cut cement M1. The blebs in this sample from the "I" zone are similar to those in the "J" zone, and are interpreted to have formed at the same time in both zones. (Carbonate unit, "I" zone; Demuth #4, 3805 feet.)

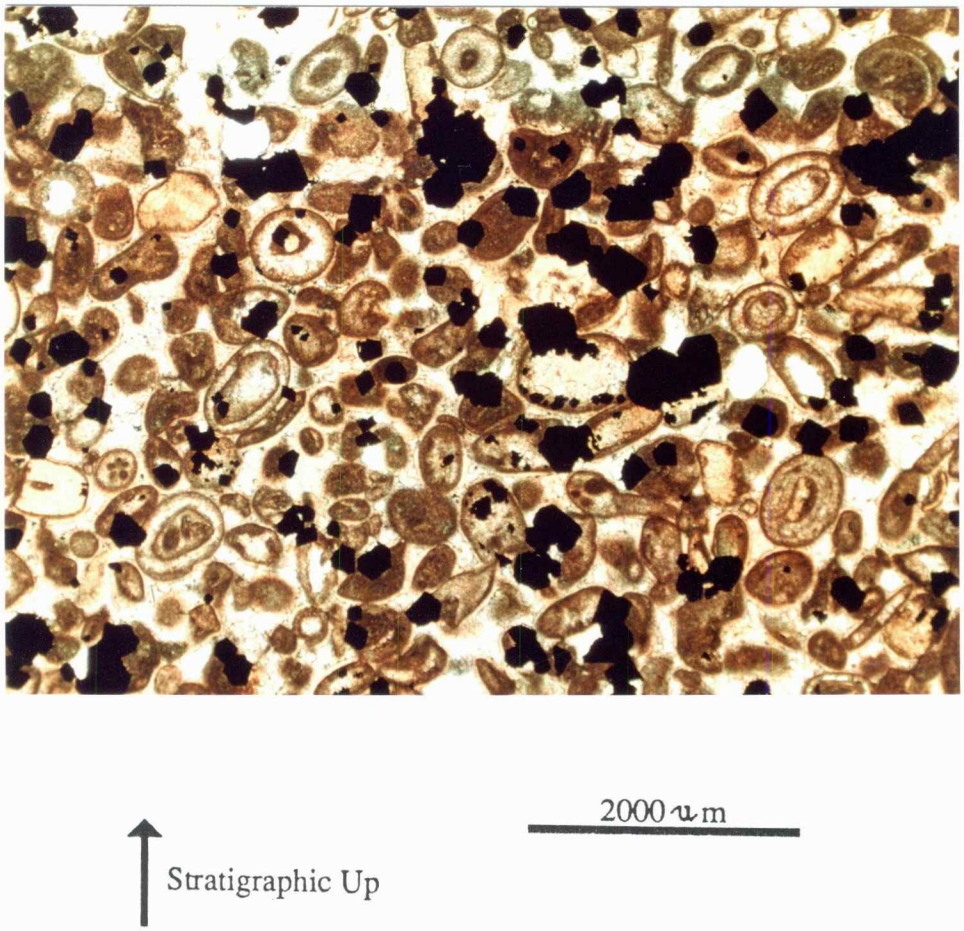

Figure 55. Unpolarized-light photomicrograph of pyrite replacement. (Thin section stained with Alizarin Red-S.) Well-defined cubic, hexagonal, and octahedral crystal aspects are most common. The replacement pyrite typically cuts across grain and cement boundaries. (Alpha grainstone subunit, upper carbonate unit, "J" zone; Rogers #1, 3802 feet.)

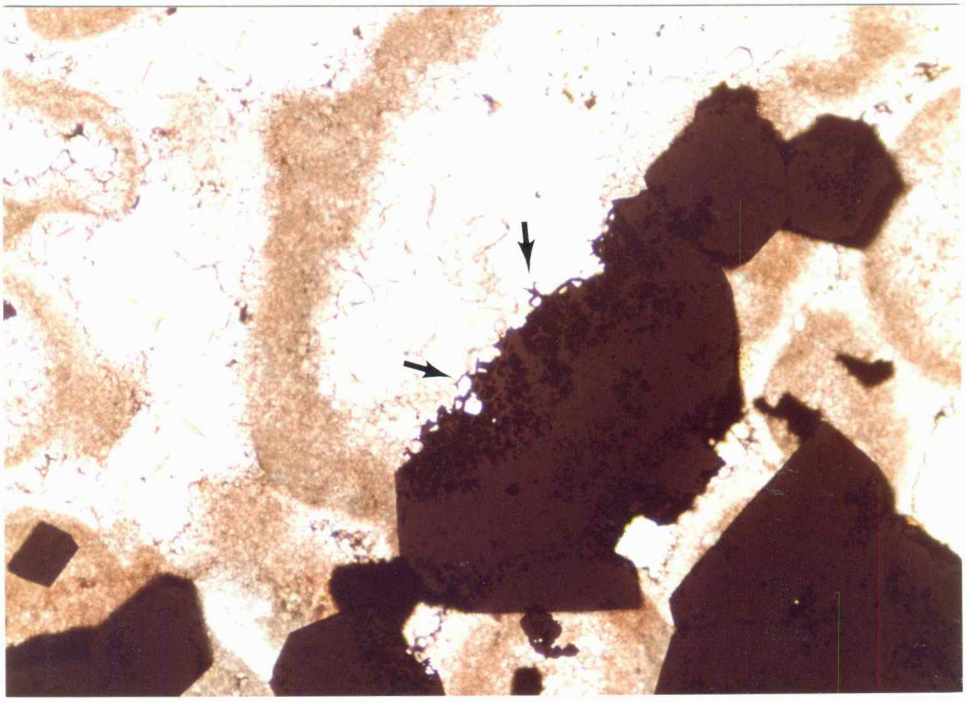

Figure 56. Unpolarized-light photomicrograph of pyrite replacement "tendrils". (Thin section stained with Alizarin Red-S.) Pyrite replacement clearly post-dates cement M1 because replacive tendrils are preferentially located along the intercrystalline boundaries of the cement (arrows). (Alpha grainstone subunit, upper carbonate unit, "J" zone; Rogers #1, 3802 feet.)

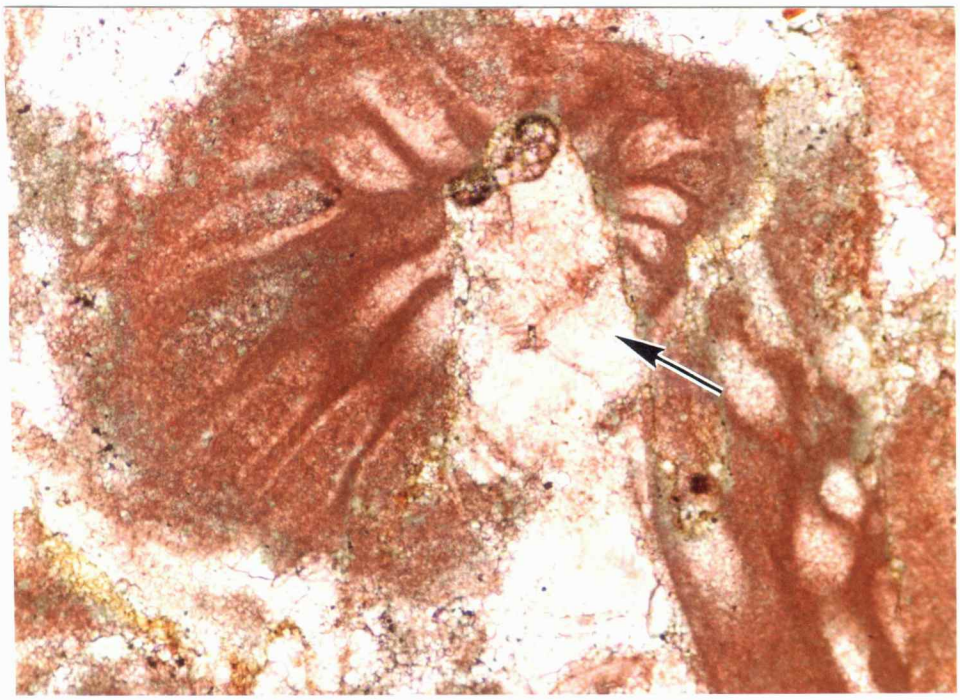

Figure 57. Unpolarized-light photomicrograph of cement M1 in a stylolite. (Thin section stained with Alizarin Red-S and potassium ferricyanide.) The cement within the stylolite suture (arrow) indicates that some amount of pressure solution post-dates precipitation of cement M1. (Beta grainstone-packstone subunit, upper carbonate unit, "J" zone; Rogers #1, 3804 feet.)

FLUID INCLUSION STUDY OF SELECTED CEMENTS IN THE "J" ZONE

Fluid inclusions in sedimentary rocks provide a direct, rather than inferred, record of diagenetic fluids. Primary fluid inclusions in cement minerals can actually preserve the original fluid from the time of cement precipitation. This fluid, and its physical conditions at the time of trapping, may provide an accurate method of determining the diagenetic environment of cementation.

Fluid Inclusion Petrography

Only cements J1, J3, and M1 contain abundant fluid inclusions. Two areas of cement M1 and one area of cement J3 containing fluid inclusions with good evidence of primary entrapment were chosen for study. In cement J1, the individual cement blades and the fluid inclusions themselves were too small to obtain accurate data.

Population A

Population A is from several crystals of cement J3 that contain abundant inclusions where the cement occludes a skeletal mold. The fluid inclusions are interpreted as primary because their occurrence is strongly related to crystal growth boundaries and growth zonations (Roedder, 1984). The crystals exhibit thin zones of inclusions that mimic the outer growth

boundaries (Fig. 58). For each crystal, the zones of inclusions occur within a single growth band as delineated by cathodoluminescence.

These fluid inclusions range up to 40 micrometers in size across the longest dimension, but most of the inclusions with acceptable optics are in the range of 3-15 micrometers. Shapes are generally simple polygons with angular to gently rounded outlines. Most of the inclusions consist of a single liquid phase, although a few exhibit a small vapor bubble.

Population B

Several inclusion-rich crystals of cement M1 occur where the cement fills a large shelter pore. These inclusions make up population B. The occurrence of the fluid inclusions is related to crystal growth orientation, indicating the inclusions are primary. These inclusions occur in a zone adjacent to the growth substrate for all crystals growing from the pore wall. Each crystal becomes progressively clearer toward the center of the pore as the number of inclusions sharply declines.

These crystals contain inclusions up to 100 micrometers in size, but the majority of inclusions with good optics range in size from 8-40 micrometers. Shapes range from simple polygons to complex figures with

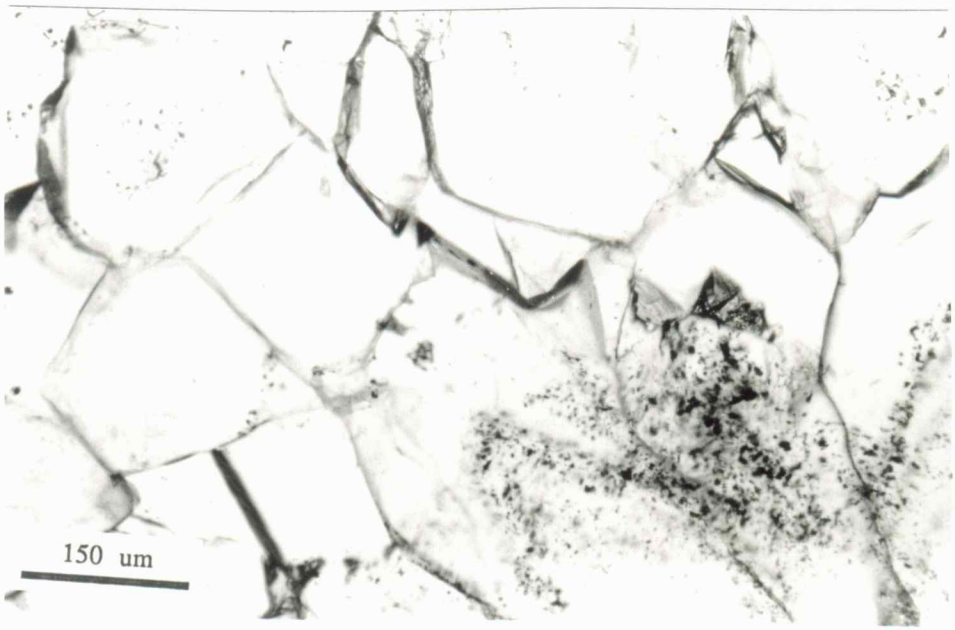

Figure 58. Plane polarized-light photomicrograph of primary fluid inclusions in cement J3 mimicking outlines of crystal terminations. (Lower carbonate unit, "J" zone; White #1, 3791 feet.)

broadly curving re-entrants of the host mineral into the inclusion and pinched embayments of the inclusion into the host. The inclusions exhibit variable vapor to liquid ratios. Many inclusions contain only a single liquid phase, but nearly half of the inclusions exhibit a small- to moderate-sized vapor bubble.

Population C

Two crystals of cement M1 contain a thin band of inclusions at the edge of the crystals where the cement fills a burrow. These inclusions make up population C. The bands of inclusions parallel the crystal terminations (Fig. 59). The inclusions are interpreted as primary on the basis of their occurrence relative to crystal growth orientation.

The crystals contain fluid inclusions up to 150 micrometers in size, but most with good optics range in size from 8-50 micrometers. Shapes range from simple to slightly more complex polygons. Many of the inclusions are slightly elongated, the longest dimension paralleling the nearest crystal boundary. The outlines of the inclusions range from angular to rounded. A few inclusions exhibit only a single liquid phase, but most show a small- to moderate-sized vapor bubble.

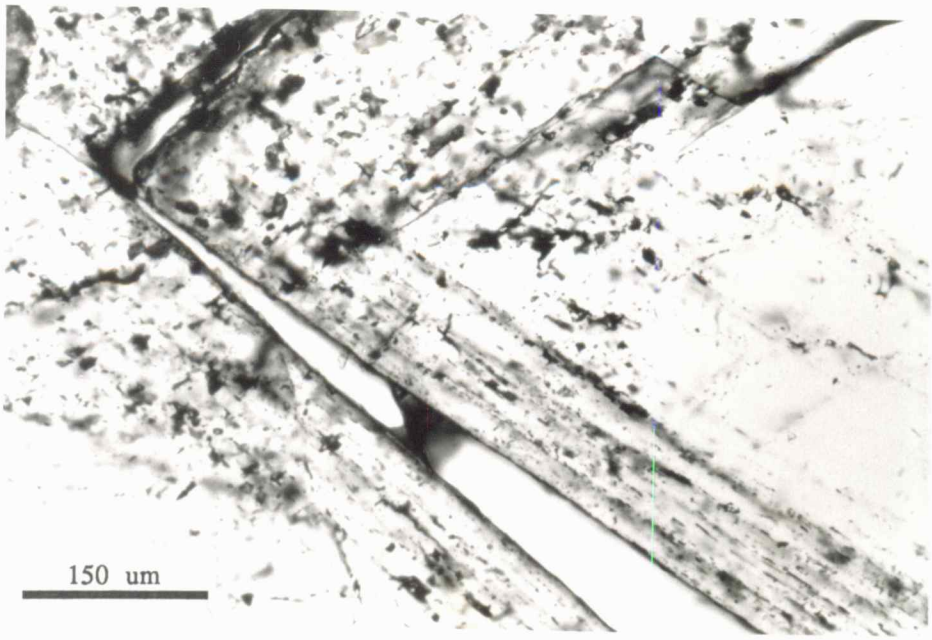

Figure 59. Plane polarized-light photomicrograph of primary fluid inclusions of cement M1 in thin growth zones adjacent to crystal terminations. (Alpha micrite-rich subunit, upper carbonate unit, "J" zone; Demuth #1, 3816 feet.)

Fluid Inclusion Microthermometry

Population A

One of the inclusions in population A that originally had a small vapor bubble homogenized at a temperature of 62.2° C. Freezing data were obtained on four inclusions. Final melting temperatures of ice range from -.5 to -1.8° C. A vapor bubble was present for all freezing runs. Sample preparation is described in Appendix 8. No eutectic melting event was observed. Microthermometric data are summarized in Table 1.

Population B

In population B, homogenization temperatures for four inclusions with vapor bubbles range from 58.6 to 89.4° C (Fig. 60). Final melting temperatures of ice range from -10.2 to -22.1° C with a vapor bubble present. Eutectic melting behavior was observed at approximately -52° C. Data are summarized in Table 1.

Population C

In population C, nine inclusions with vapor bubbles homogenized at temperatures ranging from 51.6 to 75.0° C (Fig. 60). Final melting temperatures of ice range from -12.7 to -23.7° C with a vapor bubble present. Eutectic melting occurred around -52° C (Table 1).

Pop.	Th	Tm-ice	Salinity (wt. %)	Te
A	1 phase	- 0.5	0.9	?
	1 phase	- 0.7	1.2	?
	1 phase	- 0.7	1.2	?
	1 phase	- 1.8	3.1	?
	62.2	--	--	--
B	1 phase	-11.8	15.9	-52
	1 phase	-13.0	17.0	-52
	58.6	--	--	--
	62.8	-10.2	14.2	-52
	74.6	-12.9	16.9	-52
	89.9	-22.1	24.1	-52
C	51.6	-12.7	16.7	-52
	51.6	-14.2	18.1	-52
	54.6	-13.0	17.0	-52
	59.5	-23.7	25.2	-52
	60.0	--	--	--
	67.0	--	--	--
	67.5	--	--	--
	69.0	-21.4	23.6	-52
	75.0	--	--	--

All temperatures in degrees centigrade.
Pop. - Population
Th - Homogenization temperature
Tm-ice - Final melting temperature of ice
Salinity (wt. %) - Salinity in weight percent NaCl equivalent (See Appendix 9)
Te - Eutectic melting temperature

Table 1. Microthermometry data.

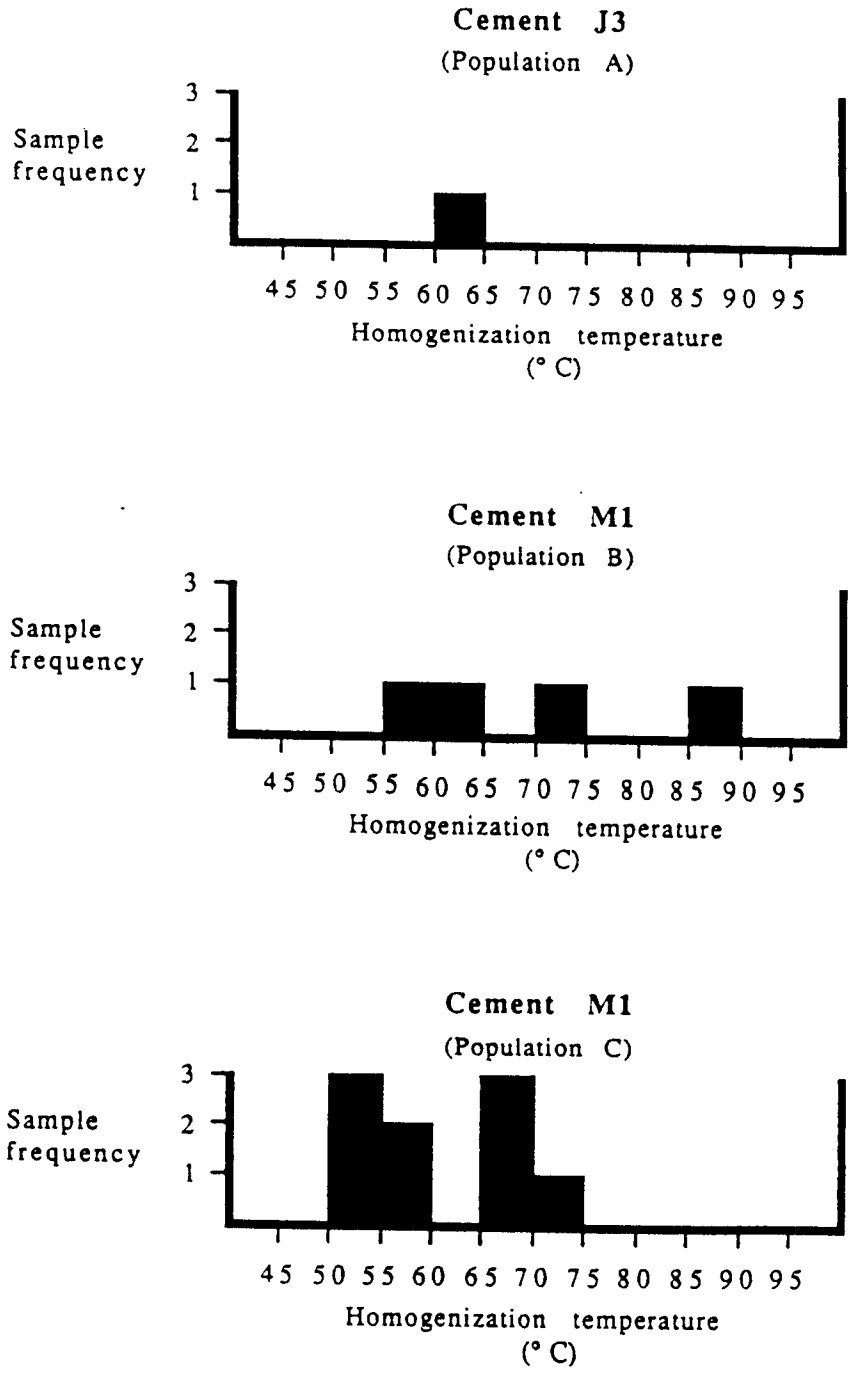

Figure 60. Frequency histograms of homogenization temperatures for selected fluid inclusions that originally had a vapor bubble.

Interpretation of Fluid Inclusion Data

Excellent evidence supporting a primary origin for the fluid inclusions of all three populations, combined with the lack of evidence for necking down in the inclusions selected for measurements, indicates the microthermometric data can be used to reliably interpret the temperature and type of fluid present during precipitation of these calcite cements. The only caveat is the possible re-equilibration of the fluid inclusions after trapping. Inclusions may have stretched after trapping which would elevate the homogenization temperature. Inclusions may also leak and exchange fluids with later fluids in the rock system. This would alter both the freezing data, which are dependent on the dissolved salts in the inclusion, and the homogenization temperature (Goldstein, 1986). Re-equilibration will be considered in the interpretation of the two cements.

Cement J3

Most of the fluid inclusions from cement J3 contain only a single liquid phase, although a few inclusions exhibit a vapor bubble. The final melting temperatures of ice exhibit a very narrow range. The number of inclusions with only a single liquid phase and the narrow range of final ice melting temperatures indicate that most of these inclusions have not re-equilibrated.

The preponderance of inclusions with a single liquid phase indicates that the cement formed at a temperature of less than about 40-50° C (Goldstein, 1990). One of the two-phase inclusions homogenized at 62.2° C, indicating a few of the inclusions in cement J3 re-equilibrated after original trapping.

Final melting temperatures of ice indicate the freezing point depression due to the ions in solution. Clynne and Potter (1977) showed that the freezing point depression of naturally occurring brines can be converted to salinity, expressed in terms of weight percent NaCl equivalent, with an error of 5% or less for low salinity solutions. Salinities for population A range from 0.9 to 3.1 weight percent NaCl equivalent (Table 1), (Appendix 9). These values are intermediate between fresh water (0.0 wt. %), and seawater (3.5 wt. %). The low temperatures of homogenization and the brackish salinities suggest that cement J3 precipitated in a "mixing zone" environment.

Cement M1

The B population in cement M1 consists of abundant inclusions containing only a single liquid phase. The C population exhibits a scarcity of one-phase inclusions. The C population is present at crystal terminations, so these inclusions were probably entrapped slightly later

than those in population B. This relative timing is necessarily speculative, because the two occurrences are not from a single crystal. However, the transition from abundant to scarce one-phase inclusions provides a useful bracket, and suggests that cement M1 precipitated at temperatures near the 40-50° C range, the maximum temperature for the preservation of one-phase inclusions.

A plot of final melting temperature of ice versus homogenization temperature reveals two distinct groupings of fluid salinity (Fig. 61). The fluid group marked I on the figure exhibits a relatively narrow range of salinities from 14.2 to 18.1 weight percent NaCl equivalent. The fluid group marked II appears to represent a separate family with much higher salinities, again with a narrow range from 23.6 to 25.2 weight percent.

The only geologically reasonable explanation for this distribution with two distinct salinity groups in individual growth zones, and a broad range of homogenization temperatures, is that many of the inclusions have re-equilibrated. Some inclusions have stretched, resulting in elevated homogenization temperatures. Other inclusions have leaked and exchanged fluid with a later pore fluid.

The predominance of fluid inclusions containing only a single liquid phase in the B population of cement M1

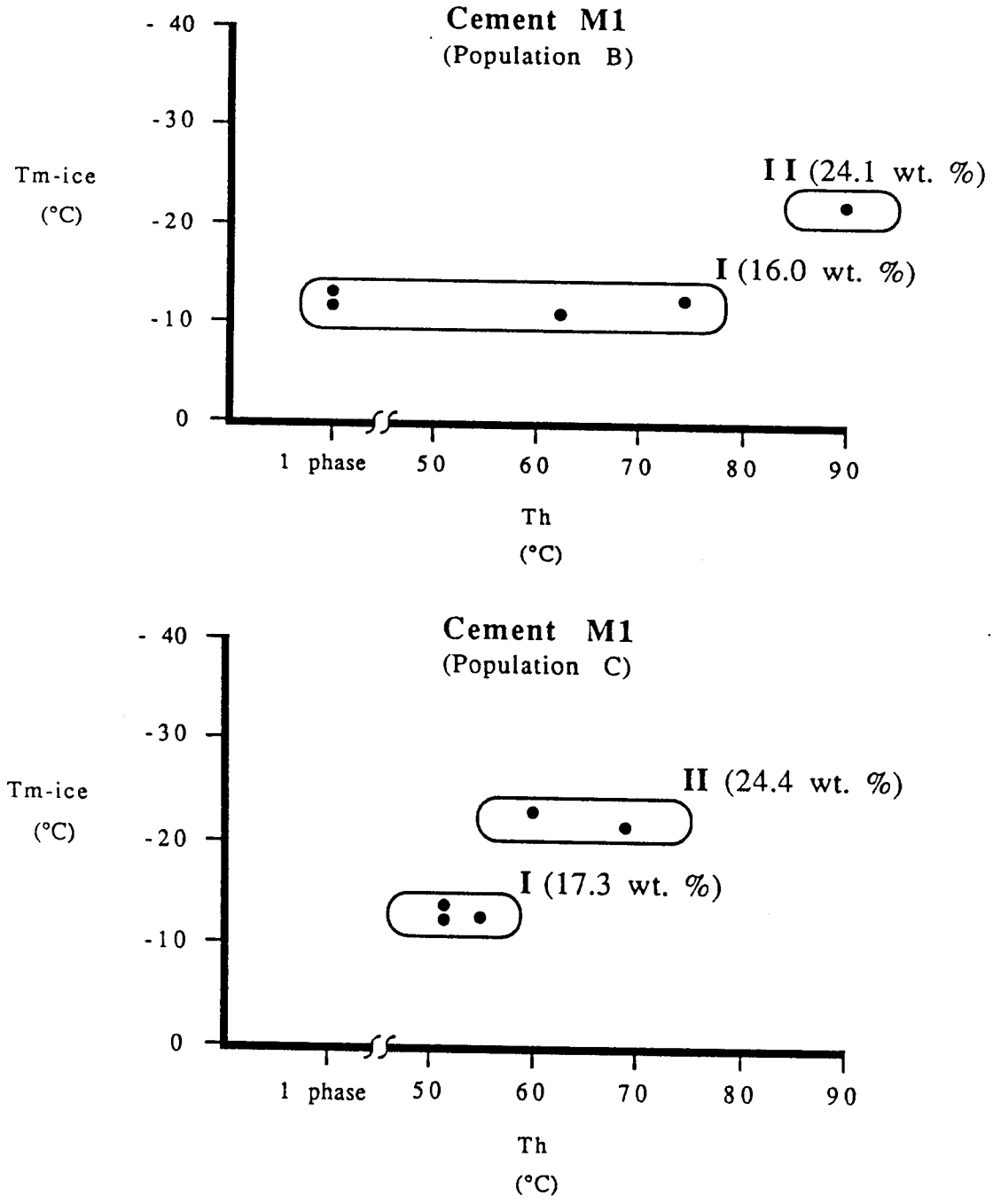

Figure 61. Plots of final melting temperature of ice (Tm-ice) versus homogenization temperature (Th), for the two populations from cement M1. Numbers in parentheses represent average salinity in NaCl equivalent for the indicated group. The narrow range of salinities for each fluid group probably indicates two distinct fluids. Eutectic melting at -52° C observed for all inclusions.

indicates this cement began to precipitate at a temperature of less than about 40-50° C. The preponderance of two-phase inclusions in the C population of cement M1 suggests this portion of the cement generation precipitated at a temperature above 40-50° C. The peak at 50-55° C probably represents the temperature of entrapment for population C (uncorrected for pressure). The rare all-liquid inclusions in this population may have also been trapped at this temperature and failed to nucleate a bubble, or may have necked down.

Examination of Figure 61 reveals that no inclusions with group II salinities are one-phase inclusions or homogenized at temperatures in the range of 40 to 55° C. Therefore it would appear that group II salinities occur only in inclusions that have re-equilibrated, since they homogenize at temperatures above those of original entrapment for either population of cement M1. Consequently, cement M1 must have precipitated from a fluid with salinity of approximately 16.5 weight percent NaCl equivalent, over slightly increasing temperatures. Cement precipitation began at less than 40 to 50° C, and continued to at least 50 to 55° C. The temperatures and salinities reflected in the fluid inclusion data indicate cement M1 is a burial cement.

After cementation, the pore fluid became much more saline, to approximately 24.3 weight percent NaCl

equivalent. A number of inclusions in both populations of cement M1 have re-equilibrated. Many re-equilibrated by fluid exchange with this later, more saline pore fluid, and show group II salinities and homogenization temperatures of greater the 55° C. Other fluid inclusions re-equilibrated by stretching, and exhibit group I salinities, but elevated homogenization temperatures of greater than 55° C.

Eutectic melting occurred at -52° C for both fluid I and II. This indicates that Na^{+}, Ca^{++}, and Cl^{-}, were the major species of ions in both fluids (Crawford, 1981).

INTERPRETATION OF THE DIAGENETIC ENVIRONMENTS OF THE "J" ZONE

This discussion is divided into pre-burial and post-burial features because the regionally extensive "J" upper shale which marks the onset of burial apparently sealed the "J" zone carbonates from near-surface diagenetic environments. Consequently, burial marks a significant transition in the types of paragenetic features in the "J" zone.

Pre-burial Features

The diagenetic environment that resulted in the altered zone at the top of the upper carbonate unit was by far the most significant in terms of diversity of paragenetic features in the "J" zone. These related features provide the best means of determining relative timing for the pre-burial features. For these reasons, the environment of the alteration and related features is discussed first; the other paragenetic features are then discussed within this framework.

Alteration Features, Root Molds, and Rhizocretions

The alteration features and root structures indicate the altered zone at the top of the upper carbonate unit is the result of subaerial exposure. Root molds and rhizocretions are reliable indicators of subaerial exposure because marine plant root structures are rarely

preserved (Esteban and Klappa, 1983).

The subvertical, cylindrical "pipes" resemble modern-day taproots (Fig. 31). The pipes could be a microkarst feature, but the association with root molds, the nearly circular aspects of the pipes, and the depth of penetration support the taproot interpretation.

The tabular "fissures" could have formed by several possible processes such as jointing, wetting and drying, root penetration, or microkarsting. The presence of sediment and root structures in the fissures indicates the fissures are a pre-burial feature, and not formed by tectonic jointing. There are no diagenetic indicators to differentiate between the other processes, but circumgranular cracks in the fissure-fill indicate wetting and drying, and the root molds indicate root penetration into the fissures. Both of these processes may have been responsible for the initial opening of the fissures, and their subsequent enlargement. However, the unfitted fissure edges indicate dissolution was certainly an important factor in fissure formation (Fig. 23). The fissures are therefore interpreted as a microkarst feature, even though other processes may have contributed to fissure development.

Autoclastic brecciation (Fig. 29) may be caused by a variety of processes such as wetting and drying, root penetration, dissolution, or even compaction. The "J"

zone brecciation is probably to some degree a result of all of these processes; the root molds and rhizocretions indicate root penetration, the circumgranular cracks indicate wetting and drying, and the rounded clasts suggest dissolution.

Autoclastic brecciation is a common product of subaerial exposure, but its occurrence is not restricted to exposure surfaces. However, the association of autoclastic breccias, root molds and rhizocretions, microkarst features, and circumgranular cracks confirm that the altered zone and the related paragenetic features formed in response to subaerial exposure.

Cement J2

Cement J2 typically occurs in alteration pores, and is rarely present in interparticle pores in the alpha grainstone subunit. The cement post-dates the onset of exposure because it occurs in alteration pores, but the patchy, point-contact distribution and curved meniscus boundaries (Fig. 32) indicate this cement formed in the vadose zone. This vadose zone probably occurred in a meteoric environment during subaerial exposure because cement J2 is closely associated with alteration features.

Skeletal Molds, Oomolds, and Vugs

Except for cement J2, the sequence of cements in the

skeletal molds, oomolds, and vugs matches that in the root molds and alteration pores, suggesting all of these pore types are penecontemporaneous. In fact, several of the infilling cement generations are interpreted to have formed during subaerial exposure (discussed below). Therefore the majority of the skeletal molds, oomolds, and vugs formed during the period of subaerial exposure, as did the alteration pores and root molds. The allochem molds and vugs probably formed as a result of contact with undersaturated meteoric water.

Cement J3

Cement J3 only occurs in the skeletal molds and interparticle pores of the lower carbonate unit. The bladed crystals and rimming to pore-filling distribution of the cement suggest it formed in phreatic conditions. The brackish salinities and low temperatures of formation exhibited by the fluid inclusions indicate this cement formed in a mixing zone environment. The formation of cement J3 is therefore related to an exposure event because mixing zones require an exposure surface for meteoric water influx.

The time of formation of this cement cannot be determined relative to the other J-cements because there are no cross-cutting relationships. However, cement J3 post-dates mold formation and pre-dates chalcedony

replacement (discussed below) and compaction. These relationships indicate cement J3 formed during the subaerial exposure event that occurred at the top of the "J" upper carbonate unit, because chalcedony replacement is interpreted to have formed during this period of exposure.

Cement J4

The lack of distinct crystals and the continuous luminescence bands of cement J4 (Fig. 30) are not features ascribed to the cements commonly forming in any of the typical diagenetic environments (Longman, 1980; Heckel, 1983). A specific interpretation for cement J4 is therefore difficult. However, the intimate association of bands of cement J4 with continuous bands of dolomite, suggests cement J4 probably formed in the same environment as the dolomite cement (J5), or a closely related environment.

Cement J5

The pore rimming distribution and distinct luminescence zonations of the dolomite rhombohedra of cement J5 indicate they represent a true primary dolomite cement (Fig. 40; 41). The dolomite cement post-dates the alteration pores as well as the skeletal molds and oomolds, indicating the dolomite formed after the onset

of subaerial exposure. Cement J5 pre-dates compaction, and clearly pre-dates burial by the upper shale unit because the cement is in places covered with clay and quartz silt (Fig. 24; 25). The dolomite cement therefore formed in a near-surface diagenetic environment, following the onset of subaerial exposure. A mixing zone is the only environment that meets these requirements and is capable of producing significant amounts of dolomite (Badiozamani, 1973; Land, 1973), although there is no direct evidence cement J5 formed in a mixing zone. However, an exposed body of grainstone with excellent permeability, as existed in the Pen Field, would provide ideal conditions for the development of a mixing zone. The differing distributions of cements J3 and J5 indicate either two unrelated mixing zones, or a mixing zone with a great change in water chemistry from the top to the bottom of the zone.

Dolomite Replacement

No relative timing was determined for the dolomite replacement of micrite. However, the vertical distribution of replacement dolomite in the "J" zone roughly corresponds to the distribution of dolomite cement J5. The luminescence patterns are also similar (Fig. 40), therefore the two forms of dolomite are probably from the same environment.

Chalcedony Cement (J6) and Chalcedony Replacement

The simplest interpretation for chalcedony cement J6 and chalcedony replacement is that they formed during the same diagenetic event. The factors controlling precipitation of chalcedony are not well understood, but the presence of hematite inclusions (Fig. 44) indicates oxidizing conditions, with ferric iron in the precipitating water. Eh values high enough for ferric iron are usually indicative of near-surface water (Harris, et al., 1985), therefore the chalcedony probably formed in the meteoric environment. The fact that the chalcedony phases occur only in the "J" zone supports the interpretation that it formed in a near-surface diagenetic environment because all of the multi-zone cements (M-prefix) formed in a burial environment (discussed below). It was not possible to determine if the chalcedony precipitated in the vadose or phreatic zone since it occurred as either a pore-filling cement, or as a replacive phase. Chalcedony replacement is the only pre-burial paragenetic feature that occurs in both the "J" upper and lower carbonate units. The replacement in cement J3 is the only means of showing that cement J3 pre-dates burial (Fig. 45).

Carbonate Sediment Infilling

The evidence that carbonate sediment infilling may

both pre-date and post-date a given cement generation indicates the infilling was episodic, rather than a single discrete event. The presence of allochems similar to those in the alpha grainstone subunit suggests the infilling carbonate sediment is probably the result of local re-working of the upper carbonate unit during subaerial exposure.

Cement J1

Cement J1 occurs only in the interparticle pores of the alpha grainstone. The alteration pores, skeletal molds, and oomolds in the "J" zone presumably formed relatively early during subaerial exposure because they pre-date the majority of the other exposure features. However, no occurrence of cement J1 was observed in the extensive network of alteration pores in the cap subunit, and the formation of cement J1 clearly pre-dates the abundant skeletal molds and oomolds in the alpha grainstone subunit. This evidence suggests cement J1 pre-dates subaerial exposure.

The bladed, generally isopachous rims of cement J1 (Fig. 26) are typical of the marine phreatic environment, but are not an exclusive indicator (Longman, 1980). The distribution of cement J1 exclusively within the alpha grainstone subunit is suggestive, because marine cements are typically localized, and commonly form in carbonate

sands (Longman, 1980). Based on the morphology and distribution of the cement, and the fact that it appears to pre-date subaerial exposure, cement J1 is interpreted as a marine phreatic cement that was penecontemporaneous with deposition of the alpha grainstone.

Post-burial Features

Shale Infilling

The infilling of clay and quartz silt generally matches the silty shale of the overlying upper shale unit (Fig. 23). Infilling is associated with the alteration features in the upper carbonate unit, but no clear examples were observed of alteration features post-dating shale infilling. Consequently, shale infilling is interpreted to mark the onset of deposition of the upper shale unit. There is no direct evidence to indicate if the infilling was subaerial or subaqueous, but the infilling environment must have matched the depositional environment of the "J" upper shale unit (discussed previously).

Cement J7

Cement J7 is a burial cement because it post-dates deposition of the upper shale unit. However, even though this cement formed in the "burial" environment, it must

have formed at a relatively shallow depth because it predates compaction (Fig. 47). It is not possible to determine the exact nature of the fluids in this shallow burial environment because no fluid inclusions from cement J7 were analyzed. However, staining indicates the cement is nonferroan. At least trace amounts of iron are present in most burial environments, but carbonate cements tend only to incorporate iron when it is present in the ferrous state (Evamy, 1969). Consequently, cement J7 probably precipitated from a relatively well oxygenated fluid with iron in the ferric state.

Cement M1

Cement M1 is moderately to highly ferroan, and may exist as large poikilotopic crystals (Fig. 48). Scholle and Halley (1985) cite these two features as typical of burial cements, though not definitive indicators. This cement occurs in both the "I" and "J" zones, indicating it formed during a period when the two zones were subject to the same conditions, which would be unlikely in a near-surface diagenetic environment. The temperature and salinity of precipitation derived from the fluid inclusion data complement the petrographic observations, and confirm that cement M1 formed in a burial environment. Cement M1 probably precipitated from a brine with salinity of approximately 16.5 weight percent

NaCl equivalent. Precipitation began at temperatures of less than 40-50° C and continued at least to 50-55° C.

Cement M2

Cement M2 consists of highly ferroan, baroque dolomite, which is typical of the burial environment, though not unique (Scholle and Halley; 1985). However, the cross-cutting relationship with cement M1 confirms that cement M2 must have also formed in a burial environment.

Quartz Cement (M3) and Quartz Replacement

Quartz cement (M3) and quartz replacement do not exhibit any features diagnostic of the burial environment, but quartz cement M3 must have precipitated in the burial environment because it post-dates burial cements M1 and M2 (Fig. 52). Likewise, quartz replacement must have formed in the burial environment because it bridges fractures that cut cement M1 (Fig. 54).

Pyrite Replacement

Pyrite replacement indicates reducing conditions, but this alone is not diagnostic of any particular environment. However, pyrite replacement clearly post-dates cement M1 (Fig. 56), and therefore must have occurred in the burial environment.

Conclusions

The "J" zone exhibits a great variety of paragenetic features from several different diagenetic environments. Severe alteration of the top of the upper carbonate unit occurred during subaerial exposure. Most of the secondary porosity in the "J" zone formed during this exposure event, as well as most of the generations of cement. Cement J1 is abundant in the alpha grainstone subunit, and apparently formed in a marine, phreatic environment prior to exposure. After burial, subsidence of the depositional basin and an evolving pore water chemistry led to four distinct burial cements, as well as replacive mineralization.

GEOLOGY OF THE LANSING-KANSAS CITY "I" ZONE IN THE PEN FIELD

LITHOLOGY OF THE "I" ZONE

The "I" zone is a relatively thin cyclothem in the Pen Field area, ranging in thickness from only 8 to 13.5 feet (2.4 - 4.1 m) (Fig. 62). It does not exhibit the four units of the ideal cyclothem (Fig. 3), instead consisting only of a carbonate unit overlain by a shale unit (Fig. 12).

Carbonate Unit

The thickness of the carbonate unit ranges from 2.5 to 8 feet (.8 - 2.4 m) (Fig. 63). The unit ranges in color from cream or light gray to medium brown, but the bulk is light brown in color. Facies development is highly irregular and even adjacent wells show differing vertical sequences of lithologies.

The basal portion of the unit alternately consists of carbonate grainstone, intermixed grainstone and packstone, packstone, intermixed wackestone and packstone, wackestone, or carbonate mudstone, the grainstone lithology being the most common. The various lithologic units generally range from 0.5 to 3 feet (.2 - .9 m) in thickness. Some of the wells lacking a basal grainstone exhibit a grainstone lithology higher within the carbonate unit, but grainstone is completely

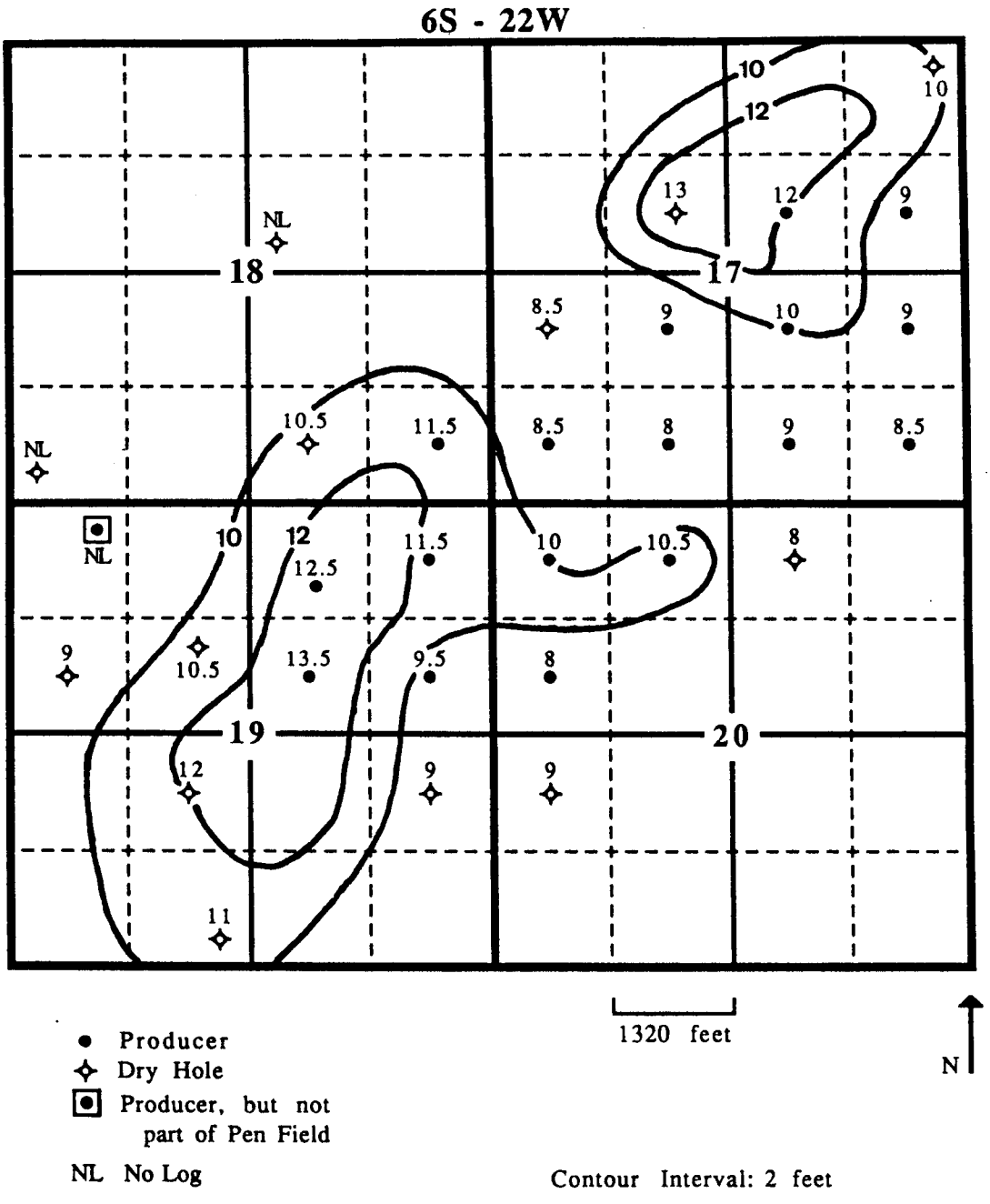

Figure 62. Isopach map of the entire "I" zone interval.

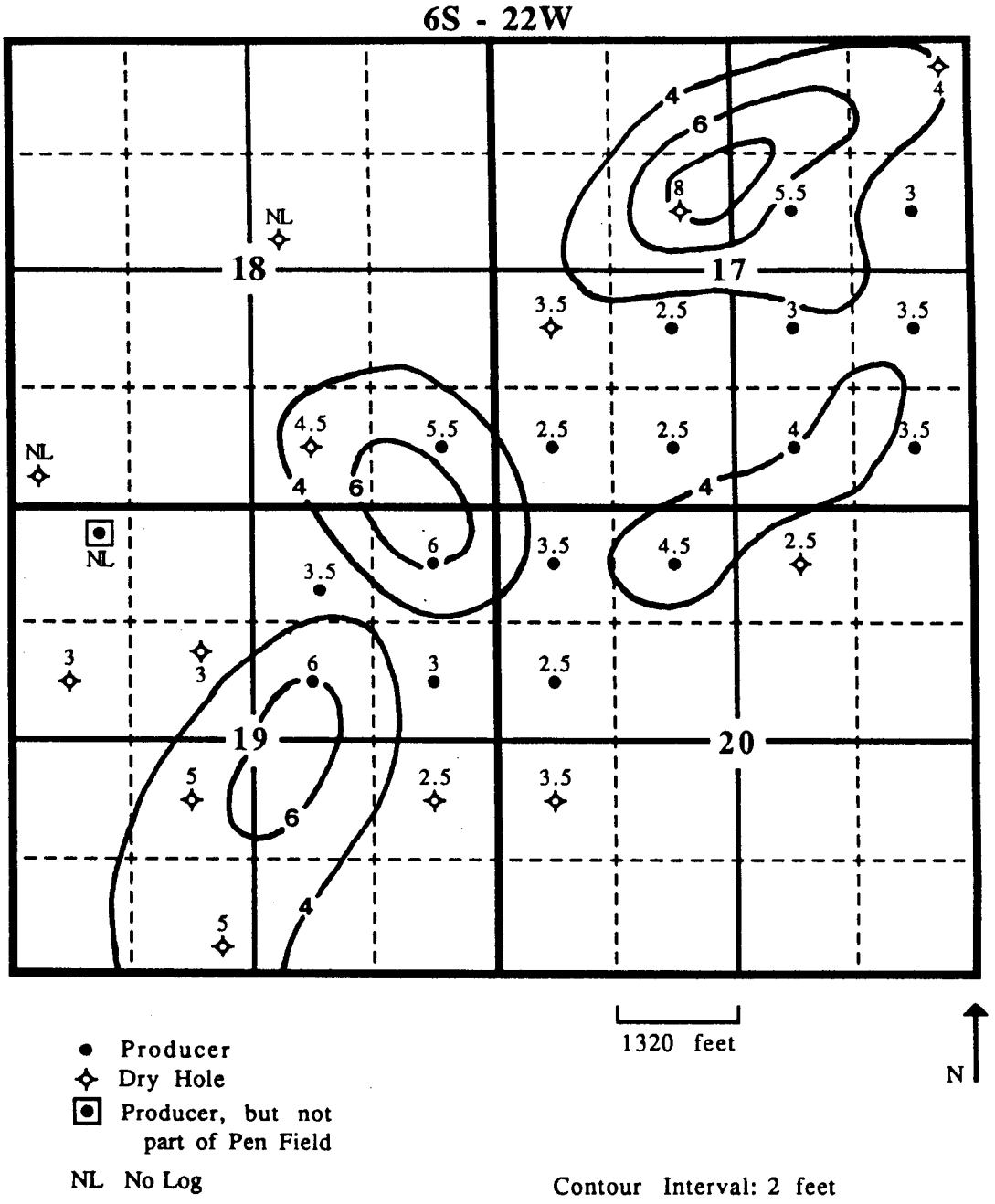

Figure 63. Isopach map of the carbonate unit of the "I" zone.

absent in three cored wells, the Bethell #5, Rogers #2, and White #5. Where present, the grainstones range in thickness from 0.5 to 3 feet (.2 - .9 m). The uppermost portion of the carbonate unit is exclusively composed of muddy lithologies. These are typically carbonate mudstones or wackestones, but intermixed wackestone and packstone occurs in three wells, the Bethell #3, Shuck #4, and White #1.

Peloids, articulate brachiopods, bivalves, fusilinids, echinoderm fragments, and intraclasts are the most common allochems in the carbonate unit. Osagia-coated grains are also common in the packstones and grainstones of some wells. A few ostracodes, dasycladacean algae, phyloid algae, and gastropods are present throughout the unit.

Allochems in the grainstone do show some variability from well to well, most notably, the presence or absence of Osagia-coated grains. The presence of coated grains does not relate to the stratigraphic position of the grainstone; these grains are present in some of the basal grainstones and in some of the grainstones that occur higher in the carbonate unit. It is not possible to determine if the grainstones represent a single genetically-related deposit, or if several unrelated grainstone bodies developed locally.

Shale Unit

The thickness of the shale unit generally ranges from 5 to 7.5 feet (1.5 - 2.3 m), although it reaches a thickness of 9 feet (2.7 m) in one well, the Demuth #2 (Fig. 64). The contact between the shale unit and the underlying carbonate unit is not a typical sedimentary contact. The top of the carbonate unit exhibits pervasive autoclastic brecciation and sediment from the overlying shale unit has partially to completely filled most of the breccia pores, resulting in a highly irregular contact surface.

The shale unit exhibits a fairly regular vertical sequence of facies, although the full sequence is not present in every well. The lowermost portion typically consists of 2 to 4 inches (5.1 - 10.2 cm) of medium green, silty shale. In two wells this shale exhibits shiny, slightly undulatory slickensides that penetrate the entire width of the core.

An interval of red silty shale overlies the green shale, or forms the basal facies where the green shale is absent. The contact with the green shale is typically color mottled. In one well that lacks green shale (the Bethell #5), the lowermost 7 inches (18 cm) of the red shale consists of a polymict conglomerate (Fig. 65). The matrix-supported conglomerate contains angular to rounded carbonate clasts up to 3 cm long in a matrix of red silty

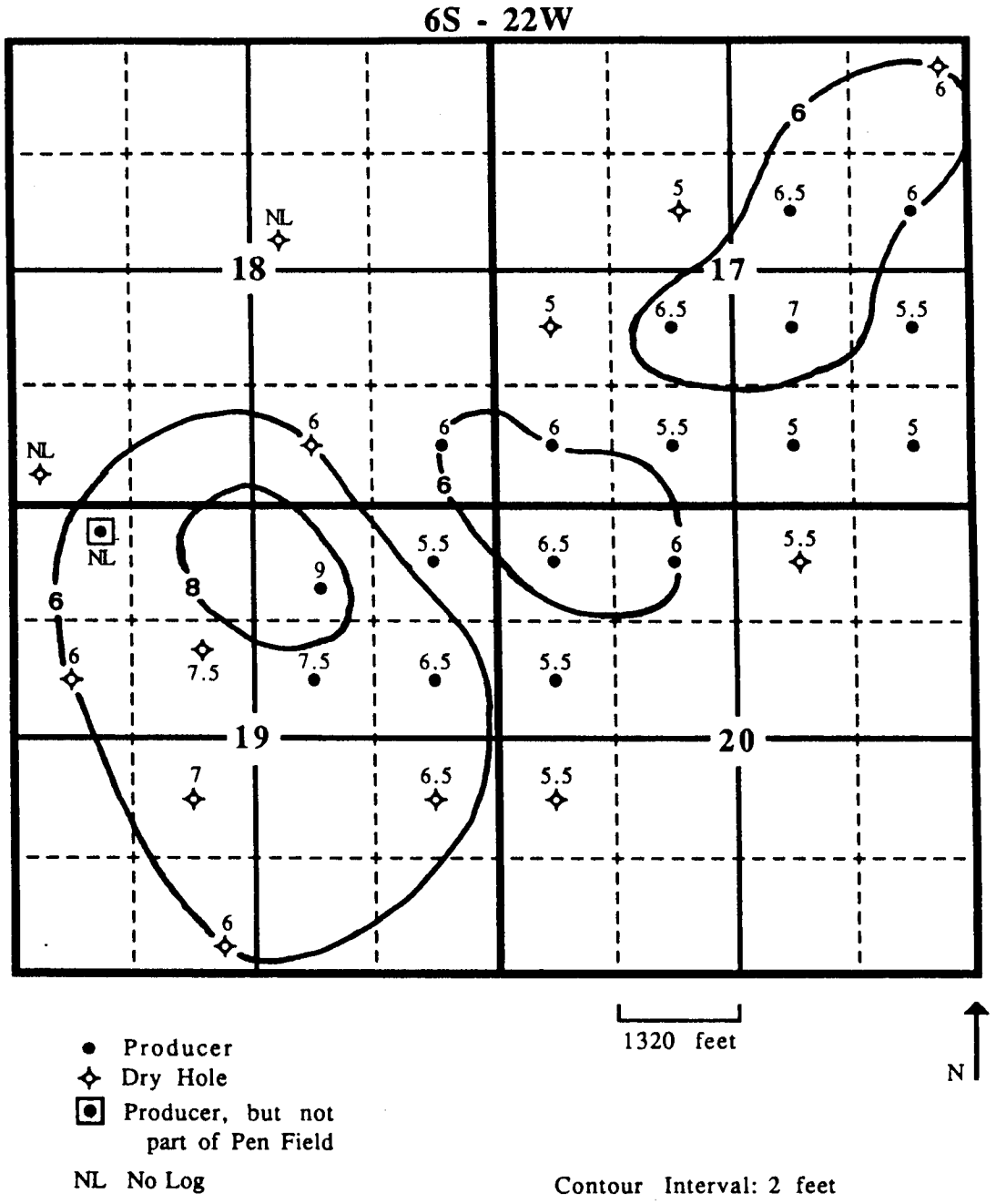

Figure 64. Isopach map of the shale unit of the "I" zone.

Figure 65. Core photo of a polymict conglomerate at the base of the shale unit. (Shale unit, "I" zone; Bethell #5, 3751 feet.)

shale. The light brown to dark gray clasts exhibit a range of carbonate textures.

The red shale is 22 to 45 inches (56 - 114 cm) thick, and also may exhibit shiny slickensides that penetrate the entire width of the core. The red shale interval contains scattered clasts composed of black carbonate with polished, concave facets, similar to those in the "J" zone upper shale unit. These clasts range in size from .5 to 4 mm.

Dark silty shale 20 to 35 inches (51 - 89 cm) thick overlies the red silty shale. Most of the dark shale is medium gray, but intervals of black or medium green silty shale also occur. Black, polished, carbonate clasts up to 1 cm long are present throughout the interval. Only rarely does this dark shale exhibit slickensides. It does contain a few carbonized plant fragments.

INTERPRETATION OF THE DEPOSITIONAL ENVIRONMENTS OF THE "I" ZONE

The carbonate unit contains diverse fossils with many stenohaline fauna and some green alga, indicating deposition in a relatively shallow, open marine environment. It is difficult to determine the specific environment because distinctive sedimentary structures were not observed, and without cores outside of the Pen Field it is not possible to evaluate the areal distribution of the facies. However, it is clear a subaerial exposure surface occurs at the top of the carbonate unit. The exposure features will be described in the paragenesis section.

The shale unit consists of a regular sequence of different colored shales. The basal transition from green shale to red shale indicates a change in oxidation conditions, but it was not possible to determine if the shale colors reflect depositional or diagenetic conditions.

If the sequence of different colored shales is depositional, the shale unit may be an amalgamation of several separate shale deposits that could have formed under greatly different conditions. However, without distinctive fossils, sedimentary structures, or comprehensive regional study, it is not possible to interpret the specific depositional environments of the shale unit.

The "I" zone represents a deviation from the ideal cyclothem because it contains only a carbonate unit and a shale unit. This deviation is a problem for regional study, but is probably due to the proximity of the Pen Field to the northern limit of the areal distribution of the "I" zone carbonate unit (Watney, personal communication, 1989).

PARAGENESIS OF THE "I" CARBONATE UNIT

The "I" zone carbonate unit exhibits seven generations of cement, several replacive minerals, and a distinct alteration zone (Fig. 66). Pervasive shale infilling provides the best means of determining relative timing of the paragenetic features in the carbonate unit. This infilling of clay and silt probably marks the onset of deposition of the shale unit, which eventually resulted in burial of the carbonate unit. Consequently, this section is subdivided into pre-burial and post-burial features.

Pre-burial Features

These features pre-date deposition of the "I" shale unit, and also pre-date compaction. Most features are described individually, but the descriptions are grouped for features that typically from in close association.

Alteration Features

Autoclastic brecciation is the most common alteration feature and occurs in every cored well. The brecciation is best developed at the top of the carbonate unit, but the entire unit is brecciated in two wells.

Fissures are also well developed in the carbonate unit (Fig. 67). Some wells even show delicate, segmented "pillars" formed by major vertical fissures and minor

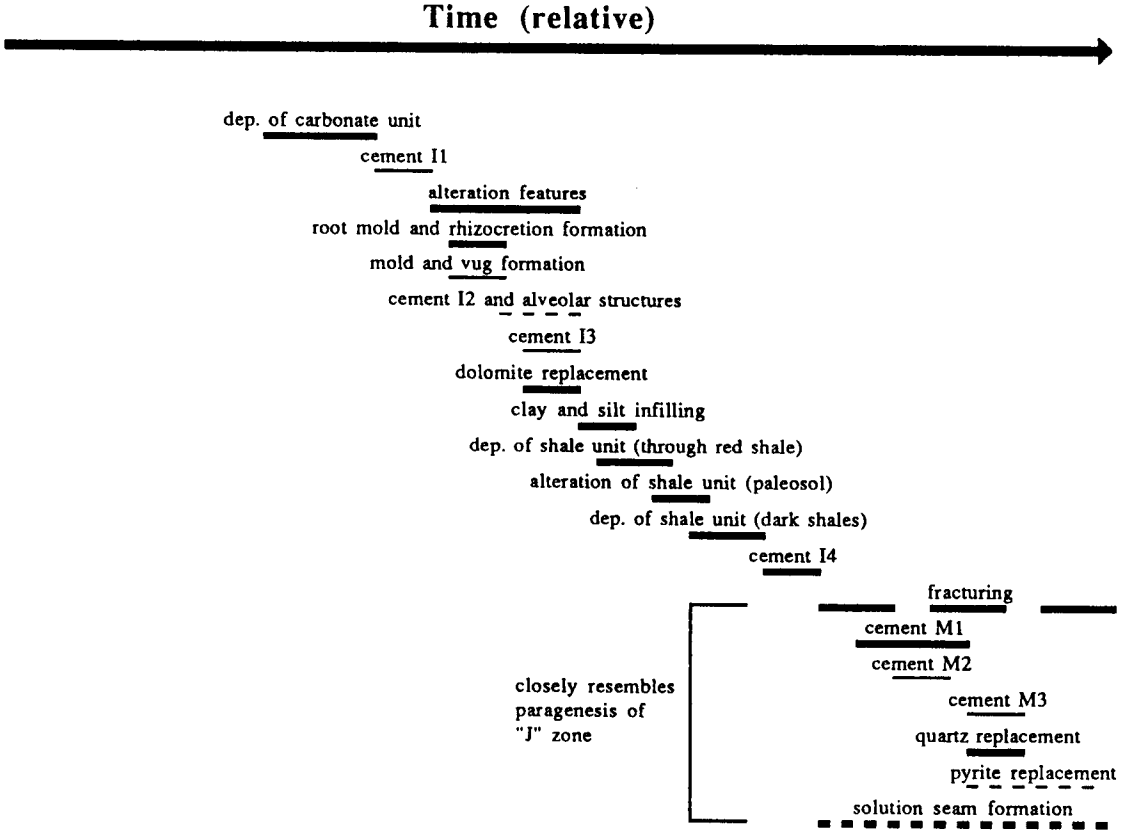

Figure 66. Paragenetic sequence of the "I" zone. The thick lines denote "major" features, that are either pervasive throughout the zone or particularly abundant. The thin lines denote "minor" features.

Figure 67. Core photo of a sample with abundant vertical and horizontal fissures. Several well-developed rhizocretions are present in the fissures of this sample, appearing as dark brown areas (arrows). (Carbonate unit, "I" zone; Rogers #1, 3790 feet.)

horizontal fissures (Fig. 68). Circumgranular cracks and glaebules are commonly associated with the fissures and brecciated intervals (Fig. 69).

Root Molds and Rhizocretions

Root molds and rhizocretions are also present in the upper portions of the carbonate unit (Fig. 67; 68). They formed in close association with the alteration features, as indicated by cracked rhizocretions and root molds, and the presence of rhizocretions in fissures and breccia pores.

Cement I1

Cement I1 consists of roughly isopachous rims of bladed to equant, nonferroan calcite (Fig. 70). This cement is present only in the grainstones, and then only in a few wells. Cement I1 is erratically developed even on a small scale, varying from well-developed rims to completely absent in the distance of a few pores. The cement crystals range from 7 - 20 micrometers long, and from 5 - 15 micrometers wide. Under cathodoluminescence, cement I1 exhibits an initial dark zone, and dull luminescence in the outer portions of the crystals (Fig. 71).

This cement pre-dates compaction and appears to pre-date the alteration features, because the cement was not

Figure 68. Core photo showing the delicate "pillars" formed by major vertical fissures and minor horizontal fissures. The arrow points to a large, well-developed rhizocretion. (Carbonate unit, "I" zone; Demuth #4, 3804 feet.)

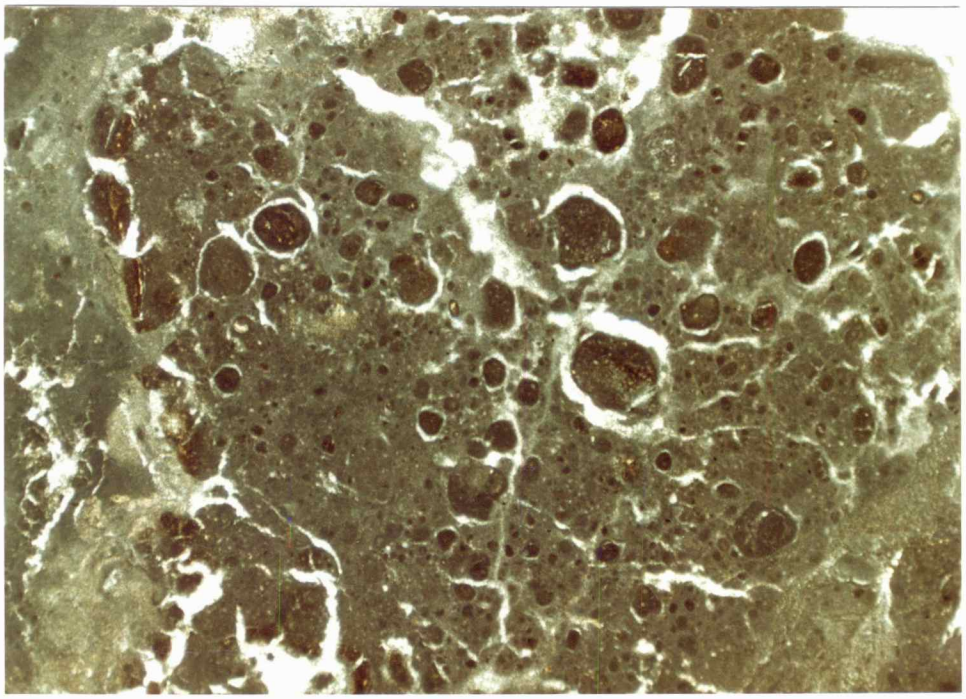

Figure 69. Plane polarized-light photomicrograph of well-developed glaebules and circumgranular cracks. The glaebules occur in a completely dolomitized matrix of carbonate mud that fills alteration pores. All of the large glaebules are surrounded by circumgranular cracks. (Carbonate unit, "I" zone; Rogers #2, 3814 feet.)

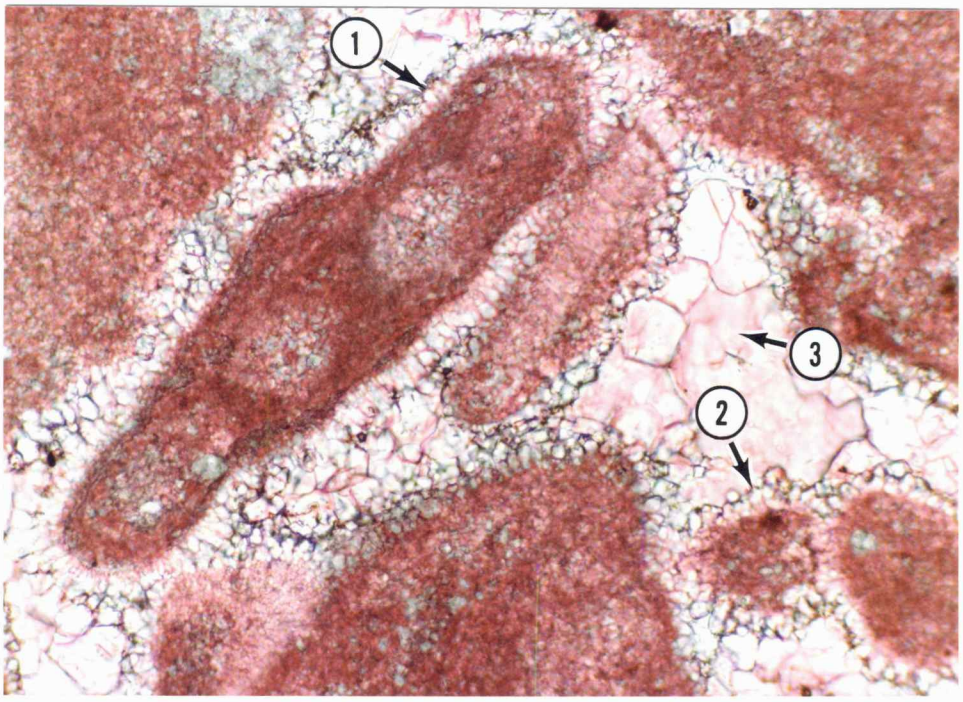

Figure 70. Plane polarized-light photomicrograph of cements I1 and I4. (Thin section stained with Alizarin Red-S and potassium ferricyanide.) Cement I1 forms isopachous rims of bladed crystals in this photo (arrows 1 and 2), but is absent from nearby pores in the same thin section. The centers of the pores are filled with cement I4 in this sample (arrow 3). (Carbonate unit, "I" zone; Rogers #1, 3792 feet.)

Figure 71. Paired plane polarized-light (A) and cathodoluminescent (B) photomicrographs of cements I1 and M1. (Thin section impregnated with blue epoxy and stained with Alizarin Red-S and potassium ferricyanide.) Arrow 1 on photo A points to a well-developed rim of cement I1. On photo B, arrow 1 points to the dark cores and dully luminescent outer portions of cement I1. Arrows 2 and 3 both point to crystals of cement M1. Crystal 3 shows a slightly more purple tinted stain (obscured in photo) than crystal 2, indicating crystal 3 is more ferroan. This subtle staining pattern is striking under cathodoluminescence, crystal 2 exhibits moderately bright luminescence while crystal 3 exhibits very dull (almost dark) luminescence. (Carbonate unit, "I" zone; Demuth #1, 3803 feet.)

A

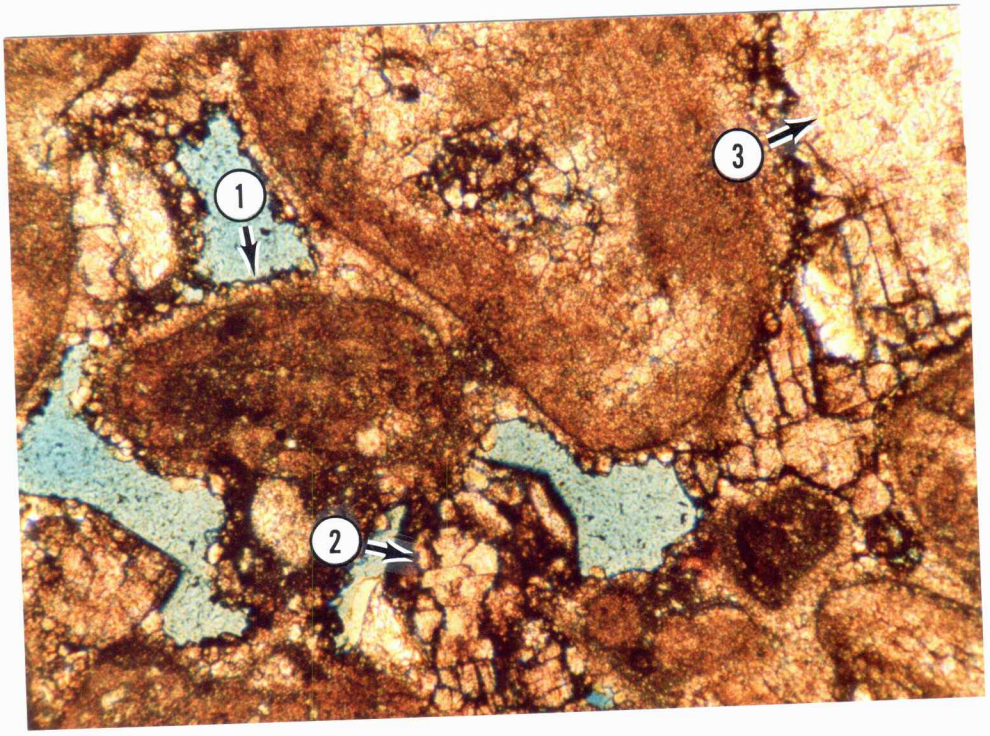

B

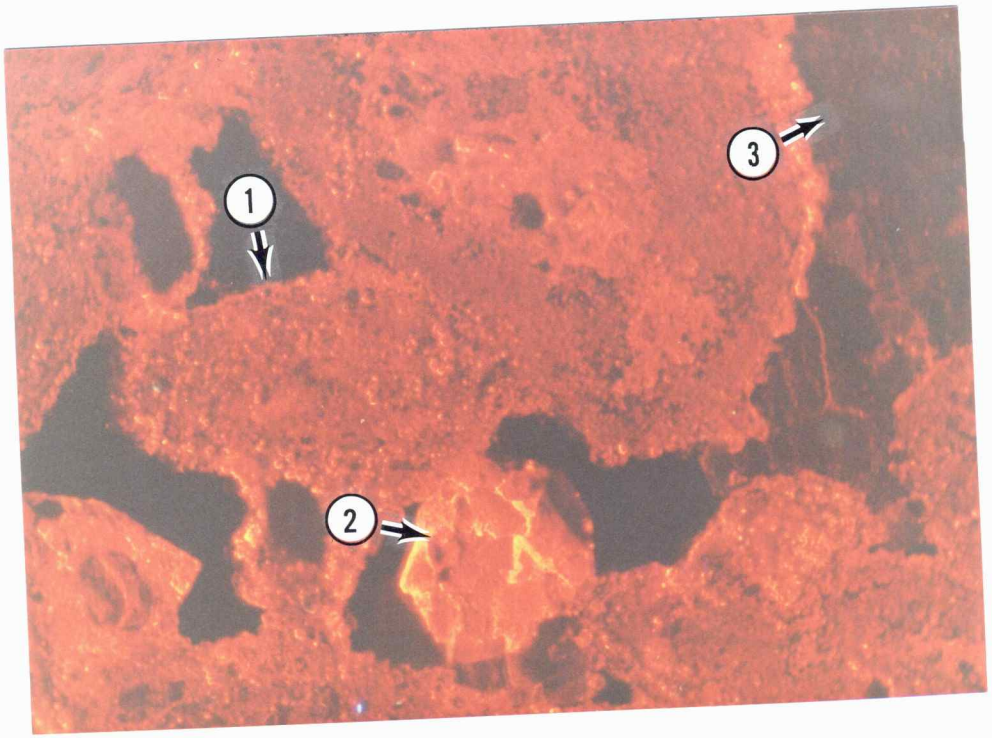

300 μm

Stratigraphic Up

observed in the alteration pores or root molds. However, no alteration features were observed cross-cutting cement I1 to confirm the inferred relative timing.

Skeletal Molds and Vugs

Molds of bivalves, gastropods, and algal fragments, as well as a few vugs, are present in the grainstones and muddy sediments. The skeletal molds and vugs pre-date compaction, and appear to be coeval with the alteration features and root molds, based on the similar sequence of infilling cements. The "I" zone grainstones generally exhibit far fewer molds than the "J" zone grainstones, primarily due to the lack of oomolds in the "I" zone.

Cement I2

Cement I2 is composed of tangential needle-fibers of calcite (Fig. 72). This cement is present only in the upper portions of the carbonate unit, usually in the alteration pores. Cement I2 post-dates the onset of the development of alteration features, and pre-dates compaction. It also pre-dates shale infilling.

The needles of cement I2 are approximately 20 micrometers long and 3 micrometers wide. The cement usually forms an irregular lining around large pores, but also forms well developed alveolar structures (Fig. 73) (Esteban and Klappa, 1983). Cement I2 exhibits very dull

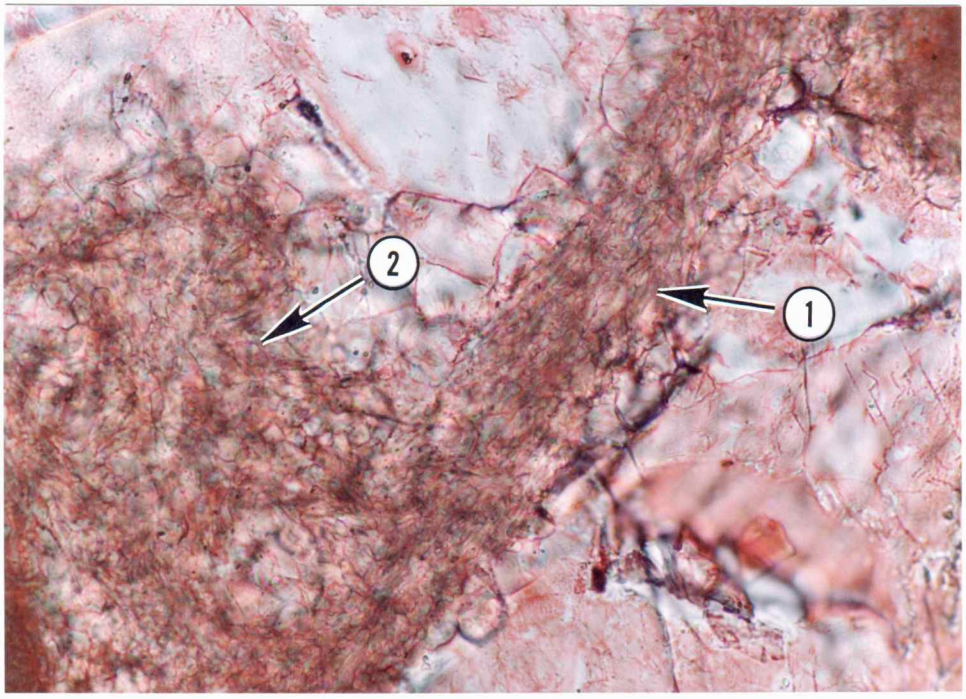

Figure 72. Unpolarized-light photomicrograph of tangential needle-fiber cement I2. (Thin section stained with Alizarin Red-S.) The needles are typically well aligned, as in the pore bridge marked by arrow 1. However, in a few places the needles show variable alignment, as in the grain coating marked by arrow 2. (Carbonate unit, "I" zone; Demuth #1, 3799 feet.)

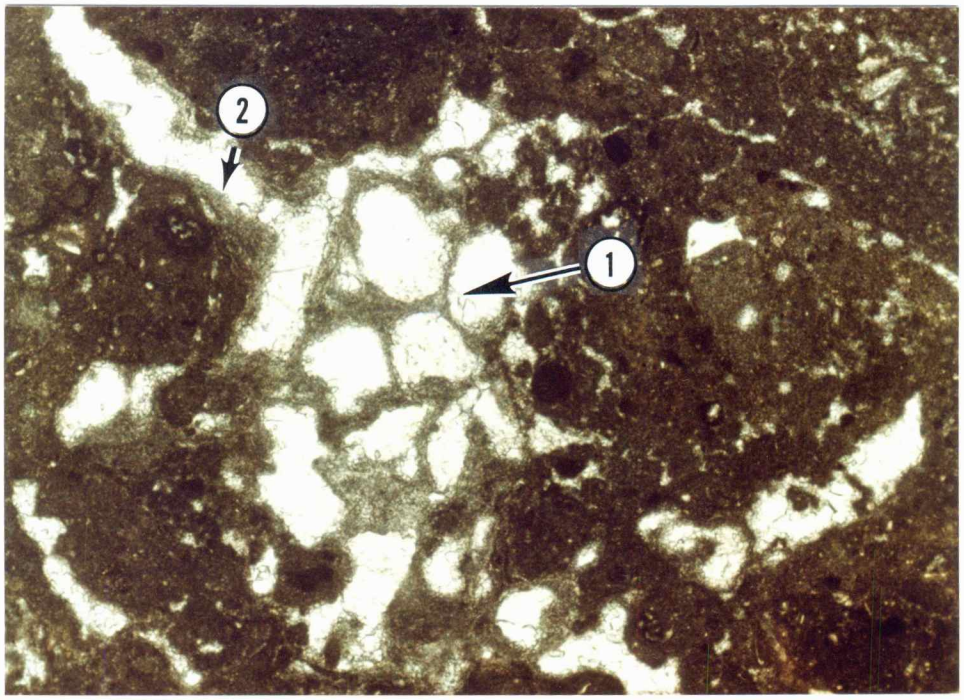

Figure 73. Plane polarized-light photomicrograph of an alveolar structure (arrow 1) in the center of an alteration pore. The alveolar structure is composed of tangential needle fiber cement (I2), which also forms an irregular lining around many of the large pores in this sample (arrow 2). (Carbonate unit, "I" zone; Demuth #1, 3799 feet.)

luminescence with a few moderately bright speckles (Fig. 74).

Cement I3

Cement I3 consists of equant rhombohedra of nonferroan dolomite. This cement generally occurs as single, scattered rhombohedra, but may form sparse, roughly isopachous rims (Fig. 75). The rhombohedra range in length from 7 to 50 micrometers, and typically exhibit a brownish, inclusion-rich core. Cement I3 is absent in several wells, and is only a minor constituent where it does occur. As in the "J" zone dolomite cement, luminescence patterns in dolomite cement I3 are variable, from a core with dark to dull luminescence and a rim of moderately bright luminescence, to rhombohedra with uniform, moderately bright luminescence throughout (Fig. 75).

Cement I3 post-dates the onset of the development of alteration features, and appears to pre-date compaction. It does not occur in association with cement I2 and therefore no timing relative to this cement can be inferred. Cement I3 does pre-date shale infilling.

Dolomite Replacement

Although no cross-cutting relationships for dating were observed, dolomite replacement of micrite is probably related to the event that formed the dolomite cement, based on the similarities of the crystals and

Figure 74. Paired plane polarized-light (A) and cathodoluminescent (B) photomicrographs of cements I2, I4, and M1. In this sample, cement I2 forms pore coatings and a pore bridge. This cement exhibits very dull luminescence with a few moderately bright speckles (arrow 1). A few crystals of cement I4 are present, and exhibit alternating bands of dull and moderately bright luminescence (arrow 2). Large crystals of cement M1 fill the pore centers and exhibit moderately bright luminescence. (Carbonate unit, "I" zone; Demuth #1, 3799 feet.)

A

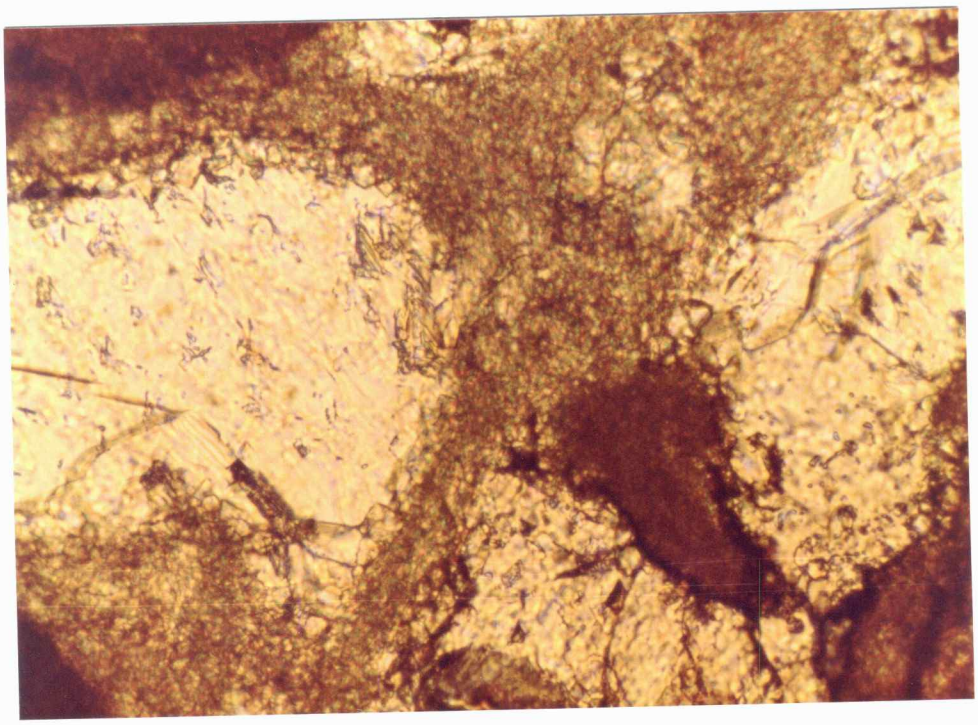

B

100 um

Stratigraphic Up

Figure 75. Photomicrographs of dolomite cement (I3) and dolomite replacement; unpolarized-light (A) photomicrograph of a stained section in oil with a cover slip, and paired plane polarized-light (B) and cathodoluminescent (C) photomicrographs. (Thin section stained with Alizarin Red-S and potassium ferricyanide.) Rhombohedra of dolomite cement I3 are scattered around the wall of the large pore in the center of photo A. Irregular blebs of replacement dolomite are also present in the matrix of this sample (arrows 2, 3, and 5). Luminescence patterns in the replacement dolomite are similar to those in the dolomite cement, but both show some variability. In places, dolomite cement (arrow 1) and replacement (arrows 2 and 3) exhibit a core with dark to dull luminescence and a rim of moderately bright luminescence. Alternatively, the dolomite cement (arrow 4) and replacement (arrow 5) may exhibit uniform, moderately bright luminescence. (Carbonate unit, "I" zone; Demuth #4, 3807 feet.)

A

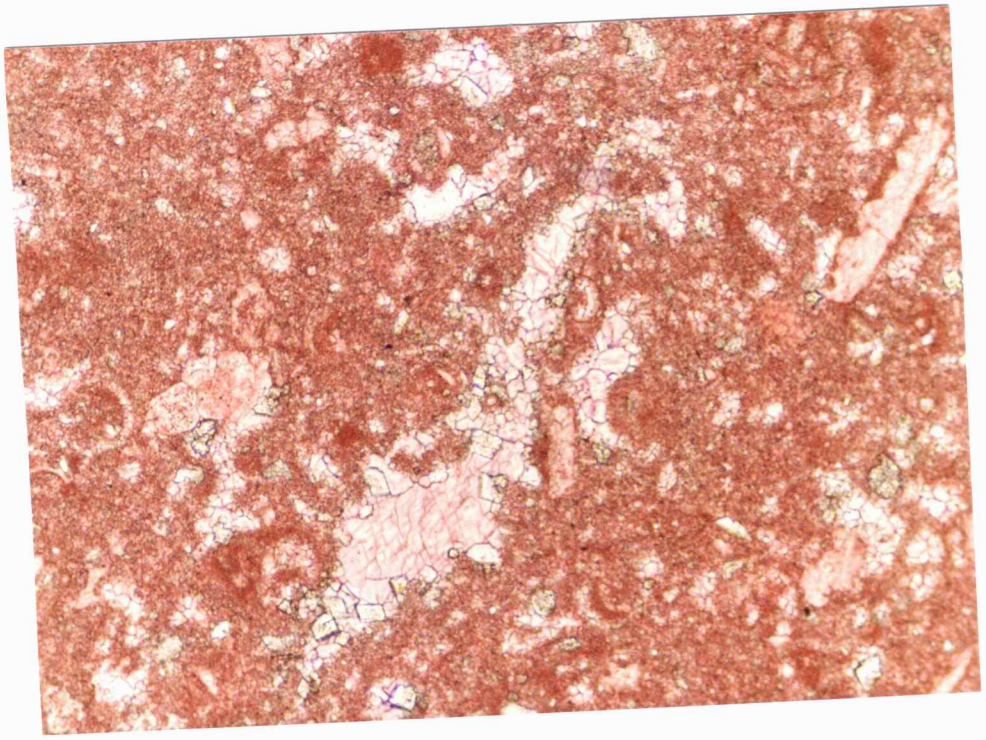

300 μm

Stratigraphic Up

B

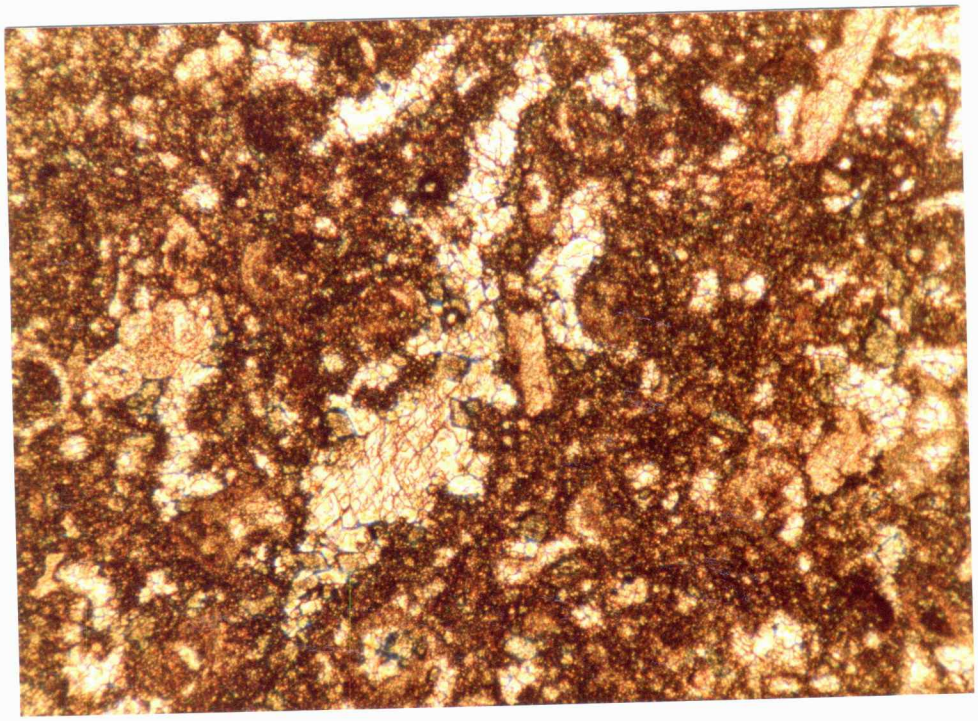

C

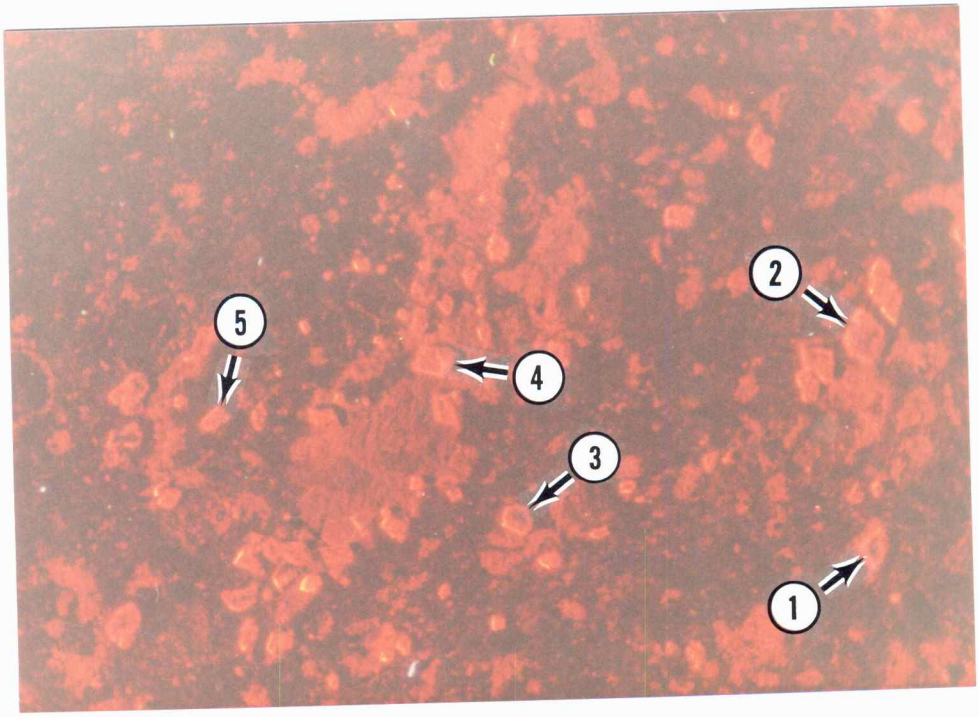

300 μm

Stratigraphic Up

luminescence. The replacement dolomite ranges from generally well-developed rhombohedra to partially developed rhombohedra to irregular blebs. The rhombohedra and blebs range in size from 5 to 20 micrometers, and exhibit a brownish core similar to that of the cement. The luminescence patterns are similar to those of the dolomite cement (Fig. 75).

Dolomite replacement in the "I" zone is far less pervasive than in the "J" zone, although at least slight replacement occurs in every well. The most striking difference is in the autoclastic brecciated carbonate mudstones and wackestones. In the "J" zone breccias, the carbonate strata are typically completely dolomitized, whereas they range from slightly to moderately dolomitized in the "I" zone.

Post-burial Features

The shale unit is regionally extensive and forms a seal over the "I" carbonate unit, effectively isolating the carbonate rocks from near-surface diagenetic environments. Shale infilling marks the onset of burial, but not necessarily the onset of significant compaction.

Shale Infilling

The majority of pores in the alteration features are filled with clay and minor amounts of quartz silt. This

infill sediment is also rarely present in the interparticle pores of the grainstones. Like the "J" zone infilling, this sediment is similar to the sediment of the lower portions of the overlying shale. Shale infilling generally extends to the base of the fissures, indicating the fissure system was connected to the surface.

Cement I4

Cement I4 consists of equant crystals of nonferroan calcite with a roughly pore-lining to pore-filling distribution (Fig. 70). The cement crystals range in size from 10 to 300 micrometers. Under cathodoluminescence, cement I4 exhibits alternating bands of dull and moderately bright luminescence (Fig. 76; 74). Cement I4 is the most common cement in the carbonate unit. It pre-dates compaction and post-dates shale infilling.

Multi-zone Features

The rest of the paragenetic features observed in the carbonate unit post-date compaction, and closely resemble the post-compactional features observed in the "J" zone (Fig. 22; 66). Several generations of fractures are present, cement M1 is common throughout the unit, and minor amounts of cements M2 and M3 are present.

Figure 76. Paired plane polarized-light (A) and cathodoluminescent (B) photomicrographs of cements I4 and M1. Arrows 1 and 2 point to crystals of cement I4 growing from echinoderm fragments. Cement I4 exhibits alternating bands of dull and moderately bright luminescence. Cement M1 fills the remaining pore space, and exhibits dull luminescence in this sample (arrow 3). (Carbonate unit, "I" zone; Shuck #1, 3736 feet.)

A

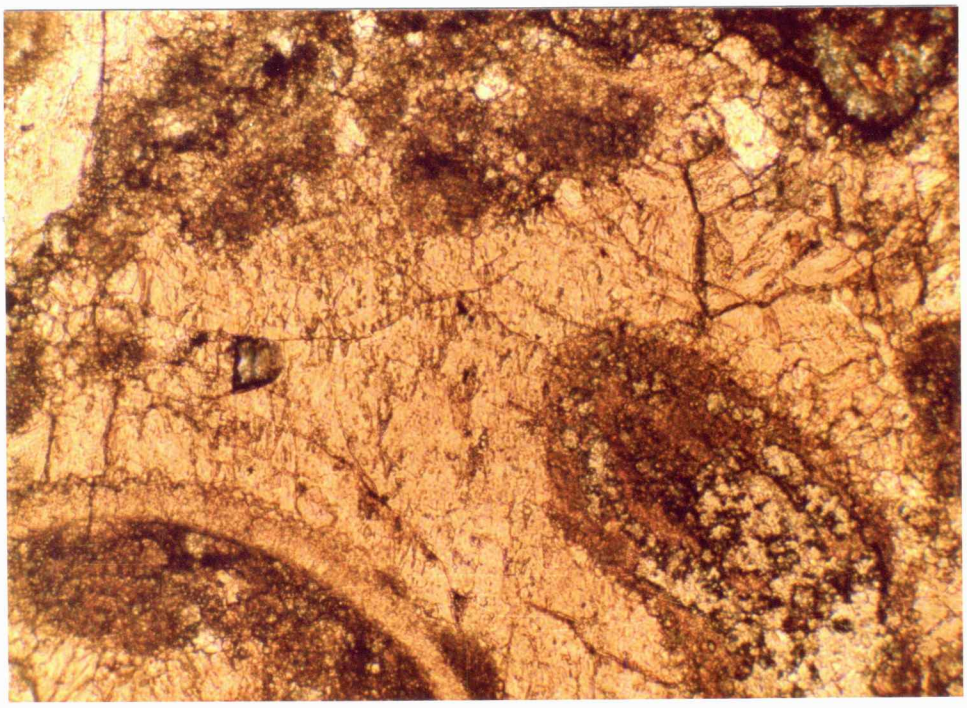

B

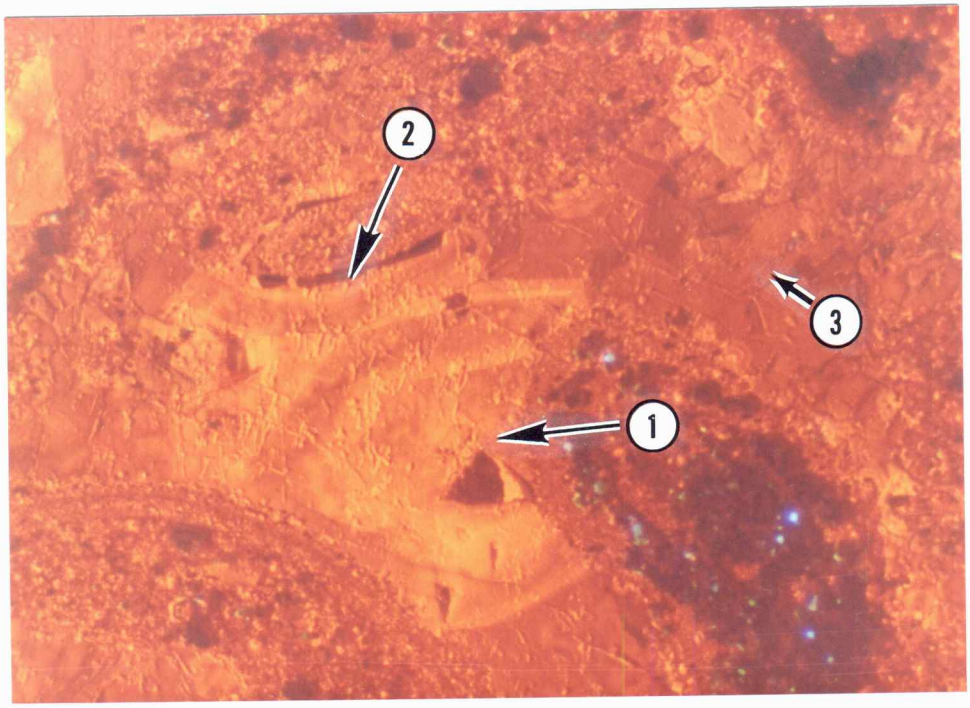

200 μm

Stratigraphic Up

Scattered quartz replacement occurs throughout the muddy sediments, and pyrite replacement is present, but is much less abundant than in the "J" zone. The four types of solution seams observed in the "J" zone are also present.

PARAGENESIS OF THE "I" SHALE UNIT

The "I" zone shale unit contains several paragenetic features that appear to be unrelated to diagenesis in the carbonate unit. The upper 6 to 20 inches (15 - 51 cm) of the red shale exhibits a distinctive pattern of alteration in every well. One feature of this alteration is the presence of irregular white blebs of carbonate ranging in size from 1 to 10 mm. These blebs typically exhibit delicate or even hazy outlines that gradationally merge into the shale (Fig. 77). The centers tend more toward unadulterated carbonate.

Silt-filled subvertical and subhorizontal stringers are another characteristic feature (Fig. 77). The stringers range in width from 2 to 20 mm and generally taper downwards. They may be up to 12 cm in length. A few stringers show a thin line of carbonized material 1 to 3 mm wide paralleling the long axis of the stringer (Fig. 78). The shape, orientation, and presence of organic material indicate the stringers are root structures.

Bright olive mottles appear to be associated with the alteration zone (Fig. 77). These mottles range from only 2 mm wide to completely coalesced, forming a distinct interval of olive silty shale. The olive mottles are most common in the obvious alteration zone at the top of the red silty shale, but may extend up into

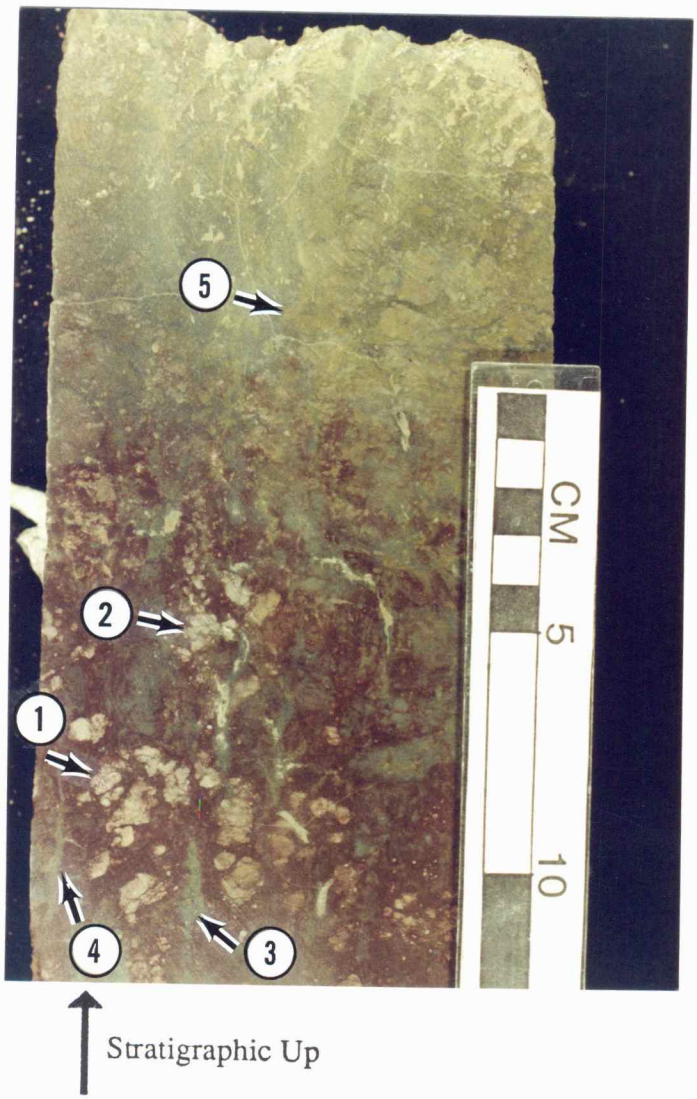

Figure 77. Core photo of the alteration zone in the shale unit. This sample contains fragments of carbonate mudstone which are probably altered clasts. However, it also contains irregular white blebs of carbonate with delicate outlines that gradationally merge into the shale (arrows 1 and 2). This sample contains many silt-filled stringers (arrows 3 and 4), as well as an interval of bluish-gray shaley siltstone just above the red shale. The sample also exhibits numerous olive mottles (arrow 5). (Shale unit, "I" zone; Rogers #2, 3810 feet.)

Plane of photo is parallel to bedding.

Blocks on scale equal one centimeter.

Figure 78. Core photo of bluish-gray silt stringers, with a thin line of carbonized material paralleling the long axis of the stringers (arrows). The tapering shape of the silt stringers, the subvertical and subhorizontal orientations, and the presence of organic material, all indicate the stringers are root structures. (Shale unit, "I" zone; Bethell #5, 3748 feet.)

the dark shales. Three wells also exhibit a few carbonate blebs in the dark shale. The relationship between the alteration zone and the deposition of the dark shales is not completely clear.

The associated alteration features form a discrete horizon, and the abundance of any single feature decreases downwards. No alteration features extend through the red shale interval; 1.5 - 4 feet (.5 - 1.2 m) of unaltered shale separates the shale alteration zone from the top of the carbonate unit.

INTERPRETATION OF THE DIAGENETIC ENVIRONMENTS OF THE "I" CARBONATE UNIT

The diagenetic history of the carbonate unit is discussed separately from the shale unit because many of the carbonate paragenetic features pre-date burial, and therefore pre-date deposition of the shale unit. The post-burial features in the carbonate unit differ greatly from the paragenetic features in the shale unit. Apparently the two units were effectively isolated by the red shale interval of the shale unit.

Pre-burial Features

Alteration Features, Root Molds, and Rhizocretions

Several of the alteration features, as well as other less pervasive features, indicate the carbonate unit was subaerially exposed. Tangential needle-fiber cement (I2), alveolar textures, root molds, rhizocretions, glaebules, and circumgranular cracks are all diagnostic indicators of paleosol formation according to Esteban and Klappa (1983) (Fig. 67; 68; 69; 72; 73). The accumulation of calcium carbonate in the alteration horizon, as evidenced by tangential needle-fiber cement (I2) and carbonate glaebules, is indicative of a caliche paleosol. The formation of caliche is not only evidence of subaerial exposure, but indicates the paleosol formed in a semiarid environment (Esteban and Klappa, 1983).

Fissures and autoclastic breccias are the two most pervasive alteration features in the carbonate unit (Fig. 67; 68). These two features are common in paleosols, although not diagnostic. However, the close association with the previously mentioned paragenetic features indicates the fissures and autoclastic breccias formed during subaerial exposure and development of the paleosol.

Cement I1

The formation of cement I1 is interpreted to pre-date subaerial exposure because this cement is not present in the alteration pores or root molds. The generally isopachous rims of equant, nonferroan calcite (Fig. 70) are typical of the meteoric phreatic environment, although hardly diagnostic (Longman, 1980). However, this interpretation is supported by the subsequent development of caliche, which confirms meteoric diagenesis.

Skeletal Molds

There are no cross-cutting relationships, but the sequence of cements in the skeletal molds matches that in the root molds and alteration pores, suggesting all of the pore types are penecontemporaneous. Cement I3 occurs in the root molds and alteration pores, as well as the

skeletal molds. This cement is interpreted to have formed during subaerial exposure (discussed below), indicating the majority of the skeletal molds, as well as the alteration pores and root molds, formed during exposure. The skeletal molds probably formed as a result of contact with undersaturated meteoric water.

Cement I2

Cement I2 post-dates the onset of subaerial exposure because it occurs primarily in alteration pores. However, this cement almost certainly formed during the period of exposure because the tangential needle fibers and alveolar textures (Fig. 72; 73) are characteristic of paleosol development (Esteban and Klappa, 1983).

Dolomite Cement and Dolomite Replacement

The dolomite cement (I3) and dolomite replacement in the "I" zone look petrographically similar to that in the "J" zone (Fig. 40; 41; 42; 75). However, the "J" zone dolomite clearly pre-dates clay and silt infilling of the "J" upper carbonate unit, and therefore formed before deposition of the "I" zone sediments. The similarities between the two generations of cement are probably the result of re-establishment of similar conditions, most likely a mixing zone environment.

Post-burial Features

Shale Infilling

The infilling of clay and quartz silt is somewhat variable, but generally matches the silty shale of the overlying shale unit. Infilling is associated with the alteration features in the carbonate unit, but no clear examples were observed of alteration features post-dating shale infilling. Consequently, shale infilling is interpreted to mark the onset of deposition of the shale unit. There is no direct evidence to indicate if the infilling was subaerial or subaqueous, but the infilling environment probably matched the depositional environment of the lower intervals of the shale unit. This environment will be discussed further in the section on diagenetic environments in the shale unit.

Cement I4

Cement I4 post-dates shale infilling and therefore probably precipitated from a fluid isolated from near-surface diagenetic environments. This cement is petrographically similar to cement J7, and probably formed in a similar shallow burial environment (Fig. 46; 47; 70; 76).

Multi-zone Features

The rest of the paragenetic features observed in the carbonate unit closely resemble the post-compactional features in the "J" zone carbonates, although the abundances of the various phases differ in the two zones. For instance, the ferroan, baroque dolomite cement (M2) preferentially forms as overgrowths on previous dolomite cement. As a consequence it is more prevalent in the "J" zone since far more crystals of the abundant dolomite cement J5 were exposed to the burial fluids than those of the relatively sparse dolomite cement I3. Although conditions sometimes manifested a little differently in the two zones, it is clear that by the onset of precipitation of cement M1, both the "I" and "J" zone were part of the deep burial environment, and were subject to similar conditions from that point to the present.

INTERPRETATION OF THE DIAGENETIC ENVIRONMENTS OF THE "I" SHALE UNIT

The alteration zone within the shale unit contains root structures and therefore is probably the result of another subaerial exposure event (Fig. 77; 78). The fragile, indistinct outlines of the carbonate blebs suggests they are autochthonous, indicating in situ accumulation of calcium carbonate (Fig. 77). Consequently, the alteration zone within the shale unit probably represents another paleosol, albeit poorly developed.

This paleosol horizon is separated from the paleosol horizon developed at the top of the carbonate unit by at least 1.5 feet (0.5 m) of unaltered red silty shale (unless the red color itself indicates alteration). It is certainly possible for diagenetic fluids evolved during paleosol development in the shale unit to pass through a few feet of fractured shale and alter the underlying carbonate unit. However, the evidence from the abundant cores suggests this is not the case. The top of the carbonate unit contains abundant root molds and rhizocretions. The paleosol horizon in the shale unit also exhibits abundant root structures, but none of the observed structures came close to penetrating to the base of the shale unit, indicating the two separate root horizons probably represent separate exposure surfaces. The size and number of carbonate blebs in the shale unit

also diminish rapidly below the paleosol horizon, and no nodules were observed in the lower two feet of the shale unit. The paragenetic features therefore indicate that two distinct paleosol horizons developed in the "I" zone.

This observation has obvious implications as to the depositional environment of the shale unit. In his regional study, Watney (1980) noted the absence of fossils, the oxidized appearance of the typically red-brown strata, and the presence of possible paleosol features in the upper shales. He interpreted the typical upper shale units to be subaerially exposed continental deposits.

The presence of a paleosol horizon at the base of the "I" shale unit, and another paleosol horizon at the top of the red shale interval, suggests the intervening shale is a subaerial deposit. The clasts of the polymict conglomerate in the Bethell #5 (Fig. 65) are probably regoliths formed from adjacent exposures of the carbonate unit. With the available data, it was not possible to determine the origin of the dark shale interval above the shale unit paleosol horizon.

CONCLUSIONS

Carbonate Unit

The "I" zone exhibits a variety of paragenetic features from several different diagenetic environments. Severe alteration of the top of the carbonate unit occurred during subaerial exposure. Most of the secondary porosity in the "I" zone formed during this exposure event. However, the resulting pore network in the "I" grainstones does not resemble that in the "J" alpha grainstone due to the different types of cement, the greater abundance of skeletal molds in the "J" zone, and the oomoldic pores in the "J" zone.

A paleosol with some caliche features was part of the alteration at the top of the "I" carbonate unit, and indicates the climate was semi-arid. The post-burial, post-compactional paragenetic features closely resemble those in the "J" zone carbonates, although the quantities of the various cements and replacive phases differ. The close similarity indicates that after significant burial, the two zones were essentially part of the same diagenetic environments. The differences in abundance of the features appears to be largely a function of the nature of the precursor substrate, rather than the burial fluids themselves.

Shale Unit

A paleosol horizon exists within the "I" shale unit, and is unrelated to the paleosol developed at the top of the carbonate unit. The existence of two paleosol horizons within a single cyclothem is not a typical occurrence in the Midcontinent. Apparently a number of factors control cyclothem deposition and diagenesis; interpretation should not be based on the simple scenario of the sea came in, the sea went out.

RESERVOIR CHARACTERIZATION OF THE MAIN PAY - "J" ZONE ALPHA GRAINSTONE SUBUNIT

After examination of the distribution and diagenesis of the lithofacies in the Pen Field, it is possible to use the available drillstem tests, production tests, and production history to determine the continuity of the reservoir rock. The abundant core measurements and comprehensive log suites, combined with the continuity information, can then be used to determine the relationship between the geologic history of the reservoir and the petrophysical properties of porosity, permeability, and water saturation.

CONTINUITY AND COMMUNICATION

The restricted distribution of the alpha grainstone subunit suggests a localized deposit (Fig. 20). Static reservoir pressure derived from drillstem test data indicates a virgin reservoir pressure of 1342 psi for the grainstone pay interval (Appendix 10). Initial static pressures in each subsequent producing well showed a marked decrease from the previously completed well, indicating that communication in the alpha grainstone exists from the Shuck #1 in the northeast of the field, to the Demuth #4 in the southwest (Fig. 79). The Rogers #1 and Rogers #2 are exceptions to this pattern, exhibiting initial static reservoir pressures

Figure 79. Map of initial static reservoir pressure in the alpha grainstone subunit. The map indicates communication between wells, since each well drilled into the alpha grainstone shows a progressively lower pressure. The Rogers #1 and Rogers #2 in the south half of section 19 are notable exceptions, exhibiting pressures far greater than those in previously drilled wells. These two wells are therefore in poor communication with the main body of the alpha grainstone. The mapped pressures are derived from Horner plot extrapolations of drillstem test data (Appendix 10). Only those tests that measured just the alpha grainstone were used for the map. The Bethell #5 is the only exception, in addition to the alpha grainstone, two feet of porous wackestone in the beta micrite-rich subunit of the "J" zone was open to the test. However, core measurements indicate this thin interval only has a permeability of 4 md, and does not appear to have affected the drillstem test results.

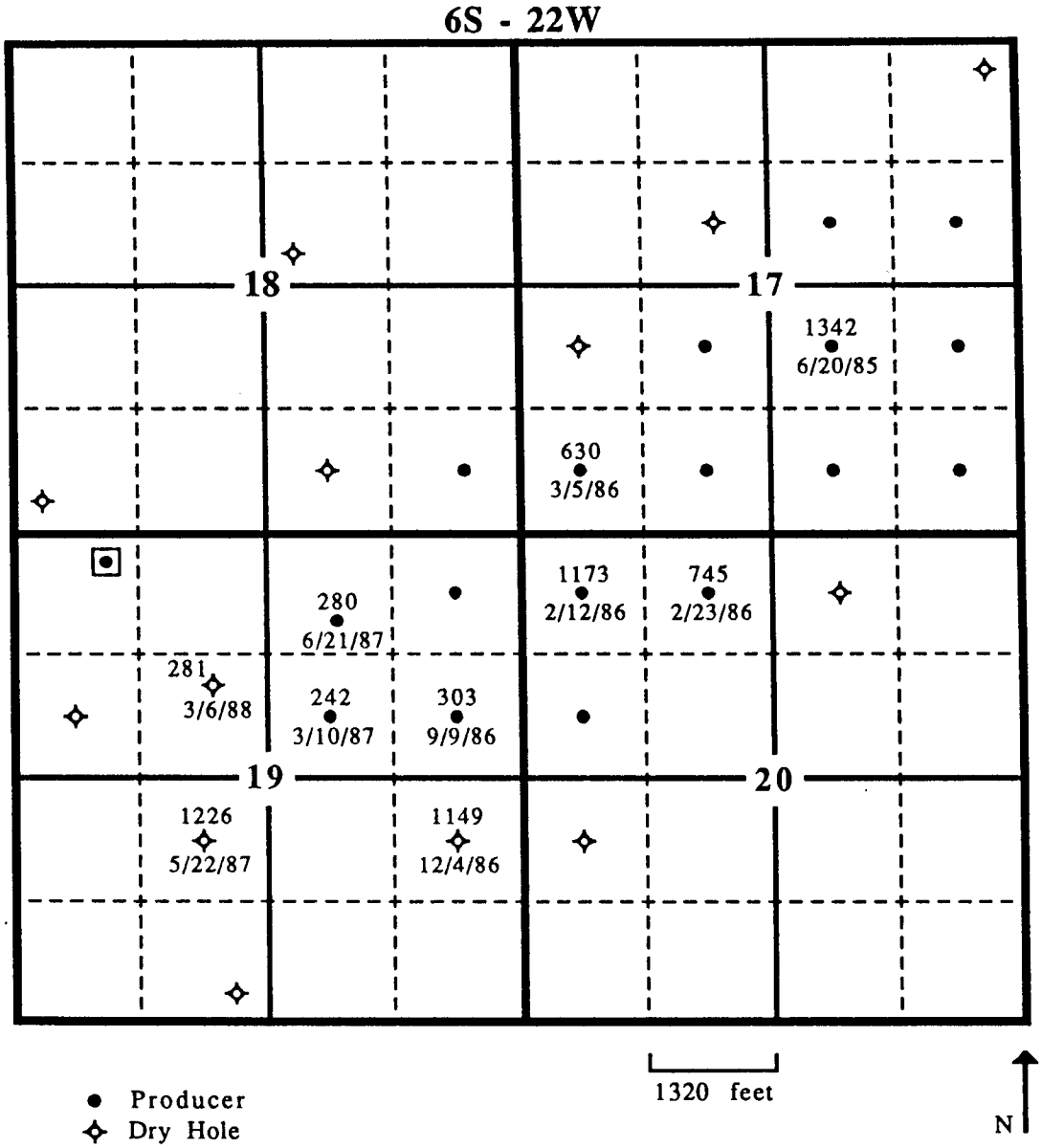
6S - 22W
18
17
19
20
1342
6/20/85
630
3/5/86
1173
2/12/86
745
2/23/86
280
6/21/87
281
3/6/88
242
3/10/87
303
9/9/86
1226
5/22/87
1149
12/4/86
1320 feet
N
Producer
Dry Hole
Producer, but not part of Pen Field
303 ← Pressure (psi)
9/9/86 ← Date of drillstem test

significantly higher than those of the previously drilled wells.

A plot of initial static reservoir pressure in the alpha grainstone versus cumulative field production indicates the pressure response due to depletion of the field (Fig. 80). The results are striking, showing a high degree of correlation. This correlation indicates that not only were the producing wells in the alpha grainstone exhibiting communication, but that the pressure disturbance of the early producers was almost completely distributed throughout the reservoir.

The plot also shows an abrupt change in the relationship between pressure and production that occurs at a cumulative production of approximately 63,000 barrels of oil. This slope change is interpreted to mark the bubble point pressure. Above this pressure, fluid expansion was the primary drive mechanism, and relatively few barrels of oil were produced for a given pressure drop. Below this pressure, gas began to come out of solution, augmenting the fluid expansion drive. This resulted in a significant change in slope as many more barrels of oil were produced for a given pressure drop. The intersection of the two lines defines the bubble point pressure, which is estimated to be 285 psi (Fig. 80).

Examination of the plot reveals the two Rogers wells are distant outliers, suggesting they are separated from

Figure 80. Crossplot of initial static reservoir pressure (P_s) in the alpha grainstone versus cumulative field production (all zones). The fit of the lines indicates the alpha grainstone has excellent communication between wells. The perturbations due to depletion by the producing wells are effectively transmitted to the entire alpha grainstone body except for the Rogers #1 and Rogers #2. These two wells are obviously isolated from the main body of the alpha grainstone. The intersection of the two regression lines marks the bubble point, which occurred at 285 psi. The slopes of the two lines also show the relative efficiency of the drive mechanisms. Fluid expansion was the primary drive mechanism to the bubble point, and only 63,000 barrels of oil were produced for a pressure drop from 1342 to 285 psi. After the bubble point, solution gas drive augmented the fluid expansion, and approximately 330,000 barrels of oil were produced with only a minor pressure decrease.

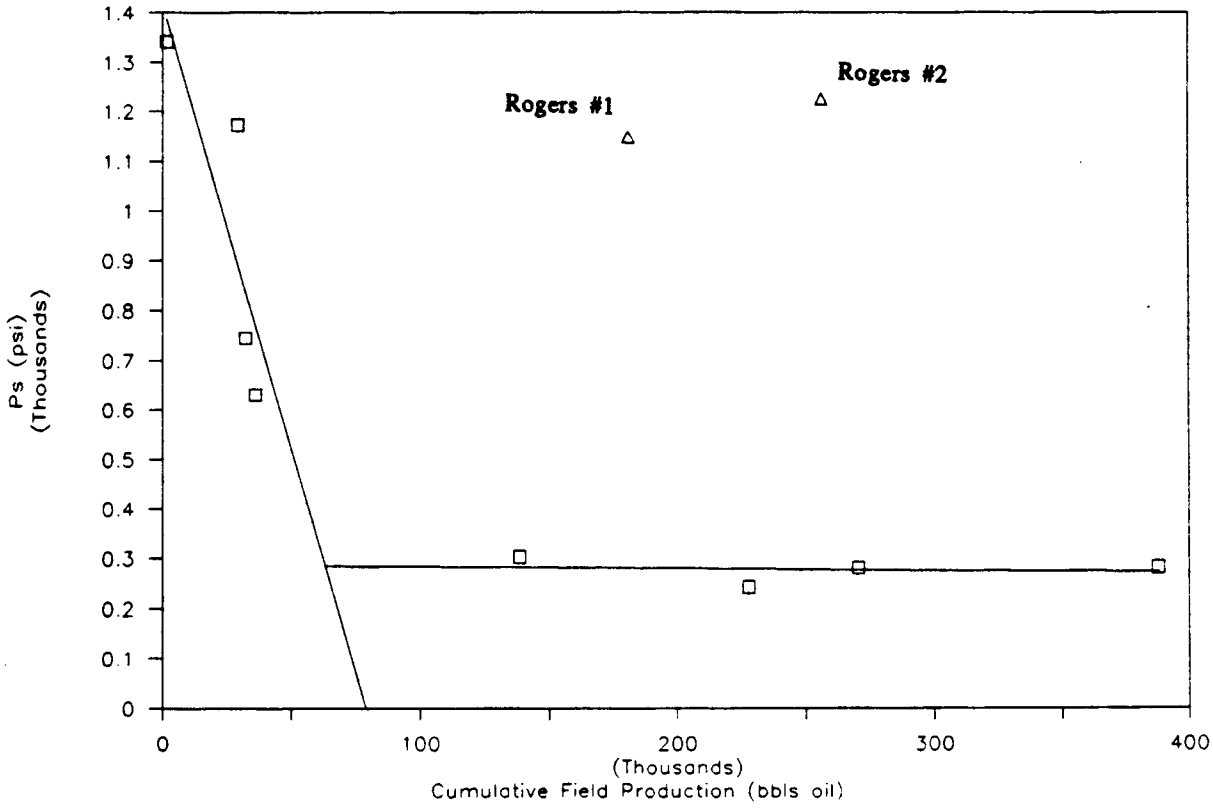
Rogers #1
Rogers #2
Ps (psi)
(Thousands)
1.4
1.3
1.2
1.1
1
0.9
0.8
0.7
0.6
0.5
0.4
0.3
0.2
0.1
0
0
100
200
300
400
(Thousands)
Cumulative Field Production (bbls oil)

the main body of the grainstone by a permeability barrier, or are in very poor communication. The drillstem test of the Rogers #2 had no show of oil and recovered 62 feet of mud and 248 feet of muddy water, the only alpha grainstone test in the field to recover water (Appendix 3). The producing "J" zone wells have not shown any water encroachment, therefore a permeability barrier must isolate the Rogers #2 from the main body of the field.

The core from the Rogers #1 exhibits a uniform oil stain throughout the grainstone interval, and porosities ranging from 7.5 to 11% (Appendix 2). This well was cased, then perforated in the "J" zone and acidized, but swabbing recovered only acid water. This was not surprising because the grainstone exhibits horizontal permeabilities ranging from only 0.5 to 1.3 md. The operator decided to fracture the well in an attempt to reach a region of higher permeability, but only small amounts of oil and water were recovered on post-fracture swab tests. The well eventually stabilized at 100% oil cut and a swab rate of .3 barrels of fluid per hour, whereupon it was abandoned as non-commercial (Appendix 3). The lack of success from the fracture treatment suggests the area of low permeability encountered in the well extends a significant distance away from the well bore. The drillstem test for this well indicated an initial

static pressure 200 psi below virgin grainstone pressure, but well above the prevailing pressure in the main body of the alpha grainstone. Therefore, this well is either in a separate reservoir compartment, or only in partial communication with the main grainstone reservoir.

POROSITY AND PERMEABILITY

The alpha grainstone subunit is generally well sorted and exhibits only moderate cement reduction of the interparticle porosity in most wells (Fig. 81). Abundant skeletal molds and oomolds, along with a few root molds and vugs, add to the porosity. This combination results in good porosity by Kansas standards; three of the cored wells exhibit porosities of 20% or greater. However, the development of porosity throughout the alpha grainstone body is far from uniform, due to the complex diagenetic history of the "J" zone. Core porosities range from 2 to 29%, but most of the variation is from well to well, with only minor variation in any single well. All of the core measurements are given in Appendix 2.

Determining the Net-pay Cut-off

Net-pay cut-offs are arbitrarily defined in many reservoir studies, but the abundant cores in the Pen Field allow resolution of the minimum permeability required for reservoir fluid movement. The production

Figure 81. Plane polarized-light photomicrograph (A) of excellent interparticle porosity and plane polarized-light photomicrograph (B) of a "mold-dominated" pore system with virtually no interparticle porosity. (Thin section in A impregnated with blue epoxy. Thin section in B impregnated with blue epoxy and stained with Alizarin Red-S.) In photo A, the interparticle porosity shows a moderate reduction by rims of cement J1 (arrow 1), and insignificant reduction by cement M1 (arrow 2). The interparticle porosity is supplemented by a few moldic pores. This pore network results in excellent porosity and permeability; for this sample the whole core porosity is 22% and maximum horizontal permeability is 257 md.

Photo B shows cement J1 completely filling most of the interparticle pores (arrows 3 and 4). Mold formation post-dates precipitation of cement J1. Consequently, many of the molds show only minor reduction by later cements, although the large oomolds are reduced or filled with cement M1 (arrow 5). This type of mold-dominated pore network typically shows very poor permeability, even where significant porosity exists. This sample exhibits a whole core porosity of 11%, but a maximum horizontal permeability of only .5 md. (A - Alpha grainstone subunit, upper carbonate unit, "J" zone; Bethell #5, 3763 feet.) (B - Alpha grainstone subunit, upper carbonate unit, "J" zone; Rogers #1, 3801 feet.)

A

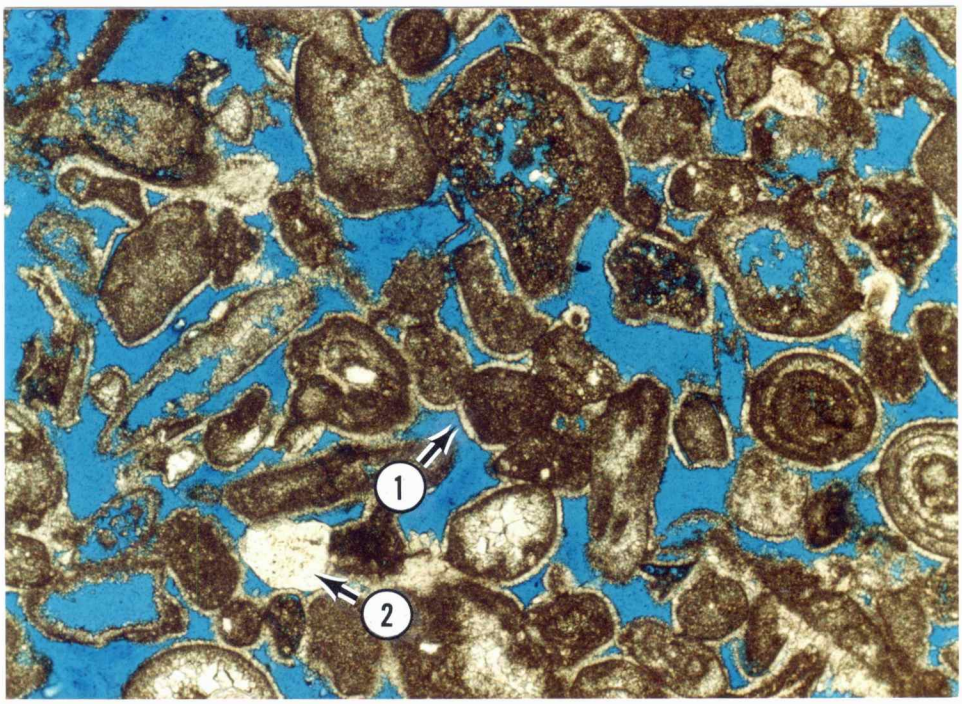

B

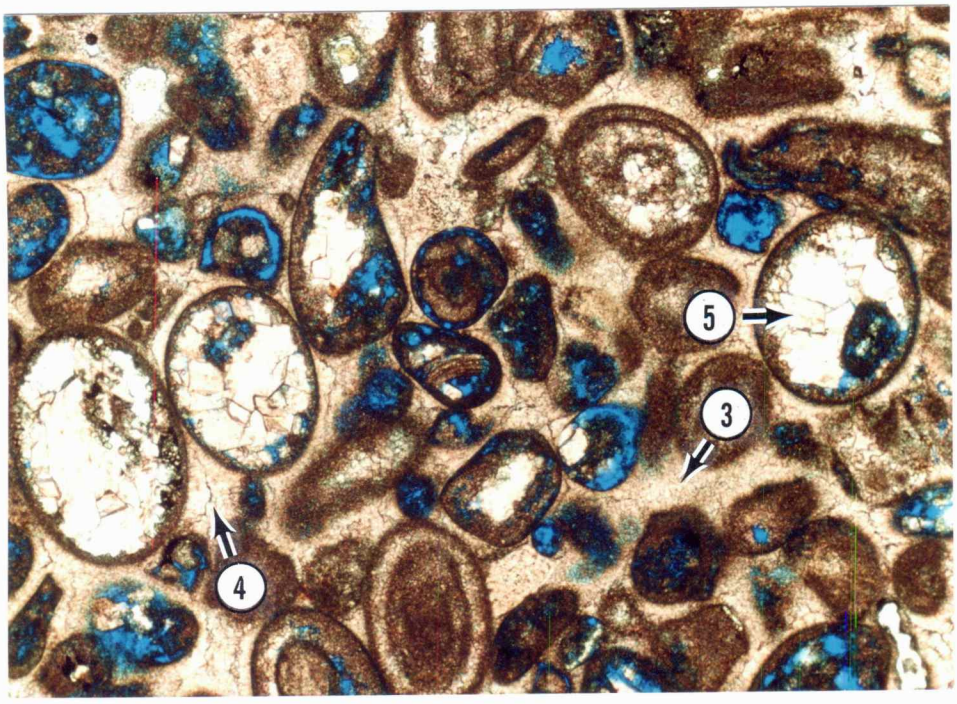

1000 μm

Stratigraphic Up

tests of the Rogers #1 indicate it was a marginal well, but they show that production from a reservoir with this temperature, pressure, and oil type, can be obtained down to permeabilities of approximately one md. This value was therefore adopted as the net-pay cut-off for all zones.

Determining the Relationship Between Porosity and Permeability

A crossplot of the logarithm of horizontal permeability versus core porosity was constructed to determine if there is a correlation between porosity and permeability for the alpha grainstone subunit (Fig. 82). The values exhibit considerable scatter, but show a definite trend of increasing permeability with increasing porosity. Thin section examination reveals that the outliers below the correlation line (low permeability for given porosity) contain greater amounts of cement J1 than the other samples. This cement reduces or completely fills most of the interparticle pores. The outliers also contain abundant skeletal molds and oomolds that post-date cement J1, and are only slightly reduced by later cements (Fig. 81). The combination of abundant molds and significant reduction of the interparticle pores with cement J1 results in a "mold-dominated" pore network. This network may have porosity as high as 11%, but the molds are poorly connected, resulting in very low

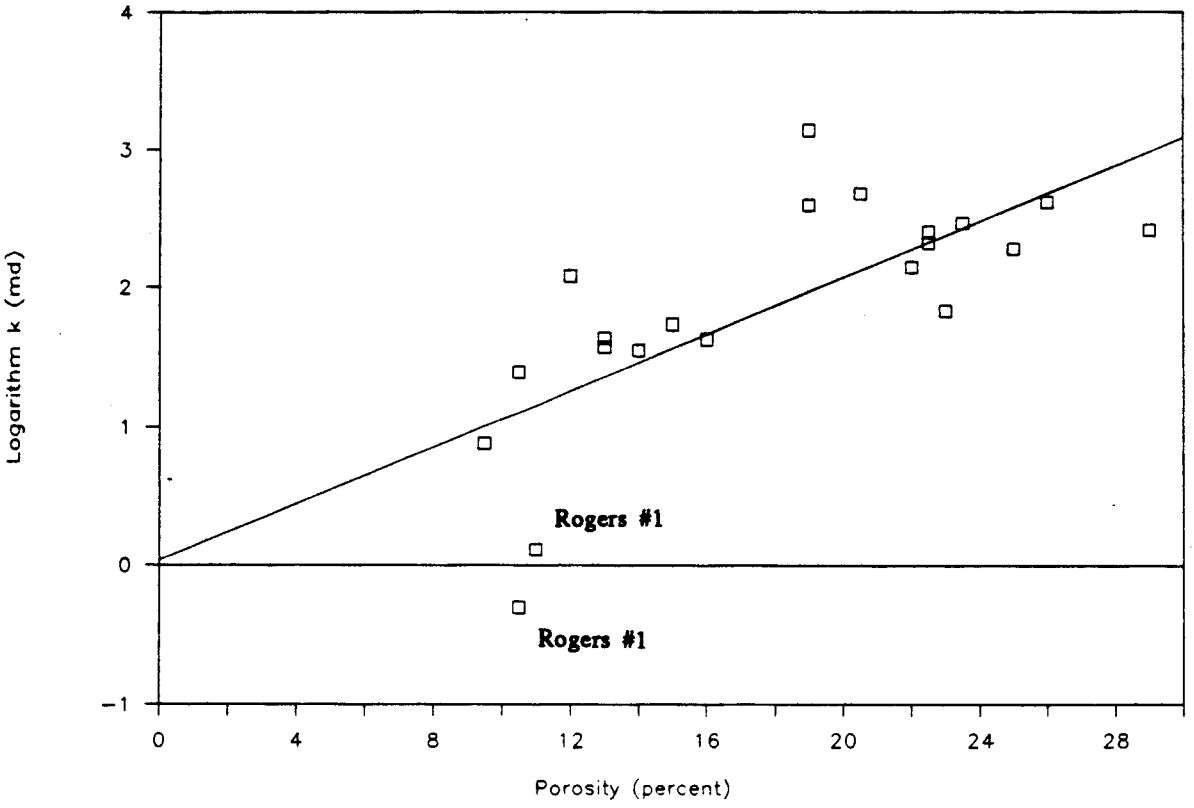

Figure 82. Crossplot of the logarithm of horizontal permeability versus core porosity for the alpha grainstone subunit, with linear regression line calculated by least-squareds method. The plot shows a fair degree of correlation. All core samples used for the crossplot were carefully examined to determine if they were representative of the actual pore network. The samples with elevated porosity values due to shale wash-out, and the samples with induced fractures due to dehydration of clay in the solution seams, were discarded.

Thin section examination of the notable outliers beneath the regression line reveals that these samples all exhibit an anomalous "mold-dominated" pore network. The two samples from the Rogers #1 are by far the most distant outliers.

permeabilities in the range of 0.5 to 4 md.

The two most distant outliers are both from the Rogers #1, a dry hole which lies in an area of the field with anomalous low permeability that apparently isolates this well from the main grainstone reservoir. Several producing wells contain significant amounts of cement J1, but the static reservoir pressures indicate all of the wells producing from the alpha grainstone are in communication. This suggests the pore network in the area of abundant cement J1 in the vicinity of the Rogers #1 is not representative of the field as a whole. Consequently, the Rogers #1 values were removed from the crossplot, and a new correlation line was calculated to determine a more precise porosity-permeability relationship for the main body of the alpha grainstone subunit (Fig. 83).

Several samples that plot below the correlation line on the new crossplot do exhibit fairly significant amounts of cement J1, though not as much as the Rogers #1 samples. These remaining samples of mold-dominated porosity do not form any mappable distribution, or exhibit a characteristic log response. A number of methods exist for estimating the tortuosity of the pore system as defined by the Archie cementation exponent "m" (e.g. Asquith, 1985), but none of these methods are applicable to the Pen Field.

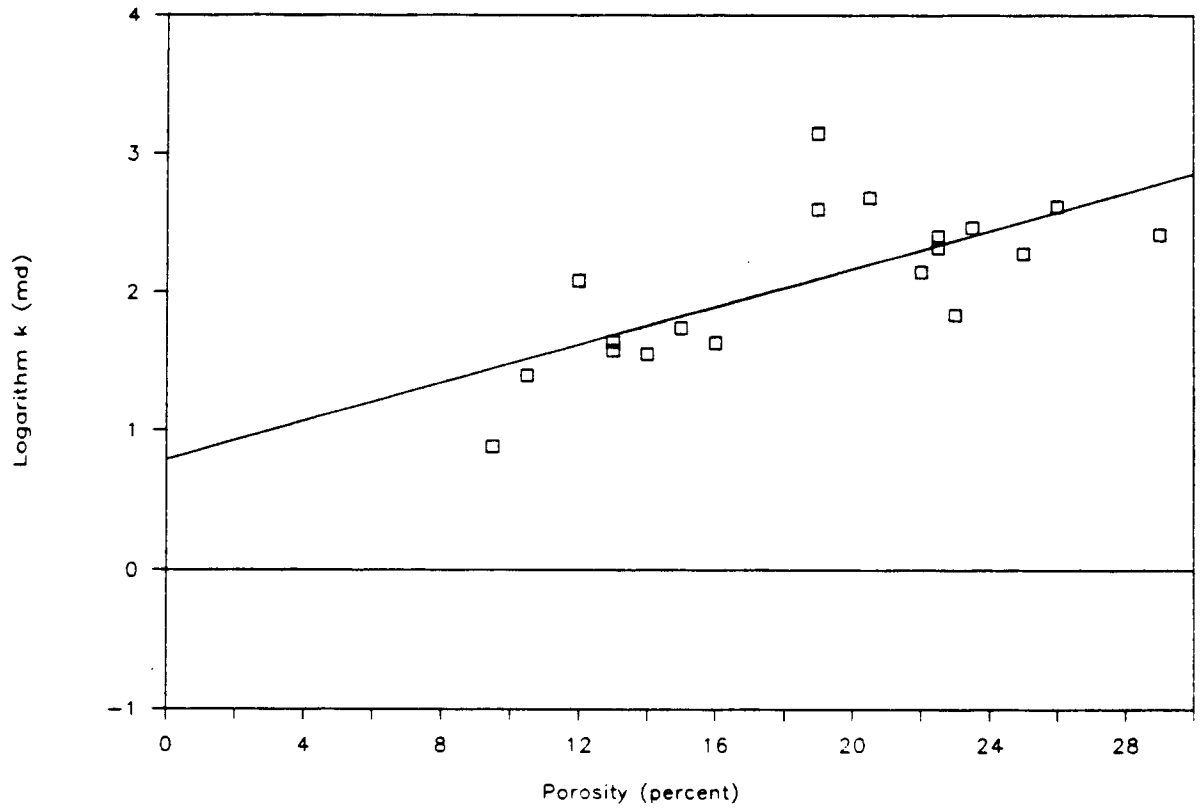

Figure 83. Crossplot of the logarithm of horizontal permeability versus core porosity for the alpha grainstone subunit, with linear regression line calculated by least-squareds method. The data values for the anomalous Rogers #1 are excluded, and this plot reveals a good correlation between permeability and porosity.

Even though regions of mold-dominated porosity exist in the main body of the alpha grainstone reservoir, they are neither large enough, nor sufficiently contiguous to compartmentalize this portion of the reservoir. Unfortunately, the locations of these mold-dominated regions cannot be identified with the available reservoir data. Consequently, the grid block permeability values derived from the porosity correlation may be substantially above the actual values in certain small areas of the field. However, in general the permeability values will be a close approximation of the true permeability in the areas with accurate estimates of porosity.

Log Porosity Versus Core Porosity

Only half of the wells are cored, but compensated neutron and compensated density logs are available for every well in the field. Consequently, reservoir characterization would require less interpolation and probably be more accurate if the log measurements were utilized.

The alpha grainstone subunit contains variable amounts of dolomite which affects porosity log measurements. To compensate for this variable, the log measurements were input into a computer program (T-Log from Terrasciences, Inc.) that utilizes a matrix algebra

equation to solve for the proportions of calcite, dolomite, and porosity. The resulting log porosities show a good correlation to the core porosities, and an even better correlation when the core porosities are described by a three-foot running average to compensate for the vertical resolution of the logging tools (Fig. 84).

Porosity in the alpha grainstone is quite variable across the field, but the grainstone interval typically shows only minor vertical variation of porosity in a single well. Over the alpha grainstone interval as a whole, the averaging of the log porosity tool would tend to compensate for any core porosity variation around the mean for the well. For this reason, no transform was considered necessary for converting log porosity to core porosity. Consequently, the porosity-permeability relationship derived in Figure 83 is considered to be valid for log porosity values. This relationship provides a means of calculating the horizontal permeability of the alpha grainstone interval for every well in the Pen Field.

Alternate Methods of Estimating Permeability

The actual productivity of the reservoir can provide an independent means of estimating permeability, and a test for the validity of the previously derived porosity-permeability relationship. Permeability can be derived

Figure 84. Crossplot of core porosity versus log porosity (A) and crossplot of three-foot running average of core porosity versus log porosity (B). The line at 45° represents core porosity equal to log porosity. Plot A shows a good correspondence between core porosity and log porosity. In plot B the core porosities are described by a three-foot running average to compensate for the vertical resolution of the logging tools. This adjusted plot shows and even better correspondence between core porosity and log porosity.

A

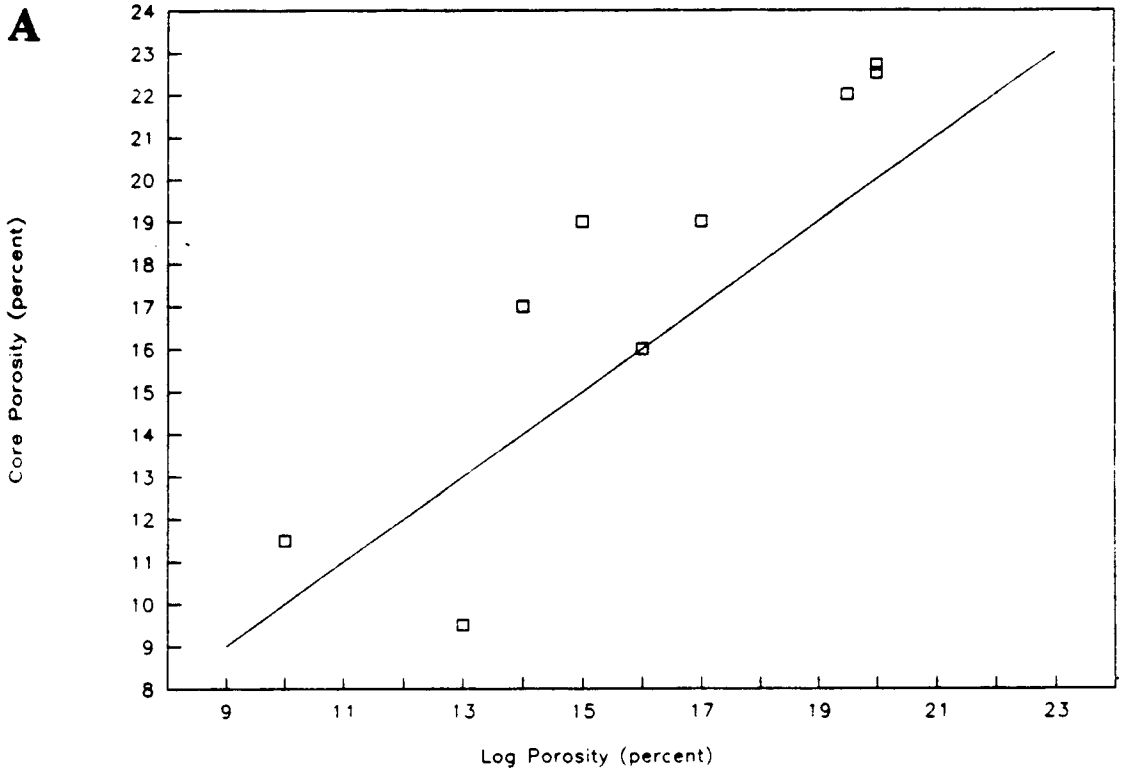
Core Porosity (percent)
Log Porosity (percent)
24
23
22
21
20
19
18
17
16
15
14
13
12
11
10
9
8
9
11
13
15
17
19
21
23

B

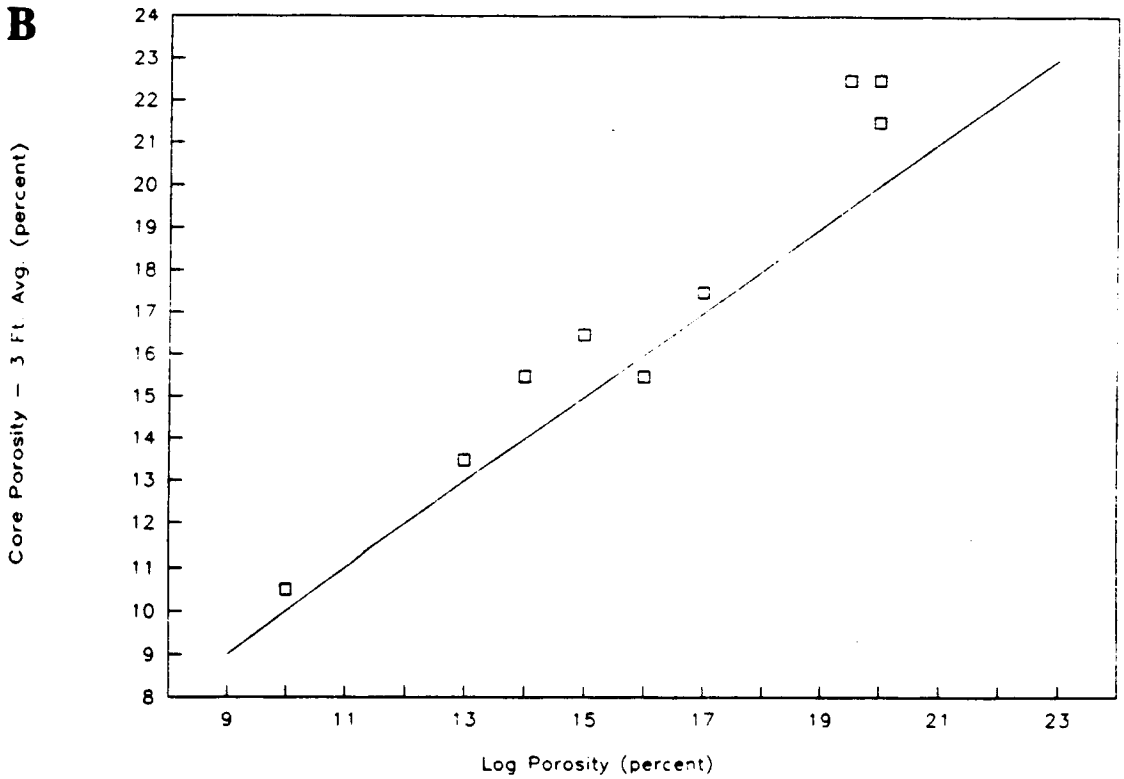
Core Porosity – 3 Ft Avg. (percent)
Log Porosity (percent)
24
23
22
21
20
19
18
17
16
15
14
13
12
11
10
9
8
9
11
13
15
17
19
21
23

from both drillstem tests and initial potential tests by integrating Darcy's equation for radial flow. These methods have the added benefit of measuring permeability over a significant areal distance, rather than only 4 1/2 inches of core. The drawback is that these equations depend on several variables other than permeability.

Utilizing Drillstem Tests

Transmissivity (kh/u) is the most common expression of the effect of permeability on drillstem test recoveries. However, within a small, stratigraphic trap like the Pen Field, viscosity (u) of the oil should be relatively constant. The variables of interest can then be simplified to kh, which can be derived from drillstem test pressure build-up data by the following equation (Maier, 1962):

$$kh = \frac{162.6\, q\, B\, u}{m} \qquad \text{Equation 1.}$$

where, k = permeability, millidarcys
h = net reservoir thickness, feet
q = production rate, stock tank barrels per day
B = formation volume factor, reservoir barrels per stock tank barrel
u = viscosity, centipoise
m = slope of pressure build-up plot, psi per cycle

Many of the drillstem tests in the Pen Field lack useful pressure information because multiple zones were open to the testing tool, so these tests were not analyzed. Kh values were calculated for all of the tests that isolated the alpha grainstone (Appendix 11). Figure 85 shows a comparison of kh derived from core measurements, and kh derived from drillstem tests. The two sets of values exhibit a very poor correlation, and the number of variables makes it difficult to determine the cause of the variations. Consequently, the permeabilities derived from drillstem test data were given little consideration in characterizing the reservoir.

Utilizing Initial Potential Tests

Initial potential is also a function of permeability, and the applicable equation (Amyx, et al., 1960) can be rearranged as:

$$kh = \frac{141.2\, q\mu \ln (re / rw)}{(Pe - Pw)} \qquad \text{Equation 2.}$$

where, k = permeability, millidarcys
h = net reservoir thickness, feet
q = production rate, stock tank barrels per day
μ = viscosity, centipoise
re = radius of external boundary, (units consistent with rw)
rw = radius of well bore, (units consistent with re)
Pe = pressure at external boundary, psi
Pw = pressure at well bore, psi

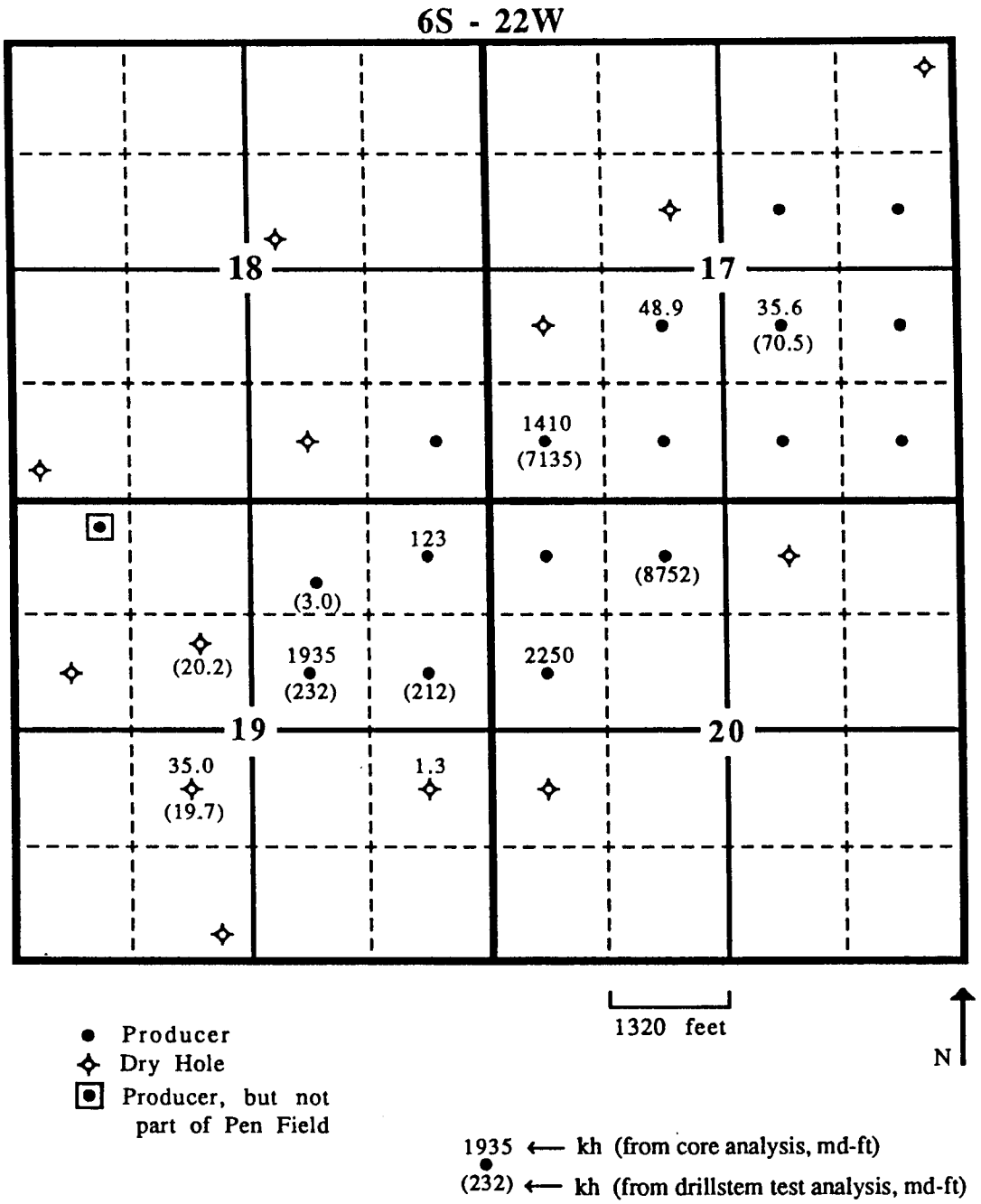

Figure 85. Map of kh values in the alpha grainstone subunit comparing the values derived from core analysis to those derived from drillstem test analysis. The two sets of values show a very poor correlation.

However, a plot of kh derived from initial potential versus kh derived from the porosity relationship shows no apparent correlation (Fig. 86). The commingling of production from multiple pay zones is one obvious source of error, because all of the zones contribute to the initial potential. The multiple pay zones themselves do not increase the estimation error because a unique porosity correlation was used for each reservoir interval (derivations shown in subsequent reservoir characterization sections). Uncertainty in the reservoir pressure term (Pe) utilized in equation 2 is the main source of error. Reservoir pressure at the time of each initial potential test was derived from the alpha grainstone pressure decline plot (Fig. 80) because this interval is the main pay zone of the field, and provides the only available pressure data versus time (Appendix 12). The substitution of the alpha grainstone interval pressure for the true pressures results in a relatively small error when the other zones have been depleted concomitantly with the alpha grainstone and the pressures reduced accordingly. However, wells that open a new zone or compartment will encounter virgin pressures and show an erroneously high kh derived from initial potential. Reservoir characterization of the field identifies three wells that apparently opened new pay. These wells all plotted in the upper left of the data cloud (Fig. 86).

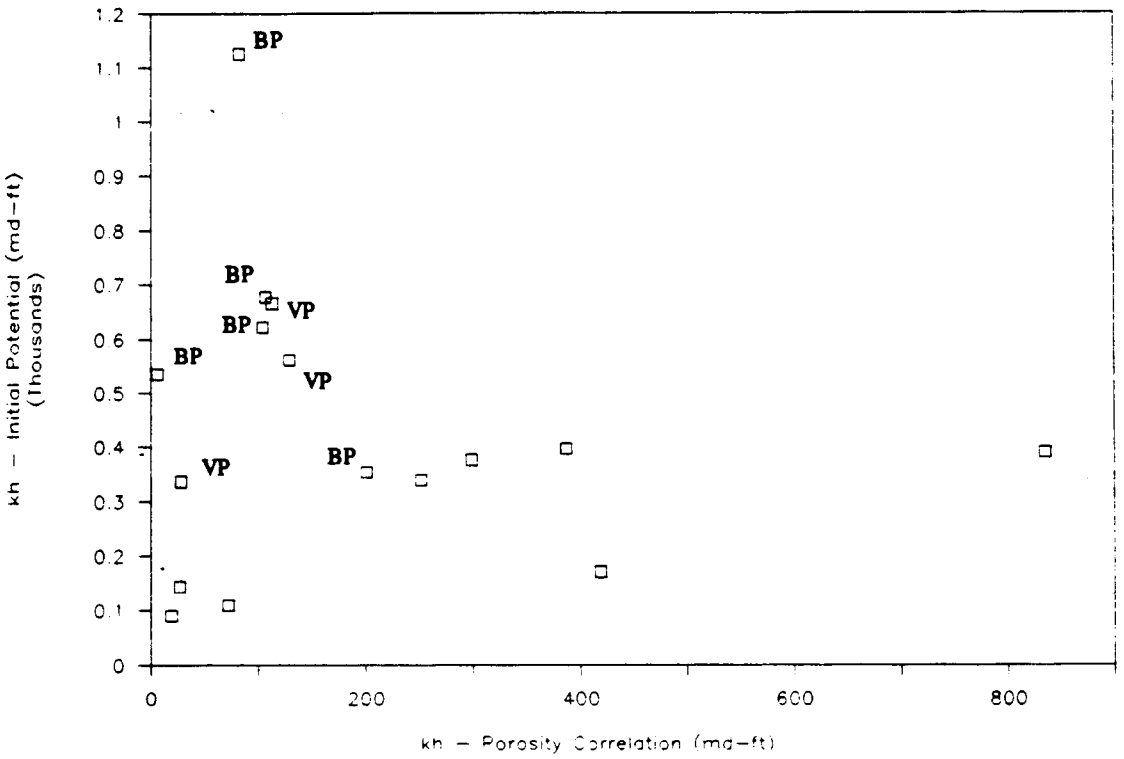

Figure 86. Crossplot of kh values (for all completed zones) derived from initial potential versus those derived from the porosity correlations. The scatter of data suggests there is no correlation. However, the three points marked VP were all completed in a new zone or compartment, and therefore encountered virgin pressures. The five points marked BP were all completed after the bubble point pressure was reached in the alpha grainstone subunit. All of the marked points lie in the upper left corner of the data cloud.

Values for kh derived from initial potential were calculated using equation 2. Values for kh derived from log porosity were calculated using the linear regression equation from the crossplot of logarithm of permeability versus log porosity for each interval. The porosity-permeability correlations for the reservoir intervals are shown in Table 3.

Examination of the data for other factors resulting in a relatively high kh derived from initial potential revealed one other significant anomaly. Every well drilled after the bubble point was reached in the "J" alpha grainstone also plotted in the upper left of the data cloud (Fig. 86). Many of these wells were drillstem tested, and were producing only from the alpha grainstone. Therefore, the reservoir pressure term (Pe) for each well was known quite accurately.

If these wells, and the wells encountering virgin pressures are excluded, the remaining points show a good linear correlation (Fig. 87). However, no theoretical basis exists for exclusion of the post-bubble point wells. High kh values were calculated for these wells because they exhibit anomalous high initial potentials. The opposite should occur as the gas going into solution increases the oil viscosity and decreases the effective permeability to oil. Because of these inexplicable results, the permeability data derived from initial potentials were not used in the reservoir characterization.

Conclusions

The crossplot constructed from core measurements reveals a good correlation between porosity and permeability in the alpha grainstone subunit. Calculated

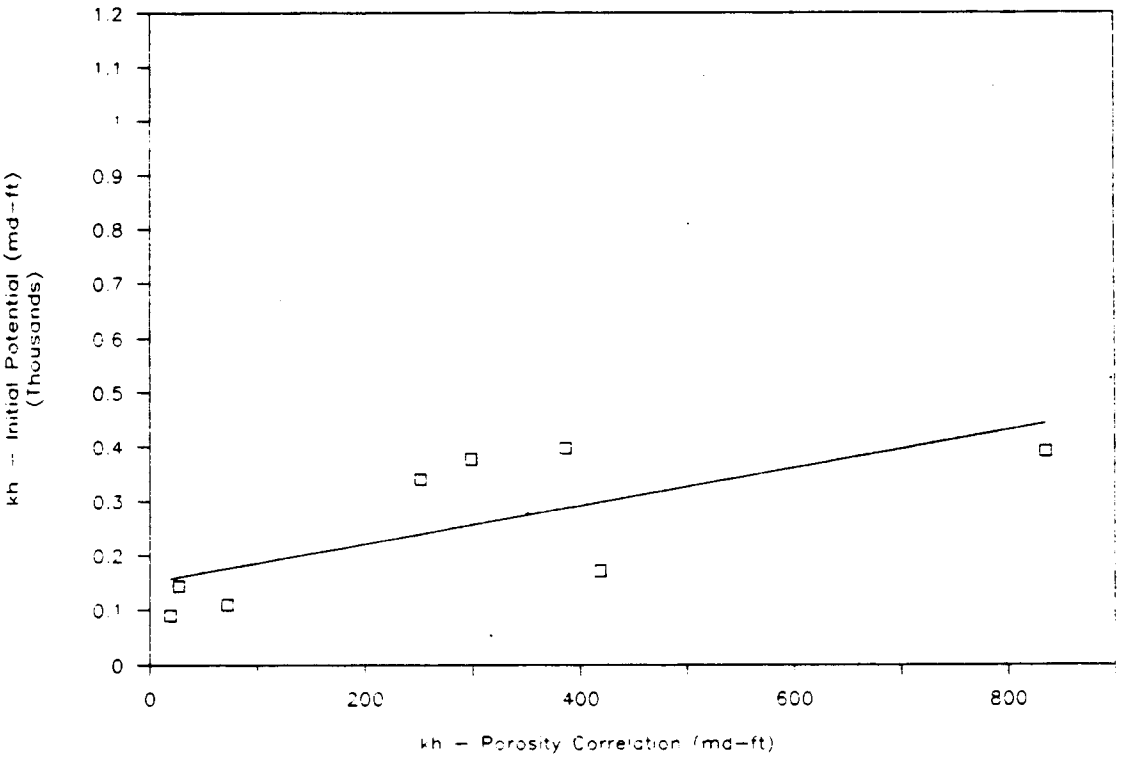

Figure 87. Crossplot of kh values derived from initial potential versus those derived from the porosity correlations, discarding the values for wells encountering virgin pressures, and those drilled after the bubble point was reached in the alpha grainstone subunit. Linear regression line calculated by least-squareds method. The data show a good degree of correlation, but no theoretical basis exists for discarding the post-bubble point wells.

log porosities show fairly good agreement with the core porosities, so the derived porosity-permeability relationship is considered to be valid for log porosity values. Permeability can also be calculated from initial potential tests and drillstem tests, but these values significantly vary from the permeabilities derived from the porosity correlations. The cause of the variations could not be determined, so it appears that the correlation with porosity is the only valid means of estimating permeability in the Pen Field.

The nature of the pore network in the alpha grainstone can significantly alter the relationship between porosity and permeability. The alpha grainstone typically exhibits abundant interparticle porosity supplemented by skeletal molds and oomolds. However, the combination of significant reduction of the interparticle pores with cement J1 and abundant molds, results in a "mold-dominated" pore network that exhibits very low permeability for a given porosity. The occurrence of mold-dominated porosity appears to be restricted primarily to the Rogers lease in the southwest corner of the field. Other areas of mold-dominated porosity cannot be readily mapped, but this type of pore network appears to be volumetrically insignificant in the main body of the alpha grainstone. Consequently, a new porosity-permeability correlation was derived, excluding the

obviously anomalous mold-dominated values from the Rogers #1. This correlation should yield a close approximation of the true permeability in the areas with accurate estimates of porosity.

WATER SATURATION

Reservoir simulation not only requires grid block values for porosity and permeability, but also fluid saturation values. Modern logging tools generally provide accurate means of calculating water saturation. Unfortunately, most of the reservoir intervals in the Pen Field are three feet thick or less. This is below the vertical resolution of deep-investigating resistivity tools which usually have vertical resolution on the order of five feet (Asquith and Gibson, 1982).

Water Saturation Calculated From Wire-Line Logs

In spite of this limitation, water saturations were calculated on a foot-by-foot basis using the Archie equation for all "pay quality" intervals at least three feet thick (Appendix 13). Pay quality is defined as rock with porosity greater than or equal to the porosity in each reservoir interval that corresponds to the one md permeability net-pay cut-off. In general, the calculated water saturations are in agreement with oil shows from the cores. Core saturations typically provide only a

crude indication of water saturations due to flushing of oil ahead of the core bit, and the loss of fluids between the reservoir and the core lab. However, the agreement with the saturations calculated from logs indicates that the logs can provide at least a rough estimate of water saturations in the reservoir.

The comparison of core and log calculated saturations does reveal several anomalies. The one foot intervals of pay adjacent to shale units consistently exhibit calculated water saturations of 100%. Core analysis of these intervals reveals significant oil saturation. Apparently, the low resistivity of the shale affects the measurements of the deep resistivity tool, resulting in erroneous saturation values.

The one foot intervals of pay adjacent to tight carbonate also exhibit anomalous values. These one foot intervals of pay exhibit extremely low calculated water saturations that are not consistent with the other calculated water saturations. The low values are apparently due to the high resistivity of the adjacent impermeable carbonate. However, the one foot intervals of pay adjacent to intervals of porous, but non-pay carbonate (3-7% porosity), exhibit calculated water saturations that are consistent with the core data and the other water saturation values calculated from logs.

Therefore, with certain exceptions, it appears that

foot-by-foot water saturation values can be calculated for zones at least three feet thick in the Pen Field. The values for one foot intervals adjacent to either shale or tight carbonate, and certain intervals obviously at odds with core and test data were discarded.

Water Saturation Calculated From A Porosity Correlation

Even resolution of intervals with only three feet of pay is insufficient for estimating water saturation for the thin porous zones that make up the bulk of the Pen Field pay. Although no general correlation is applicable to all fields, "an approximately linear correlation between [water saturation] and the logarithm of permeability exists for each individual field" according to Amyx, et al. (1960, p. 152). However, serious departures from linearity commonly occur because water saturation is also strongly affected by the capillary pressure relationships in the reservoir.

Capillary pressure is a function of height above the free water surface, saturation history, the fluids and solids involved, the size and distribution of pores, and the fluid saturation itself. Saturation history and the fluids and solids involved can be regarded as relatively invariant for a single reservoir. Saturation can be disregarded since it is the object of the analysis, leaving only height and pore type as the main variables.

Figure 88 shows that, in the region above the transition zone, permeability is the dominant control on water saturation whereas height above the free water surface is of only minor importance.

Unfortunately, permeability cannot be calculated directly from log data. However, it was previously demonstrated for the "J" alpha grainstone subunit that the logarithm of permeability is a function of porosity. Consequently, water saturation should also be a function of porosity for intervals with relatively invariant capillary conditions. Obviously if capillary conditions in an interval are variable, saturations for a given porosity could vary from irreducible water saturation to 100% water saturation. The resulting crossplot would exhibit a random scatter.

To test if water saturation is a function of porosity in the Pen Field, a plot of water saturation versus porosity was constructed for the alpha grainstone subunit, and for all other zones with sufficient data. The resulting plots are not linear, instead exhibiting tails at both very low and very high porosity values, yielding a concave-upwards distribution. To eliminate these tails, the plots were reconstructed with water saturation versus the inverse of porosity. These plots exhibit a surprising degree of correlation (Fig. 89; 90; 91; 92). The high degree of correlation for each

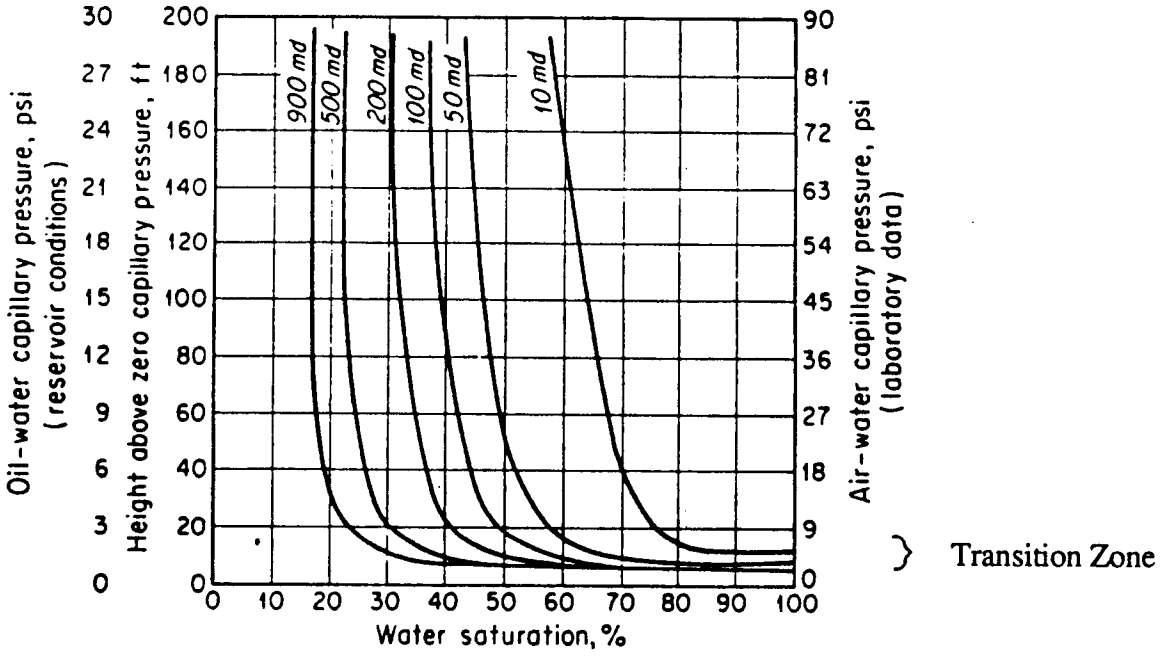

Figure 88. Reservoir fluid distribution curves. For the region above the transition zone, permeability is the dominant control on water saturation, whereas height above the free water surface (level of zero capillary pressure) is of only minor importance. The ordinate on the right reflects values of capillary pressure determined by displacing water with air in the laboratory. The ordinates on the left include the corresponding oil-water capillary pressure that would exist at reservoir conditions and the corresponding height above the free water surface. (Adapted from Amyx, et al., 1960.)

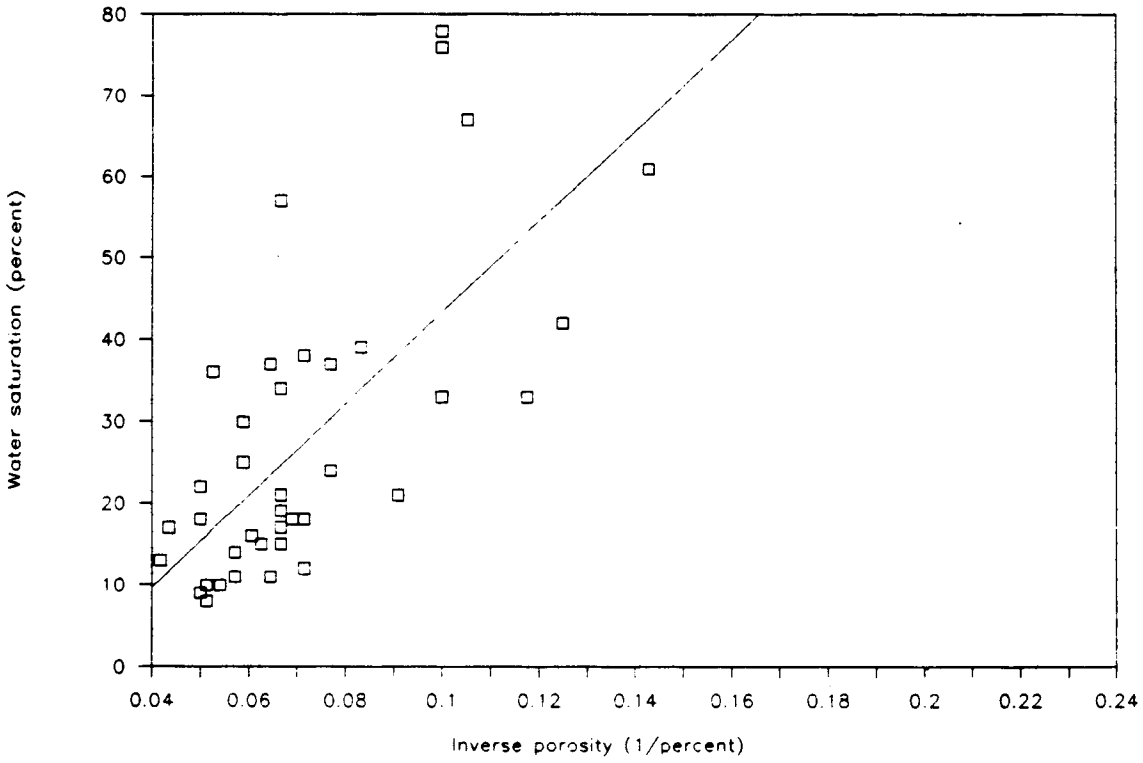

Figure 89. Crossplot of water saturation versus inverse porosity for the alpha grainstone subunit, with linear regression line calculated by least-squareds method. Both values are calculated from wire-line logs. Water saturation shows a correlation with inverse porosity, but there is a significant amount of scatter.

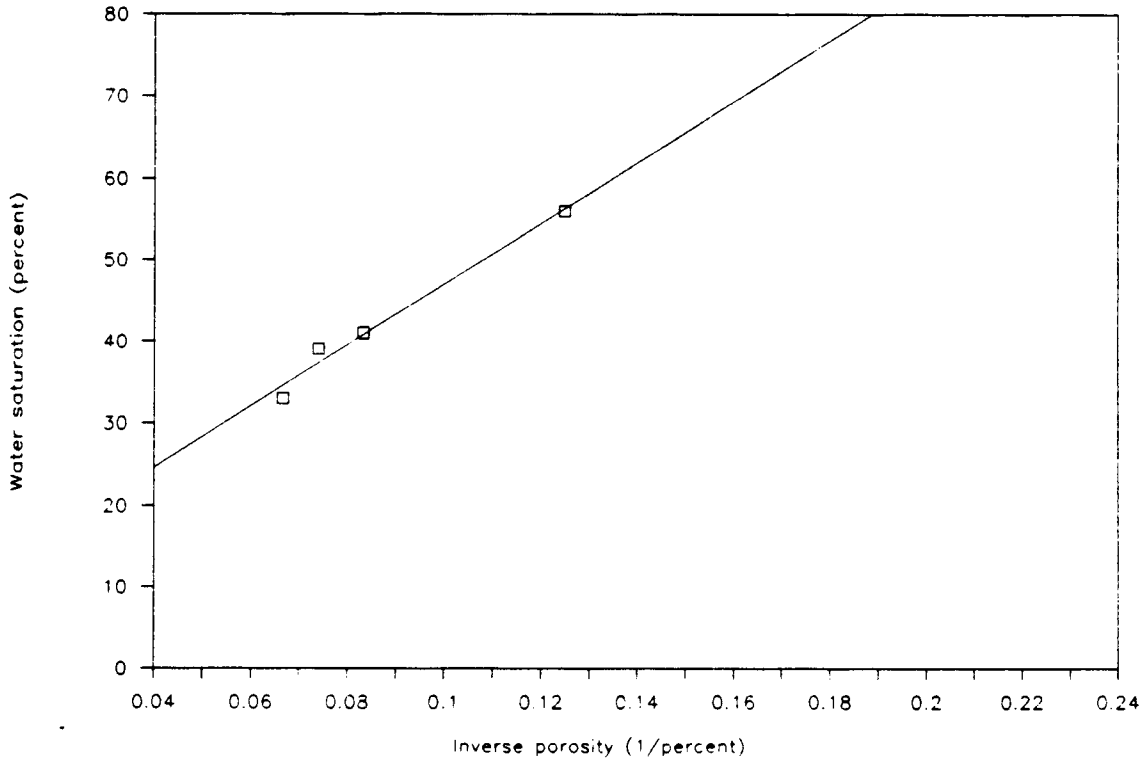

Figure 90. Crossplot of water saturation versus inverse porosity for the "D" zone, with linear regression line calculated by least-squareds method. Both values are calculated from wire-line logs. This plot reveals a good correlation for the four available data points.

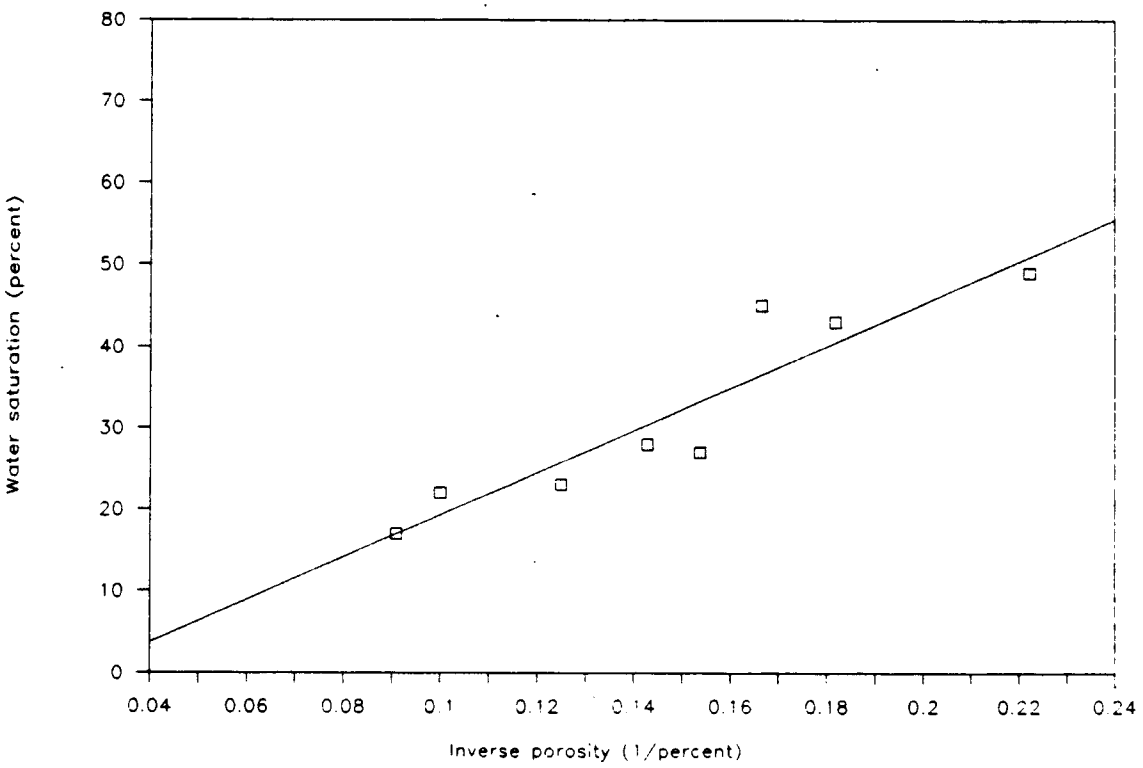

Figure 91. Crossplot of water saturation versus inverse porosity for all lithologies in the "I" zone, with linear regression line calculated by least-squareds method. Both values are calculated from wire-line logs. This plot reveals a good correlation, though the data are obviously few.

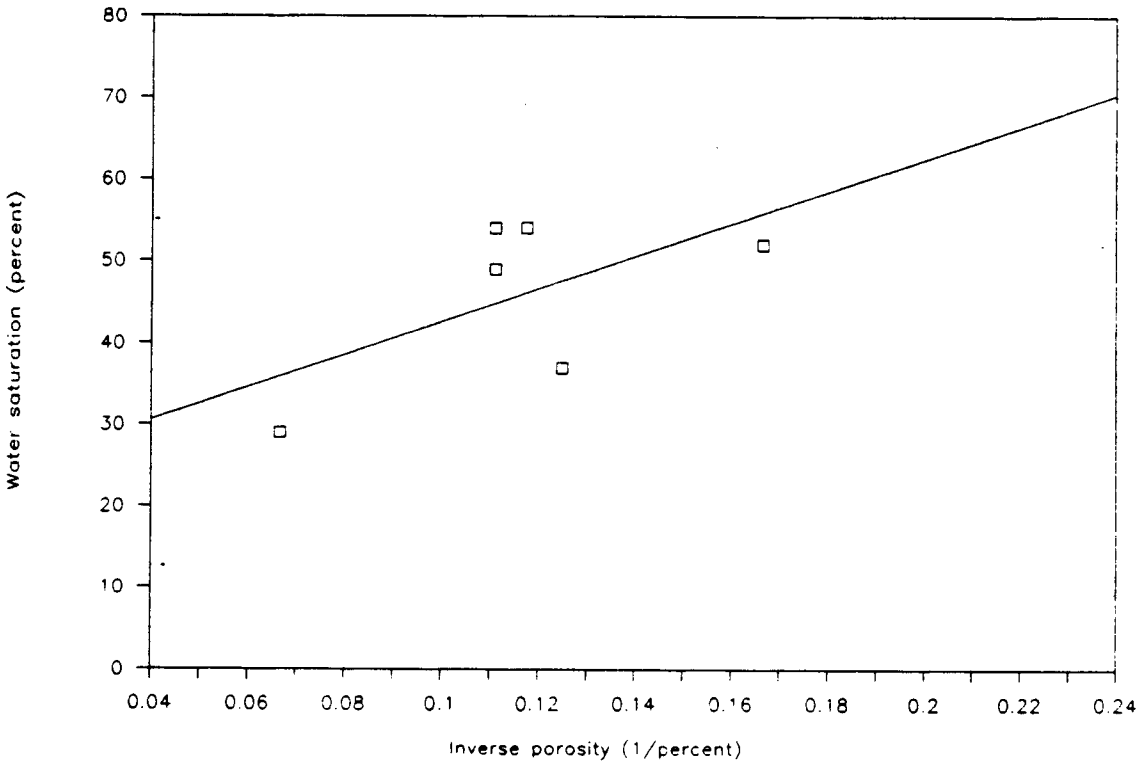

Figure 92. Crossplot of water saturation versus inverse porosity for both productive subunits in the "K" zone, with linear regression line calculated by least-squareds method. Both values are calculated from wire-line logs. This plot reveals a fair correlation.

reservoir interval suggests the foot-by-foot water saturations calculated from the logs are very reliable estimates of the true water saturations. If the estimates were only approximate due to measurement errors in the log values of porosity and Rt, the plotted values would exhibit a degree of random scatter and the plots would show only low degrees of correlation.

The high degree of correlation also indicates the intervals exhibit relatively invariant capillary conditions, because it was previously shown that water saturation is not a function of porosity for intervals with variable capillary conditions. The alpha grainstone produces little water and lacks a water leg, suggesting it does not lie in the transition zone, and the reservoir is at irreducible water saturation. In this state, capillary pressure will increase with increasing height above the free water table, but the capillary distribution of water will not change. Consequently, the water saturation-inverse porosity crossplot should accurately reflect only the saturation changes due to changes in the pore network. At irreducible water saturation, the only pore water exists as an immobile boundary layer that is of relatively uniform thickness for a given oil-water-mineral system. Because the water is in boundary layers, the water saturation is dependent on the surface area in the pores. Porosity is dependent

on the volume of the pores. For roughly spherical pores, the volume increases with the cube of the pore size, whereas the surface area only increases with the square of the pore size. Other pore geometries have slightly different relationships, but overall, as porosity increases, the percentage of pore volume occupied by the bound water layer shows a relative decrease, resulting in a lower water saturation. The correlation equation for each reservoir interval quantifies the rate of relative decrease in water saturation for increasing porosity for the pore network unique to that interval.

Figure 89 shows the crossplot for the "J" zone alpha grainstone and the corresponding correlation line, but also reveals some scatter of the data. As previously shown in Figure 88, water saturation not only depends on the pore system, but also height above the free water table. If capillary conditions in the interval are near the slope change at the top of the transition zone, structural elevation may be a secondary control on water saturation and cause the scatter observed in Figure 89. A function herein termed "relative water saturation" was derived to determine if the scatter in the water saturation correlation is due to height above the free water surface.

$$S_{W(R)} = \frac{S_{W(ACH)} - S_{W(CRL)}}{S_{W(ACH)}} \qquad \text{Equation 3.}$$

where, $S_{W(R)}$ = relative water saturation, dimensionless

$S_{W(ACH)}$ = water saturation calculated from wireline logs using Archie equation, fractional

$S_{W(CRL)}$ = water saturation calculated from the porosity correlation, fractional

If water saturation is strongly dependent upon height in the reservoir, high elevations should exhibit water saturations calculated from the Archie equation less than the porosity correlation estimate, resulting in large negative values for relative water saturation. At low elevations the converse should be true, resulting in large positive values for relative water saturation. A plot of elevation versus relative water saturation is shown in Figure 93, and exhibits a seemingly random scatter. Therefore, water saturation is not significantly affected by height in the reservoir. Apparently, the scatter in the water saturation-inverse porosity crossplot is due to measurement errors in the log-derived values of porosity and Rt, as well as variations in the pore network of the alpha grainstone subunit.

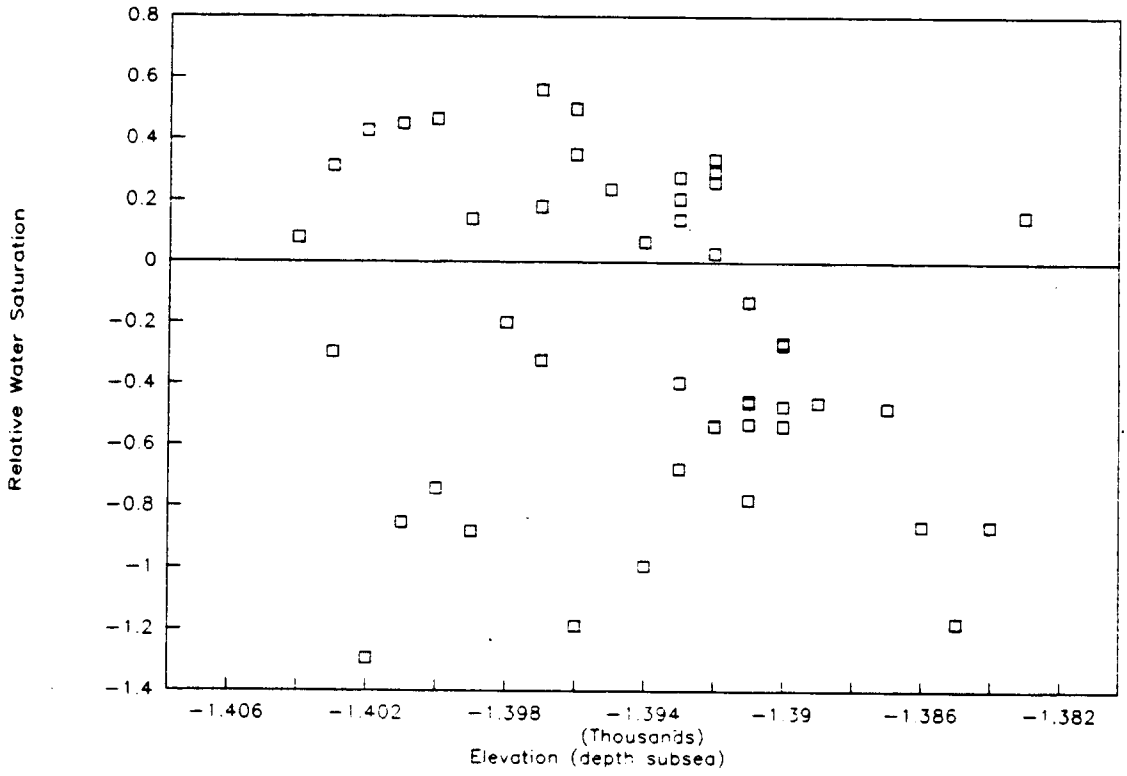

Figure 93. Crossplot of "relative water saturation" ($Sw_{(R)}$) versus elevation for the alpha grainstone subunit. If water saturation is dependent on height in the reservoir, then the plot should show negative relative water saturation values at high elevations and positive values at low elevations. The data cloud shows an essentially random scatter, indicating water saturation is a dependent variable of porosity, and is not significantly affected by height in the reservoir.

Conclusions

The agreement between the core saturations and the saturations calculated from logs indicates water saturation can be roughly estimated on a foot-by-foot basis for intervals of porous rock at least three feet thick. Unfortunately, most of the pay intervals in the Pen Field are less than three feet thick. However, water saturation appears to be a function of porosity. Crossplots of water saturation versus inverse porosity exhibit a good correlation for every reservoir interval with sufficient data for a plot. The high degree of correlation suggests that the foot-by-foot water saturations calculated from logs are very reliable estimates of the true water saturations. A test of the data for the alpha grainstone subunit indicates that water saturation is not significantly affected by height in the reservoir.

RESERVOIR CHARACTERIZATION OF THE "I" ZONE

CONTINUITY AND COMMUNICATION

Like the "J" zone, production in the "I" zone comes mainly from a grainstone facies with primary interparticle porosity. The isopach map of the "I" zone grainstone shows three distinct depositional lobes, indicating the grainstone is not continuous across the field (Fig. 94). Further, the development of grainstone in the "I" zone does not necessarily indicate pay quality rock. Cements may reduce porosity to only 2 to 3 percent as in the Shuck #1 and White #1, or shale infilling in alteration pores may reduce permeability to less than one millidarcy as in the Rogers #1.

The net-pay map reflects the loss of these areas of "non-pay" grainstone, and suggests the eastern depositional lobe may be divided into two separate compartments by diagenetic effects (Fig. 95). Reservoir pressure measurements from drillstem tests could confirm this compartmentalization, but no tests were taken with the "I" zone isolated. However, the initial potential tests might outline possible compartments. It was previously shown that anomalous high permeability derived from initial potential tests indicates compartments with virgin pressures.

The field discovery well (the Pennington #1) was

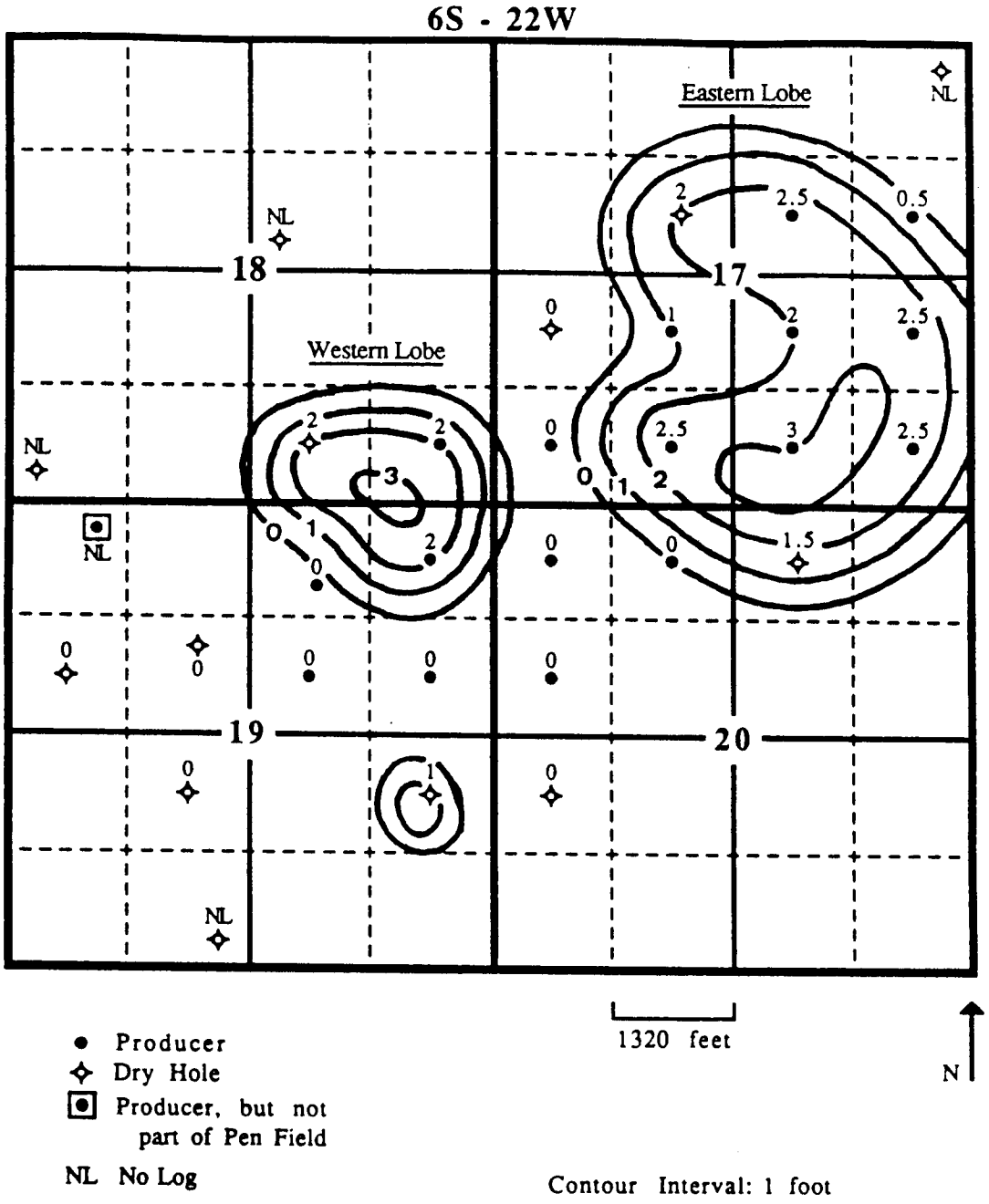

Figure 94. Isopach map of the grainstone interval of the "I" zone. Intervals in uncored wells with log porosity of 5% or greater, and permeability on the microlog, were interpreted as grainstone.

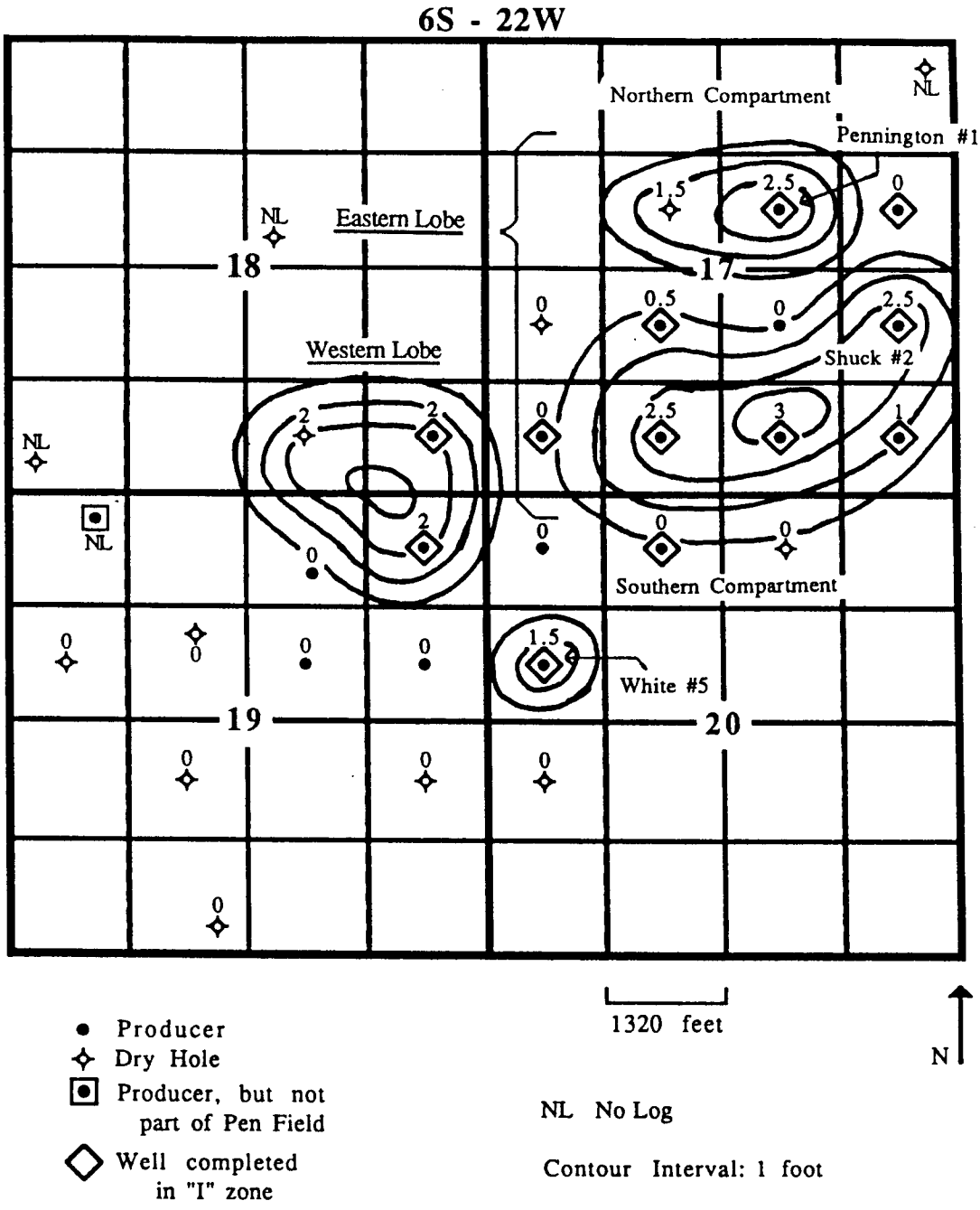

Figure 95. Net-pay map of the "I" zone with a porosity cut-off of 5%. Cementation and shale-infilling result in areas of non-pay grainstone with less than 5% porosity. This porosity reduction appears to have divided the eastern depositional lobe of grainstone into two separate reservoir compartments.

completed in the "I" and "J" zones, draining the northern compartment of the eastern lobe of the "I" zone. The Shuck #2 was also completed in the "I" and "J" zones, but was the first well draining the large southern compartment of the "I" zone (Fig. 95). The Shuck #2 showed an anomalous high kh derived from initial potential, because the well had an initial potential of 120 BOPD, the third highest value in the field. The total reservoir volume of net pay for this well is relatively low (Fig. 107), so the high initial potential is probably due to encountering virgin pressure in the "I" zone. This is consistent with the interpreted diagenetic compartmentalization of the eastern lobe of grainstone.

The net-pay map (Fig. 95) also reveals 1.5 feet of pay in the White #5, even though this well lacks grainstone. The wackestone in the well has sufficient vugs and skeletal molds to provide "pay quality" rock, with 6% porosity and a permeability of 5 md. The grainstone isopach map was primarily constructed from core observations, but for uncored wells it was assumed that any well exhibiting log porosity of 5% or greater, and an indication of permeability on the microlog, contained grainstone. The White #5 opens the possibility that some of the mapped net pay for the uncored wells may be from porous wackestones.

A final complication arises from the well-to-well variability of the allochems and the stratigraphic position of the "I" zone grainstones. Cored wells in the middle of the field that lack grainstone indicate the "I" grainstone was apparently deposited as three distinct depositional lobes (Fig. 94). However, the variability of the grainstones in adjacent wells suggests the grainstones within a "depositional lobe" might not even be genetically related. If several unrelated grainstones do occur within a depositional lobe, and the grainstone bodies are not at all superposed, the generally impermeable muddy lithologies of the "I" carbonate unit would form a permeability barrier between these grainstones.

The geologic nature of the "I" zone therefore results in great uncertainty in the reservoir characterization of this interval. The possibility of diagenetic compartmentalization, wackestone "pay" being mistakenly mapped as grainstone, and genetically unrelated grainstone bodies may result in compartmentalization of the "I" reservoir interval in addition to that already shown in Figure 95. The three possible types of compartments are graphically depicted in Figure 96.

Single-zone drillstem tests provide a means of outlining the reservoir compartments, but the common

Figure 96. Three types of compartmentalization in the "I" reservoir interval. The geologic nature of the "I" zone indicates a number of processes may alter the continuity and communication of the reservoir interval in the Pen Field. The examples depict the possibilities that exist for a cored well with two feet of porous grainstone adjacent to an uncored well with a two foot interval exhibiting log porosity greater than 5% and an indication of permeability on the microlog.

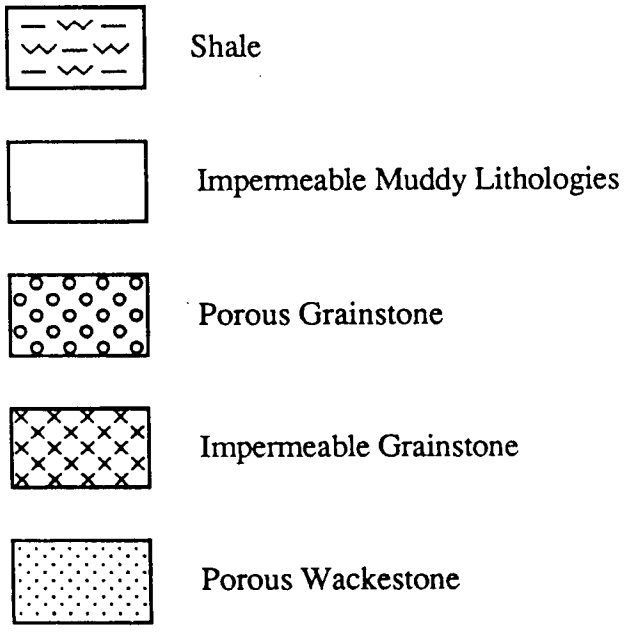

Cored Well Uncored Well

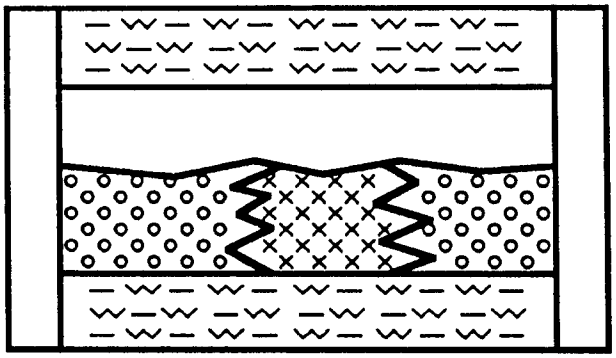

Region of impermeable grainstone formed by cement reduction of interparticle pores (as in Shuck #1 and White #1), or by formation of autoclastic breccia and fissures and subsequent infilling with shale (as in Rogers #1).

A. Unrecognized Compartment Formed by Diagenetic Effects Not Encountered by a Well-Bore

Cored Well Uncored Well

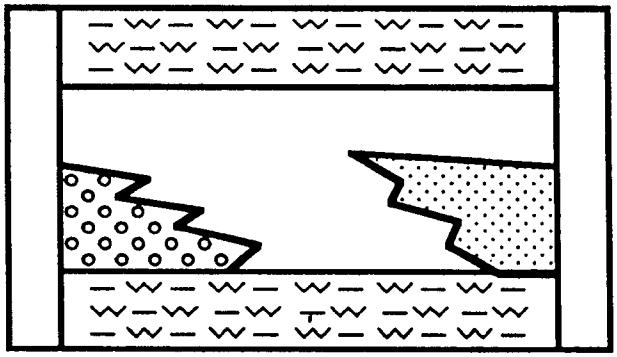

Porous wackestone (as in White #5) separated from the grainstone by the impermeable muddy lithologies that make up the bulk of the "I" carbonate unit.

B. Unrecognized Compartment Because Wackestone Pay in an Uncored Well Was Erroneously Mapped as Grainstone.

Cored Well Uncored Well

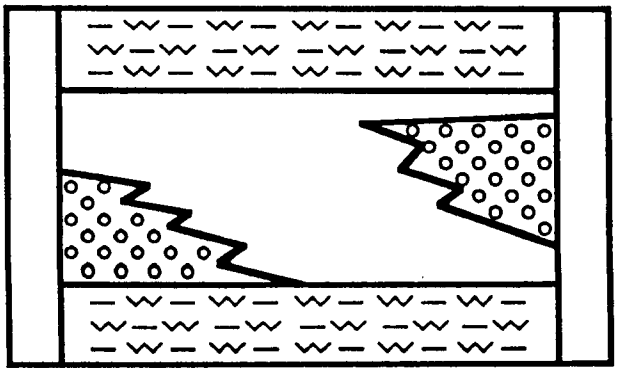

Unrelated grainstones are separated by the impermeable muddy lithologies that make up the bulk of the "I" carbonate unit.

C. Unrecognized Compartment Because Grainstone Deposits Were Not Identified as Genetically Unrelated.

practice in western Kansas is to take multiple-zone tests in the Lansing-Kansas City. Lacking pressure data, a reservoir interval with complications similar to those in the "I" zone could still be effectively exploited during waterflooding. By restricting injection to a single zone, the areas of communication could be readily delineated by careful monitoring of the production response and perhaps a few simple tracer tests.

POROSITY AND PERMEABILITY

The grainstones in the "I" zone all exhibit significant cement reduction of the interparticle pore space. Porosity is somewhat enhanced by a moderate number of skeletal molds and a few vugs. The maximum core porosity in the "I" zone is 9%, but one uncored well exhibits log porosity up to 11%. The maximum horizontal permeability is 43 md.

The pore network in the grainstone is composed primarily of partially occluded interparticle pores. This results in relatively small pores, but the porosity is very well connected, so significant permeability may exist at low porosities (Fig. 97). Consequently, the net-pay cut-off as defined by 1 md of permeability occurs at approximately 5% porosity. Only four good measurements of porosity and permeability were available for the "I" zone grainstones, but a plot of the logarithm of

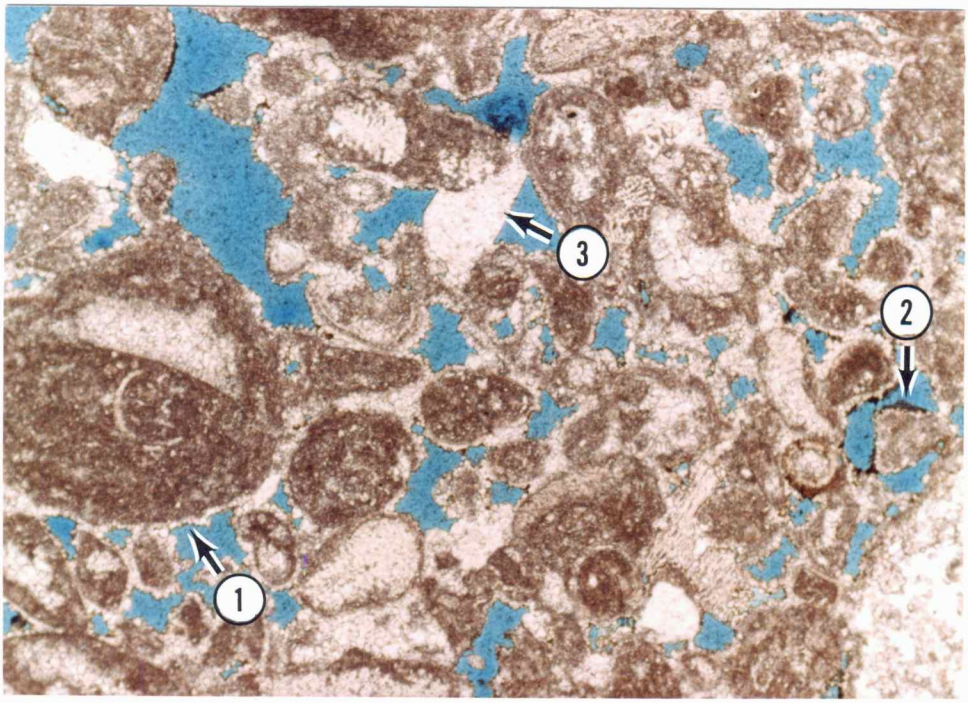

Figure 97. Plane polarized-light photomicrograph of the pore network in an "I" zone grainstone. (Thin section impregnated with blue epoxy.) In this photo, the interparticle porosity is only moderately reduced by rims of cement I1 (arrow 1), clay and silt (arrow 2), and cement M1 (arrow 3). The resulting pore network is very well connected, so significant permeability may exist at low porosities. This sample has a whole core porosity of only 5.6%, yet it still exceeds the permeability cut-off with a whole core horizontal permeability of 4.7 md.

This photo does not show any molds, although a few exist throughout the "I" zone grainstones. The grainstones in both the "I" and "J" zone exhibit only moderately reduced interparticle porosity. However, the "J" alpha grainstone subunit typically exhibits much better sorting, and consequently, significantly higher interparticle porosity. (Carbonate unit, "I" zone; Demuth #1, 3803 feet.)

permeability versus core porosity does show an excellent correlation (Fig. 98).

The wackestone pay of the White #5 exhibits a pore network of abundant small vugs with a few large molds, which superficially resembles the pore network in the grainstones. The core measurement for the wackestone was added to the permeability-porosity crossplot, and showed a good correlation to the grainstone data (Fig. 98). It is not possible to differentiate between grainstone and wackestone in the uncored wells in the "I" zone, so this combination plot probably gives the most useful relationship for permeability as a function of porosity.

WATER SATURATION

The assumptions that water saturation can be accurately calculated from wire-line logs on a foot-by-foot basis in relatively homogenous intervals of three feet or more, and that water saturation is primarily a function of porosity, appear to be valid in the alpha grainstone subunit of the "J" zone. Consequently, the methods used in the characterization of the "J" alpha grainstone were applied to the "I" zone. The crossplot of water saturation versus inverse porosity for both "I" zone productive lithologies shows a good degree of correlation and supports the validity of the assumptions (Fig. 91).

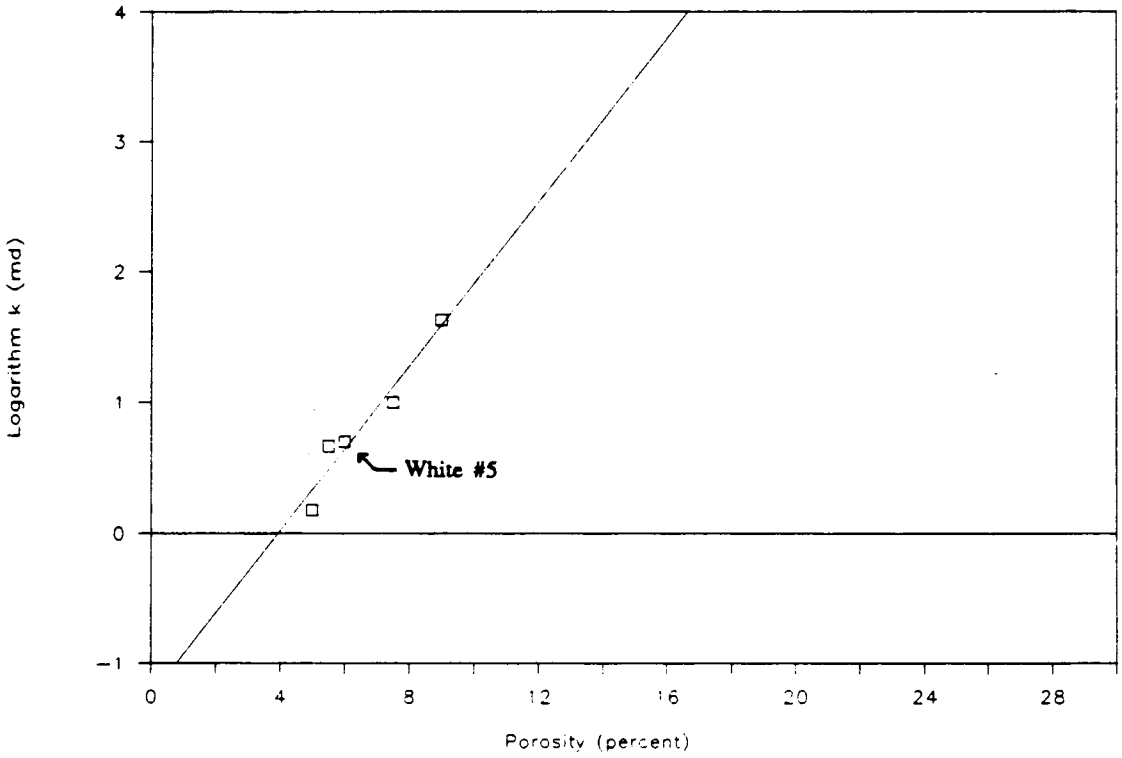

Figure 98. Crossplot of the logarithm of horizontal permeability versus core porosity for all productive lithologies in the "I" zone, with linear regression line calculated by least-squareds method. Four of the data points are from grainstones, but the porous wackestone from the White #5 is included. Surprisingly, the porosity-permeability relationship in the wackestone closely matches the relationship for the grainstones. All core samples used for the crossplot were carefully examined to determine if they were representative of the actual pore network. The samples with elevated porosity values due to shale wash-out, and the samples with induced fractures due to dehydration of clay in the solution seams, were discarded. This plot reveals an excellent correlation between permeability and porosity, though the data are obviously few.

RESERVOIR CHARACTERIZATION OF THE MINOR PAY INTERVALS

"D" ZONE

The "D" zone is only productive in one well, the Pennington #2 (Fig. 99). No cores were available for the zone, but the Pennington #2 log shows four feet of pay with porosities ranging from 8 - 15%. The calculated water saturations range from 33 - 56%.

The Pennington #2 had an initial potential (IP) of 20 barrels of oil and 21 barrels of water per day, the only IP test in the field exhibiting significant water production. The "D" and "J" zones are commingled in the well-bore, but the "J" zone shows no water elsewhere in the field, so the water production must come from the "D" zone.

The crossplot of water saturation versus inverse porosity shows a good degree of correlation, though only four data points were available (Fig. 90). It was previously shown that water saturation is a function of porosity only for intervals with relatively invariant capillary conditions. Water production indicates the "D" zone is not at irreducible water saturation. However, the data points in the crossplot are from a single well, representing four continuous feet of pay. Except for the very base of the transition zone, capillary pressure changes across a four foot increase in height above the

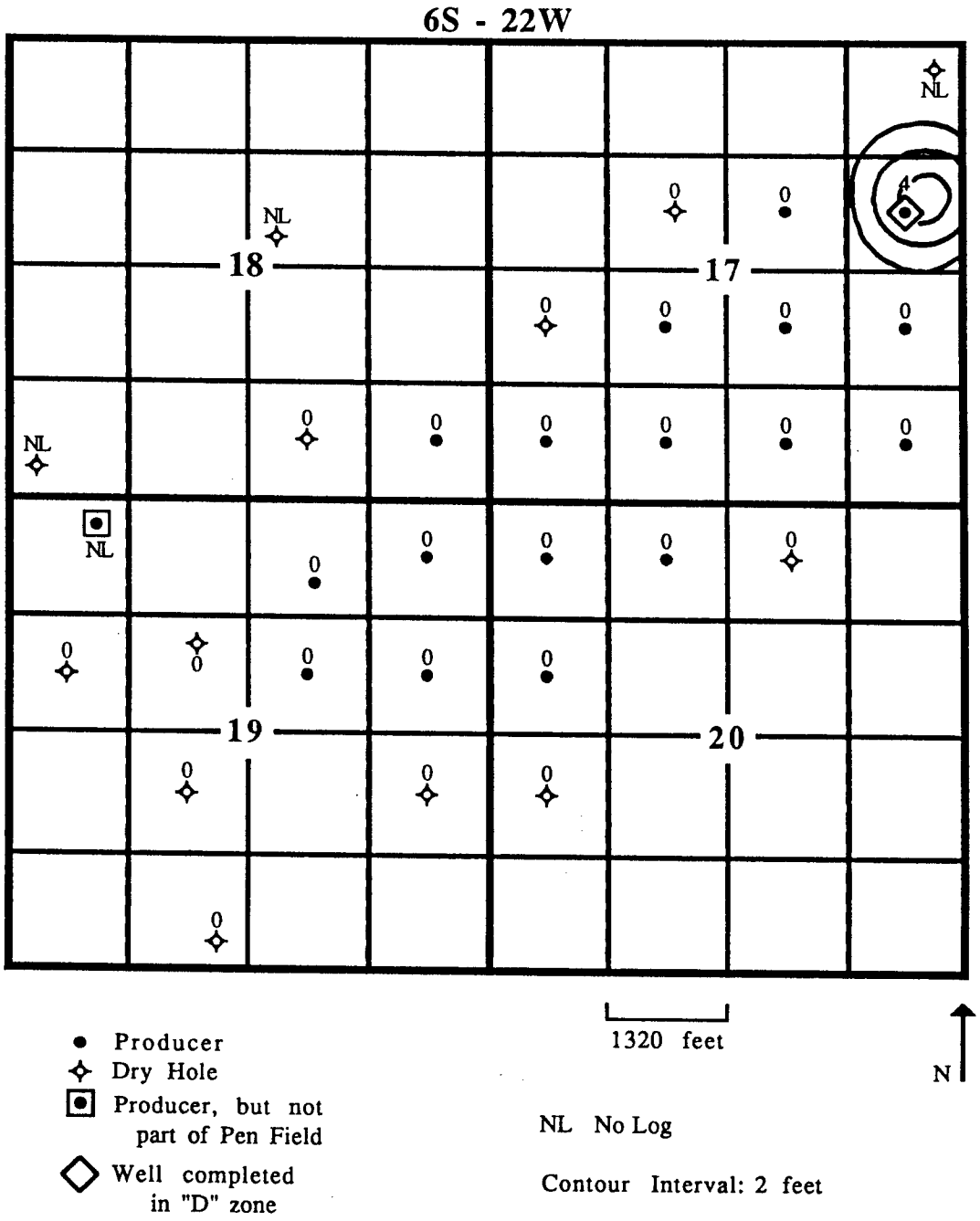

Figure 99. Net-pay map of the "D" zone. The Pennington #2 is the only well in the field that exhibits porosity in the "D" zone.

free water surface would be minor (Fig. 88).

The "D" zone is probably porous over only 10-30 acres around the well-bore of the Pennington #2. The "D" zone exhibits gentle structural relief in the Pen Field, so the relief across the small porous area is probably less than five feet. Consequently, capillary conditions are probably relatively invariant across this area, and the water saturation-inverse porosity correlation can be applied to this pore volume.

The potential productivity of the "D" zone is difficult to determine because no drillstem test covered the zone. The "D" zone was swab tested separately in the Pennington #2 and had a final rate of four barrels of fluid per hour with an oil cut of 40%. It is not possible to determine the exact "D" zone contribution in the Pennington #2 since the production is commingled, but the "D" zone contribution to cumulative field production is insignificant because the well has only produced 6,300 barrels of oil through April, 1990.

"J" CAP SUBUNIT

Several lithologies in the "J" upper carbonate unit other than the alpha grainstone are productive. However, these pay intervals are thin, with relatively low porosity and permeability. The contribution to cumulative field production from these intervals is

insignificant.

The cap subunit contains pay in only three wells. The Pennington #1 and Shuck #4 each have a pay interval only one foot thick. The pay interval is only .5 feet thick in the Bethell #5 (Fig. 100).

The core of the Shuck #4 indicates the pay interval consists of a dolomite wackestone with moldic, vug, and a little intercrystalline porosity. The core measurements are not representative of the pore network due to wash-out from some shale-filled alteration pores. Porosity is roughly 8%, estimated visually from the core and thin sections. Permeability is probably only in the 1 - 10 md range due to the poorly-connected pore network and the shale-filled fissures.

The Pennington #1 and Shuck #4 both lack the alpha grainstone subunit. The cap subunit pay in these wells is probably isolated from the main body of alpha grainstone by impermeable, micrite-rich carbonate lithologies. As a result, these areas of pay in the cap subunit form discrete, one-well compartments that have no waterflood potential.

The pay in the Bethell #5 also consists of a dolomite wackestone with moldic and vug porosity. The core measurements are not representative of the pore network because the whole core sample included two lithologies. The cap subunit pay in this well lies

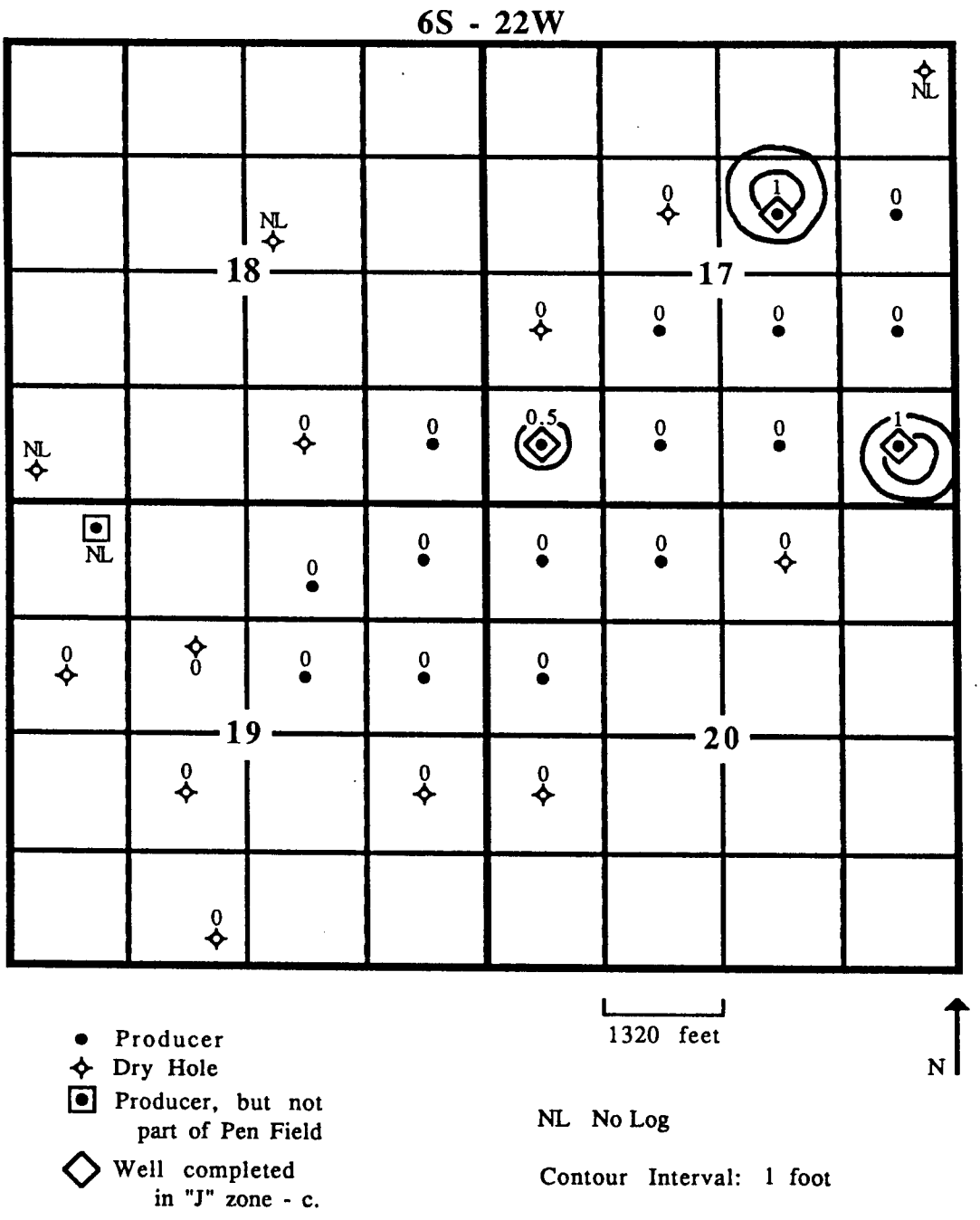

Figure 100. Net-pay map of the "J" zone cap subunit. This map reveals three compartments of pay, which occur in the Pennington #1, Shuck #4, and Bethell #5. The pay interval in the Bethell #5 directly overlies pay in the alpha grainstone subunit. These two intervals are interpreted to be communicating in the well, therefore the cap subunit pay in the Bethell #5 is deleted from the cap subunit interval in the simulation grid, but included in the alpha grainstone subunit interval.

directly on top of pay in the alpha grainstone subunit. The two intervals appear to be in communication, so the cap subunit pay in this well was not assigned to the separate reservoir interval reserved for the cap subunit in the simulation grid. Instead, it was simply added to the alpha grainstone interval.

"J" BETA MICRITE-RICH AND BETA GRAINSTONE-PACKSTONE SUBUNITS

The "J" subunits below the alpha grainstone are productive in two wells, the Bethell #5 and Pennington #2 (Fig. 101). The Bethell #5 exhibits two feet of pay in the beta micrite-rich subunit. The pay consists of wackestone with 8 to 9.5% moldic and vug porosity and 4 to 5 md horizontal permeability. This pay is isolated from the alpha grainstone in the well by 3.5 feet of tight carbonate with horizontal permeabilities ranging from .07 - .39 md and vertical permeabilities ranging from .02 - .04 md.

The Pennington #2 contains 1 foot of pay in the beta micrite-rich subunit similar to the pay in the Bethell #5, and .5 feet of pay from the beta grainstone-packstone subunit. The core measurements were not representative of the pore network, but porosity is visually estimated to be 8% in the beta micrite-rich subunit, and 12% in the beta grainstone-packstone subunit. These two intervals

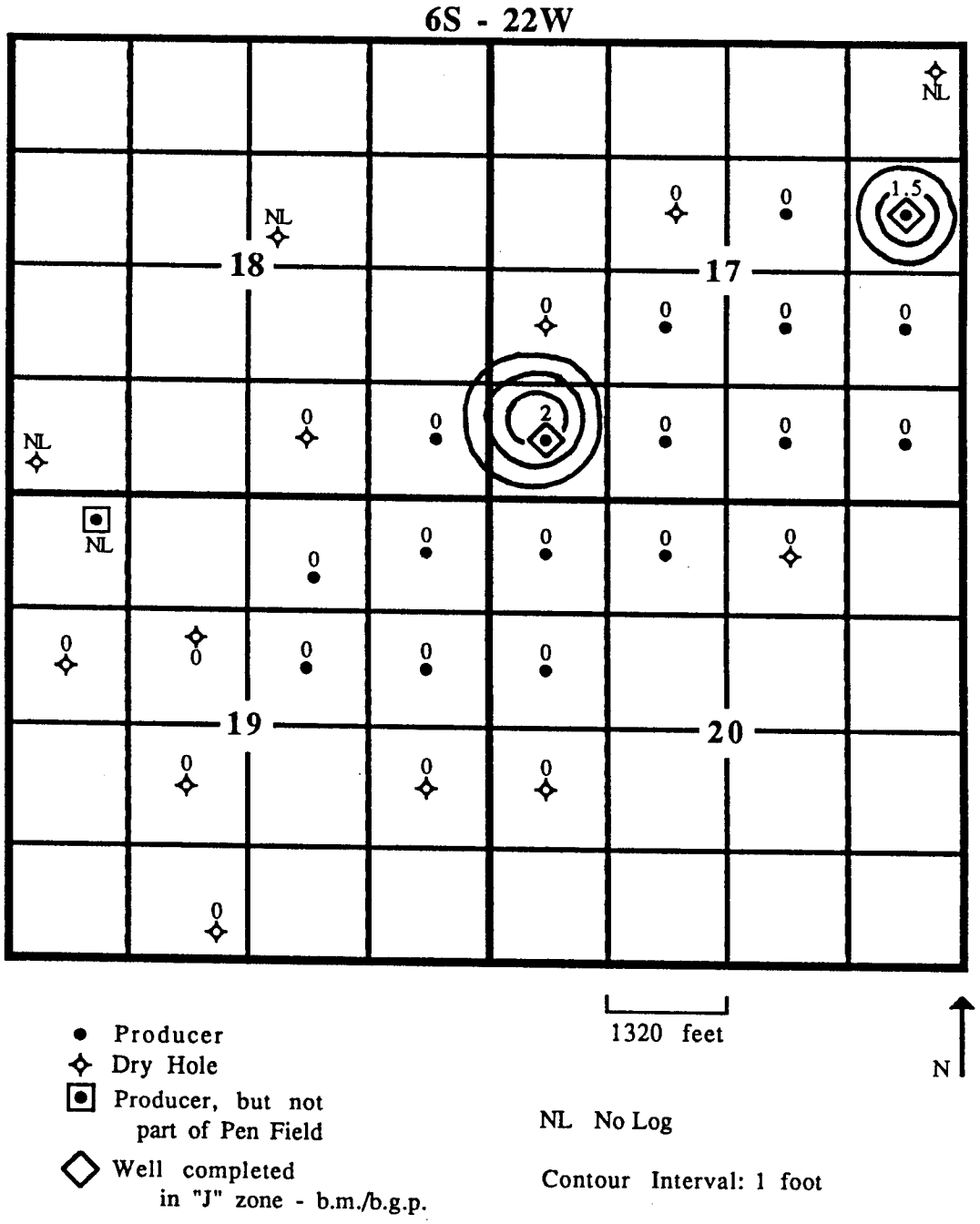

Figure 101. Net-pay map of the "J" zone beta micrite-rich and beta grainstone-packstone subunits. This map reveals two isolated compartments of pay, which occur in the Pennington #2 and the Bethell #5.

are isolated from each other by tight carbonate, and probably isolated from the alpha grainstone body since it is absent in this well. Like the "J" cap subunit pay intervals, the "J" pay intervals below the alpha grainstone appear to form isolated, one well compartments.

Evidence from the Sleepy Hollow Field in Red Willow County, Nebraska indicates the intervals of tight carbonate can form effective seals between reservoir intervals within a single carbonate unit. Lower "beta" porosity developments in some of the Lansing-Kansas City upper carbonate units were not originally perforated during development of the field. On recent rework operations, Amoco perforated the "beta" porosity and encountered virgin reservoir conditions (Watney, personal communication, 1990).

"K" ZONE

Production in the "K" zone is obtained from two separate intervals in the upper carbonate unit, the capping carbonate subunit and the basal carbonate subunit (Fig. 12). In both subunits, pay is from a grainstone with small interparticle pores and a few molds. These two subunits form separate reservoirs since they are separated by the shale subunit that is continuous across the field.

The basal carbonate subunit is productive in three wells, the White #2, #4, and #5 (Fig. 102). The capping carbonate subunit is only productive in the White #4 and #5 (Fig. 103). Core analysis in the "K" zone indicates 6.5% porosity corresponds to the 1 md net-pay cut-off for both reservoir intervals. The net-pay map of the basal carbonate subunit indicates that porous grainstone extends well beyond the area drained by the three wells completed in this interval (Fig. 102). The grainstones occur at the same stratigraphic position in each well, and probably represent only two large grainstone bodies. The larger eastern lobe (Fig. 102) provides a possible target for additional oil; primary recovery through recompletions, and secondary recovery through waterflooding.

The grainstone of the capping carbonate subunit is of only limited areal extent (Fig. 103). The two White lease completions will probably recover most of the primary reserves, and the interval is probably too thin for economic waterflooding.

The quality of pay in the two "K" zone grainstone intervals is difficult to evaluate with the available core data and limited petrographic study. The maximum core porosity is 11.5% and the maximum horizontal permeability is 22 md. No drillstem tests isolating the "K" zone were taken, but swab tests during completion

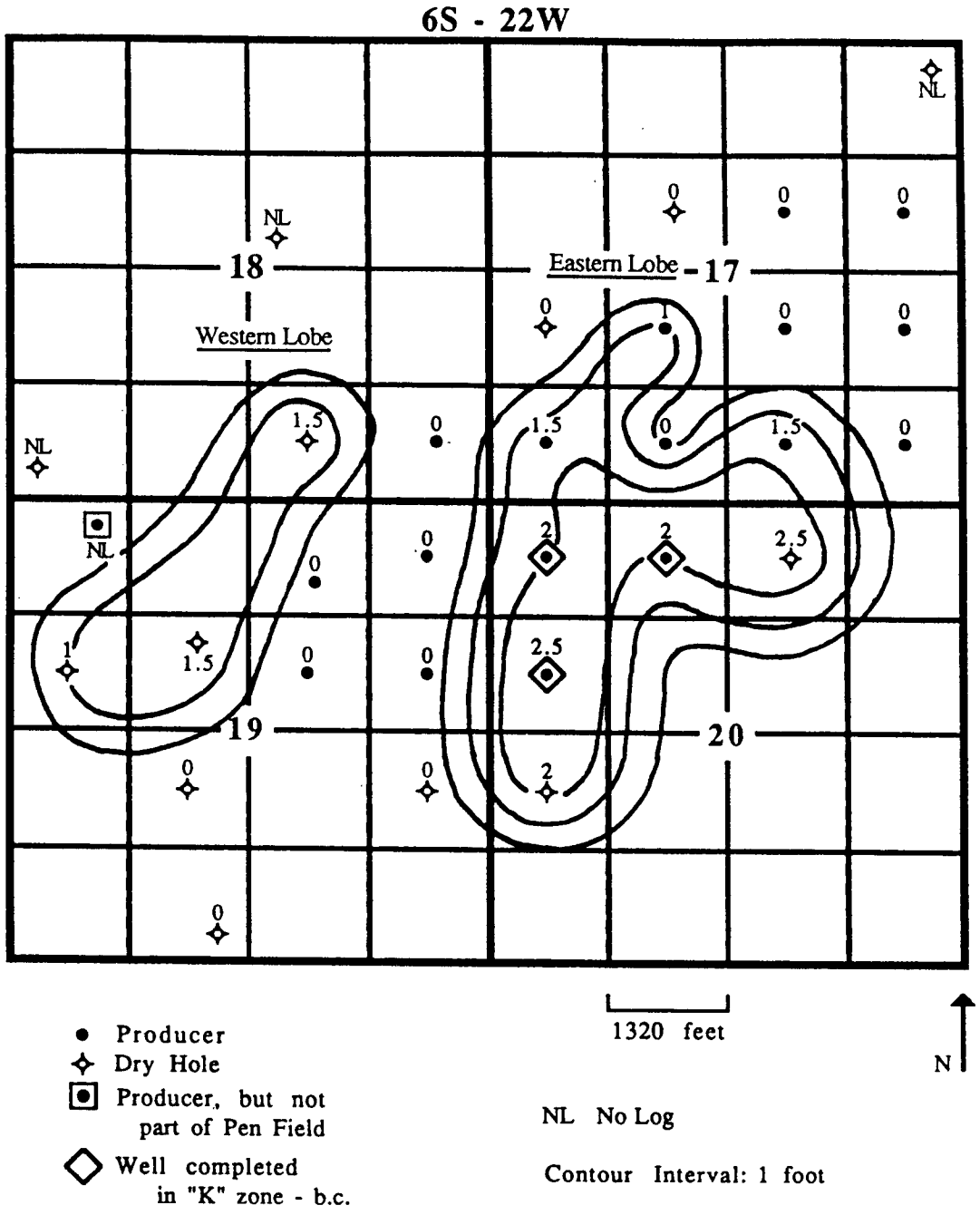

Figure 102. Net-pay map of the "K" zone basal carbonate subunit. This map reveals two distinct bodies of grainstone pay.

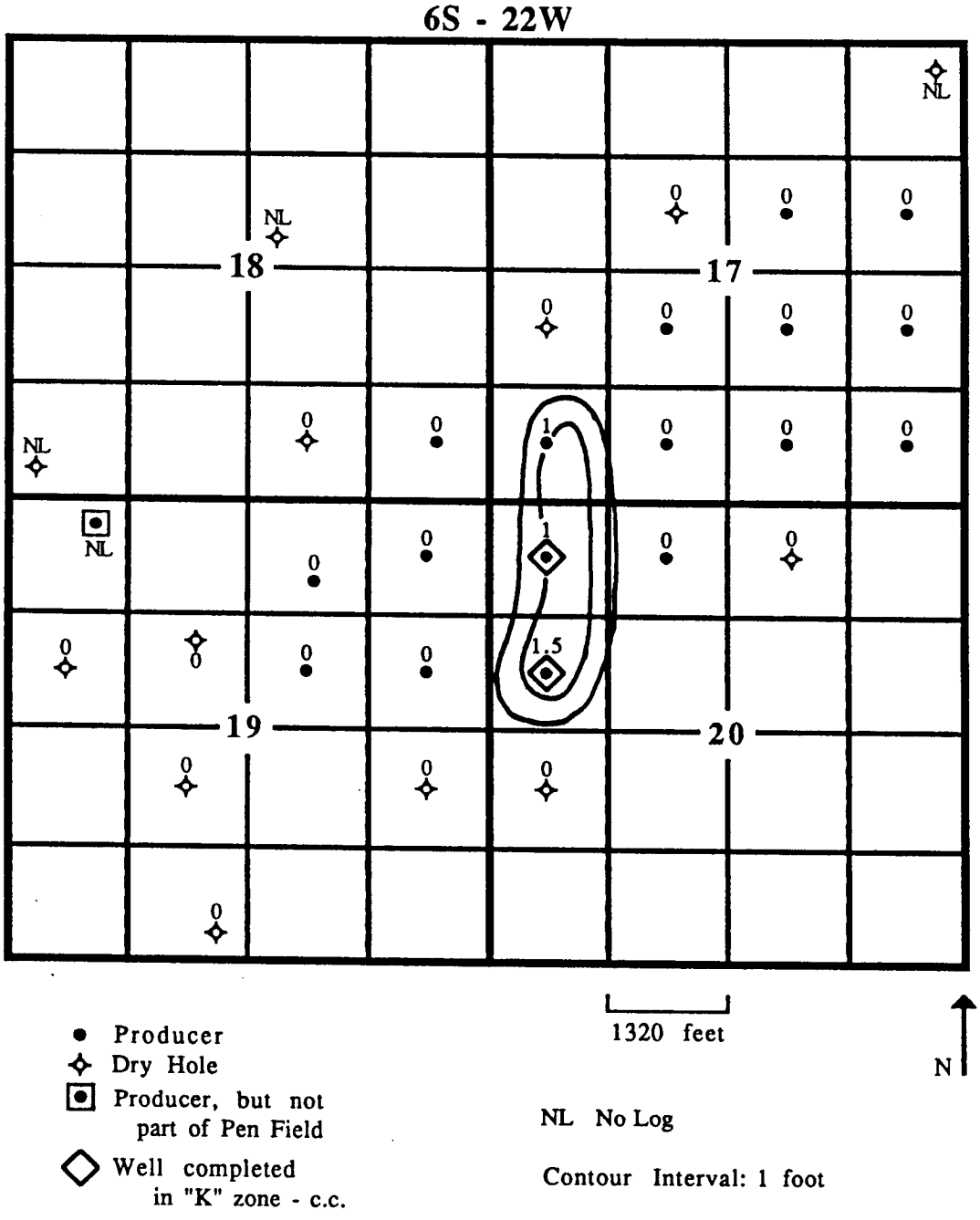

Figure 103. Net-pay map of the "K" zone capping carbonate subunit. This map reveals a single continuous body of grainstone pay.

operations showed good oil recoveries. The final test in the White #4 recovered 27 barrels of oil per hour (BOPH) with both intervals open. In the White #5 the final test recovered 19 BOPH with both intervals open. The "K" and "L" zones were tested together in the White #2, and the final test recovered 25 BOPH. These recoveries indicate the "K" zone makes a significant contribution to cumulative field production, but it is not possible to determine the exact production due to commingling with other zones.

Data for correlations relating permeability and water saturation to porosity are sparse for the "K" zone, so the data from the two reservoir intervals were combined. Figure 104 shows wide scatter of the permeability data, but it does reveal a definite trend of increasing permeability with increasing porosity, similar to the relationships observed in the grainstones of the "I" and "J" zones. Figure 92 shows some scatter of the water saturation data, but the trend is similar to the trends in the "D", "I", and "J" zones, so was interpreted as a valid relationship. The correlations from the two crossplots are only rough approximations, but they provide the best means of estimating "K" zone permeability and water saturation across the field.

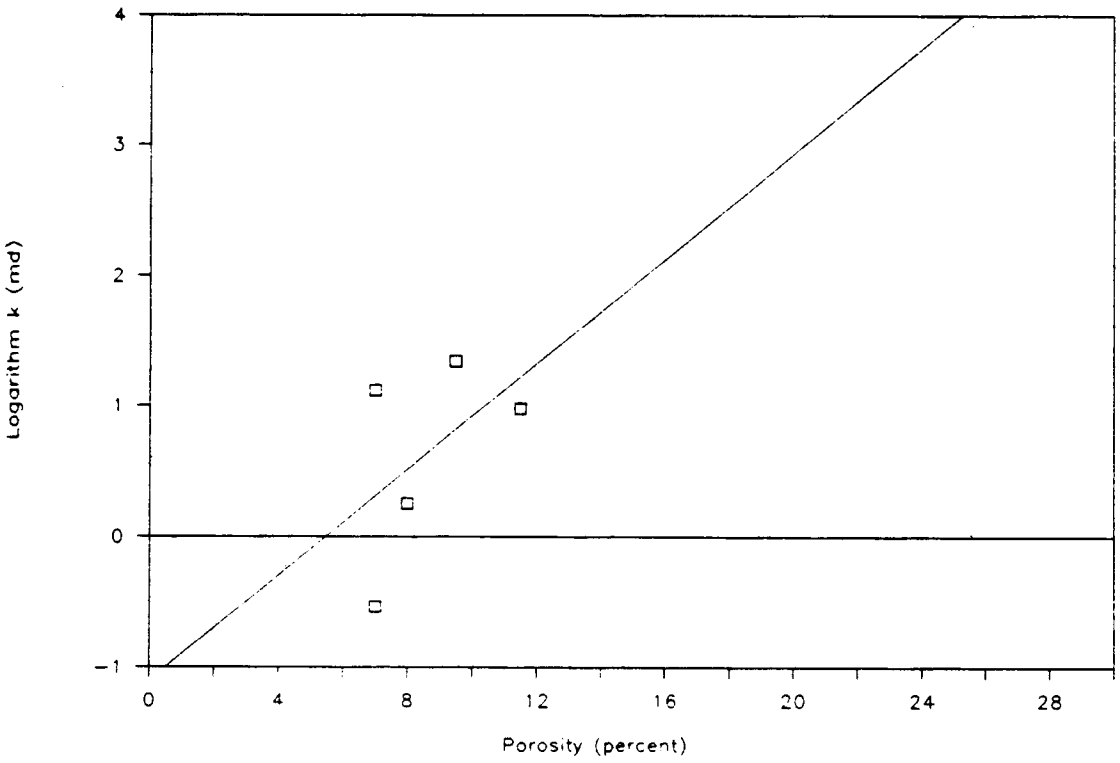

Figure 104. Crossplot of the logarithm of horizontal permeability versus core porosity for both productive grainstone subunits in the "K" zone, with linear regression line calculated by least-squareds method. All core samples used for the crossplot were carefully examined to determine if they were representative of the actual pore network. The samples with elevated porosity values due to shale wash-out, and the samples with induced fractures due to dehydration of clay in the solution seams, were discarded. The data for this plot are few, but there is a trend of increasing permeability with increasing porosity similar to the relationships observed in the grainstones of the "I" and "J" zones.

"L" ZONE

The "L" zone is productive in only two wells, the Bethell #3 and White #2 (Fig. 105). Neither well was cored in the "L" zone, but cores were available for study from the Bethell #5 and Demuth #1. Both of these wells contain an interval of pay-quality grainstone in the upper carbonate unit of the "L" zone, but no completion was attempted in either well. The grainstone intervals exhibit distinct patches and layers of small interparticle pores and a few molds, but are surrounded by areas of completely cemented grainstone with no porosity. This heterogeneous pore network has a maximum whole core porosity of 13.5% and a maximum horizontal permeability of 139 md.

The patches of porosity have a relatively well-connected pore network within a given patch, resulting in a net-pay cut-off of only 5% porosity corresponding to one md permeability. The crossplot of the logarithm of permeability versus core porosity shows a good correlation (Fig. 106). There is not sufficient data to calculate representative water saturations for this zone.

The net-pay map of the "L" zone indicates a continuous grainstone body along the northwest edge of the field (Fig. 105). Several drillstem tests were run in this grainstone interval, with the best test in the Bethell #1. This test recovered 6 inches of free oil;

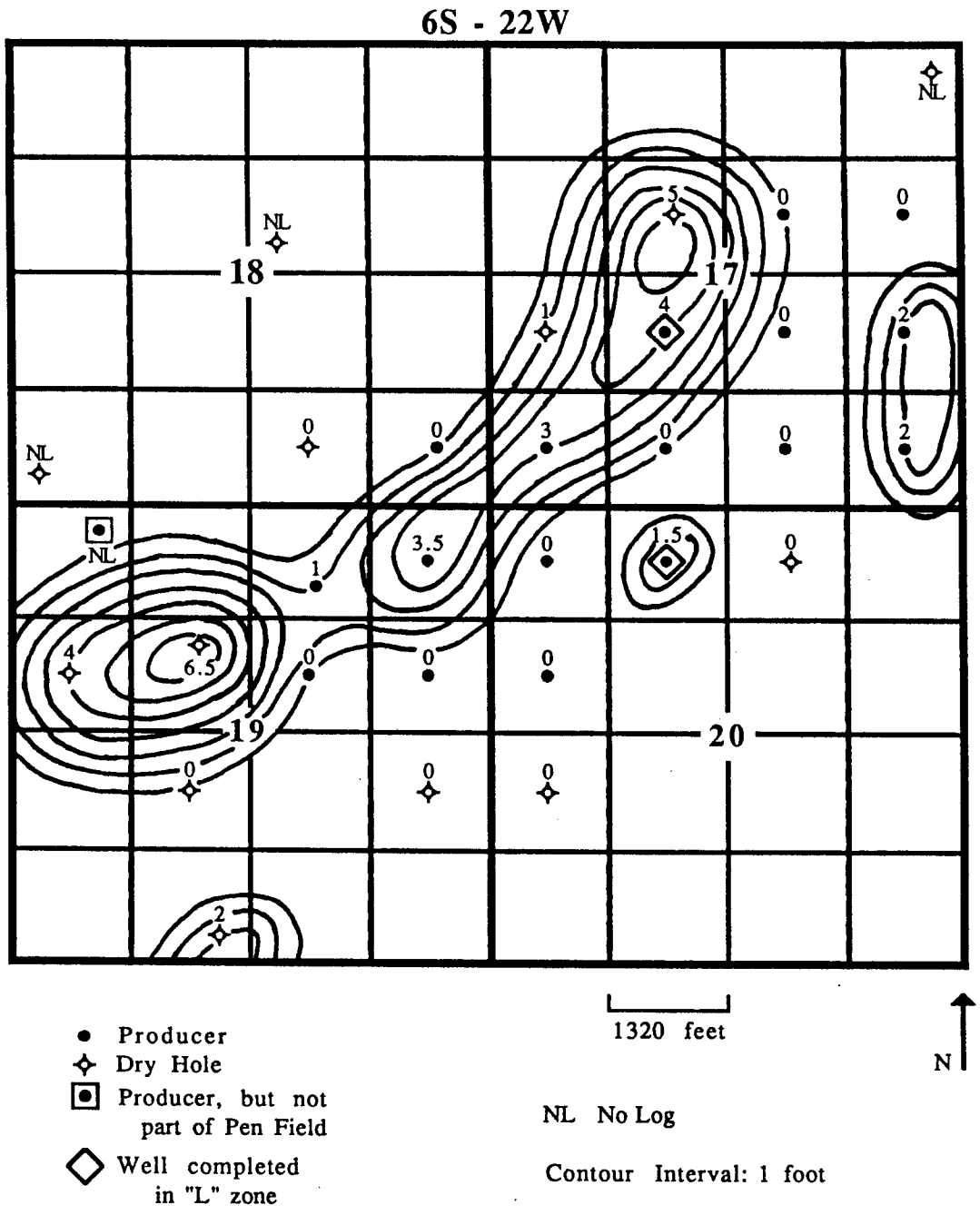

Figure 105. Net-pay map of the "L" zone. The map reveals a large body of porous grainstone along the northwest edge of the field. However, core examination indicates porosity in the grainstone is developed only in local patches, the bulk of the grainstone is tightly cemented. The drillstem and production tests indicate very small drainage volumes, and confirm the core observations. Essentially no oil flow between adjacent grid blocks is interpreted, based on the fact that the "L" zone grainstone probably does not form a commercial reservoir.

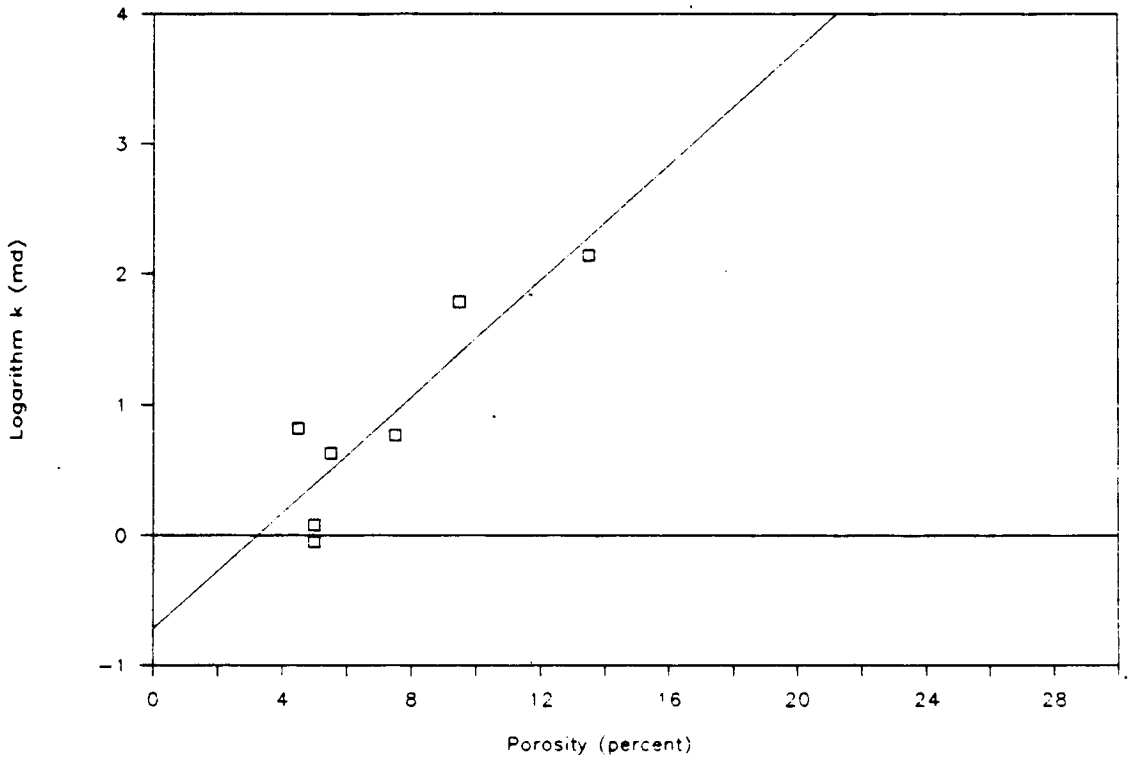

Figure 106. Crossplot of the logarithm of horizontal permeability versus core porosity for the grainstone lithology in the "L" zone, with linear regression line calculated by least-squareds method. All core samples used for the crossplot were carefully examined to determine if they were representative of the actual pore network. The samples with elevated porosity values due to shale wash-out, and the samples with induced fractures due to dehydration of clay in the solution seams, were discarded. This plot reveals a good correlation between permeability and porosity.

40 feet of oil cut mud (20% oil); 62 feet of oil-spotted mud; 62 feet of oil-spotted, water cut mud; and 144 feet of muddy water. However, the remainder of the tests recovered only small amounts of mud or oil-spotted mud. These results suggest that, while a well may encounter porous and permeable grainstone in the "L" zone, the erratic, patchy nature of the pore network results in only small volumes of grainstone connected to the well-bore. These localized drainage volumes appear to be far too small for commercial production.

In the White #2, the "L" zone was swab tested with the "K" zone for 25 BOPH. Most of this oil probably came from the "K" zone, which proved to be highly productive in swab tests of the other White lease wells. The "L" zone was separately swab tested in the Bethell #3, but showed a poor oil recovery, with swab runs varying from 1 - 4 barrels of fluid per hour with an oil cut of 45 - 66%.

Production from the "L" zone probably makes only a minor contribution to total field production. The White #2 has recovered 42,000 barrels of oil but most of this is probably from the "J" and "K" zones. The Bethell #3 exhibits a thick interval of pay in the "L" zone, but has produced only 4,600 barrels of oil from the "I", "J", and "L" zones. Though the "L" zone cores and logs may indicate porosity and permeability, this zone is at best marginally productive, and probably has no recompletion

or waterflood potential.

REVISING THE NET-PAY MAPS BY RECOGNITION OF WELLS WITH ANOMALOUS PERFORMANCE

The chapter on reservoir characterization of the "J" alpha grainstone subunit shows the difficulty in estimating permeability and reservoir productivity in the inter-well areas. Porosity, as calculated from wire-line logs, is the only direct measurement available for every well, and seems to be the only reliable indicator of the pore network. A net-pay cut-off in terms of the log porosity that best corresponds to the permeability cut-off was determined for each productive interval using the available core data. The net pay in each interval was then calculated for every well, and used to construct the initial net-pay maps exhibited in the reservoir characterization sections.

One final attempt was made to estimate inter-well properties and improve the accuracy of the net-pay maps. A reservoir volume map was constructed for all completed intervals (Fig. 107). On the assumption that each well is draining 40 acres, the reservoir volume map and water saturations were used to calculate the apparent original oil in place for every producing well (Table 2). A crossplot of cumulative well production versus apparent original oil in place shows a fair correlation (Fig. 108), indicating that the log measurements of porosity and

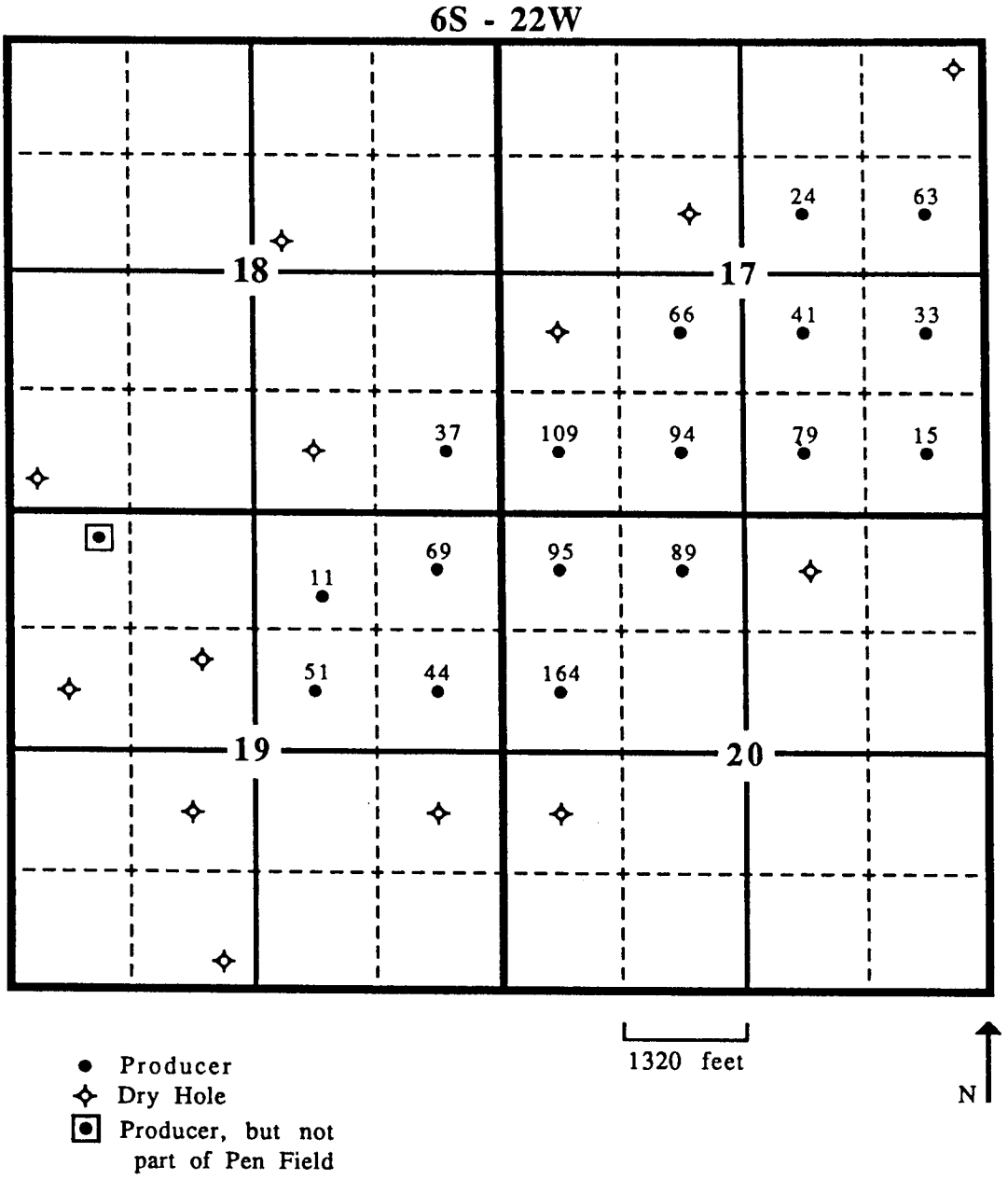

Figure 107. Reservoir volume map (porosity-feet, values in percent-ft) for all completed intervals within a given well. The values represent log porosity, although measurements of some thin intervals were modified based on core values. The map is not contoured since the variation is a function of pay development in the eight separate pay intervals.

well	Cum (stock tank bbls)	AOOIP (rsvr bbls)	Rec %
Demuth #2	12,100	10,800	112
Shuck #2	33,600	61,000	55
Pennington #1	20,300	51,500	39
Griffey #1	28,600	85,000	34
Bethell #4	74,000	222,200	33
White #4	60,100	181,700	33
Shuck #1	28,100	89,900	31
Demuth #3	24,900	90,600	27
Demuth #1	44,500	165,700	27
Shuck #3	47,500	185,900	26
White #2	42,200	221,600	19
Bethell #5	47,800	284,100	17
White #5	45,400	347,700	13
Pennington #2	6,300	123,800	5
Bethell #3	4,600	118,200	4
Shuck #4	900	33,600	3
Demuth #4	2,600	112,500	2
Field	523,500	2,385,800	22

Table 2. Cumulative well production (Cum), apparent original oil in place (AOOIP), and recovery percentage (Rec %). Apparent original oil in place values were calculated by assuming the porosity and water saturation values at the well could be applied over a drainage area of 40 acres. Typical recovery percentages range from 13 to 55%. However, four wells exhibit notably low recoveries on the order of 2 to 5%, and one well exhibits an impossibly high recovery of 112% of the apparent original oil in place.

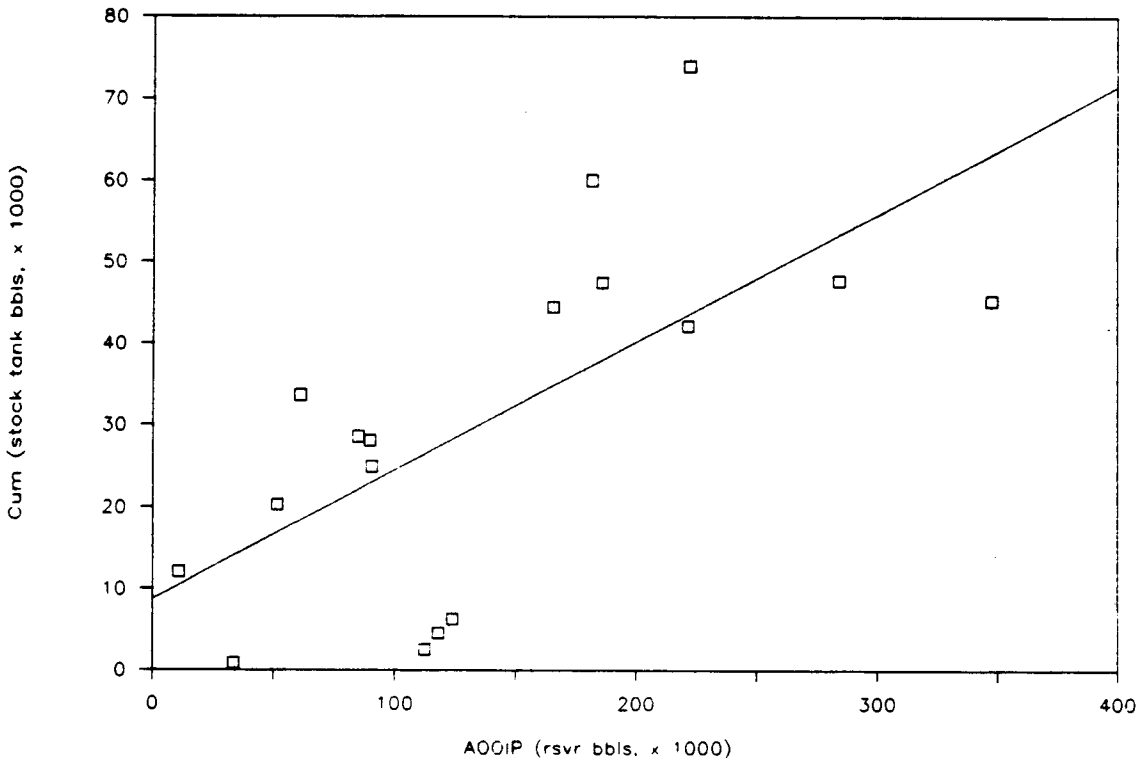

Figure 108. Crossplot of cumulative well production (Cum) versus apparent original oil in place (AOOIP), with linear regression line calculated by least-squareds method. Apparent original oil in place values were calculated by assuming the porosity and water saturation values at the well could be applied over a drainage area of 40 acres. The plot shows a fair correlation.

water saturation provide a reasonably accurate extrapolation of reservoir properties over a 40 acre area.

These data can also be represented in tabular form by expressing cumulative well production as a percentage of apparent original oil in place (Table 2). For the entire field, 22% of the apparent original oil in place has been recovered through April, 1990. Typical recovery percentages for individual wells range from 13 to 55%. However, four wells exhibit notably low recoveries on the order of 2 to 5%, and one well exhibits an impossibly high recovery of 112% of the apparent original oil in place. An attempt was then made to reconcile these obviously anomalous wells with the geologic observations and the porosity distribution reflected in the net-pay maps.

Shuck #4

The Shuck #4 recovered only 3% of the apparent original oil in place, from one foot of pay in the "I" zone, and one foot in the "J" cap subunit. This low recovery percentage is largely a data artifact due to economic considerations. The well only produced for three months before it was abandoned as non-commercial. Like the other wells in the field, production in the Shuck #4 was declining rapidly prior to the bubble point,

but this well was only a marginal producer. At the rapid rate of decline it appeared that the Shuck #4 would quickly become uneconomic to operate, so the well was abandoned even though it was still producing 4 BOPD. After the bubble point pressure was reached in the alpha grainstone, field production stabilized and declined only 10% in the next year. If economic considerations were waived and the Shuck #4 had continued pumping, production probably would have stabilized, and on a 10% decline the well would have produced 5,700 barrels through April, 1990, compared to 900 barrels of actual production.

The size of the compartment in the "J" cap subunit is another consideration. Pay in the cap subunit does not extend to the adjacent wells and is only one foot thick, so only 18 acres of "J" zone pay were attributed to this well on the initial net-pay map (Fig. 100). This adjustment to the assumed 40 acre drainage area, combined with the previous adjustment for early abandonment, would correspond to a 24% recovery factor, which would fall in the range of typical recovery percentages for the field. Consequently, no modification of the "I" zone or "J" cap subunit net-pay maps is indicated.

Bethell #3

The Bethell #3 also exhibits an anomalous low recovery factor of only 4% of the apparent original oil

in place, from completions in the "I" zone, "J" alpha grainstone subunit, and "L" zone. However, most of the pay attributed to this well is from the "L" zone (Fig. 105). In the reservoir characterization of the "L" zone section, it was noted that this zone produces from erratically developed patches of porous rock, and wells completed in this zone might not recover any significant amount of oil. The poor performance of the Bethell #3 supports this assessment of the "L" zone.

If 90% of the pay from the "L" zone is excluded as undrainable, the Bethell #3 would have a recovery of 8% of the apparent original oil in place. This value is still quite low, and indicates poor recovery from either the "I" or "J" zone, or both. Examination of the "I" zone net-pay map indicates the Bethell #3 is at the edge of a compartment, and only has about 13 acres of "I" zone pay (Fig. 95). Additionally, poor recovery from the "J" alpha grainstone in the area of the Bethell #3 would be consistent with the geologic observations. This well shows by far the most extensive development of alteration features in the "J" zone. The pipes, fissures, and autoclastic breccia intervals in this well are filled with impermeable sediment, and tend to reduce both the volume of pore space, and the continuity of the pore space drained by the well.

The removal of 22 acres (5 grid blocks) from the

40 acre drainage area in the "J" alpha grainstone, combined with the reduced drainage areas in the "L" and "I" zones, would result in a recovery factor of 15% of the apparent original oil in place, which is within the range of typical recoveries. No pressure data are available to determine if the Bethell #3 is in a separate compartment in the "J" alpha grainstone, so the initial net pay map was modified by the random removal of five grid blocks from the drainage area to simulate the loss of drainable pore volume due to alteration pores filled with impermeable sediment (Fig. 109).

Pennington #2

The Pennington #2 exhibits a low recovery factor of only 5%, from completions in the "D" zone and the beta micrite-rich and beta grainstone-packstone subunits of the "J" zone. Most of the pay in this well is attributed to the "D" zone, but no reservoir characterization data are available for the "D" zone because no cores were taken from this zone.

The lack of "D" zone pay in wells surrounding the Pennington #2 indicates the area of porous and permeable rock is limited. One simple explanation for the poor recovery in the Pennington #2 is that the well is draining less than 40 acres of "D" zone porosity. Consequently, the initial net-pay map was modified to

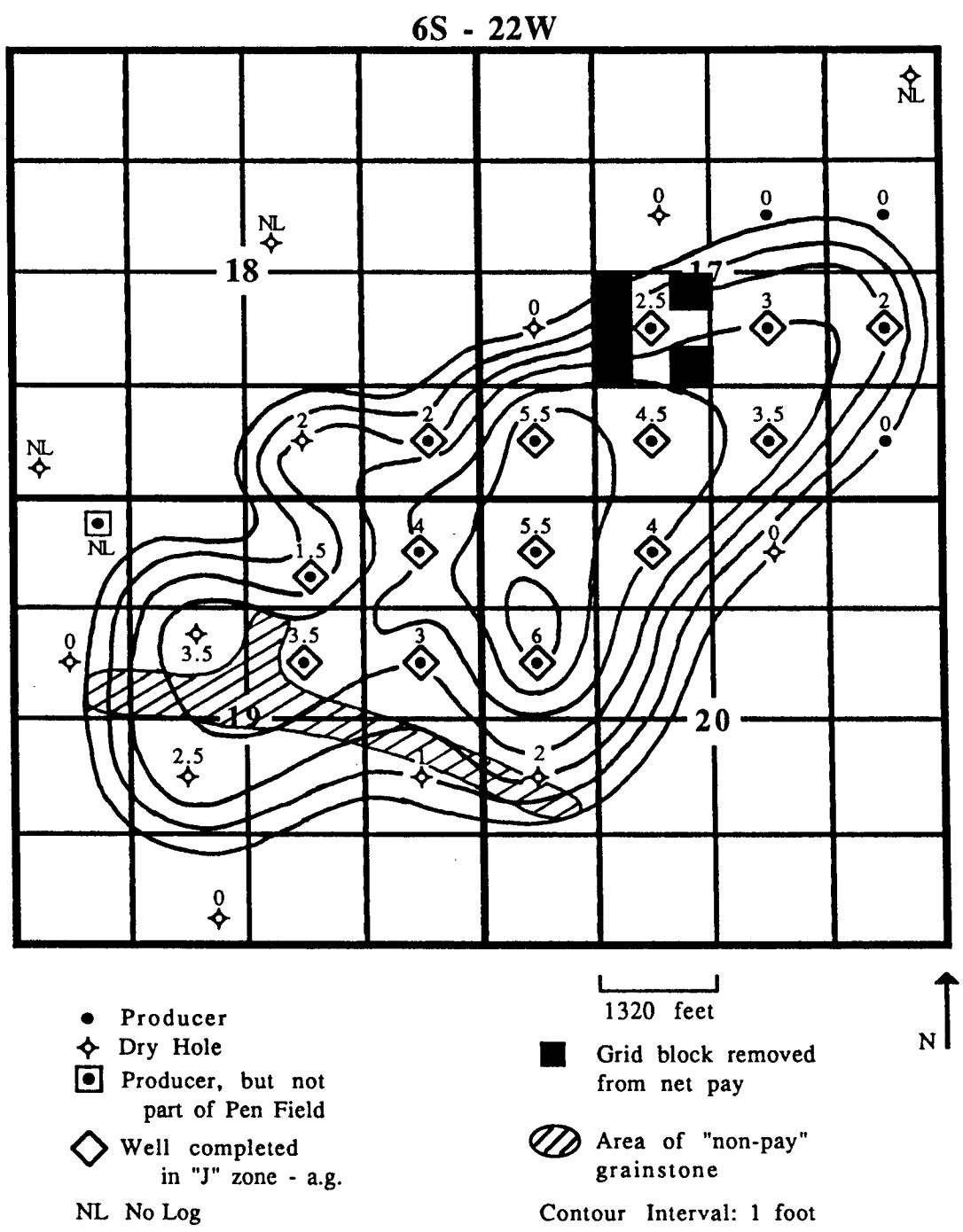

Figure 109. Revised net-pay map of the "J" zone alpha grainstone subunit. Five grid blocks were randomly removed from the 40 acres surrounding the Bethell #3 to simulate the loss of drainable pore volume due to alteration pores filled with impermeable sediment. An area of "non-pay" grainstone with permeability of less than 1 md is interpreted to traverse the Rogers and Demuth leases.

reflect a "D" zone drainage area of only 10 acres (Fig. 110).

The initial net-pay map for the "J" zone pay interval only attributed 20 acres to this well, due to the thin pay intervals (Fig. 101). The resulting recovery factor for 10 acres of "D" zone pay and 20 acres of "J" zone pay is 16% of the apparent original oil in place. This value is within the range of typical recoveries, so no modification of the "J" beta micrite-rich and beta grainstone-packstone subunit net-pay map is indicated, but the poor recovery in this well could be the result of limited pay in both the "D" and "J" intervals.

Demuth #4

The Demuth #4 is the fourth of the wells exhibiting a low recovery. This well recovered only 2% of the apparent original oil in place from its only pay interval, the "J" alpha grainstone subunit. Examination of the alpha grainstone isopach map reveals the Demuth #4 lies along the axis of the grainstone body; the areal distribution of this pay interval extends far beyond the 40 acre drainage area attributed to the well (Fig. 20). The extent of the grainstone suggests it is the continuity of the pay that is the problem in the area of the Demuth #4.

This observation is consistent with the analysis in

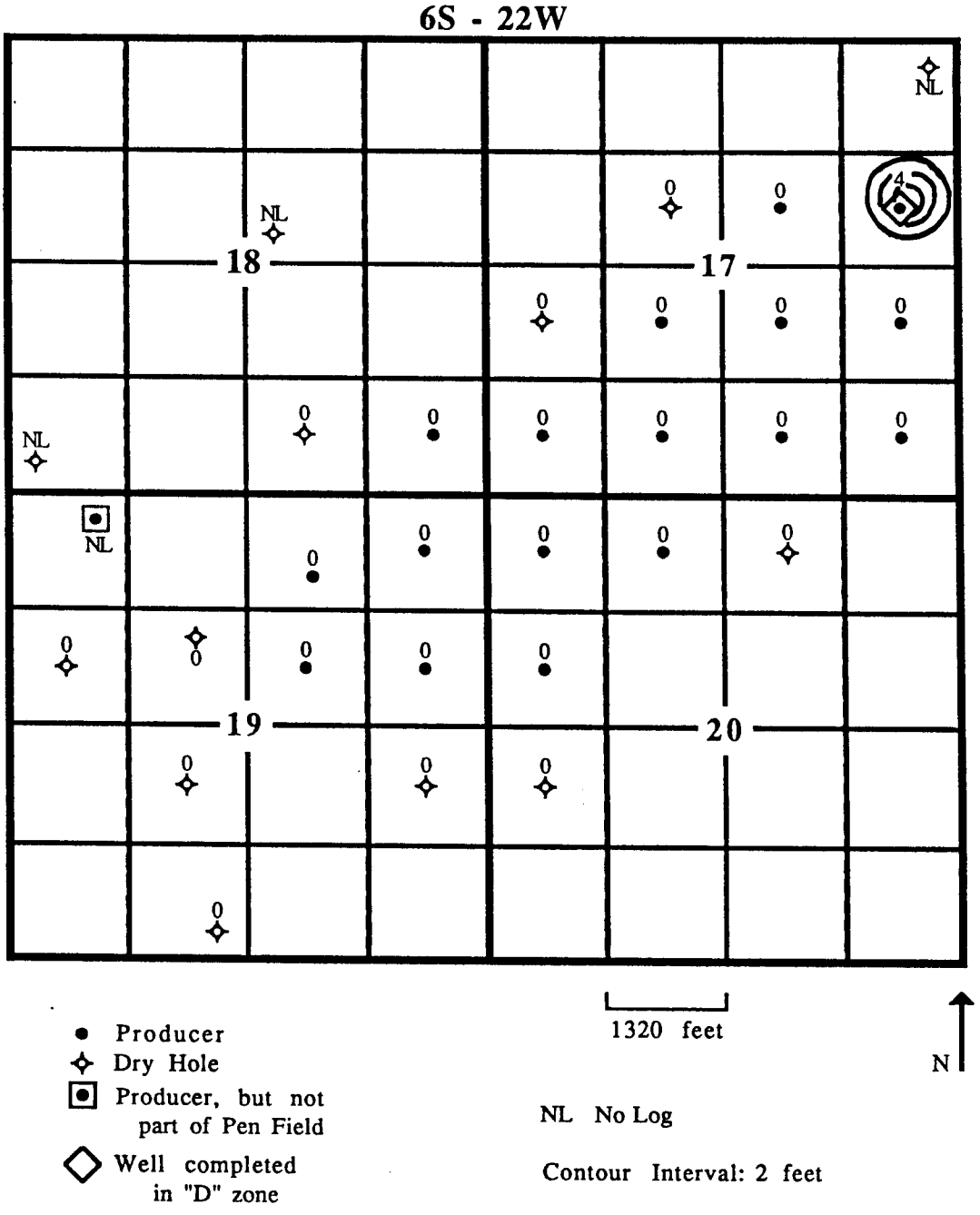

Figure 110. Revised net-pay map of the "D" zone. The Pennington #2 is the only well in the field that exhibits porosity in the "D" zone. The well recovered only 5% of the apparent original oil in place assuming a 40 acre drainage area. It was therefore interpreted that the well was draining significantly less than 40 acres of pay in the "D" zone, as reflected in this map.

the reservoir characterization section about the Rogers lease and the degree of communication within the alpha grainstone body for this area of the field. Pressure measurements indicate the Rogers lease is isolated from the main body of the alpha grainstone, probably by an area with significant reduction of the interparticle pores by cement J1. The resulting pore network is interpreted to have permeability of less than 1 md. This area of low permeability probably extends into the 40 acres attributed to the Demuth #4, effectively removing some pay from the well's drainage area, which contributes to the low recovery factor.

The Demuth #4 was the next to last producing well completed in the field. The drillstem test for this well indicated an original reservoir pressure for the vicinity of the well-bore of only 242 psi. The Demuth #4 obviously suffered some drainage from the prolific producers that lie to the east and north. The amount of offset drainage, and its contribution to the low recovery factor of the Demuth #4, is impossible to calculate without a computer simulation.

Demuth #2

Surprisingly, the Demuth #2, which lies one location north of the Demuth #4, exhibits an impossibly high recovery factor of 112% of the apparent original oil in

place. This is probably the result of several factors. First, the thickness of the alpha grainstone increases in three directions away from the well-bore of the Demuth #2 (Fig. 20). The 1.5 feet of pay encountered in the well-bore is probably not representative of the average pay thickness across the attributed 40 acres. Second, the Demuth #2 lies adjacent to abundant potential pay attributed to two dry holes. Drainage from the area of the Griffey #2 and the area of the Jacobs #1 may contribute to the high recovery factor of the Demuth #2. The drillstem test in the Jacobs #1 indicates a definite connection to the main body of the alpha grainstone, since the original reservoir pressure in the vicinity of the well-bore was only 281 psi.

The net-pay map of the alpha grainstone subunit was therefore modified by the addition of a "non-pay" area of low permeability to reflect the drainage patterns observed in the Rogers and Demuth leases. This non-pay area of grainstone apparently has less than 1 md of permeability, due primarily to an abundance of cement J1 filling the interparticle pore space. The resulting "mold-dominated" pore network may have up to 11% porosity as in the Rogers #1. Consequently, the net-pay contours were not modified to deflect around the area of low permeability because large pore volumes of oil exist adjacent to the non-pay area, and would probably be

effectively drained where permeability is greater than 1 md.

The inferred area of low permeability was positioned to fit several observations:

1. It must isolate the Rogers lease from the main body of the alpha grainstone.
2. It probably traverses part of the 40 acre area around the Demuth #4, thereby reducing the pay attributable to this well.
3. A spur of low permeability probably bisects the area between the Demuth #4 and the Jacobs #1. This prevents the Demuth #4 from draining the pay on the Jacobs lease, but leaves the Jacobs lease pay connected to the main body of the alpha grainstone, and allows for drainage by the Demuth #2 (Fig. 109).

GENERATING THE SIMULATION GRID

Examination of the distribution of net pay indicates two grid blocks between wells would allow for reasonable interpolation, and the grid system should be centered on the wells since the simulation model is based primarily on direct well-bore measurements. These two conditions result in a grid system with nine blocks per 40 acres, for a total of 260 blocks that contain pay in the Pen Field (Fig. 111). A one foot cell thickness was selected since porosity and water saturation values were calculated for one foot intervals.

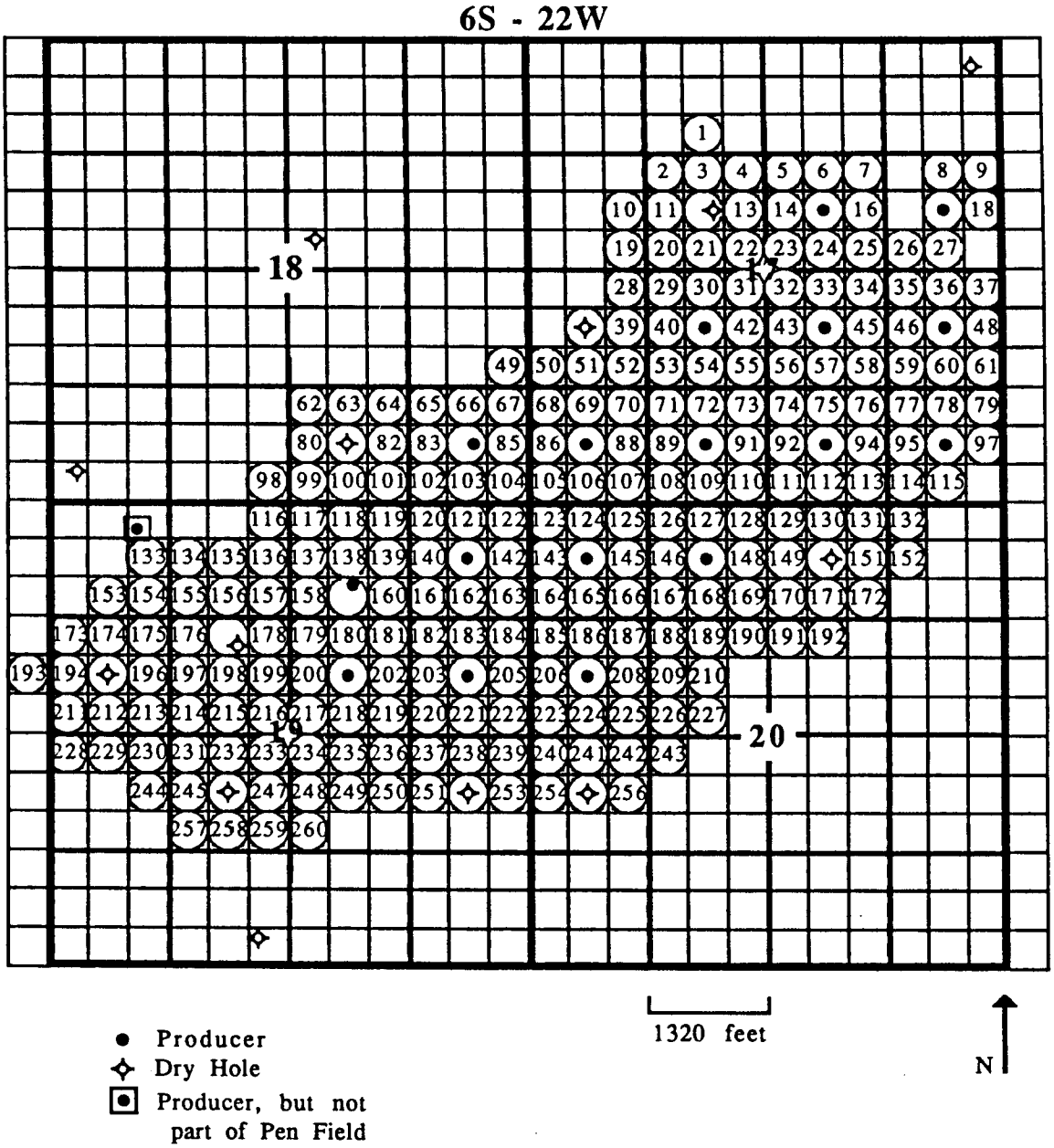

Figure 111. Areal grid blocks of the Pen Field. The grid system is based on a well at the center of a 40 acre spacing unit. A grid block size was selected such that two blocks exist between adjacent wells. The resulting grid system has nine blocks per 40 acres, for a block size of 4.44 acres. A total of 260 blocks contain pay from some interval in the Pen Field. The slightly irregular outline of the block map reflects the distribution of pay from the various net-pay maps.

The reservoir characterization of the various zones indicates that eight separate reservoir intervals occur in the Pen Field; the "D" zone, "I" zone, "J" cap subunit, "J" alpha grainstone subunit, "J" beta micrite-rich and beta grainstone-packstone subunits, "K" capping carbonate subunit, "K" basal carbonate subunit, and the "L" zone. The depth axis for the simulation grid was then calculated by adding the maximum feet of net pay in each interval, plus one cell per interval to represent the impermeable rocks separating the reservoir intervals. The resulting depth axis contains 33 one foot blocks. The combination of surface blocks and depth blocks forms a three-dimensional simulation grid with 8,580 cells (Appendix 15).

The first step in generating grid values was to calculate the feet of net pay in each reservoir interval for every grid block not containing a well. This was easily accomplished by overlaying a grid on the net-pay maps and selecting the nearest one foot contour. The porosity distribution was then estimated across the field by direct linear interpolation of the values from adjacent wells. The values for permeability and water saturation were then calculated from the correlation functions derived for each reservoir interval. The relevant equations are shown in Table 3.

Sufficient data for the correlations are not

Reservoir Interval	Permeability Correlation	Water Saturation Correlation
D Zone	$10^{[(.193 \times \text{porosity}) - .693]}$	100 x [(3.72 / porosity) + .098]
I Zone	$10^{[(.315 \times \text{porosity}) - 1.243]}$	100 x [(2.59 / porosity) - .0661]
J Capping Subunit	(same as I zone)	(same as I zone)
J Alpha Grainstone Subunit	$10^{[(.069 \times \text{porosity}) + .793]}$	100 x [(5.59 / porosity) - .126]
J Beta Micrite-Rich and Beta Grainstone-Packstone Subunits	(same as I zone)	(same as I zone)
K Capping Carbonate Subunit	$10^{[(.202 \times \text{porosity}) - 1.102]}$	100 x [(1.99 / porosity) + .227]
K Basal Carbonate Subunit	(same as K capping carbonate subunit)	(same as K capping carbonate subunit)
L Zone	$10^{[(.222 \times \text{porosity}) - .717]}$	(same as K capping carbonate subunit)

Table 3. Equations for each reservoir interval relating permeability and water saturation to porosity. Porosity is in percent, yielding permeability in md and water saturation in percent.

available for every reservoir interval. The correlations of the most similar pore network were applied to these zones, as described below.

"D" Zone

No cores of the "D" zone were taken, so both the lithology and permeability of the pay interval were unknown. Consequently, a crossplot of the logarithm of maximum horizontal permeability versus core porosity was constructed using all available values from the "I", "K", and "L" zones. The resulting "average" Lansing-Kansas City porosity-permeability relationship showed a good correlation (Fig. 112), and was used for generating "D" zone permeability values. The "J" alpha grainstone values were excluded from the plot due to the unusual nature of the "mold-dominated" pore network developed in portions of this interval.

"J" Cap, Beta Grainstone-Packstone, and Beta Micrite-Rich Subunits

No representative core measurements are available for the limited samples of pay from the "J" zone cap, beta grainstone-packstone, and beta micrite-rich subunits. However, the pore network in the grainstone-packstone subunit consists of cement reduced interparticle pores augmented by a few molds. This network closely resembles the pore network in the "I"

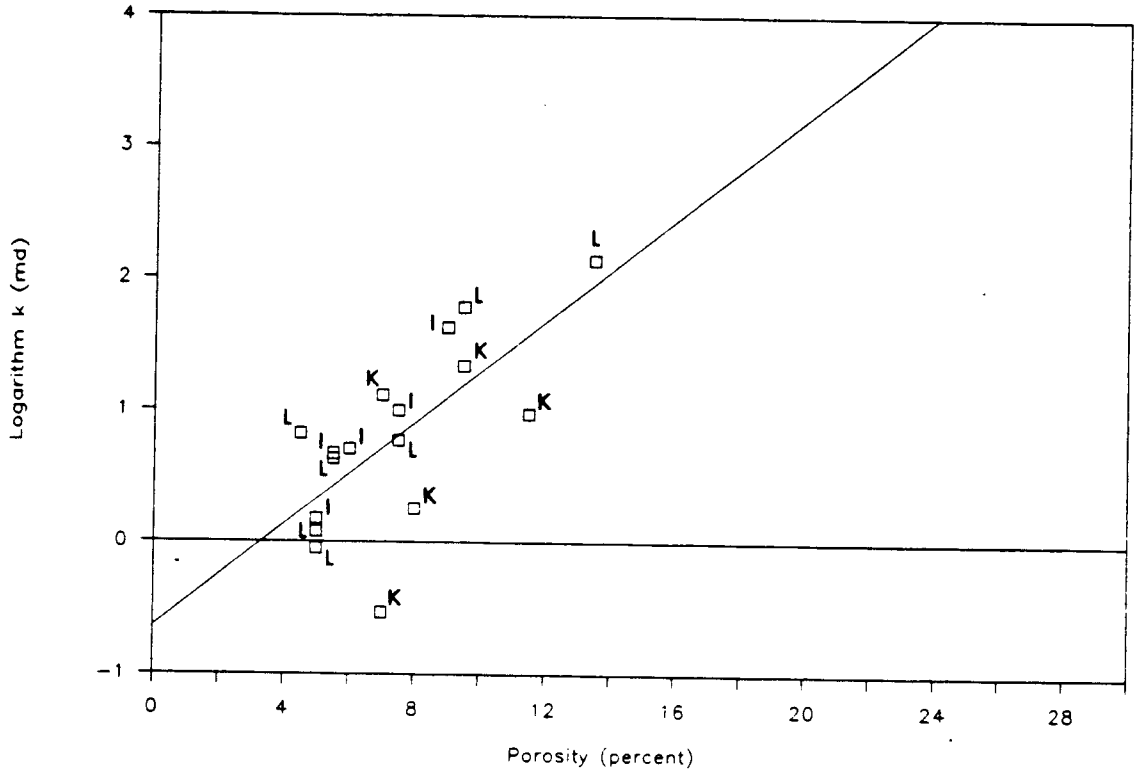

Figure 112. Crossplot of the logarithm of horizontal permeability versus core porosity for the "I", "K", and "L" zones, with linear regression line calculated by least-squareds method. Data points are labeled by zone. The resulting "average" Lansing-Kansas City porosity-permeability relationship shows a good correlation, and was used for generating "D" zone permeability values.

zone grainstones. Also, the pore network of small vugs with a few molds in the wackestones of the cap and beta micrite-rich subunits is similar to that in the wackestone of the "I" zone. It was previously shown that the porosity-permeability relationship in the "I" zone wackestone closely matched that of the "I" zone grainstones. The similarity of the "J" zone pore networks is close enough to those in the "I" zone that the porosity-permeability and porosity-water saturation correlations derived for the "I" zone were applied to the "J" zone subunits.

"K" Zone

The pore networks in the two productive subunits of the "K" zone looked similar during core examination. Consequently, all values from the subunits were examined together, and only one set of correlations was derived for the "K" zone.

"L" Zone

No water saturation values were available for the "L" zone. The "L" zone grainstone has a pore network of fine interparticle pores with a few molds, which closely resembles the network in the "K" zone. The "K" zone water saturation correlation was therefore applied to the "L" zone.

The drillstem and production tests of the "L" zone indicate very small drainage volumes. This supports the core observations that porosity exists as unconnected patches. This pore network probably results in essentially no oil flow between adjacent grid blocks, so the "L" zone probably does not form a commercial reservoir interval in the Pen Field area.

All equations in Table 3 not discussed above, are derived only from values taken from the represented interval. The derivations of these correlation equations are fully described in the reservoir characterization chapters.

COMPARING PRODUCTION TO THE REVISED OIL IN PLACE ESTIMATES

In the calculations of apparent original oil in place (AOOIP), the point estimates of porosity and water saturation at the well-bore were extrapolated over the 40 acres surrounding the well. Comparisons using the grid values of porosity and water saturation should result in a more accurate evaluation of reservoir performance because these values reflect local trends. To incorporate this "conditioned" data, the grid values and modified net-pay maps were used to recalculate the original oil in place for each well. These new estimates were termed revised original oil in place (ROOIP) (Table 4).

A crossplot of cumulative well production versus

well	Cum (stock tank bbls)	ROOIP (rsvr bbls)	Rec %
Pennington #1	20,300	21,000	97
Shuck #2	33,600	46,000	73
Demuth #2	12,100	25,400	48
Bethell #4	74,000	204,000	36
Shuck #1	28,100	78,000	36
Griffey #1	28,600	81,100	35
Demuth #1	44,500	144,700	31
Pennington #2	6,300	20,200	31
Shuck #3	47,500	158,500	30
White #4	60,100	201,400	30
White #2	42,200	152,600	28
Demuth #3	24,900	108,300	23
Bethell #5	47,800	228,200	21
White #5	45,400	252,600	18
Bethell #3	4,600	37,500	12
Demuth #4	2,600	51,300	5
Shuck #4	900	24,600	4
Field	523,500	1,835,400	29

Table 4. Cumulative well production (Cum), revised original oil in place (ROOIP), and recovery percentage (Rec %). The grid values and modified net-pay maps were used to recalculate the original oil in place.

ROOIP (Fig. 113) shows a better correlation than the previous plot using AOOIP (Fig. 108), indicating the grid values provide improved accuracy in the estimates of the inter-well properties. However, the degree of accuracy cannot be quantified because cumulative production from a well is not only dependent on the oil in place, but also the permeability, completion method, completion date, and many other factors.

It was previously shown that there exists a strong positive correlation between permeability and porosity for every reservoir interval in the Pen Field. Higher porosities result in higher permeabilities, so the porosity term in the ROOIP values largely accommodates the permeability variation between wells.

Completion methods were similar across the field, so this factor probably does not significantly affect cumulative well production. However, completion date can have a significant impact, especially in fields driven by fluid expansion and solution gas. These fields tend to exhibit rapid pressure declines during the early production history, as does the Pen Field. Consequently, early wells recover more oil because the large pressure difference between the reservoir and well-bore results in higher flow rates relative to later wells with smaller pressure differences. The three wells that plot farthest above the correlation line (high cumulative production

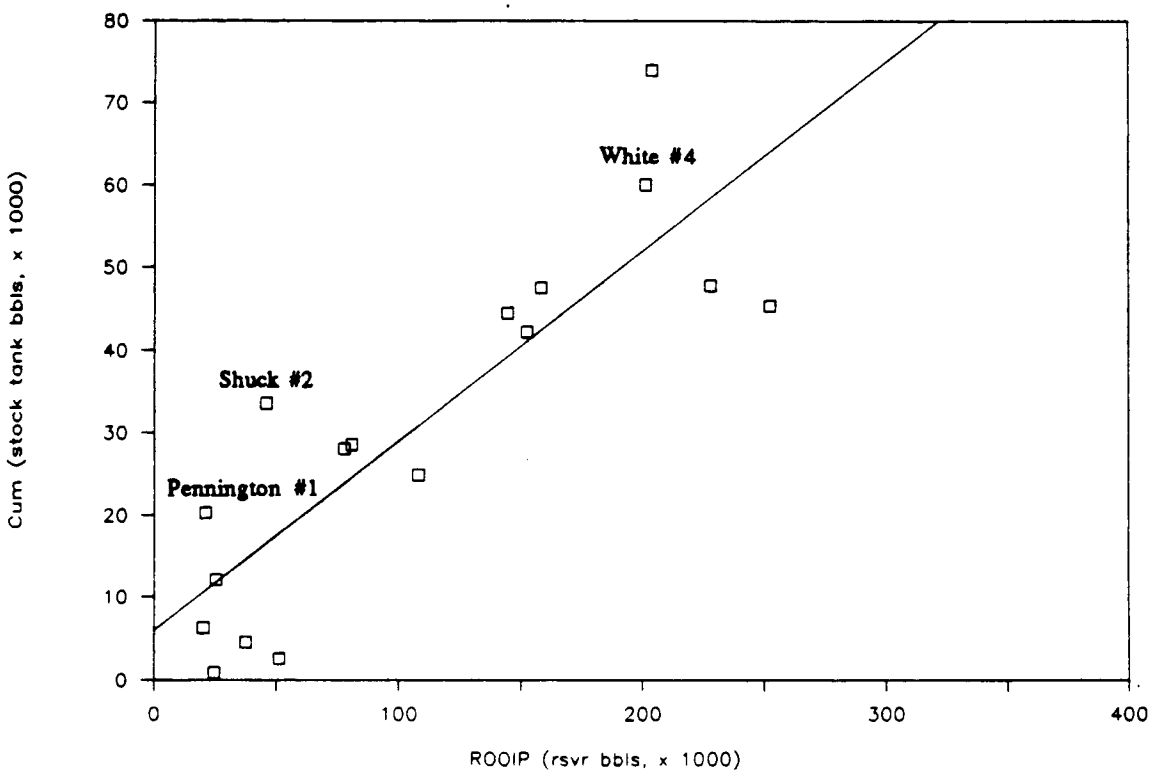

Figure 113. Crossplot of cumulative well production (Cum) versus revised original oil in place (ROOIP), with linear regression line calculated by least-squareds method. This plot shows a greater degree of correlation than the plot using AOOIP (Fig. 108). The three marked outliers all opened a new pay zone or compartment.

for a given ROOIP) all were the first well completed in a new compartment or reservoir interval, and therefore encountered virgin pressures. The Pennington #1 was completed in the "I" and "J" zones and was the field discovery well, so it necessarily encountered virgin pressures in both zones. The Shuck #2 was also completed in the "I" and "J" zones, but it opened a large, separate "I" zone compartment and encountered virgin pressure in this zone. The White #4 was completed in the "I", "J", and "K" zones and encountered virgin pressure in the "K" zone because it was the first well completed in the zone.

Obviously, the degree of correlation in the cumulative production versus ROOIP crossplot could be improved if the pressures in each reservoir interval were known throughout the field's production history. These data are rarely available for oil fields, but the previous discussion illustrates that the scatter in the ROOIP crossplot is not necessarily due to errors in the inter-well estimates of porosity and water saturation. In fact, the high degree of correlation, and the response of the few wells for which qualitative pressure data are available, suggests the grid values give very reliable estimates of the inter-well properties.

PERFORMANCE OF THE INDIVIDUAL RESERVOIR INTERVALS

The correlation between individual well performance and ROOIP indicates the ROOIP values accurately reflect the properties of each reservoir interval when sampled over areas as large as well drainage areas. To evaluate the field-wide production performance of each reservoir interval, the ROOIP was calculated for every grid cell and summed by interval (Table 5). [The total ROOIP is significantly higher than that previously calculated by individual wells because some of the reservoir volume lies outside of the inferred 40 acre drainage area of any producing well, and some wells were not completed in all of the potentially productive reservoir intervals they encountered.]

The ROOIP for all zones in the Pen Field is 2,584,000 reservoir barrels. The interval share by percentage shows the "I" zone (10.4%) and the "J" alpha grainstone subunit (66.1%) are major contributors to the field ROOIP. The "K" (9.1%) and "L" (12.7%) zones are also major contributors to ROOIP, yet the reservoir characterization of these zones indicates they make only minor contributions to Pen Field cumulative production.

The discrepancy in the "K" zone is the result of several factors. The "K" basal carbonate subunit contains pay in eleven wells (Fig. 102), yet was completed in only three wells. Five of the wells not

Interval	ROOIP (rsvr bbls)	Share	DOIP (rsvr bbls)	Share	DOIP/ROOIP
D	18,100	0.7%	18,100	1.0%	100%
I	267,600	10.4%	210,800	11.5%	79%
J c	12,300	0.5%	12,300	0.7%	100%
J ag	1,707,400	66.1%	1,484,000	80.9%	87%
J b	15,500	0.6%	15,500	0.8%	100%
K cc	15,400	0.6%	11,100	0.6%	72%
K bc	220,200	8.5%	75,200	4.1%	34%
L	327,900	12.7%	8,200	0.4%	5%
Field	2,584,400	100.1%	1,835,200	100.0%	71%

Table 5. Pay interval, revised original oil in place (ROOIP), interval share of ROOIP, drainable oil in place (DOIP), and interval share of DOIP. ROOIP is calculated from the simulation grid porosity and water saturation values for the nine areal grid blocks that subdivide each 40 acre spacing unit. The DOIP values are derived from the ROOIP values, but discount those pay intervals for which the well on the 40 acre spacing unit lacks a completion. The "L" zone has the further assumption that only the single 4.44 acre grid block containing the well is being drained. The intervals with low DOIP/ROOIP percentages are probably not being effectively drained by the current well completions. Interval abbreviations: J c - "J" cap subunit, J ag - "J" alpha grainstone subunit, J b - "J" beta micrite-rich and beta grainstone-packstone subunits, K cc - "K" capping carbonate subunit, K bc - "K" basal carbonate subunit.

completed were dry holes, and the pay interval in the "K" basal carbonate subunit was insufficient for an economic well completion from only this interval. The three producing wells that were not completed in the "K" basal carbonate subunit contain only 1 - 1.5 feet of pay in this interval, but it is not known why no completion was attempted. Additionally, only two wells were completed in the "K" capping carbonate subunit, out of three wells containing pay in this interval (Fig. 103). Consequently, a large portion of the reserves in place in the "K" zone will not be recovered due to the lack of completions in wells containing pay in this interval.

The reserves in the "L" zone are even more poorly exploited. Eleven wells contain "L" zone pay, but only two wells are completed in this interval (Fig. 105). The lack of completions is due primarily to the nature of the pore network. The patches of porous grainstone in the "L" zone tend to be unconnected. Consequently, the drainage area of any well-bore is very small, probably on the order of four acres or less. This interpretation is supported by the drillstem tests of the "L" zone which typically recover only oil-spotted mud, even in wells with porous grainstone in the core, or good indications of porosity and permeability on the logs.

A new value termed "drainable oil in place" (DOIP) was calculated to express the efficiency of exploitation

of a given pay interval (Table 5). Several assumptions are required. First, it is assumed that each well is draining the 40 acre spacing unit on which it is located. This is a reasonable assumption based on the degree of correlation between cumulative well production and revised original oil in place for 40 acre units, shown previously in Figure 113 and Table 4, and on the spacings typical of Lansing-Kansas City fields in central and western Kansas. Second, due to the apparent lack of continuous pay and the corresponding poor well performance, "L" zone completions are interpreted to drain only the single 4.44 acre grid block containing the well. With the first assumption, the pay in a given interval attributed to a well's ROOIP is not considered drainable, if the well is not completed in that pay interval. With the second assumption, only two blocks of "L" zone pay are considered drainable because only two well are completed in the interval.

The drainable oil in place values are shown in Table 5. The intervals with low DOIP/ROOIP percentages are probably not being effectively drained by the current well completions. The DOIP for the entire field is 1,835,000 reservoir barrels, which is only 70% of the ROOIP. The DOIP values clearly show that the "I" zone (11.5%) and "J" alpha grainstone subunit (80.9%) are the main producing horizons in the Pen Field, which matches

the conclusions drawn in the reservoir characterization sections. However, the DOIP values cannot be converted to actual zone production estimates without knowledge of the recovery efficiency from each reservoir interval. This recovery efficiency is dependent on both large scale continuity and the specific pore network.

The completions in the "J" alpha grainstone subunit are probably efficiently draining this interval. The reservoir characterization of this subunit indicates the interval generally has high permeability and excellent communication between wells. This should result in a high recovery efficiency of the drainable oil in place. These same factors also make the "J" alpha grainstone subunit an excellent candidate for waterflooding.

The ROOIP for the "I" zone is 268,000 reservoir barrels, which is a large enough target to make waterflooding attractive. The well completions appear to effectively exploit this interval since the DOIP is 79% of the ROOIP. However, the reservoir characterization of the "I" zone indicates at least four discrete compartments of pay. A number of geologic factors have modified the "I" reservoir interval, and there is a good possibility of additional compartmentalization that could not be identified with the available data. Consequently, the "I" zone should be considered a waterflooding target, but exploitation will require careful planning and

monitoring of the waterflood. Information derived from the early responses of the "I" zone waterflood will probably indicate modifications that will optimize recovery.

The other zones have little potential for additional oil recovery because the remaining reserves are not drainable with the current completions, and the thin intervals probably do not contain sufficient reserves to economically justify recompletions. The areally extensive and relatively thick eastern lobe of the "K" basal carbonate subunit is a possible exception.

CONCLUSIONS

Reservoir characterization of the Pen Field indicates that permeability and water saturation are strongly dependent on the nature of the pore network. It appears that reliable estimates of permeability and water saturation can be obtained by a correlation to log porosity using a simple linear regression. Unfortunately, the rock properties show significant lateral variation in the Pen Field, so the values of porosity, permeability, and water saturation are only accurate in the vicinity of the well-bore.

However, the abundance and diversity of information for the field provides a number of means of indirectly evaluating the inter-well properties. The reservoir

performance of the portion of each pay interval attributed to a well is controlled by the properties within the entire drainage radius. Several specific conclusions about inter-well properties can be drawn from analysis of the reservoir performance.

A knowledge of the geologic history was used to contour the net-pay maps with an interpretive bias, thus providing the first rough estimate of inter-well properties. These net-pay maps were further modified by reconciling the depositional and paragenetic features with drainage anomalies indicated by gross differences between oil in place and cumulative recovery. This was the first step in analyzing the reservoir performance.

The field was then subdivided into a three-dimensional grid. Grid cell values for porosity were interpolated between adjacent wells. The grid cell values for permeability and water saturation were then calculated from the porosity correlations. These grid values provide more accurate estimates of inter-well properties for reservoir performance evaluation because the values reflect local trends, rather than extrapolation over 40 acres of the point estimates at the well-bore. The oil in place estimates were then revised using the grid values. The revised original oil in place figures show a good correlation to cumulative well production, suggesting they accurately reflect the inter-

well properties.

An analysis of the ROOIP values by interval indicated anomalous reservoir performance in both the "K" and "L" zones. In the "L" zone, poor continuity of the pay results in the poor reservoir performance. In the "K" zone, the poor performance appears to be due to the lack of completions in this interval. The control exerted by completion practices affects the other intervals to some degree, so the control was quantified in a value termed drainable oil in place. The analysis of the reservoir characterization, reservoir performance, and drainable oil in place suggests the "J" alpha grainstone subunit and the "I" carbonate unit are respectively excellent and good candidates for waterflooding.

CONCLUSIONS

The "I" and "J" zone both contain carbonate strata, including locally-developed grainstones, that formed in a shallow, open marine environment. The "J" zone carbonates exhibit a complex paragenetic sequence. Most of the features formed during a period of subaerial exposure that occurred after deposition of the upper carbonate unit. However, diagenesis of this zone continued as the basin subsided, and several features formed after burial.

The "I" zone also exhibits a complex paragenetic sequence, again dominated by a period of subaerial exposure after deposition of the carbonate unit. The carbonate unit also exhibits some features that formed after burial, and all of the post-compactional features closely resemble those in the "J" zone. A second episode of subaerial exposure occurred during deposition of the "I" shale unit, but did not affect the underlying carbonates.

A grainstone interval in the "J" zone, termed the alpha grainstone, is the main producing horizon in the Pen Field, and exhibits excellent continuity and communication between producing wells. A good correlation exists between porosity and permeability, and water saturation also appears to be a function of porosity.

The grainstones in the "I" zone exhibit a significantly different relationship between porosity and permeability, but again show a high degree of correlation. The "I" zone water saturation correlation also shows a marked difference to the "J" alpha grainstone correlation. Unlike the alpha grainstone, porosity is erratically developed in the "I" zone, and there may be very poor continuity between producing wells.

Analysis of individual well production suggests the extrapolation of porosity, permeability, and water saturation into the inter-well areas is generally very accurate. However, the analysis identifies several wells with drainage anomalies. The anomalies were easily resolved because the nature of the anomaly typically coincided with the reservoir characterization.

Analysis of the production by zone indicates the "J" alpha grainstone contributes by far the most Pen Field production, although the "I" zone makes a significant contribution. Both of these zones are attractive waterflood candidates. The "K" zone contributes some production, but is poorly exploited by the original completions. The "L" zone has good porosity and saturation on the logs and in the available cores. However, this pore network exhibits very poor continuity, so the "L" zone probably does not form a commercial reservoir in the Pen Field.

BIBLIOGRAPHY

Amyx, J.W., Bass, D.M., Jr., and Whiting, R.L., 1960, Petroleum reservoir engineering: New York, McGraw-Hill, 610 p.

Anderson, J.E., 1989, Diagenesis of the Lansing and Kansas City Groups (Upper Pennsylvanian), northwestern Kansas and southwestern Nebraska: University of Kansas, M.S. thesis, 259 p.

Asquith, G.B., 1985, Handbook of log evaluation techniques for carbonate reservoirs: Amer. Assoc. of Petroleum Geol., Methods in Exploration Series No. 5, 47 p.

Asquith, G.B., and Gibson, C.R., 1982, Basic well log analysis for geologists: Amer. Assoc. of Petroleum Geol., Methods in Exploration Series No. 3, 216 p.

Badiozamani, K., 1973, The Dorag dolomitization model - application to the Middle Ordovician of Wisconsin: Jour. of Sedimentary Petrology, v. 43, p. 965-984.

Blatt, H., Middleton, G., and Murray, R., 1980, Origin of sedimentary rocks: Englewood Cliffs, New Jersey, Prentice-Hall, 782 p.

Brown, H.A., 1962, Preliminary investigation of Lansing-Kansas City carbonate reservoirs of western Kansas: Kansas Geol. Survey, Open File Report, AMOCO-13.

_____, 1963, Examination of Pennsylvanian carbonate banks in southwestern Kansas: Kansas Geol. Survey, Open File Report, AMOCO-13-A.

_____, 1984a, Adell field and vicinity - Sheridan and Decatur Counties, Kansas: Oil and Gas Jour., v.42, Oct. 29, p. 129-134.

_____, 1984b, Lansing-Kansas City carbonate reservoirs of Haskell County, Kansas, in, Hyne, N.J., (ed.), Limestones of the Mid-Continent: Tulsa, Tulsa Geol. Soc., p. 75-84.

Clynne, M.A., and Potter, R.W., II, 1977, Freezing point depression of synthetic brines (abst.): Geol. Soc. of Amer., Abst. with Programs, v. 9, p. 930.

Crawford, M.L., 1981, Phase equilibria in aqueous fluid inclusions, in, Hollister, L.S., and Crawford, M.L., (eds.), Fluid inclusions: applications to petrology: Mineralogical Assoc. of Canada, Short Course Handbook 6, p. 75-100.

Dickson, J.A.D., 1965, A modified staining technique for carbonates in thin section: Nature, v. 205, p. 587.

Dubois, M.K., 1979, Factors controlling the development of porosity in the Lansing-Kansas City "E" zone, Hitchcock, County, Nebraska: University of Kansas, M.S. thesis, 100 p.

_____, 1985, Application of cores in development of an exploration strategy for the Lansing-Kansas City "E" zone, Hitchcock County, Nebraska, in, Watney, W.L., Walton, A.W., and Doveton, J.H., (compilers), Core studies in Kansas, sedimentology and diagenesis of economically important rock strata in Kansas: Kansas Geol. Survey, Subsurface Geology Series 6, p. 120-132.

Dunham, R.J., 1962, Classification of carbonate rocks according to depositional texture, in, Ham, W.E., (ed.), Classification of carbonate rocks: Amer. Assoc. of Petroleum Geol., Memoir 1, p. 108-121.

Ebanks, W.J., and Watney, W.L., 1985, Geology of Upper Pennsylvanian carbonate oil reservoirs, Happy and Seberger Fields, northwestern Kansas, in, Roehl, P.O., and Choquette, P.W., (eds.), Carbonate petroleum reservoirs: New York, Springer-Verlag, p. 237-250.

Esteban, M., and Klappa, C.F., 1983, Subaerial exposure environment, in, Scholle, P.A., Bebout, D.G., and Moore, C.H., (eds.), Carbonate depositional environments: Amer. Assoc. of Petroleum Geol., Memoir 33, p. 1-95.

Evamy, B.D., 1969, The precipitational environment and correlation of some calcite cements deduced from artificial staining: Jour. of Sedimentary Petrology, v. 39, p. 787-793.

Goldstein, R.H., 1986, Reequilibration of fluid inclusions in low-temperature calcium-carbonate cement: Geology, v. 14, p. 792-795.

_____, 1990, Petrographic and geochemical evidence for origin of paleospeleothems, New Mexico: implications for the application of fluid inclusions to studies of diagenesis: Jour. of Sedimentary Petrology, v. 60, p. 282-292.

Harbaugh, J.W., and Davie, W., Jr., 1964, Upper Pennsylvanian calcareous rocks cored in two wells in Rawlins and Stafford Counties: Kansas Geol. Survey, Bull. 170, pt. 6, p. 1-18.

Harris, P.M., 1979, Facies anatomy and diagenesis of a Bahamian ooid shoal: University of Miami (Florida), Division of Marine Geology and Geophysics, Sedimenta VII, 163 p.

Harris, P.M., Kendall, C.G.St.C., and Lerche, I., 1985, Carbonate cementation - a brief review, in, Schneidermann, N., and Harris, P.M., (eds.), Carbonate cements: Soc. of Economic Paleontologists and Mineralogists, Special Publication no. 36, p. 79-95.

Heckel, P.H., 1977, Origin of phosphatic black shale facies in Pennsylvanian cyclothems of Mid-Continent North America: Amer. Assoc. of Petroleum Geol. Bull., v. 61, p. 1045-1068.

_____, 1983, Diagenetic model for carbonate rocks in Midcontinent Pennsylvanian eustatic cyclothems: Jour. of Sedimentary Petrology, v. 53, p. 733-759.

Hopkins, R.T., 1977, Reservoir geology of the Captain Creek Limestone, Wilson Creek Oil Field, Ellsworth and Russell Counties, Kansas: University of Kansas, M.S. thesis, 89 p.

Kintner, H.B., 1984, A subsurface study of the "F" zone (Pennsylvanian System) in Hitchcock County, Nebraska: University of Nebraska, M.S. thesis, 227 p.

Klappa, C.F., 1980, Rhizoliths in terrestrial carbonates; classification, recognition, genesis and significance: Sedimentology, v. 27, p. 613-629.

Land, L.S., 1973, Holocene meteoric dolomitization of Pleistocene limestones, north Jamaica: Sedimentology, v. 20, p. 411-422.

Longman, M.W., 1980, Carbonate diagenetic textures from nearsurface diagenetic environments: Amer. Assoc. of Petroleum Geol. Bull., v. 64, p. 461-487.

Maher, J.C., 1953, Permian and Pennsylvanian rocks of southeastern Colorado: Amer. Assoc. of Petroleum Geol. Bull., v. 37, p. 913-939.

Maier, L.F., 1962, Recent developments in the interpretation and application of DST data: Jour. of Petroleum Technology, v. 14, p. 1213-1222.

Malinky, J.M., 1982, Paleontology and depositional environments of Pennsylvanian low-oxygen shales, Mid-Continent North America (abst.): Geol. Soc. of Amer., Abst. with Programs, v. 14, p. 554.

Martin, C.A., 1965, Denver Basin: Amer. Assoc. of Petroleum Geol. Bull., v. 49, p. 1908-1925.

Merriam, D.F., 1963, The geologic history of Kansas: Kansas Geol. Survey Bull. 162, 317 p.

Moore, R.C., 1936, Stratigraphic classification of Pennsylvanian rocks of Kansas: Kansas Geol. Survey, Bull. 22, 256 p.

_____, 1949, Divisions of the Pennsylvanian System in Kansas: Kansas Geol. Survey, Bull. 83, 203 p.

Morgan, J.V., 1952, Correlation of radioactive logs of the Lansing and Kansas City Groups in central Kansas: Jour. of Petroleum Technology, v. 4, p. 111-118.

Mossler, J.H., 1973, Carbonate facies of the Swope Limestone Formation (Upper Pennsylvanian), southeast Kansas: Kansas Geol. Survey, Bull. 206, pt. 1, p. 1-17.

Payton, C.E., 1966, Petrology of the carbonate members of the Swope and Dennis Formations (Pennsylvanian), Missouri and Iowa: Jour. of Sedimentary Petrology, v. 36, p. 576-601.

Potter, R.W., II, Clynne, M.A., and Brown, D.L., 1978, Freezing point depression of aqueous sodium chloride solutions: Economic Geol., v. 73, p. 284-285.

Prather, B.E., 1981, Petrology and diagenesis of the D-zone megacyclothem of the Lansing-Kansas City Groups, Hitchcock County, Nebraska: University of New Orleans, M.S. thesis, 97 p.

_____, 1984, Deposition and diagenesis of an Upper Pennsylvanian cyclothem from the Lansing-Kansas City Groups, Hitchcock County, Nebraska, in, Hyne, N.J., (ed.), Limestones of the Mid-Continent: Tulsa, Tulsa Geol. Soc., p. 394-419.

_____, 1985a, An Upper Pennsylvanian desert paleosol in the D-zone of the Lansing-Kansas City Groups, Hitchcock County, Nebraska: Jour. of Sedimentary Petrology, v. 55, p. 218-221.

_____, 1985b, Depositional facies and diagenetic fabrics of the D-zone cyclothem Lansing-Kansas City Groups, Hitchcock County, Nebraska, in, Watney, W.L., Walton, A.W., and Doveton, J.H., (compilers), Core studies in Kansas, sedimentology and diagenesis of economically important rock strata in Kansas: Kansas Geol. Survey, Subsurface Geology Series 6, p. 133-144.

Rascoe, B., Jr., and Adler, F.J., 1983, Permo-Carboniferous hydrocarbon accumulations, Mid-Continent, U.S.A.: Amer. Assoc. of Petroleum Geol. Bull., v. 67, p. 979-1001.

Reid, H.W., 1986, DST interpretation for geologists (short course notes): Calgary, Canada, Hugh W. Reid & Associates, 216p.

Roedder, E., 1967, Metastable superheated ice in liquid-water inclusions under high negative pressure: Science, v. 155, p. 1413-1417.

_____, 1984, Fluid inclusions: Mineralogical Soc. of Amer., Reviews in Mineralogy, v. 12, 646 p.

Scholle, P.A., 1978, A color illustrated guide to carbonate rock constituents, textures, cements, and porosities: Amer. Assoc. of Petroleum Geol., Memoir 27, 241 p.

Scholle, P.A., and Halley, R.B., 1985, Burial diagenesis: out of sight, out of mind, in, Schneidermann, N., and Harris, P.M., (eds.), Carbonate cements: Soc. of Economic Paleontologists and Mineralogists, Special Publication no. 36, p. 309-334.

Wanless, H.R., 1967, Eustatic shifts in sea level during the deposition of Late Paleozoic sediments in the central United States, in, Elam, J.G., and Chuber, S., (eds.), Cyclic sedimentation in the Permian Basin: W. Texas Geol. Soc. Publication 69-56, p. 41-54 (reprinted 1972 as Publ. 72-60).

Wanless, H.R., and Shepard, F.P., 1936, Sea level and climatic changes related to Late Paleozoic cycles: Geol. Soc. of Amer. Bull., v. 47, p. 1177-1206.

Watney, W.L., 1980, Cyclic sedimentation of the Lansing-Kansas City Groups in northwestern Kansas and southwestern Nebraska: Kansas Geol. Survey, Bull. 220, 70 p.

_____, 1984, Recognition of favorable reservoir trends in Upper Pennsylvanian cyclic carbonates in western Kansas, in, Hyne, N.J., (ed.), Limestones of the Mid-Continent: Tulsa, Tulsa Geol. Soc., p. 201-246.

_____, 1985, Evaluation of the significance of tectonic, sedimentary control versus eustatic control of Upper Pennsylvanian cyclothems in the western Midcontinent, in, Watney, W.L., Kaesler, R.L., and Newell, K.D., (convenors), Recent interpretations of Late Paleozoic cyclothems: Kansas Geol. Survey, Proceedings of the Third Annual Meeting and Field Conference, Mid-Continent Section, Soc. of Economic Paleontologists and Mineralogists, p. 105-140.

_____, 1986, Petroleum reservoir characterization of Upper Pennsylvanian cyclic carbonates in the Hugoton Embayment: Kansas Geol. Survey, short course, v. I and II, 130 p.

Watney, W.L., and Ebanks, W.J., Jr., 1978, Early subaerial exposure and freshwater diagenesis of Upper Pennsylvanian cyclic sediments in northern Kansas and southern Nebraska (abst.): Amer. Assoc. of Petroleum Geol. Bull., v.62, p. 570-571.

Wilson, J.L., and Jordan, C., 1983, Middle shelf environment, in, Scholle, P.A., Bebout, D.G., and Moore, C.H., (eds.), Carbonate depositional environments: Amer. Assoc. of Petroleum Geol., Memoir 33, p. 297-343.

APPENDIX 1

CORE DESCRIPTIONS

Key to Symbols Used in Core Descriptions:

Interval

Divisions in feet, inches
Scale 1" = 2.4'

Analysis

W - whole core
P - core plug

Pore Types (extant)

BP - Interparticle
WP - Intraparticle
BC - Intercrystal
MO - Moldic
FE - Fenestral
SH - Shelter
GF - Growth Framework
FR - Fracture
CH - Channel
VG - Vug
CV - Cavern
BR - Breccia
BO - Boring
BU - Burrow
SK - Shrinkage
T - Tight

Composition


Porosity

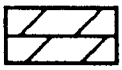
Dolostone

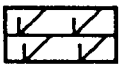
Limey Dolostone

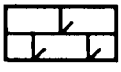
Dolomitic Limestone

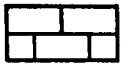
Limestone


Argillaceous Limestone


Very Argillaceous Limestone


Silty Shale (structureless)


Silty Shale (laminated)

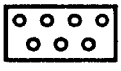
Conglomerate


Missing Interval

Nature of Contact

S - Sharp
SI - Sharp irregular
SC - Sharp conformable
SD - Sharp disconformable
G - Gradational
B - Gradational - interbedded

VS - Visibly scoured
BU - Burrowed
ST - Stylolite
MS - Microstylolite
MSS - Microstylolite swarm
CS - Clay seam
SS - Slickenside

Paragenesis

■ - Pyrite
Ch - Chert
Cd - Chalcedony

Ph - Phosphatic material
Calcite cement
S - Silica cement

Structures

- slickensides
- stylolite
- microstylolite
- microstylolite swarm
- clay seam
- vertical fracture
- horizontal fracture
- planar lamination
- wavy lamination
- discontinuous lamination

- crossbedding
- autoclastic brecciation
- vertical burrow
- horizontal burrow
- bioturbation
- root trace
- plant debris
- carbonate lithoclast
- pipes or fissures
- alveolar structure

Texture


Ooids


Coated Grains


Lithoclasts


Intraclasts

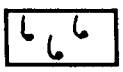
Skeletal Grains

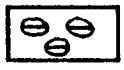
Peloids


Crust


Micrite


Highly Altered (superimposed over interpreted texture)

Fabric

M - mudstone
W - wackestone
P - packstone
G - grainstone

Allochems

- present
- common
- abundant

Color

G - gray
B - brown
R - red
Gn - green
Bl - blue
C - cream
W - white
Bk - black
Ol - olive

modifiers

L - light
M - medium
D - dark

Example: LBG = light brownish gray

Well Bethel #3 Interval Lke I-J Date 8/2/88

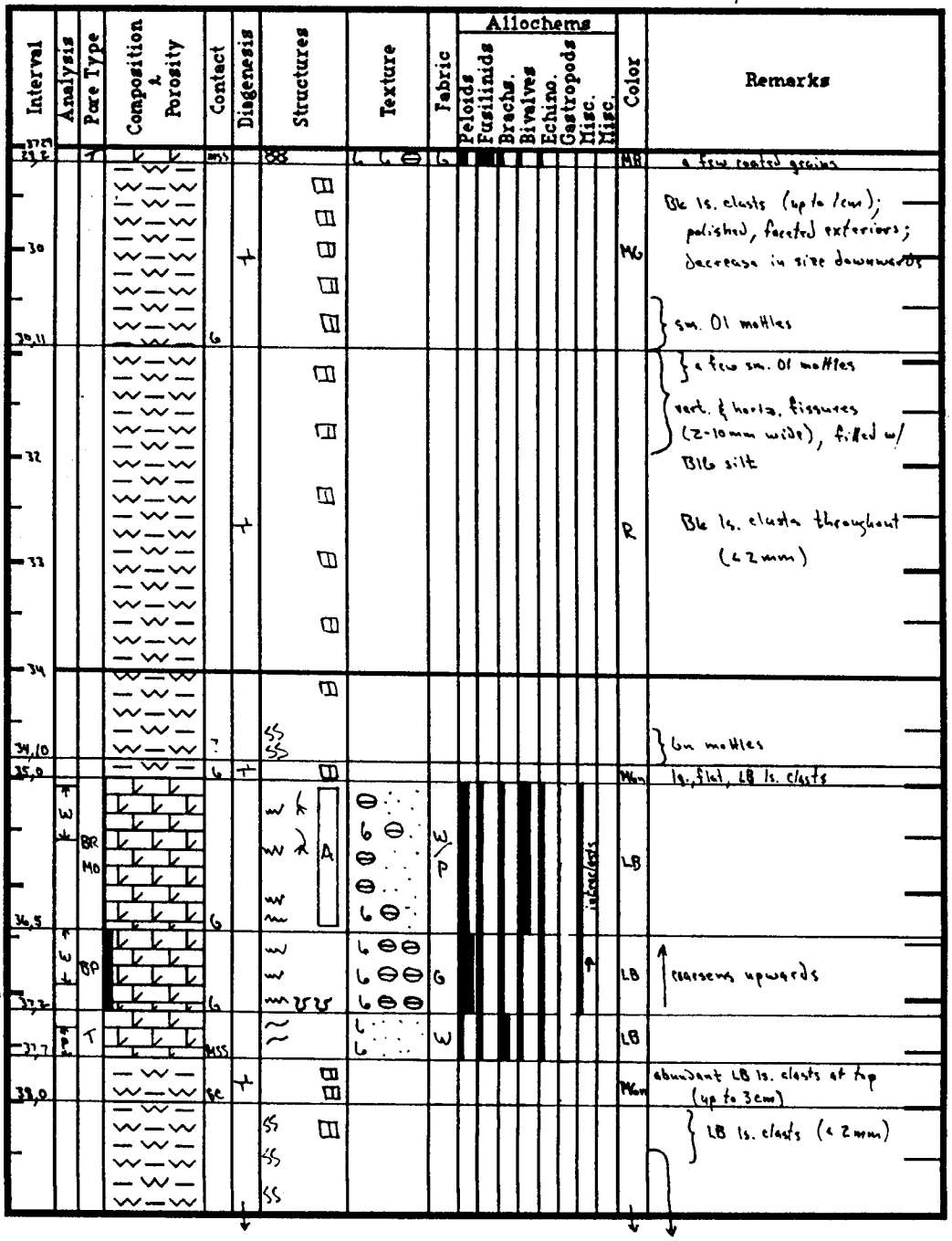

Well Bethel #3 Interval LKC I-I Date 3/2/88 p.2

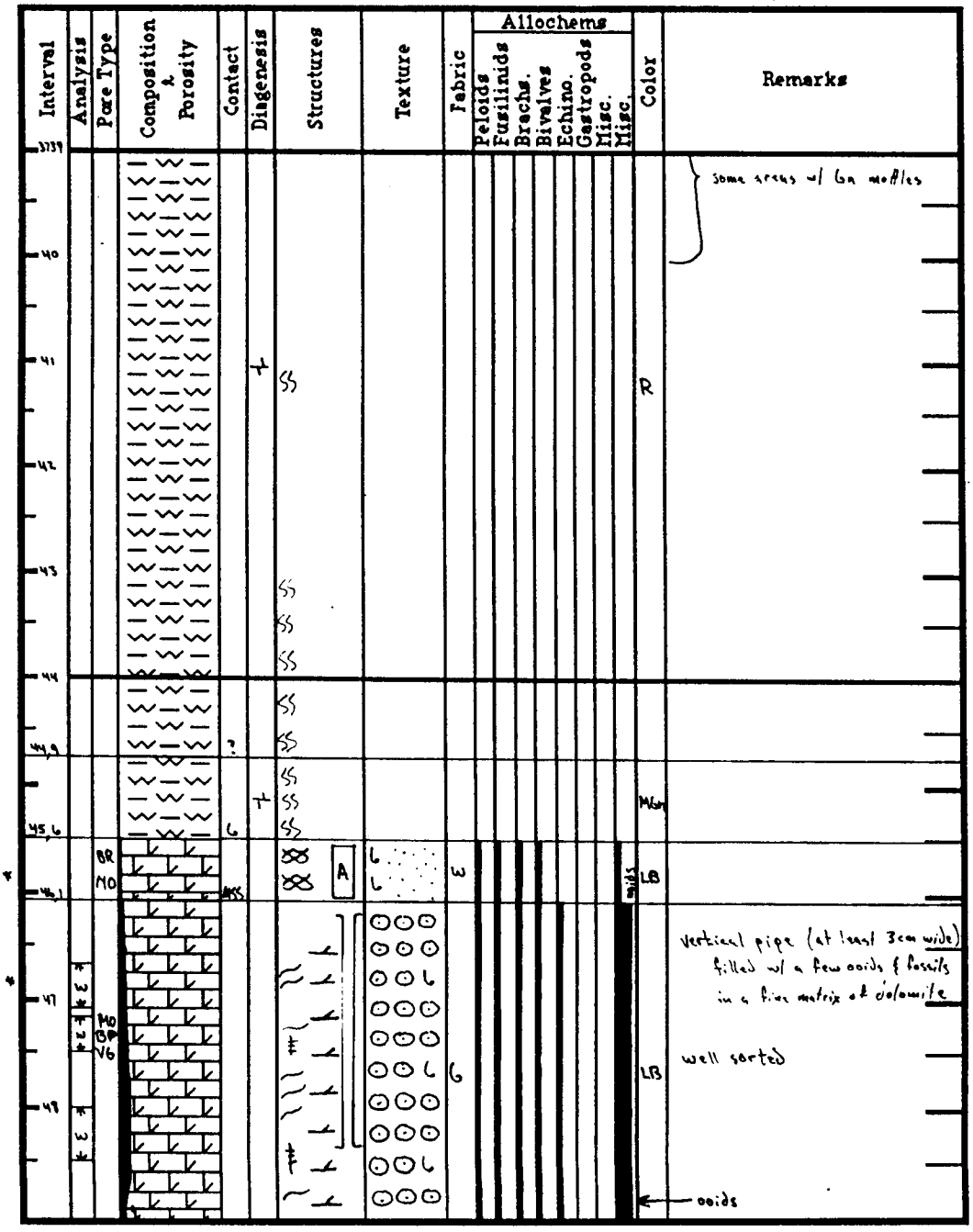

Well Bethel #3 Interval LWC I-J Date 8/2/88 p.3

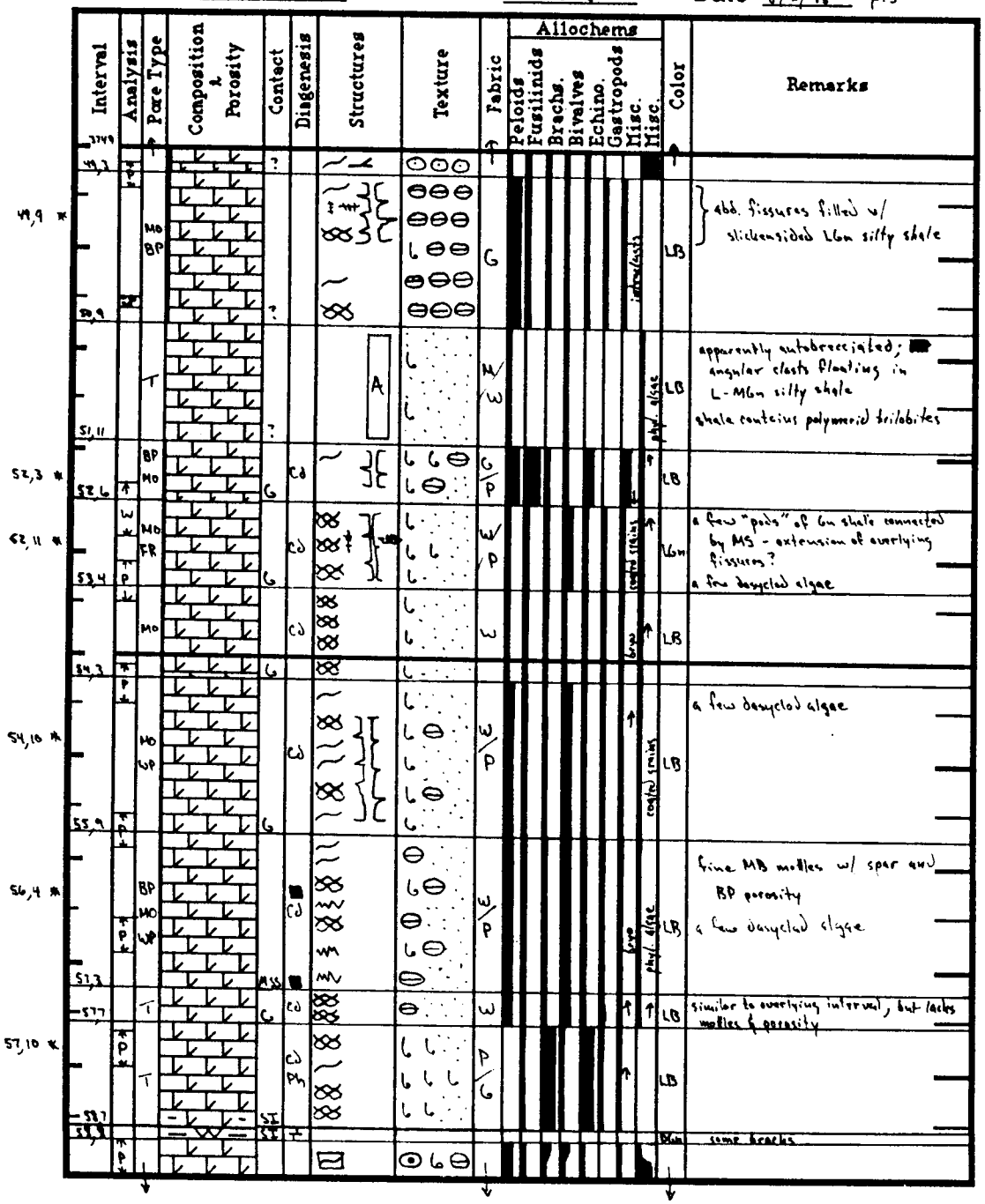

Well Bethel #3 Interval Lkc I-J Date 8/2/88 p.4

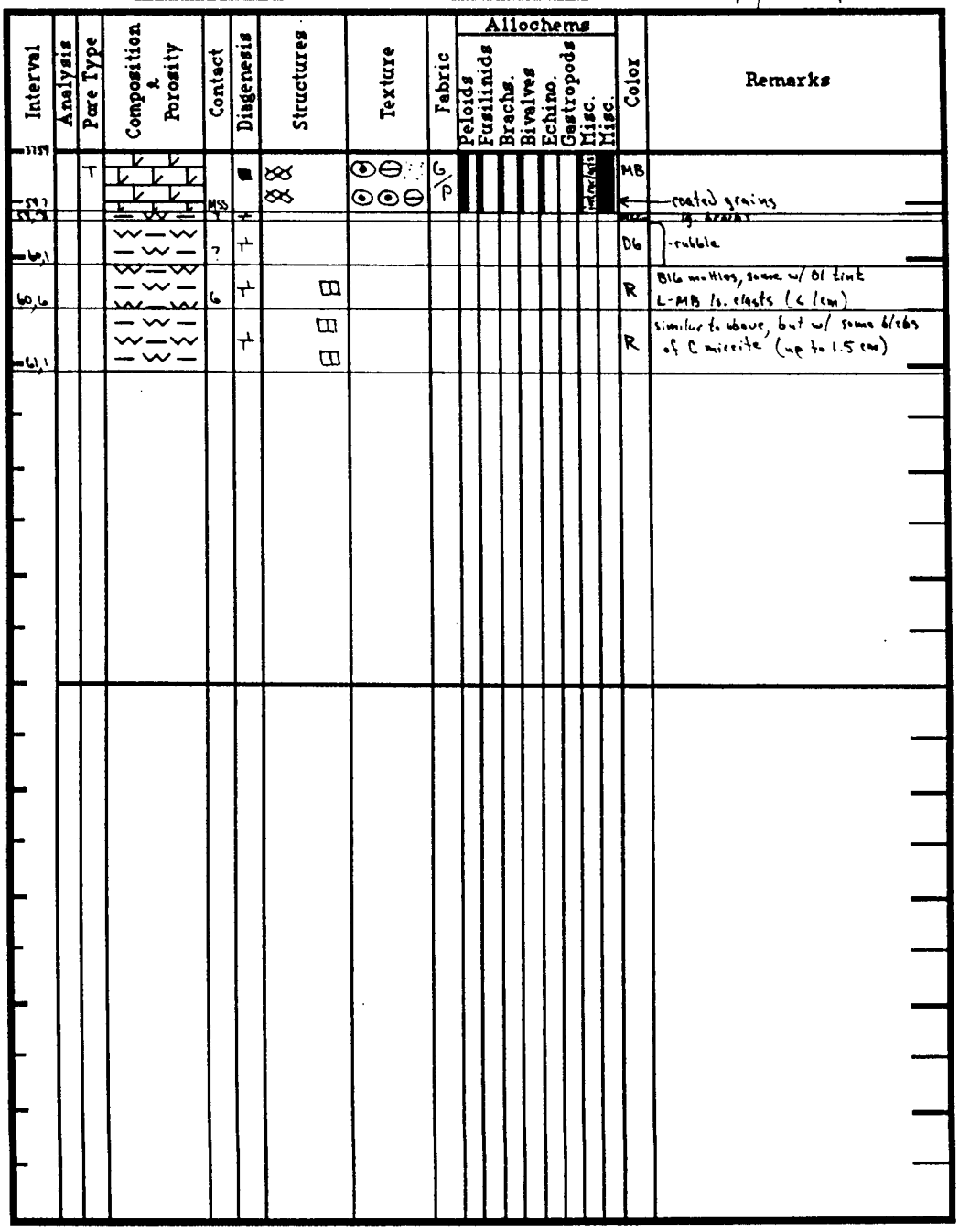

Well Bethel #5 Interval LKC I-J Date 7/26/88 p. 1

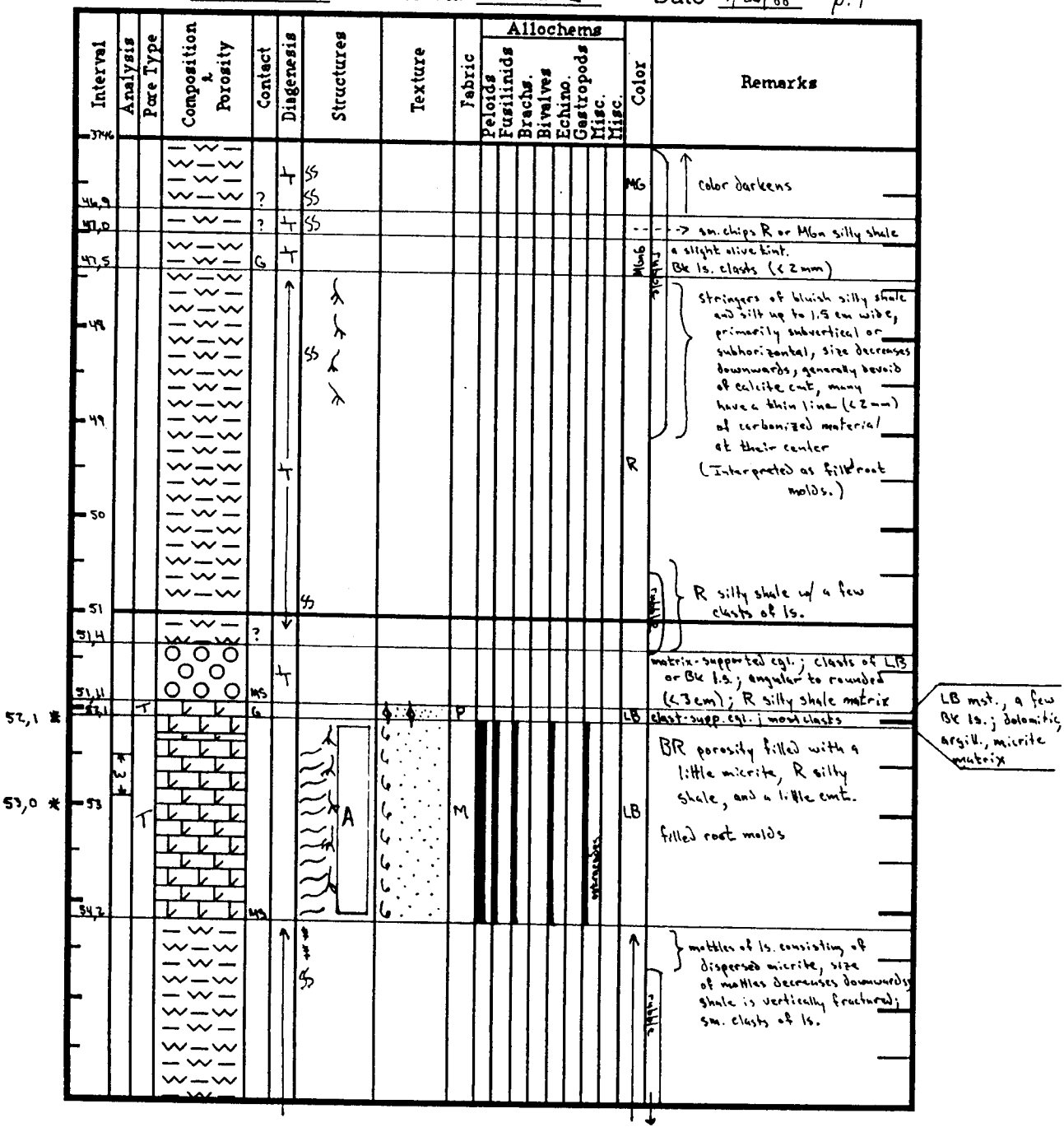

Well Bethel #5 Interval LKC I-J Date 7/26/88 p. 2

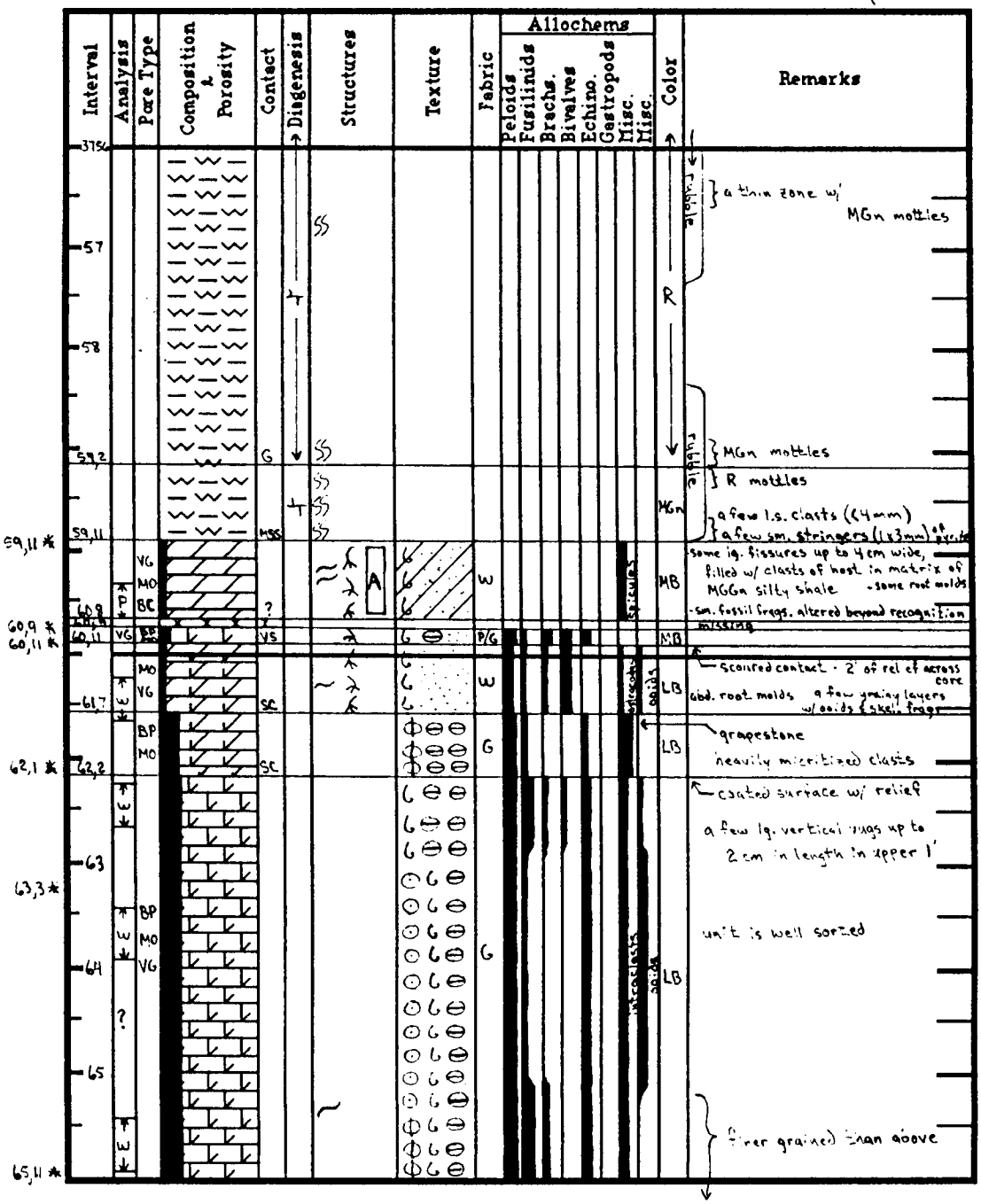

Well Bethel #5 Interval LVL I-J Date 7/26/88 p.3

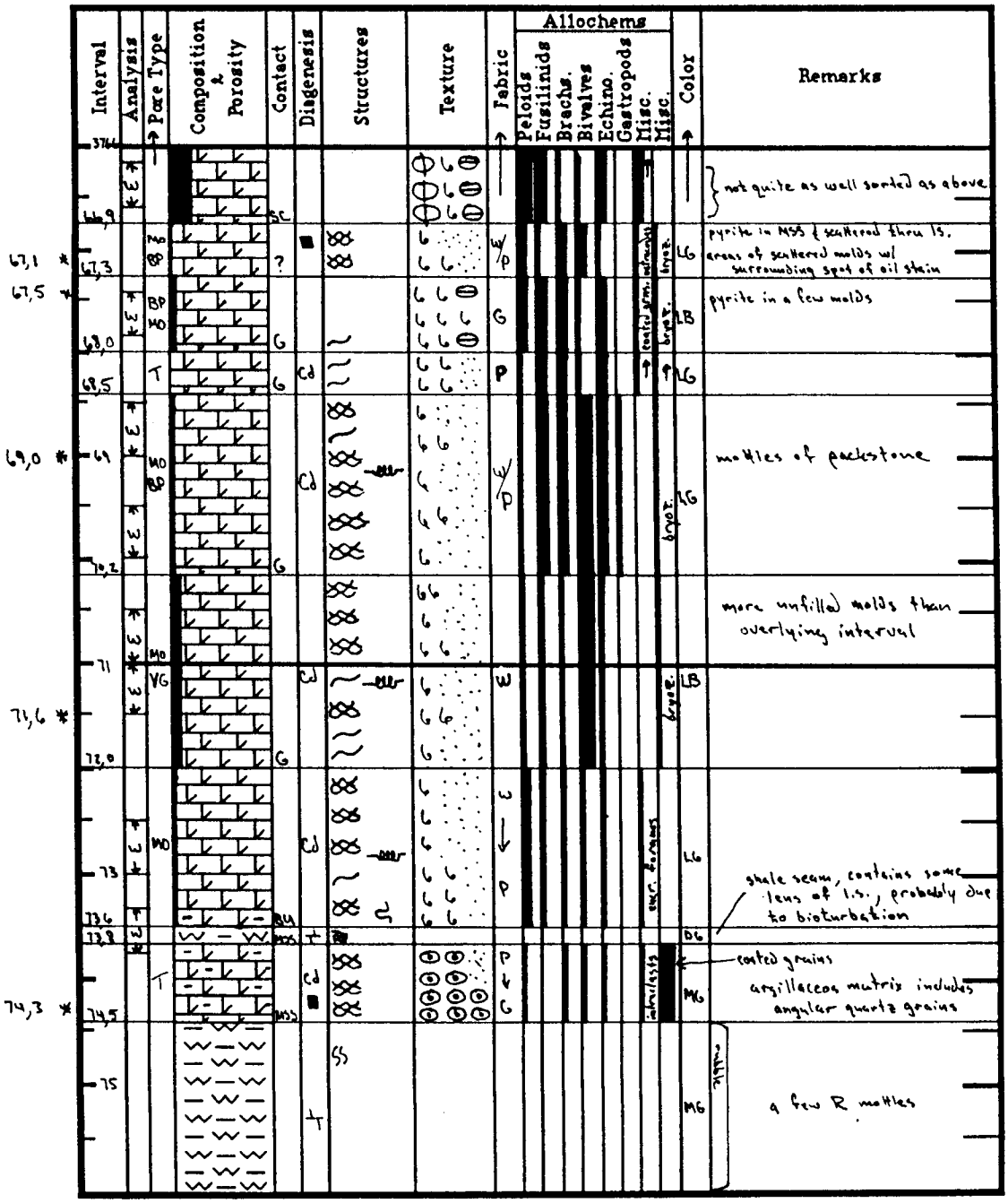

Well Demuth #1 Interval LKC I-J Date 7/21/88

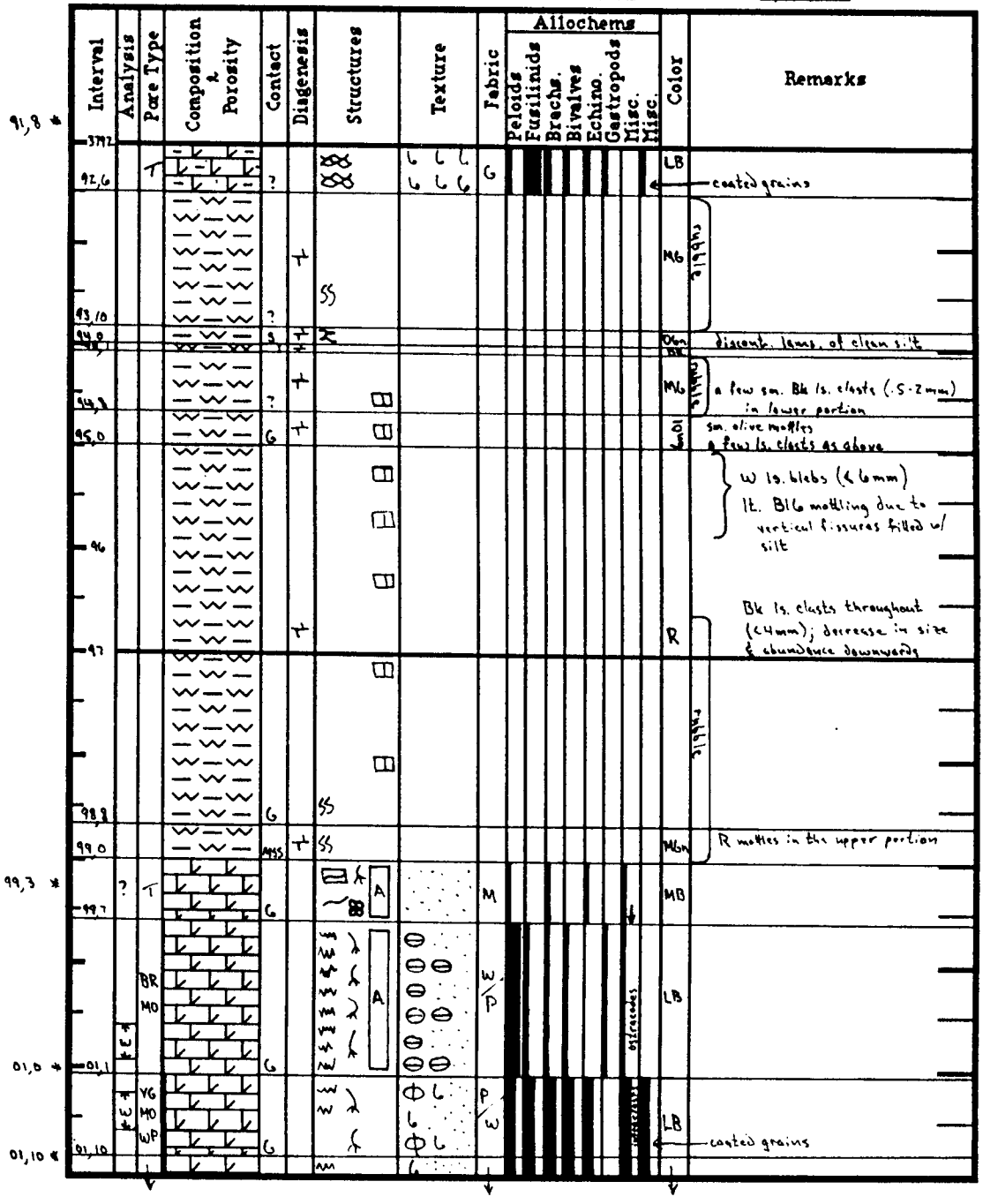

Well Demuth #1 Interval LKC I-J Date 7/21/98 p.2

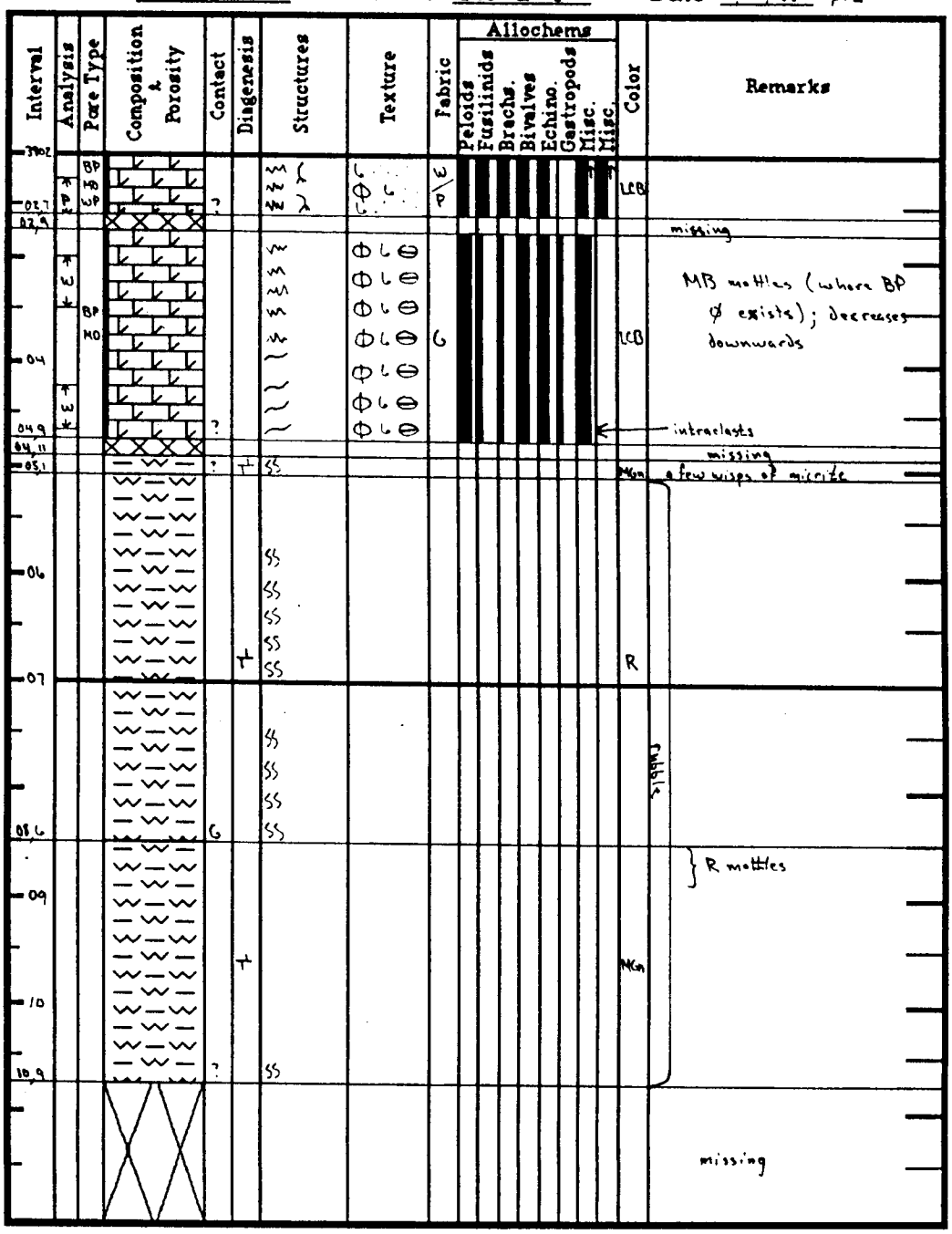

Well Demuth #1 Interval LKC I-J Date 7/21/88 p. 3

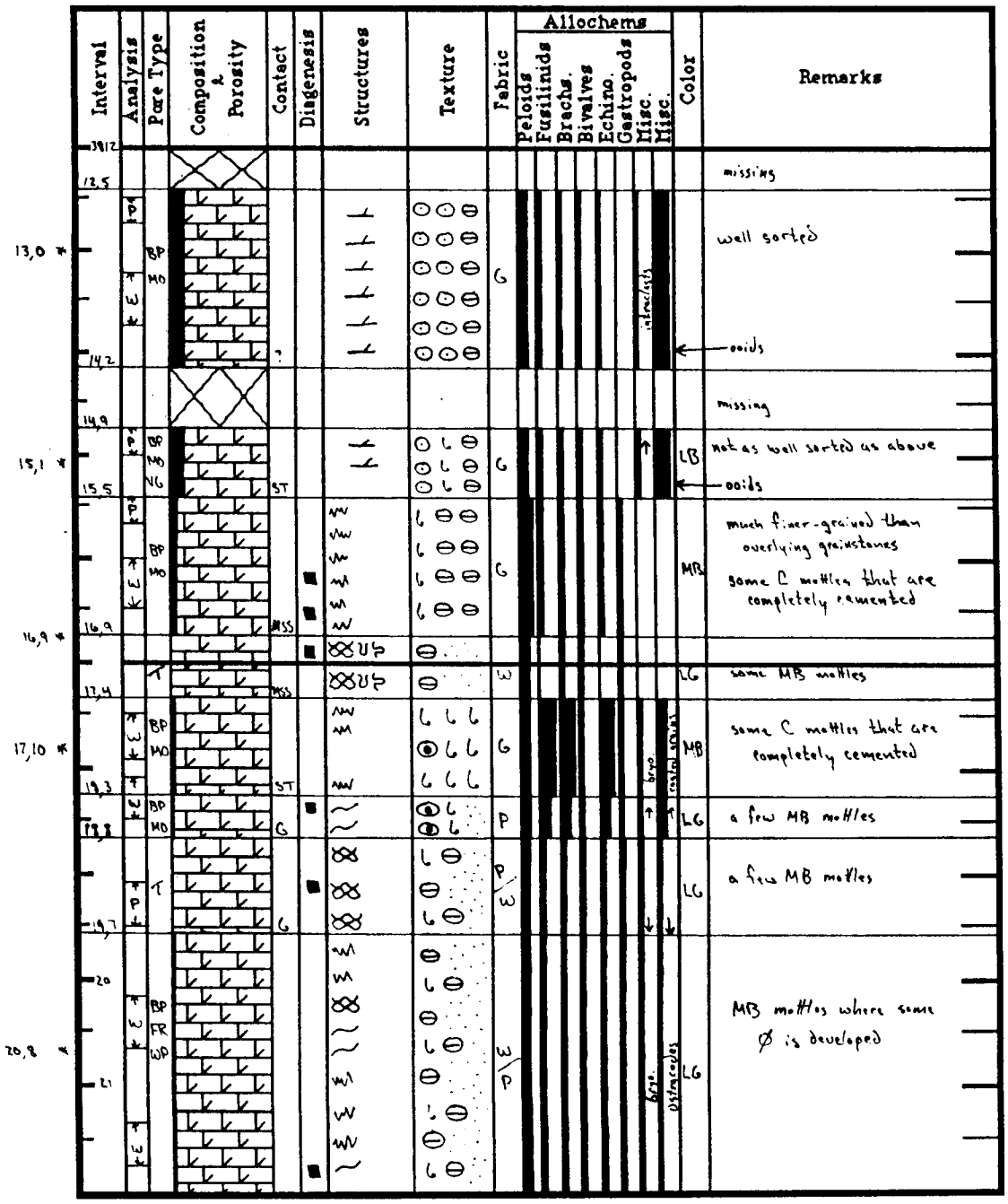

Well Demuth #1 Interval LKC I-J Date 7/21/88 p. 4

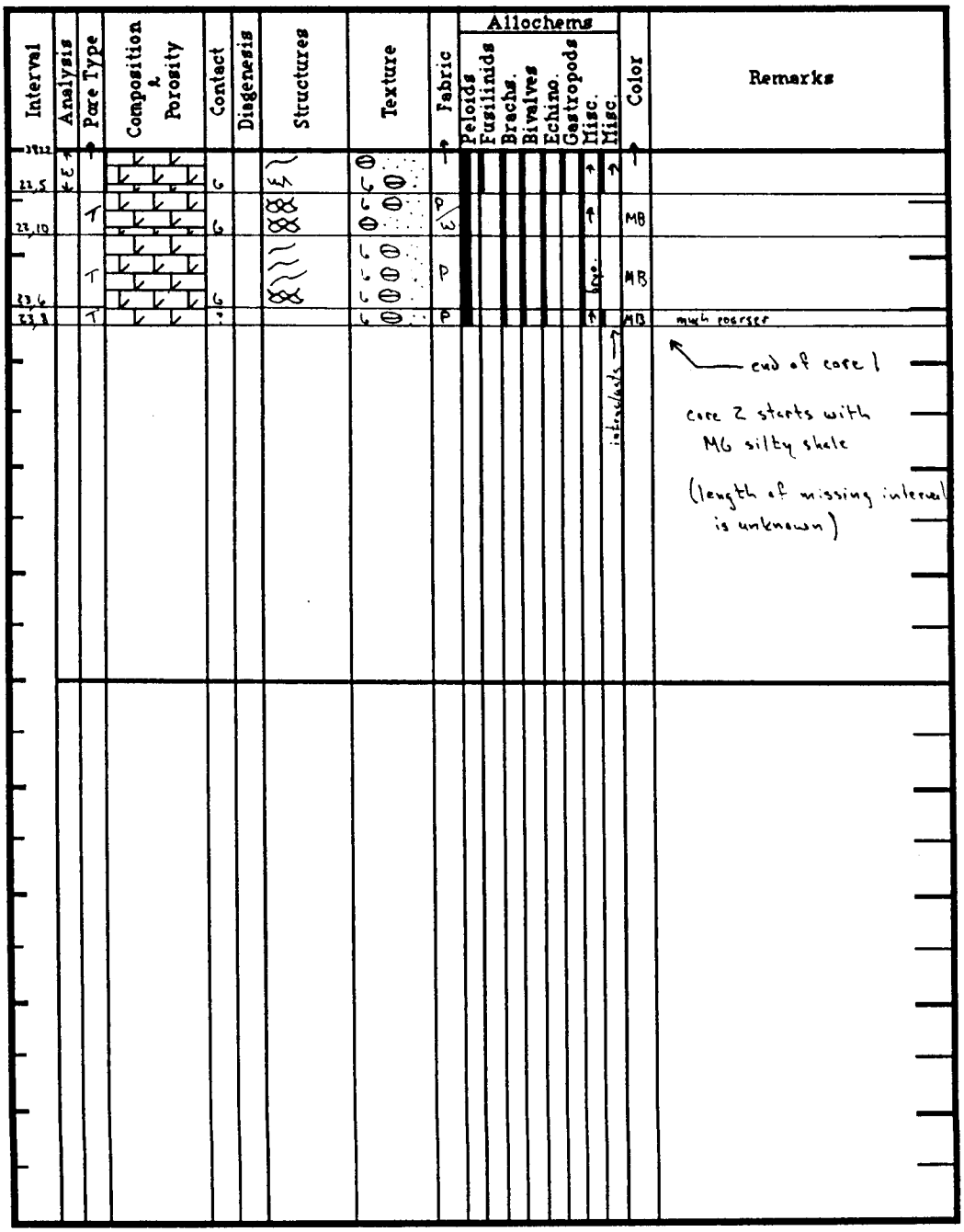

Well Demuth #4 Interval LVC I-J Date 8/30/88

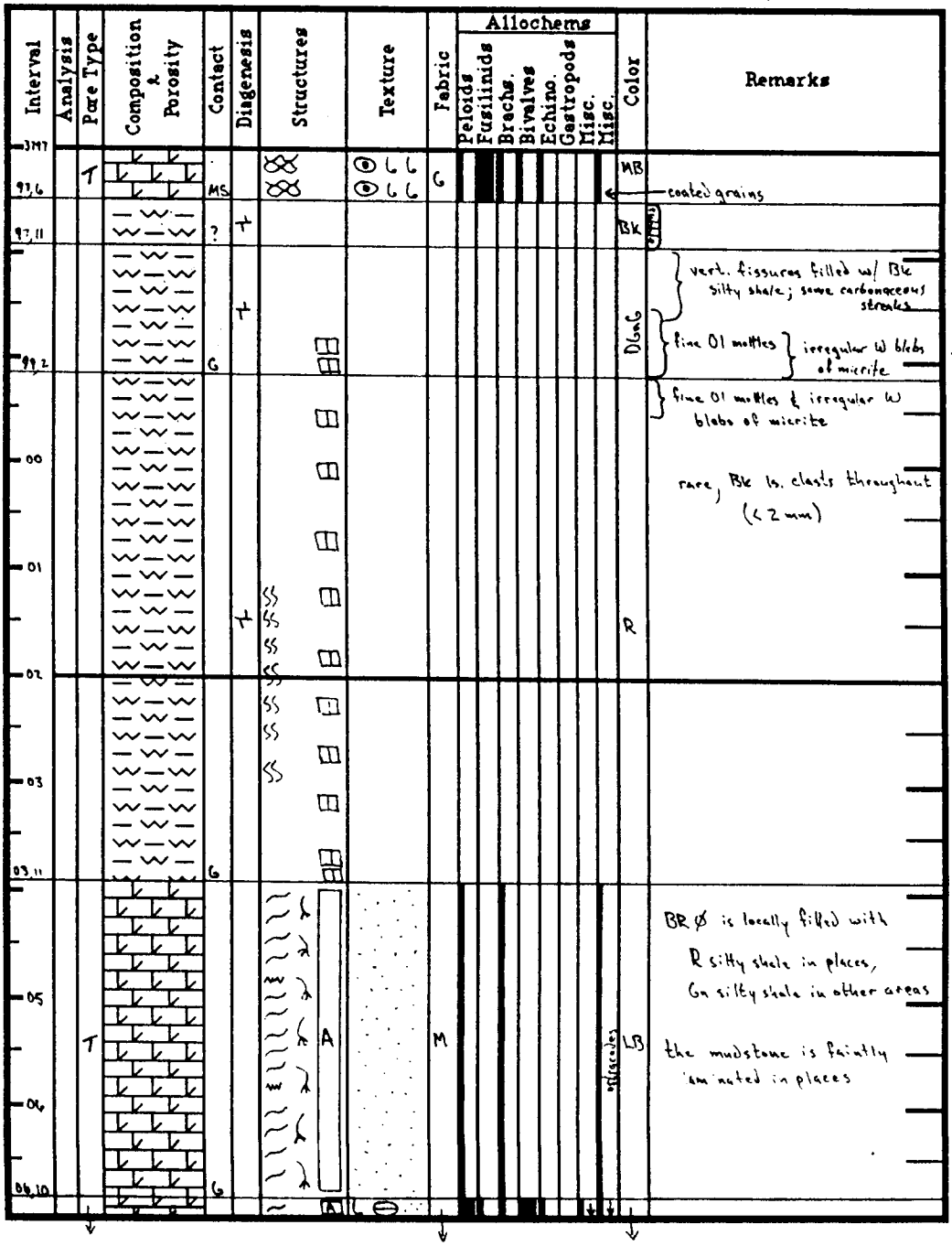

Well Demuth #4 Interval LKC I-J Date 8/30/98 p.2

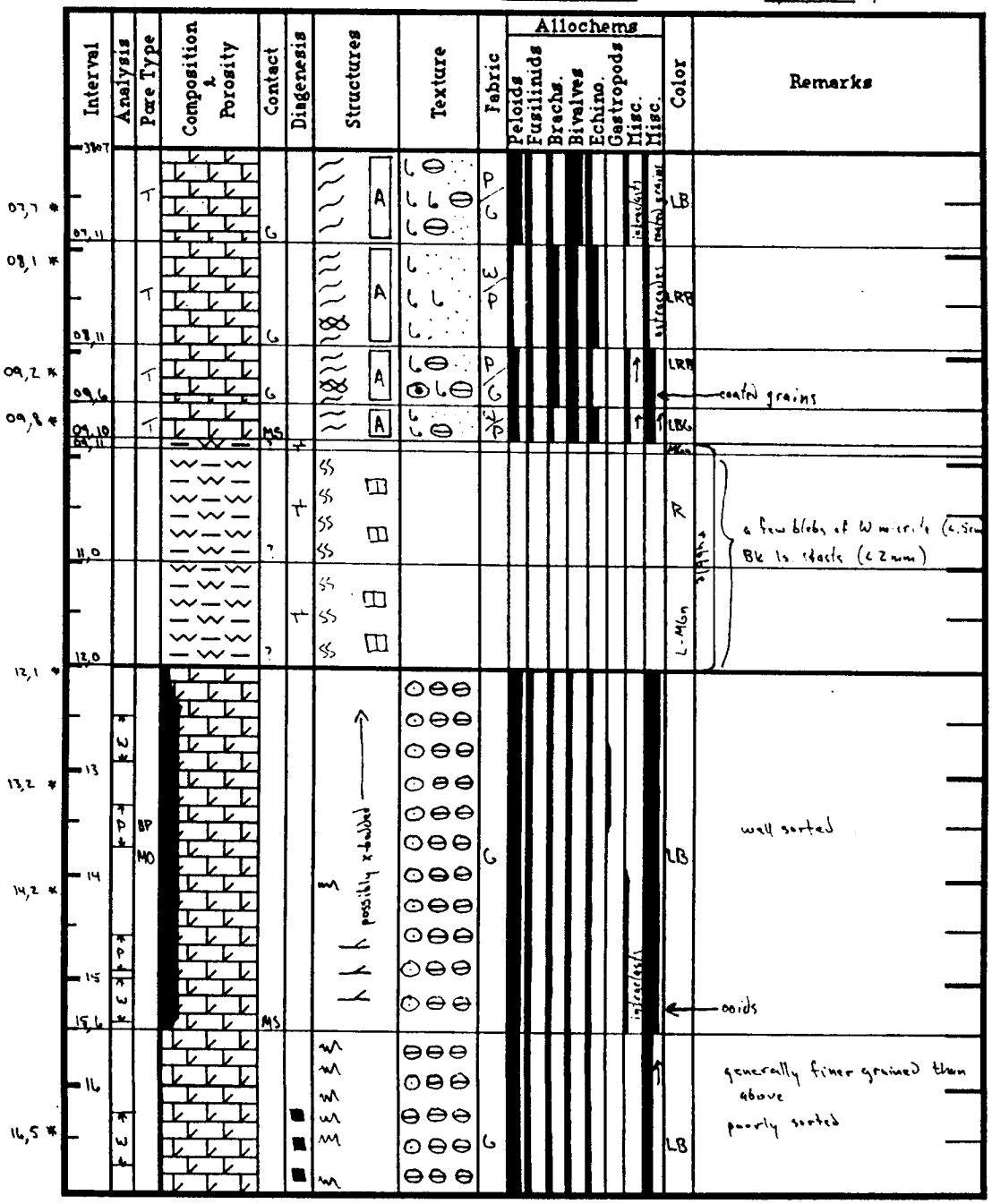

Well Nemaha #4 Interval LKC I-J Date 8/30/88 p. 3

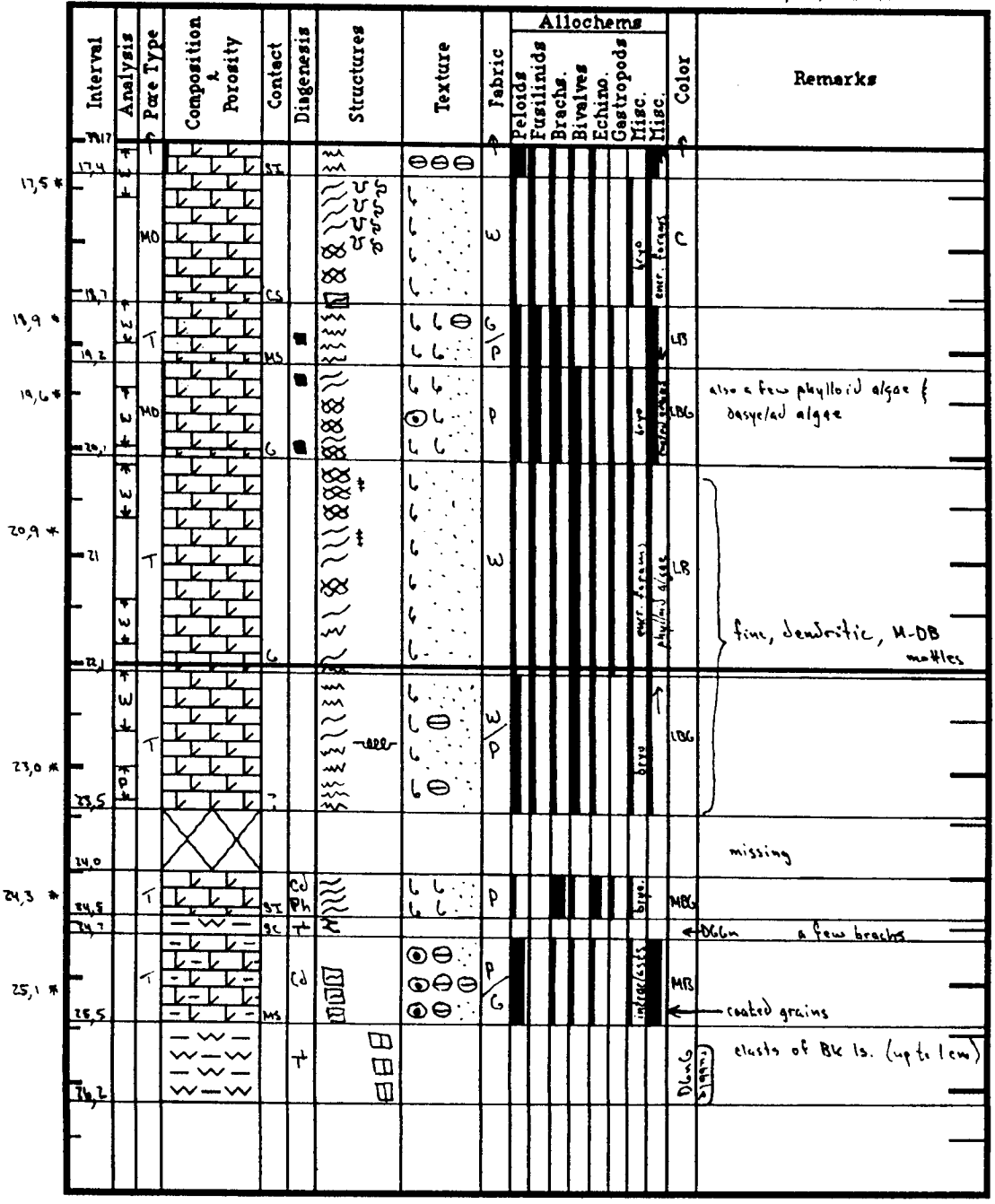

Well Pennington #2 Interval LKC I-J Date 8/12/18 p.1

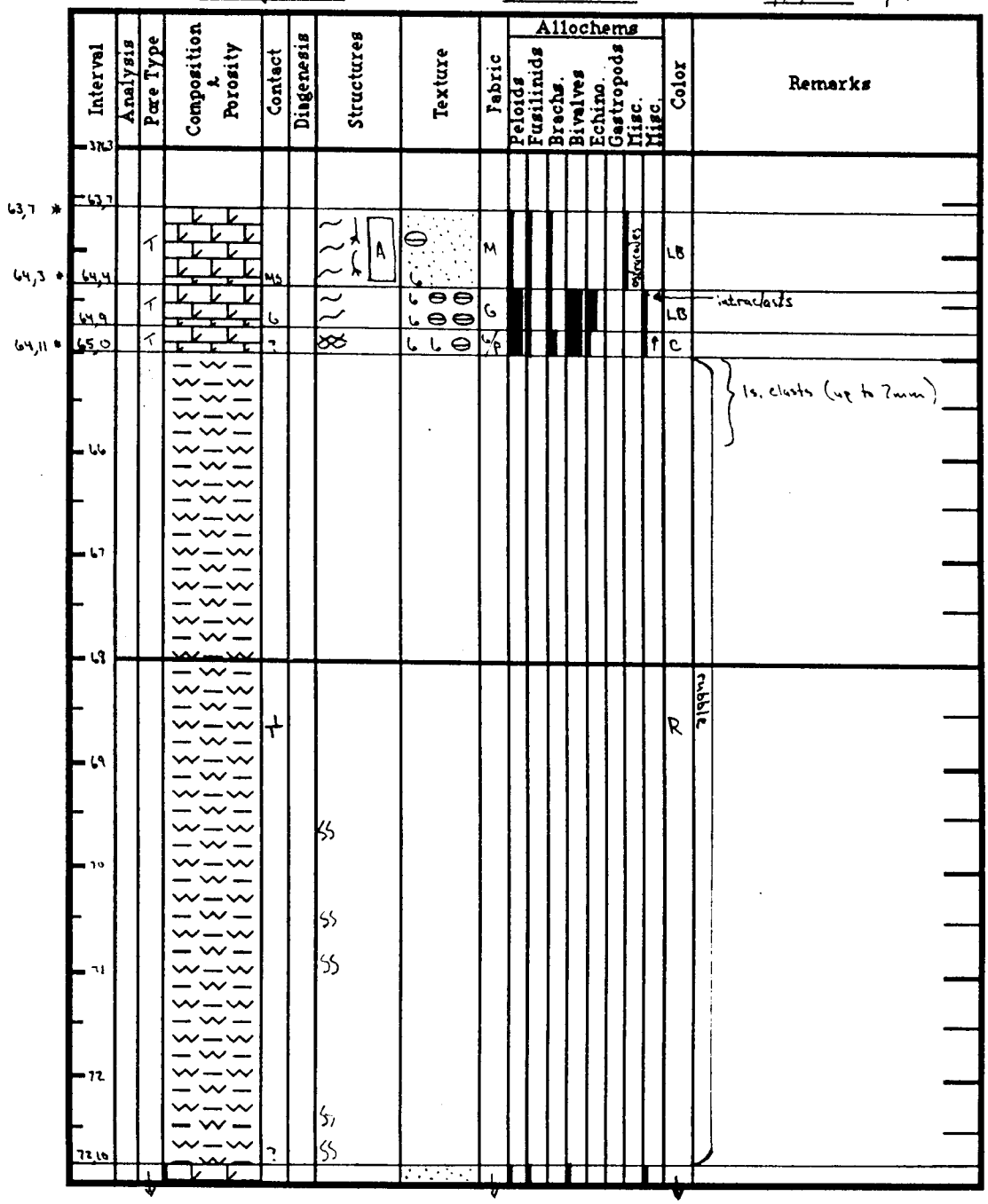

Well Pennington #2 Interval LKC I-J Date 8/12/98 p. 2

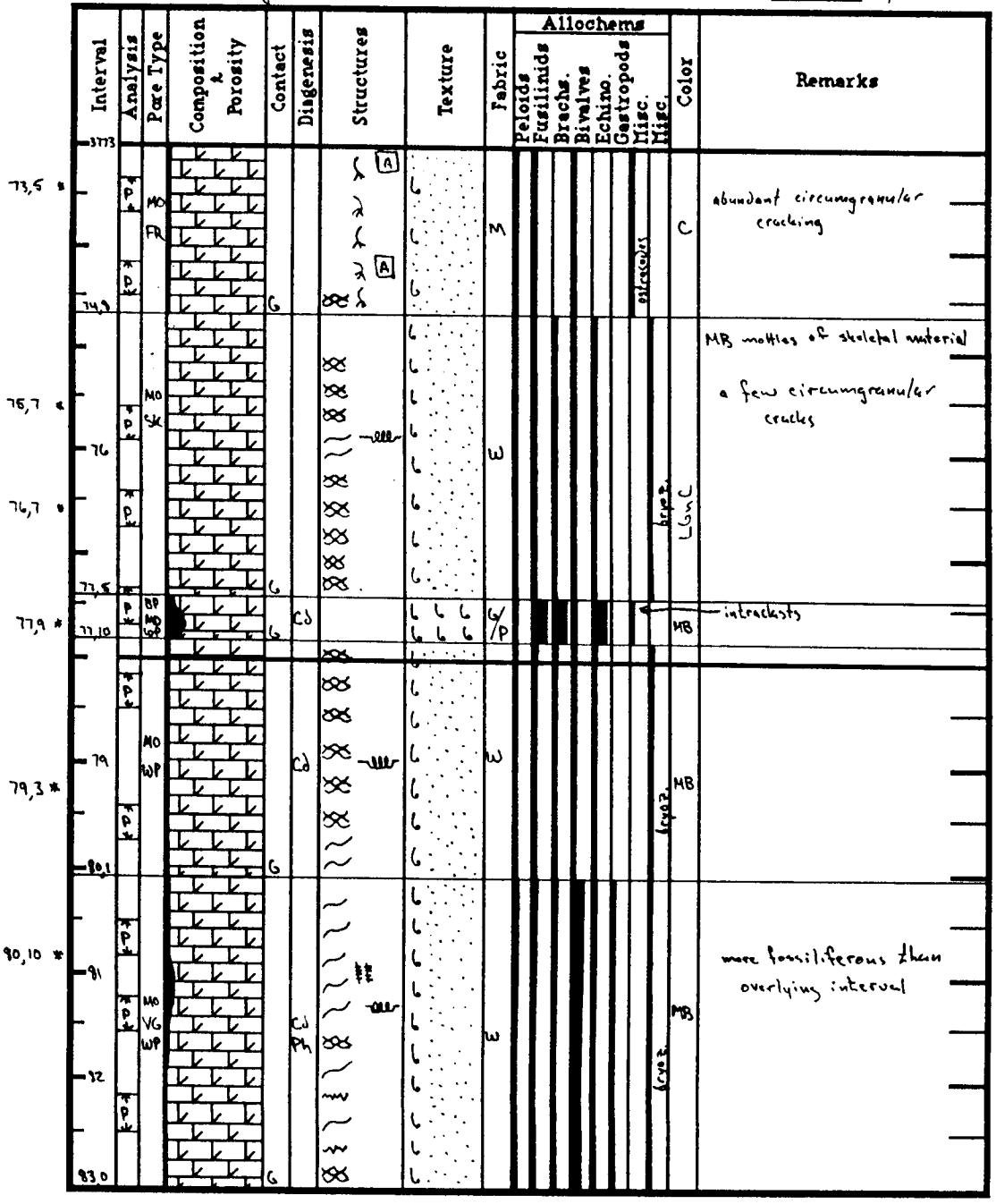

Well Pennington #2 Interval Lwr. I-J Date 9/12/88 p. 3

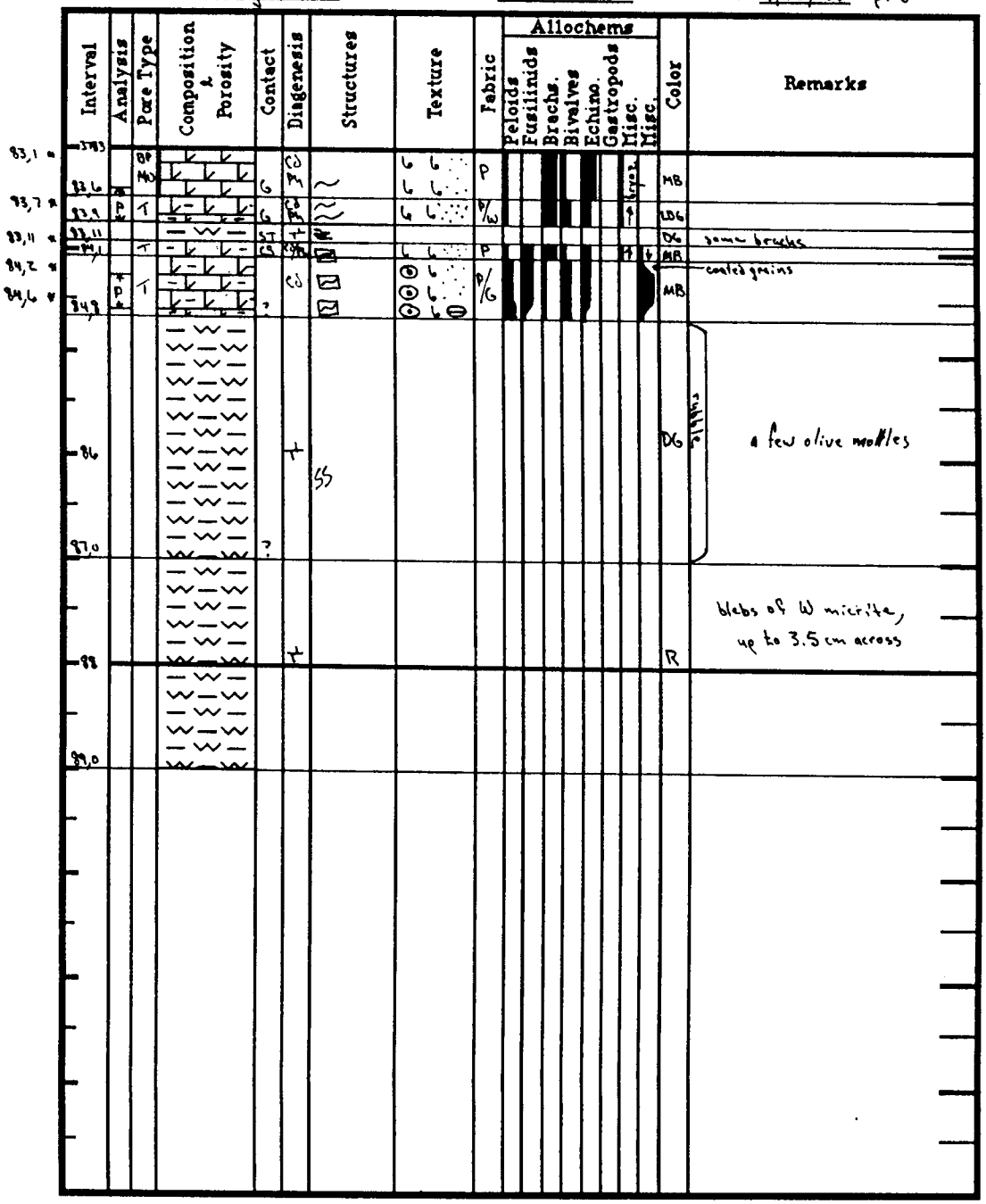

Well Rogers #1 Interval Lkc I-J Date 8/14/88 p.1

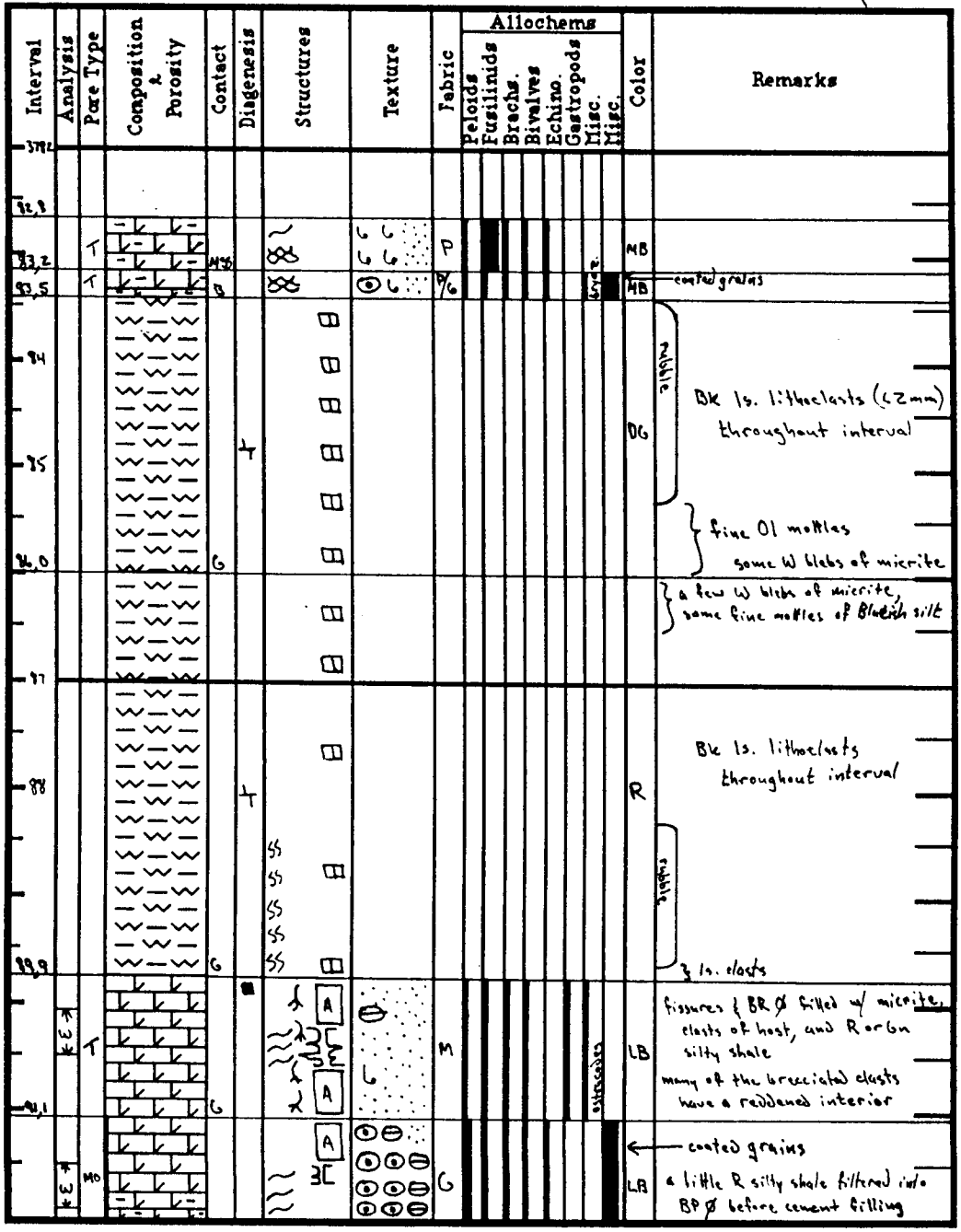

Well Rogers #1 Interval Lkc I-J Date 8/16/88 p. 2

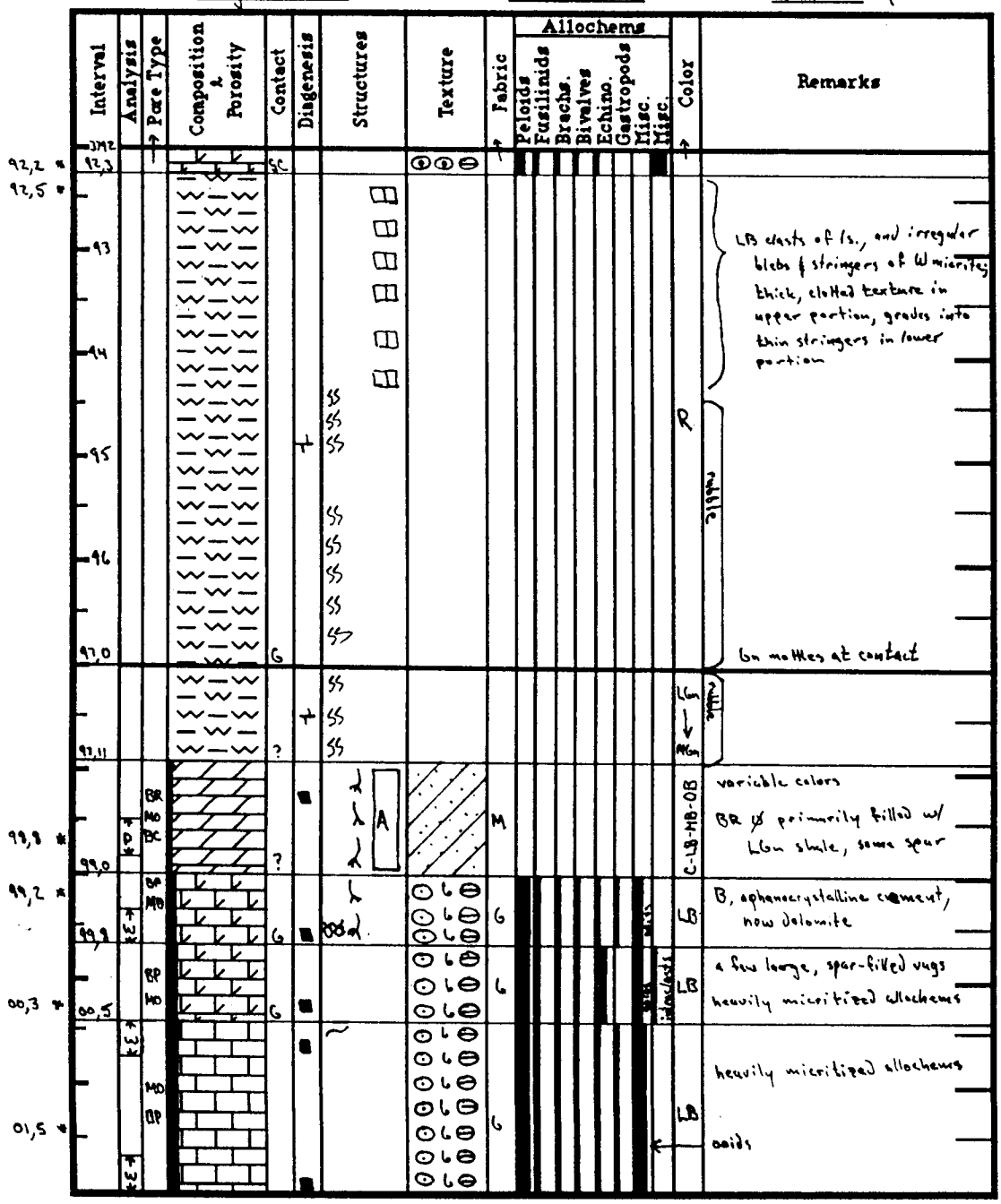

Well Rogers #1 Interval Lwr T-J Date 8/16/88 p.3

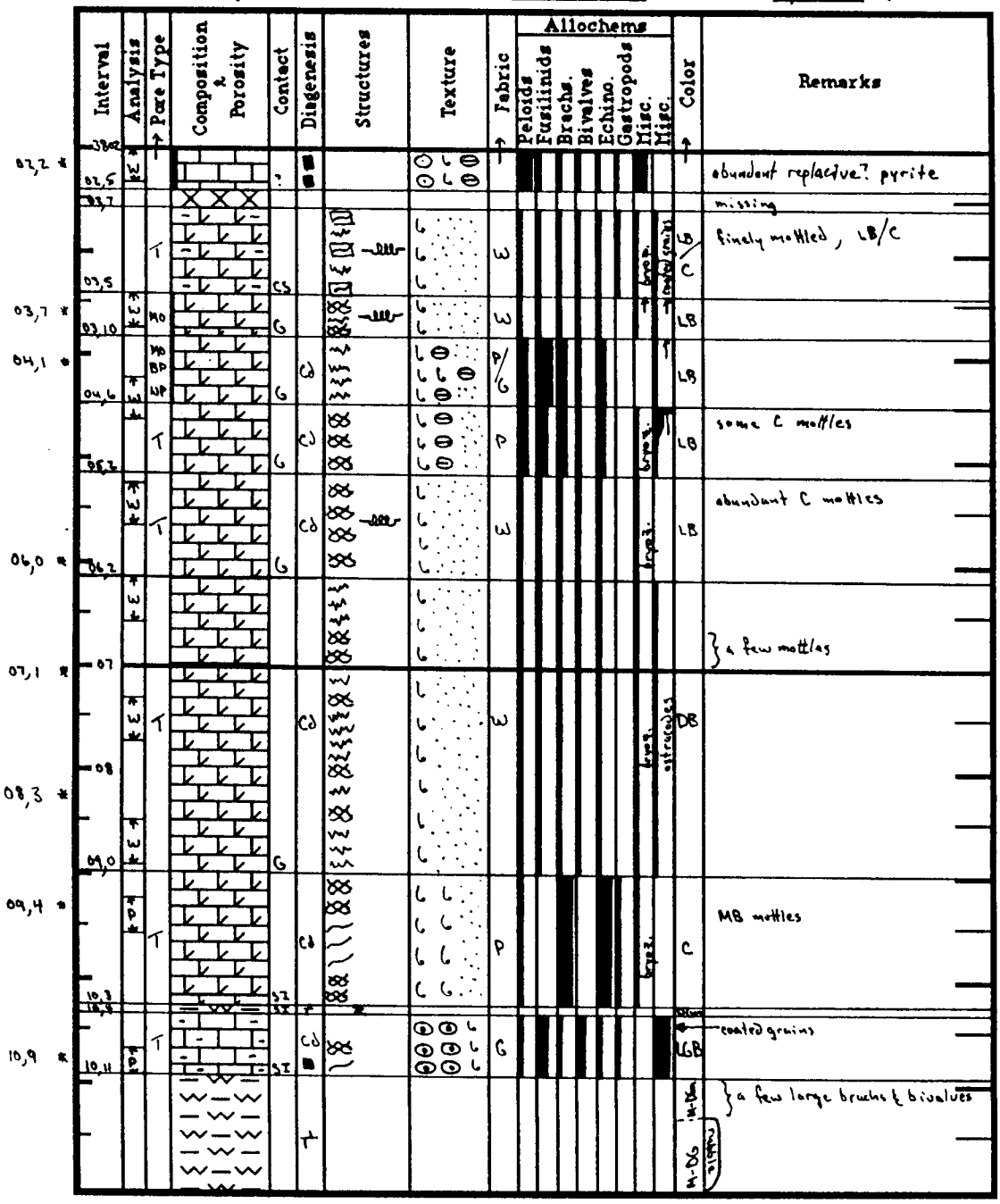

Well Rogers #2 Interval LKC I-J Date 7/15/98 p.1

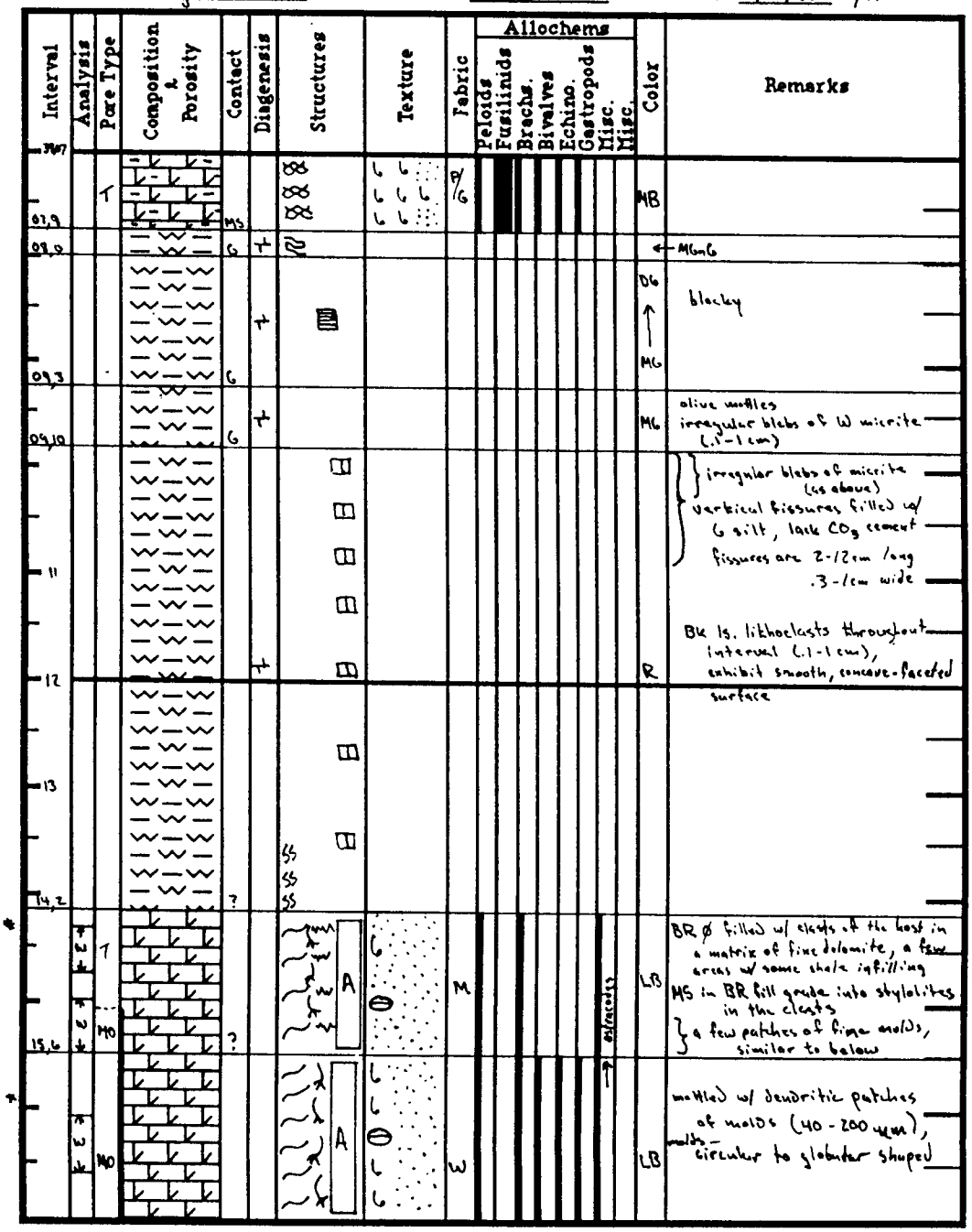

Well Rogers #2 Interval LKC I-J Date 7/15/88 p. 2

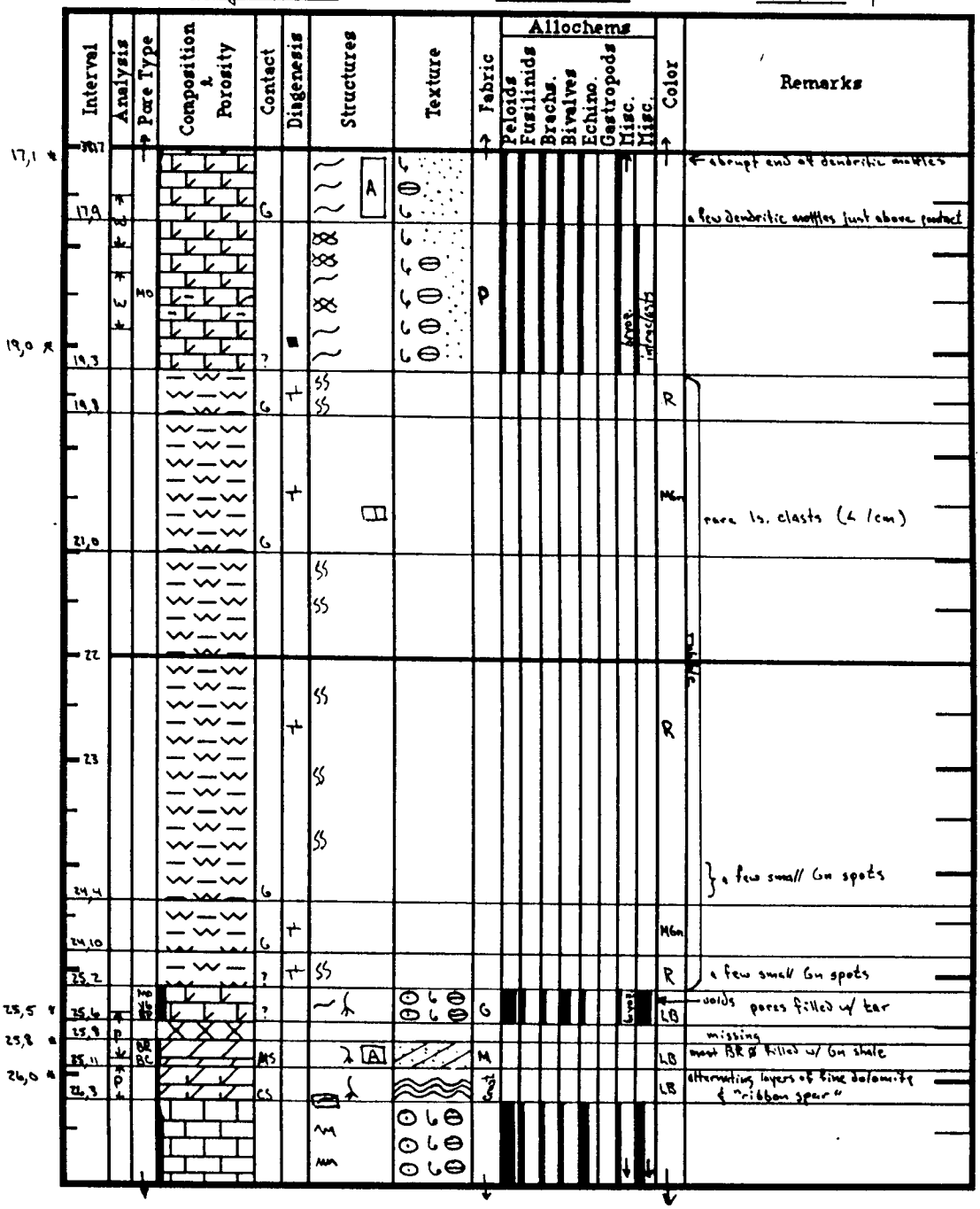

Well Rogers #2 Interval LKC I-J Date 7/15/88 p. 3

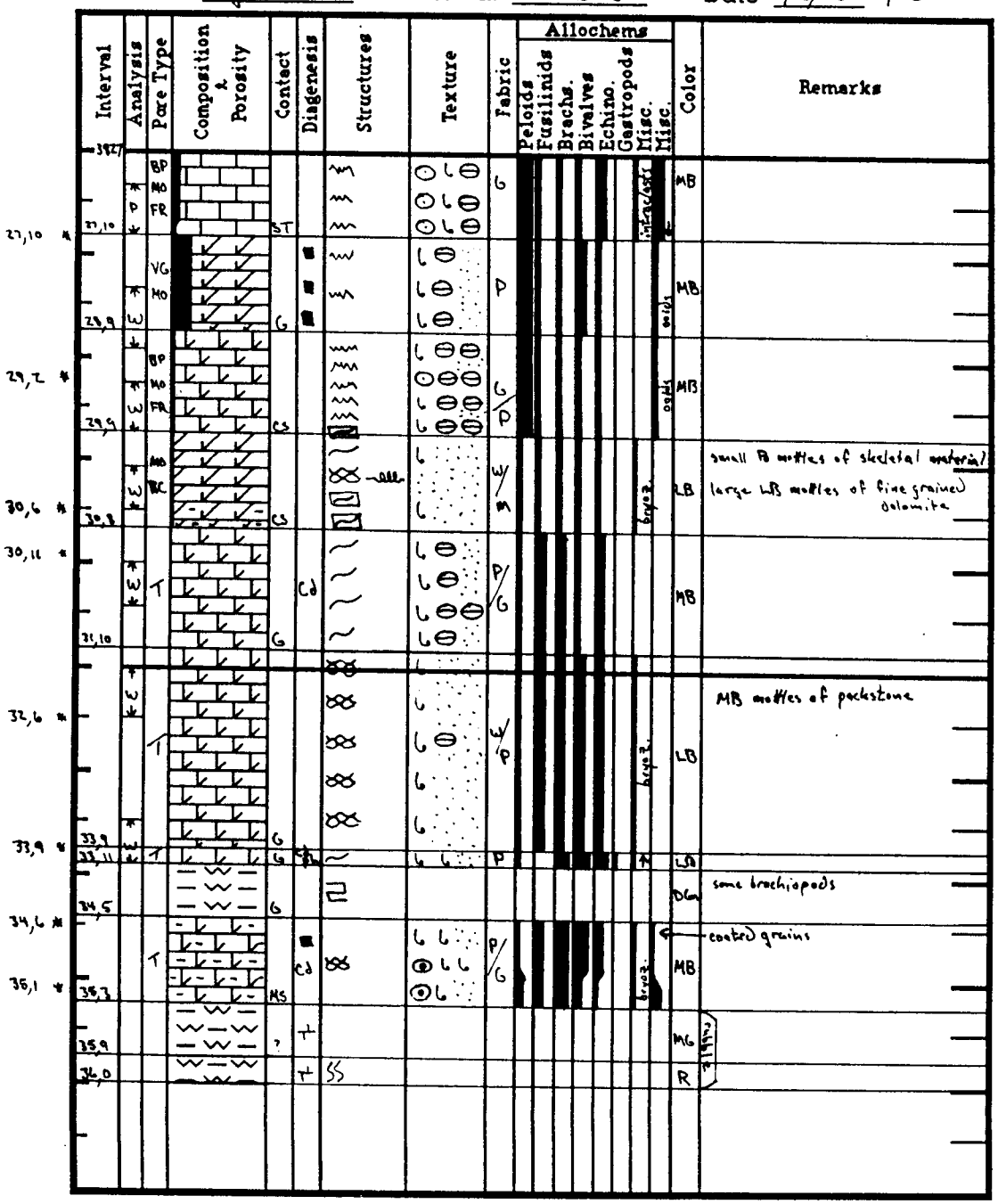

Well Shuck #1 Interval LKC I-J Date 8/11/88

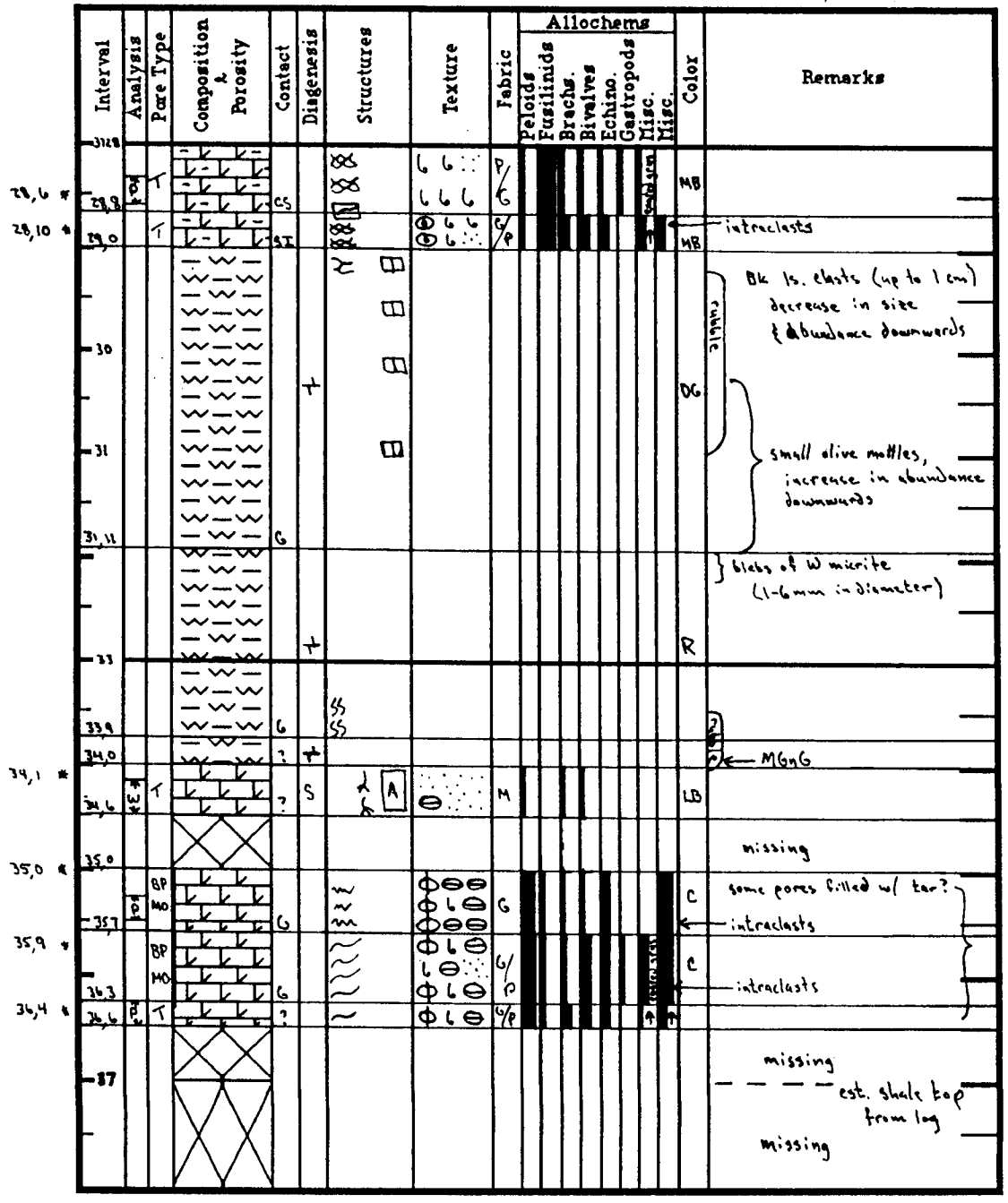

Well Shuck #1 Interval LKC I-J Date 8/11/88 p.2

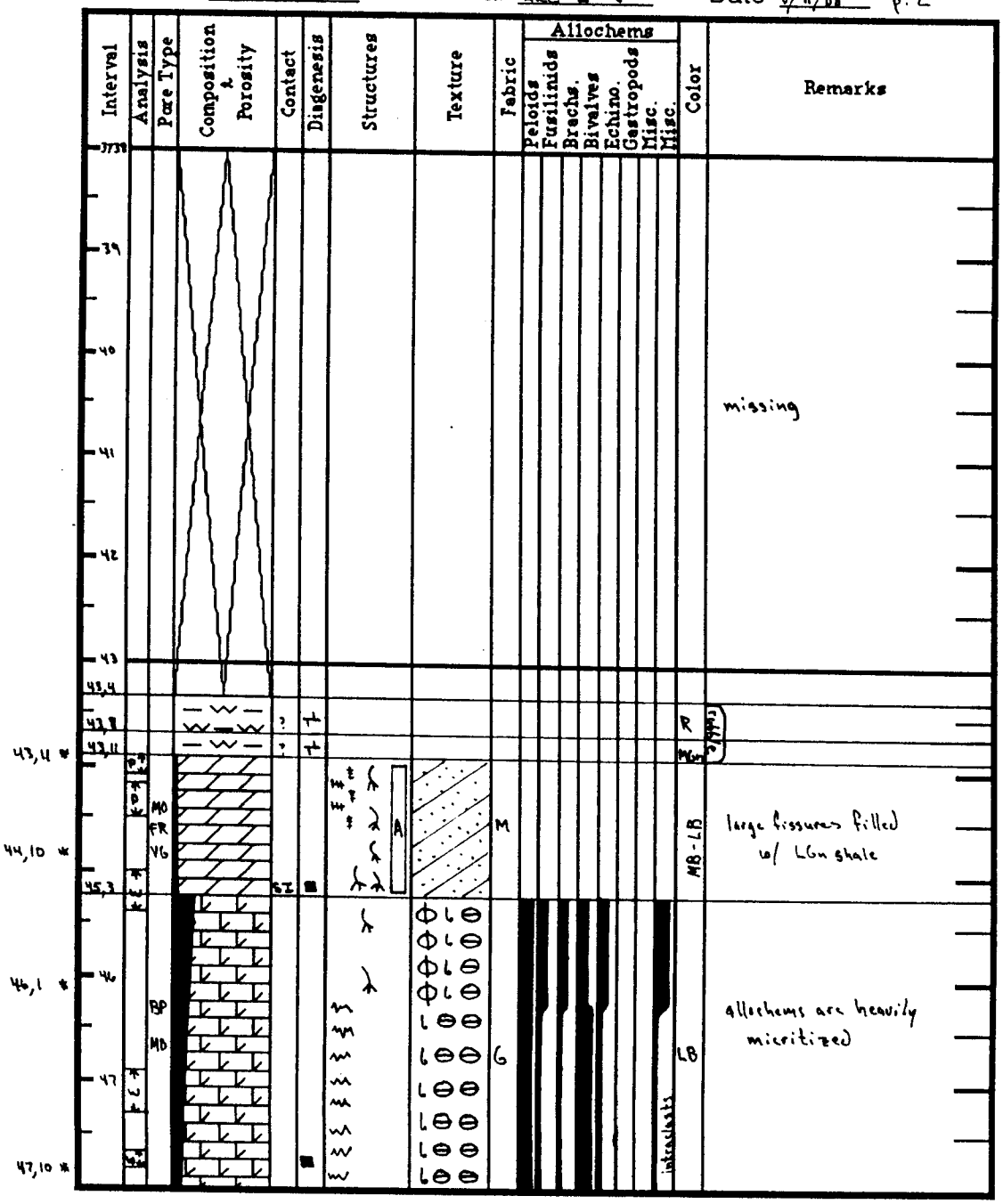

Well Shuck #1 Interval Lkc I-J Date 8/11/88 p.3

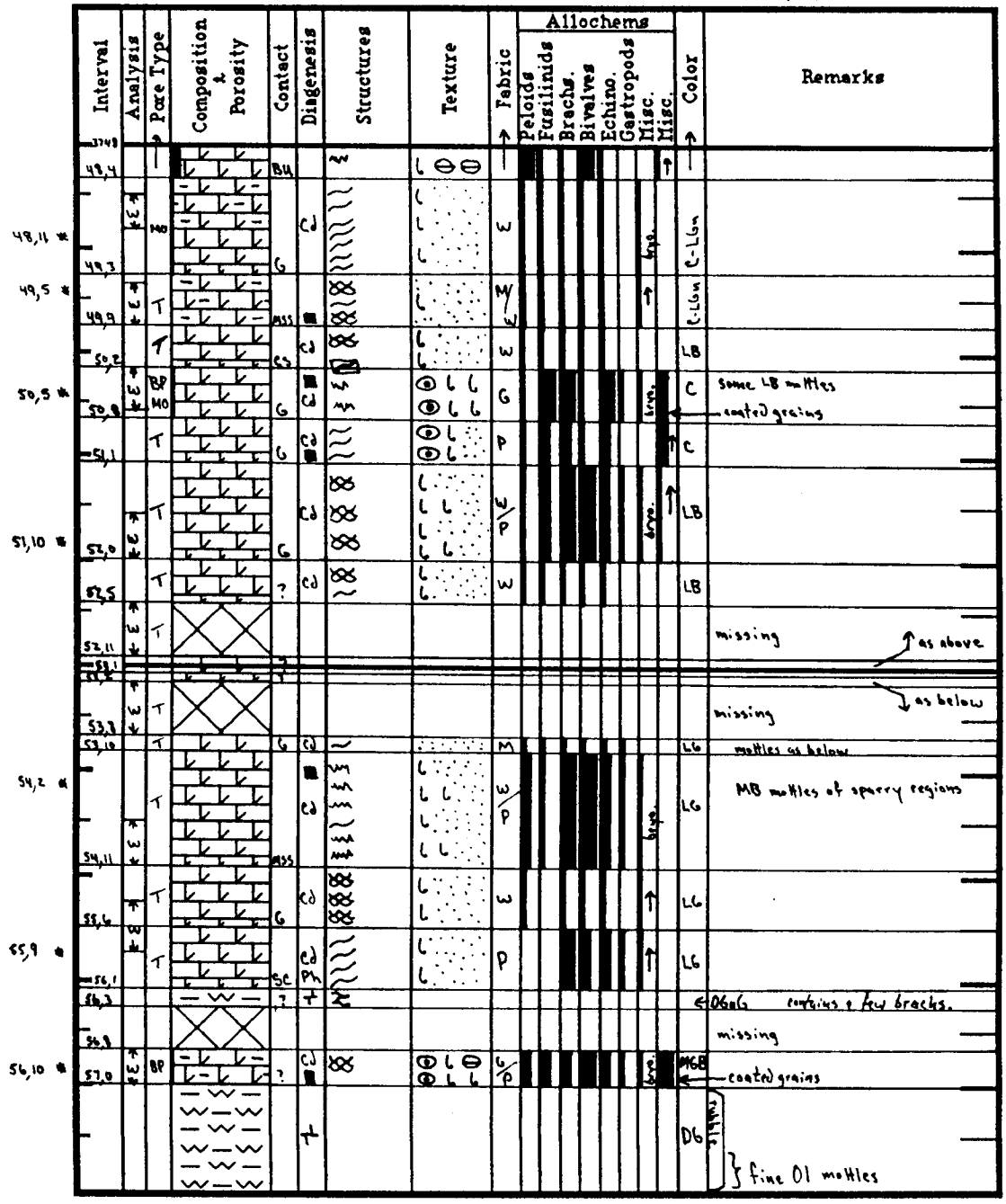

Well Shuck #4 Interval LKC I-J Date 8/1/88

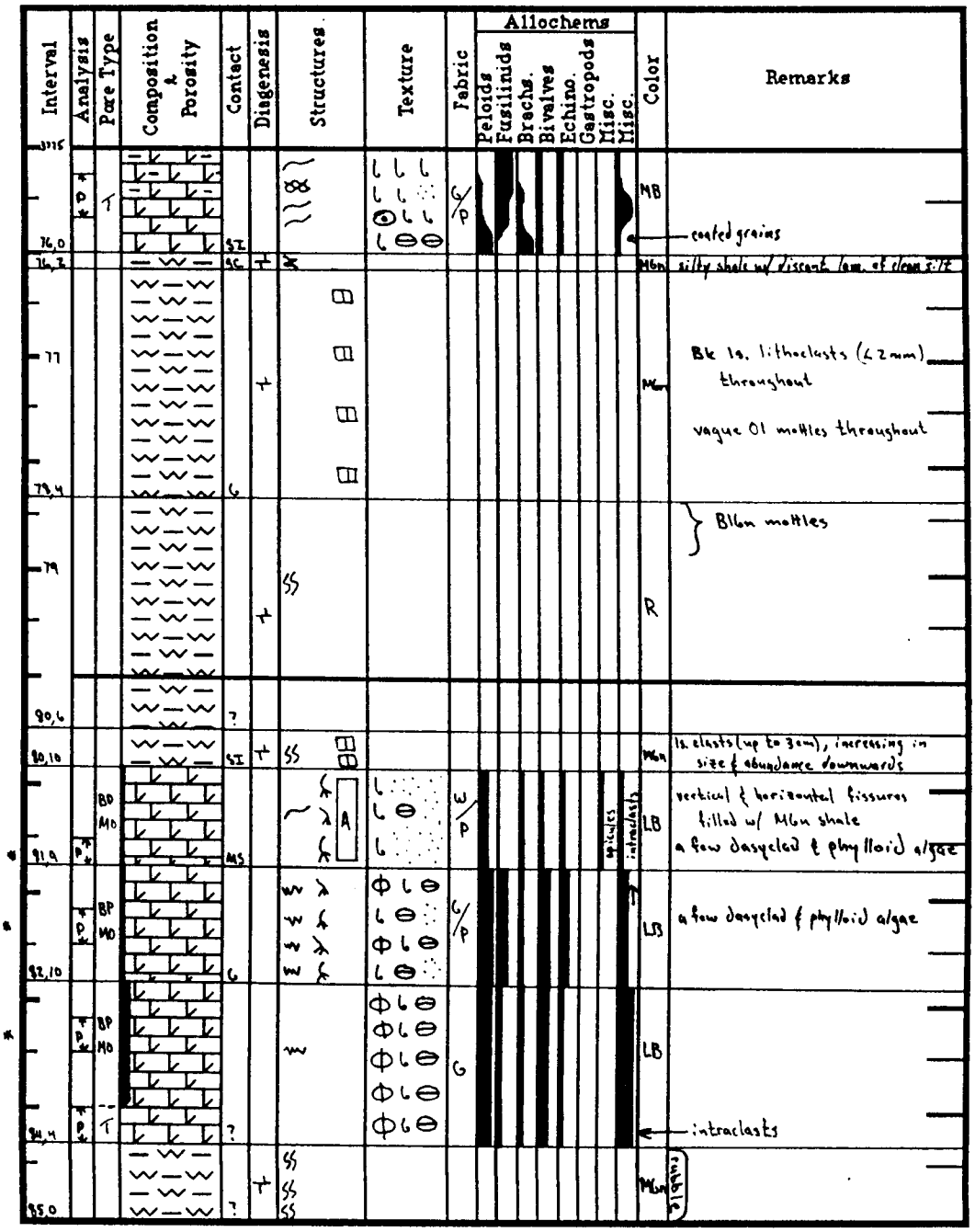

Well Shuck #4 Interval Lec I-I Date 8/1/88 p. 2

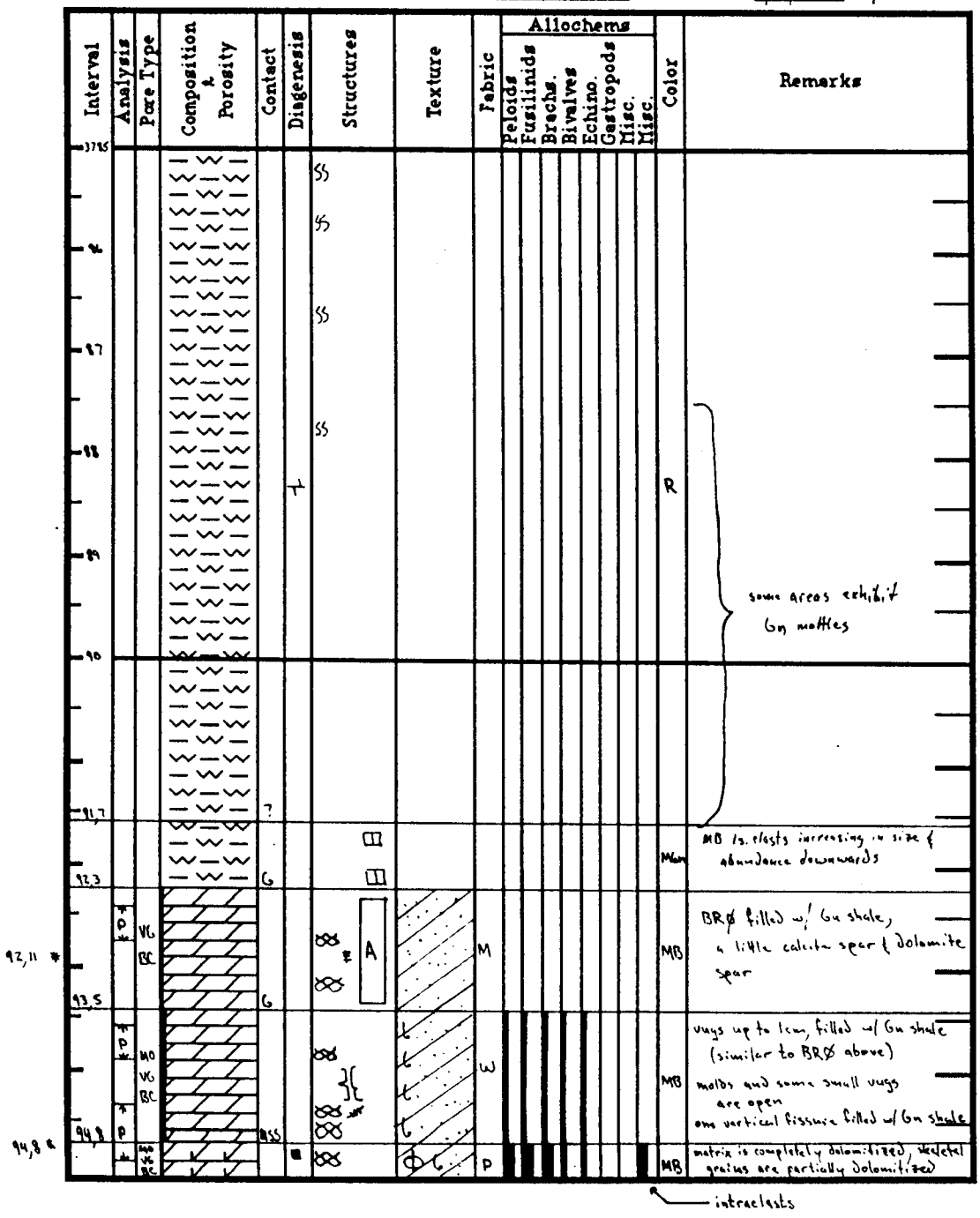

Well Shuck #4 Interval LKC I-J Date 8/1/88 p. 3

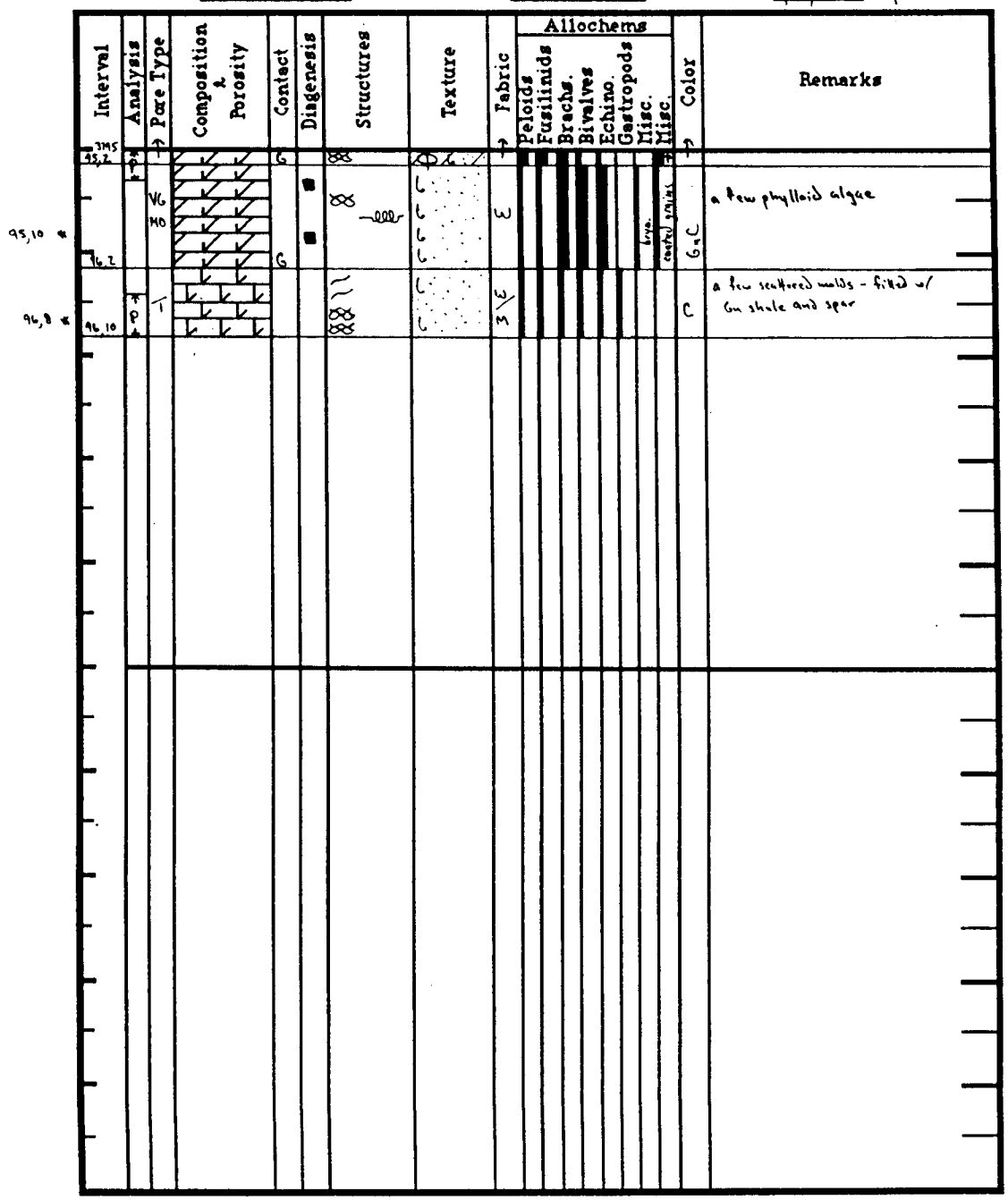

Well White #1 Interval Lkc. I-J Date 7/28/88

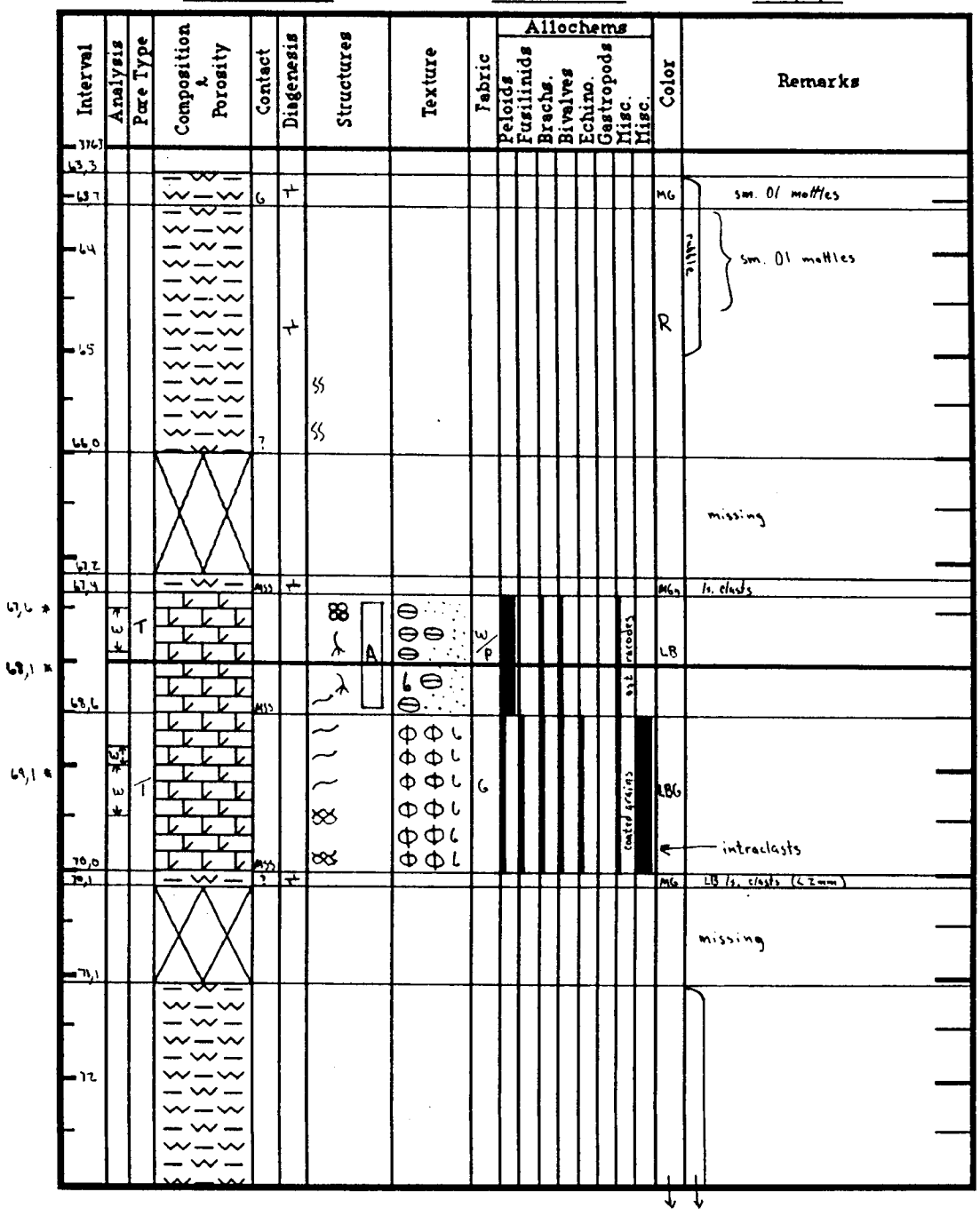

Well White #1 Interval Lkc I-J Date 7/29/88 p.2

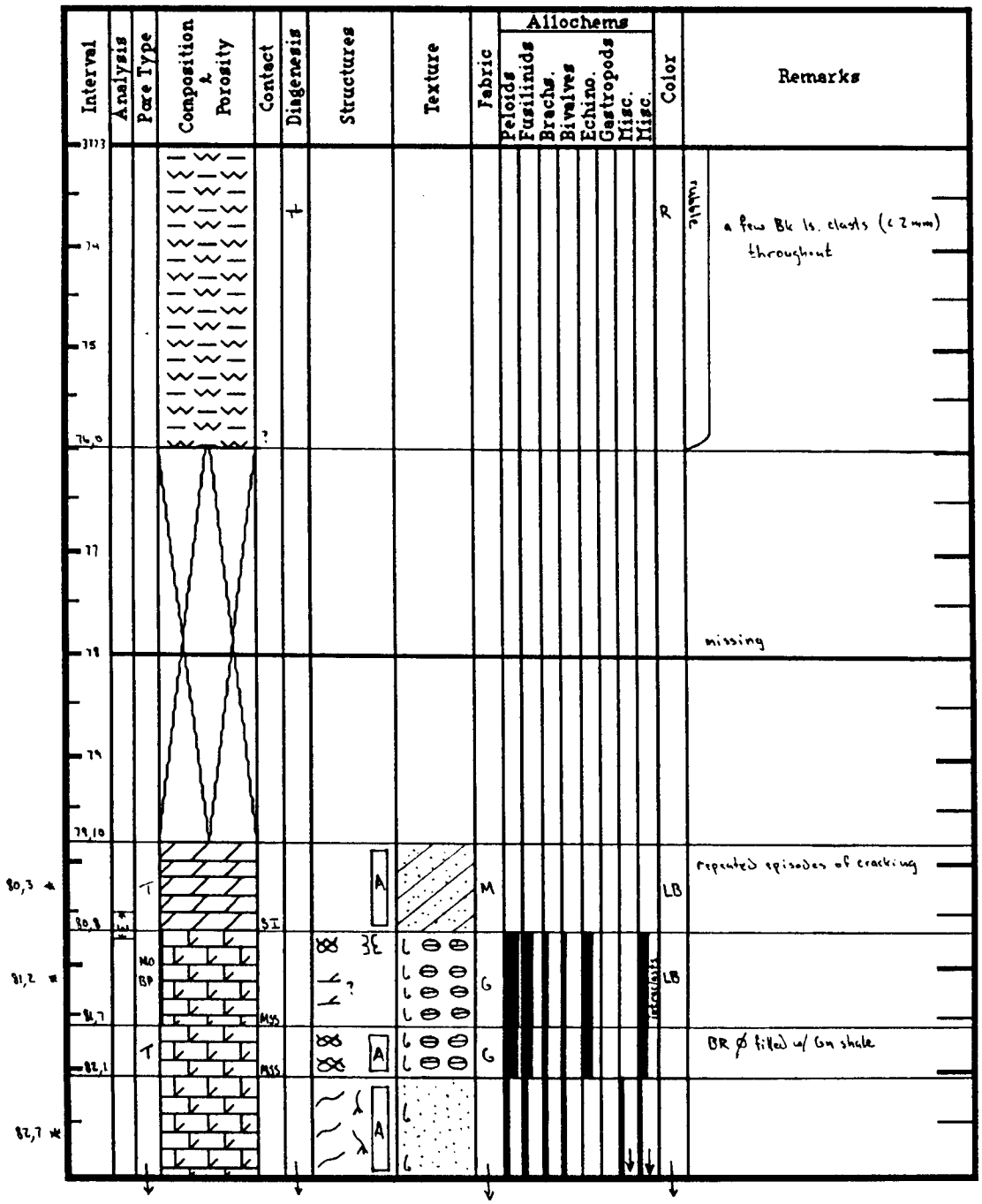

Well White #1 Interval LKC I-J Date 7/28/88 p.3

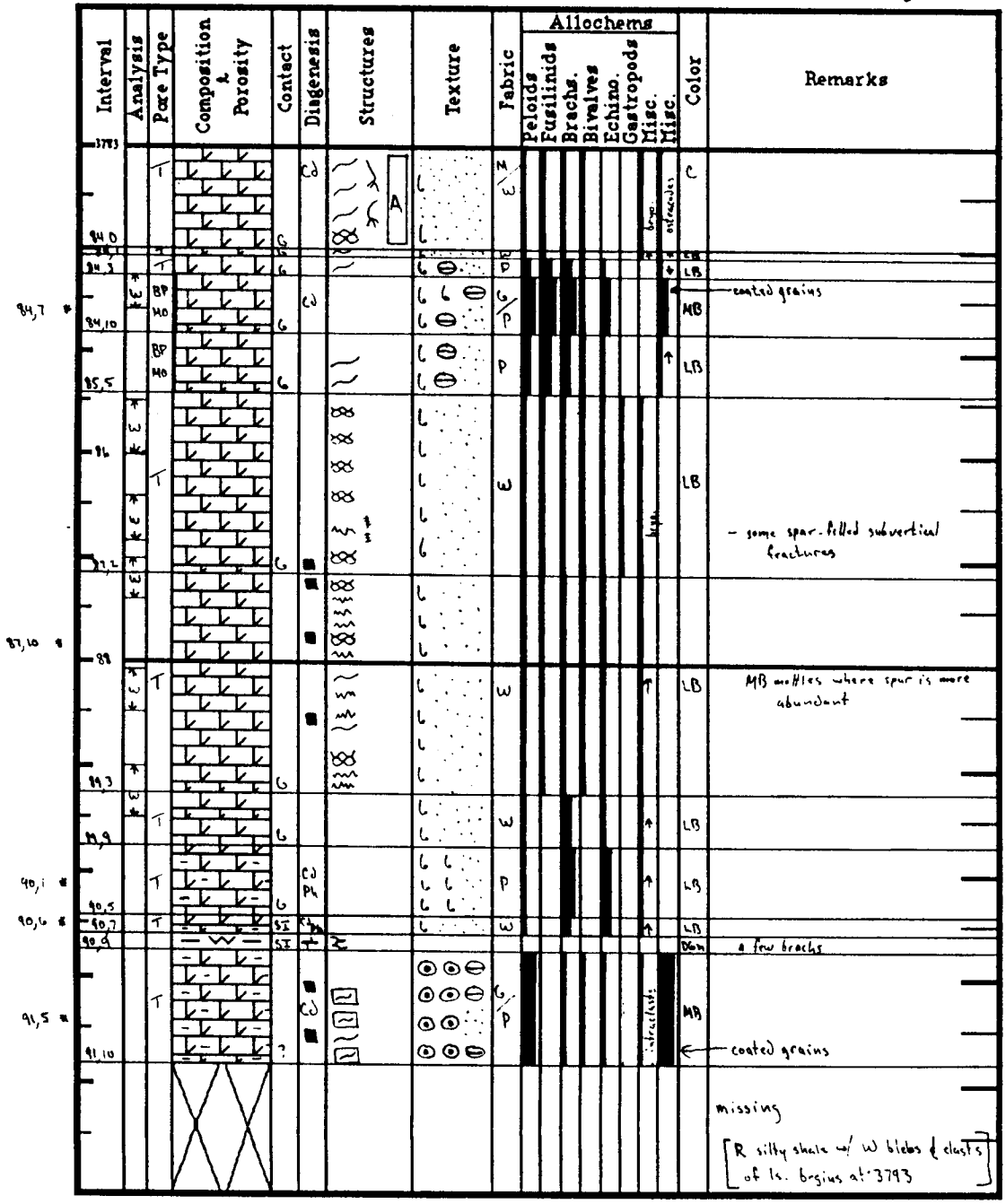

Well White #5 Interval LKC I-J Date 7/19/88

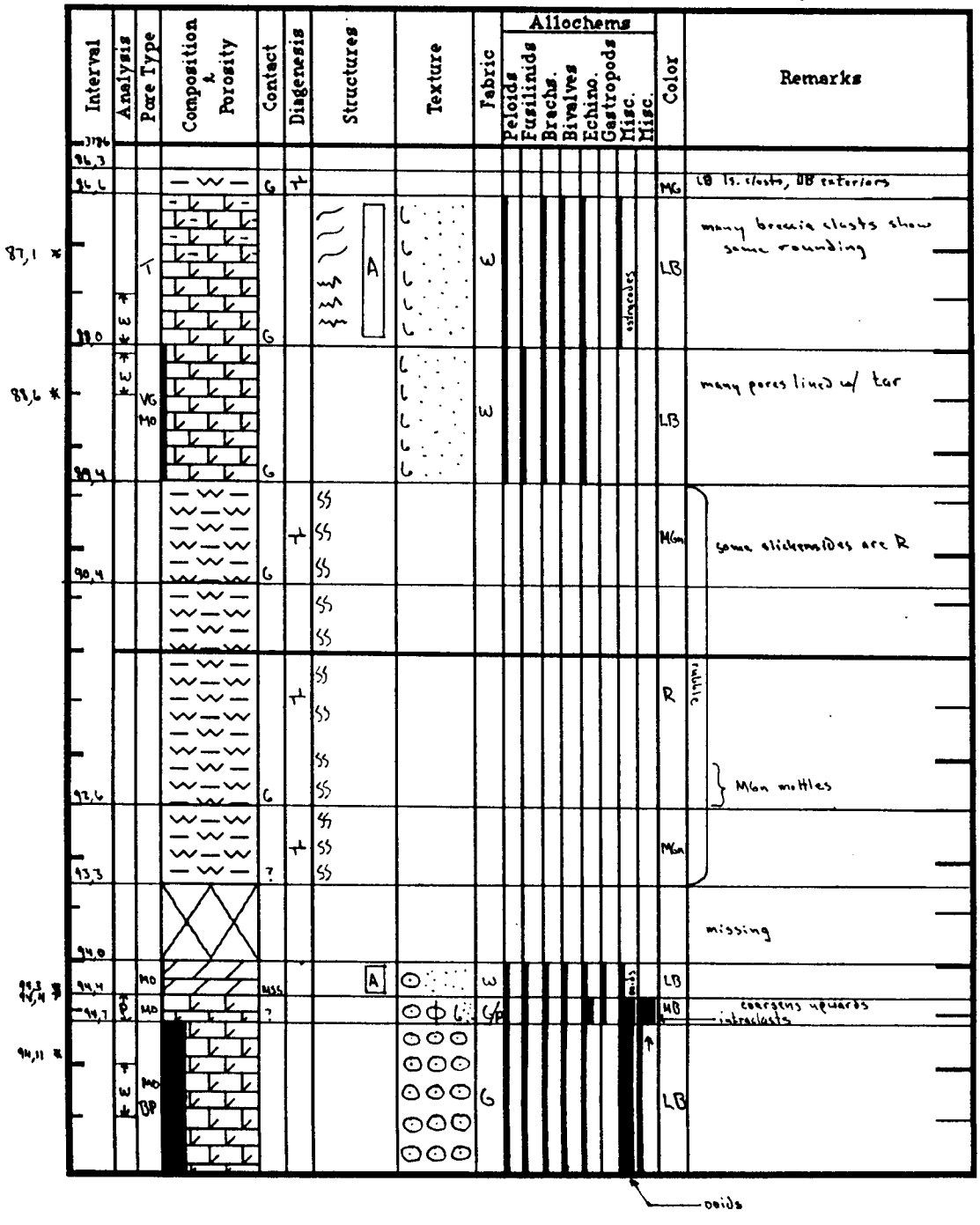

Well White #5 Interval LKC I-J Date 7/19/88 p. 2

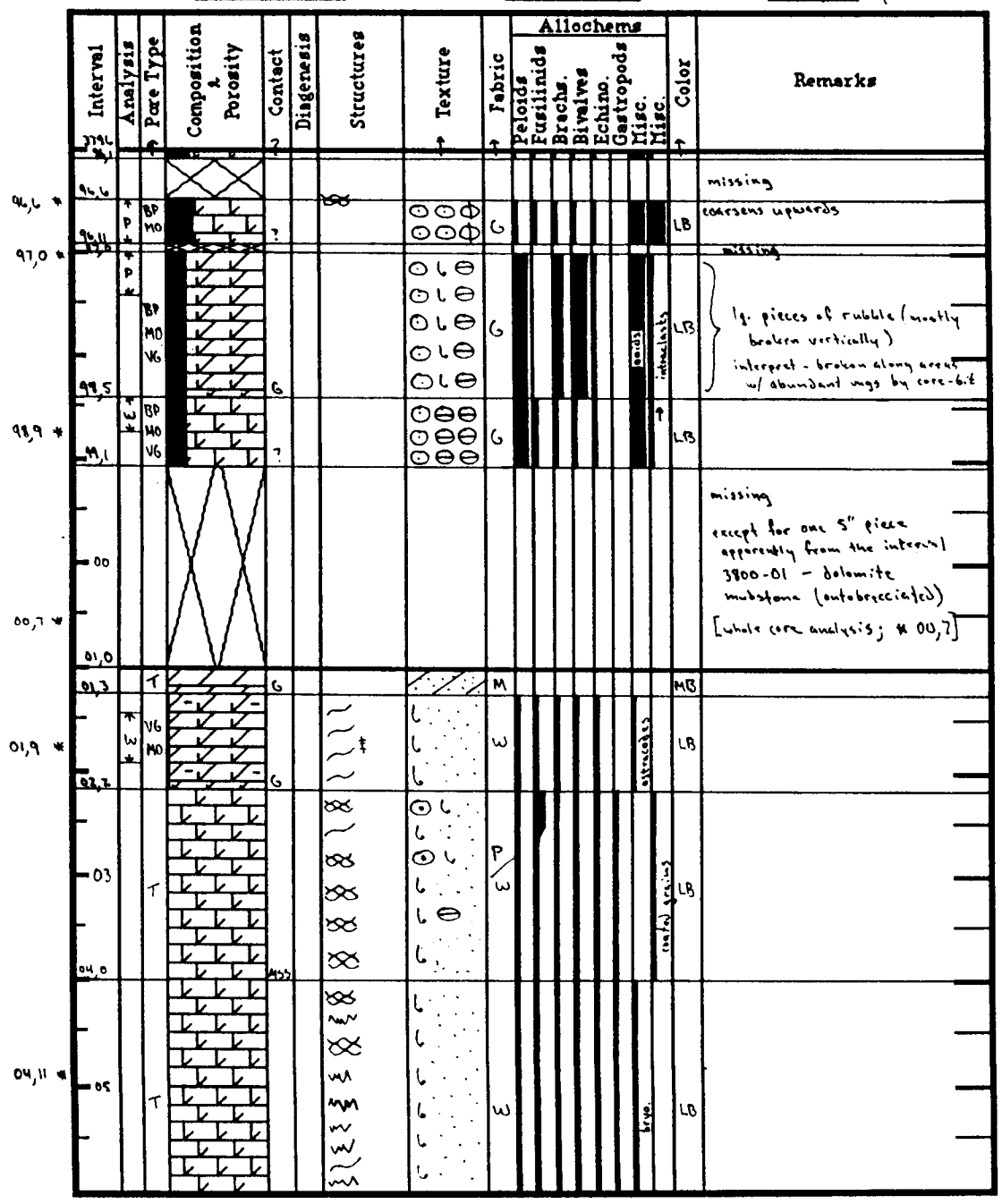

Well White #5 Interval LKC I-J Date 7/19/88 p. 3

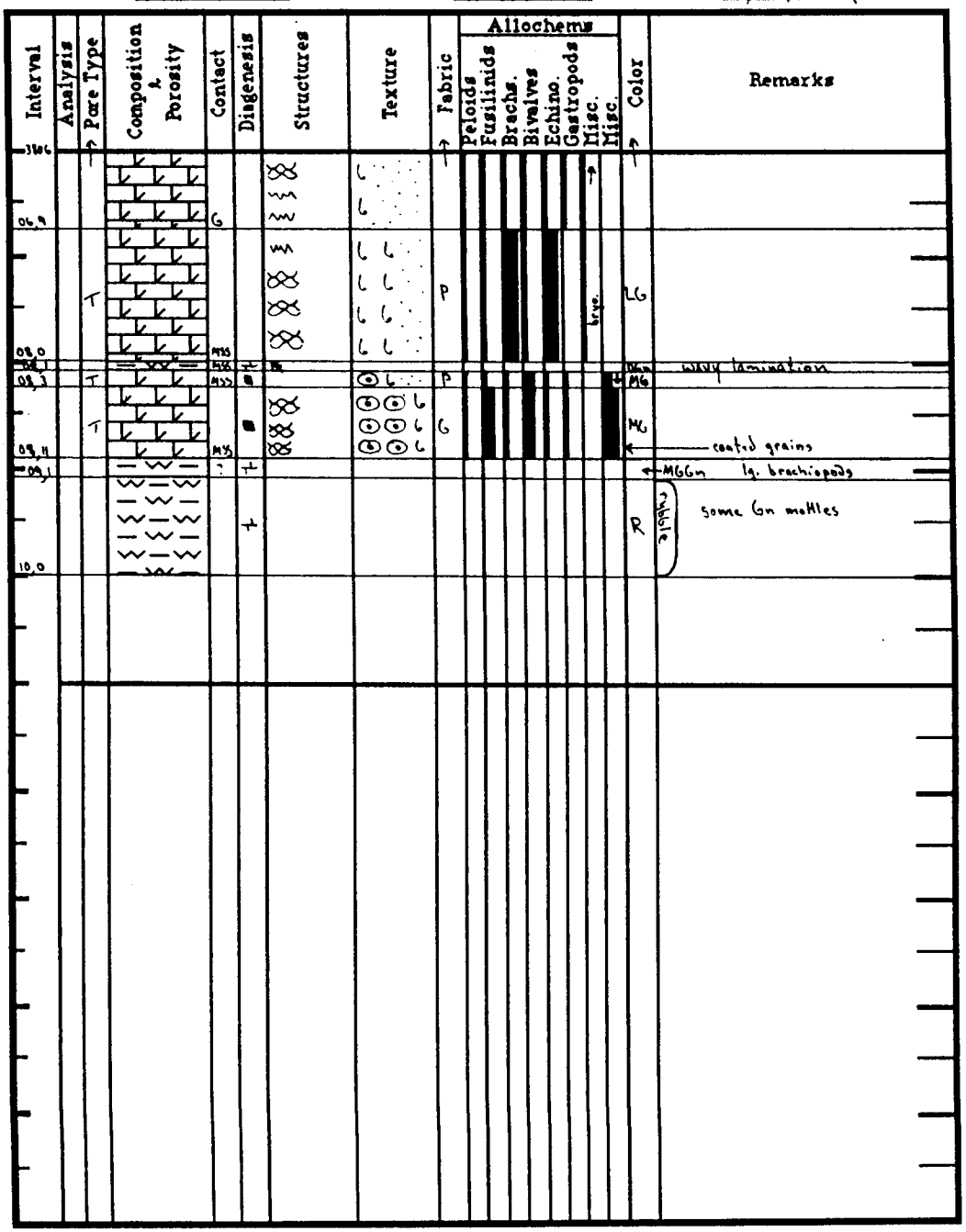

APPENDIX 2

CORE MEASUREMENTS

All values except those for the Shuck #4 represent whole core measurements, unless noted otherwise. Only plug samples were taken from the Shuck #4.

Abbreviations:

#	Core sample not examined to determine if measurements are representative of the actual pore network
I-S	"I" Shale Unit
I-C	"I" Carbonate Unit
J-US	"J" Upper Shale Unit
J-UC	"J" Upper Carbonate Unit
J-LS	"J" Lower Shale Unit
J-LC	"J" Lower Carbonate Unit
C	Cap Subunit
AG	Alpha Grainstone Subunit
AM	Alpha Micrite-Rich Subunit
BGP	Beta Grainstone/Packstone Subunit
BM	Beta Micrite-Rich Subunit
K-US	"K" Upper Shale Unit
K-UC	"K" Upper Carbonate Unit
K-LS	"K" Lower Shale Unit
K-LC	"K" Lower Carbonate Unit
CC	Capping Carbonate Subunit
S	Shale Subunit
BC	Basal Carbonate Subunit
L-US	"L" Upper Shale Unit
L-UC	"L" Upper Carbonate Unit
L-LS	"L" Lower Shale Unit
L-LC	"L" Lower Carbonate Unit
PLS	Pleasanton Group
Kmax	Horizontal permeability (md) [maximum (greater) of two measurements taken 90 degrees apart]
K90	Horizontal permeability (md) [lesser of two measurements]
Kv	Vertical permeability (md)
Poro	Porosity (%)
So	Oil saturation (% of pore volume)
Sw	Water saturation (% of pore volume)
Rho-G	Grain density (grams/cubic centimeters)
**	Horizontal permeability at 90 degrees not performed because only a plug could be taken from this sample
***	Sample unsuitable for permeability measurement
[ ]	Examination of the sample indicates this measurement is not representative of the actual pore network

Bethell #3 C NE SW 17-6S-22W

Depth	Interval	Kmax	K90	Kv	Poro	So	Sw	Rho-G
3702.0-13.0	H Zone	No Analysis						
#3713.0-14.0	H Zone	0.22	**	0.65	7.5	19.6	31.4	2.81
#3714.0-15.0	"	81	**	2.8	11.1	6.6	60.0	2.71
#3715.0-16.0	"	0.15	**	0.03	5.6	0.0	56.2	2.71
#3716.0-17.0	"	<0.01	**	<0.01	2.3	0.0	41.3	2.71
#3717.0-18.0	"	0.03	**	<0.01	3.6	0.0	61.3	2.70
#3718.0-19.0	"	<0.01	**	0.11	2.2	10.5	52.7	2.71
#3719.0-20.0	"	<0.01	**	<0.01	1.3	0.0	40.4	2.70
#3720.0-21.0	"	<0.01	**	<0.01	4.6	0.0	91.1	2.71
#3721.0-22.0	"	<0.01	**	<0.01	1.1	0.0	49.9	2.71
#3722.0-23.0	"	<0.01	**	<0.01	1.0	0.0	62.8	2.71
#3723.0-24.0	"	<0.01	**	<0.01	3.0	0.0	74.3	2.71
#3724.0-25.0	"	<0.01	**	<0.01	0.7	0.0	50.1	2.71
#3725.0-26.0	"	<0.01	**	<0.01	1.2	0.0	63.0	2.71
#3726.0-27.0	"	<0.01	**	<0.01	1.4	0.0	90.4	2.71
#3727.0-28.0	"	<0.01	**	<0.01	2.3	0.0	61.1	2.71
#3728.0-29.0	"	0.08	**	<0.01	6.6	0.0	76.3	2.72
3729.0-35.0	I-S	No Analysis						
3735.0-36.0	I-C	0.04	0.04	<0.01	1.9	14.3	35.8	2.71
3736.0-37.0	"	10	8.8	3.3	7.6	22.7	19.0	2.72
3737.0-37.5	"	<0.01	**	<0.01	1.7	0.0	33.0	2.71
3737.5-46.0	J-US	No Analysis						
3746.0-47.0	J-UC;AG	[.50]	[.48]	[1.2]	[6.9]	5.1	15.2	2.70
3747.0-48.0	"	4.4	1.9	3.0	[11.6]	10.5	44.1	2.67
3748.0-49.0	"	44	23	58	13.0	32.9	17.7	2.70
3749.0-50.0	"	***	**	***	[9.9]	28.2	22.6	2.72
3750.0-51.0	"	<0.01	**	***	3.3	28.5	24.5	2.70
3751.0-52.0	J-UC;AM	No Analysis						
3752.0-53.0	J-UC;BGP/BM	[5.3]	[1.7]	<0.01	3.4	0.0	27.7	2.69
3753.0-54.0	J-UC;BM	0.03	**	<0.01	3.2	0.0	61.1	2.70
3754.0-55.0	"	<0.01	**	<0.01	0.5	0.0	40.1	2.70
3755.0-56.0	"	0.02	**	<0.01	3.2	34.1	28.5	2.70
3756.0-57.0	"	<0.01	**	<0.01	1.9	0.0	38.1	2.71
3757.0-58.0	"	<0.01	**	<0.01	2.4	0.0	27.4	2.71
3758.0-59.0	J-LC	<0.01	**	<0.01	1.6	0.0	69.0	2.71
3759.0-64.0	K-US	No Analysis						

Bethell #5 C SW SW 17-6S-22W

Depth	Interval	Kmax	K90	Kv	Poro	So	Sw	Rho-G
3746.0-52.0	I-S	No Analysis						
3752.0-53.0	I-C	0.56	0.53	0.05	3.3	0.0	47.2	2.71
3753.0-54.0	"	No Analysis						
3754.0-60.0	J-US	No Analysis						
3760.0-61.0	J-UC;C	[0.10]	**	[11]	[9.0]	6.9	54.2	2.70
3761.0-62.0	J-UC;C/AG	[16]	[13]	[1.6]	[15.0]	8.9	49.6	2.78
3762.0-63.0	J-AG	300	224	2300	23.6	20.8	29.7	2.73
3763.0-64.0	"	257	70	372	22.3	25.0	37.9	2.72
3764.0-65.0	"	143	100	795	22.2	33.4	34.1	2.71
3765.0-66.0	"	214	51	192	22.4	34.2	32.7	2.72
3766.0-67.0	"	487	437	600	20.6	9.1	32.7	2.72
3767.0-68.0	J-UC;BGP	0.39	0.30	0.04	5.7	20.7	15.9	2.72
3768.0-69.0	J-UC;BM	0.07	0.06	0.02	3.3	12.5	26.9	2.72
3769.0-70.0	"	[1.2]	[0.95]	0.03	3.8	14.2	25.4	2.72
3770.0-71.0	"	4.0	3.3	0.20	7.8	17.0	18.9	2.72
3771.0-72.0	"	4.8	4.4	0.07	9.3	22.3	16.7	2.72
3772.0-73.0	"	0.01	0.01	0.01	2.8	23.4	29.7	2.71
3773.0-74.0	J-UC/LS/LC	[0.04]	[0.03]	<0.01	[4.3]	0.0	68.2	2.73
3774.0-82.0	K-US	No Analysis						
3782.0-83.0	K-UC;CC	No Analysis						
3783.0-84.0	"	No Analysis						
3784.0-85.0	"	No Analysis						
3785.0-86.0	K-UC;S/BC	No Analysis						
3786.0-87.0	K-UC;BC	1.8	1.6	0.06	7.9	0.0	65.7	2.78
3787.0-88.0	"	No Analysis						
3788.0-89.0	"	No Analysis						
3789.0-90.0	K-LS/LC	No Analysis						
3790.0-91.0	L-UC	61	60	9.7	9.3	0.0	37.6	2.71
3791.0-92.0	"	139	**	5.1	13.5	13.9	32.5	2.71
3792.0-93.0	"	4.3	1.3	0.43	5.4	12.0	42.7	2.71
3793.0-94.0	"	0.89	0.71	0.23	4.8	8.1	61.1	2.70
3794.0-95.0	"	1.2	1.1	0.13	4.9	4.2	61.4	2.71
3795.0-96.0	"	5.9	1.4	1.7	7.4	6.4	39.1	2.72
3796.0-97.0	"	<0.01	**	[0.44]	1.7	8.5	33.3	2.71
3797.0-98.0	"	[0.31]	**	[0.05]	[13.8]	1.0	82.7	2.74
3798.0-99.0	"	0.02	0.02	0.02	[6.3]	0.0	75.2	2.75
3799.0-02.0	"	No Analysis						
3802.0-03.0	L-LS	No Analysis						
3803.0-07.0	PLS	No Analysis						

Demuth #1 C NE NE 19-6S-22W

Depth	Interval	Kmax	K90	Kv	Poro	So	Sw	Rho-G
3791.0-92.5	H Zone	No Analysis						
3792.5-99.0	I-S	No Analysis						
3799.0-00.0	I-C	<0.01	**	<0.01	2.5	0.0	62.0	2.70
3800.0-01.0	"	0.13	0.09	<0.01	2.8	14.2	42.7	2.71
3801.0-02.0	"	0.85	0.46	0.21	4.0	8.5	47.0	2.70
3802.0-03.0	"	0.85	**	0.23	4.4	15.8	43.0	2.71
3803.0-04.0	"	4.7	4.3	0.38	5.6	13.3	47.6	2.69
3804.0-05.0	"	1.5	1.3	0.11	4.8	13.7	51.7	2.69
3805.0-11.0	J-US	No Analysis						
3811.0-12.0	J-UC;AG	38	**	65	12.9	30.4	28.3	2.71
3812.0-13.0	"	2.0	**	0.80	17.2	21.1	22.2	2.70
3813.0-14.0	"	43	9.3	446	16.0	22.6	31.1	2.70
3814.0-15.0	"	36	**	[304]	13.8	24.3	24.4	2.71
3815.0-16.0	"	[3.6]	**	0.15	[9.4]	28.8	20.6	2.71
3816.0-17.0	"	0.56	0.45	0.52	5.4	12.5	35.8	2.71
3817.0-18.0	J-UC;BGP	0.06	0.05	<0.01	3.9	8.0	32.1	2.70
3818.0-19.0	J-UC;BGP/BM	[0.14]	[0.10]	[<0.01]	[3.5]	0.0	41.4	2.70
3819.0-20.0	J-UC;BM	<0.01	**	<0.01	1.0	23.1	38.5	2.70
3820.0-21.0	"	[0.13]	[0.11]	0.03	1.9	32.0	19.7	2.69
3821.0-22.0	"	[0.06]	[0.06]	<0.01	1.1	39.0	26.0	2.69
3822.0-23.0	"	[0.22]	[0.15]	<0.01	1.0	0.0	61.3	2.69
3823.0-24.0	"	No Analysis						
3824.0-33.0	K-US	No Analysis						
3833.0-34.0	K-UC;CC	No Analysis						
3834.0-35.0	K-UC;S	No Analysis						
3835.0-36.0	K-UC;BC	0.29	0.21	<0.01	7.2	19.7	48.6	2.76
3836.0-37.0	"	[1.7]	**	[0.04]	[18.3]	0.0	69.5	2.78
3837.0-38.0	"	***	**	***	1.5	0.0	57.9	--
3838.0-39.0	"	***	**	***	[3.5]	0.0	77.0	--
3839.0-40.0	K-LS/LC/L-US	No Analysis						
3840.0-41.0	L-UC	***	**	***	[3.7]	0.0	68.4	--
3841.0-42.0	"	***	**	***	3.4	0.0	30.8	--
3842.0-43.0	"	***	**	***	1.5	0.0	56.2	--
3843.0-44.0	"	***	**	***	2.9	0.0	35.9	--
3844.0-45.0	"	6.6	6.4	1.4	4.3	0.0	40.9	2.72
3845.0-46.0	"	0.04	**	2.0	8.7	1.1	38.9	2.72
3846.0-47.0	"	***	**	***	2.7	0.0	39.2	--
3847.0-48.0	"	***	**	***	2.3	4.6	54.8	--
3848.0-49.0	"	***	**	***	[7.6]	0.0	87.7	--
3849.0-50.0	"	***	**	***	1.6	0.0	40.7	--
3850.0-51.0	"	***	**	***	1.9	0.0	64.4	--
3851.0-52.0	L-LS	No Analysis						
3852.0-53.0	L-LC/PLS	No Analysis						

Demuth #4 C SW NE 19-6S-22W

Depth	Interval	Kmax	K90	Kv	Poro	So	Sw	Rho-G
3794.0-98.0	H Zone	No Analysis						
3798.0-04.0	I-S	No Analysis						
3804.0-10.0	I-C	No Analysis						
3810.0-12.0	J-US	No Analysis						
3812.0-13.0	J-UC;AG	54.6	54.6	252	14.8	28.0	34.0	2.73
3813.0-14.0	"	401	**	1165	19.0	14.8	49.8	2.70
3814.0-15.0	"	1418	**	688	18.9	23.5	48.8	2.70
3815.0-16.0	"	122	117	0.56	12.1	21.6	35.0	2.72
3816.0-17.0	"	0.06	0.06	<0.01	4.8	27.0	23.2	2.74
3817.0-18.0	J-UC;AG/AM	[0.38]	[0.33]	[<0.01]	[2.8]	12.1	57.8	2.71
3818.0-19.0	J-UC;BGP	<0.01	<0.01	<0.01	1.9	11.8	58.8	2.72
3819.0-20.0	J-UC;BM	0.10	0.05	<0.01	2.3	1.4	43.3	2.72
3820.0-21.0	"	0.11	0.06	<0.01	2.1	0.0	36.9	2.72
3821.0-22.0	"	0.14	0.06	<0.01	1.2	9.8	19.6	2.71
3822.0-23.0	"	0.21	0.18	<0.01	1.3	0.0	19.3	2.70
3823.0-24.0	"	<0.01	**	0.01	0.2	0.0	18.3	2.71
3824.0-25.0	J-UC/LS/LC	No Analysis						
3825.0-35.0	K-US	No Analysis						
3835.0-36.0	K-UC;CC	No Analysis						
3836.0-37.0	K-UC;S	No Analysis						
#3837.0-38.0	K-UC;BC	0.02	0.02	<0.01	6.6	0.0	78.4	2.79
#3838.0-39.0	"	0.08	<0.01	0.26	3.0	0.0	19.3	2.73
3839.0-40.0	K-LS	No Analysis						
3840.0-41.0	K-LC/L-US	No Analysis						
3841.0-45.0	L-UC	No Analysis						
#3845.0-46.0	"	0.01	**	0.02	0.4	0.0	22.7	2.71
#3846.0-47.0	"	0.02	<0.01	<0.01	3.1	0.0	50.5	2.74
#3847.0-48.0	"	0.63	0.49	0.37	4.4	7.7	46.1	2.72
#3848.0-49.0	"	1.56	1.37	0.60	4.8	0.0	27.6	2.71
#3849.0-50.0	"	<0.01	<0.01	<0.01	0.8	0.0	51.2	2.70
#3850.0-51.0	"	<0.01	<0.01	<0.01	1.0	0.0	17.4	2.71
#3851.0-52.0	"	<0.01	<0.01	<0.01	0.9	0.0	31.9	2.71
#3852.0-53.0	"	<0.01	<0.01	<0.01	0.3	0.0	22.5	2.70
#3853.0-54.0	"	<0.01	<0.01	<0.01	0.6	0.0	23.9	2.70

Pennington #2 C SE NE 17-6S-22W

Depth	Interval	Kmax	K90	Kv	Poro	So	Sw	Rho-G
3763.0-65.0	I-C	No Analysis						
3765.0-72.5	J-US	No Analysis						
3772.5-73.0	J-UC;C	***	**	***	[12.2]	0.0	79.2	2.73
3773.0-74.0	"	[0.57]	**	[0.03]	[7.5]	0.0	80.2	2.75
3774.0-75.0	"	[0.41]	**	[0.05]	[12.1]	5.0	64.1	2.79
3775.0-76.0	J-UC;AM	<0.01	**	<0.01	1.3	37.9	29.1	2.71
3776.0-77.0	"	<0.01	**	<0.01	1.4	0.0	40.2	2.72
3777.0-78.0	J-UC;AM/BGP	[0.03]	**	[0.05]	[6.0]	[0.0]	42.2	2.71
3778.0-79.0	J-UC;BM	0.02	**	0.03	4.3	30.1	22.5	2.71
3779.0-80.0	"	0.03	**	<0.01	4.0	18.2	23.2	2.67
3780.0-81.0	"	0.01	**	0.05	3.4	32.7	15.7	2.66
3781.0-82.0	"	[0.35]	**	[2.3]	[6.0]	29.4	11.2	2.69
3782.0-83.0	"	0.09	**	0.01	1.0	46.7	22.3	2.68
3783.0-84.0	"	<0.01	**	<0.01	1.2	8.6	42.8	2.71
3784.0-85.0	J-LC	[0.15]	**	***	[3.6]	0.0	32.4	2.68
3785.0-93.0	K-US	No Analysis						

Rogers #1 C NE SE 19-6S-22W

Depth	Interval	Kmax	K90	Kv	Poro	So	Sw	Rho-G
3780.0-81.0	H Zone	No Analysis						
3781.0-82.0	"	[1.3]	[0.70]	<0.01	[4.3]	0.0	77.1	2.73
3782.0-83.0	"	[0.58]	[0.05]	<0.01	[3.6]	0.0	89.3	2.73
3783.0-90.0	I-S	No Analysis						
3790.0-91.0	I-C	[0.12]	[0.01]	[0.25]	3.5	0.0	64.6	2.73
3791.0-92.0	"	<0.01	<0.01	<0.01	3.3	0.0	72.5	2.73
3792.0-98.0	J-US	No Analysis						
3798.0-99.0	J-UC;C	[0.94]	**	[0.91]	[23.9]	11.5	61.5	2.78
3799.0-00.0	J-UC;AG	[0.82]	[0.65]	<0.01	7.7	24.4	41.8	2.74
3800.0-01.0	"	1.3	1.2	0.68	11.2	30.8	24.6	2.72
3801.0-02.0	"	0.50	0.44	0.18	10.6	37.0	11.0	2.73
3802.0-03.0	"	0.10	0.09	<0.01	6.5	9.2	77.5	2.96
3803.0-04.0	J-UC;AM	0.01	0.01	<0.01	4.2	23.5	37.6	2.73
3804.0-05.0	J-UC;BGP/BM	[<0.01]	[<0.01]	[<0.01]	[2.1]	43.4	21.7	2.70
3805.0-06.0	"	0.02	<0.01	<0.01	1.8	38.7	38.7	2.70
3806.0-07.0	"	<0.01	<0.01	<0.01	0.6	43.8	19.5	2.67
3807.0-08.0	"	<0.01	<0.01	<0.01	0.7	29.6	16.9	2.67
3808.0-09.0	"	<0.01	<0.01	<0.01	0.7	44.3	36.9	2.67
3809.0-10.0	"	<0.01	**	<0.01	1.6	3.6	65.0	2.70
3810.0-11.0	J-LC	[0.05]	**	<0.01	[3.9]	0.0	80.1	2.70
3811.0-20.0	K-US	No Analysis						
#3820.0-21.0	K-UC;CC	0.06	0.01	<0.01	3.9	0.0	85.4	2.73
#3821.0-22.0	"	<0.01	<0.01	<0.01	7.0	0.0	80.7	2.75
#3822.0-22.5	"	0.04	**	<0.01	5.2	11.7	73.6	2.72
3822.5-23.5	K-UC;S	No Analysis						
#3823.5-24.0	K-UC;BC	<0.01	<0.01	<0.01	2.1	0.0	47.7	2.73
#3824.0-25.0	"	0.02	0.01	<0.01	4.1	5.1	51.3	2.75
#3825.0-26.0	"	0.01	<0.01	<0.01	1.9	7.7	53.9	2.72
#3826.0-27.0	"	[23]	[16]	<0.01	1.7	0.0	44.7	2.71
#3827.0-28.0	"	0.04	<0.01	<0.01	2.2	0.0	75.7	2.72
3828.0-30.0	K-LS/LC/L-US	No Analysis						
#3830.0-31.0	L-UC	[11]	[0.97]	<0.01	8.2	0.0	90.3	2.76
#3831.0-32.0		0.32	0.29	0.09	9.0	1.0	73.3	2.75
#3832.0-33.0		0.02	<0.01	<0.01	1.4	9.0	44.9	2.72
#3833.0-34.0		<0.01	<0.01	<0.01	1.4	0.0	34.0	2.72
#3834.0-35.0		[0.78]	[0.59]	<0.01	2.0	0.0	43.9	2.72
#3835.0-36.0		<0.01	<0.01	<0.01	1.3	0.0	65.4	2.71
#3836.0-37.0		<0.01	**	<0.01	0.5	0.0	58.7	2.71

Rogers #2 C NE SW 19-6S-22W

Depth	Interval	Kmax	K90	Kv	Poro	So	Sw	Rho-G
3803.5-07.0	H Zone	No Analysis						
3807.0-14.0	I-S	No Analysis						
3814.0-15.0	I-C	<0.01	<0.01	<0.01	1.6	0.0	90.1	2.71
3815.0-16.0	"	0.10	0.08	0.28	3.5	47.1	18.8	2.70
3816.0-17.0	"	0.07	0.06	0.37	3.6	35.9	25.6	2.71
3817.0-18.0	"	0.01	<0.01	<0.01	1.5	0.0	62.3	2.71
3818.0-19.0	"	0.10	0.07	0.22	2.0	0.0	80.6	2.72
3819.0-25.5	J-US	No Analysis						
3825.5-26.0	J-UC;C	[0.65]	**	<0.01	[10.0]	13.7	55.0	2.81
3826.0-27.0	"	[3.31]	**	<0.01	[14.0]	7.8	53.7	2.79
3827.0-28.0	J-UC;AG	3.99	**	2.25	7.8	6.5	48.4	2.72
3828.0-29.0	"	31.0	20.0	1.20	14.7	7.7	72.8	2.78
3829.0-30.0	"	0.01	<0.01	0.01	1.8	8.5	39.8	2.69
3830.0-31.0	J-UC;AM	0.04	0.03	0.02	2.8	23.9	44.8	2.79
3831.0-32.0	J-UC;BGP	0.01	<0.01	<0.01	0.5	15.1	45.3	2.68
3832.0-33.0	J-UC;BM	0.18	0.08	0.23	1.5	2.1	42.7	2.70
3833.0-34.0	"	<0.01	<0.01	<0.01	1.5	0.0	62.7	2.71
3834.0-35.0	J-LS/LC	No Analysis						
3835.0-43.0	K-US	No Analysis						
#3843.0-44.0	K-UC;CC	1.10	0.88	0.26	4.7	0.0	90.9	2.79
3844.0-45.0	K-UC;S	No Analysis						
#3845.0-46.0	K-UC;BC	0.01	<0.01	<0.01	6.1	0.0	96.7	2.74
#3846.0-47.0	"	<0.01	<0.01	<0.01	0.4	44.9	30.0	2.69
#3847.0-48.0	"	0.07	<0.01	0.23	2.3	0.0	38.7	2.72
#3848.0-49.0	K-LS	0.01	<0.01	<0.01	2.7	0.0	48.9	2.72
#3849.0-50.0	K-LC/L-US	0.10	0.08	0.09	2.9	0.0	61.3	2.76
#3850.0-51.0	L-UC	0.66	0.28	0.21	3.8	45.3	30.2	2.70
#3851.0-52.0	"	0.01	**	<0.01	1.6	3.3	53.4	2.70
#3852.0-53.0	"	0.02	**	0.17	2.1	0.0	74.0	2.71
#3853.0-54.0	"	0.06	**	0.01	1.9	0.0	74.1	2.71
#3854.0-55.0	"	0.06	0.06	<0.01	1.3	0.0	54.7	2.77
#3855.0-56.0	"	0.04	0.02	<0.01	1.1	0.0	41.8	2.70
#3856.0-57.0	"	0.96	**	<0.01	1.6	0.0	71.5	2.71
#3857.0-58.0	"	0.33	0.31	0.01	2.4	0.0	54.4	2.80
#3858.0-59.0	"	0.02	0.02	0.01	1.6	0.0	25.1	2.72
#3859.0-60.0	"	0.38	0.29	0.01	1.7	0.0	36.4	2.71
#3860.0-61.0	L-LS/LC	0.01	<0.01	<0.01	0.5	0.0	25.6	2.71
#3861.0-62.0	PLS	0.24	0.23	0.36	1.7	0.0	79.8	2.71
#3862.0-63.0	"	0.32	0.29	0.31	10.8	0.0	65.3	2.70

Shuck #1 C NW SE 17-6S-22W

Depth	Interval	Kmax	K90	Kv	Poro	So	Sw	Rho-G
#3718.0-19.0	H Zone	0.01	0.01	<0.01	1.1	0.0	25.9	2.72
#3719.0-20.0	"	0.01	<0.01	<0.01	1.9	0.0	48.4	2.74
#3720.0-21.0	"	0.41	0.15	<0.01	5.5	0.0	79.3	2.75
#3721.0-22.0	"	0.01	<0.01	<0.01	2.0	0.0	76.3	2.72
#3722.0-23.0	"	0.02	0.02	<0.01	3.2	0.0	65.1	2.75
#3723.0-24.0	"	0.07	0.05	<0.01	3.7	0.0	73.4	2.75
#3724.0-25.0	"	0.03	<0.01	<0.01	1.6	0.0	68.5	2.73
#3725.0-26.0	"	<0.01	<0.01	<0.01	2.0	0.0	72.8	2.73
#3726.0-27.0	"	0.06	0.01	<0.01	2.1	0.0	92.3	2.72
#3727.0-28.0	"	0.01	<0.01	<0.01	3.2	0.0	86.4	2.74
3728.0-29.0	"	[0.55]	**	<0.01	[7.6]	0.0	82.4	2.72
3729.0-34.0	I-S	No Analysis						
3734.0-35.0	I-C	0.10	0.01	<0.01	1.5	0.0	84.8	2.67
3735.0-36.0	"	<0.01	**	<0.01	1.9	37.3	13.3	2.71
3736.0-36.5	"	<0.01	**	<0.01	1.3	0.0	53.1	2.70
3736.5-43.0	I-C/J-US	Lost Core						
3743.0-43.5	J-US	No Analysis						
3743.5-44.0	J-UC;C	***	**	[0.24]	[7.5]	7.9	78.5	2.82
3744.0-45.0	"	[0.05]	**	[0.03]	[7.3]	7.8	67.2	2.81
3745.0-46.0	J-UC;C/AG	[2.9]	[2.7]	[0.07]	[13.5]	10.1	38.5	2.78
3747.0-47.5	J-UC;AG	7.7	7.1	0.12	9.4	35.0	56.0	2.71
3747.5-48.0	"	25	23	10	10.4	15.3	39.2	2.71
3748.0-49.0	J-UC;AM	0.11	0.05	<0.01	[5.4]	15.9	39.9	2.74
3749.0-50.0	"	0.05	0.01	<0.01	[3.5]	0.0	85.5	2.74
3750.0-51.0	J-UC;BGP	<0.01	<0.01	<0.01	1.8	0.0	62.1	2.71
3751.0-52.0	J-UC;BM	0.01	<0.01	<0.01	1.1	0.0	39.7	2.70
3752.0-53.0	"	0.02	0.02	<0.01	1.0	0.0	63.0	2.71
3753.0-54.0	"	<0.01	<0.01	<0.01	0.9	0.0	71.2	2.70
3754.0-55.0	"	0.01	<0.01	<0.01	0.8	0.0	40.5	2.70
3755.0-56.0	"	0.03	<0.01	<0.01	1.3	0.0	44.6	2.71
3756.0-57.0	J-LC	[0.19]	[0.03]	<0.01	[3.5]	6.4	64.3	2.70
3757.0-65.0	K-US	No Analysis						
#3765.0-66.0	K-UC;CC	0.15	0.10	<0.01	4.7	0.0	92.2	2.72
#3766.0-67.0	"	0.02	0.02	<0.01	2.0	0.0	82.4	2.71
#3767.0-68.0	K-UC;S/BC	[0.23]	[0.04]	<0.01	[5.6]	1.1	87.8	2.72
#3768.0-69.0	K-UC;BC	<0.01	**	<0.01	1.3	0.0	94.2	2.71
3769.0-70.0	K-UC;BC	Lost Core						

Shuck #4 C SE SE 17-6S-22W

Depth	Interval	Kmax	K90	Kv	Poro	So	Sw	Rho-G
#3768.0-69.0	H Zone	<0.01	**	<0.01	1.6	0.0	68.7	2.71
#3769.0-70.0	"	<0.01	**	<0.01	2.8	0.0	71.3	2.71
#3770.0-71.0	"	<0.01	**	<0.01	0.8	0.0	71.5	2.70
#3771.0-72.0	"	[0.66]	**	<0.01	1.6	0.0	46.0	2.70
#3772.0-73.0	"	<0.01	**	<0.01	1.8	0.0	71.8	2.71
#3773.0-74.0	"	0.01	**	<0.01	2.5	0.0	63.1	2.71
#3774.0-75.0	"	0.01	**	0.01	2.3	0.0	59.4	2.71
3775.0-76.0	"	[0.02]	**	<0.01	[3.3]	0.0	82.7	2.72
3776.0-81.0	I-S	No Analysis						
3781.0-82.0	I-C	<0.01	**	0.01	0.8	16.6	27.7	2.70
3782.0-83.0	"	0.08	**	0.01	3.3	22.7	28.3	2.70
3783.0-84.0	"	43	**	14	8.9	19.1	31.8	2.72
3784.0-84.5	"	<0.01	**	<0.01	1.4	0.0	74.8	2.71
3784.5-92.0	J-US	No Analysis						
3792.0-93.0	J-UC;C	[2.1]	**	[0.91]	[12.1]	2.0	89.9	2.89
3793.0-94.0	"	[0.51]	**	[1.7]	[10.2]	32.8	43.8	2.77
3794.0-95.0	"	[0.01]	**	[0.72]	[2.9]	6.6	69.8	2.74
3795.0-96.0	J-UC;C/AM	[0.01]	**	[0.02]	[1.7]	20.7	51.0	2.72
3796.0-97.0	J-UC;AM	0.01	**	0.01	2.1	0.0	61.6	2.72
3797.0-98.0	"	Lost Core						

White #1 60'E, C NW NE 20-6S-22W

Depth	Interval	Kmax	K90	Kv	Poro	So	Sw	Rho-G
3763.5-67.5	I-S	No Analysis						
3767.5-68.0	I-C	<0.01	<0.01	***	0.4	9.4	76.9	2.70
3768.0-69.0	"	[0.17]	[0.04]	***	[3.2]	26.2	46.8	2.70
3769.0-70.0	"	<0.01	<0.01	***	1.7	32.4	51.7	2.70
3970.0-80.0	J-US	No Analysis						
3780.0-81.0	J-UC;C/AG	[0.78]	[0.51]	***	[12.6]	0.0	85.3	2.75
3781.0-82.0	J-UC;AG	No Analysis						
3782.0-83.0	J-UC;AM	No Analysis						
3783.0-84.0	"	No Analysis						
3784.0-85.0	J-UC;BGP	[22]	[0.01]	***	[2.8]	34.6	46.8	2.71
3785.0-86.0	J-UC;BM	[0.69]	[0.36]	***	[2.9]	17.8	72.5	2.71
3786.0-87.0	"	0.03	0.02	***	1.6	14.4	76.6	2.71
3787.0-88.0	"	0.03	0.03	***	2.3	20.4	62.2	2.71
3788.0-89.0	"	0.16	0.11	***	1.2	10.5	80.0	2.70
3789.0-90.0	"	0.01	0.01	***	1.2	6.6	78.1	2.71
3790.0-91.0	J-UC/LS/LC	No Analysis						
3791.0-92.0	J-LC	No Analysis						
3792.0-94.5	K-US	No Analysis						

White #5 C SW NW 20-6S-22W

Depth	Interval	Kmax	K90	Kv	Poro	So	Sw	Rho-G
3786.0-86.5	I-S	No Analysis						
3786.5-87.0	I-C	No Analysis						
3787.0-88.0	"	0.01	<0.01	<0.01	2.2	3.3	33.3	2.71
3788.0-89.0	"	5.1	3.9	0.82	6.0	61.3	13.1	2.68
3789.0-94.0	J-US	No Analysis						
3794.0-94.5	J-UC;C	No Analysis						
3794.5-95.0	J-UC;AG	0.01	**	<0.01	5.0	27.0	21.3	2.72
3795.0-96.0	"	69	60	40	23.2	35.3	18.5	2.70
3796.0-97.0	"	266	**	925	28.8	26.8	31.3	2.76
3797.0-98.0	"	1280	**	***	28.2	32.0	30.0	2.74
3798.0-99.0	"	193	151	780	25.0	35.4	31.8	2.73
3799.0-00.0	"	426	143	690	26.2	31.2	28.0	2.75
3800.0-01.0	J-UC;AM	[16]	[11]	[4.8]	[22.4]	25.7	40.4	2.79
3801.0-02.0	J-UC;BM	[0.47]	[0.24]	[0.41]	[9.3]	22.3	53.0	2.77
3802.0-08.0	J-UC;BM	No Analysis						
3808.0-09.0	J-LS/LC	No Analysis						
3809.0-16.5	K-US	No Analysis						
3816.5-17.0	K-UC;CC	No Analysis						
3817.0-18.0	"	No Analysis						
3718.0-18.5	"	13	11	0.08	7.1	34.4	32.7	2.71
3718.5-19.0	K-UC;S	No Analysis						
3819.0-20.0	K-UC;BC	[0.14]	[0.08]	<0.01	[7.2]	18.7	14.4	2.73
3820.0-21.0	"	22	20	14	9.4	32.9	29.9	2.72
3821.0-22.0	"	9.5	7.6	9.5	11.6	15.0	20.8	2.72
3822.0-23.0	"	0.04	0.01	<0.01	3.2	10.1	43.3	2.71
3823.0-25.0	K-UC;BC	No Analysis						
3825.0-26.0	K-LS	No Analysis						
3826.0-27.0	K-LC/L-US	No Analysis						
3827.0-28.0	L-UC	No Analysis						
3828.0-29.0	"	No Analysis						
3829.0-30.0	"	[4.3]	[0.55]	<0.01	[6.0]	20.1	43.9	2.75
3830.0-31.0	"	0.27	0.26	<0.01	2.5	0.0	39.6	2.73
3831.0-37.0	L-UC	No Analysis						
3837.0-38.0	L-LS/LC	No Analysis						
3838.0-45.0	PLS	No Analysis						

APPENDIX 3

WELL FILES

Glossary of well file abbreviations:

AC	Acidize
AMT	Amount
ARB	Arbuckle Group
BO	Barrels of oil
BOPD	Barrels of oil per day
BP	Bridge plug
BTM	Bottom
BWPD	Barrels of water per day
CC	Cubic centimeters
CD HILL	Cedar Hill Formation
CGL SD	Conglomerate Sand (local formation name)
CIBP	Cast iron bridge plug
CLN	Clean
CMP	Completion date
CO	Cleaned out
CSG	Casing (diameter, footage/amount of cement)
DST	Drillstem test
DVT	Diverting tool
DWN	Down
D&A	Drilled and abandoned
FEL	From east line
FNL	From north line
FP	Flow pressures
FRAC	Fracture
FWL	From west line
GAL	Gallons
GIP	Gas in pipe
GR	Gravity
GSO	Good show of oil
GSY	Gassy
GTSTM	Gas too small to measure
HCL	Hydrochloric acid
HMCO	Heavily mud cut oil
HOCM	Heavily oil cut mud
HP	Hydrostatic pressures
HWCM	Heavily water cut mud

Glossary (continued)

Inj.	Injection
INTV	Interval
IP	Initial potential (pumping/flowing, rate, fluid)
L PENN	Undifferentiated Lower Pennsylvanian formations
LD	Load
LKC	Lansing-Kansas City groups
M	Mud
MCA	Mud clean-up acid
MDY	Muddy
MICT	Moved in cable tools
MO	Muddy oil
MSC	Multi-stage collar
MW	Muddy water
NA	Not available
Non-Comm	Non-commercial
NS	No show
NSO	No show of oil
NW	No water
O	Oil
OCM	Oil cut mud
OCMW	Oil cut muddy water
OP	Open
OWWO	Old well work-over
P	Pumping
PF	Perforate
PFS	Perforations
PKR	Packer
POP	Put on pump
Pot.	Potential
PRD	Production
REC	Recovered
Rept.	Reported
RE-AC	Re-acidize
RNT	Re-entry date
Satis.	Satisfactory
SHW	Shawnee Group
SIP	Shut-in pressures
Sl	Slightly
SO	Show of oil
SOCM	Slightly oil cut mud

Glossary (continued)

SPD	Spud date (operations commence)
SPF	Shots per foot
SPKS	Specks
SPLR	Sampler
SPTD	Spotted
SW	Salt water
SWB	Swab
SWDW	Salt water disposal well
sx	Sacks (of cement)
TBG	Tubing
Tr	Trace
TRT	Toronto Formation
WCM	Water cut mud
WM	Watery mud
WTR	Water
WTRY	Watery
w/	With
#	Pounds per square inch (psi)

Bethell #1 Oper: B & R Drlg. and Wilcox Loc: NE NE NE
17-6S-22W

IP: D&A Interval:

SPD: 7/29/48 CMP: 8/20/48 CSG: 8" 162

Cores: None

DST (1) 3576-3585 OP 35"; 7' OCM

Bethell #1 Oper: PanCanadian Petroleum Co. Loc: 100' E, C SE NW 17-6S-22W

IP: D&A Interval:

SPD: 9/15/85 CMP: 10/1/85 CSG: 8 5/8" 296/225 sx

Cores: None

DST (1) 3551-3572 [TRT, LKC "A"] 15-45-45-90; 25' O SPTD M
SIP 1255-1255#, FP 32-21 / 21-21#, HP 1844-1833#

DST (2) 3700-3730 [LKC "I", "J"] 15-45-45-90; 30' OCM (5% O, 95% M)
SIP 434-478#, FP 43-32 / 32-32#, HP 1950-1940#

DST (3) 3730-3772 [LKC "K", "L"] 15-45-45-90; 6" O, 40' OCM (20% O),
62' O SPTD M, 62' O SPTD WCM, 144' MW
SIP 1223-1180#, FP 54-54 / 97-152#, HP 1982-1961#

Bethell #3 Oper: PanCanadian Petroleum Co. Loc: C NE SW
17-6S-22W

IP: P 29 BO & 4 BWPD Interval: 3734-3740 LKC "I"
3746-3756 LKC "J"
3776-3782 LKC "L"

SPD: 6/14/86 CMP: 7/17/86 CSG: 8 5/8" 295/195 sx
4 1/2" 3874/245 sx
DVT @ 2018/375 sx

Cores: (1) 3702-3724 LKC "H"
(2) 3724-3754 LKC "H", "I", "J"
(3) 3754-3762 LKC "J"

DST (1) 3724-3754 [LKC "H", "I", "J"] 10-45-60-90; 10' Free O,
20' OCM (30% O, 70% M), 60' OCM (10% O, 90% M)
SIP 592-360#, FP 105-105 / 105-105#, HP 1937-1843#

MICT - CO, PF 3776-3782 w/ 2 SPF, AC 1082 GAL (15% HCL), SO;
PF 3734-3740, 3746-3756 w/ 2 SPF, AC 2918 GAL (15% HCL), SO;
Set 2 3/8" TBG @ 3821, POP, P 29 BO & 4 BWPD, GTSTM (GR 38)

Bethell #4 Oper: PanCanadian Petroleum Co. Loc: C SE SW
17-6S-22W

IP: P 108 BOPD, NW Interval: 3750-3754 LKC "I"
3759-3766 LKC "J"

SPD: 12/6/85 CMP: 1/18/86 CSG: 8 5/8" 305/225 sx
4 1/2" 4009/800 sx

Cores: None

DST (1) 3745-3780 [LKC "I", "J"] 15-45-60-90; 1200' GIP,
2010' CLN GSY O, 120' OCM
SIP 1095-1095#, FP 470-490 / 599-817#, HP 2040-1920#

DST (2) 3782-3808 [LKC "K", "L"] Times NA; 240' M
Pressures NA, Misrun

DST (3) 3775-3808 [LKC "K", "L"] 15-45-60-90; 10' M
SIP 795-726#, FP 70-70 / 70-70#, HP 2068-1980#

MICT - CO, PF 3750-3754 w/ 2 SPF & 3759-3766 w/ 2 SPF,
AC (all PFS) 2750 GAL, GSO;
Set 2 3/8" TBG @ 3839, POP, P 108 BOPD, NW

Bethell #5 Oper: PanCanadian Petroleum Co. Loc: C SW SW
17-6S-22W

IP: P 70 BOPD, NW Interval: 3750-3752 LKC "I"
3758-3765 LKC "J"

SPD: 2/28/86 CMP: 3/26/86 CSG: 8 5/8" 302/225 sx
4 1/2" 4064/265 sx
DVT @ 2040/410 sx

Cores: (1) 3746-3776 LKC "I", "J"
(2) 3776-3807 LKC "K", "L"

DST (1) 3742-3776 [LKC "I", "J"] 10-45-60-90; 1220' GIP,
1300' CLN GSY O, 60' MCO (10% M, 90% O),
60' SOCM (90% M, 10% O)
SIP 596-596#, FP 131-151 / 263-495#, HP 1927-1899#

MICT - CO, PF 3750-3752 w/ 2 SPF, AC 500 GAL, GSO;
PF 3758-3765 w/ 2 SPF, AC 1750 GAL, GSO;
Set 2 3/8" TBG @ 3825, POP, P 70 BOPD, NW, GTSTM, (GR 38)

Bethell #6 Oper: PanCanadian Petroleum Co. Loc: C NW SW
17-6S-22W

IP: D&A Interval:

SPD: 11/23/86 CMP: 11/30/86 CSG: 8 5/8" 304/205 sx

Cores: None

DST (1) 3738-3773 [LKC "I", "J"] 15-30-30-30; 5' M
SIP 127-127#, FP 105-105 / 84-127#, HP 1937-1812#

DST (2) 3770-3803 [LKC "K", "L"] 15-45-30-30; 5' M
SIP 116-95#, FP 105-105 / 105-105#, HP 1937-1802#

DST (3) 3844-3866 [CGL SD] 10-45-60-90; 60' M, 20' MCW
SIP 987-904#, FP 42-42 / 42-52#, HP 1989-1958#

Pennington #1 Oper: PanCanadian Petroleum Co. Loc: C SW NE
17 6S-22W

IP: P 60 BOPD, NW Interval: 3707-3723 LKC "I", "J"

SPD: 4/22/85 CMP: 5/21/85 CSG: 8 5/8" 275/225 sx
4 1/2" 3890/240 sx
MSC @ 1996/450 sx

Cores: None

DST (1) 3522-3618 [TRT, LKC "A", "C", "D"] 10-45-45-90; 340' Sl O SPTD HWCM
SIP 1279-1207#, FP 132-132 / 204-234#

DST (2) 3678-3736 [LKC "H", "I", "J", "K"] 10-45-45-90; 840' GIP,
60' Free O, 480' MCO
SIP 1228-1146#, FP 142-153 / 173-255#

DST (3) 3737-3770 [LKC "K", "L"] 10-30-30-60; 40' O SPTD M
SIP 817-530#, FP 61-61 / 61-71#

DST (4) 3785-3832 [L PENN, CGL SD] 10-30-30-60; 20' O SPTD HWCM
SIP 1022-1043#, FP 61-61 / 71-71#

MICT - CO, PF 3810-3816 [CGL SD] w/ 2 SPF, AC 300 GAL, SWB DWN, NS;
Set Plug (Depth NA)
PF 3707-3723 w/ 2 SPF, AC 800 GAL, SWB DWN, GSO;
Set TBG, POP, P 60 BOPD, NW (GR 41.4)

Pennington #2 Oper: PanCanadian Petroleum Co. Loc: C SE NE
17-6S-22W

IP: P 20 BO & 21 BWPD Interval: 3673-3678 LKC "D"
3764-3767 LKC "I"
3774-3784 LKC "J"

SPD: 12/6/85 CMP: 1/30/86 CSG: 8 5/8" 296/225 sx
4 1/2" 4021/825 sx
DVT @ 2035/475 sx

Cores: (1) 3763-3793 LKC "I", "J"

DST (1) 3531-3568 [SHW] 22-45-60-90; 30' OCMW, 2230' sulphur WTR
SIP 1235-1204#, FP 164-370 / 473-1039#

DST (2) 3617-3630 [TRT, LKC "A"] 15-45-60-90; 1450' SW w/ scum of O
SIP 1028-925#, FP 144-277 / 380-648#, HP 1792-1740#

DST (3) 3759-3793 [LKC "I", "J"] 15-45-60-90; 150' GIP,
60' CLN GSY O, 60' OCM
SIP 925-823#, FP 51-51 / 61-72#, HP 1925-1905#

MICT - CO, PF 3673-3678 w/ 2 SPF, AC 1250 GAL;
PF 3764-3767 & 3774-3784 w/ 2 SPF, AC 3250 GAL, GSO;
Set 2 3/8" TBG @ 3845, POP, P 20 BO & 21 BWPD (GR 38)

Shuck #1 Oper: PanCanadian Petroleum Co. Loc: C NW SE
17-6S-22W

IP: P 46 BOPD, NW Interval: 3742-3750 LKC "J"

SPD: 6/14/85 CMP: 7/9/85 CSG: 8 5/8" 306/215 sx
4 1/2" 3927/670 sx

Cores: (1) 3718-3742 LKC "H", "I"
(2) 3742-3770 LKC "J", "K"

DST (1) 3539-3580 [TRT] 15-45-45-90; 1370' MW, 40' Heavy M
SIP 1332-1310#, FP 114-360 / 426-709#, HP 1880-1848#

DST (2) 3579-3598 [TRT, LKC "A"] 15-45-45-90; 2' Free O,
1300' GSY MCW, 40' Heavy M on BTM
SIP 1320-1310#, FP 171-360 / 470-688#, HP 1891-1848#

DST (3) 3716-3772 [LKC "H", "I", "J", "K"] 15-45-45-90; 60' GIP,
120' GSY SOCM, 180' GSY OCM, 60' MO
SIP 1310-1278#, FP 103-114 / 159-227#, HP 1988-1945#

MICT - CO, PF 3742-3750 w/ 2 SPF, AC 800 GAL, SWB DWN, GSO;
Set TBG, POP, P 46 BOPD, NW (GR 41)

Shuck #2 Oper: PanCanadian Petroleum Co. Loc: C NE SE
17-6S-22W

IP: P 120 BO & 1 BWPD Interval: 3754-3758 LKC "I"
3764-3768 LKC "J"

SPD: 10/14/85 CMP: 12/3/85 CSG: 8 5/8" 303/225 sx
4 1/2" 3993/850 sx

Cores: None

DST (1) 3606-3650 [TRT, LKC "A", "C"] 15-45-45-90; 150' GIP,
30' CLN GSY O, 120' O & WCM, 105' SW
SIP 1313-1293#, FP 130-190 / 330-559#, HP 1911-1793#

DST (2) 3653-3690 [LKC "C", "D", "E", "F"] 15-45-45-90; 2' O,
98' WCM, 180' SW
SIP 1225-1157#, FP 70-90 / 120-180#, HP 1891-1783#

DST (3) 3744-3780 [LKC "H", "I", "J"] 15-45-45-90; 960' GIP,
400' CLN GSY O, 120' MCO
SIP 1069-971#, FP 90-110 / 130-220#

DST (4) INTV NA, Misrun

DST (5) 3774-3810 [LKC "K", "L"] 15-45-45-90; 10' M
SIP 1127-1098, FP 50-50 / 50-60#, HP 1940-1861#

MICT - CO, PF 3795-3798 w/ 2 SPF, AC 750 GAL, SWB DWN, NSO;
PF 3764-3768 w/ 2 SPF, AC 1000 GAL, SO;
PF 3754-3758 w/ 2 SPF, AC 1000 GAL, SO;
Set 2 3/8" TBG @ 3864, POP, P 120 BO & 1 BWPD (GR 37)

Shuck #3 Oper: PanCanadian Petroleum Co. Loc: C SW SE
17-6S-22W

IP: P 59 BO & 1 BWPD Interval: 3730-3734 LKC "I"
3741-3745 LKC "J"

SPD: 11/14/85 CMP: 12/29/85 CSG: 8 5/8" 302/210 sx
4 1/2" 4017/805 sx

Cores: None

DST (1) 3586-3596 [LKC "A"] 15-45-60-90; 1891' SW
SIP 1323-1323#, FP 40-607 / 617-1005#

DST (2) 3613-3634 [LKC "C"] 15-45-60-90; 213' MW, 976' SW
SIP 1303-1263#, 172-248 / 335-577#

DST (3) 3688-3727 [LKC "H"] 15-45-60-90; 450' MW
SIP 1273-1244#, FP 60-91 / 121-233#

DST (4) 3727-3756 [LKC "I", "J"] 15-45-60-90; 1736' CLN GSY O, 124' MCO
SIP 1199-1122#, FP 306-352 / 443-712#, HP 1906-1852#

MICT - CO, PF 3962-3966 [ARB] w/ 2 SPF, AC 1000 GAL, NS;
Set CIBP @ 3900
PF 3741-3745 w/ 2 SPF, AC 1000 GAL, SO;
PF 3730-3734 w/ 2 SPF, AC 1000 GAL, GSO;
Set 2 3/8" TBG @ 3811, POP, P 59 BO & 1 BWPD, GTSTM (GR 37)

Shuck #4 Oper: PanCanadian Petroleum Co. Loc: C SE SE
17-6S-22W

IP: P 30 BO & 1 BWPD Interval: 3780-3786 LKC "I"
3792-3802 LKC "J"

SPD: 11/24/85 CMP: 1/6/86 CSG: 8 5/8" 298/210 sx
4 1/2" 4048/805 sx

Cores: (1) 3768-3798 LKC "H", "I", "J"

DST (1) 3615-3645 [TRT, LKC "A"] Times NA, 120 M w/ few O SPKS
Pressures NA, Misrun

DST (2) 3620-3645 [TRT, LKC "A"] 15-45-60-90; 1' CLN O
4' WTRY OCM, 60' Oily WCM
SIP 1286-1256#, FP 51-51 / 51-51#, HP 1952-1901#

DST (3) 3765-3798 [LKC "H", "I", "J"] 15-45-60-90;
20' OCM w/ CLN O on top of tool
SIP 1000-846#, FP 51-51 / 62-62#, HP 2211-2004#

MICT - CO, PF 3866-3871 (L PENN) w/ 2 SPF, AC 1250 GAL, NS;
PF 3824-3830 (LKC "L") w/ 2 SPF, AC 1500 GAL, NS;
Set CIBP @ 3820
PF 3792-3802 w/ 2 SPF, AC 2500 GAL, GSO;
PF 3780-3786 w/ 2 SPF, AC 1500 GAL, GSO;
Set 2 3/8" TBG @ 3809, POP, P 30 BO & 1 BWPD (GR 37)

Billips #1 Oper: Wood River Oil & Refining Loc: SW SW NE 18-6S-22W

IP: D&A Interval:

SPD: NA CMP: 2/9/51 CSG: 8" 268

Cores: None

DST (1) 3629-3652 OP 60; 49' SW

Griffey #1 Oper: Ritchie Exploration Loc: SW SW SW
18-6S-22W

IP: (OWWO) SWDW Interval: 1750-1770 CD HILL

RNT: 12/20/89 CMP: 1/9/90 CSG: 8 5/8" 246/160 sx
4 1/2" 2050/600 sx

Old Info:

IP: D&A Interval:

SPD: 10/04/75 CMP: 11/12/75 CSG: 8 5/8" 246/160 sx

Cores: None

DST (1) 3684-3696 30-30-30-30; 60' CLN O,
180' SOCM, 1790' WTR w/ screen O
SIP 1199-1199#, FP 102-701 / 745-979#

DST (2) 3696-3705 30-30-30-30; 60' MW, 1140' SW
SIP 1202-1202#, FP 10-353 / 405-541#

DST (3) 3730-3770 30-30-30-30; 10' M
SIP 135-114#, FP 31-31# / 41-31#

DST (4) 3771-3785 30-30-30-60; 5' OCM, 2' Free O in tool
SIP 93-104#, FP 20-20 / 31-31#

DST (5) 3787-3820 30-30-30-30; 5' SOCM
SIP 1130-944#, FP 31-31 / 31-31#

New Info:

WSH DWN; Set 4 1/2" 2050/600 sx
MICT - CO, PF 1750-1770 w/ 1 SPF;
Set 2 3/8" TBG @ 2050 & PKR @ 1735, SWDW, Inj. Rate Satis.

Griffey #1 Oper: Ritchie Exploration Loc: 100' E, C SE SE
18-6S-22W

IP: P 60 BOPD, NW Interval: 3774-3778 LKC "I"
3782.5-3786.5 LKC "J"

SPD: 4/17/86 CMP: 5/13/86 CSG: 8 5/8" 260/185 sx
4 1/2" 3877/130 sx

Cores: None

DST (1) 3540-3580 [SHW] 30-30-30-30; 150' WM, 2280' MDY SW w/ Scum O
SIP 1271-1271#, FP 216-926 / 961-1156#

DST (2) 3584-3643 [TRT, LKC "A"] 30-30-30-30; 140' WM, 2380' SW, NSO
SIP 1290-1290#, FP 251-972 / 1006-1179#

DST (3) 3731-3795 [LKC "H", "I", "J"] 30-45-30-45; 240' GIP, 280' MCO
SIP 1149-1145#, FP 45-93 / 114/139#

DST (4) 3869-3904 [CGL SD] 15-30-0-0; 100' M w/ O spots,
260' MW w/ O spots, 1140' SW
SIP 1142, FP 367-848#

MICT - CO PF 3785, 3777 w/ 1 shot each, AC 1500 GAL, SWB LD, SO;
PF 3782.5-3786.5 & 3774-3778 w/ 2 SPF, GSO;
Set TBG, POP, P 60 BOPD, NW

Griffey #2 Oper: Ritchie Exploration Loc: C SW SE
18-6S-22W

IP: D&A Interval:

SPD: 12/17/86 CMP: 12/23/86 CSG: 8 5/8" 249/185 sx

Cores: None

DST (1) 3756-3792 [LKC "I", "J"] 30-30-30-30; 15' O SPTD M w/ scum O on top
SIP 65-34#, FP 10-10 / 20-20#

DST (2) 3866-3910 [L PENN, CGL SD] 15-30-0-0; 186' MW, 1626' SW
SIP 1169#, FP 489-770#

DST (3) 3580-3640 30-30-30-30; 243' MW, 1200' SW, NSO
SIP 1266-1266#, FP 97-445 / 500-629#

Demuth #1 Oper: PanCanadian Petroleum Co. Loc: C NE NE
19-6S-22W

IP: P 87 BOPD, NW Interval: 3800-3804 LKC "I"
3809-3820 LKC "J"

SPD: 3/19/86 CMP: 4/10/86 CSG: 8 5/8" 295/250 sx
4 1/2" 4039/350 sx
DVT @ 2097/375 sx

Cores: (1) 3791-3823 LKC "I", "J"
(2) 3823-3852 LKC "K", "L"

DST (1) 3789-3822 [LKC "I", "J"] 10-45-60-90; 640' GIP
980' O, 120' MCO (75% O, 25% M)
SIP 846-846#, FP 108-152 / 239-391#, HP 2100-2068#

DST (2) 3821-3852 [LKC "K", "L"] 15-45-60-90; 5' M
SIP 173-173#, FP 21-21 / 21-21#, HP 2057-2046#

MICT - CO, PF 3800-3804 w/ 2 SPF, AC 1000 GAL;
PF 3809-3820 w/ 2 SPF, AC 2750 GAL, GSO;
Set 2 3/8" TBG @ 3868, POP, P 87 BOPD, NW (GR 38)

Demuth #2 Oper: PanCanadian Petroleum Co. Loc: 950 FNL 1900 FEL
19-6S-22W

IP: P 46 BO & 2 BWPD Interval: 3790-3800 LKC "J"

SPD: 6/16/87 CMP: 7/26/87 CSG: 8 5/8" 313/200 sx
4 1/2" 2949/270 sx
MSC @ 2702/385 sx

Cores: None

DST (1) 3768-3781 [LKC "H"] 15-45-60-90; SPLR 2000 CC M
SIP 42-42#, FP 42-42 / 42-42#, HP 1974-1974#

DST (2) 3781-3796 [LKC "I", "J"] 15-45-60-90; SPLR 1000 CC O, 1000 CC M
SIP 158-180#, FP 52-63 / 62-63#, HP 2038-2027#

DST (3) 3796-3825 [LKC "J", "K", "L"] 15-45-60-90; SPLR 2000 CC M w/ Tr O
SIP 902-985#, FP 63-63 / 63-63#, HP 2048-2027#

MICT - CO, PF 3790-3800 w/ 4 SPF, AC 1000 GAL, SO;
RE-AC 1500 GAL, GSO;
Set 2 3/8" TBG @ 3841, No PKR, POP, P 46 BO & 2 BWPD, GTSTM (GR 40)

Demuth #3 Oper: PanCanadian Petroleum Co. Loc: C SE NE
19-6S-22W

IP: P 99 BOPD, NW Interval: 3816-3824 LKC "J"

SPD: 9/3/86 CMP: 9/21/86 CSG: 8 5/8" 301/205 sx
4 1/2" 4014/285 sx
MSC @ 1778/240 sx

Cores: None

DST (1) 3580-3615 [SHW] 10-45-45-90; 60' WCM w/ SPKS O, 60' MW
SIP 1287-1255#, 54-54 / 65-76#, HP 1950-1940#

DST (2) 3797-3828 [LKC "I", "J"] 10-45-60-90; 140' GIP
2' O, 45' MCO (70% O, 20% M, 10% G), 124' MCO
SIP 255-255#, FP 68-69 / 78-88#, HP 1976-1976#

DST (3) 3827-3853 [LKC "J", "K", "L"] 10-45-30-30; 1' M
SIP 76-70#, FP 21-21 / 21-21#, HP 1950-1940#

MICT - CO, PF 3816-3824 w/ 2 SPF, AC 2400 GAL, GSO;
Set TBG, POP, P 99 BOPD, NW (GR 38)

Demuth #4 Oper: PanCanadian Petroleum Co. Loc: C SW NE
19-6S-22W

IP: P 54 BO & 4 BWPD Interval: 3812-3817 LKC "J"

SPD: 3/5/87 CMP: 3/20/87 CSG: 8 5/8" 309/250 sx
4 1/2" 3974/290 sx
MSC @ 2086/210 sx

Cores: (1) 3794-3824 LKC "I", "J"
(2) 3824-3854 LKC "K", "L"

DST (1) 3698-3738 [LKC "C", "D", "E", "F"] 10-45-60-90; 240'MW (40% M),
2220' MW (5% M)
SIP 1205-1205#, FP 353-674 / 743-1170#, HP 1940-1905#

DST (2) 3789-3824 [LKC "H", "I", "J"] 10-45-60-90; 110' CLN O,
120' OCM (20% O), 180' HOCM (35% O)
SIP 228-228#, FP 79-83 / 134-189#, HP 1974-1951#

DST (3) 3819-3854 [LKC "J", "K", "L"] 15-45-60-90; 10' M w/ O SPKS
SIP 1248-1202#, FP 20-20 / 22-26#, HP 2087-2032#

MICT - CO, PF 3812-3817 w/ 2 SPF, AC 4250 GAL (15% HCL) & 4000 GAL Gel, GSO;
Set 2 3/8" TBG @ 3815, POP, P 54 BO & 4 BWPD, GTSTM (GR 38)

Jacobs #1 Oper: Three G Oil Loc: C SW NW
19-6S-22W

IP: D&A Interval:

SPD: 6/27/69 CMP: 7/17/69 CSG: 8 5/8" 249/185 sx

Cores: None

DST (1) 3593-3610 [SHW] OP 60; 65' WM w/ O SPKS
SIP 1271-1255#, FP 15-39#

DST (2) 3628-3659 [TRT] OP 40; 10' M
SIP 20-20#, FP 20-20#

DST (3) 3657-3673 [TRT, LKC "A"] OP 40; 20' M
SIP 791-624#, FP 31-31#

DST (4) 3678-3720 [LKC "A", "C", "D"] OP 90; 2500' WTR
SIP 1311-1311#, FP 275-1239#

DST (5) 3768-3830 [LKC "H", "I", "J"] OP 40; 30' M
SIP 1142-1094#, FP 55-5#

Jacobs #1 Oper: PanCanadian Petroleum Co. Loc: 1650' FNL 2086' FWL
19-6S-22W

IP: D&A Interval:

SPD: 3/3/88 CMP: 6/22/88 CSG: 8 5/8" 312/215 sx
4 1/2" 3949/40 sx
MSC @ 2161/425 sx

Cores: None

DST (1) 3810-3840 [LKC "I", "J"] 15-45-60-90; 30' Sl O SPTD M
SIP 222-222#, FP 47-84 / 84-84#, HP 1920-1899#

DST (2) 3568-3605 [SHW] 15-45-60-90; 120' MW
SIP 1236-1248#, FP 52-52 / 84-90#, HP 1805-1794#

MICT - CO, PF 3852-3864 (LKC "L") w/ 4 SPF, AC 3000 GAL, SWB LD, NS;
Set BP @ 3848
PF 3824-3826 (LKC "J") w/ 4 SPF, SWB DWN, Non-Comm

V. Jacobs #1 Oper: Ritchie Exploration Loc: NE NW NW
19-6S-22W

IP: Oil Interval: INTV NA LKC

SPD: 8/2/89 CMP: 12/20/89 CSG: 8 5/8" 269
PRD CSG NA
MSC @ 2018/385 sx

Cores: None

MICT - CO, PF INTV NA (LKC), GSO;
Set TBG, POP, Oil Well, Pot. not Rept.

Rogers #1 Oper: Herndon Drilling Co. Loc: SE SE SW
19-6S-22W

IP: D&A Interval:

SPD: CMP: 8/31/51 CSG:

Cores: None

No DSTs

Rogers #1 Oper: PanCanadian Petroleum Co. Loc: C NE SE
19-6S-22W

IP: D&A Interval:

SPD: 11/30/86 CMP: 12/15/86 CSG: 8 5/8" 302/205 sx
4 1/2" 3939/515 sx

Cores: (1) 3780-3810 LKC "H", "I", "J"
(2) 3810-3837 LKC "K", "L"

DST (1) 3774-3810 [LKC "H", "I", "J"] 15-45-30-30; 5' M w/ O SPKS
SIP 674-175#, FP 33-35 / 33-33#, HP 1930-1922#

DST (2) 3810-3838 [LKC "K", "L"] 15-45-30-30; 3' M
SIP 582-158#, FP 25-25 / 25-25#, HP 1963-1941#

MICT - CO, PF 3798-3804 (LKC "J") w/ 2 SPF, AC 2300 GAL, SWB DWN, REC Acid WTR; FRAC 2000 GAL Gel WTR & Sand (AMT NA), SWB DWN, SSO, Non-Comm

Rogers #2 Oper: PanCanadian Petroleum Co. Loc: C NE SW
19-6S-22W

IP: D&A Interval:

SPD: 5/14/87 CMP: 5/25/87 CSG: 8 5/8" 304/200 sx

Cores: (1) 3803-3833 LKC "I", "J"
(2) 3833-3863 LKC "K", "L"

DST (1) 3662-3683 [LKC "A"] 15-45-30-60; 10' M w/ O SPKS (60% M, 39% WTR, 1% O)
SIP 1133-1112#, FP 10-10 / 20-10#, HP 1860-1799#

DST (2) 3710-3752 [LKC "D", "E", "F", "G"] 10-45-30-60; 124' M,
124' MW (80% WTR, 20% M), 310' MW (95% WTR, 5% M)
SIP 1133-1102#, FP 51-62 / 93-165#, HP 2045-1952#

DST (3) 3798-3833 [LKC "H", "I", "J"] 15-45-60-90; 62' M, 248' MW (90% WTR, 10% M)
SIP 1051-969#, FP 51-62 / 93-145#, HP 1952-1901#

DST (4) 3833-3863 [LKC "K", "L"] 15-45-60-90; 62' M, 133' WTR
SIP 1235-1194#, FP 10-10 / 31-72#, HP 1911-1829#

DST (5) 3900-3950 [L PENN, CGL SD] PKR Failure, Misrun

DST (6) 3876-3950 [L PENN, CGL SD] 10-45-60-90; 500' MW (85% WTR, 15% M),
460' MW (95% WTR, 5% M), 962' SW
SIP 1112-1081#, FP 414-425 / 363-877#, HP 2066-1963#

Brown #1 Oper: PanCanadian Petroleum Co. Loc: C NW SW
20-6S-22W

IP: D&A Interval:

SPD: 11/7/86 CMP: 11/12/86 CSG: 8 5/8" 302/205 sx

Cores: None

DST (1) 3777-3808 [LKC "I", "J"] 15-45-15-15; 5' OCM
SIP 94-42#, FP 42-31 / 31-31#, HP 1993-1980#

DST (2) 3777-3835 [LKC "I", "J", "K", "L"] 15-45-60-90; 62' M
SIP 941-875#, FP 42-42 / 42-43#, HP 1993-1972#

White #1 Oper: PanCanadian Petroleum Co. Loc: 60' E, C NW NE
20-6S-22W

IP: D&A Interval:

SPD: 1/29/86 CMP: 2/4/86 CSG: 8 5/8" 303/250 sx

Cores: (1) 3763-3795 LKC "I", "J"

DST (1) 3757-3793 [LKC "H", "I", "J"] 15-45-60-90; 5' OCM (10% O, 90% M)
SIP 30-20#, FP 20-20 / 20-20#, HP 1913-1895#

White #2 Oper: PanCanadian Petroleum Co. Loc: C NE NW
20-6S-22W

IP: P 85 BO & 2 BWPD Interval: 3775-3779 LKC "I"
3785-3791 LKC "J"
3806-3813 LKC "K"
3819-3823 LKC "L"

SPD: 2/17/86 CMP: 3/10/86 CSG: 8 5/8" 302/250 sx
4 1/2" 4057/280 sx
DVT @ 2045/450 sx

Cores: None

DST (1) 3531-3570 [SHW] 15-45-30-90; 245' MW
SIP 1147-1137#, FP 70-80 / 130-150#, HP 1881-1783#

DST (2) 3605-3630 [TRT] 15-45-60-90; 335' WM w/ Few O SPKS
SIP 1303-1293#, FP 60-70 / 90-160#, HP 1891-1783#

DST (3) 3770-3806 [LKC "I", "J"] 15-30-60-90; 1055' GIP
745' O, 185' MCO (65% O, 25% M, 10% G), 310' MCO (55% O, 35% M, 10% G)
SIP 716-716#, FP 130-190 / 290-440#, HP 1979-1901#

MICT - CO, PF 3819-3823 w/ 2 SPF, AC 1000 GAL;
PF 3806-3813 w/ 2 SPF, AC 1750 GAL;
PF 3785-3791 w/ 2 SPF, AC 1500 GAL;
PF 3775-3779 w/ 2 SPF, AC 1000 GAL, GSO;
Set 2 3/8" TBG @ 3871, POP, P 85 BO & 2 BWPD (GR 38)

White #4 Oper: PanCanadian Petroleum Co. Loc: C NW NW
20-6S-22W

IP: P 140 BOPD, NW Interval: 3774-3779 LKC "J"
3796-3802 LKC "K"

SPD: 2/6/86 CMP: 3/1/86 CSG: 8 5/8" 302/250 sx
4 1/2" 4074/230 sx
MSC @ 2021/460 sx

Cores: None

DST (1) 3518-3552 [SHW] 15-45-60-90; 125' WM
SIP 1259-1216#, FP 32-32 / 54-75#, HP 1809-1748#

DST (2) 3608-3628 [TRT, LKC "A"] 15-45-60-90; 2280' MDY SW
SIP 1312-1280#, FP 365-615 / 165-1141#, HP 1863-1830#

DST (3) 3680-3690 [LKC "D", "E"] 15-45-60-90; 75' Sl WM
SIP 969-1002#, FP 21-21 / 32-32#, HP 1906-1863#

DST (4) 3749-3785 [LKC "H", "I", "J"] 15-45-60-90; 600' GIP, 195' O,
300' MCO (70% O, 20% G, 10% M), 300' MCO (70% O, 20% M, 10% G),
300' MCO (60% O, 40% M)
SIP 991-862#, FP 194-216 / 216-335#, HP 1960-1939#

DST (5) 3742-4007 [LKC "H", "I", "J", "K", "L", L PENN, CGL SD, ARB] 10-45-30-90;
930' MW
SIP 1162-1162#, FP 216-248 / 345-540#, HP 2123-2069#

MICT - CO, PF 3796-3802 w/ 2 SPF, AC 1500 GAL, GSO;
PF 3774-3779 w/ 2 SPF, AC 1250 GAL, GSO;
Set 2 3/8" TBG @ 3852, POP, P 140 BOPD, NW, GTSTM (GR 38)

White #5 Oper: PanCanadian Petroleum Co. Loc: C SW NW
20-6S-22W

IP: P 68 BO & 2 BWPD Interval: 3784-3788 LKC "I"
3792-3799 LKC "J"
3814-3820 LKC "K"

SPD: 3/9/86 CMP: 3/27/86 CSG: 8 5/8" 302/250 sx
4 1/2" 4028/330 sx
DVT @ 2056/420 sx

Cores: (1) 3786-3814 LKC "I", "J"
(2) 3814-3845 LKC "K", "L"

DST (1) 2935-2966 15-60-60-90; 70' MW
SIP 1094-1094#, FP 33-37 / 41-66#, HP 1471-1451#

DST (2) 3776-3844 [LKC "I", "J", "K", "L"] 10-45-60-90; 700' GIP,
1100' O, 200' Sl MCO (85% O), 45' HMCO (60% O, 40% M)
SIP 598-598#, FP 248-328 / 312-533#, HP 1986-1936#

MICT - CO, PF 3814-3820 w/ 2 SPF, AC 1500 GAL (15% MCA), GSO;
PF 3792-3799 w/ 2 SPF, AC 1750 GAL (15% MCA), GSO;
PF 3784-3788 w/ 2 SPF, AC 1000 GAL (15% MCA), GSO;
Set 2 3/8" TBG @ 3843, POP, P 68 BO & 2 BWPD, GTSTM (GR 38)

APPENDIX 4

MONTHLY PRODUCTION BY LEASE

Figures are from sales data. Each lease had a separate tank battery through April, 1990, prior to waterflood unitization. Consequently, these figures accurtely reflect the lease production.

Date	Bethell	Demuth	Griffey	Pennington	Shuck	White
May-85				673		
Jun-85				990		
Jul-85				988	628	
Aug-85				633	1877	
Sep-85				860	837	
Oct-85				854	823	
Nov-85				861	2157	
Dec-85				423	3848	
Jan-86	1266			418	5333	
Feb-86	2524			1056	4442	
Mar-86	3295			796	4012	5767
Apr-86	4529	1362		782	3331	8058
May-86	3912	1863	961	765	3539	8006
Jun-86	3443	1623	1723	764	4530	6449
Jul-86	2474	1418	1461	523	3878	4977
Aug-86	1988	1313	1466	258	4092	4124
Sep-86	2649	1302	1294	783	3604	4773
Oct-86	2963	1320	1425	788	3163	4505
Nov-86	4035	3015	1117	264	3811	3510
Dec-86	3663	3395	1142	522	3149	3730
Jan-87	2059	3806	1001	535	2582	3824
Feb-87	3091	3134	819	538	1652	4613
Mar-87	1783	2828	998	242	2238	3155
Apr-87	2748	1437	887	533	2862	2542
May-87	3198	3657	925	515	3061	3911
Jun-87	3547	2351	812	264	2635	3913
Jul-87	3121	2692	816	519	1186	3390
Aug-87	3725	2716	866	263	1405	4504
Sep-87	3088	4535	748	504	1044	3762
Oct-87	3064	3980	637	247	1294	4610
Nov-87	4447	3103	620	536	3087	4264
Dec-87	4577	3314	655	536	2525	4287

Date	Bethell	Demuth	Griffey	Pennington	Shuck	White
Jan-88	4432	2882	489	268	2613	3867
Feb-88	3967	2350	487	540	2093	3368
Mar-88	3964	2144	494	269	2377	3441
Apr-88	3496	1841	331	266	2044	3362
May-88	3050	1841	497	237	1549	3179
Jun-88	3001	1834	370	530	1556	3042
Jul-88	2302	1238	164	260	1310	2251
Aug-88	2062	1300	484	265	1047	2366
Sep-88	2098	1055	165	262	1322	1822
Oct-88	1841	1066	317	528	1062	2104
Nov-88	1566	1066	332	270	801	1335
Dec-88	1604	806	334	269	1066	1558
Jan-89	1590	1059	322	271	800	1343
Feb-89	1076	533	169	269	536	809
Mar-89	1318	786	325	268	539	1337
Apr-89	1299	773	167	243	756	1064
May-89	1418	744	330	241	530	1061
Jun-89	1053	530	166	0	774	1060
Jul-89	1306	792	330	263	790	1051
Aug-89	1048	778	165	265	528	1054
Sep-89	1056	532	165	266	452	797
Oct-89	796	531	333	270	534	798
Nov-89	1061	788	166	266	531	803
Dec-89	1067	541	337	0	524	1054
Jan-90	1025	539	169	0	257	809
Feb-90	797	523	163	248	521	797
Mar-90	792	535	162	247	267	537
Apr-90	1055	535	330	247	266	1074
Cumulative Production	126329	84106	28636	26561	110070	147817

Cumulative Field Production 523519

APPENDIX 5

MONTHLY PRODUCTION BY WELL

Lease production was apportioned to each well on the basis of periodic barrel tests.

Bethell Lease

Date	#3	#4	#5	Total
May-85	0	0	0	0
Jun-85	0	0	0	0
Jul-85	0	0	0	0
Aug-85	0	0	0	0
Sep-85	0	0	0	0
Oct-85	0	0	0	0
Nov-85	0	0	0	0
Dec-85	0	0	0	0
Jan-86	0	1266	0	1266
Feb-86	0	2524	0	2524
Mar-86	0	2786	509	3295
Apr-86	0	3627	902	4529
May-86	0	2963	949	3912
Jun-86	0	2454	989	3443
Jul-86	80	1602	792	2474
Aug-86	118	1172	698	1988
Sep-86	320	1350	979	2649
Oct-86	225	1520	1218	2963
Nov-86	251	2165	1619	4035
Dec-86	190	1978	1495	3663
Jan-87	107	1038	914	2059
Feb-87	159	1521	1411	3091
Mar-87	77	914	792	1783
Apr-87	86	1494	1168	2748
May-87	85	1789	1324	3198
Jun-87	155	1964	1428	3547
Jul-87	135	1735	1251	3121
Aug-87	142	2159	1424	3725
Sep-87	107	1786	1195	3088
Oct-87	99	1713	1252	3064
Nov-87	133	2424	1890	4447
Dec-87	133	2503	1941	4577
Jan-88	119	2441	1872	4432
Feb-88	100	2198	1669	3967
Mar-88	143	2204	1617	3964
Apr-88	211	1941	1344	3496
May-88	143	1596	1311	3050
Jun-88	84	1480	1437	3001
Jul-88	70	1157	1075	2302
Aug-88	37	1082	943	2062
Sep-88	89	1083	926	2098
Cumulative Production	3598	61629	38334	103561

Demuth Lease

Date	#1	#2	#3	#4	Total
May-85	0	0	0	0	0
Jun-85	0	0	0	0	0
Jul-85	0	0	0	0	0
Aug-85	0	0	0	0	0
Sep-85	0	0	0	0	0
Oct-85	0	0	0	0	0
Nov-85	0	0	0	0	0
Dec-85	0	0	0	0	0
Jan-86	0	0	0	0	0
Feb-86	0	0	0	0	0
Mar-86	0	0	0	0	0
Apr-86	1362	0	0	0	1362
May-86	1863	0	0	0	1863
Jun-86	1623	0	0	0	1623
Jul-86	1418	0	0	0	1418
Aug-86	1313	0	0	0	1313
Sep-86	1302	0	0	0	1302
Oct-86	1320	0	0	0	1320
Nov-86	1579	0	1436	0	3015
Dec-86	1187	0	2208	0	3395
Jan-87	1412	0	2394	0	3806
Feb-87	1312	0	1822	0	3134
Mar-87	1381	0	1447	0	2828
Apr-87	716	0	684	37	1437
May-87	1733	0	1653	271	3657
Jun-87	1074	0	1089	188	2351
Jul-87	1212	0	1265	215	2692
Aug-87	989	553	1050	124	2716
Sep-87	1714	1261	1410	150	4535
Oct-87	1825	1057	949	149	3980
Nov-87	1626	782	568	127	3103
Dec-87	1794	772	606	142	3314
Jan-88	1548	646	552	136	2882
Feb-88	1117	586	504	143	2350
Mar-88	980	542	489	133	2144
Apr-88	922	417	417	85	1841
May-88	1000	401	368	72	1841
Jun-88	1026	440	313	55	1834
Jul-88	625	402	201	10	1238
Aug-88	628	441	225	6	1300
Sep-88	492	380	164	19	1055
Cumulative Production	38093	8680	21814	2062	70649

Pennington Lease

Date	#1	#2	Total
May-85	673	0	673
Jun-85	990	0	990
Jul-85	988	0	988
Aug-85	633	0	633
Sep-85	860	0	860
Oct-85	854	0	854
Nov-85	861	0	861
Dec-85	423	0	423
Jan-86	374	44	418
Feb-86	549	507	1056
Mar-86	514	282	796
Apr-86	521	261	782
May-86	520	245	765
Jun-86	521	243	764
Jul-86	357	166	523
Aug-86	176	82	258
Sep-86	537	246	783
Oct-86	541	247	788
Nov-86	189	75	264
Dec-86	368	154	522
Jan-87	416	119	535
Feb-87	432	106	538
Mar-87	184	58	242
Apr-87	371	162	533
May-87	346	169	515
Jun-87	184	80	264
Jul-87	387	132	519
Aug-87	194	69	263
Sep-87	369	135	504
Oct-87	181	66	247
Nov-87	389	147	536
Dec-87	380	156	536
Jan-88	185	83	268
Feb-88	362	178	540
Mar-88	177	92	269
Apr-88	174	92	266
May-88	158	79	237
Jun-88	356	174	530
Jul-88	168	92	260
Aug-88	179	86	265
Sep-88	161	101	262
Cumulative Production	17202	4928	22130

Shuck Lease

Date	#1	#2	#3	#4	Total
May-85	0	0	0	0	0
Jun-85	0	0	0	0	0
Jul-85	628	0	0	0	628
Aug-85	1877	0	0	0	1877
Sep-85	837	0	0	0	837
Oct-85	823	0	0	0	823
Nov-85	2157	0	0	0	2157
Dec-85	985	2671	192	0	3848
Jan-86	1712	1846	1335	440	5333
Feb-86	1202	1852	1101	287	4442
Mar-86	1071	1870	939	132	4012
Apr-86	871	1733	727	0	3331
May-86	853	1322	1364	0	3539
Jun-86	1239	1795	1496	0	4530
Jul-86	1024	1528	1326	0	3878
Aug-86	1145	1352	1595	0	4092
Sep-86	879	1416	1309	0	3604
Oct-86	743	1227	1193	0	3163
Nov-86	913	1305	1593	0	3811
Dec-86	731	1004	1414	0	3149
Jan-87	604	872	1106	0	2582
Feb-87	395	563	694	0	1652
Mar-87	513	765	960	0	2238
Apr-87	606	936	1320	0	2862
May-87	600	997	1464	0	3061
Jun-87	511	859	1265	0	2635
Jul-87	232	395	559	0	1186
Aug-87	274	473	658	0	1405
Sep-87	186	304	554	0	1044
Oct-87	194	277	823	0	1294
Nov-87	386	469	2232	0	3087
Dec-87	268	358	1899	0	2525
Jan-88	229	352	2032	0	2613
Feb-88	146	268	1679	0	2093
Mar-88	148	283	1946	0	2377
Apr-88	141	223	1680	0	2044
May-88	133	205	1211	0	1549
Jun-88	163	242	1151	0	1556
Jul-88	152	199	959	0	1310
Aug-88	140	161	746	0	1047
Sep-88	201	190	931	0	1322
Cumulative Production	25912	30312	41453	859	98536

White Lease

Date	#2	#4	#5	Total
May-85	0	0	0	0
Jun-85	0	0	0	0
Jul-85	0	0	0	0
Aug-85	0	0	0	0
Sep-85	0	0	0	0
Oct-85	0	0	0	0
Nov-85	0	0	0	0
Dec-85	0	0	0	0
Jan-86	0	0	0	0
Feb-86	0	0	0	0
Mar-86	1546	3783	438	5767
Apr-86	1918	3288	2852	8058
May-86	1907	3265	2834	8006
Jun-86	1535	2631	2283	6449
Jul-86	1184	2031	1762	4977
Aug-86	982	1682	1460	4124
Sep-86	1137	1947	1689	4773
Oct-86	1163	1759	1583	4505
Nov-86	883	1400	1227	3510
Dec-86	903	1492	1335	3730
Jan-87	821	1656	1347	3824
Feb-87	872	2057	1684	4613
Mar-87	597	1422	1136	3155
Apr-87	483	1182	877	2542
May-87	708	1871	1332	3911
Jun-87	662	1921	1330	3913
Jul-87	581	1714	1095	3390
Aug-87	779	2270	1455	4504
Sep-87	867	1767	1128	3762
Oct-87	1504	1915	1191	4610
Nov-87	1696	1591	977	4264
Dec-87	1685	1582	1020	4287
Jan-88	1477	1419	971	3867
Feb-88	1254	1232	882	3368
Mar-88	1308	1232	901	3441
Apr-88	1436	1119	807	3362
May-88	1542	808	829	3179
Jun-88	1583	569	890	3042
Jul-88	1101	465	685	2251
Aug-88	1259	565	542	2366
Sep-88	955	414	453	1822
Cumulative Production	36328	52049	38995	127372

APPENDIX 6

CUMULATIVE PRODUCTION BY WELL

Estimated cumulative production through April, 1990.

Periodic barrel tests by well are not available for the period after September, 1988, so the subsequent well production history must be estimated. The early production history for each well was used to calculate the percentage of production the well contributed to overall lease production. This "early production history" is defined as the first month after the bubble point was surpassed in the "J" zone (May, 1986), through September, 1988. For leases developed after the bubble point was surpassed, the start date for the early production history is the first full month of production after all wells on the lease were producing.

Key

EP	Early Production (bbls)
WC	Well Contribution to Lease Production
LP	Actual Late Production for the Lease – 10/88 through 4/90 (bbls)
CLP	Calculated Late Production for the Well (bbls)
Cum	Calculated Cumulative Production for the Well Through 4/90 (bbls)

Early production period used for each lease

Bethell	7/86 – 9/88
Demuth	8/87 – 9/88
Pennington	5/86 – 9/88
Shuck	5/86 – 9/88
White	5/86 – 9/88

Well	EP	WC	LP	CLP	Cum
Bethell #3	3598	4.2%		956	4554
Bethell #4	46009	54.4%		12386	74015
Bethell #5	34985	41.4%		9426	47760
Lease Total	84592	100.0%	22768		126329
Demuth #1	16286	47.7%		6419	44512
Demuth #2	8680	25.4%		3418	12098
Demuth #3	7816	22.9%		3082	24896
Demuth #4	1351	4.0%		538	2600
Lease Total	34133	100.0%	13457		84106
Pennington #1	8962	70.0%		3102	20304
Pennington #2	3834	30.0%		1329	6257
Lease Total	12796	100.0%	4431		26561
Shuck #1	13749	19.3%		2226	28138
Shuck #2	20340	28.5%		3287	33599
Shuck #3	37159	52.2%		6021	47474
Shuck #4	0	0.0%		0	859
Lease Total	71248	100.0%	11534		110070
White #2	32864	28.9%		5909	42237
White #4	44978	39.6%		8096	60145
White #5	35705	31.5%		6440	45435
Lease Total	113547	100.0%	20445		147817

APPENDIX 7

PRODUCTION IN THE PEN FIELD REGION

The Pen Field is part of a local trend of oil fields that produce only from the Toronto Formation and the Lansing-Kansas City groups (Fig. 114). This trend of fields occurs in an area of low-relief structures (Fig. 115).

Field	IWD	Wells	Productive Intervals	1989 Production (bbls)	Cumulative Production (bbls)
Houston	8/47	2	LKC "A", "F"	0	19,516
Houston S & Springbird (coalesced)	7/81	17	TRT, LKC "A", "H", "I", "J", "L"	61,212	348,691
Mt. Vernon N	4/63	3	LKC "A", "E", "J"	325	5,743
Mt. Vernon NW	5/84	1	TRT, LKC "A"	0	1,358
Pen	5/85	17	LKC "D", "I", "J", "K", "L"	47,597	529,138

IWD = initial withdrawal date
Wells = total wells in the field
Cumulative production through 6/90

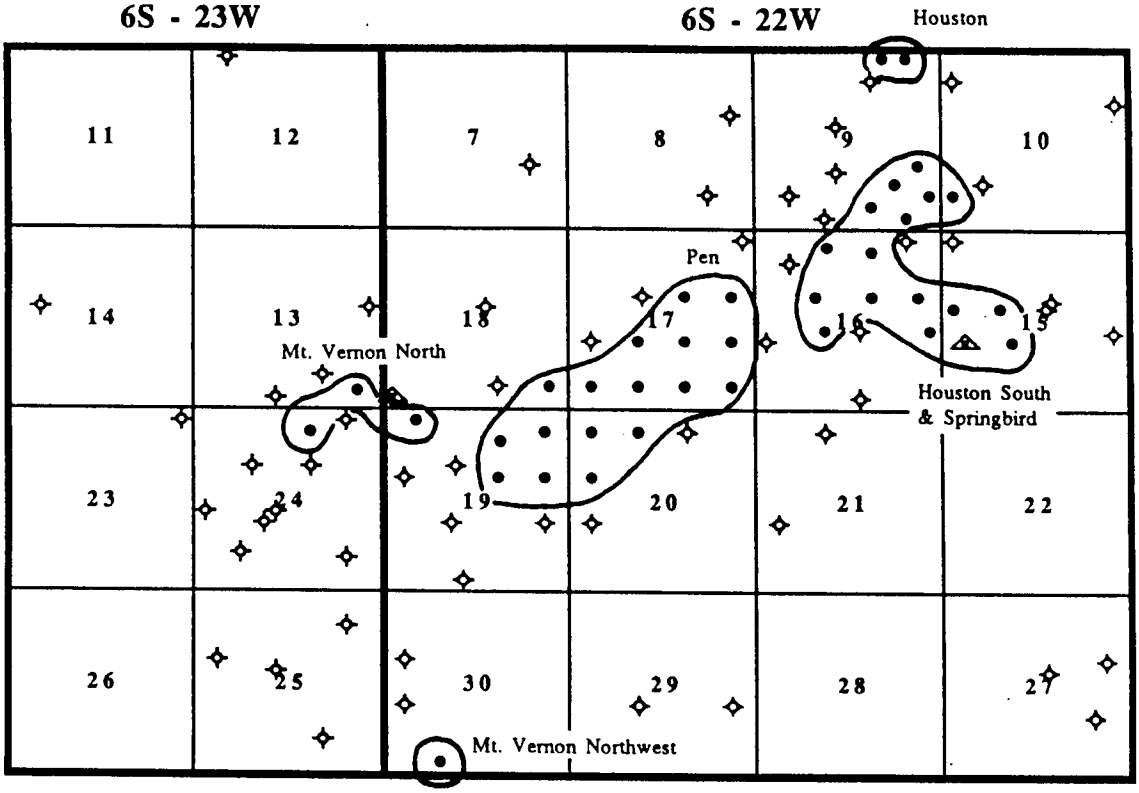

Figure 114. Map of oil fields in the Pen Field region.

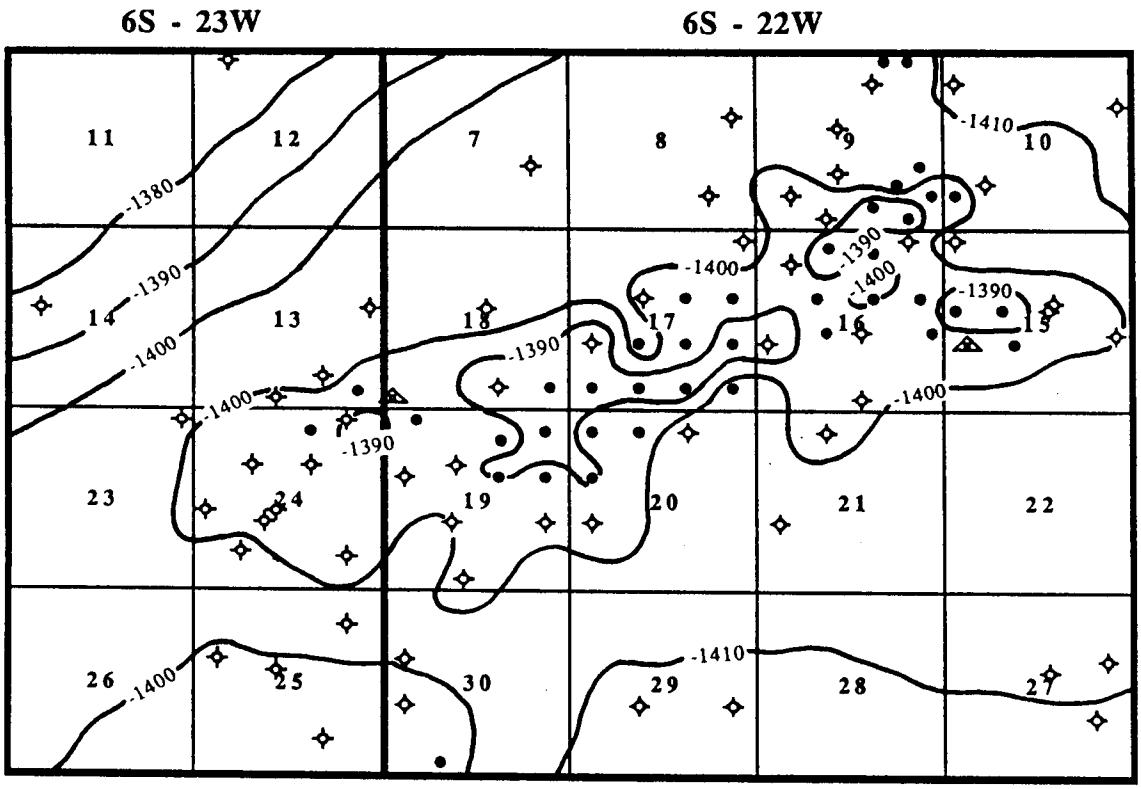

Figure 115. Structure map of the top of the "J" upper carbonate unit in the Pen Field region. (Contour interval = 10 feet. All depths in feet below datum of mean sea level.)

APPENDIX 8

FLUID INCLUSION SAMPLE PREPARATION

Billets were hand polished to avoid frictional heating, and then affixed to microscope slides using cold-mounting techniques. The thin section was then hand polished to a thickness of approximately 150 micrometers.

Fluid inclusion petrography was performed on whole sections, but microthermometry was performed on small chips to preserve the rest of the sample for later study. The area containing the population of interest was cut from the thin section using a slow-cut diamond saw. Heating runs to determine the homogenization temperatures of the inclusions were performed first.

As an inclusion is cooled, the fluid contracts and may result in an internal "negative pressure". If no vapor bubble is present during freezing runs, the negative pressure may lead to metastable superheated ice (Roedder, 1967). This results in erroneously high melting temperature of ice measurements.

Consequently, all inclusions that originally contained only a single liquid phase were heated to stretch the inclusions sufficiently to ensure a vapor bubble would be present during final melting of ice in freezing runs. These chips were slowly heated to a target temperature, and then sustained at that

temperature for two minutes. The chip was then cooled to room temperature. The process was repeated with increasingly higher target temperatures until vapor bubbles were observed at room temperature for all inclusions of interest. The maximum required target temperature for any sample chip was 167° C.

APPENDIX 9

CALCULATING FLUID INCLUSION SALINITY FROM THE FREEZING POINT DEPRESSION

The liquidus for ice in the NaCl-H_2O system has been determined experimentally by Potter, et al. (1978). The liquidus line represents the freezing point depression of water with the addition of NaCl. Using a linear least-squares regression they derived the following equation to calculate weight percent NaCl in solution:

$$W_S = 0.00 + 1.76958(D) - 0.042384(D)^2 + 0.00052778(D)^3$$

where, W_S = weight percent NaCl in solution

D = freezing point depression in degrees centigrade

APPENDIX 10

CALCULATING STATIC RESERVOIR PRESSURE FROM DRILLSTEM TEST MEASUREMENTS

Static reservoir pressure is herein defined as the pressure that exists in the vicinity of the well-bore. For drillstem tests, "in the vicinity" means within the radius of investigation of the test.

A "Horner plot" is the preferred method to extrapolate shut-in buildup pressures to static reservoir conditions (Reid, 1986). To construct a Horner plot, shut-in pressure is plotted versus the logarithm of the "dimensionless time function". The later time values should plot as a straight line. The extrapolation of this line to infinite shut-in time (logarithm of dimensionless time = 0.0) yields the static reservoir pressure. The first well completed in a reservoir provides a unique case where static reservoir pressure in the vicinity of the well-bore equals virgin reservoir pressure.

The dimensionless time function is given by the equation:

$$\Theta = \frac{T + \Delta t}{\Delta t}$$

where, Θ = Horner dimensionless time
T = cumulative flow time of the drillstem test (minutes)
Δt = time of pressure measurement since start of shut-in period (minutes)

APPENDIX 11

CALCULATING kh (MILLIDARCY-FEET) FROM DRILLSTEM TEST MEASUREMENTS

Kh values were calculated from the following equation (equation 1 in text):

$$kh = \frac{162.6\, q\, B\, \mu}{m} \qquad \text{Equation 1.}$$

where, k = permeability, millidarcys
h = net reservoir thickness, feet
q = production rate, stock tank barrels per day
B = formation volume factor, reservoir barrels per stock tank barrel
μ = viscosity, centipoise
m = slope of pressure build-up plot, psi per cycle

The values utilized for each well are shown in the following calculations:

Bethell #5 $kh = \frac{(162.6)\,(409.55)\,(1.0)\,(3.0)}{28} = 7135$ md-ft

Demuth #2 $kh = \frac{(162.6)\,(2.04)\,(1.0)\,(3.5)}{385} = 3.0$ md-ft

Demuth #3 $kh = \frac{(162.6)\,(43.55)\,(1.0)\,(1.5)}{50} = 212$ md-ft

Demuth #4 $kh = \frac{(162.6)\,(41.46)\,(1.0)\,(3.0)}{87} = 232$ md-ft

Jacobs #1 $kh = \frac{(162.6)\,(4.08)\,(1.0)\,(2.5)}{82} = 20.2$ md-ft

Rogers #2 $kh = \frac{(162.6)\,(118.39)\,(1.0)\,(1.0)}{977} = 19.7$ md-ft

Shuck #1 $kh = \frac{(162.6)\,(45.63)\,(1.0)\,(2.5)}{263} = 70.5$ md-ft

White #2 $kh = \frac{(162.6)\,(269.11)\,(1.0)\,(3.0)}{15} = 8751$ md-ft

APPENDIX 12

CALCULATING kh (MILLIDARCY FEET) FROM INITIAL POTENTIAL

Kh values were calculated from the following equation (equation 2 in text):

$$kh = \frac{141.2\ q\mu \ln (re / rw)}{(Pe - Pw)} \qquad \text{Equation 2.}$$

where, k = permeability, millidarcys
h = net reservoir thickness, feet
q = production rate, stock tank barrels per day
μ = viscosity, centipoise
re = radius of external boundary, (units consistent with rw)
rw = radius of well bore, (units consistent with re)
Pe = pressure at external boundary, psi
Pw = pressure at well bore, psi

The following values were assumed to be constant across the field:

μ = 3.0 centipoise
re = 660 feet (radial drainage - 40 acre spacing)
rw = .33 feet
Pw = 20 psi

Because reservoir pressures were not available for most wells, pressures at the external boundary (Pe) were estimated from the pressure decline for the main pay, the alpha grainstone subunit of the "J" upper carbonate unit (Fig. 80). Cumulative field production on the completion date of a given well was utilized in the correlation equation derived in Figure 80. The calculated pressure was then used as the best estimate of Pe.

APPENDIX 13

CALCULATING WATER SATURATION FROM LOG MEASUREMENTS USING THE ARCHIE EQUATION

Water saturation is most commonly calculated using the Archie equation (Asquith and Gibson, 1982, p. 2):

$$S_w = \left(\frac{F \times R_w}{R_t}\right)^{1/n}$$

where, S_w = water saturation of uninvaded zone, proportional
F = formation factor
R_w = formation water resistivity, ohm-meters
R_t = formation resistivity of uninvaded zone, ohm-meters
n = saturation exponent

Rw values for each zone were as follows:

"D" Zone = .08 ohm-meters
"I" Zone = .08 ohm-meters
"J" Zone = .08 ohm-meters
"K" Zone = .10 ohm-meters

These values were temperature corrected from measurements of formation water recovered on drillstem tests.

The saturation exponent (n) was assumed to be equal to 2.0, the value generally used for carbonates (Asquith and Gibson, 1982, p. 5).

The most commonly used expression for the formation factor in carbonate rocks is given by the following equation (Asquith and Gibson, 1982, p. 5):

$$F = \frac{1}{\phi^2}$$

where, F = formation factor
ϕ = porosity, proportional

APPENDIX 14

RESERVOIR VOLUME (POROSITY-FEET) MAPS FOR EACH RESERVOIR INTERVAL

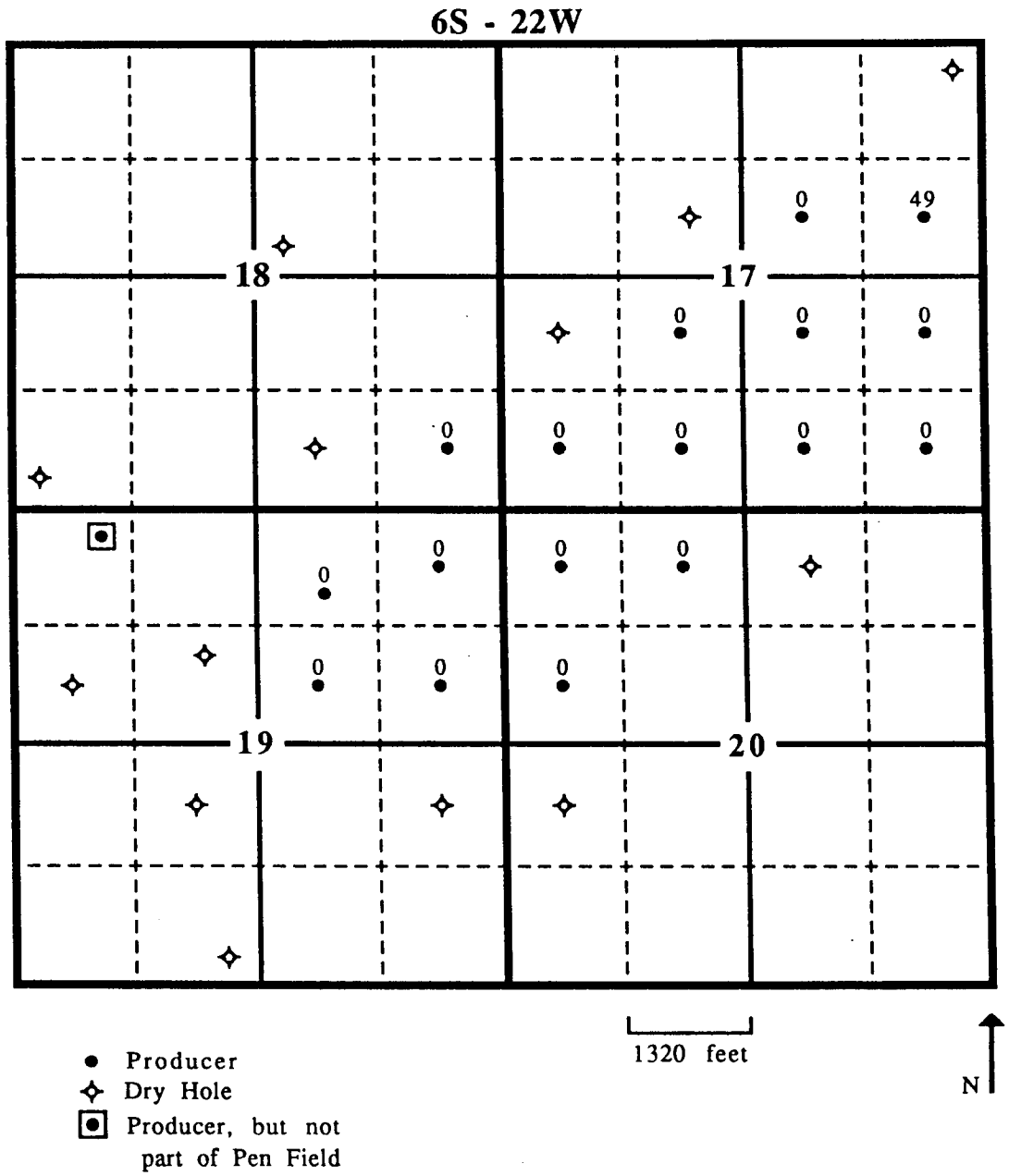

Figure 116. "D" zone reservoir volume map (porosity-feet, values in percent-ft) for all wells completed in this interval.

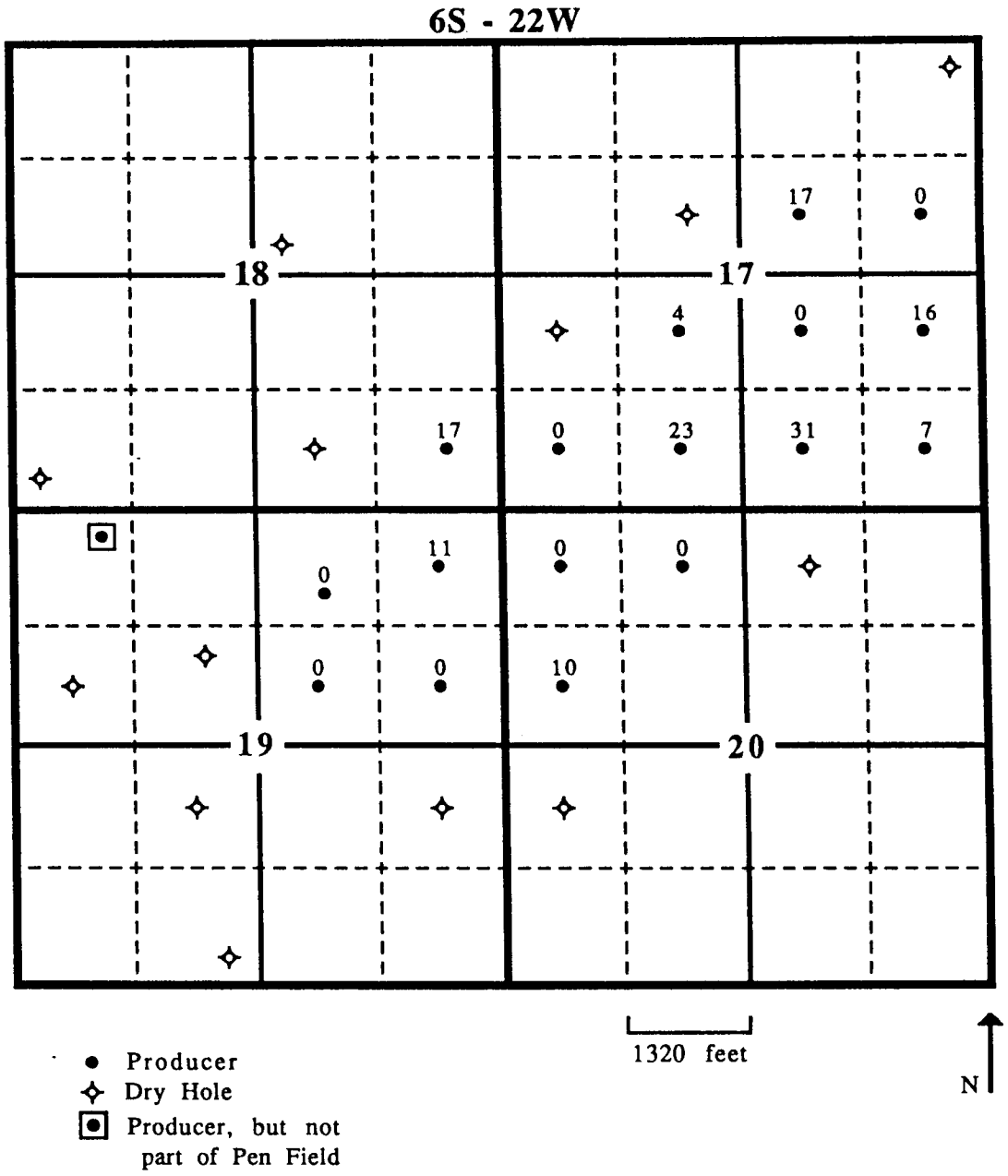

Figure 117. "I" zone reservoir volume map (porosity-feet, values in percent-ft) for all wells completed in this interval.

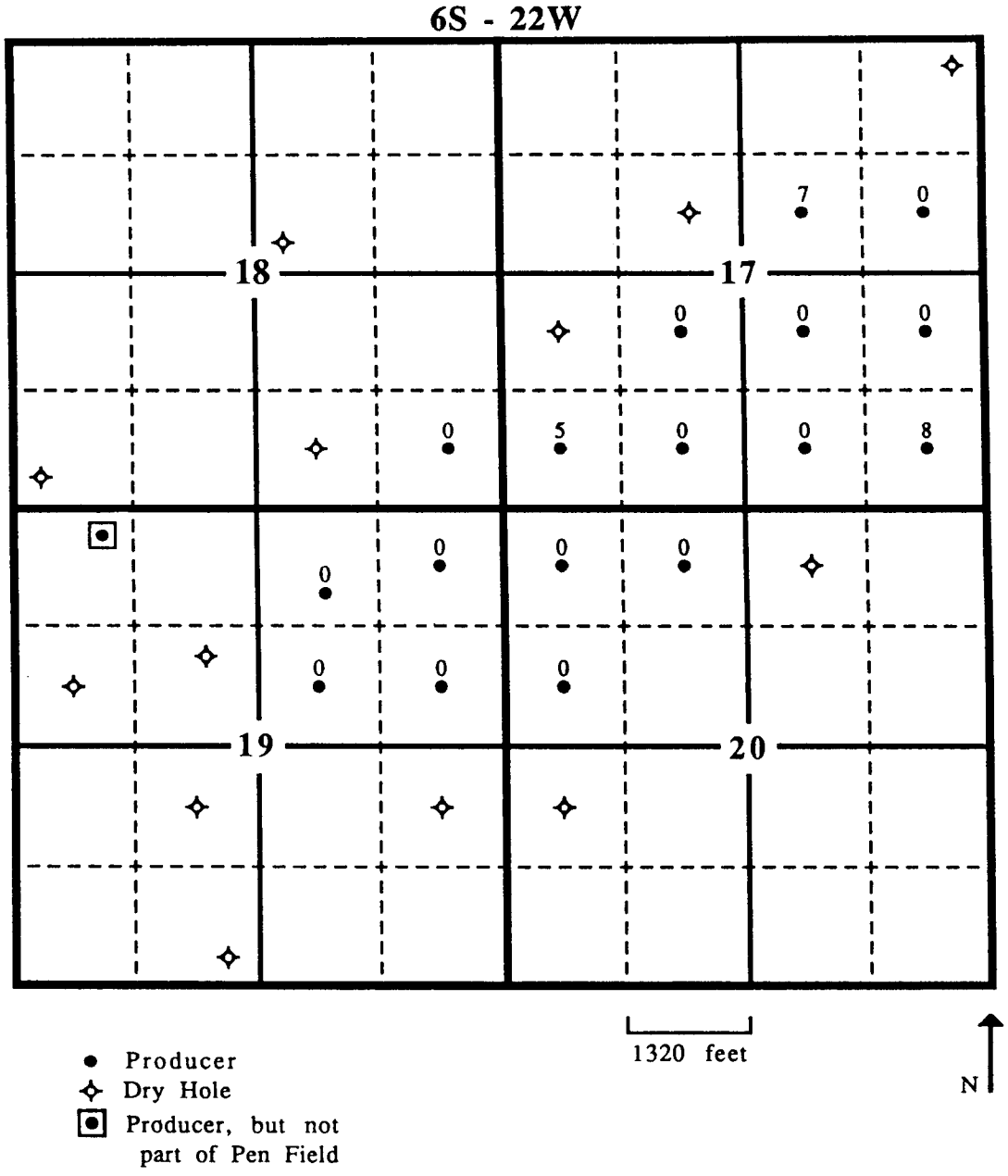

Figure 118. "J" cap subunit reservoir volume map (porosity-feet, values in percent-ft) for all wells completed in this interval.

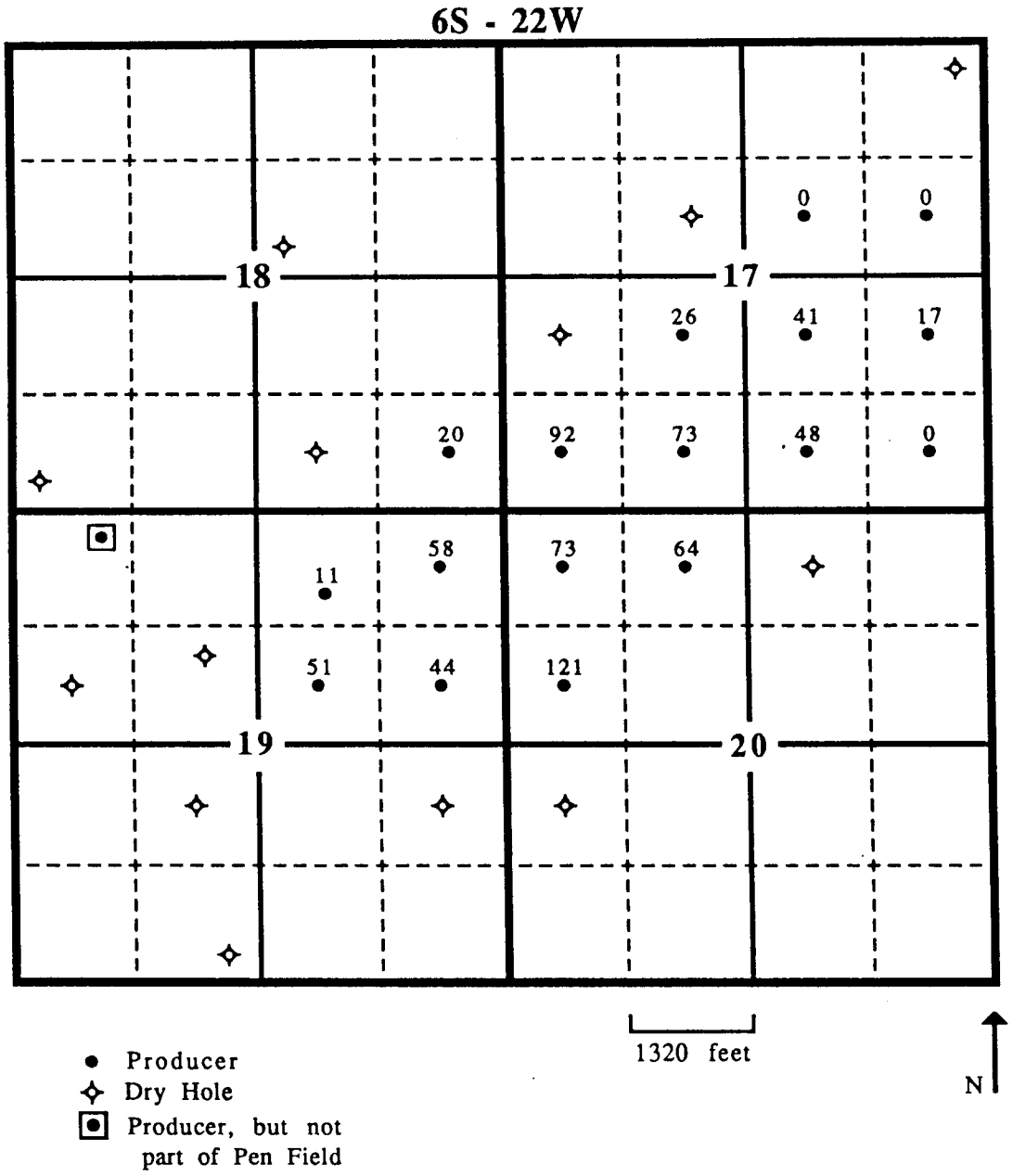

Figure 119. "J" alpha grainstone reservoir volume map (porosity-feet, values in percent-ft) for all wells completed in this interval.

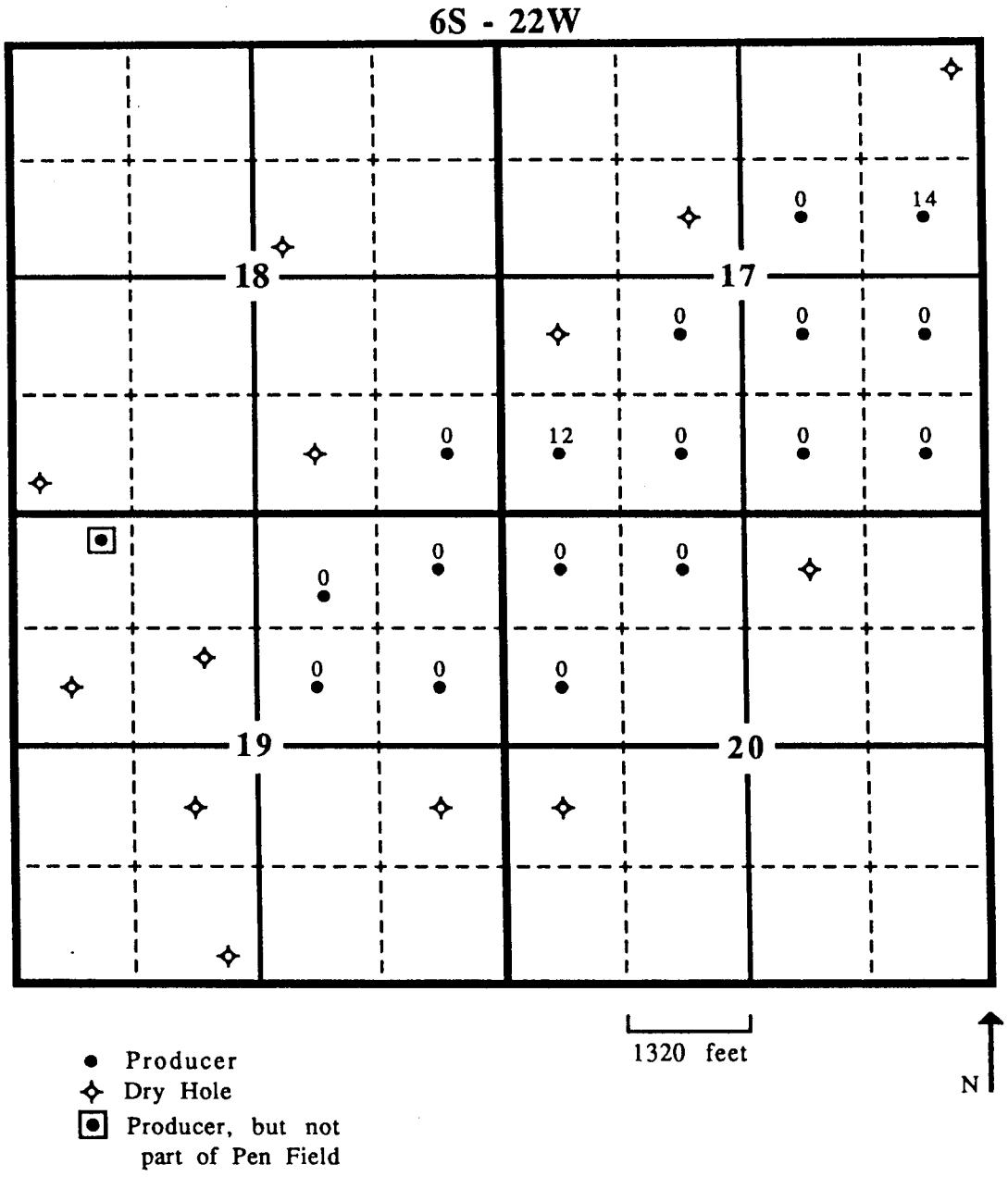

Figure 120. "J" beta grainstone-packstone and beta micrite-rich subunits reservoir volume map (porosity-feet, values in percent-ft) for all wells completed in this interval.

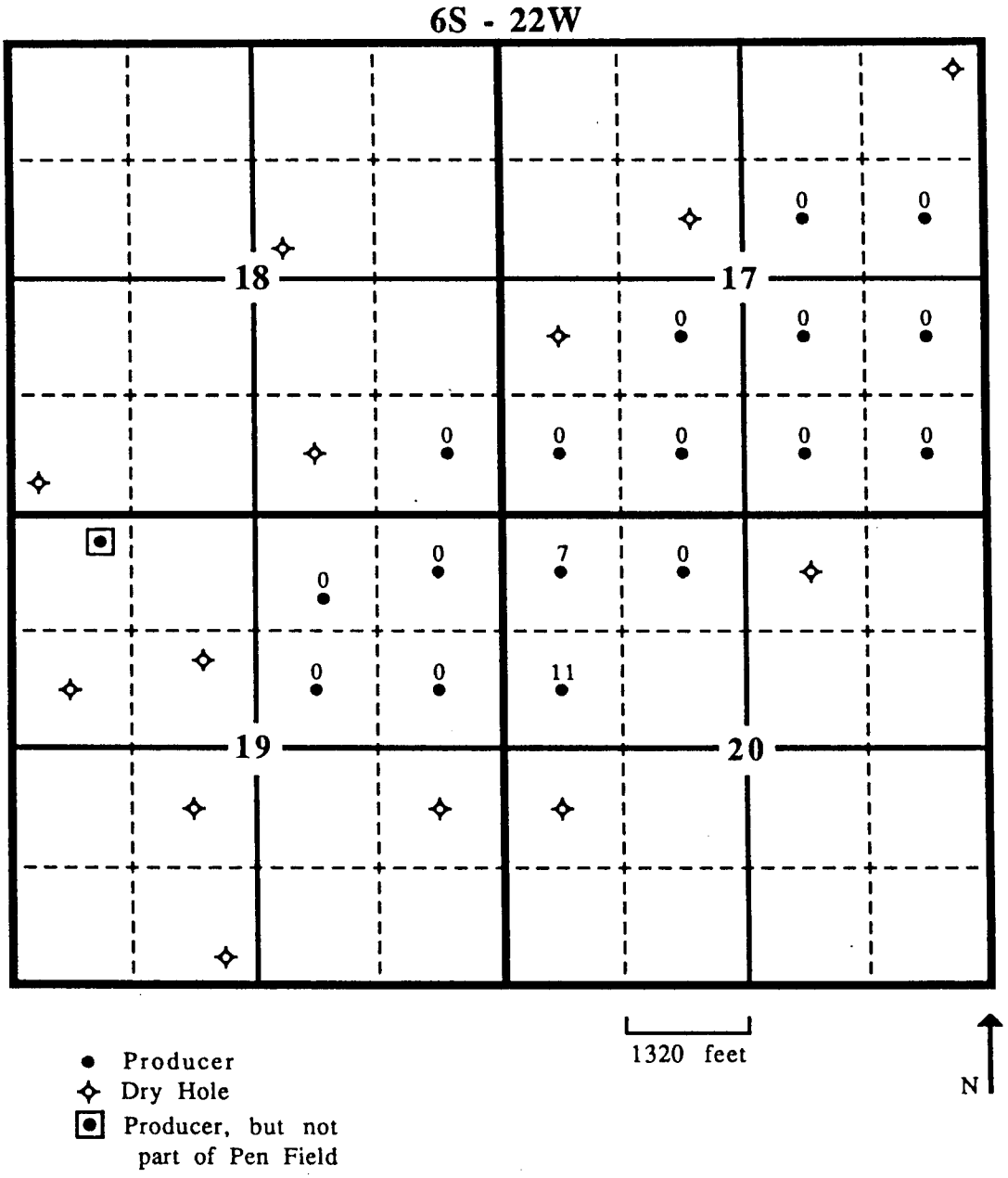

Figure 121. "K" capping carbonate subunit reservoir volume map (porosity-feet, values in percent-ft) for all wells completed in this interval.

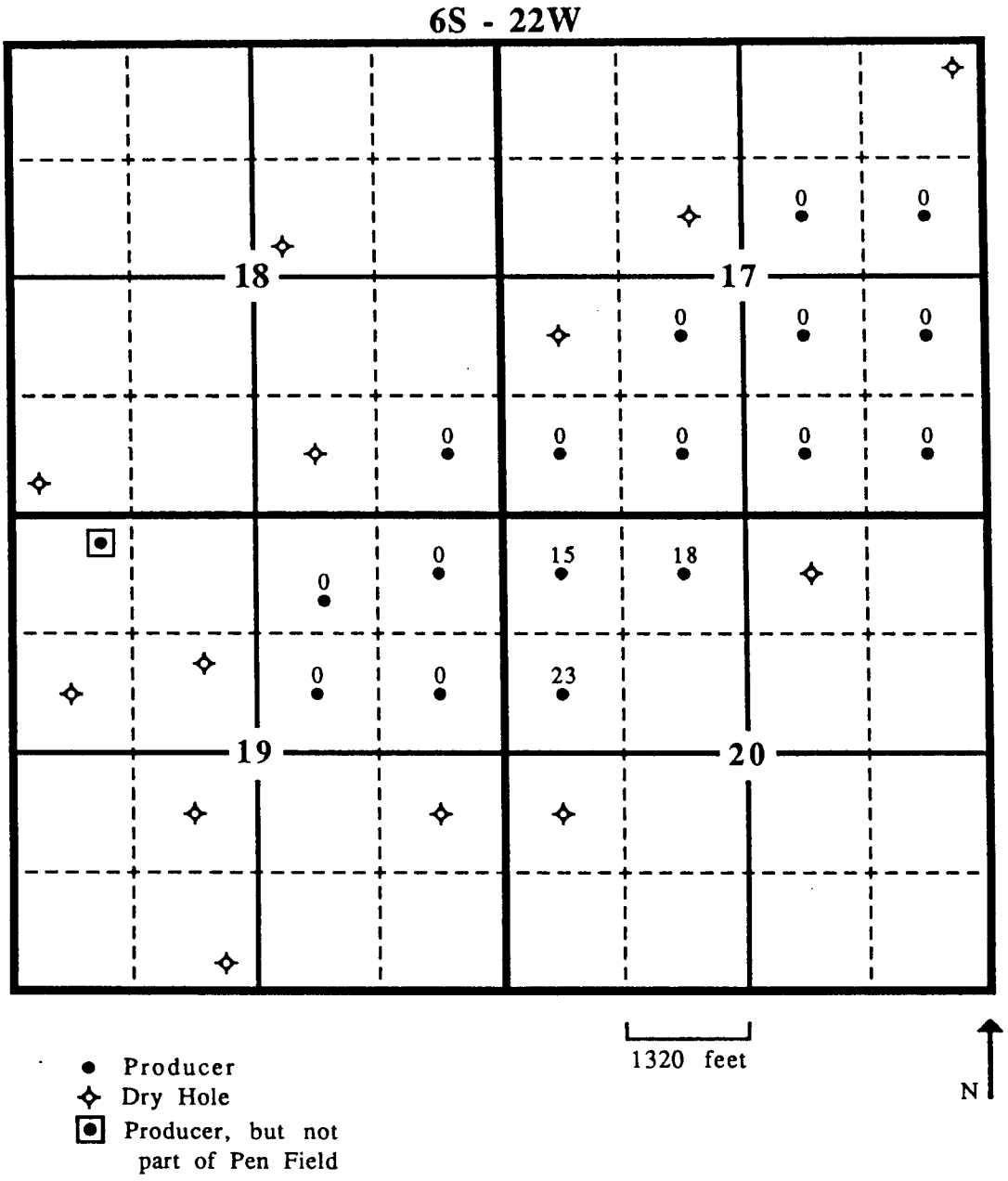

Figure 122. "K" basal carbonate subunit reservoir volume map (porosity-feet, values in percent-ft) for all wells completed in this interval.

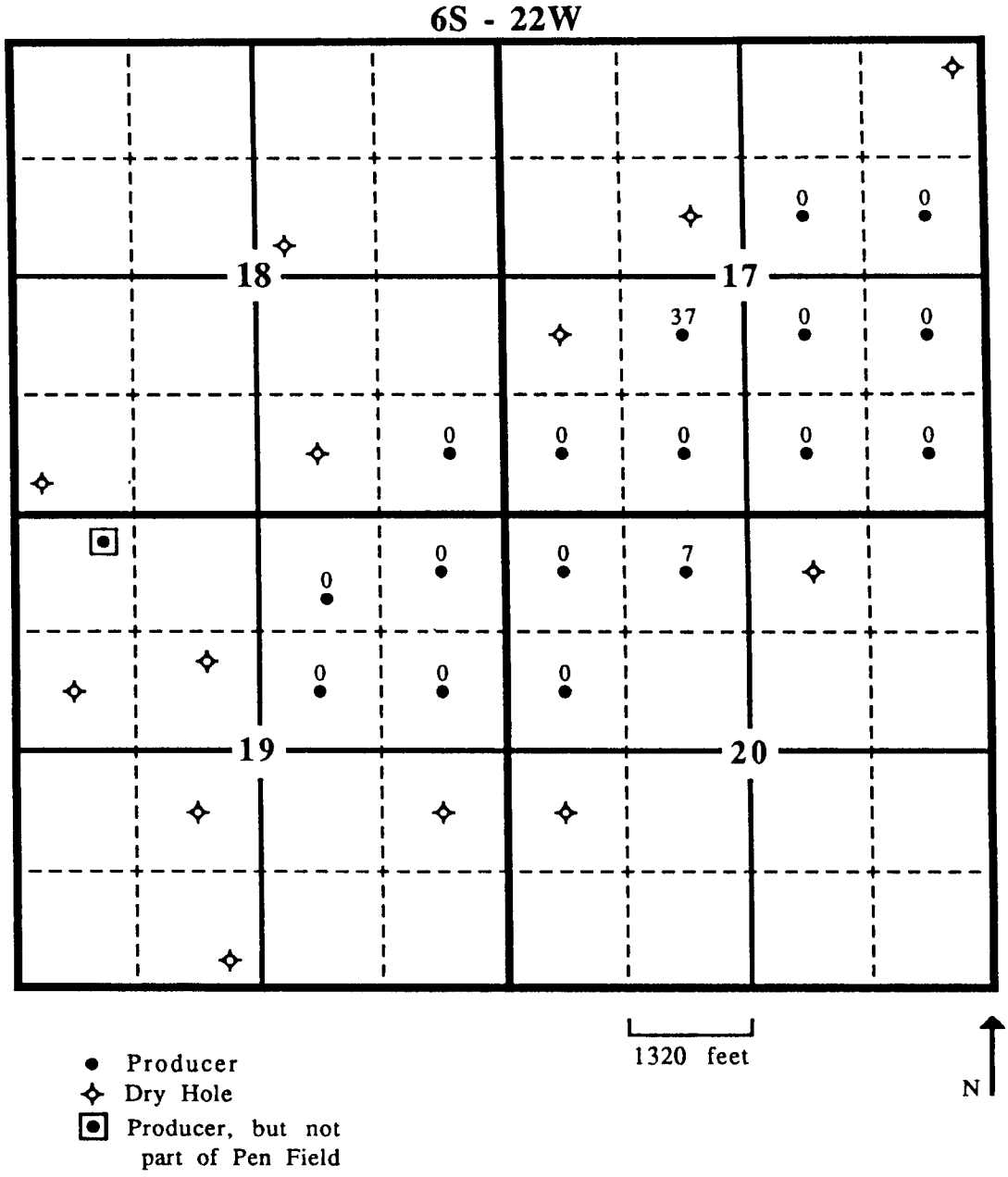

Figure 123. "L" zone reservoir volume map (porosity-feet, values in percent-ft) for all wells completed in this interval.

APPENDIX 15

SIMULATION GRID VALUES

Key

Cell numbers refer to the cells illustrated in Figure 111.

poro	porosity (%)
perm	permeability (md)
Sw	water saturation (%)

Depth cell abbreviations:

D	"D" Zone
(I S)	"I" Shale Unit
I	"I" Carbonate Unit
(J US)	"J" Upper Shale Unit
J c	"J" Upper Carbonate Unit (cap subunit)
(i.c.)	impermeable carbonate
J ag	"J" Upper Carbonate Unit (alpha grainstone subunit)
J b	"J" Upper Carbonate Unit (beta micrite-rich and beta grainstone-packstone subunits)
(K US)	"K" Upper Shale Unit
K cc	"K" Upper Carbonate Unit (capping carbonate subunit)
(K s)	"K" Upper Carbonate Unit (shale subunit)
K bc	"K" Upper Carbonate Unit (basal carbonate subunit)
(L US)	"L" Upper Shale Unit
L	"L" Upper Carbonate Unit

Cell designations in parentheses represent impermeable strata that separate the reservoir intervals. In some cases the designated impermeable unit is a simplification, for example, the "I" Shale Unit is just one of several impermeable layers that separate the "D" Zone and "I" Carbonate Unit reservoir intervals.

Cell values in boxes (e.g. parts of column 29) represent values that were removed from reservoir calculations as lost drainable pore volume in the "J" alpha grainstone subunit (Fig. 109).

Cell	1			2			3			4		
	poro	perm	Sw	poro	perm	Sw	poro	perm	Sw	poro	perm	Sw
D	0.0	0	0	0.0	0	0	0.0	0	0	0.0	0	0
D	0.0	0	0	0.0	0	0	0.0	0	0	0.0	0	0
D	0.0	0	0	0.0	0	0	0.0	0	0	0.0	0	0
D	0.0	0	0	0.0	0	0	0.0	0	0	0.0	0	0
(I S)	–	–	–	–	–	–	–	–	–	–	–	–
I	0.0	0	0	0.0	0	0	0.0	0	0	5.5	3	40
I	0.0	0	0	0.0	0	0	0.0	0	0	0.0	0	0
I	0.0	0	0	0.0	0	0	0.0	0	0	0.0	0	0
(J US)	–	–	–	–	–	–	–	–	–	–	–	–
J c	0.0	0	0	0.0	0	0	0.0	0	0	0.0	0	0
(i.c.)	–	–	–	–	–	–	–	–	–	–	–	–
J ag	0.0	0	0	0.0	0	0	0.0	0	0	0.0	0	0
J ag	0.0	0	0	0.0	0	0	0.0	0	0	0.0	0	0
J ag	0.0	0	0	0.0	0	0	0.0	0	0	0.0	0	0
J ag	0.0	0	0	0.0	0	0	0.0	0	0	0.0	0	0
J ag	0.0	0	0	0.0	0	0	0.0	0	0	0.0	0	0
J ag	0.0	0	0	0.0	0	0	0.0	0	0	0.0	0	0
(i.c.)	–	–	–	–	–	–	–	–	–	–	–	–
J b	0.0	0	0	0.0	0	0	0.0	0	0	0.0	0	0
J b	0.0	0	0	0.0	0	0	0.0	0	0	0.0	0	0
(K US)	–	–	–	–	–	–	–	–	–	–	–	–
K cc	0.0	0	0	0.0	0	0	0.0	0	0	0.0	0	0
(K s)	–	–	–	–	–	–	–	–	–	–	–	–
K bc	0.0	0	0	0.0	0	0	0.0	0	0	0.0	0	0
K bc	0.0	0	0	0.0	0	0	0.0	0	0	0.0	0	0
K bc	0.0	0	0	0.0	0	0	0.0	0	0	0.0	0	0
(L US)	–	–	–	–	–	–	–	–	–	–	–	–
L	5.0	2	63	8.0	11	48	11.0	53	41	8.5	15	46
L	0.0	0	0	8.0	11	48	9.0	19	45	8.0	11	48
L	0.0	0	0	0.0	0	0	7.0	7	51	0.0	0	0
L	0.0	0	0	0.0	0	0	0.0	0	0	0.0	0	0
L	0.0	0	0	0.0	0	0	0.0	0	0	0.0	0	0
L	0.0	0	0	0.0	0	0	0.0	0	0	0.0	0	0

Cell		5			6			7			8	
	poro	perm	Sw	poro	perm	Sw	poro	perm	Sw	poro	perm	Sw
D	0.0	0	0	0.0	0	0	0.0	0	0	8.0	8	56
D	0.0	0	0	0.0	0	0	0.0	0	0	9.0	13	51
D	0.0	0	0	0.0	0	0	0.0	0	0	0.0	0	0
D	0.0	0	0	0.0	0	0	0.0	0	0	0.0	0	0
(I S)	–	–	–	–	–	–	–	–	–	–	–	–
I	6.0	4	37	6.5	6	33	6.0	4	37	0.0	0	0
I	0.0	0	0	0.0	0	0	0.0	0	0	0.0	0	0
I	0.0	0	0	0.0	0	0	0.0	0	0	0.0	0	0
(J US)	–	–	–	–	–	–	–	–	–	–	–	–
J c	0.0	0	0	7.0	9	30	0.0	0	0	0.0	0	0
(i.c.)	–	–	–	–	–	–	–	–	–	–	–	–
J ag	0.0	0	0	0.0	0	0	0.0	0	0	0.0	0	0
J ag	0.0	0	0	0.0	0	0	0.0	0	0	0.0	0	0
J ag	0.0	0	0	0.0	0	0	0.0	0	0	0.0	0	0
J ag	0.0	0	0	0.0	0	0	0.0	0	0	0.0	0	0
J ag	0.0	0	0	0.0	0	0	0.0	0	0	0.0	0	0
J ag	0.0	0	0	0.0	0	0	0.0	0	0	0.0	0	0
(i.c.)	–	–	–	–	–	–	–	–	–	–	–	–
J b	0.0	0	0	0.0	0	0	0.0	0	0	0.0	0	0
J b	0.0	0	0	0.0	0	0	0.0	0	0	0.0	0	0
(K US)	–	–	–	–	–	–	–	–	–	–	–	–
K cc	0.0	0	0	0.0	0	0	0.0	0	0	0.0	0	0
(K s)	–	–	–	–	–	–	–	–	–	–	–	–
K bc	0.0	0	0	0.0	0	0	0.0	0	0	0.0	0	0
K bc	0.0	0	0	0.0	0	0	0.0	0	0	0.0	0	0
K bc	0.0	0	0	0.0	0	0	0.0	0	0	0.0	0	0
(L US)	–	–	–	–	–	–	–	–	–	–	–	–
L	5.0	2	63	0.0	0	0	0.0	0	0	0.0	0	0
L	0.0	0	0	0.0	0	0	0.0	0	0	0.0	0	0
L	0.0	0	0	0.0	0	0	0.0	0	0	0.0	0	0
L	0.0	0	0	0.0	0	0	0.0	0	0	0.0	0	0
L	0.0	0	0	0.0	0	0	0.0	0	0	0.0	0	0
L	0.0	0	0	0.0	0	0	0.0	0	0	0.0	0	0

Cell	9			10			11			12		
	poro	perm	Sw	poro	perm	Sw	poro	perm	Sw	poro	perm	Sw
D	8.0	8	56	0.0	0	0	0.0	0	0	0.0	0	0
D	9.0	13	51	0.0	0	0	0.0	0	0	0.0	0	0
D	0.0	0	0	0.0	0	0	0.0	0	0	0.0	0	0
D	0.0	0	0	0.0	0	0	0.0	0	0	0.0	0	0
(I S)	–	–	–	–	–	–	–	–	–	–	–	–
I	0.0	0	0	0.0	0	0	5.0	2	45	6.0	4	37
I	0.0	0	0	0.0	0	0	0.0	0	0	0.0	0	0
I	0.0	0	0	0.0	0	0	0.0	0	0	0.0	0	0
(J US)	–	–	–	–	–	–	–	–	–	–	–	–
J c	0.0	0	0	0.0	0	0	0.0	0	0	0.0	0	0
(i.c.)	–	–	–	–	–	–	–	–	–	–	–	–
J ag	0.0	0	0	0.0	0	0	0.0	0	0	0.0	0	0
J ag	0.0	0	0	0.0	0	0	0.0	0	0	0.0	0	0
J ag	0.0	0	0	0.0	0	0	0.0	0	0	0.0	0	0
J ag	0.0	0	0	0.0	0	0	0.0	0	0	0.0	0	0
J ag	0.0	0	0	0.0	0	0	0.0	0	0	0.0	0	0
J ag	0.0	0	0	0.0	0	0	0.0	0	0	0.0	0	0
(i.c.)	–	–	–	–	–	–	–	–	–	–	–	–
J b	0.0	0	0	0.0	0	0	0.0	0	0	0.0	0	0
J b	0.0	0	0	0.0	0	0	0.0	0	0	0.0	0	0
(K US)	–	–	–	–	–	–	–	–	–	–	–	–
K cc	0.0	0	0	0.0	0	0	0.0	0	0	0.0	0	0
(K s)	–	–	–	–	–	–	–	–	–	–	–	–
K bc	0.0	0	0	0.0	0	0	0.0	0	0	0.0	0	0
K bc	0.0	0	0	0.0	0	0	0.0	0	0	0.0	0	0
K bc	0.0	0	0	0.0	0	0	0.0	0	0	0.0	0	0
(L US)	–	–	–	–	–	–	–	–	–	–	–	–
L	0.0	0	0	7.0	7	51	11.5	69	40	16.0	684	35
L	0.0	0	0	0.0	0	0	9.5	25	44	14.0	246	37
L	0.0	0	0	0.0	0	0	7.5	9	49	8.0	11	48
L	0.0	0	0	0.0	0	0	0.0	0	0	5.5	3	59
L	0.0	0	0	0.0	0	0	0.0	0	0	7.0	7	51
L	0.0	0	0	0.0	0	0	0.0	0	0	0.0	0	0

Cell	13			14			15			16		
	poro	perm	Sw	poro	perm	Sw	poro	perm	Sw	poro	perm	Sw
D	0.0	0	0	0.0	0	0	0.0	0	0	0.0	0	0
D	0.0	0	0	0.0	0	0	0.0	0	0	0.0	0	0
D	0.0	0	0	0.0	0	0	0.0	0	0	0.0	0	0
D	0.0	0	0	0.0	0	0	0.0	0	0	0.0	0	0
(I S)	–	–	–	–	–	–	–	–	–	–	–	–
I	6.5	6	33	6.5	6	33	7.0	9	30	6.5	6	33
I	6.0	4	37	6.5	6	33	7.5	13	28	6.0	4	37
I	0.0	0	0	0.0	0	0	0.0	0	0	0.0	0	0
(J US)	–	–	–	–	–	–	–	–	–	–	–	–
J c	0.0	0	0	0.0	0	0	7.0	9	30	0.0	0	0
(i.c.)	–	–	–	–	–	–	–	–	–	–	–	–
J ag	0.0	0	0	0.0	0	0	0.0	0	0	0.0	0	0
J ag	0.0	0	0	0.0	0	0	0.0	0	0	0.0	0	0
J ag	0.0	0	0	0.0	0	0	0.0	0	0	0.0	0	0
J ag	0.0	0	0	0.0	0	0	0.0	0	0	0.0	0	0
J ag	0.0	0	0	0.0	0	0	0.0	0	0	0.0	0	0
J ag	0.0	0	0	0.0	0	0	0.0	0	0	0.0	0	0
(i.c.)	–	–	–	–	–	–	–	–	–	–	–	–
J b	0.0	0	0	0.0	0	0	0.0	0	0	0.0	0	0
J b	0.0	0	0	0.0	0	0	0.0	0	0	0.0	0	0
(K US)	–	–	–	–	–	–	–	–	–	–	–	–
K cc	0.0	0	0	0.0	0	0	0.0	0	0	0.0	0	0
(K s)	–	–	–	–	–	–	–	–	–	–	–	–
K bc	0.0	0	0	0.0	0	0	0.0	0	0	0.0	0	0
K bc	0.0	0	0	0.0	0	0	0.0	0	0	0.0	0	0
K bc	0.0	0	0	0.0	0	0	0.0	0	0	0.0	0	0
(L US)	–	–	–	–	–	–	–	–	–	–	–	–
L	13.0	148	38	8.0	11	48	0.0	0	0	0.0	0	0
L	11.0	53	41	8.0	11	48	0.0	0	0	0.0	0	0
L	7.5	9	49	0.0	0	0	0.0	0	0	0.0	0	0
L	6.0	4	56	0.0	0	0	0.0	0	0	0.0	0	0
L	0.0	0	0	0.0	0	0	0.0	0	0	0.0	0	0
L	0.0	0	0	0.0	0	0	0.0	0	0	0.0	0	0

Cell	17			18			19			20		
	poro	perm	Sw	poro	perm	Sw	poro	perm	Sw	poro	perm	Sw
D	13.5	93	37	8.0	8	56	0.0	0	0	0.0	0	0
D	15.0	180	35	9.0	13	51	0.0	0	0	0.0	0	0
D	12.0	48	41	0.0	0	0	0.0	0	0	0.0	0	0
D	8.0	8	56	0.0	0	0	0.0	0	0	0.0	0	0
(I S)	–	–	–	–	–	–	–	–	–	–	–	–
I	0.0	0	0	0.0	0	0	0.0	0	0	0.0	0	0
I	0.0	0	0	0.0	0	0	0.0	0	0	0.0	0	0
I	0.0	0	0	0.0	0	0	0.0	0	0	0.0	0	0
(J US)	–	–	–	–	–	–	–	–	–	–	–	–
J c	0.0	0	0	0.0	0	0	0.0	0	0	0.0	0	0
(i.c.)	–	–	–	–	–	–	–	–	–	–	–	–
J ag	0.0	0	0	0.0	0	0	0.0	0	0	0.0	0	0
J ag	0.0	0	0	0.0	0	0	0.0	0	0	0.0	0	0
J ag	0.0	0	0	0.0	0	0	0.0	0	0	0.0	0	0
J ag	0.0	0	0	0.0	0	0	0.0	0	0	0.0	0	0
J ag	0.0	0	0	0.0	0	0	0.0	0	0	0.0	0	0
J ag	0.0	0	0	0.0	0	0	0.0	0	0	0.0	0	0
(i.c.)	–	–	–	–	–	–	–	–	–	–	–	–
J b	8.0	19	26	0.0	0	0	0.0	0	0	0.0	0	0
J b	0.0	0	0	0.0	0	0	0.0	0	0	0.0	0	0
(K US)	–	–	–	–	–	–	–	–	–	–	–	–
K cc	0.0	0	0	0.0	0	0	0.0	0	0	0.0	0	0
(K s)	–	–	–	–	–	–	–	–	–	–	–	–
K bc	0.0	0	0	0.0	0	0	0.0	0	0	0.0	0	0
K bc	0.0	0	0	0.0	0	0	0.0	0	0	0.0	0	0
K bc	0.0	0	0	0.0	0	0	0.0	0	0	0.0	0	0
(L US)	–	–	–	–	–	–	–	–	–	–	–	–
L	0.0	0	0	0.0	0	0	8.0	11	48	11.0	53	41
L	0.0	0	0	0.0	0	0	8.0	11	48	11.0	53	41
L	0.0	0	0	0.0	0	0	0.0	0	0	8.5	15	46
L	0.0	0	0	0.0	0	0	0.0	0	0	6.5	5	53
L	0.0	0	0	0.0	0	0	0.0	0	0	0.0	0	0
L	0.0	0	0	0.0	0	0	0.0	0	0	0.0	0	0

Cell	21			22			23			24		
	poro	perm	Sw	poro	perm	Sw	poro	perm	Sw	poro	perm	Sw
D	0.0	0	0	0.0	0	0	0.0	0	0	0.0	0	0
D	0.0	0	0	0.0	0	0	0.0	0	0	0.0	0	0
D	0.0	0	0	0.0	0	0	0.0	0	0	0.0	0	0
D	0.0	0	0	0.0	0	0	0.0	0	0	0.0	0	0
(I S)	–	–	–	–	–	–	–	–	–	–	–	–
I	5.0	2	45	6.0	4	37	6.0	4	37	6.5	6	33
I	0.0	0	0	0.0	0	0	0.0	0	0	0.0	0	0
I	0.0	0	0	0.0	0	0	0.0	0	0	0.0	0	0
(J US)	–	–	–	–	–	–	–	–	–	–	–	–
J c	0.0	0	0	0.0	0	0	0.0	0	0	0.0	0	0
(i.c.)	–	–	–	–	–	–	–	–	–	–	–	–
J ag	0.0	0	0	0.0	0	0	7.0	19	67	8.0	22	57
J ag	0.0	0	0	0.0	0	0	0.0	0	0	0.0	0	0
J ag	0.0	0	0	0.0	0	0	0.0	0	0	0.0	0	0
J ag	0.0	0	0	0.0	0	0	0.0	0	0	0.0	0	0
J ag	0.0	0	0	0.0	0	0	0.0	0	0	0.0	0	0
J ag	0.0	0	0	0.0	0	0	0.0	0	0	0.0	0	0
(i.c.)	–	–	–	–	–	–	–	–	–	–	–	–
J b	0.0	0	0	0.0	0	0	0.0	0	0	0.0	0	0
J b	0.0	0	0	0.0	0	0	0.0	0	0	0.0	0	0
(K US)	–	–	–	–	–	–	–	–	–	–	–	–
K cc	0.0	0	0	0.0	0	0	0.0	0	0	0.0	0	0
(K s)	–	–	–	–	–	–	–	–	–	–	–	–
K bc	0.0	0	0	0.0	0	0	0.0	0	0	0.0	0	0
K bc	0.0	0	0	0.0	0	0	0.0	0	0	0.0	0	0
K bc	0.0	0	0	0.0	0	0	0.0	0	0	0.0	0	0
(L US)	–	–	–	–	–	–	–	–	–	–	–	–
L	14.0	246	37	11.0	53	41	8.0	11	48	0.0	0	0
L	13.5	191	37	11.0	53	41	8.0	11	48	0.0	0	0
L	9.0	19	45	8.5	15	46	0.0	0	0	0.0	0	0
L	6.5	5	53	6.5	5	53	0.0	0	0	0.0	0	0
L	6.5	5	53	0.0	0	0	0.0	0	0	0.0	0	0
L	0.0	0	0	0.0	0	0	0.0	0	0	0.0	0	0

Cell	25			26			27			28		
	poro	perm	Sw	poro	perm	Sw	poro	perm	Sw	poro	perm	Sw
D	0.0	0	0	0.0	0	0	0.0	0	0	0.0	0	0
D	0.0	0	0	0.0	0	0	0.0	0	0	0.0	0	0
D	0.0	0	0	0.0	0	0	0.0	0	0	0.0	0	0
D	0.0	0	0	0.0	0	0	0.0	0	0	0.0	0	0
(I S)	–	–	–	–	–	–	–	–	–	–	–	–
I	6.0	4	37	0.0	0	0	0.0	0	0	0.0	0	0
I	0.0	0	0	0.0	0	0	0.0	0	0	0.0	0	0
I	0.0	0	0	0.0	0	0	0.0	0	0	0.0	0	0
(J US)	–	–	–	–	–	–	–	–	–	–	–	–
J c	0.0	0	0	0.0	0	0	0.0	0	0	0.0	0	0
(i.c.)	–	–	–	–	–	–	–	–	–	–	–	–
J ag	8.0	22	57	8.0	22	57	7.0	19	67	0.0	0	0
J ag	0.0	0	0	0.0	0	0	0.0	0	0	0.0	0	0
J ag	0.0	0	0	0.0	0	0	0.0	0	0	0.0	0	0
J ag	0.0	0	0	0.0	0	0	0.0	0	0	0.0	0	0
J ag	0.0	0	0	0.0	0	0	0.0	0	0	0.0	0	0
J ag	0.0	0	0	0.0	0	0	0.0	0	0	0.0	0	0
(i.c.)	–	–	–	–	–	–	–	–	–	–	–	–
J b	0.0	0	0	0.0	0	0	0.0	0	0	0.0	0	0
J b	0.0	0	0	0.0	0	0	0.0	0	0	0.0	0	0
(K US)	–	–	–	–	–	–	–	–	–	–	–	–
K cc	0.0	0	0	0.0	0	0	0.0	0	0	0.0	0	0
(K s)	–	–	–	–	–	–	–	–	–	–	–	–
K bc	0.0	0	0	0.0	0	0	0.0	0	0	0.0	0	0
K bc	0.0	0	0	0.0	0	0	0.0	0	0	0.0	0	0
K bc	0.0	0	0	0.0	0	0	0.0	0	0	0.0	0	0
(L US)	–	–	–	–	–	–	–	–	–	–	–	–
L	0.0	0	0	0.0	0	0	0.0	0	0	8.5	15	46
L	0.0	0	0	0.0	0	0	0.0	0	0	8.5	15	46
L	0.0	0	0	0.0	0	0	0.0	0	0	0.0	0	0
L	0.0	0	0	0.0	0	0	0.0	0	0	0.0	0	0
L	0.0	0	0	0.0	0	0	0.0	0	0	0.0	0	0
L	0.0	0	0	0.0	0	0	0.0	0	0	0.0	0	0

Cell	29			30			31			32		
	poro	perm	Sw	poro	perm	Sw	poro	perm	Sw	poro	perm	Sw
D	0.0	0	0	0.0	0	0	0.0	0	0	0.0	0	0
D	0.0	0	0	0.0	0	0	0.0	0	0	0.0	0	0
D	0.0	0	0	0.0	0	0	0.0	0	0	0.0	0	0
D	0.0	0	0	0.0	0	0	0.0	0	0	0.0	0	0
(I S)	–	–	–	–	–	–	–	–	–	–	–	–
I	0.0	0	0	0.0	0	0	0.0	0	0	0.0	0	0
I	0.0	0	0	0.0	0	0	0.0	0	0	0.0	0	0
I	0.0	0	0	0.0	0	0	0.0	0	0	0.0	0	0
(J US)	–	–	–	–	–	–	–	–	–	–	–	–
J c	0.0	0	0	0.0	0	0	0.0	0	0	0.0	0	0
(i.c.)	–	–	–	–	–	–	–	–	–	–	–	–
J ag	0.0	0	0	7.0	19	67	9.0	26	50	14.0	57	27
J ag	0.0	0	0	0.0	0	0	11.0	36	38	12.0	42	34
J ag	0.0	0	0	0.0	0	0	0.0	0	0	0.0	0	0
J ag	0.0	0	0	0.0	0	0	0.0	0	0	0.0	0	0
J ag	0.0	0	0	0.0	0	0	0.0	0	0	0.0	0	0
J ag	0.0	0	0	0.0	0	0	0.0	0	0	0.0	0	0
(i.c.)	–	–	–	–	–	–	–	–	–	–	–	–
J b	0.0	0	0	0.0	0	0	0.0	0	0	0.0	0	0
J b	0.0	0	0	0.0	0	0	0.0	0	0	0.0	0	0
(K US)	–	–	–	–	–	–	–	–	–	–	–	–
K cc	0.0	0	0	0.0	0	0	0.0	0	0	0.0	0	0
(K s)	–	–	–	–	–	–	–	–	–	–	–	–
K bc	0.0	0	0	0.0	0	0	0.0	0	0	0.0	0	0
K bc	0.0	0	0	0.0	0	0	0.0	0	0	0.0	0	0
K bc	0.0	0	0	0.0	0	0	0.0	0	0	0.0	0	0
(L US)	–	–	–	–	–	–	–	–	–	–	–	–
L	9.0	19	45	10.5	41	42	8.5	15	46	7.0	7	51
L	12.0	89	39	13.0	148	38	11.0	53	41	7.0	7	51
L	9.5	25	44	10.0	32	43	8.5	15	46	0.0	0	0
L	7.0	7	51	7.0	7	51	6.5	5	53	0.0	0	0
L	0.0	0	0	6.5	5	53	0.0	0	0	0.0	0	0
L	0.0	0	0	0.0	0	0	0.0	0	0	0.0	0	0

Cell		33			34			35			36	
	poro	perm	Sw	poro	perm	Sw	poro	perm	Sw	poro	perm	Sw
D	0.0	0	0	0.0	0	0	0.0	0	0	0.0	0	0
D	0.0	0	0	0.0	0	0	0.0	0	0	0.0	0	0
D	0.0	0	0	0.0	0	0	0.0	0	0	0.0	0	0
D	0.0	0	0	0.0	0	0	0.0	0	0	0.0	0	0
(I S)	–	–	–	–	–	–	–	–	–	–	–	–
I	0.0	0	0	0.0	0	0	5.0	2	45	6.0	4	37
I	0.0	0	0	0.0	0	0	0.0	0	0	0.0	0	0
I	0.0	0	0	0.0	0	0	0.0	0	0	0.0	0	0
(J US)	–	–	–	–	–	–	–	–	–	–	–	–
J c	0.0	0	0	0.0	0	0	0.0	0	0	0.0	0	0
(i.c.)	–	–	–	–	–	–	–	–	–	–	–	–
J ag	14.5	62	26	14.0	57	27	11.0	36	38	9.5	28	46
J ag	12.0	42	34	12.0	42	34	8.5	24	53	7.0	19	67
J ag	0.0	0	0	0.0	0	0	0.0	0	0	0.0	0	0
J ag	0.0	0	0	0.0	0	0	0.0	0	0	0.0	0	0
J ag	0.0	0	0	0.0	0	0	0.0	0	0	0.0	0	0
J ag	0.0	0	0	0.0	0	0	0.0	0	0	0.0	0	0
(i.c.)	–	–	–	–	–	–	–	–	–	–	–	–
J b	0.0	0	0	0.0	0	0	0.0	0	0	0.0	0	0
J b	0.0	0	0	0.0	0	0	0.0	0	0	0.0	0	0
(K US)	–	–	–	–	–	–	–	–	–	–	–	–
K cc	0.0	0	0	0.0	0	0	0.0	0	0	0.0	0	0
(K s)	–	–	–	–	–	–	–	–	–	–	–	–
K bc	0.0	0	0	0.0	0	0	0.0	0	0	0.0	0	0
K bc	0.0	0	0	0.0	0	0	0.0	0	0	0.0	0	0
K bc	0.0	0	0	0.0	0	0	0.0	0	0	0.0	0	0
(L US)	–	–	–	–	–	–	–	–	–	–	–	–
L	0.0	0	0	0.0	0	0	0.0	0	0	5.5	3	59
L	0.0	0	0	0.0	0	0	0.0	0	0	0.0	0	0
L	0.0	0	0	0.0	0	0	0.0	0	0	0.0	0	0
L	0.0	0	0	0.0	0	0	0.0	0	0	0.0	0	0
L	0.0	0	0	0.0	0	0	0.0	0	0	0.0	0	0
L	0.0	0	0	0.0	0	0	0.0	0	0	0.0	0	0

Cell	37			38			39			40		
	poro	perm	Sw	poro	perm	Sw	poro	perm	Sw	poro	perm	Sw
D	0.0	0	0	0.0	0	0	0.0	0	0	0.0	0	0
D	0.0	0	0	0.0	0	0	0.0	0	0	0.0	0	0
D	0.0	0	0	0.0	0	0	0.0	0	0	0.0	0	0
D	0.0	0	0	0.0	0	0	0.0	0	0	0.0	0	0
(I S)	–	–	–	–	–	–	–	–	–	–	–	–
I	5.0	2	45	0.0	0	0	0.0	0	0	0.0	0	0
I	0.0	0	0	0.0	0	0	0.0	0	0	0.0	0	0
I	0.0	0	0	0.0	0	0	0.0	0	0	0.0	0	0
(J US)	–	–	–	–	–	–	–	–	–	–	–	–
J c	0.0	0	0	0.0	0	0	0.0	0	0	0.0	0	0
(i.c.)	–	–	–	–	–	–	–	–	–	–	–	–
J ag	0.0	0	0	0.0	0	0	7.0	19	67	9.0	26	50
J ag	0.0	0	0	0.0	0	0	0.0	0	0	11.0	36	38
J ag	0.0	0	0	0.0	0	0	0.0	0	0	0.0	0	0
J ag	0.0	0	0	0.0	0	0	0.0	0	0	0.0	0	0
J ag	0.0	0	0	0.0	0	0	0.0	0	0	0.0	0	0
J ag	0.0	0	0	0.0	0	0	0.0	0	0	0.0	0	0
(i.c.)	–	–	–	–	–	–	–	–	–	–	–	–
J b	0.0	0	0	0.0	0	0	0.0	0	0	0.0	0	0
J b	0.0	0	0	0.0	0	0	0.0	0	0	0.0	0	0
(K US)	–	–	–	–	–	–	–	–	–	–	–	–
K cc	0.0	0	0	0.0	0	0	0.0	0	0	0.0	0	0
(K s)	–	–	–	–	–	–	–	–	–	–	–	–
K bc	0.0	0	0	0.0	0	0	0.0	0	0	6.5	2	53
K bc	0.0	0	0	0.0	0	0	0.0	0	0	0.0	0	0
K bc	0.0	0	0	0.0	0	0	0.0	0	0	0.0	0	0
(L US)	–	–	–	–	–	–	–	–	–	–	–	–
L	6.0	4	56	5.0	2	63	6.0	4	56	7.0	7	51
L	0.0	0	0	0.0	0	0	9.0	19	45	12.5	114	39
L	0.0	0	0	0.0	0	0	8.0	11	48	10.5	41	42
L	0.0	0	0	0.0	0	0	0.0	0	0	7.0	7	51
L	0.0	0	0	0.0	0	0	0.0	0	0	0.0	0	0
L	0.0	0	0	0.0	0	0	0.0	0	0	0.0	0	0

Cell	41			42			43			44		
	poro	perm	Sw	poro	perm	Sw	poro	perm	Sw	poro	perm	Sw
D	0.0	0	0	0.0	0	0	0.0	0	0	0.0	0	0
D	0.0	0	0	0.0	0	0	0.0	0	0	0.0	0	0
D	0.0	0	0	0.0	0	0	0.0	0	0	0.0	0	0
D	0.0	0	0	0.0	0	0	0.0	0	0	0.0	0	0
(I S)	–	–	–	–	–	–	–	–	–	–	–	–
I	7.5	13	28	0.0	0	0	0.0	0	0	0.0	0	0
I	0.0	0	0	0.0	0	0	0.0	0	0	0.0	0	0
I	0.0	0	0	0.0	0	0	0.0	0	0	0.0	0	0
(J US)	–	–	–	–	–	–	–	–	–	–	–	–
J c	0.0	0	0	0.0	0	0	0.0	0	0	0.0	0	0
(i.c.)	–	–	–	–	–	–	–	–	–	–	–	–
J ag	10.0	30	43	12.0	42	34	14.0	57	27	16.5	85	21
J ag	12.0	42	34	12.0	42	34	12.5	45	32	13.0	49	30
J ag	0.0	0	0	11.5	39	36	11.5	39	36	11.0	36	38
J ag	0.0	0	0	0.0	0	0	0.0	0	0	0.0	0	0
J ag	0.0	0	0	0.0	0	0	0.0	0	0	0.0	0	0
J ag	0.0	0	0	0.0	0	0	0.0	0	0	0.0	0	0
(i.c.)	–	–	–	–	–	–	–	–	–	–	–	–
J b	0.0	0	0	0.0	0	0	0.0	0	0	0.0	0	0
J b	0.0	0	0	0.0	0	0	0.0	0	0	0.0	0	0
(K US)	–	–	–	–	–	–	–	–	–	–	–	–
K cc	0.0	0	0	0.0	0	0	0.0	0	0	0.0	0	0
(K s)	–	–	–	–	–	–	–	–	–	–	–	–
K bc	6.5	2	53	0.0	0	0	0.0	0	0	0.0	0	0
K bc	0.0	0	0	0.0	0	0	0.0	0	0	0.0	0	0
K bc	0.0	0	0	0.0	0	0	0.0	0	0	0.0	0	0
(L US)	–	–	–	–	–	–	–	–	–	–	–	–
L	7.0	7	51	8.5	15	46	5.0	2	63	0.0	0	0
L	12.5	114	39	8.5	15	46	0.0	0	0	0.0	0	0
L	10.5	41	42	0.0	0	0	0.0	0	0	0.0	0	0
L	7.0	7	51	0.0	0	0	0.0	0	0	0.0	0	0
L	0.0	0	0	0.0	0	0	0.0	0	0	0.0	0	0
L	0.0	0	0	0.0	0	0	0.0	0	0	0.0	0	0

Cell		45			46			47			48	
	poro	perm	Sw	poro	perm	Sw	poro	perm	Sw	poro	perm	Sw
D	0.0	0	0	0.0	0	0	0.0	0	0	0.0	0	0
D	0.0	0	0	0.0	0	0	0.0	0	0	0.0	0	0
D	0.0	0	0	0.0	0	0	0.0	0	0	0.0	0	0
D	0.0	0	0	0.0	0	0	0.0	0	0	0.0	0	0
(I S)	–	–	–	–	–	–	–	–	–	–	–	–
I	5.0	2	45	6.5	6	33	7.0	9	30	6.5	6	33
I	0.0	0	0	6.0	4	37	6.0	4	37	6.0	4	37
I	0.0	0	0	0.0	0	0	6.0	4	37	0.0	0	0
(J US)	–	–	–	–	–	–	–	–	–	–	–	–
J c	0.0	0	0	0.0	0	0	0.0	0	0	0.0	0	0
(i.c.)	–	–	–	–	–	–	–	–	–	–	–	–
J ag	14.0	57	27	12.0	42	34	10.0	30	43	0.0	0	0
J ag	11.0	36	38	9.0	26	50	7.0	19	67	0.0	0	0
J ag	9.0	26	50	7.0	19	67	0.0	0	0	0.0	0	0
J ag	0.0	0	0	0.0	0	0	0.0	0	0	0.0	0	0
J ag	0.0	0	0	0.0	0	0	0.0	0	0	0.0	0	0
J ag	0.0	0	0	0.0	0	0	0.0	0	0	0.0	0	0
(i.c.)	–	–	–	–	–	–	–	–	–	–	–	–
J b	0.0	0	0	0.0	0	0	0.0	0	0	0.0	0	0
J b	0.0	0	0	0.0	0	0	0.0	0	0	0.0	0	0
(K US)	–	–	–	–	–	–	–	–	–	–	–	–
K cc	0.0	0	0	0.0	0	0	0.0	0	0	0.0	0	0
(K s)	–	–	–	–	–	–	–	–	–	–	–	–
K bc	0.0	0	0	0.0	0	0	0.0	0	0	0.0	0	0
K bc	0.0	0	0	0.0	0	0	0.0	0	0	0.0	0	0
K bc	0.0	0	0	0.0	0	0	0.0	0	0	0.0	0	0
(L US)	–	–	–	–	–	–	–	–	–	–	–	–
L	0.0	0	0	0.0	0	0	8.0	11	48	8.0	11	48
L	0.0	0	0	0.0	0	0	8.0	11	48	8.0	11	48
L	0.0	0	0	0.0	0	0	0.0	0	0	0.0	0	0
L	0.0	0	0	0.0	0	0	0.0	0	0	0.0	0	0
L	0.0	0	0	0.0	0	0	0.0	0	0	0.0	0	0
L	0.0	0	0	0.0	0	0	0.0	0	0	0.0	0	0

Cell		49			50			51			52	
	poro	perm	Sw	poro	perm	Sw	poro	perm	Sw	poro	perm	Sw
D	0.0	0	0	0.0	0	0	0.0	0	0	0.0	0	0
D	0.0	0	0	0.0	0	0	0.0	0	0	0.0	0	0
D	0.0	0	0	0.0	0	0	0.0	0	0	0.0	0	0
D	0.0	0	0	0.0	0	0	0.0	0	0	0.0	0	0
(I S)	–	–	–	–	–	–	–	–	–	–	–	–
I	0.0	0	0	0.0	0	0	0.0	0	0	0.0	0	0
I	0.0	0	0	0.0	0	0	0.0	0	0	0.0	0	0
I	0.0	0	0	0.0	0	0	0.0	0	0	0.0	0	0
(J US)	–	–	–	–	–	–	–	–	–	–	–	–
J c	0.0	0	0	0.0	0	0	0.0	0	0	0.0	0	0
(i.c.)	–	–	–	–	–	–	–	–	–	–	–	–
J ag	7.0	19	67	10.5	33	41	10.5	33	41	10.5	33	41
J ag	0.0	0	0	10.0	30	43	12.0	42	34	12.5	45	32
J ag	0.0	0	0	0.0	0	0	11.0	36	38	11.0	36	38
J ag	0.0	0	0	0.0	0	0	0.0	0	0	0.0	0	0
J ag	0.0	0	0	0.0	0	0	0.0	0	0	0.0	0	0
J ag	0.0	0	0	0.0	0	0	0.0	0	0	0.0	0	0
(i.c.)	–	–	–	–	–	–	–	–	–	–	–	–
J b	0.0	0	0	0.0	0	0	0.0	0	0	0.0	0	0
J b	0.0	0	0	0.0	0	0	0.0	0	0	0.0	0	0
(K US)	–	–	–	–	–	–	–	–	–	–	–	–
K cc	0.0	0	0	0.0	0	0	0.0	0	0	0.0	0	0
(K s)	–	–	–	–	–	–	–	–	–	–	–	–
K bc	0.0	0	0	0.0	0	0	0.0	0	0	6.5	2	53
K bc	0.0	0	0	0.0	0	0	0.0	0	0	0.0	0	0
K bc	0.0	0	0	0.0	0	0	0.0	0	0	0.0	0	0
(L US)	–	–	–	–	–	–	–	–	–	–	–	–
L	0.0	0	0	0.0	0	0	8.0	11	48	8.0	11	48
L	0.0	0	0	0.0	0	0	8.0	11	48	11.0	53	41
L	0.0	0	0	0.0	0	0	0.0	0	0	10.5	41	42
L	0.0	0	0	0.0	0	0	0.0	0	0	7.0	7	51
L	0.0	0	0	0.0	0	0	0.0	0	0	0.0	0	0
L	0.0	0	0	0.0	0	0	0.0	0	0	0.0	0	0

Cell	53			54			55			56		
	poro	perm	Sw	poro	perm	Sw	poro	perm	Sw	poro	perm	Sw
D	0.0	0	0	0.0	0	0	0.0	0	0	0.0	0	0
D	0.0	0	0	0.0	0	0	0.0	0	0	0.0	0	0
D	0.0	0	0	0.0	0	0	0.0	0	0	0.0	0	0
D	0.0	0	0	0.0	0	0	0.0	0	0	0.0	0	0
(I S)	–	–	–	–	–	–	–	–	–	–	–	–
I	7.5	13	28	8.0	19	26	8.5	27	24	9.0	39	22
I	0.0	0	0	0.0	0	0	0.0	0	0	0.0	0	0
I	0.0	0	0	0.0	0	0	0.0	0	0	0.0	0	0
(J US)	–	–	–	–	–	–	–	–	–	–	–	–
J c	0.0	0	0	0.0	0	0	0.0	0	0	0.0	0	0
(i.c.)	–	–	–	–	–	–	–	–	–	–	–	–
J ag	11.5	39	36	12.0	42	34	12.5	45	32	17.0	92	20
J ag	13.5	53	29	14.0	57	27	14.5	62	26	14.5	62	26
J ag	11.5	39	36	12.0	42	34	12.5	45	32	12.5	45	32
J ag	0.0	0	0	0.0	0	0	0.0	0	0	12.0	42	34
J ag	0.0	0	0	0.0	0	0	0.0	0	0	0.0	0	0
J ag	0.0	0	0	0.0	0	0	0.0	0	0	0.0	0	0
(i.c.)	–	–	–	–	–	–	–	–	–	–	–	–
J b	0.0	0	0	0.0	0	0	0.0	0	0	0.0	0	0
J b	0.0	0	0	0.0	0	0	0.0	0	0	0.0	0	0
(K US)	–	–	–	–	–	–	–	–	–	–	–	–
K cc	0.0	0	0	0.0	0	0	0.0	0	0	0.0	0	0
(K s)	–	–	–	–	–	–	–	–	–	–	–	–
K bc	7.0	2	51	6.5	2	53	0.0	0	0	0.0	0	0
K bc	0.0	0	0	0.0	0	0	0.0	0	0	0.0	0	0
K bc	0.0	0	0	0.0	0	0	0.0	0	0	0.0	0	0
(L US)	–	–	–	–	–	–	–	–	–	–	–	–
L	8.5	15	46	10.5	41	42	5.0	2	63	0.0	0	0
L	11.5	69	40	10.5	41	42	0.0	0	0	0.0	0	0
L	10.5	41	42	7.0	7	51	0.0	0	0	0.0	0	0
L	7.0	7	51	0.0	0	0	0.0	0	0	0.0	0	0
L	0.0	0	0	0.0	0	0	0.0	0	0	0.0	0	0
L	0.0	0	0	0.0	0	0	0.0	0	0	0.0	0	0

Cell	57			58			59			60		
	poro	perm	Sw	poro	perm	Sw	poro	perm	Sw	poro	perm	Sw
D	0.0	0	0	0.0	0	0	0.0	0	0	0.0	0	0
D	0.0	0	0	0.0	0	0	0.0	0	0	0.0	0	0
D	0.0	0	0	0.0	0	0	0.0	0	0	0.0	0	0
D	0.0	0	0	0.0	0	0	0.0	0	0	0.0	0	0
(I S)	–	–	–	–	–	–	–	–	–	–	–	–
I	9.0	39	22	9.0	39	22	8.5	27	24	7.0	9	30
I	9.0	39	22	9.0	39	22	7.5	13	28	6.0	4	37
I	0.0	0	0	0.0	0	0	7.5	13	28	0.0	0	0
(J US)	–	–	–	–	–	–	–	–	–	–	–	–
J c	0.0	0	0	0.0	0	0	0.0	0	0	0.0	0	0
(i.c.)	–	–	–	–	–	–	–	–	–	–	–	–
J ag	16.5	85	21	15.5	73	23	12.0	42	34	9.5	28	46
J ag	13.5	53	29	12.5	45	32	10.0	30	43	7.0	19	67
J ag	12.5	45	32	11.5	39	36	8.0	22	57	0.0	0	0
J ag	0.0	0	0	0.0	0	0	0.0	0	0	0.0	0	0
J ag	0.0	0	0	0.0	0	0	0.0	0	0	0.0	0	0
J ag	0.0	0	0	0.0	0	0	0.0	0	0	0.0	0	0
(i.c.)	–	–	–	–	–	–	–	–	–	–	–	–
J b	0.0	0	0	0.0	0	0	0.0	0	0	0.0	0	0
J b	0.0	0	0	0.0	0	0	0.0	0	0	0.0	0	0
(K US)	–	–	–	–	–	–	–	–	–	–	–	–
K cc	0.0	0	0	0.0	0	0	0.0	0	0	0.0	0	0
(K s)	–	–	–	–	–	–	–	–	–	–	–	–
K bc	0.0	0	0	0.0	0	0	0.0	0	0	0.0	0	0
K bc	0.0	0	0	0.0	0	0	0.0	0	0	0.0	0	0
K bc	0.0	0	0	0.0	0	0	0.0	0	0	0.0	0	0
(L US)	–	–	–	–	–	–	–	–	–	–	–	–
L	0.0	0	0	0.0	0	0	0.0	0	0	8.0	11	48
L	0.0	0	0	0.0	0	0	0.0	0	0	8.0	11	48
L	0.0	0	0	0.0	0	0	0.0	0	0	0.0	0	0
L	0.0	0	0	0.0	0	0	0.0	0	0	0.0	0	0
L	0.0	0	0	0.0	0	0	0.0	0	0	0.0	0	0
L	0.0	0	0	0.0	0	0	0.0	0	0	0.0	0	0

Cell	61			62			63			64		
	poro	perm	Sw	poro	perm	Sw	poro	perm	Sw	poro	perm	Sw
D	0.0	0	0	0.0	0	0	0.0	0	0	0.0	0	0
D	0.0	0	0	0.0	0	0	0.0	0	0	0.0	0	0
D	0.0	0	0	0.0	0	0	0.0	0	0	0.0	0	0
D	0.0	0	0	0.0	0	0	0.0	0	0	0.0	0	0
(I S)	–	–	–	–	–	–	–	–	–	–	–	–
I	6.0	4	37	0.0	0	0	0.0	0	0	6.0	4	37
I	0.0	0	0	0.0	0	0	0.0	0	0	0.0	0	0
I	0.0	0	0	0.0	0	0	0.0	0	0	0.0	0	0
(J US)	–	–	–	–	–	–	–	–	–	–	–	–
J c	0.0	0	0	0.0	0	0	0.0	0	0	0.0	0	0
(i.c.)	–	–	–	–	–	–	–	–	–	–	–	–
J ag	0.0	0	0	0.0	0	0	0.0	0	0	7.0	19	67
J ag	0.0	0	0	0.0	0	0	0.0	0	0	0.0	0	0
J ag	0.0	0	0	0.0	0	0	0.0	0	0	0.0	0	0
J ag	0.0	0	0	0.0	0	0	0.0	0	0	0.0	0	0
J ag	0.0	0	0	0.0	0	0	0.0	0	0	0.0	0	0
J ag	0.0	0	0	0.0	0	0	0.0	0	0	0.0	0	0
(i.c.)	–	–	–	–	–	–	–	–	–	–	–	–
J b	0.0	0	0	0.0	0	0	0.0	0	0	0.0	0	0
J b	0.0	0	0	0.0	0	0	0.0	0	0	0.0	0	0
(K US)	–	–	–	–	–	–	–	–	–	–	–	–
K cc	0.0	0	0	0.0	0	0	0.0	0	0	0.0	0	0
(K s)	–	–	–	–	–	–	–	–	–	–	–	–
K bc	0.0	0	0	6.5	2	53	6.5	2	53	0.0	0	0
K bc	0.0	0	0	0.0	0	0	0.0	0	0	0.0	0	0
K bc	0.0	0	0	0.0	0	0	0.0	0	0	0.0	0	0
(L US)	–	–	–	–	–	–	–	–	–	–	–	–
L	8.0	11	48	0.0	0	0	0.0	0	0	0.0	0	0
L	8.0	11	48	0.0	0	0	0.0	0	0	0.0	0	0
L	0.0	0	0	0.0	0	0	0.0	0	0	0.0	0	0
L	0.0	0	0	0.0	0	0	0.0	0	0	0.0	0	0
L	0.0	0	0	0.0	0	0	0.0	0	0	0.0	0	0
L	0.0	0	0	0.0	0	0	0.0	0	0	0.0	0	0

Cell	65			66			67			68		
	poro	perm	Sw	poro	perm	Sw	poro	perm	Sw	poro	perm	Sw
D	0.0	0	0	0.0	0	0	0.0	0	0	0.0	0	0
D	0.0	0	0	0.0	0	0	0.0	0	0	0.0	0	0
D	0.0	0	0	0.0	0	0	0.0	0	0	0.0	0	0
D	0.0	0	0	0.0	0	0	0.0	0	0	0.0	0	0
(I S)	–	–	–	–	–	–	–	–	–	–	–	–
I	7.0	9	30	7.5	13	28	0.0	0	0	0.0	0	0
I	0.0	0	0	0.0	0	0	0.0	0	0	0.0	0	0
I	0.0	0	0	0.0	0	0	0.0	0	0	0.0	0	0
(J US)	–	–	–	–	–	–	–	–	–	–	–	–
J c	0.0	0	0	0.0	0	0	0.0	0	0	0.0	0	0
(i.c.)	–	–	–	–	–	–	–	–	–	–	–	–
J ag	0.0	0	0	7.0	19	67	11.0	36	38	17.0	92	20
J ag	0.0	0	0	0.0	0	0	8.5	24	53	15.5	73	23
J ag	0.0	0	0	0.0	0	0	0.0	0	0	13.0	49	30
J ag	0.0	0	0	0.0	0	0	0.0	0	0	11.5	39	36
J ag	0.0	0	0	0.0	0	0	0.0	0	0	0.0	0	0
J ag	0.0	0	0	0.0	0	0	0.0	0	0	0.0	0	0
(i.c.)	–	–	–	–	–	–	–	–	–	–	–	–
J b	0.0	0	0	0.0	0	0	0.0	0	0	6.0	4	37
J b	0.0	0	0	0.0	0	0	0.0	0	0	6.0	4	37
(K US)	–	–	–	–	–	–	–	–	–	–	–	–
K cc	0.0	0	0	0.0	0	0	0.0	0	0	0.0	0	0
(K s)	–	–	–	–	–	–	–	–	–	–	–	–
K bc	0.0	0	0	0.0	0	0	0.0	0	0	0.0	0	0
K bc	0.0	0	0	0.0	0	0	0.0	0	0	0.0	0	0
K bc	0.0	0	0	0.0	0	0	0.0	0	0	0.0	0	0
(L US)	–	–	–	–	–	–	–	–	–	–	–	–
L	0.0	0	0	0.0	0	0	0.0	0	0	7.5	9	49
L	0.0	0	0	0.0	0	0	0.0	0	0	8.0	11	48
L	0.0	0	0	0.0	0	0	0.0	0	0	0.0	0	0
L	0.0	0	0	0.0	0	0	0.0	0	0	0.0	0	0
L	0.0	0	0	0.0	0	0	0.0	0	0	0.0	0	0
L	0.0	0	0	0.0	0	0	0.0	0	0	0.0	0	0

Cell		69			70			71			72	
	poro	perm	Sw	poro	perm	Sw	poro	perm	Sw	poro	perm	Sw
D	0.0	0	0	0.0	0	0	0.0	0	0	0.0	0	0
D	0.0	0	0	0.0	0	0	0.0	0	0	0.0	0	0
D	0.0	0	0	0.0	0	0	0.0	0	0	0.0	0	0
D	0.0	0	0	0.0	0	0	0.0	0	0	0.0	0	0
(I S)	–	–	–	–	–	–	–	–	–	–	–	–
I	0.0	0	0	0.0	0	0	7.5	13	28	8.0	19	26
I	0.0	0	0	0.0	0	0	0.0	0	0	8.5	27	24
I	0.0	0	0	0.0	0	0	0.0	0	0	0.0	0	0
(J US)	–	–	–	–	–	–	–	–	–	–	–	–
J c	0.0	0	0	0.0	0	0	0.0	0	0	0.0	0	0
(i.c.)	–	–	–	–	–	–	–	–	–	–	–	–
J ag	16.0	79	22	16.0	79	22	16.0	79	22	15.0	67	25
J ag	19.0	127	17	19.0	127	17	18.0	108	18	16.5	85	21
J ag	18.5	117	18	18.5	117	18	17.5	100	19	16.0	79	22
J ag	19.0	127	17	19.0	127	17	16.0	79	22	13.0	49	30
J ag	14.0	57	27	14.0	57	27	0.0	0	0	0.0	0	0
J ag	0.0	0	0	0.0	0	0	0.0	0	0	0.0	0	0
(i.c.)	–	–	–	–	–	–	–	–	–	–	–	–
J b	6.0	4	37	6.0	4	37	0.0	0	0	0.0	0	0
J b	6.5	6	33	0.0	0	0	0.0	0	0	0.0	0	0
(K US)	–	–	–	–	–	–	–	–	–	–	–	–
K cc	0.0	0	0	0.0	0	0	0.0	0	0	0.0	0	0
(K s)	–	–	–	–	–	–	–	–	–	–	–	–
K bc	6.5	2	53	7.5	3	49	7.0	2	51	0.0	0	0
K bc	0.0	0	0	0.0	0	0	0.0	0	0	0.0	0	0
K bc	0.0	0	0	0.0	0	0	0.0	0	0	0.0	0	0
(L US)	–	–	–	–	–	–	–	–	–	–	–	–
L	10.0	32	43	10.5	41	42	10.5	41	42	7.0	7	51
L	11.0	53	41	11.5	69	40	10.5	41	42	7.0	7	51
L	7.5	9	49	7.5	9	49	7.0	7	51	0.0	0	0
L	0.0	0	0	0.0	0	0	0.0	0	0	0.0	0	0
L	0.0	0	0	0.0	0	0	0.0	0	0	0.0	0	0
L	0.0	0	0	0.0	0	0	0.0	0	0	0.0	0	0

Cell		73			74			75			76	
	poro	perm	Sw	poro	perm	Sw	poro	perm	Sw	poro	perm	Sw
D	0.0	0	0	0.0	0	0	0.0	0	0	0.0	0	0
D	0.0	0	0	0.0	0	0	0.0	0	0	0.0	0	0
D	0.0	0	0	0.0	0	0	0.0	0	0	0.0	0	0
D	0.0	0	0	0.0	0	0	0.0	0	0	0.0	0	0
(I S)	–	–	–	–	–	–	–	–	–	–	–	–
I	8.5	27	24	10.0	81	19	10.5	116	18	10.5	116	18
I	9.0	39	22	9.5	56	21	9.5	56	21	9.5	56	21
I	0.0	0	0	9.0	39	22	9.5	56	21	9.5	56	21
(J US)	–	–	–	–	–	–	–	–	–	–	–	–
J c	0.0	0	0	0.0	0	0	0.0	0	0	0.0	0	0
(i.c.)	–	–	–	–	–	–	–	–	–	–	–	–
J ag	15.0	67	25	15.0	67	25	14.5	62	26	15.0	67	25
J ag	16.5	85	21	16.5	85	21	16.0	79	22	15.0	67	25
J ag	16.0	79	22	15.5	73	23	15.0	67	25	12.0	42	34
J ag	13.0	49	30	11.5	39	36	11.0	36	38	0.0	0	0
J ag	0.0	0	0	0.0	0	0	0.0	0	0	0.0	0	0
J ag	0.0	0	0	0.0	0	0	0.0	0	0	0.0	0	0
(i.c.)	–	–	–	–	–	–	–	–	–	–	–	–
J b	0.0	0	0	0.0	0	0	0.0	0	0	0.0	0	0
J b	0.0	0	0	0.0	0	0	0.0	0	0	0.0	0	0
(K US)	–	–	–	–	–	–	–	–	–	–	–	–
K cc	0.0	0	0	0.0	0	0	0.0	0	0	0.0	0	0
(K s)	–	–	–	–	–	–	–	–	–	–	–	–
K bc	0.0	0	0	6.5	2	53	6.5	2	53	0.0	0	0
K bc	0.0	0	0	0.0	0	0	0.0	0	0	0.0	0	0
K bc	0.0	0	0	0.0	0	0	0.0	0	0	0.0	0	0
(L US)	–	–	–	–	–	–	–	–	–	–	–	–
L	0.0	0	0	0.0	0	0	0.0	0	0	0.0	0	0
L	0.0	0	0	0.0	0	0	0.0	0	0	0.0	0	0
L	0.0	0	0	0.0	0	0	0.0	0	0	0.0	0	0
L	0.0	0	0	0.0	0	0	0.0	0	0	0.0	0	0
L	0.0	0	0	0.0	0	0	0.0	0	0	0.0	0	0
L	0.0	0	0	0.0	0	0	0.0	0	0	0.0	0	0

Cell	77			78			79			80		
	poro	perm	Sw	poro	perm	Sw	poro	perm	Sw	poro	perm	Sw
D	0.0	0	0	0.0	0	0	0.0	0	0	0.0	0	0
D	0.0	0	0	0.0	0	0	0.0	0	0	0.0	0	0
D	0.0	0	0	0.0	0	0	0.0	0	0	0.0	0	0
D	0.0	0	0	0.0	0	0	0.0	0	0	0.0	0	0
(I S)	–	–	–	–	–	–	–	–	–	–	–	–
I	9.0	39	22	7.0	9	30	6.5	6	33	6.0	4	37
I	8.0	19	26	6.5	6	33	0.0	0	0	0.0	0	0
I	8.0	19	26	0.0	0	0	0.0	0	0	0.0	0	0
(J US)	–	–	–	–	–	–	–	–	–	–	–	–
J c	0.0	0	0	0.0	0	0	0.0	0	0	0.0	0	0
(i.c.)	–	–	–	–	–	–	–	–	–	–	–	–
J ag	10.0	30	43	7.0	19	67	0.0	0	0	7.0	19	67
J ag	7.5	20	62	0.0	0	0	0.0	0	0	0.0	0	0
J ag	0.0	0	0	0.0	0	0	0.0	0	0	0.0	0	0
J ag	0.0	0	0	0.0	0	0	0.0	0	0	0.0	0	0
J ag	0.0	0	0	0.0	0	0	0.0	0	0	0.0	0	0
J ag	0.0	0	0	0.0	0	0	0.0	0	0	0.0	0	0
(i.c.)	–	–	–	–	–	–	–	–	–	–	–	–
J b	0.0	0	0	0.0	0	0	0.0	0	0	0.0	0	0
J b	0.0	0	0	0.0	0	0	0.0	0	0	0.0	0	0
(K US)	–	–	–	–	–	–	–	–	–	–	–	–
K cc	0.0	0	0	0.0	0	0	0.0	0	0	0.0	0	0
(K s)	–	–	–	–	–	–	–	–	–	–	–	–
K bc	0.0	0	0	0.0	0	0	0.0	0	0	7.0	2	51
K bc	0.0	0	0	0.0	0	0	0.0	0	0	0.0	0	0
K bc	0.0	0	0	0.0	0	0	0.0	0	0	0.0	0	0
(L US)	–	–	–	–	–	–	–	–	–	–	–	–
L	0.0	0	0	7.5	9	49	7.5	9	49	0.0	0	0
L	0.0	0	0	7.5	9	49	7.5	9	49	0.0	0	0
L	0.0	0	0	0.0	0	0	0.0	0	0	0.0	0	0
L	0.0	0	0	0.0	0	0	0.0	0	0	0.0	0	0
L	0.0	0	0	0.0	0	0	0.0	0	0	0.0	0	0
L	0.0	0	0	0.0	0	0	0.0	0	0	0.0	0	0

Cell	81			82			83			84		
	poro	perm	Sw	poro	perm	Sw	poro	perm	Sw	poro	perm	Sw
D	0.0	0	0	0.0	0	0	0.0	0	0	0.0	0	0
D	0.0	0	0	0.0	0	0	0.0	0	0	0.0	0	0
D	0.0	0	0	0.0	0	0	0.0	0	0	0.0	0	0
D	0.0	0	0	0.0	0	0	0.0	0	0	0.0	0	0
(I S)	–	–	–	–	–	–	–	–	–	–	–	–
I	7.5	13	28	8.5	27	24	9.5	56	21	10.0	81	19
I	7.5	13	28	7.5	13	28	7.0	9	30	7.0	9	30
I	0.0	0	0	0.0	0	0	0.0	0	0	0.0	0	0
(J US)	–	–	–	–	–	–	–	–	–	–	–	–
J c	0.0	0	0	0.0	0	0	0.0	0	0	0.0	0	0
(i.c.)	–	–	–	–	–	–	–	–	–	–	–	–
J ag	10.5	33	41	11.0	36	38	11.0	36	38	11.0	36	38
J ag	12.0	42	34	12.0	42	34	9.5	28	46	8.5	24	53
J ag	0.0	0	0	0.0	0	0	0.0	0	0	0.0	0	0
J ag	0.0	0	0	0.0	0	0	0.0	0	0	0.0	0	0
J ag	0.0	0	0	0.0	0	0	0.0	0	0	0.0	0	0
J ag	0.0	0	0	0.0	0	0	0.0	0	0	0.0	0	0
(i.c.)	–	–	–	–	–	–	–	–	–	–	–	–
J b	0.0	0	0	0.0	0	0	0.0	0	0	0.0	0	0
J b	0.0	0	0	0.0	0	0	0.0	0	0	0.0	0	0
(K US)	–	–	–	–	–	–	–	–	–	–	–	–
K cc	0.0	0	0	0.0	0	0	0.0	0	0	0.0	0	0
(K s)	–	–	–	–	–	–	–	–	–	–	–	–
K bc	7.5	3	49	6.5	2	53	0.0	0	0	0.0	0	0
K bc	0.0	0	0	0.0	0	0	0.0	0	0	0.0	0	0
K bc	0.0	0	0	0.0	0	0	0.0	0	0	0.0	0	0
(L US)	–	–	–	–	–	–	–	–	–	–	–	–
L	0.0	0	0	0.0	0	0	0.0	0	0	0.0	0	0
L	0.0	0	0	0.0	0	0	0.0	0	0	0.0	0	0
L	0.0	0	0	0.0	0	0	0.0	0	0	0.0	0	0
L	0.0	0	0	0.0	0	0	0.0	0	0	0.0	0	0
L	0.0	0	0	0.0	0	0	0.0	0	0	0.0	0	0
L	0.0	0	0	0.0	0	0	0.0	0	0	0.0	0	0

Cell	85			86			87			88		
	poro	perm	Sw	poro	perm	Sw	poro	perm	Sw	poro	perm	Sw
D	0.0	0	0	0.0	0	0	0.0	0	0	0.0	0	0
D	0.0	0	0	0.0	0	0	0.0	0	0	0.0	0	0
D	0.0	0	0	0.0	0	0	0.0	0	0	0.0	0	0
D	0.0	0	0	0.0	0	0	0.0	0	0	0.0	0	0
(I S)	–	–	–	–	–	–	–	–	–	–	–	–
I	7.5	13	28	0.0	0	0	0.0	0	0	7.5	13	28
I	0.0	0	0	0.0	0	0	0.0	0	0	0.0	0	0
I	0.0	0	0	0.0	0	0	0.0	0	0	0.0	0	0
(J US)	–	–	–	–	–	–	–	–	–	–	–	–
J c	0.0	0	0	0.0	0	0	0.0	0	0	0.0	0	0
(i.c.)	–	–	–	–	–	–	–	–	–	–	–	–
J ag	14.0	57	27	16.0	79	22	10.0	81	19	17.0	92	20
J ag	12.0	42	34	19.0	127	17	17.0	92	20	20.0	149	15
J ag	10.0	30	43	18.5	117	18	20.0	149	15	19.5	138	16
J ag	0.0	0	0	19.0	127	17	19.5	138	16	20.0	149	15
J ag	0.0	0	0	14.0	57	27	20.0	149	15	15.0	67	25
J ag	0.0	0	0	0.0	0	0	15.0	67	25	0.0	0	0
(i.c.)	–	–	–	–	–	–	–	–	–	–	–	–
J b	0.0	0	0	6.0	4	37	6.0	4	37	6.0	4	37
J b	0.0	0	0	6.0	4	37	6.5	6	33	0.0	0	0
(K US)	–	–	–	–	–	–	–	–	–	–	–	–
K cc	0.0	0	0	0.0	0	0	6.5	2	53	6.5	2	53
(K s)	–	–	–	–	–	–	–	–	–	–	–	–
K bc	0.0	0	0	6.5	2	53	8.0	3	48	8.0	3	48
K bc	0.0	0	0	0.0	0	0	8.0	3	48	8.0	3	48
K bc	0.0	0	0	0.0	0	0	0.0	0	0	0.0	0	0
(L US)	–	–	–	–	–	–	–	–	–	–	–	–
L	6.0	4	56	10.0	32	43	10.0	32	43	8.5	15	46
L	0.0	0	0	11.0	53	41	11.0	53	41	8.5	15	46
L	0.0	0	0	7.5	9	49	7.5	9	49	0.0	0	0
L	0.0	0	0	0.0	0	0	0.0	0	0	0.0	0	0
L	0.0	0	0	0.0	0	0	0.0	0	0	0.0	0	0
L	0.0	0	0	0.0	0	0	0.0	0	0	0.0	0	0

Cell	89			90			91			92		
	poro	perm	Sw	poro	perm	Sw	poro	perm	Sw	poro	perm	Sw
D	0.0	0	0	0.0	0	0	0.0	0	0	0.0	0	0
D	0.0	0	0	0.0	0	0	0.0	0	0	0.0	0	0
D	0.0	0	0	0.0	0	0	0.0	0	0	0.0	0	0
D	0.0	0	0	0.0	0	0	0.0	0	0	0.0	0	0
(I S)	–	–	–	–	–	–	–	–	–	–	–	–
I	8.0	19	26	8.0	19	26	9.0	39	22	10.0	81	19
I	8.5	27	24	9.0	39	22	9.5	56	21	9.5	56	21
I	0.0	0	0	8.0	19	26	8.5	27	24	9.5	56	21
(J US)	–	–	–	–	–	–	–	–	–	–	–	–
J c	0.0	0	0	0.0	0	0	0.0	0	0	0.0	0	0
(i.c.)	–	–	–	–	–	–	–	–	–	–	–	–
J ag	16.5	85	21	16.0	79	22	15.5	73	23	15.5	73	23
J ag	18.0	108	18	17.5	100	19	17.0	92	20	16.5	85	21
J ag	18.5	117	18	17.0	92	20	16.5	85	21	15.0	67	25
J ag	18.5	117	18	14.0	57	27	13.5	53	29	12.5	45	32
J ag	14.5	62	26	0.0	0	0	0.0	0	0	0.0	0	0
J ag	0.0	0	0	0.0	0	0	0.0	0	0	0.0	0	0
(i.c.)	–	–	–	–	–	–	–	–	–	–	–	–
J b	0.0	0	0	0.0	0	0	0.0	0	0	0.0	0	0
J b	0.0	0	0	0.0	0	0	0.0	0	0	0.0	0	0
(K US)	–	–	–	–	–	–	–	–	–	–	–	–
K cc	0.0	0	0	0.0	0	0	0.0	0	0	0.0	0	0
(K s)	–	–	–	–	–	–	–	–	–	–	–	–
K bc	7.0	2	51	0.0	0	0	6.5	2	53	7.5	3	49
K bc	0.0	0	0	0.0	0	0	0.0	0	0	7.5	3	49
K bc	0.0	0	0	0.0	0	0	0.0	0	0	0.0	0	0
(L US)	–	–	–	–	–	–	–	–	–	–	–	–
L	5.5	3	59	0.0	0	0	0.0	0	0	0.0	0	0
L	0.0	0	0	0.0	0	0	0.0	0	0	0.0	0	0
L	0.0	0	0	0.0	0	0	0.0	0	0	0.0	0	0
L	0.0	0	0	0.0	0	0	0.0	0	0	0.0	0	0
L	0.0	0	0	0.0	0	0	0.0	0	0	0.0	0	0
L	0.0	0	0	0.0	0	0	0.0	0	0	0.0	0	0

Cell	93			94			95			96		
	poro	perm	Sw	poro	perm	Sw	poro	perm	Sw	poro	perm	Sw
D	0.0	0	0	0.0	0	0	0.0	0	0	0.0	0	0
D	0.0	0	0	0.0	0	0	0.0	0	0	0.0	0	0
D	0.0	0	0	0.0	0	0	0.0	0	0	0.0	0	0
D	0.0	0	0	0.0	0	0	0.0	0	0	0.0	0	0
(I S)	–	–	–	–	–	–	–	–	–	–	–	–
I	11.0	167	17	9.5	56	21	8.0	19	26	7.0	9	30
I	10.0	81	19	8.0	19	26	7.5	13	28	0.0	0	0
I	10.0	81	19	0.0	0	0	0.0	0	0	0.0	0	0
(J US)	–	–	–	–	–	–	–	–	–	–	–	–
J c	0.0	0	0	0.0	0	0	0.0	0	0	8.0	19	26
(i.c.)	–	–	–	–	–	–	–	–	–	–	–	–
J ag	15.5	73	23	13.5	53	29	7.0	19	67	0.0	0	0
J ag	15.5	73	23	13.5	53	29	0.0	0	0	0.0	0	0
J ag	12.0	42	34	10.0	30	43	0.0	0	0	0.0	0	0
J ag	0.0	0	0	0.0	0	0	0.0	0	0	0.0	0	0
J ag	0.0	0	0	0.0	0	0	0.0	0	0	0.0	0	0
J ag	0.0	0	0	0.0	0	0	0.0	0	0	0.0	0	0
(i.c.)	–	–	–	–	–	–	–	–	–	–	–	–
J b	0.0	0	0	0.0	0	0	0.0	0	0	0.0	0	0
J b	0.0	0	0	0.0	0	0	0.0	0	0	0.0	0	0
(K US)	–	–	–	–	–	–	–	–	–	–	–	–
K cc	0.0	0	0	0.0	0	0	0.0	0	0	0.0	0	0
(K s)	–	–	–	–	–	–	–	–	–	–	–	–
K bc	7.5	3	49	6.5	2	53	0.0	0	0	0.0	0	0
K bc	7.5	3	49	0.0	0	0	0.0	0	0	0.0	0	0
K bc	0.0	0	0	0.0	0	0	0.0	0	0	0.0	0	0
(L US)	–	–	–	–	–	–	–	–	–	–	–	–
L	0.0	0	0	0.0	0	0	0.0	0	0	7.0	7	51
L	0.0	0	0	0.0	0	0	0.0	0	0	7.0	7	51
L	0.0	0	0	0.0	0	0	0.0	0	0	0.0	0	0
L	0.0	0	0	0.0	0	0	0.0	0	0	0.0	0	0
L	0.0	0	0	0.0	0	0	0.0	0	0	0.0	0	0
L	0.0	0	0	0.0	0	0	0.0	0	0	0.0	0	0

Cell	97			98			99			100		
	poro	perm	Sw	poro	perm	Sw	poro	perm	Sw	poro	perm	Sw
D	0.0	0	0	0.0	0	0	0.0	0	0	0.0	0	0
D	0.0	0	0	0.0	0	0	0.0	0	0	0.0	0	0
D	0.0	0	0	0.0	0	0	0.0	0	0	0.0	0	0
D	0.0	0	0	0.0	0	0	0.0	0	0	0.0	0	0
(I S)	–	–	–	–	–	–	–	–	–	–	–	–
I	0.0	0	0	0.0	0	0	6.0	4	37	7.5	13	28
I	0.0	0	0	0.0	0	0	0.0	0	0	7.5	13	28
I	0.0	0	0	0.0	0	0	0.0	0	0	0.0	0	0
(J US)	–	–	–	–	–	–	–	–	–	–	–	–
J c	8.0	19	26	0.0	0	0	0.0	0	0	0.0	0	0
(i.c.)	–	–	–	–	–	–	–	–	–	–	–	–
J ag	0.0	0	0	0.0	0	0	7.5	20	62	11.0	36	38
J ag	0.0	0	0	0.0	0	0	0.0	0	0	12.5	45	32
J ag	0.0	0	0	0.0	0	0	0.0	0	0	0.0	0	0
J ag	0.0	0	0	0.0	0	0	0.0	0	0	0.0	0	0
J ag	0.0	0	0	0.0	0	0	0.0	0	0	0.0	0	0
J ag	0.0	0	0	0.0	0	0	0.0	0	0	0.0	0	0
(i.c.)	–	–	–	–	–	–	–	–	–	–	–	–
J b	0.0	0	0	0.0	0	0	0.0	0	0	0.0	0	0
J b	0.0	0	0	0.0	0	0	0.0	0	0	0.0	0	0
(K US)	–	–	–	–	–	–	–	–	–	–	–	–
K cc	0.0	0	0	0.0	0	0	0.0	0	0	0.0	0	0
(K s)	–	–	–	–	–	–	–	–	–	–	–	–
K bc	0.0	0	0	6.5	2	53	7.5	3	49	6.5	2	53
K bc	0.0	0	0	0.0	0	0	0.0	0	0	0.0	0	0
K bc	0.0	0	0	0.0	0	0	0.0	0	0	0.0	0	0
(L US)	–	–	–	–	–	–	–	–	–	–	–	–
L	7.0	7	51	0.0	0	0	0.0	0	0	0.0	0	0
L	6.5	5	53	0.0	0	0	0.0	0	0	0.0	0	0
L	0.0	0	0	0.0	0	0	0.0	0	0	0.0	0	0
L	0.0	0	0	0.0	0	0	0.0	0	0	0.0	0	0
L	0.0	0	0	0.0	0	0	0.0	0	0	0.0	0	0
L	0.0	0	0	0.0	0	0	0.0	0	0	0.0	0	0

Cell		101			102			103			104	
	poro	perm	Sw	poro	perm	Sw	poro	perm	Sw	poro	perm	Sw
D	0.0	0	0	0.0	0	0	0.0	0	0	0.0	0	0
D	0.0	0	0	0.0	0	0	0.0	0	0	0.0	0	0
D	0.0	0	0	0.0	0	0	0.0	0	0	0.0	0	0
D	0.0	0	0	0.0	0	0	0.0	0	0	0.0	0	0
(I S)	–	–	–	–	–	–	–	–	–	–	–	–
I	9.0	39	22	10.0	81	19	8.5	27	24	6.0	4	37
I	8.0	19	26	9.0	39	22	7.5	13	28	0.0	0	0
I	7.5	13	28	8.0	19	26	7.0	9	30	0.0	0	0
(J US)	–	–	–	–	–	–	–	–	–	–	–	–
J c	0.0	0	0	0.0	0	0	0.0	0	0	0.0	0	0
(i.c.)	–	–	–	–	–	–	–	–	–	–	–	–
J ag	9.0	26	50	10.0	30	43	11.5	39	36	13.0	49	30
J ag	11.5	39	36	12.5	45	32	12.0	42	34	14.0	57	27
J ag	13.5	53	29	14.0	57	27	14.0	57	27	16.0	79	22
J ag	0.0	0	0	0.0	0	0	0.0	0	0	15.0	67	25
J ag	0.0	0	0	0.0	0	0	0.0	0	0	0.0	0	0
J ag	0.0	0	0	0.0	0	0	0.0	0	0	0.0	0	0
(i.c.)	–	–	–	–	–	–	–	–	–	–	–	–
J b	0.0	0	0	0.0	0	0	0.0	0	0	0.0	0	0
J b	0.0	0	0	0.0	0	0	0.0	0	0	0.0	0	0
(K US)	–	–	–	–	–	–	–	–	–	–	–	–
K cc	0.0	0	0	0.0	0	0	0.0	0	0	0.0	0	0
(K s)	–	–	–	–	–	–	–	–	–	–	–	–
K bc	0.0	0	0	0.0	0	0	0.0	0	0	0.0	0	0
K bc	0.0	0	0	0.0	0	0	0.0	0	0	0.0	0	0
K bc	0.0	0	0	0.0	0	0	0.0	0	0	0.0	0	0
(L US)	–	–	–	–	–	–	–	–	–	–	–	–
L	0.0	0	0	0.0	0	0	6.5	5	53	7.5	9	49
L	0.0	0	0	0.0	0	0	5.5	3	59	9.0	19	45
L	0.0	0	0	0.0	0	0	0.0	0	0	7.0	7	51
L	0.0	0	0	0.0	0	0	0.0	0	0	0.0	0	0
L	0.0	0	0	0.0	0	0	0.0	0	0	0.0	0	0
L	0.0	0	0	0.0	0	0	0.0	0	0	0.0	0	0

Cell		105			106			107			108	
	poro	perm	Sw	poro	perm	Sw	poro	perm	Sw	poro	perm	Sw
D	0.0	0	0	0.0	0	0	0.0	0	0	0.0	0	0
D	0.0	0	0	0.0	0	0	0.0	0	0	0.0	0	0
D	0.0	0	0	0.0	0	0	0.0	0	0	0.0	0	0
D	0.0	0	0	0.0	0	0	0.0	0	0	0.0	0	0
(I S)	–	–	–	–	–	–	–	–	–	–	–	–
I	0.0	0	0	0.0	0	0	6.0	4	37	7.0	9	30
I	0.0	0	0	0.0	0	0	0.0	0	0	0.0	0	0
I	0.0	0	0	0.0	0	0	0.0	0	0	0.0	0	0
(J US)	–	–	–	–	–	–	–	–	–	–	–	–
J c	0.0	0	0	0.0	0	0	0.0	0	0	0.0	0	0
(i.c.)	–	–	–	–	–	–	–	–	–	–	–	–
J ag	16.0	79	22	16.5	85	21	16.5	85	21	16.5	85	21
J ag	19.0	127	17	19.5	138	16	19.5	138	16	17.5	100	19
J ag	18.5	117	18	19.0	127	17	19.0	127	17	18.5	117	18
J ag	19.0	127	17	19.5	138	16	19.5	138	16	18.0	108	18
J ag	14.0	57	27	14.5	62	26	14.5	62	26	14.0	57	27
J ag	0.0	0	0	0.0	0	0	0.0	0	0	0.0	0	0
(i.c.)	–	–	–	–	–	–	–	–	–	–	–	–
J b	0.0	0	0	0.0	0	0	0.0	0	0	0.0	0	0
J b	0.0	0	0	0.0	0	0	0.0	0	0	0.0	0	0
(K US)	–	–	–	–	–	–	–	–	–	–	–	–
K cc	0.0	0	0	6.5	2	53	6.5	2	53	0.0	0	0
(K s)	–	–	–	–	–	–	–	–	–	–	–	–
K bc	6.5	2	53	8.0	3	48	8.0	3	48	8.0	3	48
K bc	0.0	0	0	8.0	3	48	8.5	4	46	8.0	3	48
K bc	0.0	0	0	0.0	0	0	0.0	0	0	0.0	0	0
(L US)	–	–	–	–	–	–	–	–	–	–	–	–
L	8.5	15	46	6.0	4	56	0.0	0	0	0.0	0	0
L	9.5	25	44	0.0	0	0	0.0	0	0	0.0	0	0
L	7.5	9	49	0.0	0	0	0.0	0	0	0.0	0	0
L	0.0	0	0	0.0	0	0	0.0	0	0	0.0	0	0
L	0.0	0	0	0.0	0	0	0.0	0	0	0.0	0	0
L	0.0	0	0	0.0	0	0	0.0	0	0	0.0	0	0

Cell	109			110			111			112		
	poro	perm	Sw	poro	perm	Sw	poro	perm	Sw	poro	perm	Sw
D	0.0	0	0	0.0	0	0	0.0	0	0	0.0	0	0
D	0.0	0	0	0.0	0	0	0.0	0	0	0.0	0	0
D	0.0	0	0	0.0	0	0	0.0	0	0	0.0	0	0
D	0.0	0	0	0.0	0	0	0.0	0	0	0.0	0	0
(I S)	–	–	–	–	–	–	–	–	–	–	–	–
I	7.5	13	28	7.5	13	28	8.5	27	24	8.5	27	24
I	8.5	27	24	8.5	27	24	8.0	19	26	8.0	19	26
I	0.0	0	0	0.0	0	0	0.0	0	0	0.0	0	0
(J US)	–	–	–	–	–	–	–	–	–	–	–	–
J c	0.0	0	0	0.0	0	0	0.0	0	0	0.0	0	0
(i.c.)	–	–	–	–	–	–	–	–	–	–	–	–
J ag	16.0	79	22	16.0	79	22	16.0	79	22	15.0	67	25
J ag	17.5	100	19	17.5	100	19	17.0	92	20	16.0	79	22
J ag	17.0	92	20	16.5	85	21	15.5	73	23	13.5	53	29
J ag	14.0	57	27	13.0	49	30	12.0	42	34	0.0	0	0
J ag	0.0	0	0	0.0	0	0	0.0	0	0	0.0	0	0
J ag	0.0	0	0	0.0	0	0	0.0	0	0	0.0	0	0
(i.c.)	–	–	–	–	–	–	–	–	–	–	–	–
J b	0.0	0	0	0.0	0	0	0.0	0	0	0.0	0	0
J b	0.0	0	0	0.0	0	0	0.0	0	0	0.0	0	0
(K US)	–	–	–	–	–	–	–	–	–	–	–	–
K cc	0.0	0	0	0.0	0	0	0.0	0	0	0.0	0	0
(K s)	–	–	–	–	–	–	–	–	–	–	–	–
K bc	7.5	3	49	8.0	3	48	8.0	3	48	8.0	3	48
K bc	8.0	3	48	8.0	3	48	8.5	4	46	8.0	3	48
K bc	0.0	0	0	0.0	0	0	0.0	0	0	0.0	0	0
(L US)	–	–	–	–	–	–	–	–	–	–	–	–
L	0.0	0	0	0.0	0	0	0.0	0	0	0.0	0	0
L	0.0	0	0	0.0	0	0	0.0	0	0	0.0	0	0
L	0.0	0	0	0.0	0	0	0.0	0	0	0.0	0	0
L	0.0	0	0	0.0	0	0	0.0	0	0	0.0	0	0
L	0.0	0	0	0.0	0	0	0.0	0	0	0.0	0	0
L	0.0	0	0	0.0	0	0	0.0	0	0	0.0	0	0

Cell	113			114			115			116		
	poro	perm	Sw	poro	perm	Sw	poro	perm	Sw	poro	perm	Sw
D	0.0	0	0	0.0	0	0	0.0	0	0	0.0	0	0
D	0.0	0	0	0.0	0	0	0.0	0	0	0.0	0	0
D	0.0	0	0	0.0	0	0	0.0	0	0	0.0	0	0
D	0.0	0	0	0.0	0	0	0.0	0	0	0.0	0	0
(I S)	–	–	–	–	–	–	–	–	–	–	–	–
I	7.5	13	28	7.0	9	30	0.0	0	0	0.0	0	0
I	0.0	0	0	0.0	0	0	0.0	0	0	0.0	0	0
I	0.0	0	0	0.0	0	0	0.0	0	0	0.0	0	0
(J US)	–	–	–	–	–	–	–	–	–	–	–	–
J c	0.0	0	0	0.0	0	0	8.0	19	26	0.0	0	0
(i.c.)	–	–	–	–	–	–	–	–	–	–	–	–
J ag	7.0	19	67	0.0	0	0	0.0	0	0	0.0	0	0
J ag	0.0	0	0	0.0	0	0	0.0	0	0	0.0	0	0
J ag	0.0	0	0	0.0	0	0	0.0	0	0	0.0	0	0
J ag	0.0	0	0	0.0	0	0	0.0	0	0	0.0	0	0
J ag	0.0	0	0	0.0	0	0	0.0	0	0	0.0	0	0
J ag	0.0	0	0	0.0	0	0	0.0	0	0	0.0	0	0
(i.c.)	–	–	–	–	–	–	–	–	–	–	–	–
J b	0.0	0	0	0.0	0	0	0.0	0	0	0.0	0	0
J b	0.0	0	0	0.0	0	0	0.0	0	0	0.0	0	0
(K US)	–	–	–	–	–	–	–	–	–	–	–	–
K cc	0.0	0	0	0.0	0	0	0.0	0	0	0.0	0	0
(K s)	–	–	–	–	–	–	–	–	–	–	–	–
K bc	7.5	3	49	0.0	0	0	0.0	0	0	7.0	2	51
K bc	0.0	0	0	0.0	0	0	0.0	0	0	0.0	0	0
K bc	0.0	0	0	0.0	0	0	0.0	0	0	0.0	0	0
(L US)	–	–	–	–	–	–	–	–	–	–	–	–
L	0.0	0	0	0.0	0	0	5.5	3	59	0.0	0	0
L	0.0	0	0	0.0	0	0	0.0	0	0	0.0	0	0
L	0.0	0	0	0.0	0	0	0.0	0	0	0.0	0	0
L	0.0	0	0	0.0	0	0	0.0	0	0	0.0	0	0
L	0.0	0	0	0.0	0	0	0.0	0	0	0.0	0	0
L	0.0	0	0	0.0	0	0	0.0	0	0	0.0	0	0

Cell	117			118			119			120		
	poro	perm	Sw	poro	perm	Sw	poro	perm	Sw	poro	perm	Sw
D	0.0	0	0	0.0	0	0	0.0	0	0	0.0	0	0
D	0.0	0	0	0.0	0	0	0.0	0	0	0.0	0	0
D	0.0	0	0	0.0	0	0	0.0	0	0	0.0	0	0
D	0.0	0	0	0.0	0	0	0.0	0	0	0.0	0	0
(I S)	–	–	–	–	–	–	–	–	–	–	–	–
I	0.0	0	0	6.0	4	37	6.0	4	37	7.0	9	30
I	0.0	0	0	0.0	0	0	6.5	6	33	7.0	9	30
I	0.0	0	0	0.0	0	0	0.0	0	0	7.5	13	28
(J US)	–	–	–	–	–	–	–	–	–	–	–	–
J c	0.0	0	0	0.0	0	0	0.0	0	0	0.0	0	0
(i.c.)	–	–	–	–	–	–	–	–	–	–	–	–
J ag	0.0	0	0	7.0	19	67	10.0	30	43	10.5	33	41
J ag	0.0	0	0	7.5	20	62	11.0	36	38	13.0	49	30
J ag	0.0	0	0	0.0	0	0	0.0	0	0	11.5	39	36
J ag	0.0	0	0	0.0	0	0	0.0	0	0	0.0	0	0
J ag	0.0	0	0	0.0	0	0	0.0	0	0	0.0	0	0
J ag	0.0	0	0	0.0	0	0	0.0	0	0	0.0	0	0
(i.c.)	–	–	–	–	–	–	–	–	–	–	–	–
J b	0.0	0	0	0.0	0	0	0.0	0	0	0.0	0	0
J b	0.0	0	0	0.0	0	0	0.0	0	0	0.0	0	0
(K US)	–	–	–	–	–	–	–	–	–	–	–	–
K cc	0.0	0	0	0.0	0	0	0.0	0	0	0.0	0	0
(K s)	–	–	–	–	–	–	–	–	–	–	–	–
K bc	7.0	2	51	0.0	0	0	0.0	0	0	0.0	0	0
K bc	0.0	0	0	0.0	0	0	0.0	0	0	0.0	0	0
K bc	0.0	0	0	0.0	0	0	0.0	0	0	0.0	0	0
(L US)	–	–	–	–	–	–	–	–	–	–	–	–
L	0.0	0	0	0.0	0	0	5.0	2	63	6.5	5	53
L	0.0	0	0	0.0	0	0	0.0	0	0	5.5	3	59
L	0.0	0	0	0.0	0	0	0.0	0	0	0.0	0	0
L	0.0	0	0	0.0	0	0	0.0	0	0	0.0	0	0
L	0.0	0	0	0.0	0	0	0.0	0	0	0.0	0	0
L	0.0	0	0	0.0	0	0	0.0	0	0	0.0	0	0

Cell		121			122			123			124	
	poro	perm	Sw	poro	perm	Sw	poro	perm	Sw	poro	perm	Sw
D	0.0	0	0	0.0	0	0	0.0	0	0	0.0	0	0
D	0.0	0	0	0.0	0	0	0.0	0	0	0.0	0	0
D	0.0	0	0	0.0	0	0	0.0	0	0	0.0	0	0
D	0.0	0	0	0.0	0	0	0.0	0	0	0.0	0	0
(I S)	–	–	–	–	–	–	–	–	–	–	–	–
I	7.5	13	28	5.5	3	40	0.0	0	0	0.0	0	0
I	7.0	9	30	0.0	0	0	0.0	0	0	0.0	0	0
I	7.5	13	28	0.0	0	0	0.0	0	0	0.0	0	0
(J US)	–	–	–	–	–	–	–	–	–	–	–	–
J c	0.0	0	0	0.0	0	0	0.0	0	0	0.0	0	0
(i.c.)	–	–	–	–	–	–	–	–	–	–	–	–
J ag	13.0	49	30	14.0	57	27	14.0	57	27	15.5	73	23
J ag	14.0	57	27	14.5	62	26	14.5	62	26	16.0	79	22
J ag	16.0	79	22	15.5	73	23	15.5	73	23	16.0	79	22
J ag	15.0	67	25	14.0	57	27	14.0	57	27	14.0	57	27
J ag	0.0	0	0	10.0	30	43	10.0	30	43	10.5	33	41
J ag	0.0	0	0	0.0	0	0	0.0	0	0	0.0	0	0
(i.c.)	–	–	–	–	–	–	–	–	–	–	–	–
J b	0.0	0	0	0.0	0	0	0.0	0	0	0.0	0	0
J b	0.0	0	0	0.0	0	0	0.0	0	0	0.0	0	0
(K US)	–	–	–	–	–	–	–	–	–	–	–	–
K cc	0.0	0	0	0.0	0	0	0.0	0	0	6.5	2	53
(K s)	–	–	–	–	–	–	–	–	–	–	–	–
K bc	0.0	0	0	0.0	0	0	6.5	2	53	8.0	3	48
K bc	0.0	0	0	0.0	0	0	0.0	0	0	8.0	3	48
K bc	0.0	0	0	0.0	0	0	0.0	0	0	0.0	0	0
(L US)	–	–	–	–	–	–	–	–	–	–	–	–
L	5.5	3	59	5.5	3	59	5.5	3	59	0.0	0	0
L	7.0	7	51	7.0	7	51	0.0	0	0	0.0	0	0
L	6.0	4	56	6.0	4	56	0.0	0	0	0.0	0	0
L	0.0	0	0	0.0	0	0	0.0	0	0	0.0	0	0
L	0.0	0	0	0.0	0	0	0.0	0	0	0.0	0	0
L	0.0	0	0	0.0	0	0	0.0	0	0	0.0	0	0

Cell	125			126			127			128		
	poro	perm	Sw	poro	perm	Sw	poro	perm	Sw	poro	perm	Sw
D	0.0	0	0	0.0	0	0	0.0	0	0	0.0	0	0
D	0.0	0	0	0.0	0	0	0.0	0	0	0.0	0	0
D	0.0	0	0	0.0	0	0	0.0	0	0	0.0	0	0
D	0.0	0	0	0.0	0	0	0.0	0	0	0.0	0	0
(I S)	–	–	–	–	–	–	–	–	–	–	–	–
I	0.0	0	0	0.0	0	0	6.0	4	37	6.0	4	37
I	0.0	0	0	0.0	0	0	0.0	0	0	0.0	0	0
I	0.0	0	0	0.0	0	0	0.0	0	0	0.0	0	0
(J US)	–	–	–	–	–	–	–	–	–	–	–	–
J c	0.0	0	0	0.0	0	0	0.0	0	0	0.0	0	0
(i.c.)	–	–	–	–	–	–	–	–	–	–	–	–
J ag	16.0	79	22	16.5	85	21	16.5	85	21	16.0	79	22
J ag	16.5	85	21	17.0	92	20	17.0	92	20	16.5	85	21
J ag	16.5	85	21	16.5	85	21	16.5	85	21	16.0	79	22
J ag	14.0	57	27	14.0	57	27	14.0	57	27	13.5	53	29
J ag	10.5	33	41	11.0	36	38	0.0	0	0	0.0	0	0
J ag	0.0	0	0	0.0	0	0	0.0	0	0	0.0	0	0
(i.c.)	–	–	–	–	–	–	–	–	–	–	–	–
J b	0.0	0	0	0.0	0	0	0.0	0	0	0.0	0	0
J b	0.0	0	0	0.0	0	0	0.0	0	0	0.0	0	0
(K US)	–	–	–	–	–	–	–	–	–	–	–	–
K cc	6.5	2	53	0.0	0	0	0.0	0	0	0.0	0	0
(K s)	–	–	–	–	–	–	–	–	–	–	–	–
K bc	8.0	3	48	8.0	3	48	8.0	3	48	8.0	3	48
K bc	8.5	4	46	8.5	4	46	8.5	4	46	8.5	4	46
K bc	0.0	0	0	0.0	0	0	0.0	0	0	0.0	0	0
(L US)	–	–	–	–	–	–	–	–	–	–	–	–
L	0.0	0	0	0.0	0	0	0.0	0	0	0.0	0	0
L	0.0	0	0	0.0	0	0	0.0	0	0	0.0	0	0
L	0.0	0	0	0.0	0	0	0.0	0	0	0.0	0	0
L	0.0	0	0	0.0	0	0	0.0	0	0	0.0	0	0
L	0.0	0	0	0.0	0	0	0.0	0	0	0.0	0	0
L	0.0	0	0	0.0	0	0	0.0	0	0	0.0	0	0

Cell	129			130			131			132		
	poro	perm	Sw	poro	perm	Sw	poro	perm	Sw	poro	perm	Sw
D	0.0	0	0	0.0	0	0	0.0	0	0	0.0	0	0
D	0.0	0	0	0.0	0	0	0.0	0	0	0.0	0	0
D	0.0	0	0	0.0	0	0	0.0	0	0	0.0	0	0
D	0.0	0	0	0.0	0	0	0.0	0	0	0.0	0	0
(I S)	–	–	–	–	–	–	–	–	–	–	–	–
I	6.0	4	37	6.0	4	37	0.0	0	0	0.0	0	0
I	0.0	0	0	0.0	0	0	0.0	0	0	0.0	0	0
I	0.0	0	0	0.0	0	0	0.0	0	0	0.0	0	0
(J US)	–	–	–	–	–	–	–	–	–	–	–	–
J c	0.0	0	0	0.0	0	0	0.0	0	0	0.0	0	0
(i.c.)	–	–	–	–	–	–	–	–	–	–	–	–
J ag	14.0	57	27	7.0	19	67	0.0	0	0	0.0	0	0
J ag	14.0	57	27	0.0	0	0	0.0	0	0	0.0	0	0
J ag	11.0	36	38	0.0	0	0	0.0	0	0	0.0	0	0
J ag	0.0	0	0	0.0	0	0	0.0	0	0	0.0	0	0
J ag	0.0	0	0	0.0	0	0	0.0	0	0	0.0	0	0
J ag	0.0	0	0	0.0	0	0	0.0	0	0	0.0	0	0
(i.c.)	–	–	–	–	–	–	–	–	–	–	–	–
J b	0.0	0	0	0.0	0	0	0.0	0	0	0.0	0	0
J b	0.0	0	0	0.0	0	0	0.0	0	0	0.0	0	0
(K US)	–	–	–	–	–	–	–	–	–	–	–	–
K cc	0.0	0	0	0.0	0	0	0.0	0	0	0.0	0	0
(K s)	–	–	–	–	–	–	–	–	–	–	–	–
K bc	8.5	4	46	8.0	3	48	7.5	3	49	6.5	2	53
K bc	8.5	4	46	8.5	4	46	7.5	3	49	0.0	0	0
K bc	0.0	0	0	0.0	0	0	0.0	0	0	0.0	0	0
(L US)	–	–	–	–	–	–	–	–	–	–	–	–
L	0.0	0	0	0.0	0	0	0.0	0	0	0.0	0	0
L	0.0	0	0	0.0	0	0	0.0	0	0	0.0	0	0
L	0.0	0	0	0.0	0	0	0.0	0	0	0.0	0	0
L	0.0	0	0	0.0	0	0	0.0	0	0	0.0	0	0
L	0.0	0	0	0.0	0	0	0.0	0	0	0.0	0	0
L	0.0	0	0	0.0	0	0	0.0	0	0	0.0	0	0

Cell	133			134			135			136		
	poro	perm	Sw	poro	perm	Sw	poro	perm	Sw	poro	perm	Sw
D	0.0	0	0	0.0	0	0	0.0	0	0	0.0	0	0
D	0.0	0	0	0.0	0	0	0.0	0	0	0.0	0	0
D	0.0	0	0	0.0	0	0	0.0	0	0	0.0	0	0
D	0.0	0	0	0.0	0	0	0.0	0	0	0.0	0	0
(I S)	–	–	–	–	–	–	–	–	–	–	–	–
I	0.0	0	0	0.0	0	0	0.0	0	0	0.0	0	0
I	0.0	0	0	0.0	0	0	0.0	0	0	0.0	0	0
I	0.0	0	0	0.0	0	0	0.0	0	0	0.0	0	0
(J US)	–	–	–	–	–	–	–	–	–	–	–	–
J c	0.0	0	0	0.0	0	0	0.0	0	0	0.0	0	0
(i.c.)	–	–	–	–	–	–	–	–	–	–	–	–
J ag	0.0	0	0	0.0	0	0	7.0	19	67	7.0	19	67
J ag	0.0	0	0	0.0	0	0	0.0	0	0	0.0	0	0
J ag	0.0	0	0	0.0	0	0	0.0	0	0	0.0	0	0
J ag	0.0	0	0	0.0	0	0	0.0	0	0	0.0	0	0
J ag	0.0	0	0	0.0	0	0	0.0	0	0	0.0	0	0
J ag	0.0	0	0	0.0	0	0	0.0	0	0	0.0	0	0
(i.c.)	–	–	–	–	–	–	–	–	–	–	–	–
J b	0.0	0	0	0.0	0	0	0.0	0	0	0.0	0	0
J b	0.0	0	0	0.0	0	0	0.0	0	0	0.0	0	0
(K US)	–	–	–	–	–	–	–	–	–	–	–	–
K cc	0.0	0	0	0.0	0	0	0.0	0	0	0.0	0	0
(K s)	–	–	–	–	–	–	–	–	–	–	–	–
K bc	0.0	0	0	6.5	2	53	7.0	2	51	7.5	3	49
K bc	0.0	0	0	0.0	0	0	0.0	0	0	0.0	0	0
K bc	0.0	0	0	0.0	0	0	0.0	0	0	0.0	0	0
(L US)	–	–	–	–	–	–	–	–	–	–	–	–
L	5.0	2	63	5.0	2	63	5.5	3	59	5.0	2	63
L	0.0	0	0	0.0	0	0	0.0	0	0	0.0	0	0
L	0.0	0	0	0.0	0	0	0.0	0	0	0.0	0	0
L	0.0	0	0	0.0	0	0	0.0	0	0	0.0	0	0
L	0.0	0	0	0.0	0	0	0.0	0	0	0.0	0	0
L	0.0	0	0	0.0	0	0	0.0	0	0	0.0	0	0

Cell		137			138			139			140	
	poro	perm	Sw	poro	perm	Sw	poro	perm	Sw	poro	perm	Sw
D	0.0	0	0	0.0	0	0	0.0	0	0	0.0	0	0
D	0.0	0	0	0.0	0	0	0.0	0	0	0.0	0	0
D	0.0	0	0	0.0	0	0	0.0	0	0	0.0	0	0
D	0.0	0	0	0.0	0	0	0.0	0	0	0.0	0	0
(I S)	–	–	–	–	–	–	–	–	–	–	–	–
I	0.0	0	0	0.0	0	0	5.0	2	45	5.0	2	45
I	0.0	0	0	0.0	0	0	0.0	0	0	5.5	3	40
I	0.0	0	0	0.0	0	0	0.0	0	0	0.0	0	0
(J US)	–	–	–	–	–	–	–	–	–	–	–	–
J c	0.0	0	0	0.0	0	0	0.0	0	0	0.0	0	0
(i.c.)	–	–	–	–	–	–	–	–	–	–	–	–
J ag	7.0	19	67	7.5	20	62	8.0	22	57	10.0	30	43
J ag	0.0	0	0	0.0	0	0	8.5	24	53	11.0	36	38
J ag	0.0	0	0	0.0	0	0	0.0	0	0	12.0	42	34
J ag	0.0	0	0	0.0	0	0	0.0	0	0	0.0	0	0
J ag	0.0	0	0	0.0	0	0	0.0	0	0	0.0	0	0
J ag	0.0	0	0	0.0	0	0	0.0	0	0	0.0	0	0
(i.c.)	–	–	–	–	–	–	–	–	–	–	–	–
J b	0.0	0	0	0.0	0	0	0.0	0	0	0.0	0	0
J b	0.0	0	0	0.0	0	0	0.0	0	0	0.0	0	0
(K US)	–	–	–	–	–	–	–	–	–	–	–	–
K cc	0.0	0	0	0.0	0	0	0.0	0	0	0.0	0	0
(K s)	–	–	–	–	–	–	–	–	–	–	–	–
K bc	6.5	2	53	0.0	0	0	0.0	0	0	0.0	0	0
K bc	0.0	0	0	0.0	0	0	0.0	0	0	0.0	0	0
K bc	0.0	0	0	0.0	0	0	0.0	0	0	0.0	0	0
(L US)	–	–	–	–	–	–	–	–	–	–	–	–
L	0.0	0	0	0.0	0	0	6.0	4	56	5.0	2	63
L	0.0	0	0	0.0	0	0	0.0	0	0	7.0	7	51
L	0.0	0	0	0.0	0	0	0.0	0	0	6.0	4	56
L	0.0	0	0	0.0	0	0	0.0	0	0	0.0	0	0
L	0.0	0	0	0.0	0	0	0.0	0	0	0.0	0	0
L	0.0	0	0	0.0	0	0	0.0	0	0	0.0	0	0

Cell		141			142			143			144	
	poro	perm	Sw	poro	perm	Sw	poro	perm	Sw	poro	perm	Sw
D	0.0	0	0	0.0	0	0	0.0	0	0	0.0	0	0
D	0.0	0	0	0.0	0	0	0.0	0	0	0.0	0	0
D	0.0	0	0	0.0	0	0	0.0	0	0	0.0	0	0
D	0.0	0	0	0.0	0	0	0.0	0	0	0.0	0	0
(I S)	–	–	–	–	–	–	–	–	–	–	–	–
I	5.0	2	45	5.0	2	45	0.0	0	0	0.0	0	0
I	5.5	3	40	0.0	0	0	0.0	0	0	0.0	0	0
I	0.0	0	0	0.0	0	0	0.0	0	0	0.0	0	0
(J US)	–	–	–	–	–	–	–	–	–	–	–	–
J c	0.0	0	0	0.0	0	0	0.0	0	0	0.0	0	0
(i.c.)	–	–	–	–	–	–	–	–	–	–	–	–
J ag	13.0	49	30	14.0	57	27	15.0	67	25	15.5	73	23
J ag	14.0	57	27	14.5	62	26	14.5	62	26	15.0	67	25
J ag	16.0	79	22	15.5	73	23	15.5	73	23	15.0	67	25
J ag	15.0	67	25	14.0	57	27	13.0	49	30	12.0	42	34
J ag	0.0	0	0	10.0	30	43	10.0	30	43	10.0	30	43
J ag	0.0	0	0	0.0	0	0	0.0	0	0	0.0	0	0
(i.c.)	–	–	–	–	–	–	–	–	–	–	–	–
J b	0.0	0	0	0.0	0	0	0.0	0	0	0.0	0	0
J b	0.0	0	0	0.0	0	0	0.0	0	0	0.0	0	0
(K US)	–	–	–	–	–	–	–	–	–	–	–	–
K cc	0.0	0	0	0.0	0	0	0.0	0	0	6.5	2	53
(K s)	–	–	–	–	–	–	–	–	–	–	–	–
K bc	0.0	0	0	0.0	0	0	7.0	2	51	8.0	3	48
K bc	0.0	0	0	0.0	0	0	0.0	0	0	8.0	3	48
K bc	0.0	0	0	0.0	0	0	0.0	0	0	0.0	0	0
(L US)	–	–	–	–	–	–	–	–	–	–	–	–
L	5.0	2	63	6.5	5	53	0.0	0	0	0.0	0	0
L	7.0	7	51	5.5	3	59	0.0	0	0	0.0	0	0
L	6.0	4	56	0.0	0	0	0.0	0	0	0.0	0	0
L	5.0	2	63	0.0	0	0	0.0	0	0	0.0	0	0
L	0.0	0	0	0.0	0	0	0.0	0	0	0.0	0	0
L	0.0	0	0	0.0	0	0	0.0	0	0	0.0	0	0

Cell	145			146			147			148		
	poro	perm	Sw	poro	perm	Sw	poro	perm	Sw	poro	perm	Sw
D	0.0	0	0	0.0	0	0	0.0	0	0	0.0	0	0
D	0.0	0	0	0.0	0	0	0.0	0	0	0.0	0	0
D	0.0	0	0	0.0	0	0	0.0	0	0	0.0	0	0
D	0.0	0	0	0.0	0	0	0.0	0	0	0.0	0	0
(I S)	–	–	–	–	–	–	–	–	–	–	–	–
I	0.0	0	0	0.0	0	0	0.0	0	0	0.0	0	0
I	0.0	0	0	0.0	0	0	0.0	0	0	0.0	0	0
I	0.0	0	0	0.0	0	0	0.0	0	0	0.0	0	0
(J US)	–	–	–	–	–	–	–	–	–	–	–	–
J c	0.0	0	0	0.0	0	0	0.0	0	0	0.0	0	0
(i.c.)	–	–	–	–	–	–	–	–	–	–	–	–
J ag	16.5	85	21	18.0	108	18	19.0	127	17	15.0	67	25
J ag	16.0	79	22	17.0	92	20	18.5	117	18	15.0	67	25
J ag	15.0	67	25	15.5	73	23	15.5	73	23	12.0	42	34
J ag	12.0	42	34	12.0	42	34	11.0	36	38	0.0	0	0
J ag	10.0	30	43	9.0	26	50	0.0	0	0	0.0	0	0
J ag	0.0	0	0	0.0	0	0	0.0	0	0	0.0	0	0
(i.c.)	–	–	–	–	–	–	–	–	–	–	–	–
J b	0.0	0	0	0.0	0	0	0.0	0	0	0.0	0	0
J b	0.0	0	0	0.0	0	0	0.0	0	0	0.0	0	0
(K US)	–	–	–	–	–	–	–	–	–	–	–	–
K cc	6.5	2	53	0.0	0	0	0.0	0	0	0.0	0	0
(K s)	–	–	–	–	–	–	–	–	–	–	–	–
K bc	8.0	3	48	8.0	3	48	8.0	3	48	8.0	3	48
K bc	8.5	4	46	8.0	3	48	8.0	3	48	8.5	4	46
K bc	0.0	0	0	0.0	0	0	0.0	0	0	0.0	0	0
(L US)	–	–	–	–	–	–	–	–	–	–	–	–
L	0.0	0	0	0.0	0	0	7.0	7	51	0.0	0	0
L	0.0	0	0	0.0	0	0	0.0	0	0	0.0	0	0
L	0.0	0	0	0.0	0	0	0.0	0	0	0.0	0	0
L	0.0	0	0	0.0	0	0	0.0	0	0	0.0	0	0
L	0.0	0	0	0.0	0	0	0.0	0	0	0.0	0	0
L	0.0	0	0	0.0	0	0	0.0	0	0	0.0	0	0

Cell		149			150			151			152	
	poro	perm	Sw	poro	perm	Sw	poro	perm	Sw	poro	perm	Sw
D	0.0	0	0	0.0	0	0	0.0	0	0	0.0	0	0
D	0.0	0	0	0.0	0	0	0.0	0	0	0.0	0	0
D	0.0	0	0	0.0	0	0	0.0	0	0	0.0	0	0
D	0.0	0	0	0.0	0	0	0.0	0	0	0.0	0	0
(I S)	–	–	–	–	–	–	–	–	–	–	–	–
I	0.0	0	0	0.0	0	0	0.0	0	0	0.0	0	0
I	0.0	0	0	0.0	0	0	0.0	0	0	0.0	0	0
I	0.0	0	0	0.0	0	0	0.0	0	0	0.0	0	0
(J US)	–	–	–	–	–	–	–	–	–	–	–	–
J c	0.0	0	0	0.0	0	0	0.0	0	0	0.0	0	0
(i.c.)	–	–	–	–	–	–	–	–	–	–	–	–
J ag	7.0	19	67	0.0	0	0	0.0	0	0	0.0	0	0
J ag	0.0	0	0	0.0	0	0	0.0	0	0	0.0	0	0
J ag	0.0	0	0	0.0	0	0	0.0	0	0	0.0	0	0
J ag	0.0	0	0	0.0	0	0	0.0	0	0	0.0	0	0
J ag	0.0	0	0	0.0	0	0	0.0	0	0	0.0	0	0
J ag	0.0	0	0	0.0	0	0	0.0	0	0	0.0	0	0
(i.c.)	–	–	–	–	–	–	–	–	–	–	–	–
J b	0.0	0	0	0.0	0	0	0.0	0	0	0.0	0	0
J b	0.0	0	0	0.0	0	0	0.0	0	0	0.0	0	0
(K US)	–	–	–	–	–	–	–	–	–	–	–	–
K cc	0.0	0	0	0.0	0	0	0.0	0	0	0.0	0	0
(K s)	–	–	–	–	–	–	–	–	–	–	–	–
K bc	8.5	4	46	8.5	4	46	8.0	3	48	6.5	2	53
K bc	8.5	4	46	9.0	5	45	8.0	3	48	0.0	0	0
K bc	0.0	0	0	8.5	4	46	0.0	0	0	0.0	0	0
(L US)	–	–	–	–	–	–	–	–	–	–	–	–
L	0.0	0	0	0.0	0	0	0.0	0	0	0.0	0	0
L	0.0	0	0	0.0	0	0	0.0	0	0	0.0	0	0
L	0.0	0	0	0.0	0	0	0.0	0	0	0.0	0	0
L	0.0	0	0	0.0	0	0	0.0	0	0	0.0	0	0
L	0.0	0	0	0.0	0	0	0.0	0	0	0.0	0	0
L	0.0	0	0	0.0	0	0	0.0	0	0	0.0	0	0

Cell	153			154			155			156		
	poro	perm	Sw	poro	perm	Sw	poro	perm	Sw	poro	perm	Sw
D	0.0	0	0	0.0	0	0	0.0	0	0	0.0	0	0
D	0.0	0	0	0.0	0	0	0.0	0	0	0.0	0	0
D	0.0	0	0	0.0	0	0	0.0	0	0	0.0	0	0
D	0.0	0	0	0.0	0	0	0.0	0	0	0.0	0	0
(I S)	–	–	–	–	–	–	–	–	–	–	–	–
I	0.0	0	0	0.0	0	0	0.0	0	0	0.0	0	0
I	0.0	0	0	0.0	0	0	0.0	0	0	0.0	0	0
I	0.0	0	0	0.0	0	0	0.0	0	0	0.0	0	0
(J US)	–	–	–	–	–	–	–	–	–	–	–	–
J c	0.0	0	0	0.0	0	0	0.0	0	0	0.0	0	0
(i.c.)	–	–	–	–	–	–	–	–	–	–	–	–
J ag	0.0	0	0	0.0	0	0	7.5	20	62	8.0	22	57
J ag	0.0	0	0	0.0	0	0	7.5	20	62	7.5	20	62
J ag	0.0	0	0	0.0	0	0	0.0	0	0	0.0	0	0
J ag	0.0	0	0	0.0	0	0	0.0	0	0	0.0	0	0
J ag	0.0	0	0	0.0	0	0	0.0	0	0	0.0	0	0
J ag	0.0	0	0	0.0	0	0	0.0	0	0	0.0	0	0
(i.c.)	–	–	–	–	–	–	–	–	–	–	–	–
J b	0.0	0	0	0.0	0	0	0.0	0	0	0.0	0	0
J b	0.0	0	0	0.0	0	0	0.0	0	0	0.0	0	0
(K US)	–	–	–	–	–	–	–	–	–	–	–	–
K cc	0.0	0	0	0.0	0	0	0.0	0	0	0.0	0	0
(K s)	–	–	–	–	–	–	–	–	–	–	–	–
K bc	0.0	0	0	6.5	2	53	7.0	2	51	7.5	3	49
K bc	0.0	0	0	0.0	0	0	0.0	0	0	0.0	0	0
K bc	0.0	0	0	0.0	0	0	0.0	0	0	0.0	0	0
(L US)	–	–	–	–	–	–	–	–	–	–	–	–
L	6.0	4	56	7.0	7	51	7.0	7	51	7.0	7	51
L	6.0	4	56	6.5	5	53	7.0	7	51	7.5	9	49
L	0.0	0	0	7.0	7	51	7.0	7	51	7.5	9	49
L	0.0	0	0	0.0	0	0	7.0	7	51	7.0	7	51
L	0.0	0	0	0.0	0	0	0.0	0	0	0.0	0	0
L	0.0	0	0	0.0	0	0	0.0	0	0	0.0	0	0

Cell	157			158			159			160		
	poro	perm	Sw	poro	perm	Sw	poro	perm	Sw	poro	perm	Sw
D	0.0	0	0	0.0	0	0	0.0	0	0	0.0	0	0
D	0.0	0	0	0.0	0	0	0.0	0	0	0.0	0	0
D	0.0	0	0	0.0	0	0	0.0	0	0	0.0	0	0
D	0.0	0	0	0.0	0	0	0.0	0	0	0.0	0	0
(I S)	–	–	–	–	–	–	–	–	–	–	–	–
I	0.0	0	0	0.0	0	0	0.0	0	0	0.0	0	0
I	0.0	0	0	0.0	0	0	0.0	0	0	0.0	0	0
I	0.0	0	0	0.0	0	0	0.0	0	0	0.0	0	0
(J US)	–	–	–	–	–	–	–	–	–	–	–	–
J c	0.0	0	0	0.0	0	0	0.0	0	0	0.0	0	0
(i.c.)	–	–	–	–	–	–	–	–	–	–	–	–
J ag	8.0	22	57	7.5	20	62	7.5	20	62	12.5	45	32
J ag	7.5	20	62	7.5	20	62	7.5	20	62	16.0	79	22
J ag	0.0	0	0	0.0	0	0	0.0	0	0	14.5	62	26
J ag	0.0	0	0	0.0	0	0	0.0	0	0	0.0	0	0
J ag	0.0	0	0	0.0	0	0	0.0	0	0	0.0	0	0
J ag	0.0	0	0	0.0	0	0	0.0	0	0	0.0	0	0
(i.c.)	–	–	–	–	–	–	–	–	–	–	–	–
J b	0.0	0	0	0.0	0	0	0.0	0	0	0.0	0	0
J b	0.0	0	0	0.0	0	0	0.0	0	0	0.0	0	0
(K US)	–	–	–	–	–	–	–	–	–	–	–	–
K cc	0.0	0	0	0.0	0	0	0.0	0	0	0.0	0	0
(K s)	–	–	–	–	–	–	–	–	–	–	–	–
K bc	7.0	2	51	6.5	2	53	0.0	0	0	0.0	0	0
K bc	0.0	0	0	0.0	0	0	0.0	0	0	0.0	0	0
K bc	0.0	0	0	0.0	0	0	0.0	0	0	0.0	0	0
(L US)	–	–	–	–	–	–	–	–	–	–	–	–
L	6.5	5	53	6.0	4	56	5.5	3	59	6.0	4	56
L	7.0	7	51	6.5	5	53	0.0	0	0	0.0	0	0
L	6.5	5	53	0.0	0	0	0.0	0	0	0.0	0	0
L	0.0	0	0	0.0	0	0	0.0	0	0	0.0	0	0
L	0.0	0	0	0.0	0	0	0.0	0	0	0.0	0	0
L	0.0	0	0	0.0	0	0	0.0	0	0	0.0	0	0

Cell	161			162			163			164		
	poro	perm	Sw	poro	perm	Sw	poro	perm	Sw	poro	perm	Sw
D	0.0	0	0	0.0	0	0	0.0	0	0	0.0	0	0
D	0.0	0	0	0.0	0	0	0.0	0	0	0.0	0	0
D	0.0	0	0	0.0	0	0	0.0	0	0	0.0	0	0
D	0.0	0	0	0.0	0	0	0.0	0	0	0.0	0	0
(I S)	–	–	–	–	–	–	–	–	–	–	–	–
I	5.0	2	45	5.0	2	45	0.0	0	0	0.0	0	0
I	0.0	0	0	0.0	0	0	0.0	0	0	0.0	0	0
I	0.0	0	0	0.0	0	0	0.0	0	0	0.0	0	0
(J US)	–	–	–	–	–	–	–	–	–	–	–	–
J c	0.0	0	0	0.0	0	0	0.0	0	0	0.0	0	0
(i.c.)	–	–	–	–	–	–	–	–	–	–	–	–
J ag	13.0	49	30	13.0	49	30	14.0	57	27	17.0	92	20
J ag	15.0	67	25	14.5	62	26	14.5	62	26	16.5	85	21
J ag	15.5	73	23	16.0	79	22	16.0	79	22	16.5	85	21
J ag	14.0	57	27	14.5	62	26	14.0	57	27	14.5	62	26
J ag	0.0	0	0	0.0	0	0	13.5	53	29	13.5	53	29
J ag	0.0	0	0	0.0	0	0	0.0	0	0	11.5	39	36
(i.c.)	–	–	–	–	–	–	–	–	–	–	–	–
J b	0.0	0	0	0.0	0	0	0.0	0	0	0.0	0	0
J b	0.0	0	0	0.0	0	0	0.0	0	0	0.0	0	0
(K US)	–	–	–	–	–	–	–	–	–	–	–	–
K cc	0.0	0	0	0.0	0	0	0.0	0	0	0.0	0	0
(K s)	–	–	–	–	–	–	–	–	–	–	–	–
K bc	0.0	0	0	0.0	0	0	0.0	0	0	7.5	3	49
K bc	0.0	0	0	0.0	0	0	0.0	0	0	7.5	3	49
K bc	0.0	0	0	0.0	0	0	0.0	0	0	0.0	0	0
(L US)	–	–	–	–	–	–	–	–	–	–	–	–
L	6.0	4	56	6.0	4	56	5.0	2	63	0.0	0	0
L	6.5	5	53	6.0	4	56	0.0	0	0	0.0	0	0
L	0.0	0	0	0.0	0	0	0.0	0	0	0.0	0	0
L	0.0	0	0	0.0	0	0	0.0	0	0	0.0	0	0
L	0.0	0	0	0.0	0	0	0.0	0	0	0.0	0	0
L	0.0	0	0	0.0	0	0	0.0	0	0	0.0	0	0

Cell	165			166			167			168		
	poro	perm	Sw	poro	perm	Sw	poro	perm	Sw	poro	perm	Sw
D	0.0	0	0	0.0	0	0	0.0	0	0	0.0	0	0
D	0.0	0	0	0.0	0	0	0.0	0	0	0.0	0	0
D	0.0	0	0	0.0	0	0	0.0	0	0	0.0	0	0
D	0.0	0	0	0.0	0	0	0.0	0	0	0.0	0	0
(I S)	–	–	–	–	–	–	–	–	–	–	–	–
I	0.0	0	0	0.0	0	0	0.0	0	0	0.0	0	0
I	0.0	0	0	0.0	0	0	0.0	0	0	0.0	0	0
I	0.0	0	0	0.0	0	0	0.0	0	0	0.0	0	0
(J US)	–	–	–	–	–	–	–	–	–	–	–	–
J c	0.0	0	0	0.0	0	0	0.0	0	0	0.0	0	0
(i.c.)	–	–	–	–	–	–	–	–	–	–	–	–
J ag	18.0	108	18	18.0	108	18	18.5	117	18	15.5	73	23
J ag	17.0	92	20	17.0	92	20	17.5	100	19	15.0	67	25
J ag	16.5	85	21	16.5	85	21	16.0	79	22	12.5	45	32
J ag	14.5	62	26	14.0	57	27	13.0	49	30	0.0	0	0
J ag	13.0	49	30	12.5	45	32	0.0	0	0	0.0	0	0
J ag	11.5	39	36	0.0	0	0	0.0	0	0	0.0	0	0
(i.c.)	–	–	–	–	–	–	–	–	–	–	–	–
J b	0.0	0	0	0.0	0	0	0.0	0	0	0.0	0	0
J b	0.0	0	0	0.0	0	0	0.0	0	0	0.0	0	0
(K US)	–	–	–	–	–	–	–	–	–	–	–	–
K cc	6.5	2	53	6.5	2	53	0.0	0	0	0.0	0	0
(K s)	–	–	–	–	–	–	–	–	–	–	–	–
K bc	8.0	3	48	8.0	3	48	7.5	3	49	6.5	2	53
K bc	8.5	4	46	8.5	4	46	7.5	3	49	0.0	0	0
K bc	0.0	0	0	0.0	0	0	0.0	0	0	0.0	0	0
(L US)	–	–	–	–	–	–	–	–	–	–	–	–
L	0.0	0	0	0.0	0	0	0.0	0	0	0.0	0	0
L	0.0	0	0	0.0	0	0	0.0	0	0	0.0	0	0
L	0.0	0	0	0.0	0	0	0.0	0	0	0.0	0	0
L	0.0	0	0	0.0	0	0	0.0	0	0	0.0	0	0
L	0.0	0	0	0.0	0	0	0.0	0	0	0.0	0	0
L	0.0	0	0	0.0	0	0	0.0	0	0	0.0	0	0

Cell		169			170			171			172	
	poro	perm	Sw	poro	perm	Sw	poro	perm	Sw	poro	perm	Sw
D	0.0	0	0	0.0	0	0	0.0	0	0	0.0	0	0
D	0.0	0	0	0.0	0	0	0.0	0	0	0.0	0	0
D	0.0	0	0	0.0	0	0	0.0	0	0	0.0	0	0
D	0.0	0	0	0.0	0	0	0.0	0	0	0.0	0	0
(I S)	–	–	–	–	–	–	–	–	–	–	–	–
I	0.0	0	0	0.0	0	0	0.0	0	0	0.0	0	0
I	0.0	0	0	0.0	0	0	0.0	0	0	0.0	0	0
I	0.0	0	0	0.0	0	0	0.0	0	0	0.0	0	0
(J US)	–	–	–	–	–	–	–	–	–	–	–	–
J c	0.0	0	0	0.0	0	0	0.0	0	0	0.0	0	0
(i.c.)	–	–	–	–	–	–	–	–	–	–	–	–
J ag	8.5	24	53	0.0	0	0	0.0	0	0	0.0	0	0
J ag	0.0	0	0	0.0	0	0	0.0	0	0	0.0	0	0
J ag	0.0	0	0	0.0	0	0	0.0	0	0	0.0	0	0
J ag	0.0	0	0	0.0	0	0	0.0	0	0	0.0	0	0
J ag	0.0	0	0	0.0	0	0	0.0	0	0	0.0	0	0
J ag	0.0	0	0	0.0	0	0	0.0	0	0	0.0	0	0
(i.c.)	–	–	–	–	–	–	–	–	–	–	–	–
J b	0.0	0	0	0.0	0	0	0.0	0	0	0.0	0	0
J b	0.0	0	0	0.0	0	0	0.0	0	0	0.0	0	0
(K US)	–	–	–	–	–	–	–	–	–	–	–	–
K cc	0.0	0	0	0.0	0	0	0.0	0	0	0.0	0	0
(K s)	–	–	–	–	–	–	–	–	–	–	–	–
K bc	7.0	2	51	7.5	3	49	7.5	3	49	7.0	2	51
K bc	0.0	0	0	7.5	3	49	7.5	3	49	0.0	0	0
K bc	0.0	0	0	0.0	0	0	0.0	0	0	0.0	0	0
(L US)	–	–	–	–	–	–	–	–	–	–	–	–
L	0.0	0	0	0.0	0	0	0.0	0	0	0.0	0	0
L	0.0	0	0	0.0	0	0	0.0	0	0	0.0	0	0
L	0.0	0	0	0.0	0	0	0.0	0	0	0.0	0	0
L	0.0	0	0	0.0	0	0	0.0	0	0	0.0	0	0
L	0.0	0	0	0.0	0	0	0.0	0	0	0.0	0	0
L	0.0	0	0	0.0	0	0	0.0	0	0	0.0	0	0

Cell	173			174			175			176		
	poro	perm	Sw	poro	perm	Sw	poro	perm	Sw	poro	perm	Sw
D	0.0	0	0	0.0	0	0	0.0	0	0	0.0	0	0
D	0.0	0	0	0.0	0	0	0.0	0	0	0.0	0	0
D	0.0	0	0	0.0	0	0	0.0	0	0	0.0	0	0
D	0.0	0	0	0.0	0	0	0.0	0	0	0.0	0	0
(I S)	–	–	–	–	–	–	–	–	–	–	–	–
I	0.0	0	0	0.0	0	0	0.0	0	0	0.0	0	0
I	0.0	0	0	0.0	0	0	0.0	0	0	0.0	0	0
I	0.0	0	0	0.0	0	0	0.0	0	0	0.0	0	0
(J US)	–	–	–	–	–	–	–	–	–	–	–	–
J c	0.0	0	0	0.0	0	0	0.0	0	0	0.0	0	0
(i.c.)	–	–	–	–	–	–	–	–	–	–	–	–
J ag	0.0	0	0	0.0	0	0	7.0	19	67	8.0	22	57
J ag	0.0	0	0	0.0	0	0	0.0	0	0	7.0	19	67
J ag	0.0	0	0	0.0	0	0	0.0	0	0	7.0	19	67
J ag	0.0	0	0	0.0	0	0	0.0	0	0	0.0	0	0
J ag	0.0	0	0	0.0	0	0	0.0	0	0	0.0	0	0
J ag	0.0	0	0	0.0	0	0	0.0	0	0	0.0	0	0
(i.c.)	–	–	–	–	–	–	–	–	–	–	–	–
J b	0.0	0	0	0.0	0	0	0.0	0	0	0.0	0	0
J b	0.0	0	0	0.0	0	0	0.0	0	0	0.0	0	0
(K US)	–	–	–	–	–	–	–	–	–	–	–	–
K cc	0.0	0	0	0.0	0	0	0.0	0	0	0.0	0	0
(K s)	–	–	–	–	–	–	–	–	–	–	–	–
K bc	0.0	0	0	6.5	2	53	7.0	2	51	7.5	3	49
K bc	0.0	0	0	0.0	0	0	0.0	0	0	7.5	3	49
K bc	0.0	0	0	0.0	0	0	0.0	0	0	0.0	0	0
(L US)	–	–	–	–	–	–	–	–	–	–	–	–
L	6.0	4	56	7.0	7	51	7.5	9	49	7.0	7	51
L	6.0	4	56	7.0	7	51	7.0	7	51	7.5	9	49
L	0.0	0	0	7.5	9	49	7.5	9	49	8.0	11	48
L	0.0	0	0	0.0	0	0	8.0	11	48	6.0	4	56
L	0.0	0	0	0.0	0	0	0.0	0	0	7.0	7	51
L	0.0	0	0	0.0	0	0	0.0	0	0	0.0	0	0

Cell		177			178			179			180	
	poro	perm	Sw	poro	perm	Sw	poro	perm	Sw	poro	perm	Sw
D	0.0	0	0	0.0	0	0	0.0	0	0	0.0	0	0
D	0.0	0	0	0.0	0	0	0.0	0	0	0.0	0	0
D	0.0	0	0	0.0	0	0	0.0	0	0	0.0	0	0
D	0.0	0	0	0.0	0	0	0.0	0	0	0.0	0	0
(I S)	–	–	–	–	–	–	–	–	–	–	–	–
I	0.0	0	0	0.0	0	0	0.0	0	0	0.0	0	0
I	0.0	0	0	0.0	0	0	0.0	0	0	0.0	0	0
I	0.0	0	0	0.0	0	0	0.0	0	0	0.0	0	0
(J US)	–	–	–	–	–	–	–	–	–	–	–	–
J c	0.0	0	0	0.0	0	0	0.0	0	0	0.0	0	0
(i.c.)	–	–	–	–	–	–	–	–	–	–	–	–
J ag	8.5	24	53	9.0	26	50	10.5	33	41	11.0	36	38
J ag	7.5	20	62	8.0	22	57	12.0	42	34	12.5	45	32
J ag	7.5	20	62	8.0	22	57	11.0	36	38	11.5	39	36
J ag	0.0	0	0	0.0	0	0	0.0	0	0	0.0	0	0
J ag	0.0	0	0	0.0	0	0	0.0	0	0	0.0	0	0
J ag	0.0	0	0	0.0	0	0	0.0	0	0	0.0	0	0
(i.c.)	–	–	–	–	–	–	–	–	–	–	–	–
J b	0.0	0	0	0.0	0	0	0.0	0	0	0.0	0	0
J b	0.0	0	0	0.0	0	0	0.0	0	0	0.0	0	0
(K US)	–	–	–	–	–	–	–	–	–	–	–	–
K cc	0.0	0	0	0.0	0	0	0.0	0	0	0.0	0	0
(K s)	–	–	–	–	–	–	–	–	–	–	–	–
K bc	7.5	3	49	6.5	2	53	0.0	0	0	0.0	0	0
K bc	7.5	3	49	0.0	0	0	0.0	0	0	0.0	0	0
K bc	0.0	0	0	0.0	0	0	0.0	0	0	0.0	0	0
(L US)	–	–	–	–	–	–	–	–	–	–	–	–
L	7.0	7	51	7.0	7	51	6.0	4	56	5.5	3	59
L	7.5	9	49	7.5	9	49	6.5	5	53	0.0	0	0
L	8.0	11	48	7.5	9	49	6.0	4	56	0.0	0	0
L	6.0	4	56	6.0	4	56	0.0	0	0	0.0	0	0
L	7.0	7	51	6.5	5	53	0.0	0	0	0.0	0	0
L	6.5	5	53	0.0	0	0	0.0	0	0	0.0	0	0

Cell	181			182			183			184		
	poro	perm	Sw	poro	perm	Sw	poro	perm	Sw	poro	perm	Sw
D	0.0	0	0	0.0	0	0	0.0	0	0	0.0	0	0
D	0.0	0	0	0.0	0	0	0.0	0	0	0.0	0	0
D	0.0	0	0	0.0	0	0	0.0	0	0	0.0	0	0
D	0.0	0	0	0.0	0	0	0.0	0	0	0.0	0	0
(I S)	–	–	–	–	–	–	–	–	–	–	–	–
I	0.0	0	0	0.0	0	0	0.0	0	0	0.0	0	0
I	0.0	0	0	0.0	0	0	0.0	0	0	0.0	0	0
I	0.0	0	0	0.0	0	0	0.0	0	0	0.0	0	0
(J US)	–	–	–	–	–	–	–	–	–	–	–	–
J c	0.0	0	0	0.0	0	0	0.0	0	0	0.0	0	0
(i.c.)	–	–	–	–	–	–	–	–	–	–	–	–
J ag	14.0	57	27	14.0	57	27	13.0	49	30	16.0	79	22
J ag	16.0	79	22	16.0	79	22	14.5	62	26	16.5	85	21
J ag	14.0	57	27	13.5	53	29	15.5	73	23	16.5	85	21
J ag	0.0	0	0	12.0	42	34	14.0	57	27	15.0	67	25
J ag	0.0	0	0	0.0	0	0	0.0	0	0	0.0	0	0
J ag	0.0	0	0	0.0	0	0	0.0	0	0	0.0	0	0
(i.c.)	–	–	–	–	–	–	–	–	–	–	–	–
J b	0.0	0	0	0.0	0	0	0.0	0	0	0.0	0	0
J b	0.0	0	0	0.0	0	0	0.0	0	0	0.0	0	0
(K US)	–	–	–	–	–	–	–	–	–	–	–	–
K cc	0.0	0	0	0.0	0	0	0.0	0	0	0.0	0	0
(K s)	–	–	–	–	–	–	–	–	–	–	–	–
K bc	0.0	0	0	0.0	0	0	0.0	0	0	6.5	2	53
K bc	0.0	0	0	0.0	0	0	0.0	0	0	0.0	0	0
K bc	0.0	0	0	0.0	0	0	0.0	0	0	0.0	0	0
(L US)	–	–	–	–	–	–	–	–	–	–	–	–
L	0.0	0	0	5.0	2	63	0.0	0	0	0.0	0	0
L	0.0	0	0	0.0	0	0	0.0	0	0	0.0	0	0
L	0.0	0	0	0.0	0	0	0.0	0	0	0.0	0	0
L	0.0	0	0	0.0	0	0	0.0	0	0	0.0	0	0
L	0.0	0	0	0.0	0	0	0.0	0	0	0.0	0	0
L	0.0	0	0	0.0	0	0	0.0	0	0	0.0	0	0

Cell	185			186			187			188		
	poro	perm	Sw	poro	perm	Sw	poro	perm	Sw	poro	perm	Sw
D	0.0	0	0	0.0	0	0	0.0	0	0	0.0	0	0
D	0.0	0	0	0.0	0	0	0.0	0	0	0.0	0	0
D	0.0	0	0	0.0	0	0	0.0	0	0	0.0	0	0
D	0.0	0	0	0.0	0	0	0.0	0	0	0.0	0	0
(I S)	–	–	–	–	–	–	–	–	–	–	–	–
I	0.0	0	0	0.0	0	0	0.0	0	0	0.0	0	0
I	0.0	0	0	0.0	0	0	0.0	0	0	0.0	0	0
I	0.0	0	0	0.0	0	0	0.0	0	0	0.0	0	0
(J US)	–	–	–	–	–	–	–	–	–	–	–	–
J c	0.0	0	0	0.0	0	0	0.0	0	0	0.0	0	0
(i.c.)	–	–	–	–	–	–	–	–	–	–	–	–
J ag	18.0	108	18	21.5	189	13	18.0	108	18	18.0	108	18
J ag	17.5	100	19	20.0	149	15	17.5	100	19	17.5	100	19
J ag	17.0	92	20	18.0	108	18	17.0	92	20	16.5	85	21
J ag	16.0	79	22	17.0	92	20	15.5	73	23	13.0	49	30
J ag	14.0	57	27	16.0	79	22	14.0	57	27	0.0	0	0
J ag	12.0	42	34	13.0	49	30	0.0	0	0	0.0	0	0
(i.c.)	–	–	–	–	–	–	–	–	–	–	–	–
J b	0.0	0	0	0.0	0	0	0.0	0	0	0.0	0	0
J b	0.0	0	0	0.0	0	0	0.0	0	0	0.0	0	0
(K US)	–	–	–	–	–	–	–	–	–	–	–	–
K cc	0.0	0	0	7.0	2	51	7.0	2	51	0.0	0	0
(K s)	–	–	–	–	–	–	–	–	–	–	–	–
K bc	8.0	3	48	8.5	4	46	8.0	3	48	7.0	2	51
K bc	8.0	3	48	9.0	5	45	8.5	4	46	0.0	0	0
K bc	0.0	0	0	0.0	0	0	0.0	0	0	0.0	0	0
(L US)	–	–	–	–	–	–	–	–	–	–	–	–
L	0.0	0	0	0.0	0	0	0.0	0	0	0.0	0	0
L	0.0	0	0	0.0	0	0	0.0	0	0	0.0	0	0
L	0.0	0	0	0.0	0	0	0.0	0	0	0.0	0	0
L	0.0	0	0	0.0	0	0	0.0	0	0	0.0	0	0
L	0.0	0	0	0.0	0	0	0.0	0	0	0.0	0	0
L	0.0	0	0	0.0	0	0	0.0	0	0	0.0	0	0

Cell	189			190			191			192		
	poro	perm	Sw	poro	perm	Sw	poro	perm	Sw	poro	perm	Sw
D	0.0	0	0	0.0	0	0	0.0	0	0	0.0	0	0
D	0.0	0	0	0.0	0	0	0.0	0	0	0.0	0	0
D	0.0	0	0	0.0	0	0	0.0	0	0	0.0	0	0
D	0.0	0	0	0.0	0	0	0.0	0	0	0.0	0	0
(I S)	–	–	–	–	–	–	–	–	–	–	–	–
I	0.0	0	0	0.0	0	0	0.0	0	0	0.0	0	0
I	0.0	0	0	0.0	0	0	0.0	0	0	0.0	0	0
I	0.0	0	0	0.0	0	0	0.0	0	0	0.0	0	0
(J US)	–	–	–	–	–	–	–	–	–	–	–	–
J c	0.0	0	0	0.0	0	0	0.0	0	0	0.0	0	0
(i.c.)	–	–	–	–	–	–	–	–	–	–	–	–
J ag	10.0	30	43	7.0	19	67	0.0	0	0	0.0	0	0
J ag	8.0	22	57	0.0	0	0	0.0	0	0	0.0	0	0
J ag	0.0	0	0	0.0	0	0	0.0	0	0	0.0	0	0
J ag	0.0	0	0	0.0	0	0	0.0	0	0	0.0	0	0
J ag	0.0	0	0	0.0	0	0	0.0	0	0	0.0	0	0
J ag	0.0	0	0	0.0	0	0	0.0	0	0	0.0	0	0
(i.c.)	–	–	–	–	–	–	–	–	–	–	–	–
J b	0.0	0	0	0.0	0	0	0.0	0	0	0.0	0	0
J b	0.0	0	0	0.0	0	0	0.0	0	0	0.0	0	0
(K US)	–	–	–	–	–	–	–	–	–	–	–	–
K cc	0.0	0	0	0.0	0	0	0.0	0	0	0.0	0	0
(K s)	–	–	–	–	–	–	–	–	–	–	–	–
K bc	0.0	0	0	0.0	0	0	6.5	2	53	6.5	2	53
K bc	0.0	0	0	0.0	0	0	0.0	0	0	0.0	0	0
K bc	0.0	0	0	0.0	0	0	0.0	0	0	0.0	0	0
(L US)	–	–	–	–	–	–	–	–	–	–	–	–
L	0.0	0	0	0.0	0	0	0.0	0	0	0.0	0	0
L	0.0	0	0	0.0	0	0	0.0	0	0	0.0	0	0
L	0.0	0	0	0.0	0	0	0.0	0	0	0.0	0	0
L	0.0	0	0	0.0	0	0	0.0	0	0	0.0	0	0
L	0.0	0	0	0.0	0	0	0.0	0	0	0.0	0	0
L	0.0	0	0	0.0	0	0	0.0	0	0	0.0	0	0

Cell	193			194			195			196		
	poro	perm	Sw	poro	perm	Sw	poro	perm	Sw	poro	perm	Sw
D	0.0	0	0	0.0	0	0	0.0	0	0	0.0	0	0
D	0.0	0	0	0.0	0	0	0.0	0	0	0.0	0	0
D	0.0	0	0	0.0	0	0	0.0	0	0	0.0	0	0
D	0.0	0	0	0.0	0	0	0.0	0	0	0.0	0	0
(I S)	–	–	–	–	–	–	–	–	–	–	–	–
I	0.0	0	0	0.0	0	0	0.0	0	0	0.0	0	0
I	0.0	0	0	0.0	0	0	0.0	0	0	0.0	0	0
I	0.0	0	0	0.0	0	0	0.0	0	0	0.0	0	0
(J US)	–	–	–	–	–	–	–	–	–	–	–	–
J c	0.0	0	0	0.0	0	0	0.0	0	0	0.0	0	0
(i.c.)	–	–	–	–	–	–	–	–	–	–	–	–
J ag	0.0	0	0	0.0	0	0	0.0	0	0	7.0	19	67
J ag	0.0	0	0	0.0	0	0	0.0	0	0	0.0	0	0
J ag	0.0	0	0	0.0	0	0	0.0	0	0	0.0	0	0
J ag	0.0	0	0	0.0	0	0	0.0	0	0	0.0	0	0
J ag	0.0	0	0	0.0	0	0	0.0	0	0	0.0	0	0
J ag	0.0	0	0	0.0	0	0	0.0	0	0	0.0	0	0
(i.c.)	–	–	–	–	–	–	–	–	–	–	–	–
J b	0.0	0	0	0.0	0	0	0.0	0	0	0.0	0	0
J b	0.0	0	0	0.0	0	0	0.0	0	0	0.0	0	0
(K US)	–	–	–	–	–	–	–	–	–	–	–	–
K cc	0.0	0	0	0.0	0	0	0.0	0	0	0.0	0	0
(K s)	–	–	–	–	–	–	–	–	–	–	–	–
K bc	0.0	0	0	0.0	0	0	6.5	2	53	7.0	2	51
K bc	0.0	0	0	0.0	0	0	0.0	0	0	0.0	0	0
K bc	0.0	0	0	0.0	0	0	0.0	0	0	0.0	0	0
(L US)	–	–	–	–	–	–	–	–	–	–	–	–
L	5.0	2	63	6.0	4	56	8.0	11	48	8.0	11	48
L	0.0	0	0	6.5	5	53	7.0	7	51	7.5	9	49
L	0.0	0	0	0.0	0	0	7.0	7	51	7.0	7	51
L	0.0	0	0	0.0	0	0	9.0	19	45	8.5	15	46
L	0.0	0	0	0.0	0	0	0.0	0	0	6.5	5	53
L	0.0	0	0	0.0	0	0	0.0	0	0	0.0	0	0

Cell	197			198			199			200		
	poro	perm	Sw	poro	perm	Sw	poro	perm	Sw	poro	perm	Sw
D	0.0	0	0	0.0	0	0	0.0	0	0	0.0	0	0
D	0.0	0	0	0.0	0	0	0.0	0	0	0.0	0	0
D	0.0	0	0	0.0	0	0	0.0	0	0	0.0	0	0
D	0.0	0	0	0.0	0	0	0.0	0	0	0.0	0	0
(I S)	–	–	–	–	–	–	–	–	–	–	–	–
I	0.0	0	0	0.0	0	0	0.0	0	0	0.0	0	0
I	0.0	0	0	0.0	0	0	0.0	0	0	0.0	0	0
I	0.0	0	0	0.0	0	0	0.0	0	0	0.0	0	0
(J US)	–	–	–	–	–	–	–	–	–	–	–	–
J c	0.0	0	0	0.0	0	0	0.0	0	0	0.0	0	0
(i.c.)	–	–	–	–	–	–	–	–	–	–	–	–
J ag	8.0	22	57	8.5	24	53	9.0	26	50	11.0	36	38
J ag	8.0	22	57	7.5	20	62	8.0	22	57	12.5	45	32
J ag	7.0	19	67	7.5	20	62	8.0	22	57	11.5	39	36
J ag	0.0	0	0	0.0	0	0	0.0	0	0	0.0	0	0
J ag	0.0	0	0	0.0	0	0	0.0	0	0	0.0	0	0
J ag	0.0	0	0	0.0	0	0	0.0	0	0	0.0	0	0
(i.c.)	–	–	–	–	–	–	–	–	–	–	–	–
J b	0.0	0	0	0.0	0	0	0.0	0	0	0.0	0	0
J b	0.0	0	0	0.0	0	0	0.0	0	0	0.0	0	0
(K US)	–	–	–	–	–	–	–	–	–	–	–	–
K cc	0.0	0	0	0.0	0	0	0.0	0	0	0.0	0	0
(K s)	–	–	–	–	–	–	–	–	–	–	–	–
K bc	7.5	3	49	7.5	3	49	6.5	2	53	0.0	0	0
K bc	0.0	0	0	0.0	0	0	0.0	0	0	0.0	0	0
K bc	0.0	0	0	0.0	0	0	0.0	0	0	0.0	0	0
(L US)	–	–	–	–	–	–	–	–	–	–	–	–
L	7.5	9	49	7.0	7	51	6.5	5	53	6.0	4	56
L	7.5	9	49	7.5	9	49	7.0	7	51	6.0	4	56
L	8.0	11	48	8.0	11	48	7.5	9	49	0.0	0	0
L	6.5	5	53	6.5	5	53	6.0	4	56	0.0	0	0
L	7.0	7	51	6.5	5	53	0.0	0	0	0.0	0	0
L	6.5	5	53	6.5	5	53	0.0	0	0	0.0	0	0

Cell	201			202			203			204		
	poro	perm	Sw	poro	perm	Sw	poro	perm	Sw	poro	perm	Sw
D	0.0	0	0	0.0	0	0	0.0	0	0	0.0	0	0
D	0.0	0	0	0.0	0	0	0.0	0	0	0.0	0	0
D	0.0	0	0	0.0	0	0	0.0	0	0	0.0	0	0
D	0.0	0	0	0.0	0	0	0.0	0	0	0.0	0	0
(I S)	–	–	–	–	–	–	–	–	–	–	–	–
I	0.0	0	0	0.0	0	0	0.0	0	0	0.0	0	0
I	0.0	0	0	0.0	0	0	0.0	0	0	0.0	0	0
I	0.0	0	0	0.0	0	0	0.0	0	0	0.0	0	0
(J US)	–	–	–	–	–	–	–	–	–	–	–	–
J c	0.0	0	0	0.0	0	0	0.0	0	0	0.0	0	0
(i.c.)	–	–	–	–	–	–	–	–	–	–	–	–
J ag	13.0	49	30	13.5	53	29	14.5	62	26	15.0	67	25
J ag	17.0	92	20	16.5	85	21	16.0	79	22	15.5	73	23
J ag	15.0	67	25	14.5	62	26	13.5	53	29	13.0	49	30
J ag	0.0	0	0	0.0	0	0	0.0	0	0	0.0	0	0
J ag	0.0	0	0	0.0	0	0	0.0	0	0	0.0	0	0
J ag	0.0	0	0	0.0	0	0	0.0	0	0	0.0	0	0
(i.c.)	–	–	–	–	–	–	–	–	–	–	–	–
J b	0.0	0	0	0.0	0	0	0.0	0	0	0.0	0	0
J b	0.0	0	0	0.0	0	0	0.0	0	0	0.0	0	0
(K US)	–	–	–	–	–	–	–	–	–	–	–	–
K cc	0.0	0	0	0.0	0	0	0.0	0	0	0.0	0	0
(K s)	–	–	–	–	–	–	–	–	–	–	–	–
K bc	0.0	0	0	0.0	0	0	0.0	0	0	0.0	0	0
K bc	0.0	0	0	0.0	0	0	0.0	0	0	0.0	0	0
K bc	0.0	0	0	0.0	0	0	0.0	0	0	0.0	0	0
(L US)	–	–	–	–	–	–	–	–	–	–	–	–
L	0.0	0	0	0.0	0	0	0.0	0	0	0.0	0	0
L	0.0	0	0	0.0	0	0	0.0	0	0	0.0	0	0
L	0.0	0	0	0.0	0	0	0.0	0	0	0.0	0	0
L	0.0	0	0	0.0	0	0	0.0	0	0	0.0	0	0
L	0.0	0	0	0.0	0	0	0.0	0	0	0.0	0	0
L	0.0	0	0	0.0	0	0	0.0	0	0	0.0	0	0

Cell	205			206			207			208		
	poro	perm	Sw	poro	perm	Sw	poro	perm	Sw	poro	perm	Sw
D	0.0	0	0	0.0	0	0	0.0	0	0	0.0	0	0
D	0.0	0	0	0.0	0	0	0.0	0	0	0.0	0	0
D	0.0	0	0	0.0	0	0	0.0	0	0	0.0	0	0
D	0.0	0	0	0.0	0	0	0.0	0	0	0.0	0	0
(I S)	–	–	–	–	–	–	–	–	–	–	–	–
I	0.0	0	0	0.0	0	0	6.5	6	33	0.0	0	0
I	0.0	0	0	0.0	0	0	0.0	0	0	0.0	0	0
I	0.0	0	0	0.0	0	0	0.0	0	0	0.0	0	0
(J US)	–	–	–	–	–	–	–	–	–	–	–	–
J c	0.0	0	0	0.0	0	0	0.0	0	0	0.0	0	0
(i.c.)	–	–	–	–	–	–	–	–	–	–	–	–
J ag	18.0	108	18	21.0	175	14	24.0	281	11	21.0	175	14
J ag	18.0	108	18	20.5	161	15	23.0	240	12	20.5	161	15
J ag	15.5	73	23	18.0	108	18	20.0	149	15	18.0	108	18
J ag	14.5	62	26	17.0	92	20	20.0	149	15	17.0	92	20
J ag	0.0	0	0	16.0	79	22	19.0	127	17	16.0	79	22
J ag	0.0	0	0	0.0	0	0	15.0	67	25	0.0	0	0
(i.c.)	–	–	–	–	–	–	–	–	–	–	–	–
J b	0.0	0	0	0.0	0	0	0.0	0	0	0.0	0	0
J b	0.0	0	0	0.0	0	0	0.0	0	0	0.0	0	0
(K US)	–	–	–	–	–	–	–	–	–	–	–	–
K cc	0.0	0	0	0.0	0	0	7.0	2	51	7.0	2	51
(K s)	–	–	–	–	–	–	–	–	–	–	–	–
K bc	6.5	2	53	8.0	3	48	9.0	5	45	8.5	4	46
K bc	0.0	0	0	8.0	3	48	9.5	7	44	8.5	4	46
K bc	0.0	0	0	0.0	0	0	9.0	5	45	0.0	0	0
(L US)	–	–	–	–	–	–	–	–	–	–	–	–
L	0.0	0	0	0.0	0	0	0.0	0	0	0.0	0	0
L	0.0	0	0	0.0	0	0	0.0	0	0	0.0	0	0
L	0.0	0	0	0.0	0	0	0.0	0	0	0.0	0	0
L	0.0	0	0	0.0	0	0	0.0	0	0	0.0	0	0
L	0.0	0	0	0.0	0	0	0.0	0	0	0.0	0	0
L	0.0	0	0	0.0	0	0	0.0	0	0	0.0	0	0

Cell		209			210			211			212	
	poro	perm	Sw	poro	perm	Sw	poro	perm	Sw	poro	perm	Sw
D	0.0	0	0	0.0	0	0	0.0	0	0	0.0	0	0
D	0.0	0	0	0.0	0	0	0.0	0	0	0.0	0	0
D	0.0	0	0	0.0	0	0	0.0	0	0	0.0	0	0
D	0.0	0	0	0.0	0	0	0.0	0	0	0.0	0	0
(I S)	–	–	–	–	–	–	–	–	–	–	–	–
I	0.0	0	0	0.0	0	0	0.0	0	0	0.0	0	0
I	0.0	0	0	0.0	0	0	0.0	0	0	0.0	0	0
I	0.0	0	0	0.0	0	0	0.0	0	0	0.0	0	0
(J US)	–	–	–	–	–	–	–	–	–	–	–	–
J c	0.0	0	0	0.0	0	0	0.0	0	0	0.0	0	0
(i.c.)	–	–	–	–	–	–	–	–	–	–	–	–
J ag	18.0	108	18	8.5	24	53	0.0	0	0	0.0	0	0
J ag	17.0	92	20	8.0	22	57	0.0	0	0	0.0	0	0
J ag	15.0	67	25	0.0	0	0	0.0	0	0	0.0	0	0
J ag	12.5	45	32	0.0	0	0	0.0	0	0	0.0	0	0
J ag	0.0	0	0	0.0	0	0	0.0	0	0	0.0	0	0
J ag	0.0	0	0	0.0	0	0	0.0	0	0	0.0	0	0
(i.c.)	–	–	–	–	–	–	–	–	–	–	–	–
J b	0.0	0	0	0.0	0	0	0.0	0	0	0.0	0	0
J b	0.0	0	0	0.0	0	0	0.0	0	0	0.0	0	0
(K US)	–	–	–	–	–	–	–	–	–	–	–	–
K cc	0.0	0	0	0.0	0	0	0.0	0	0	0.0	0	0
(K s)	–	–	–	–	–	–	–	–	–	–	–	–
K bc	6.5	2	53	0.0	0	0	0.0	0	0	0.0	0	0
K bc	0.0	0	0	0.0	0	0	0.0	0	0	0.0	0	0
K bc	0.0	0	0	0.0	0	0	0.0	0	0	0.0	0	0
(L US)	–	–	–	–	–	–	–	–	–	–	–	–
L	0.0	0	0	0.0	0	0	6.0	4	56	6.5	5	53
L	0.0	0	0	0.0	0	0	6.0	4	56	6.5	5	53
L	0.0	0	0	0.0	0	0	0.0	0	0	8.0	11	48
L	0.0	0	0	0.0	0	0	0.0	0	0	0.0	0	0
L	0.0	0	0	0.0	0	0	0.0	0	0	0.0	0	0
L	0.0	0	0	0.0	0	0	0.0	0	0	0.0	0	0

Cell	213			214			215			216		
	poro	perm	Sw	poro	perm	Sw	poro	perm	Sw	poro	perm	Sw
D	0.0	0	0	0.0	0	0	0.0	0	0	0.0	0	0
D	0.0	0	0	0.0	0	0	0.0	0	0	0.0	0	0
D	0.0	0	0	0.0	0	0	0.0	0	0	0.0	0	0
D	0.0	0	0	0.0	0	0	0.0	0	0	0.0	0	0
(I S)	–	–	–	–	–	–	–	–	–	–	–	–
I	0.0	0	0	0.0	0	0	0.0	0	0	0.0	0	0
I	0.0	0	0	0.0	0	0	0.0	0	0	0.0	0	0
I	0.0	0	0	0.0	0	0	0.0	0	0	0.0	0	0
(J US)	–	–	–	–	–	–	–	–	–	–	–	–
J c	0.0	0	0	0.0	0	0	0.0	0	0	0.0	0	0
(i.c.)	–	–	–	–	–	–	–	–	–	–	–	–
J ag	7.0	19	67	7.5	20	62	8.0	22	57	9.0	26	50
J ag	0.0	0	0	7.5	20	62	7.5	20	62	9.0	26	50
J ag	0.0	0	0	0.0	0	0	10.5	33	41	11.0	36	38
J ag	0.0	0	0	0.0	0	0	0.0	0	0	0.0	0	0
J ag	0.0	0	0	0.0	0	0	0.0	0	0	0.0	0	0
J ag	0.0	0	0	0.0	0	0	0.0	0	0	0.0	0	0
(i.c.)	–	–	–	–	–	–	–	–	–	–	–	–
J b	0.0	0	0	0.0	0	0	0.0	0	0	0.0	0	0
J b	0.0	0	0	0.0	0	0	0.0	0	0	0.0	0	0
(K US)	–	–	–	–	–	–	–	–	–	–	–	–
K cc	0.0	0	0	0.0	0	0	0.0	0	0	0.0	0	0
(K s)	–	–	–	–	–	–	–	–	–	–	–	–
K bc	6.5	2	53	6.5	2	53	6.5	2	53	0.0	0	0
K bc	0.0	0	0	0.0	0	0	0.0	0	0	0.0	0	0
K bc	0.0	0	0	0.0	0	0	0.0	0	0	0.0	0	0
(L US)	–	–	–	–	–	–	–	–	–	–	–	–
L	8.0	11	48	7.5	9	49	7.0	7	51	6.0	4	56
L	7.5	9	49	7.5	9	49	7.0	7	51	7.0	7	51
L	6.5	5	53	6.5	5	53	6.0	4	56	6.0	4	56
L	8.0	11	48	7.5	9	49	7.0	7	51	0.0	0	0
L	0.0	0	0	0.0	0	0	0.0	0	0	0.0	0	0
L	0.0	0	0	0.0	0	0	0.0	0	0	0.0	0	0

Cell	217			218			219			220		
	poro	perm	Sw	poro	perm	Sw	poro	perm	Sw	poro	perm	Sw
D	0.0	0	0	0.0	0	0	0.0	0	0	0.0	0	0
D	0.0	0	0	0.0	0	0	0.0	0	0	0.0	0	0
D	0.0	0	0	0.0	0	0	0.0	0	0	0.0	0	0
D	0.0	0	0	0.0	0	0	0.0	0	0	0.0	0	0
(I S)	–	–	–	–	–	–	–	–	–	–	–	–
I	0.0	0	0	0.0	0	0	0.0	0	0	0.0	0	0
I	0.0	0	0	0.0	0	0	0.0	0	0	0.0	0	0
I	0.0	0	0	0.0	0	0	0.0	0	0	0.0	0	0
(J US)	–	–	–	–	–	–	–	–	–	–	–	–
J c	0.0	0	0	0.0	0	0	0.0	0	0	0.0	0	0
(i.c.)	–	–	–	–	–	–	–	–	–	–	–	–
J ag	11.0	36	38	12.0	42	34	12.0	42	34	11.5	39	36
J ag	13.0	49	30	14.0	57	27	13.5	53	29	13.0	49	30
J ag	13.0	49	30	13.0	49	30	12.5	45	32	0.0	0	0
J ag	0.0	0	0	0.0	0	0	0.0	0	0	0.0	0	0
J ag	0.0	0	0	0.0	0	0	0.0	0	0	0.0	0	0
J ag	0.0	0	0	0.0	0	0	0.0	0	0	0.0	0	0
(i.c.)	–	–	–	–	–	–	–	–	–	–	–	–
J b	0.0	0	0	0.0	0	0	0.0	0	0	0.0	0	0
J b	0.0	0	0	0.0	0	0	0.0	0	0	0.0	0	0
(K US)	–	–	–	–	–	–	–	–	–	–	–	–
K cc	0.0	0	0	0.0	0	0	0.0	0	0	0.0	0	0
(K s)	–	–	–	–	–	–	–	–	–	–	–	–
K bc	0.0	0	0	0.0	0	0	0.0	0	0	0.0	0	0
K bc	0.0	0	0	0.0	0	0	0.0	0	0	0.0	0	0
K bc	0.0	0	0	0.0	0	0	0.0	0	0	0.0	0	0
(L US)	–	–	–	–	–	–	–	–	–	–	–	–
L	5.0	2	63	0.0	0	0	0.0	0	0	0.0	0	0
L	0.0	0	0	0.0	0	0	0.0	0	0	0.0	0	0
L	0.0	0	0	0.0	0	0	0.0	0	0	0.0	0	0
L	0.0	0	0	0.0	0	0	0.0	0	0	0.0	0	0
L	0.0	0	0	0.0	0	0	0.0	0	0	0.0	0	0
L	0.0	0	0	0.0	0	0	0.0	0	0	0.0	0	0

Cell	221			222			223			224		
	poro	perm	Sw	poro	perm	Sw	poro	perm	Sw	poro	perm	Sw
D	0.0	0	0	0.0	0	0	0.0	0	0	0.0	0	0
D	0.0	0	0	0.0	0	0	0.0	0	0	0.0	0	0
D	0.0	0	0	0.0	0	0	0.0	0	0	0.0	0	0
D	0.0	0	0	0.0	0	0	0.0	0	0	0.0	0	0
(I S)	–	–	–	–	–	–	–	–	–	–	–	–
I	0.0	0	0	0.0	0	0	0.0	0	0	0.0	0	0
I	0.0	0	0	0.0	0	0	0.0	0	0	0.0	0	0
I	0.0	0	0	0.0	0	0	0.0	0	0	0.0	0	0
(J US)	–	–	–	–	–	–	–	–	–	–	–	–
J c	0.0	0	0	0.0	0	0	0.0	0	0	0.0	0	0
(i.c.)	–	–	–	–	–	–	–	–	–	–	–	–
J ag	11.5	39	36	15.0	67	25	18.0	108	18	18.0	108	18
J ag	13.0	49	30	15.5	73	23	17.5	100	19	17.5	100	19
J ag	0.0	0	0	13.0	49	30	15.5	73	23	15.5	73	23
J ag	0.0	0	0	0.0	0	0	14.5	62	26	14.5	62	26
J ag	0.0	0	0	0.0	0	0	0.0	0	0	0.0	0	0
J ag	0.0	0	0	0.0	0	0	0.0	0	0	0.0	0	0
(i.c.)	–	–	–	–	–	–	–	–	–	–	–	–
J b	0.0	0	0	0.0	0	0	0.0	0	0	0.0	0	0
J b	0.0	0	0	0.0	0	0	0.0	0	0	0.0	0	0
(K US)	–	–	–	–	–	–	–	–	–	–	–	–
K cc	0.0	0	0	0.0	0	0	0.0	0	0	0.0	0	0
(K s)	–	–	–	–	–	–	–	–	–	–	–	–
K bc	0.0	0	0	6.5	2	53	8.0	3	48	8.5	4	46
K bc	0.0	0	0	0.0	0	0	8.0	3	48	8.5	4	46
K bc	0.0	0	0	0.0	0	0	0.0	0	0	0.0	0	0
(L US)	–	–	–	–	–	–	–	–	–	–	–	–
L	0.0	0	0	0.0	0	0	0.0	0	0	0.0	0	0
L	0.0	0	0	0.0	0	0	0.0	0	0	0.0	0	0
L	0.0	0	0	0.0	0	0	0.0	0	0	0.0	0	0
L	0.0	0	0	0.0	0	0	0.0	0	0	0.0	0	0
L	0.0	0	0	0.0	0	0	0.0	0	0	0.0	0	0
L	0.0	0	0	0.0	0	0	0.0	0	0	0.0	0	0

Cell		225			226			227			228	
	poro	perm	Sw	poro	perm	Sw	poro	perm	Sw	poro	perm	Sw
D	0.0	0	0	0.0	0	0	0.0	0	0	0.0	0	0
D	0.0	0	0	0.0	0	0	0.0	0	0	0.0	0	0
D	0.0	0	0	0.0	0	0	0.0	0	0	0.0	0	0
D	0.0	0	0	0.0	0	0	0.0	0	0	0.0	0	0
(I S)	-	-	-	-	-	-	-	-	-	-	-	-
I	0.0	0	0	0.0	0	0	0.0	0	0	0.0	0	0
I	0.0	0	0	0.0	0	0	0.0	0	0	0.0	0	0
I	0.0	0	0	0.0	0	0	0.0	0	0	0.0	0	0
(J US)	-	-	-	-	-	-	-	-	-	-	-	-
J c	0.0	0	0	0.0	0	0	0.0	0	0	0.0	0	0
(i.c.)	-	-	-	-	-	-	-	-	-	-	-	-
J ag	17.0	92	20	14.0	57	27	7.0	19	67	0.0	0	0
J ag	16.5	85	21	13.0	49	30	0.0	0	0	0.0	0	0
J ag	14.5	62	26	11.0	36	38	0.0	0	0	0.0	0	0
J ag	13.5	53	29	0.0	0	0	0.0	0	0	0.0	0	0
J ag	0.0	0	0	0.0	0	0	0.0	0	0	0.0	0	0
J ag	0.0	0	0	0.0	0	0	0.0	0	0	0.0	0	0
(i.c.)	-	-	-	-	-	-	-	-	-	-	-	-
J b	0.0	0	0	0.0	0	0	0.0	0	0	0.0	0	0
J b	0.0	0	0	0.0	0	0	0.0	0	0	0.0	0	0
(K US)	-	-	-	-	-	-	-	-	-	-	-	-
K cc	0.0	0	0	0.0	0	0	0.0	0	0	0.0	0	0
(K s)	-	-	-	-	-	-	-	-	-	-	-	-
K bc	8.0	3	48	6.5	2	53	0.0	0	0	0.0	0	0
K bc	8.5	4	46	0.0	0	0	0.0	0	0	0.0	0	0
K bc	0.0	0	0	0.0	0	0	0.0	0	0	0.0	0	0
(L US)	-	-	-	-	-	-	-	-	-	-	-	-
L	0.0	0	0	0.0	0	0	0.0	0	0	5.0	2	63
L	0.0	0	0	0.0	0	0	0.0	0	0	0.0	0	0
L	0.0	0	0	0.0	0	0	0.0	0	0	0.0	0	0
L	0.0	0	0	0.0	0	0	0.0	0	0	0.0	0	0
L	0.0	0	0	0.0	0	0	0.0	0	0	0.0	0	0
L	0.0	0	0	0.0	0	0	0.0	0	0	0.0	0	0

Cell	229			230			231			232		
	poro	perm	Sw	poro	perm	Sw	poro	perm	Sw	poro	perm	Sw
D	0.0	0	0	0.0	0	0	0.0	0	0	0.0	0	0
D	0.0	0	0	0.0	0	0	0.0	0	0	0.0	0	0
D	0.0	0	0	0.0	0	0	0.0	0	0	0.0	0	0
D	0.0	0	0	0.0	0	0	0.0	0	0	0.0	0	0
(I S)	–	–	–	–	–	–	–	–	–	–	–	–
I	0.0	0	0	0.0	0	0	0.0	0	0	0.0	0	0
I	0.0	0	0	0.0	0	0	0.0	0	0	0.0	0	0
I	0.0	0	0	0.0	0	0	0.0	0	0	0.0	0	0
(J US)	–	–	–	–	–	–	–	–	–	–	–	–
J c	0.0	0	0	0.0	0	0	0.0	0	0	0.0	0	0
(i.c.)	–	–	–	–	–	–	–	–	–	–	–	–
J ag	0.0	0	0	7.0	19	67	7.5	20	62	8.0	22	57
J ag	0.0	0	0	0.0	0	0	11.0	36	38	8.0	22	57
J ag	0.0	0	0	0.0	0	0	0.0	0	0	11.0	36	38
J ag	0.0	0	0	0.0	0	0	0.0	0	0	0.0	0	0
J ag	0.0	0	0	0.0	0	0	0.0	0	0	0.0	0	0
J ag	0.0	0	0	0.0	0	0	0.0	0	0	0.0	0	0
(i.c.)	–	–	–	–	–	–	–	–	–	–	–	–
J b	0.0	0	0	0.0	0	0	0.0	0	0	0.0	0	0
J b	0.0	0	0	0.0	0	0	0.0	0	0	0.0	0	0
(K US)	–	–	–	–	–	–	–	–	–	–	–	–
K cc	0.0	0	0	0.0	0	0	0.0	0	0	0.0	0	0
(K s)	–	–	–	–	–	–	–	–	–	–	–	–
K bc	0.0	0	0	0.0	0	0	0.0	0	0	0.0	0	0
K bc	0.0	0	0	0.0	0	0	0.0	0	0	0.0	0	0
K bc	0.0	0	0	0.0	0	0	0.0	0	0	0.0	0	0
(L US)	–	–	–	–	–	–	–	–	–	–	–	–
L	5.5	3	59	6.0	4	56	6.0	4	56	6.0	4	56
L	5.5	3	59	6.0	4	56	6.0	4	56	0.0	0	0
L	0.0	0	0	0.0	0	0	0.0	0	0	0.0	0	0
L	0.0	0	0	0.0	0	0	0.0	0	0	0.0	0	0
L	0.0	0	0	0.0	0	0	0.0	0	0	0.0	0	0
L	0.0	0	0	0.0	0	0	0.0	0	0	0.0	0	0

Cell	233			234			235			236		
	poro	perm	Sw	poro	perm	Sw	poro	perm	Sw	poro	perm	Sw
D	0.0	0	0	0.0	0	0	0.0	0	0	0.0	0	0
D	0.0	0	0	0.0	0	0	0.0	0	0	0.0	0	0
D	0.0	0	0	0.0	0	0	0.0	0	0	0.0	0	0
D	0.0	0	0	0.0	0	0	0.0	0	0	0.0	0	0
(I S)	–	–	–	–	–	–	–	–	–	–	–	–
I	0.0	0	0	0.0	0	0	0.0	0	0	0.0	0	0
I	0.0	0	0	0.0	0	0	0.0	0	0	0.0	0	0
I	0.0	0	0	0.0	0	0	0.0	0	0	0.0	0	0
(J US)	–	–	–	–	–	–	–	–	–	–	–	–
J c	0.0	0	0	0.0	0	0	0.0	0	0	0.0	0	0
(i.c.)	–	–	–	–	–	–	–	–	–	–	–	–
J ag	8.5	24	53	8.0	22	57	10.0	30	43	11.0	36	38
J ag	9.0	26	50	8.5	24	53	10.0	30	43	10.0	30	43
J ag	11.0	36	38	10.5	33	41	0.0	0	0	0.0	0	0
J ag	0.0	0	0	0.0	0	0	0.0	0	0	0.0	0	0
J ag	0.0	0	0	0.0	0	0	0.0	0	0	0.0	0	0
J ag	0.0	0	0	0.0	0	0	0.0	0	0	0.0	0	0
(i.c.)	–	–	–	–	–	–	–	–	–	–	–	–
J b	0.0	0	0	0.0	0	0	0.0	0	0	0.0	0	0
J b	0.0	0	0	0.0	0	0	0.0	0	0	0.0	0	0
(K US)	–	–	–	–	–	–	–	–	–	–	–	–
K cc	0.0	0	0	0.0	0	0	0.0	0	0	0.0	0	0
(K s)	–	–	–	–	–	–	–	–	–	–	–	–
K bc	0.0	0	0	0.0	0	0	0.0	0	0	0.0	0	0
K bc	0.0	0	0	0.0	0	0	0.0	0	0	0.0	0	0
K bc	0.0	0	0	0.0	0	0	0.0	0	0	0.0	0	0
(L US)	–	–	–	–	–	–	–	–	–	–	–	–
L	5.0	2	63	0.0	0	0	0.0	0	0	0.0	0	0
L	0.0	0	0	0.0	0	0	0.0	0	0	0.0	0	0
L	0.0	0	0	0.0	0	0	0.0	0	0	0.0	0	0
L	0.0	0	0	0.0	0	0	0.0	0	0	0.0	0	0
L	0.0	0	0	0.0	0	0	0.0	0	0	0.0	0	0
L	0.0	0	0	0.0	0	0	0.0	0	0	0.0	0	0

Cell	237			238			239			240		
	poro	perm	Sw	poro	perm	Sw	poro	perm	Sw	poro	perm	Sw
D	0.0	0	0	0.0	0	0	0.0	0	0	0.0	0	0
D	0.0	0	0	0.0	0	0	0.0	0	0	0.0	0	0
D	0.0	0	0	0.0	0	0	0.0	0	0	0.0	0	0
D	0.0	0	0	0.0	0	0	0.0	0	0	0.0	0	0
(I S)	–	–	–	–	–	–	–	–	–	–	–	–
I	0.0	0	0	0.0	0	0	0.0	0	0	0.0	0	0
I	0.0	0	0	0.0	0	0	0.0	0	0	0.0	0	0
I	0.0	0	0	0.0	0	0	0.0	0	0	0.0	0	0
(J US)	–	–	–	–	–	–	–	–	–	–	–	–
J c	0.0	0	0	0.0	0	0	0.0	0	0	0.0	0	0
(i.c.)	–	–	–	–	–	–	–	–	–	–	–	–
J ag	11.0	36	38	11.0	36	38	10.5	33	41	11.0	36	38
J ag	10.0	30	43	10.0	30	43	9.0	26	50	9.0	26	50
J ag	0.0	0	0	0.0	0	0	0.0	0	0	8.5	24	53
J ag	0.0	0	0	0.0	0	0	0.0	0	0	0.0	0	0
J ag	0.0	0	0	0.0	0	0	0.0	0	0	0.0	0	0
J ag	0.0	0	0	0.0	0	0	0.0	0	0	0.0	0	0
(i.c.)	–	–	–	–	–	–	–	–	–	–	–	–
J b	0.0	0	0	0.0	0	0	0.0	0	0	0.0	0	0
J b	0.0	0	0	0.0	0	0	0.0	0	0	0.0	0	0
(K US)	–	–	–	–	–	–	–	–	–	–	–	–
K cc	0.0	0	0	0.0	0	0	0.0	0	0	0.0	0	0
(K s)	–	–	–	–	–	–	–	–	–	–	–	–
K bc	0.0	0	0	0.0	0	0	6.5	2	53	8.0	3	48
K bc	0.0	0	0	0.0	0	0	0.0	0	0	8.0	3	48
K bc	0.0	0	0	0.0	0	0	0.0	0	0	0.0	0	0
(L US)	–	–	–	–	–	–	–	–	–	–	–	–
L	0.0	0	0	0.0	0	0	0.0	0	0	0.0	0	0
L	0.0	0	0	0.0	0	0	0.0	0	0	0.0	0	0
L	0.0	0	0	0.0	0	0	0.0	0	0	0.0	0	0
L	0.0	0	0	0.0	0	0	0.0	0	0	0.0	0	0
L	0.0	0	0	0.0	0	0	0.0	0	0	0.0	0	0
L	0.0	0	0	0.0	0	0	0.0	0	0	0.0	0	0

Cell	241			242			243			244		
	poro	perm	Sw	poro	perm	Sw	poro	perm	Sw	poro	perm	Sw
D	0.0	0	0	0.0	0	0	0.0	0	0	0.0	0	0
D	0.0	0	0	0.0	0	0	0.0	0	0	0.0	0	0
D	0.0	0	0	0.0	0	0	0.0	0	0	0.0	0	0
D	0.0	0	0	0.0	0	0	0.0	0	0	0.0	0	0
(I S)	–	–	–	–	–	–	–	–	–	–	–	–
I	0.0	0	0	0.0	0	0	0.0	0	0	0.0	0	0
I	0.0	0	0	0.0	0	0	0.0	0	0	0.0	0	0
I	0.0	0	0	0.0	0	0	0.0	0	0	0.0	0	0
(J US)	–	–	–	–	–	–	–	–	–	–	–	–
J c	0.0	0	0	0.0	0	0	0.0	0	0	0.0	0	0
(i.c.)	–	–	–	–	–	–	–	–	–	–	–	–
J ag	11.0	36	38	10.5	33	41	7.5	20	62	7.0	19	67
J ag	9.0	26	50	8.5	24	53	7.0	19	67	0.0	0	0
J ag	8.5	24	53	8.0	22	57	0.0	0	0	0.0	0	0
J ag	0.0	0	0	0.0	0	0	0.0	0	0	0.0	0	0
J ag	0.0	0	0	0.0	0	0	0.0	0	0	0.0	0	0
J ag	0.0	0	0	0.0	0	0	0.0	0	0	0.0	0	0
(i.c.)	–	–	–	–	–	–	–	–	–	–	–	–
J b	0.0	0	0	0.0	0	0	0.0	0	0	0.0	0	0
J b	0.0	0	0	0.0	0	0	0.0	0	0	0.0	0	0
(K US)	–	–	–	–	–	–	–	–	–	–	–	–
K cc	0.0	0	0	0.0	0	0	0.0	0	0	0.0	0	0
(K s)	–	–	–	–	–	–	–	–	–	–	–	–
K bc	8.0	3	48	8.0	3	48	6.5	2	53	0.0	0	0
K bc	8.5	4	46	8.0	3	48	0.0	0	0	0.0	0	0
K bc	0.0	0	0	0.0	0	0	0.0	0	0	0.0	0	0
(L US)	–	–	–	–	–	–	–	–	–	–	–	–
L	0.0	0	0	0.0	0	0	0.0	0	0	0.0	0	0
L	0.0	0	0	0.0	0	0	0.0	0	0	0.0	0	0
L	0.0	0	0	0.0	0	0	0.0	0	0	0.0	0	0
L	0.0	0	0	0.0	0	0	0.0	0	0	0.0	0	0
L	0.0	0	0	0.0	0	0	0.0	0	0	0.0	0	0
L	0.0	0	0	0.0	0	0	0.0	0	0	0.0	0	0

Cell	245			246			247			248		
	poro	perm	Sw	poro	perm	Sw	poro	perm	Sw	poro	perm	Sw
D	0.0	0	0	0.0	0	0	0.0	0	0	0.0	0	0
D	0.0	0	0	0.0	0	0	0.0	0	0	0.0	0	0
D	0.0	0	0	0.0	0	0	0.0	0	0	0.0	0	0
D	0.0	0	0	0.0	0	0	0.0	0	0	0.0	0	0
(I S)	–	–	–	–	–	–	–	–	–	–	–	–
I	0.0	0	0	0.0	0	0	0.0	0	0	0.0	0	0
I	0.0	0	0	0.0	0	0	0.0	0	0	0.0	0	0
I	0.0	0	0	0.0	0	0	0.0	0	0	0.0	0	0
(J US)	–	–	–	–	–	–	–	–	–	–	–	–
J c	0.0	0	0	0.0	0	0	0.0	0	0	0.0	0	0
(i.c.)	–	–	–	–	–	–	–	–	–	–	–	–
J ag	7.5	20	62	8.0	22	57	9.0	26	50	9.0	26	50
J ag	10.5	33	41	13.5	53	29	12.0	42	34	11.5	39	36
J ag	0.0	0	0	0.0	0	0	0.0	0	0	0.0	0	0
J ag	0.0	0	0	0.0	0	0	0.0	0	0	0.0	0	0
J ag	0.0	0	0	0.0	0	0	0.0	0	0	0.0	0	0
J ag	0.0	0	0	0.0	0	0	0.0	0	0	0.0	0	0
(i.c.)	–	–	–	–	–	–	–	–	–	–	–	–
J b	0.0	0	0	0.0	0	0	0.0	0	0	0.0	0	0
J b	0.0	0	0	0.0	0	0	0.0	0	0	0.0	0	0
(K US)	–	–	–	–	–	–	–	–	–	–	–	–
K cc	0.0	0	0	0.0	0	0	0.0	0	0	0.0	0	0
(K s)	–	–	–	–	–	–	–	–	–	–	–	–
K bc	0.0	0	0	0.0	0	0	0.0	0	0	0.0	0	0
K bc	0.0	0	0	0.0	0	0	0.0	0	0	0.0	0	0
K bc	0.0	0	0	0.0	0	0	0.0	0	0	0.0	0	0
(L US)	–	–	–	–	–	–	–	–	–	–	–	–
L	0.0	0	0	0.0	0	0	0.0	0	0	0.0	0	0
L	0.0	0	0	0.0	0	0	0.0	0	0	0.0	0	0
L	0.0	0	0	0.0	0	0	0.0	0	0	0.0	0	0
L	0.0	0	0	0.0	0	0	0.0	0	0	0.0	0	0
L	0.0	0	0	0.0	0	0	0.0	0	0	0.0	0	0
L	0.0	0	0	0.0	0	0	0.0	0	0	0.0	0	0

Cell		249			250			251			252	
	poro	perm	Sw	poro	perm	Sw	poro	perm	Sw	poro	perm	Sw
D	0.0	0	0	0.0	0	0	0.0	0	0	0.0	0	0
D	0.0	0	0	0.0	0	0	0.0	0	0	0.0	0	0
D	0.0	0	0	0.0	0	0	0.0	0	0	0.0	0	0
D	0.0	0	0	0.0	0	0	0.0	0	0	0.0	0	0
(I S)	–	–	–	–	–	–	–	–	–	–	–	–
I	0.0	0	0	0.0	0	0	0.0	0	0	0.0	0	0
I	0.0	0	0	0.0	0	0	0.0	0	0	0.0	0	0
I	0.0	0	0	0.0	0	0	0.0	0	0	0.0	0	0
(J US)	–	–	–	–	–	–	–	–	–	–	–	–
J c	0.0	0	0	0.0	0	0	0.0	0	0	0.0	0	0
(i.c.)	–	–	–	–	–	–	–	–	–	–	–	–
J ag	9.0	26	50	11.0	36	38	10.5	33	41	11.0	36	38
J ag	11.5	39	36	0.0	0	0	0.0	0	0	0.0	0	0
J ag	0.0	0	0	0.0	0	0	0.0	0	0	0.0	0	0
J ag	0.0	0	0	0.0	0	0	0.0	0	0	0.0	0	0
J ag	0.0	0	0	0.0	0	0	0.0	0	0	0.0	0	0
J ag	0.0	0	0	0.0	0	0	0.0	0	0	0.0	0	0
(i.c.)	–	–	–	–	–	–	–	–	–	–	–	–
J b	0.0	0	0	0.0	0	0	0.0	0	0	0.0	0	0
J b	0.0	0	0	0.0	0	0	0.0	0	0	0.0	0	0
(K US)	–	–	–	–	–	–	–	–	–	–	–	–
K cc	0.0	0	0	0.0	0	0	0.0	0	0	0.0	0	0
(K s)	–	–	–	–	–	–	–	–	–	–	–	–
K bc	0.0	0	0	0.0	0	0	0.0	0	0	0.0	0	0
K bc	0.0	0	0	0.0	0	0	0.0	0	0	0.0	0	0
K bc	0.0	0	0	0.0	0	0	0.0	0	0	0.0	0	0
(L US)	–	–	–	–	–	–	–	–	–	–	–	–
L	0.0	0	0	0.0	0	0	0.0	0	0	0.0	0	0
L	0.0	0	0	0.0	0	0	0.0	0	0	0.0	0	0
L	0.0	0	0	0.0	0	0	0.0	0	0	0.0	0	0
L	0.0	0	0	0.0	0	0	0.0	0	0	0.0	0	0
L	0.0	0	0	0.0	0	0	0.0	0	0	0.0	0	0
L	0.0	0	0	0.0	0	0	0.0	0	0	0.0	0	0

Cell	253			254			255			256		
	poro	perm	Sw	poro	perm	Sw	poro	perm	Sw	poro	perm	Sw
D	0.0	0	0	0.0	0	0	0.0	0	0	0.0	0	0
D	0.0	0	0	0.0	0	0	0.0	0	0	0.0	0	0
D	0.0	0	0	0.0	0	0	0.0	0	0	0.0	0	0
D	0.0	0	0	0.0	0	0	0.0	0	0	0.0	0	0
(I S)	–	–	–	–	–	–	–	–	–	–	–	–
I	0.0	0	0	0.0	0	0	0.0	0	0	0.0	0	0
I	0.0	0	0	0.0	0	0	0.0	0	0	0.0	0	0
I	0.0	0	0	0.0	0	0	0.0	0	0	0.0	0	0
(J US)	–	–	–	–	–	–	–	–	–	–	–	–
J c	0.0	0	0	0.0	0	0	0.0	0	0	0.0	0	0
(i.c.)	–	–	–	–	–	–	–	–	–	–	–	–
J ag	10.0	30	43	9.0	26	50	7.5	20	62	7.0	19	67
J ag	0.0	0	0	7.5	20	62	7.5	20	62	0.0	0	0
J ag	0.0	0	0	0.0	0	0	0.0	0	0	0.0	0	0
J ag	0.0	0	0	0.0	0	0	0.0	0	0	0.0	0	0
J ag	0.0	0	0	0.0	0	0	0.0	0	0	0.0	0	0
J ag	0.0	0	0	0.0	0	0	0.0	0	0	0.0	0	0
(i.c.)	–	–	–	–	–	–	–	–	–	–	–	–
J b	0.0	0	0	0.0	0	0	0.0	0	0	0.0	0	0
J b	0.0	0	0	0.0	0	0	0.0	0	0	0.0	0	0
(K US)	–	–	–	–	–	–	–	–	–	–	–	–
K cc	0.0	0	0	0.0	0	0	0.0	0	0	0.0	0	0
(K s)	–	–	–	–	–	–	–	–	–	–	–	–
K bc	0.0	0	0	7.5	3	49	8.0	3	48	7.5	3	49
K bc	0.0	0	0	7.5	3	49	8.0	3	48	7.5	3	49
K bc	0.0	0	0	0.0	0	0	0.0	0	0	0.0	0	0
(L US)	–	–	–	–	–	–	–	–	–	–	–	–
L	0.0	0	0	0.0	0	0	0.0	0	0	0.0	0	0
L	0.0	0	0	0.0	0	0	0.0	0	0	0.0	0	0
L	0.0	0	0	0.0	0	0	0.0	0	0	0.0	0	0
L	0.0	0	0	0.0	0	0	0.0	0	0	0.0	0	0
L	0.0	0	0	0.0	0	0	0.0	0	0	0.0	0	0
L	0.0	0	0	0.0	0	0	0.0	0	0	0.0	0	0

Cell	257			258			259			260		
	poro	perm	Sw	poro	perm	Sw	poro	perm	Sw	poro	perm	Sw
D	0.0	0	0	0.0	0	0	0.0	0	0	0.0	0	0
D	0.0	0	0	0.0	0	0	0.0	0	0	0.0	0	0
D	0.0	0	0	0.0	0	0	0.0	0	0	0.0	0	0
D	0.0	0	0	0.0	0	0	0.0	0	0	0.0	0	0
(I S)	–	–	–	–	–	–	–	–	–	–	–	–
I	0.0	0	0	0.0	0	0	0.0	0	0	0.0	0	0
I	0.0	0	0	0.0	0	0	0.0	0	0	0.0	0	0
I	0.0	0	0	0.0	0	0	0.0	0	0	0.0	0	0
(J US)	–	–	–	–	–	–	–	–	–	–	–	–
J c	0.0	0	0	0.0	0	0	0.0	0	0	0.0	0	0
(i.c.)	–	–	–	–	–	–	–	–	–	–	–	–
J ag	7.0	19	67	9.0	26	50	9.0	26	50	9.0	26	50
J ag	0.0	0	0	0.0	0	0	0.0	0	0	0.0	0	0
J ag	0.0	0	0	0.0	0	0	0.0	0	0	0.0	0	0
J ag	0.0	0	0	0.0	0	0	0.0	0	0	0.0	0	0
J ag	0.0	0	0	0.0	0	0	0.0	0	0	0.0	0	0
J ag	0.0	0	0	0.0	0	0	0.0	0	0	0.0	0	0
(i.c.)	–	–	–	–	–	–	–	–	–	–	–	–
J b	0.0	0	0	0.0	0	0	0.0	0	0	0.0	0	0
J b	0.0	0	0	0.0	0	0	0.0	0	0	0.0	0	0
(K US)	–	–	–	–	–	–	–	–	–	–	–	–
K cc	0.0	0	0	0.0	0	0	0.0	0	0	0.0	0	0
(K s)	–	–	–	–	–	–	–	–	–	–	–	–
K bc	0.0	0	0	0.0	0	0	0.0	0	0	0.0	0	0
K bc	0.0	0	0	0.0	0	0	0.0	0	0	0.0	0	0
K bc	0.0	0	0	0.0	0	0	0.0	0	0	0.0	0	0
(L US)	–	–	–	–	–	–	–	–	–	–	–	–
L	0.0	0	0	0.0	0	0	0.0	0	0	0.0	0	0
L	0.0	0	0	0.0	0	0	0.0	0	0	0.0	0	0
L	0.0	0	0	0.0	0	0	0.0	0	0	0.0	0	0
L	0.0	0	0	0.0	0	0	0.0	0	0	0.0	0	0
L	0.0	0	0	0.0	0	0	0.0	0	0	0.0	0	0
L	0.0	0	0	0.0	0	0	0.0	0	0	0.0	0	0